UNIVERSITY OF CALIFORNIA, SAN DIEGO

Organic synthesis as an effective approach to chemical, pharmaceutical, and biosynthetic investigations of natural products

A dissertation submitted in partial satisfaction of the requirements for the degree of

Doctor of Philosophy

in

Oceanography

by

Takashi L.Suyama

Committee in charge:

Professor William H. Gerwick, Chair
Professor William Fenical
Professor Yoshihisa Kobayashi
Professor Bradley S. Moore
Professor Emmanuel Theodorakis

2009

The Dissertation of Takashi L. Suyama is approved, and it is acceptable in quality and form for publication on microfilm and electronically:

_____

_____

_____

_____

_____

Chair

University of California, San Diego

2009

DEDICATION

This dissertation is dedicated to my best friend, my counselor, my strength, my inspiration, my advocate, my guide, my hope, my savior, my hero, and my Lord, Jesus Christ of Nazareth. For, “we are hard-pressed on every side, yet not crushed; we are perplexed, but not in despair; persecuted, but not forsaken; struck down, but not destroyed— always carrying about in the body the dying of the Lord Jesus, that the life of Jesus also may be manifested in our body.... Therefore we do not lose heart.... For the things which are seen are temporary, but the things which are not seen are *eternal* (2Corinthians 4:8-10, 16, 18, NKJV; emphasis mine).” Indeed, it is because of Him that even I have persevered through this doctoral program. The credit for all that follows is due unto His name.

EPIGRAPH

My Hope is Built.

My hope is built on nothing less
Than Jesus' blood and righteousness.
I dare not trust the sweetest frame,
But wholly lean on Jesus' name.

On Christ the solid rock I stand,
All other ground is sinking sand;
All other ground is sinking sand.

When darkness veils His lovely face,
I rest on His unchanging grace.
In every high and stormy gale,
My anchor holds within the veil.

On Christ the solid rock I stand,
All other ground is sinking sand;
All other ground is sinking sand.

His oath, His covenant, His blood
Supports me in the whelming flood.
When all around my soul gives way,
He then is all my hope and stay.

On Christ the solid rock I stand,
All other ground is sinking sand;
All other ground is sinking sand.

When He shall come with trumpet sound,
O may I then in Him be found!
Dressed in His righteousness alone,
Faultless to stand before the Throne!

On Christ the solid rock I stand,
All other ground is sinking sand;
All other ground is sinking sand.

— Edward Mote, 1797-1874

TABLE OF CONTENTS

Signature Page..... iii

Dedication..... iv

Epigraph..... v

Table of Contents..... vi

List of Abbreviations..... viii

List of Illustration and Figures..... x

List of Schemes..... xvi

List of Tables..... xix

Acknowledgments..... xx

Vita and Publications..... xxiv

Abstract..... xxvi

Chapter I: Introduction..... 1

Chapter II: Ichthyotoxic brominated diphenyl ethers from a mixed assemblage of a red alga and cyanobacterium: structure clarification and biological properties 60

Chapter III: Discovery of a novel vinylchloride containing fatty acid from a marine cyanobacterium *Lyngbya* sp. 101

Chapter IV: Absolute stereochemistry of novel fatty acids by synthetic introduction of a stereochemical reference 126

Chapter V: Use of biomimetic starting materials for expedient total synthesis of epiquinamide enantiomers: true identity of bioactive metabolite..... 172

Chapter VI: Stereospecific total synthesis of somocystinamide A; an extremely potent antiangiogenic marine natural product containing synthetically challenging functional groups..... 234

Chapter VII: Biomimetic total synthesis of a cyanobacterial UV-blocking natural product, scytonemin and insights into its biogenesis..... 315

Chapter VIII: Conclusions.. 368

Appendix... 375

LIST OF ABBREVIATIONS

CD	circular dichroism
CoA	coenzyme A
COSY	correlation spectroscopy
DCI	desorption chemical ionization
DDQ	2,3-dichloro-5,6-dicyano benzoquinone
EC	effective concentration
EDC	1-ethyl-3-(3-dimethylaminopropyl)-carbodiimide
EtOH	ethanol
DMAP	4-dimethylamino pyridine
EI	electron impact
ESI	electron spray ionization
FAB	fast atom bombardment
FLIPR	fluorescence laser plate reader
GCMS	gas chromatography mass spectrometry
HMBC	heteronuclear multiple bond correlation
HMG	3-hydroxy-3-methyl-glutaryl
HMQC	heteronuclear multiple quantum coherence
HPLC	high performance liquid chromatography
HR	high resolution
HSQC	heteronuclear single quantum coherence
INADEQUATE	incredible natural abundance double quantum transfer experiment
i-PrOH	isopropanol
IR	infrared spectroscopy
MeOH	methanol
MS	mass spectrometry
MsO	methanesulfonate
NCS	*N*-chlorosuccinimide
NMR	nuclear magnetic resonance

NOE	nuclear Overhauser effect
NOESY	nuclear Overhauser effect spectroscopy
NRPS	non-ribosomal peptide synthase
OR	optical rotation
PKS	polyketide synthase
ROESY	rotating Overhauser effect spectroscopy
rt	room temperature
TFA	trifluoroacetic acid
THF	tetrahydrofuran
TLC	thin layer chromatography
TMSOTf	trimethylsilyl trifluoromethanesulfonate
TBDMSOTf	*tert*-butyldimethylsilyl trifluoromethanesulfonate
TBSOTf	*tert*-butyldimethylsilyl trifluoromethanesulfonate
TsOH	toluenesulfonic acid
UV	ultra violet
VLC	vacuum liquid chromatography

LIST OF ILLUSTRATION AND FIGURES

Illustration I.1: Graphical representation of thesis research..... 4

Figure I.1: The originally assigned structure (**13**) of mururin C and its revised structure (**12**)..... 11

Figure I.2: Types of errors in natural product structure revisions..... 30

Figure I.3: Structure determination methods used in 2005-2008 for the erroneous cases..... 30

Figure I.4: Structure revision methods used in 2005-2008..... 30

Figure I.5: Discrimination of possible structures by HMBC..... 31

Figure I.6: HMBC correlations observed and recorded for the labdane diterpenoid... 31

Figure I.7: All new small chemical entities that were approved for clinical use, 01/1981-06/2006, by source..... 33

Figure I.8: Drug Development Process..... 35

Figure II.1: OH-PBDE congeners isolated from the red alga/cyanobacteria assembly (**1** and **2**) and an alternative regioisomer of **1** (**3**)..... 63

Figure II.2: X-ray crystal structure of **1**..... 68

Figure II.3: Ca^{2+} modulation assay in mouse neocortical neurons for compounds **1**-**3**..... 72

Figure II.4: Photographs of the red algal voucher sample..... 77

Figure II.5: Photograph of the red algal voucher sample..... 78

Figure II.6: Isolation scheme for **1** and **3**..... 85

Figure II.7: ^{1}H NMR Spectrum of **1** in $CDCl_3$ 86

Figure II.8: ^{13}C NMR Spectrum of **1** in $CDCl_3$ 87

Figure II.9: ^{1}H-^{1}H COSY Spectrum of **1** in $CDCl_3$ 88

Figure II.10: ^{1}H-^{13}C HSQC Spectrum of **1** in $CDCl_3$ 89

Figure II.11: ^{1}H-^{13}C HMBC Spectrum of **1** in $CDCl_3$ 90

Figure II.12: ^{1}H NMR Spectrum of **1** in $CDCl_3$ 91

Figure II.13: ^{13}C NMR Spectrum of **3** in $CDCl_3$ 92

Figure II.14: ^{1}H-^{1}H COSY Spectrum of **3** in $CDCl_3$ 93

Figure II.15: ^{1}H-^{13}C HSQC Spectrum of **3** in $CDCl_3$ 94

Figure II.16: ^{1}H-^{13}C HMBC Spectrum of **3** in $CDCl_3$ 95

Figure II.17: ^{1}H NMR Spectrum of **2** in $CDCl_3$ 96

Figure II.18: ^{1}H-^{1}H COSY Spectrum of **2** in $CDCl_3$ 97
Figure III.1: Jamaicamides A-C..... 104
Figure III.2: Malyngamides A-X..... 104
Figure III.3: Satellite Image of *Lyngbya* Collection Site..... 106
Figure III.4: Zoom-up of the Satelite Image of the *Lyngbya* Collection Site..... 106
Figure III.5: "Green *Lyngbya*" collected in Papua New Guinea..... 107
Figure III.6: ^{1}H NMR Spectrum of Credneric Acid (**38**)..... 108
Figure III.7: Credneric Acid and Credneramide..... 112
Figure III.8: *N*-Acyl Homoserine Lactones (AHLs)..... 112
Figure III.9: Credneric Acid (**38**) ^{13}C NMR Spectrum in $CDCl_3$..... 116
Figure III.10: Credneric Acid (**38**) ^{1}H-^{1}H COSY Spectrum in $CDCl_3$..... 117
Figure III.11: Credneric Acid (**38**) ^{1}H-^{13}C HSQC Spectrum in $CDCl_3$..... 118
Figure III.12: Credneric Acid (**38**) ^{1}H-^{13}C HMBC Spectrum in $CDCl_3$..... 119
Figure III.13: Credneric Acid (**38**) 1D ROESY Spectrum: Irradiated at 2.73 ppm in $CDCl_3$..... 120
Figure III.14: Credneric Acid (**38**) 1D ROESY Spectrum: Irradiated at 5.79 ppm in $CDCl_3$..... 121
Figure III.15: Credneric Acid (**38**) 1D ROESY Spectrum: Irradiated at 2.16 ppm in $CDCl_3$..... 122
Figure III.16: IR spectrum of **38**..... 123
Figure IV.1: Proposed transition state of alkylation of the enolate of 5 guided by oxazolidinone auxiliary..... 132
Figure IV.2: Dihedral angles predicted from the ^{1}H-^{1}H coupling constants and Altona equation (A) and select ROESY correlations for **7** and **8** (B)..... 135
Figure IV.3: History of the absolute stereochemical assignment of cyclopropane derivative **11**..... 136
Figure IV.4: **1**H and **13**C NMR assignments and an NOE correlation of **16** in $CDCl_3$ 138
Figure IV.5: X-ray crystal structure of **15**..... 139
Figure IV.6: Corrected stereochemistry of **1-m** and **1-c**..... 139
Figure IV.7: Synthetic Introduction of a Stereochemical Reference (SISTER) method conceptual figure..... 141
Figure IV.8: ^{1}H NMR spectrum of **7** in C_6D_6..... 146
Figure IV.9: ^{1}H NMR spectrum of **7** in $CDCl_3$..... 147
Figure IV.10: ^{13}C NMR spectrum of **7** in $CDCl_3$..... 148
Figure IV.11: ^{1}H-^{1}H Homonuclear decoupling experiment for **7** in C_6D_6 – Part 1..... 149
Figure IV.12: ^{1}H-^{1}H Homonuclear decoupling for **7** in C_6D_6 – Part 2..... 150

Figure IV.13: ^{1}H-^{1}H Homonuclear decoupling experiment for 7 in C_6D_6 – Part 3..... 151
Figure IV.14: ^{1}H-^{1}H COSY spectrum of **7** in C_6D_6..... 152
Figure IV.15: ROESY spectrum of **7** in C_6D_6..... 153
Figure IV.16: LR FAB MS spectrum of **7**..... 154
Figure IV.17: IR spectrum of **7**..... 155
Figure IV.18: ^{1}H NMR spectrum of **8** in C_6D_6..... 156
Figure IV.19: ^{1}H NMR spectrum of **8** in $CDCl_3$..... 157
Figure IV.20: ^{13}C NMR spectrum of **8** in $CDCl_3$..... 158
Figure IV.21: ^{1}H-^{1}H Homonuclear decoupling experiment for **8** in C_6D_6 – Part 1..... 159
Figure IV.22: ^{1}H-^{1}H Homonuclear decoupling experiment for **8** in C_6D_6 – Part 2..... 160
Figure IV.23: ^{1}H-^{1}H Homonulcear decoupling experiment for **8** in C_6D_6 – Part 3 161
Figure IV.24: ^{1}H-^{1}H COSY spectrum of **8** in C_6D_6..... 162
Figure IV.25: ROESY spectrum of **8** in C_6D_6..... 163
Figure IV.26: IR spectrum of **8**..... 164
Figure IV.27: ^{1}H NMR spectrum of **9** in $CDCl_3$..... 165
Figure IV.28: IR spectrum of **9**..... 166
Figure IV.29: Geometry optimized 3D structures of **7** (above) and **8** (below)..... 167
Figure IV.30: HPLC chromatogram for **4** and **7**..... 168
Figure IV.31: HPLC chromatogram for **5** and **8**..... 169
Figure IV.32: UV spectra of **7** and **8**..... 170
Figure V.1: Frog skin alkaloids of various core skeletons..... 174
Figure V.2: Skin of Epipedobates tricolor contains epibatidine and epiquinamide..... 175
Figure V.3: X-ray crystal structure of epi-epiquinamide (**15**)..... 178
Figure V.4: ^{1}H NMR Spectrum of **11** in $CDCl_3$..... 200
Figure V.5: ^{13}C NMR Spectrum of **11** in $CDCl_3$..... 201
Figure V.6: ^{1}H NMR Spectrum of **12** in $CDCl_3$..... 202
Figure V.7: ^{13}C NMR Spectrum of **12** in $CDCl_3$..... 203
Figure V.8: ^{1}H NMR Spectrum of **13** in $CDCl_3$..... 204
Figure V.9: ^{13}C NMR Spectrum of **13** in $CDCl_3$..... 205
Figure V.10: ^{1}H NMR Spectrum of **14** in $CDCl_3$..... 206
Figure V.11: ^{13}C NMR Spectrum of **14** in $CDCl_3$..... 207
Figure V.12: ^{1}H NMR Spectrum of **15** in MeOH-d_4..... 208
Figure V.13: ^{13}C NMR Spectrum of **15** in MeOH-d_4..... 209
Figure V.14: ^{1}H NMR Spctrum of **16** in $CDCl_3$..... 210

Figure V.15: ^{13}C NMR Spectrum of **16** in $CDCl_3$..... 211
Figure V.16: EI-GCMS Chromatogram and Mass Spectrum of **16**..... 212
Figure V.17: ^{1}H NMR spectrum **29** in $CDCl_3$..... 213
Figure V.18: ^{13}C NMR spectrum of **29** in $CDCl_3$..... 214
Figure V.19: ^{1}H NMR spectrum of **30** in $CDCl_3$..... 215
Figure V.20: ^{13}C NMR spectrum of **30** in $CDCl_3$..... 216
Figure V.21: ^{1}H NMR spectrum of **28** in $CDCl_3$..... 217
Figure V.22: ^{13}C NMR spectrum of **28** in $CDCl_3$..... 218
Figure V.23: ^{1}H NMR spectrum of **31** in $CDCl_3$..... 219
Figure V.24: ^{13}C NMR spectrum of **31** in $CDCl_3$..... 220
Figure V.25: ^{1}H NMR spectrum of **27** in $CDCl_3$..... 221
Figure V.26: 13C NMR spectrum of **27** in $CDCl_3$..... 222
Figure V.27: ^{1}H NMR spectrum of **32** in $CDCl_3$..... 223
Figure V.28: ^{1}H NMR NMR spectrum of **(+)-9** in $CDCl_3$..... 224
Figure V.29: ^{1}H NMR spectrum of **(+)-9** in $CDCl_3$..... 225
Figure V.30: ^{13}C NMR spectrum of **(+)-9** in $CDCl_3$..... 226
Figure V.31: ^{1}H NMR spectrum of **(-)-9** in $CDCl_3$..... 227
Figure V. 32: ^{13}C NMR spectrum of **(-)-9** in $CDCl_3$..... 228
Figure Vl.1: Antiangiogenic activity of **1** in zebrafish..... 236
Figure VI.2: Impact of somocystinamide A (**1**) on proliferation of paired neuroblastoma cells lacking caspase 8 expression (triangles) or expressing caspase 8 (squares)..... 238
Figure VI.3: Extrinsic pathway via activation of caspase-8 leading to apoptosis..... 238
Figure VI.4: Intrinsic pathway via activation of caspase-9 leading to apoptosis..... 239
Figure VI.5: Most stable conformer of somocystinamide A found through molecular modeling..... 240
Figure VI.6: Proposed biosynthesis of somocystinamide A (**1**)..... 243
Figure VI.7: Enamide containing natural products..... 244
Figure VI.8: Examples of disulfide-containing natural products..... 247
Figure VI.9: Model compounds used in the study of enamide formation..... 255
Figure VI.10: Reaction setup for enamide formation using molecular sieves and glass wool in a Soxhlet extractor..... 259
Figure VI.11: Solubility of somocystinamide A (**1**) in various media..... 261
Figure VI.12: ^{1}H NMR spectrum of **22** in $CDCl_3$..... 282
Figure VI.13: ^{13}C NMR spectrum of **22** in $CDCl_3$..... 283

Figure VI.14: ^{1}H NMR spectrum of **2** in $CDCl_3$..... 284
Figure VI.15: ^{13}C NMR spectrum of **2** in $CDCl_3$..... 285
Figure VI.16: ^{1}H NMR spectrum of **44** in $CDCl_3$..... 286
Figure VI.17: ^{13}C NMR spectrum of **44** in $CDCl_3$..... 287
Figure VI.18: ^{1}H NMR spectrum of **51** in $CDCl_3$..... 288
Figure VI.19: ^{13}C NMR spectrum of **51** in $CDCl_3$..... 289
Figure VI.20: ^{1}H NMR spectrum of **52** in $CDCl_3$..... 290
Figure VI.21: ^{13}C NMR spectrum of **52** in $CDCl_3$..... 291
Figure VI.22: ^{1}H NMR spectrum of **52-cis** in $CDCl_3$..... 292
Figure VI.23: ^{13}C NMR spectrum of **52-cis** in $CDCl_3$..... 293
Figure VI.24: ^{1}H NMR spectrum of **56** in $CDCl_3$..... 294
Figure VI.25: ^{13}C NMR spectrum of **56** in $CDCl_3$..... 295
Figure VI.26: COSY spectrum of **56** in $CDCl_3$..... 296
Figure VI.27: HMBC spectrum of **56** in $CDCl_3$..... 297
Figure VI.28: ^{1}H NMR spectrum of **57** in $CDCl_3$..... 298
Figure VI.29: ^{13}C NMR spectrum of **57** in $CDCl_3$..... 299
Figure VI.30: ^{1}H NMR spectrum of **3** in 1:1 $CDCl_3/CD_3OD$..... 300
Figure VI.31: ^{13}C NMR spectrum of **3** in 1:1 $CDCl_3/CD_3OD$..... 301
Figure VI.32: ^{1}H NMR spectrum of **1** in $CDCl_3$..... 302
Figure VI.33: ^{13}C NMR spectrum of **1** in $CDCl_3$..... 303
Figure VI.34: 1H NMR spectrum of **70** in $CDCl_3$..... 304
Figure VI.35: ^{13}C NMR spectrum of **70** in $CDCl_3$..... 305
Figure VI.36: ^{1}H NMR spectrum of **71** in $CDCl_3$..... 306
Figure VI.37: ^{13}C NMR spectrum of **71** in $CDCl_3$..... 307
Figure VI.38: ^{1}H NMR spectrum of **73** in $CDCl_3$..... 308
Figure VI.39: ^{13}C NMR spectrum of **73** in $CDCl_3$..... 309
Figure VII.1: Light absorption spectrum of scytonemin (**1**) (taken from ref. 4)..... 318
Figure VII.2: Select HMBC, COSY, and ROESY correlations of scytonemin monomer (**22**) in DMF-d_7..... 323
Figure VII.3: Scytonemin monomer (**22**): geometry optimized computer model..... 324
Figure VII.4: ^{1}H NMR spectrum of **22** in DMF-d_7..... 325
Figure VII.5: pH-dependent color change of monomer **22**..... 328
Figure VII.6: Alternative structures for scytonemin..... 335
Figure VII.7: ^{1}H NMR spectrum of **21** in $CDCl_3$..... 346
Figure VII.8: ^{13}C NMR spectrum of **21** in $CDCl_3$..... 347

Figure VII.9: ^{1}H NMR spectrum of **18** in $CDCl_3$..... 348
Figure VII.10: ^{13}C NMR spectrum of **22** in DMF-d_7..... 349
Figure VII.11: COSY NMR spectrum of **22** in DMF-d_7..... 350
Figure VII.12: HSQC NMR spectrum of **22** in DMF-d_7..... 351
Figure VII.13: HMBC NMR spectrum of **22** in DMF-d_7..... 352
Figure VII.14: NOESY NMR spectrum of **22** in DMF-d_7..... 353
Figure VII.15: HRMS (EI) spectrum of **22**..... 354
Figure VII.16: ^{1}H NMR spectrum of **29** in $CDCl_3$..... 355
Figure VII.17: ^{13}C NMR spectrum of **29** in $CDCl_3$..... 356
Figure VII.18: COSY spectrum of **29** in $CDCl_3$..... 357
Figure VII.19: HSQC spectrum of **29** in $CDCl_3$..... 358
Figure VII.20: HMBC spectrum of **29** in $CDCl_3$..... 359
Figure VII.21: ROESY spectrum of **29** in $CDCl_3$..... 360
Figure VII.22: HRMS (ESI-FT) spectrum of **29** (showing [M+Na])..... 361
Figure VII.23: ^{1}H NMR spectrum of **34** in $CDCl_3$..... 362
Figure VII.24: ^{13}C NMR spectrum of **34** in $CDCl_3$..... 363
Figure VII.25: ^{1}H NMR spectrum of **37** in $CDCl_3$..... 364
Figure VII.26: ^{13}C NMR spectrum of **37** in $CDCl_3$..... 365
Figure VIII.1: Natural products isolated during the dissertation research..... 371
Figure VIII.2: Natural products that were synthetically investigated during the disseration research..... 372

LIST OF SCHEMES

Scheme I.1: Echitamine structure elucidation efforts by chemical degradation and synthetic logic..... 8

Scheme I.2: Assigned structures by chemical investigation and X-ray crystallography..... 8

Scheme I.3: Relationship between **9** and **10** via electrocyclization..... 9

Scheme I.4: Novartis strategy for the synthesis of discodermolide (**17**)..... 37

Scheme I.5: Synthetic contributions to the study of brevianamides biosynthesis..... 40

Scheme I.6: Biomimetic synthesis of grossularine-1 (**35**)..... 42

Scheme I.7: Biomimetic synthesis of panepophenanthrin (**41**) through a Diels-Alder reaction..... 42

Scheme I.8: Scytonemin monomer does not dimerize under naturally occurring conditions..... 43

Scheme II.1: Synthesis of **3** by Marsh's route..... 71

Scheme III.1: Divergent biosyntheses of jamaicamide A and curacin A..... 105

Scheme III.2: Isolation process for credneric acid (**38**)..... 108

Scheme III.3: Substructures of Credneric Acid by 1H NMR, COSY, and HSQC..... 110

Scheme III.4: Stereochemical Assignments of Credneric Acid by 1D ROESY Correlations..... 111

Scheme III.5: Cyclopropane Fatty Acid and Lyngbyamides..... 112

Scheme IV.1: Derivatization of cyclopropane fatty acids **1-m** and **1-c**..... 131

Scheme IV.2: Total synthesis of (+)-grenadamide (**13**) by Baird et al..... 135

Scheme IV.3: Synthesis of PGME derivatives from **11**..... 137

Scheme V.1: Reduction of dehydropiperidine: two stereochemical outcomes..... 176

Scheme V.2: Applying the synthetic logic of quinolizidine biosynthesis to the synthesis of epiquinamide skeleton..... 176

Scheme V.3: Biomimetic synthesis of lupinamine by Wanner and Koomen..... 177

Scheme V.4: Initial Retrosynthetic Analysis of Epiquinamide..... 177

Scheme V.5: Total synthesis of (1R,9S)-epi-epiquinamide (**16**)..... 178

Scheme V.6: Proposed total synthesis of (+)-epiquinamide via boron nucleophilic addition to acyl imminium ion..... 180

Scheme V.7: Proposed total synthesis of (+)-epiquinamide via hetero Diels-Alder... 180

Scheme V.8: Retrosynthetic analysis of (+)-epiquinamide..... 181

Scheme V.9: Total synthesis of (+)-epiquinamide..... 182

Scheme V.10: Chelation-controlled hydride reduction of ketone (**30**)..... 183
Scheme VI.1: Enamide..... 242
Scheme VI.2: Instability of enamide as seen in the facile decomposition of somocystinamide A..... 243
Scheme VI.3: Enamide synthesis on model systems through acylation of imine..... 246
Scheme VI.4: Different approaches to enamide functional group..... 247
Scheme VI.5: Approaches to install disulfide of the epidithiapiperazinedione core.. 248
Scheme VI.6: Total synthesis of glyotoxin involving sensitive installation of disulfide..... 248
Scheme VI.7: Synthesis of psammaplin A..... 249
Scheme VI.8: Retrosynthetic Analysis of Somocystinamide A..... 249
Scheme VI.9: Synthesis of vinyl iodide for Suzuki coupling (Scheme VI.10)..... 250
Scheme VI.10: Suzuki coupling with varying coupling partners..... 250
Scheme VI.11: Ruthenium catalyzed cross metathesis approach..... 251
Scheme VI.12: Initially planned final steps to Somocystinamide (**1**)..... 254
Scheme VI.13: Possible mechanism of enamide formation..... 255
Scheme VI.14: Copper-mediated vinylation of a primary amide model compound (**65**) and attempted chemoselective methylation..... 257
Scheme VI.15: Final steps to somocystinamide A (**1**)..... 258
Scheme VI.16: Revised synthesis of the bis-methylamide **3**..... 263
Scheme VII.1: Fragmentation of the reduced form of scytonemin (**2**) through ozonolysis in its structure elucidation..... 319
Scheme VII.2: Biosynthetic gene cluster for scytonemin in Nostoc punctiforme..... 319
Scheme VII.3: Chemical synthesis of a putative biosynthetic precursor of scytonemin (**1**), soraphinol A (**S-8**)..... 320
Scheme VII.4: Proposed mechanism for the biosynthesis of scytonemin (**1**) by Balsksus and Walsh..... 321
Scheme VII.5: Initially conceived synthesis of scytonemin monomer **11**..... 322
Scheme VII.6: Predicted mechanism for regioselectivity of aldol condensation between ketone **18** and aldehyde **19**..... 322
Scheme VII.7: Synthesis of scytonemin monomer..... 323
Scheme VII.8: Absence of tautomerization and resonance characteristics of scytonemin monomer (**22**)..... 324
Scheme VII.9: Proposed mcehanism for dimerization of oxidized monomer **25** to reduced scytonemin **2**..... 328
Scheme VII.10: Synthesis of methylated monomer **29**..... 331
Scheme VII.11: Possible role of glycosylation in the biosynthesis of scytonemin.... 332

Scheme VII.12: Attempts to synthesize **30** and/or a mimic thereof (e.g. **33**)..... 333

Scheme VII.13: Attempts to perform Rubottom oxidation via doubly silylation of **22**..... 334

Scheme VII.14: Newly proposed route for the synthesis of **2**..... 336

Scheme VII.15: Highly chemo-selective DDQ oxidation of (E)-16-epinormacusine B (**45**)..... 337

Scheme VII.16: Chemo-selective oxidation of benzylic ether by DDQ in a neat mixture..... 337

Scheme VII.17: Completion of total synthesis of scytonemin albeit low yield (yield to be determined)..... 338

LIST OF TABLES

Table I.1: Use of natural products in the past and present..... 6

Table I.2: Structural revisions made in 2005-2008..... 13

Table II.1: Comparison of NMR data for two isolates of **1** and **3** ($CDCl_3$)..... 69

Table II.2: Crystal data and structure refinement for **1**..... 80

Table II.3: Atomic coordinates (x 10^4) and equivalent isotropic displacement parameters ($Å^2x10^3$) for **1**..... 80

Table II.4: Bond lengths [Å] and angles [°] for **1**..... 82

Table II.5: Anisotropic displacement parameters ($Å^2x10^3$) for **1**..... 83

Table II.6: Hydrogen coordinates (x 10^4) and isotropic displacement parameters ($Å^2x10^3$) for **1**..... 84

Table III.1: ^1H and ^{13}C NMR, COSY, HSQC, and HMBC data for credneric acid (**38**)..... 110

Table IV.1: Dihedral angles calculated or simulated by different methods for **7** and **8**..... 133

Table VI.1: Optimization of ruthenium-catalyzed cross metathesis..... 253

Table VI.2: Enamide formation via acyl chloride..... 256

Table VII.1: Oxidative dimerization conditions..... 330

ACKNOWLEDGMENTS

I would like to first thank my PhD advisor, Prof. William Gerwick, who has given me great opportunities in his laboratory. His enthusiasm and mentorship were invaluable during my graduate program. Bill has also been a great person to work for, and he has been greatly patient with me through the hard and slow times that are associated with scientific research. His approachability undoubtedly contributed to my accomplishments as well. I am very grateful for the many hours that he has spent editing, reviewing, and critiquing my manuscripts for this disseration and other publications. I would not like to ponder what would have happened without his involvement.

It was very helpful to discuss research issues with other members of my PhD committee. I sincerely thank Professors Emmanual Theodorakis, Yoshihisa Kobashi, Bradley Moore, and William Fenical for taking their time out to be my advisors. I thank Professor Fenical for allowing me to work in his laboratory while our new labs at SIO were undergoing renovation.

I am very thankful for all the postdoctoral researchers, graduate students, and staff that have worked with me over the years both at OSU and UCSD. I particularly enjoyed and benefited from bouncing various ideas off Keith Schwartz (Dr. White's lab at OSU) and my officemate, Karla Malloy. I acknowledge the technical assistance from Dr. Anthony Mrse, Dr. Yongxuan Su, Dr. Harry Gross, Dr. Arnold Rhinegold and his staff, Josh Wingerd, and Tara Byrum at UCSD and Roger Kohnert at OSU. I am especially indebted to Professor Kerry McPhail at OSU, who helped me in the early years of my scientific career.

I must not forget to thank Professor David A. Horne at OSU, who first introduced me to the joy of synthetic organic and bioorganic chemistry and taught me invaluable skills in his laboratory. Going back further in time, I am thankful for my high school biology teacher, Mr. Kudara, who inspired me to pursue a career in science back when all I ever thought about was improving my batting average and hitting a home run some day (sadly I never did in an official game).

On a more personal note, I am thankful for the ministry by Dr. Kent Hovind and his associates, who have inspired me to appreciate having a doctoral degree in science for the Kingdom of our God. I am also very grateful for the church family I have in Oceanside, CA and in Albany, OR. I cannot replace their fellowship, support, and prayers with anything else. I am extremely grateful for Pastor Ron Reed, who has been a great friend and a mentor despite the long distance between us. Knowing that he prays to our Lord for me everyday is a great treasure to me.

I am deeply thankful for my parents and other family members for their support. Thank you! I am especially grateful for my mother, who came to the Lord a few years ago and has given me much joy.

To my dear wife, Janet, I cannot thank God enough for you. Indeed, "whoso findeth a wife findeth a good thing, and obtaineth favour of the LORD (Proverbs 18:22, KJV)." You have been a great gift from the Lord. Your support, love, and friendship have been a great source of strength. Thank you, honey. I look forward to serving our Lord together with you in the years to come. I also thank you for your help with the tedious aspects of preparing this thesis manuscript.

Lastly, but most definitely not the least, I owe everything to my greatest mentor, hero, and friend, the Lord Jesus Christ. Lord, You have taken my place and sacrificed Your life for me, a wretched sinner who was a miserable atheist until six years ago, so that I may be forgiven and have an eternal life with You. Knowing this fact has been an infinite source of confidence and strength in all the situations I have faced in the last six years. Any difficult situation seemed so small compared to the hope You have given me through Your resurrection. With indescribable gratitude, all I can say is "Now unto Him [Jesus] that is able to keep you from falling, and to present you faultless before the presence of His glory with exceeding joy, to the only wise God our Savior, be glory and majesty, dominion and power, both now and ever. Amen (Jude 24-25)." Hallelujah!

The text of I, in part, will be used for a manuscript to be submitted to an academic journal. The dissertation author was the primary investigator and author of the research which forms the basis of this chapter. A coauthor will be William H. Gerwick.

The text of II, in whole, is the manuscript that has been submitted to *Toxicon* as it will appear: Takashi L. Suyama, Zhengyu Cao, Thomas F. Murray, and William H. Gerwick, Ichthyotoxic Brominated Diphenyl Ethers from a Mixed Assemblage of a Red Alga and Cyanobacterium: Structure Clarification and Biological Properties. The dissertation author was the primary investigator and author of the research which forms the basis of this chapter.

The text of III, in part, will be used for a manuscript to be submitted to an academic journal. The dissertation author was the primary investigator and author of the

research which forms the basis of this chapter. Coauthors will include Karla L. Malloy and William H. Gerwick.

The text of IV, in part, will be used for a manuscript to be submitted to an academic journal. The dissertation author was the primary investigator and author of the research which forms the basis of this chapter. Coauthors will include Kerry L. Mcphail, Christopher J. Nannini, and William H. Gerwick.

The text of V, in part, is published material as it appears: Takashi L. Suyama and William H. Gerwick, Practical Total Syntheses of Epiquinamide Enantiomers, *Organic Letters* **2006**, *8*, 4541-4543. The dissertation author was the primary investigator and author of the research which forms the basis of this chapter.

The text of VI, in part, is published material as it appears: Takashi L. Suyama and William H. Gerwick, Stereospecific Total Synthesis of Somocystinamide A, *Organic Letters* **2008**, *10,* 4449-4452. Another portion of the text of VI will be submitted to another academic journal. The dissertation author was the primary investigator and author of the research which forms the basis of this chapter. A coauthor for the second publication will be William H. Gerwick.

The text of VII, in part, will be used for two manuscripts to be submitted to two different academic journals. The dissertation author was the primary investigator and author of the research which forms the basis of this chapter. Coauthors will include William H. Gerwick and Carla Sorrels.

VITA

2001-2002	Undergraduate Research Assistant: Biomimetic Synthesis of Oroidin-derived Alkaloids and Medicinal Chemistry of Psoralens; Prof. David Horne, Oregon State University
2002-2003	Undergraduate Research Assistant: Novel Methodologies for Absolute Stereochemistry Determination of Natural Products; Prof. William Gerwick, Oregon State University
2001-2004	Teaching Assistant; Department of Chemistry, Oregon State University
2003	Bachelor of Science; Oregon State University
2003-2005	Graduate Research Assistant: Novel Methodologies for Absolute Stereochemistry Determination of Natural Products and Total Synthesis of Natural Products; Prof. William Gerwick, University of California at San Diego
2005-2009	Graduate Research Assistant: Total Synthesis of Natural Products and Natural Product Chemistry; University of California at San Diego
2009	Doctor of Philosophy; University of California at San Diego

PUBLICATIONS

- "Practical Total Syntheses of Epiquinamide Enantiomers" Takashi L. Suyama; William H. Gerwick, *Organic Letters* **2006**, *8*, 4541-4543.
- "The marine lipopeptide somocystinamide A triggers apoptosis via caspase 8" Wolf Wrasidlo; Ainhoa Mieglo; Vicente A. Torres; Simone Barbero; Konstantin Stoletov; Takashi L. Suyama; Richard L. Klemke; William H. Gerwick; Dennis A. Carson; Dwayne G. Stupack, *Proceedings of National Academy of Science* **2008**, *105*, 2313-2318.
- "Apratoxin D, a Potent Cytotoxic Cyclodepsipeptide from Papua New Guinea Collections of the Marine Cyanobacteria *Lyngbya majuscula* and *Lyngbya sordida* " Marcelino Gutierrez; Takashi L. Suyama; Nicolas Engene; Joshua S.

Wingerd; Teatulohi Matainaho; William H. Gerwick, *Journal of Natural Products* **2008**, *71*, 1099-1103.

•"Stereospecific Total Synthesis of Somocystinamide A" Takashi L. Suyama; William H. Gerwick, *Organic Letters* **2008**, *10,* 4449-4452.

•"Lipoproteins, lipopetides and analogs, and methods for making and using them." William Gerwick; Wolfgang Wrasidlo; Dennis Carson; Dwayne Stupack; Takashi Suyama. *PCT Int. Appl*. **2008**, 119pp.

•"Ichthyotoxic Brominated Diphenyl Ethers from a Mixed Assemblage of a Red Alga and Cyanobacterium: Structure Clarification and Biological Properties." Takashi L. Suyama; Zhengyu Cao; Thomas F. Murray; William H. Gerwick. *Toxicon*, **2009**, *Manuscript in review*.

•"Vinylchloride-Containing Fatty acid and its Neurotoxic Phenethylamide Derivative from a Papua New Guinea Collection of *Lyngbya* sp." Takashi L. Suyama; Karla L. Malloy; Zhengyu Cao; Thomas F. Murray; William H. Gerwick. *J. Nat. Prod.* **2009**, *Manuscript in preparation*.

•"Probing the Enzymatic Potential of Scy1263, a Hypothetical Protein from the Scytonemin Biosynthetic Gene Cluster in *Nostoc punctiforme* ATCC 29133" Carla M. Sorrels; Takashi L. Suyama; William H. Gerwick. *Manuscript in preparation*.

•"Expedient Synthesis of α,α-dimethyl-β-hydroxy Carbonyl Scaffolds via Evans' Aldol Reaction with a Tertiary Enolate" Joshawna K. Nunnery; Takashi L. Suyama; William H. Gerwick. *Manuscript in preparation*.

•"Recent Structural Revisions of Natural Products" Takashi L. Suyama; William H. Gerwick. *Manuscript in preparation*.

•"Insights into the Biosynthesis of Scytonemin through Synthetic Investigations" Takashi L. Suyama; William H. Gerwick. *Manuscript in preparation*.

•"Improved Synthesis of Somocystinamide A" Takashi L. Suyama; William H. Gerwick. *Manuscript in Preparation*.

FIELDS OF STUDY

Major field: Organic Chemistry

Studies in Natural Products Chemistry
Professors William H. Gerwick, William H. Fenical, and Bradley S. Moore

Studies in Synthetic Organic Chemistry
Professors Emmanuel Theodorakis and Yoshihisa Kobayashi

ABSTRACT OF THE DISSERTATION

Organic synthesis as an effective approach to chemical, pharmaceutical, and biosynthetic investigations of natural products

by

Takashi L. Suyama

Doctor of Philosophy in Oceanography

University of California, San Diego, 2009

Professor William H. Gerwick, Chair

The partnership between natural products and synthetic organic chemistry date back to the origin of organic chemistry itself. While natural products became a major driving force for the development of novel organic reactions and synthetic strategies, organic synthesis has contributed in many ways to the elucidation and confirmation of structure, pharmaceutical development, and biosynthetic studies of natural products. Due to the recent advances in both of these two disciplines, there are new opportunities and

issues surrounding natural products that organic synthesis can be applied to, and such studies comprise this dissertation.

Chapter I introduces the background information and rationale for the dissertation research, which is based on the history of organic chemistry and newly emerging research topics in natural products chemistry. Chapter II describes the isolation, characterization, and toxicological evaluation of polybrominated diphenyl ethers from a mixed assemblage of a marine red alga and cyanobacteria. Chapter III describes the isolation, characterization, and biological evaluation of a novel vinylchloride-containing fatty acid, credneric acid, from a *Lyngbya* sp. Chapter IV describes the conception of a method for determining the absolute stereochemistry of natural products lacking proper functional groups for derivatization. This methodology was applied to a cyclopropane-containing fatty acid and resulted in a conflict with newly published literature, which is discussed in detail. Chapter V describes the development of an expedient and efficient total synthesis of a novel alkaloid, epiquinamide, isolated from the skin of a rainforest frog, *Epipedobates tricolor*. This work contributed to clarifying the identity of a potent and selective nicotinic receptor agonistic activity observed in the extract of *E. tricolor*. Chapter VI describes the development of a total synthesis of a marine cyanobacterial metabolite, somocystinamide A, which has been shown to be a potent inhibitor of endothelial cell proliferation and angiogenesis. The synthesis was later modified for scalability to meet the need for further pharmaceutical investigations of this important natural product. Chapter VII describes the synthetic investigations on scytonemin, a cyanobacterial metabolite possessing UV-blocking properties. Through this work, many

intriguing insights into the biosynthesis of the natural product were obtained. Finally, Chapter VIII provides the conclusions drawn from this dissertation research.

Chapter I

Introduction

Abstract

Natural products chemistry and organic synthesis share a rich history of partnership. While natural products became the major driving force for development of novel organic reactions and synthetic strategies, organic synthesis has contributed in many ways to the elucidation and confirmation of structure, pharmaceutical development, and biosynthetic studies of natural products. Historical and modern examples of these contributions and the prospect of applying chemical synthesis to current problems in natural products chemistry will be discussed in detail.

I.1 Origin of Natural Product Chemistry

> "I can no longer, as it were, hold back my chemical urine; and I have to let out that I can make urea without needing a kidney, or even of an animal, whether of man or dog: the ammonium salt of cyanic acid (cyansäures Ammoniak) is urea."
>
> Friedrich Wöhler (1828)[1]

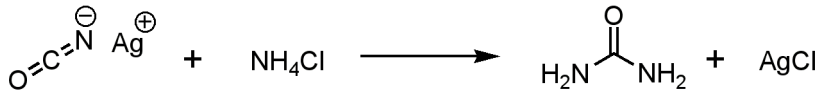

With the advent of chemical nomenclature and the acceptance of the atomic theory, chemistry emerged as a scientific discipline during the late eighteenth century.[2] Subsequently, knowledge of inorganic chemistry expanded rapidly. However, scientific study of organic compounds did not begin until Wöhler synthesized urea from ammonium cyanate in 1828.[3] Prior to this accomplishment, chemists believed that organic compounds could only be made by "vital forces" in living organisms and that they obeyed laws other than the physical laws observed for inorganic compounds.[2] The new field of organic chemistry flourished due to the developing confidence that organic compounds could be studied logically and systematically in the same way inorganic compounds were being studied. The backbone of this breakthrough was the structural theory, which explained that the diversity and chemical properties of organic compounds are due to the way the constituting atoms are connected to one another. The introduction of this theory is regarded as "of the same importance in the history of science as the development of the two laws of thermodynamics around 1850, the quantum theory and the theory of general relativity after 1900, and the explanation of the molecular basis of genetics after 1950."[4]

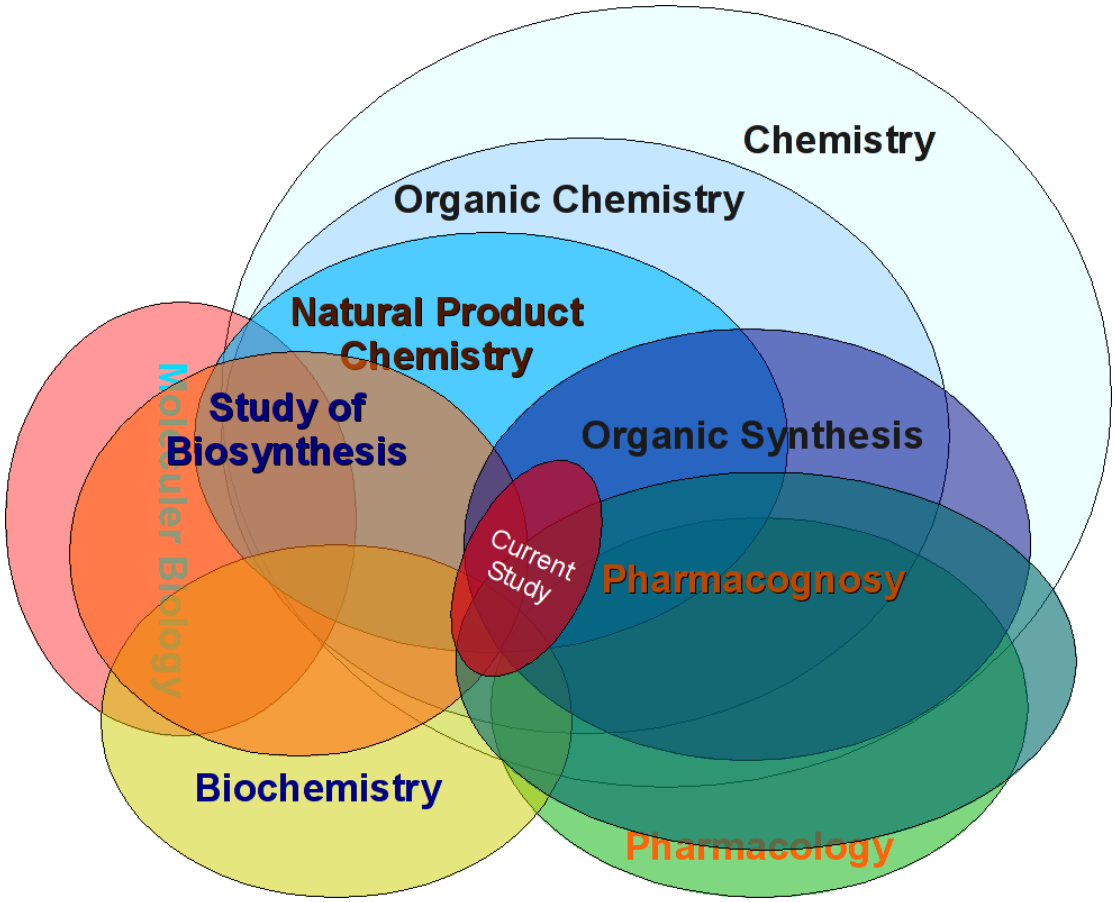

Illustration I.1: Graphical representation of thesis research

This diagram utilizes the principles of Venn diagram. Where there is an overlap between different fields, strong interdisciplinary influence is implied. The order of overlaps is meant to roughly depict the order of emergence of each discipline chronologically.

Due to scientists' constant interest in nature and health, many organic chemists of the nineteenth century chose to study biological molecules, including medicinal compounds, isolated from living organisms.[5] In time, two sub-disciplines were formed to study biological compounds. Biochemists studied primary metabolites, which are essential for normal growth, sustaining of life, and reproduction of the organism. Examples of primary metabolites include proteins, carbohydrates, fats, and nucleic acids. In contrast, natural product chemists studied secondary metabolites (Illustration I.1). Unlike primary metabolites, the absence of secondary metabolites would not result in immediate death but in long-term disadvantages.[5]

Secondary metabolites have been unwittingly used throughout the history of mankind for various purposes. They have been used as medicines for pain relief and healing of wounds, as poisons for hunting and warfare, as agents for capital punishment, as narcotics, hallucinogens, or stimulants to relieve tedium, as spice to disguise the bland flavor of food, as perfume to obscure the odor of dead bodies, and in religious worship and anointment (Table I-1).[5,6] A great many of these natural products are still used today and often for the same purposes.[7] The difference is that the full chemical identities of the natural products are now mostly known through advances in chemical sciences.

The rise of natural product chemistry not only stimulated the growth of biology, but it also had a great impact on the art and science of organic synthesis (Illustration I.1). The complex and elegant structures of many naturally occurring compounds became the favored targets of total synthesis. In its infancy, the field of organic total synthesis focused on primary metabolites. Only after a few decades, molecules, such as

Table I.1: Use of natural products in the past and present

Compound	Structure	Historical usage	Modern usage
Ephedrine	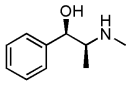	Treatment for respiratory aliments	Treatment for asthma, hay fever
Salicine	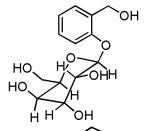	Treatment for fever	Derivative (aspirin) used for fever, pain
Strychnine	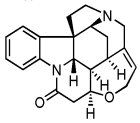	Poison	Stimulant, laxative, pesticide
Coniine	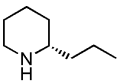	Poison (hemlock), capital punishment	
Rotenone	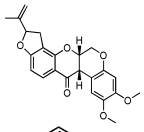	Poison, insecticide	Insecticide, pesticide
Morphine	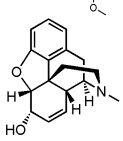	Narcotic	Narcotic
THC (tetrahydrocannabinol)	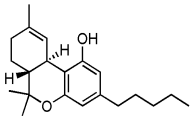	Narcotic	Narcotic
Cocaine	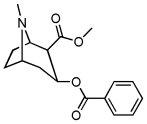	Narcotic	Narcotic
Caffeine	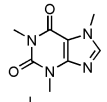	Stimulant	Stimulant, dieting
Geraniol		Perfume (rose oil)	Perfume (rose oil)
Linalol		Perfume (lavendar oil)	Perfume (lavendar oil)
Cinnamaldehyde	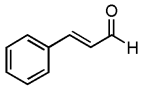	Spice (cinnamon)	Spice (cinnamon)
Eugenol	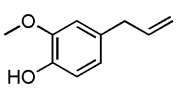	Spice (cloves)	Spice (cloves)
Diallyl sulfide	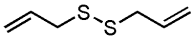	Spice (garlic)	Spice (garlic), anti-cancer agent[8]

haemin (**1**)[9] and equilenin (**2**),[10] that would be considered complex even by today's standard were being synthesized.

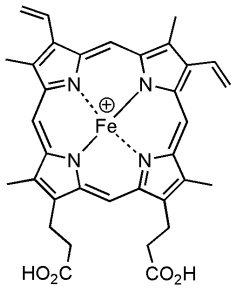

Haemin

1

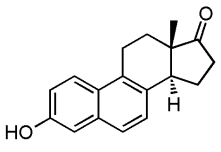

Equilenin

2

I.2 Natural Product Structure Elucidation and Organic Synthesis

> "Until the mid-1960's, structure determination was an art that could be likened to solving a complicated detective case, but with the spectacular advancement in spectroscopy it has become less inspiring, and since the mid-1980's, in most cases, structure determination has become rather 'routine'."
>
> Koji Nakanishi (1991)[11]

In the classical era, many of the natural product chemists had their primary training in synthetic organic chemistry. Often times, the only possible means of structure determination of the natural product of interest was to chemically degrade it to known substances.[12] One of the most complex structures to be elucidated by this classical method is echitamine (**8**), a tumoricidal alkaloid isolated from the bark of *Alstonia scholaris*.[13] The presence of an indole nucleus was determined by treatment with glyoxylic reagent (Scheme I.1). Treatment with aqueous base and acid revealed a methyl ester and imine-like moiety, respectively. Much structural information around the olefin

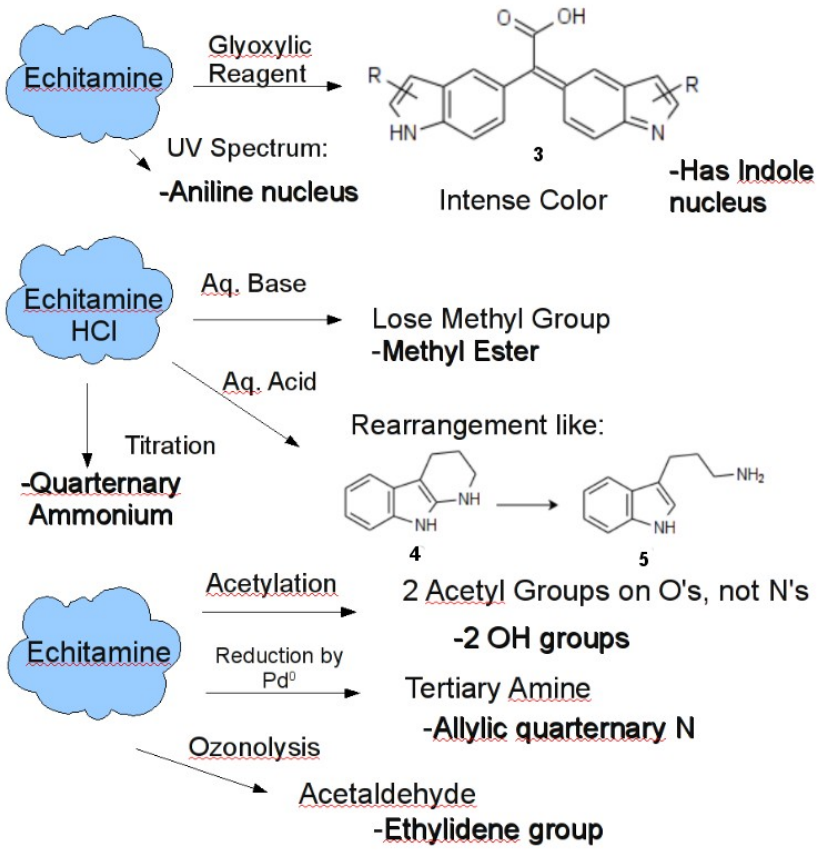

Scheme I.1: Echitamine structure elucidation efforts by chemical degradation and synthetic logic

The conclusion from each chemical reaction is shown in bold letters.

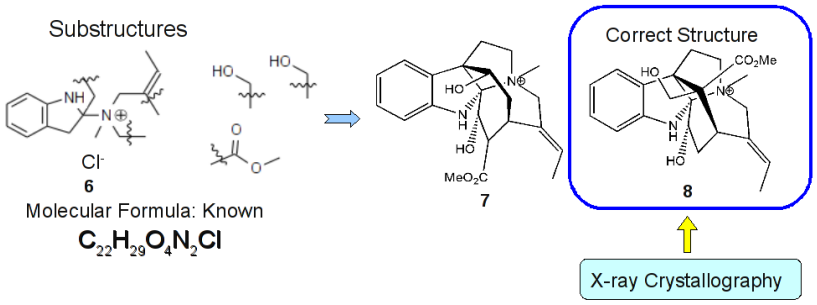

Scheme I.2: Assigned structures by chemical investigation and X-ray crystallography

was obtained by the observed reduction with palladium and the resulting fragments from ozonolysis. Acetylation added two acetate units, thereby showing that there are two hydroxyl groups. Further chemical analysis of a similar nature, the molecular formula derived by mass spectrometry, and the compound's chemical properties finally led to structure **7** (Scheme I.2).[14] Even though **7** was very similar to the correct structure **8**, the true identity of this intriguing alkaloid was not discovered until X-ray crystallography was applied in 1962. Since the initial isolation of this natural product,[15] some 85 years had passed before its structure determination.

However, with the advent of spectroscopic methodologies, specialization in the spectroscopic structural analysis of natural products appeared and consequently, the field of natural product chemistry matured.[12,16] Today, in many cases, the processes of natural product isolation and structural determination are streamlined and expeditious.[16] Subsequently, the focus of natural product chemists has shifted from merely describing the chemical properties of newly found compounds to finding biologically active

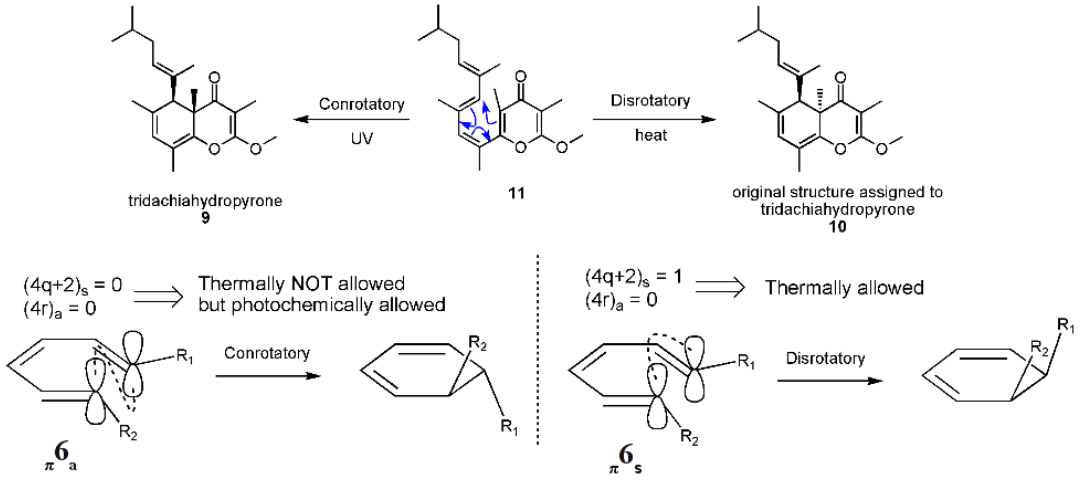

Scheme I.3: Relationship between **9** and **10** via electrocyclization

molecules.[17] However, the age old partner of natural products chemistry, chemical synthesis, still plays a major role today in confirmation of the chemical structure of the natural product, particularly its stereochemistry, and in providing a larger quantity of the compound as well as analogs for biological testing (*vide infra*).[11]

Particularly profound and interesting examples of the contribution from chemical synthesis to the structural revision of a natural product include tridachiahydropyrone (**9**) and mururin C (**12**). In the first case, the issue concerned stereochemical assignments, while an incorrect planar structure was assigned to the latter compound. Such revisions were required for 30 natural products in 2008 alone.[18] It is safe to say that the art of structure elucidation has not achieved perfection and that the partnership between natural products chemistry and synthetic organic chemistry is still very much in order.

Tridachiahydropyrone (**9**) was isolated from a marine mollusk *Tridachia crispata* by Cimino and coworkers.[19] Originally, structure **10** was proposed based on NMR and NOE spectroscopic analyses. Subsequently, the total synthesis of **10** by Perkins and coworkers suggested that the correct structure is most likely **9**.[20] A biogenetic rationale for structure **9** was inspired by Cimino and Faulkner, who noted that the extensive conjugation of tridachiahydropyrone and its congeners may serve as defense against harmful UV rays.[21] The putative precursor **11** could be converted to either **9** or **10** through 6π electrocyclization depending on the mode of activation (Scheme I-1). According to the Woodward-Hoffman rules,[22] photochemical 6π electrocyclization would yield the conrotatory product, **9**, whereas the corresponding thermal reaction would yield the disrotatory product, **10**.

Indeed, Moses and coworkers synthesized **11**, which was converted to **9** upon exposure to sunlight.[23] Furthermore, this synthetic material, **9**, had the same NMR and UV properties as the authentic sample. All attempts to convert **11** to **10** by thermal means failed.[23] These results not only confirm that **9** is the correct structure for this natural product, but also suggests that the actual biosynthetic product produced by *Tridachia* may be **11** and that it is subsequently converted to the stronger UV absorbent **9** when exposed to strong sunlight. The biomimetic synthesis of tridachiahydropyrone led to its structural revision as well as insights into its biosynthesis that could not have been easily obtained by any other approach.

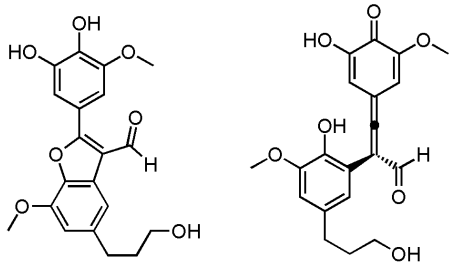

Figure I.1: The originally assigned structure (**13**) of mururin C and its revised structure (**12**)

Although the majority of structural revisions of natural products have been due to stereochemical issues involving tetrahedral carbon atoms, perhaps it is more intellectually interesting to consider the less frequent cases of incorrectly assigned planar structures. Such was the case with mururin C (**12**), a natural product isolated from the bark of *Brosimum acutifolium*. Originally, structure **13** was incorrectly assigned to this natural product based on HR-MS and 1D and 2D NMR analyses.[24] In the course of the synthesis

of **13**, however, it was found that allenes analogous to **13**, when formed *in situ*, were intercepted readily by nucleophiles in the reaction mixture and the allene species could not be isolated.[25] This observation led to the rationale that if **13** was formed at all in the course of biosynthesis, the hydroxyl group of the phenol would attack the allenic carbon and form benzofuran, thereby converting to structure **12**. Therefore it is highly unlikely that **13** was the correct structure. Moreover, comparison of predicted chemical shifts for **12** and **13** revealed that **12** is very likely the correct structure. In this work, synthetic studies of the natural product eloquently revealed the erroneous feature of the originally mis-assigned planar structure of mururin C.

In 2005, Nicolaou and Snyder published a fairly comprehensive and inspiring paper on natural product structural revisions that were made possible by total synthesis in the period of 1990 to 2004.[16] In that paper, the authors articulate the amazement, in contrast to their expectation, of discovering the large number and profoundness of structural mis-assignments made in the recent years. In Table I.2, all of the structural revisions[26] of natural products since 2005 through 2008 are summarized.

Table I.2: Structural revisions made in 2005-2008.

The year in which the initial structure was published is in parentheses. Only the structure determination methods used for the portion of the structure that is erroneous are mentioned in this table. Predict.: predictions based on molecular modeling. Mol. Mod.: use of geometry optimized structure.

Proposed Structure	Initial Structure Determination Method	Revised Structure	Structure Revision Method
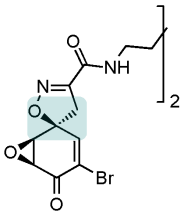 **Calafianin**[27] (2000)	NOE	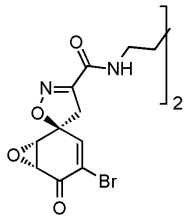	Total Synthesis[28]
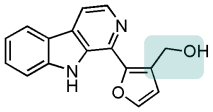 **Tribulusterine**[29] (1999)	NOESY	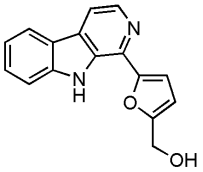	Total Synthesis[30]
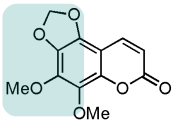 **Ayapin derivative**[31] (1999)	Absence of NOE	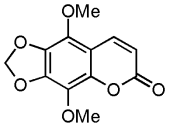	Total Synthesis[32]
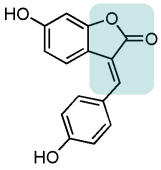 **Isoaurostatin**[33] (2001)	^{1}H & ^{13}C NMR HMBC NOE	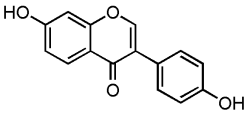	Total Synthesis[34]
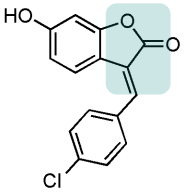 **Chloroaurone**[35] (2001)	^{1}H & ^{13}C NMR HMQC HMBC	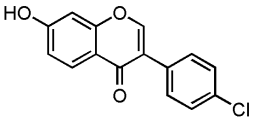	Total Synthesis[36]

Table I.1 continued

Proposed Structure	Initial Structure Determination Method	Revised Structure	Structure Revision Method
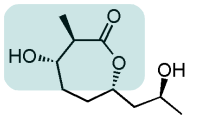 **Feigrisolide A**[37] (2000)	NOESY HMBC	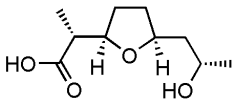	Total Synthesis[38]
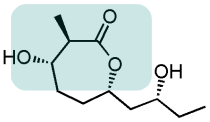 **Feigrisolide B**[37] (2000)	NOESY HMBC	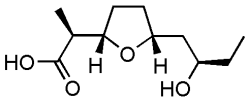	Total Synthesis[38]
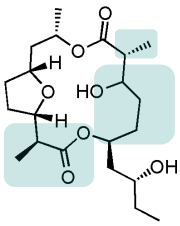 **Feigrisolide C**[39] (2000)	HMBC NOESY	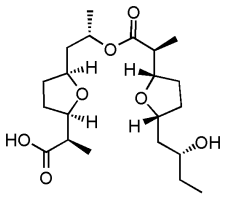	Total Synthesis[40]
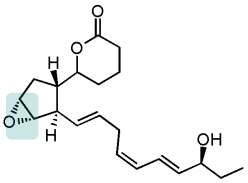 **Agardhilactone**[41] (1996)	Derivatization NMR	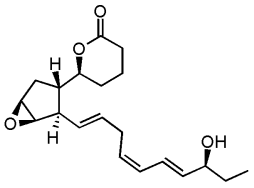	Total Synthesis[42]
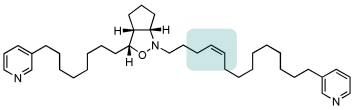 **Pyrinodemin A**[43] (2001)	EIMS Fragmentation	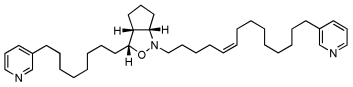	Total Synthesis[44]
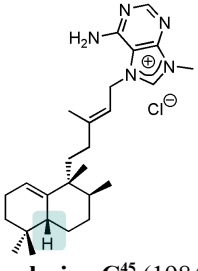 **Agelasine C**[45] (1984)	CD Comparison NMR	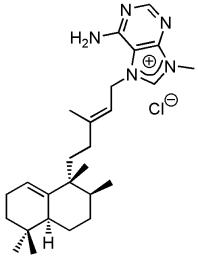	Total Synthesis[46]

Table I.1 continued

Proposed Structure	Initial Structure Determination Method	Revised Structure	Structure Revision Method
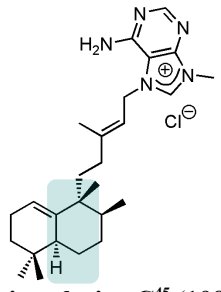 **Epi-agelasine C**[45] (1984)	CD Comparison NMR	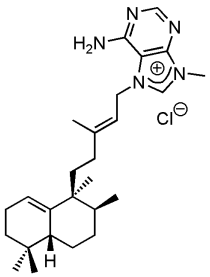	Total Synthesis[46]
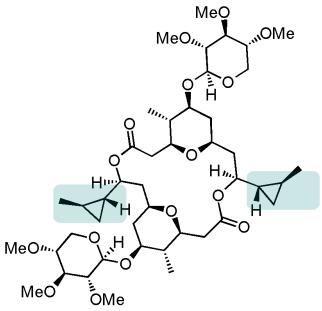 **Clavosolide A**[47] (2002)	*J*-based ROESY	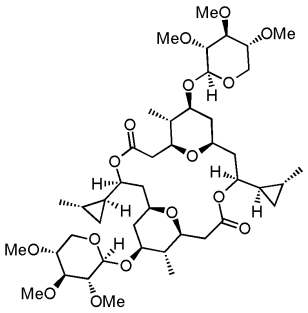	Total Synthesis[48]
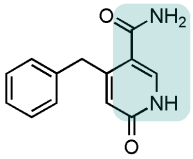 **Aspernigrin A**[49] (2004)	HMBC	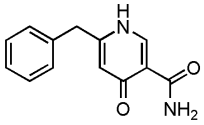	X-ray NOE[50]
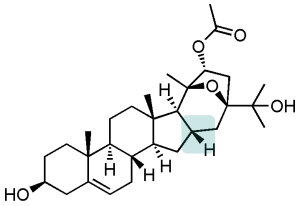 **Suberoretisteroid B**[51] (2000)	^{1}H NMR	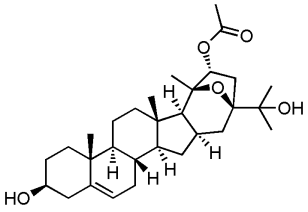	NMR Comparison[52]
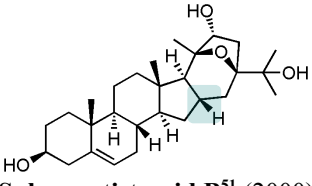 **Suberoretisteroid B**[51] (2000)	^{1}H NMR	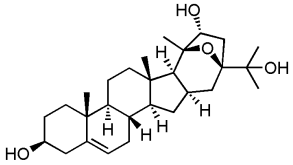	NMR Comparison[52]

Table I.1 continued

Proposed Structure	Initial Structure Determination Method	Revised Structure	Structure Revision Method
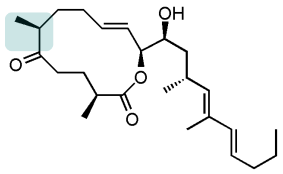 **Amphidinolide W**[53] (2002)	Derivatization *J*-based Mosher	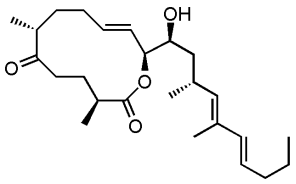	Total Synthesis[54]
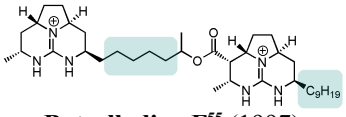 **Batzelladine F**[55] (1997)	Comparison NOE DCI-MS Fragmentation	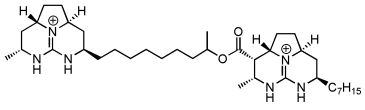	Total Synthesis[56]
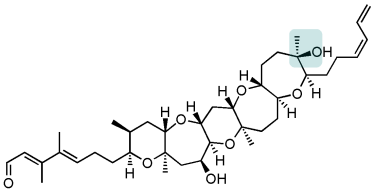 **Brevenal**[57] (2005)	NOE	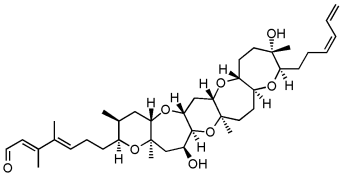	Total Synthesis[58]
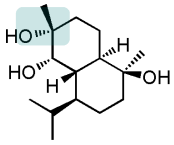 **Trihydroxycadinane**[59] (1998)	NOE	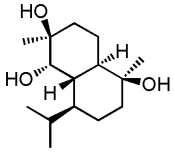	Total Synthesis[60]
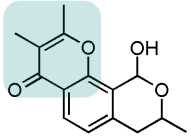 **Aspergione B**[61] (2003)	Comparison	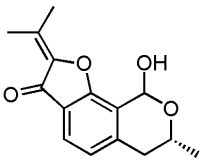	Total Synthesis[62]
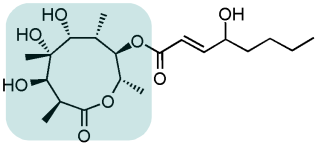 **Botcinic acid**[63] (1993) (Botcinolide)	^{1}H & ^{13}C NMR	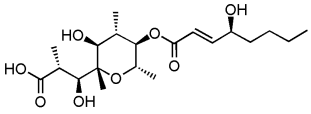	Semi-synthesis NMR Comparison[64]

Table I.1 continued

Proposed Structure	Initial Structure Determination Method	Revised Structure	Structure Revision Method
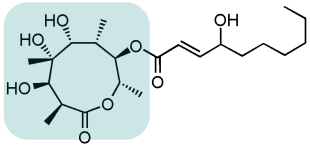 **Homobotcinic acid**[65] (1996) (Homobotcinolide)	NMR Comparison	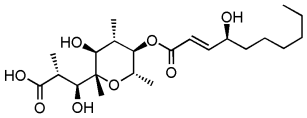	NMR Comparison[65]
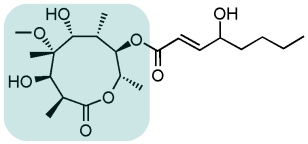 **Botcinic acid methyl ester**[66] (1996) (4-O-methylbotcinolide)	NMR Comparison	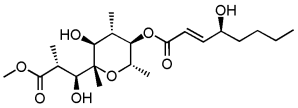	NMR Comparison[65]
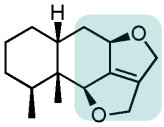 **Peribysin C**[67] (2004)	HMBC NOE	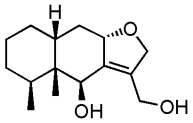	EI-MS ^{13}C Prediction NMR comparison[68]
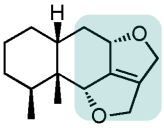 **Peribysin C**[62] (2004)	HMBC NOE	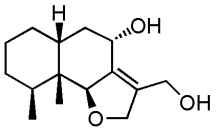	EI-MS ^{13}C Prediction NMR comparison[61]
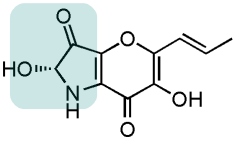 **Pyranonigrin**[69] (2004)	ROESY	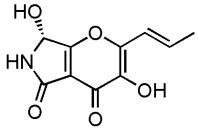	Chemical Reactivity CD predict.[70]
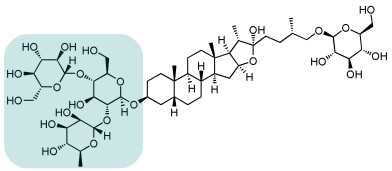 **Shatavarin I**[71] (1987)	FAB-MS Degradation	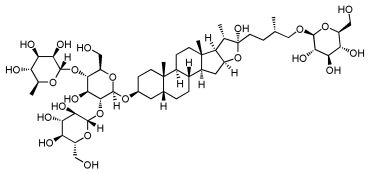	HMBC[72]

Table I.1 continued

Proposed Structure	Initial Structure Determination Method	Revised Structure	Structure Revision Method
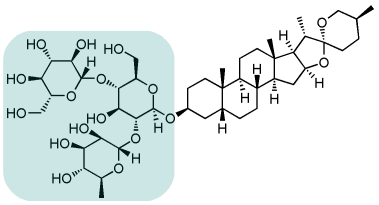 **Shatavarin IV**[58] (1987)	EI-MS Degradation OR predict	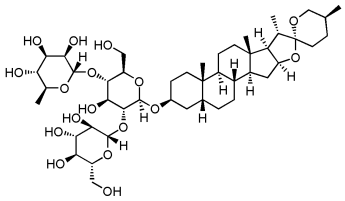	HMBC[57]
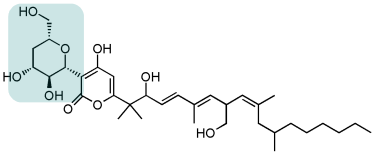 **Fusapyrone**[73] (1994)	1D & 2D NMR	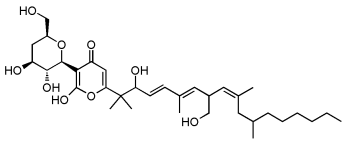	HMBC NMR Comparison[74]
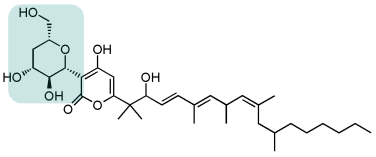 **Deoxyfusapyrone**[73] (1994)	1D & 2D NMR	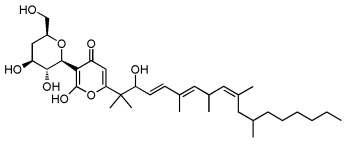	HMBC NMR Comparison[74]
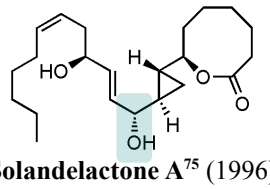 **Solandelactone A**[75] (1996)	HMQC COSY Comparison *J*-based	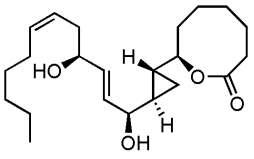	Total Synthesis[76]
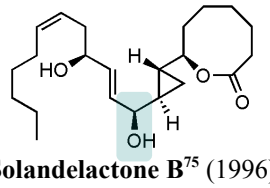 **Solandelactone B**[75] (1996)	Comparison *J*-based	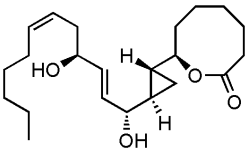	Total Synthesis[76]
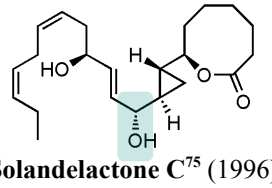 **Solandelactone C**[75] (1996)	Comparison *J*-based	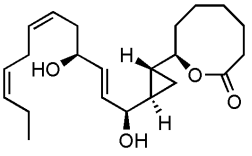	Total Synthesis[76]

Table I.1 continued

Proposed Structure	Initial Structure Determination Method	Revised Structure	Structure Revision Method
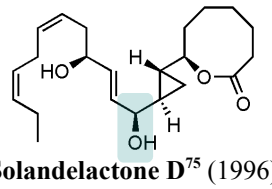 **Solandelactone D**[75] (1996)	Comparison *J*-based	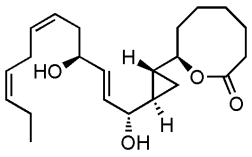	Total Synthesis[76]
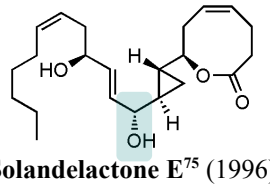 **Solandelactone E**[75] (1996)	Comparison *J*-based	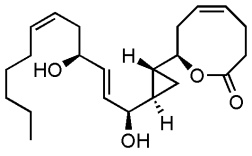	Total Synthesis[76]
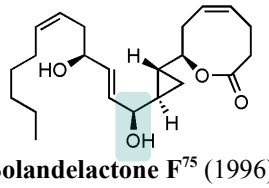 **Solandelactone F**[75] (1996)	Comparison *J*-based	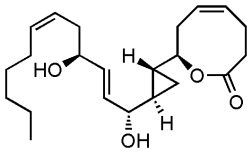	Total Synthesis[76]
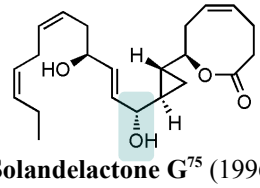 **Solandelactone G**[75] (1996)	Comparison *J*-based	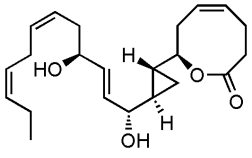	Total Synthesis[76]
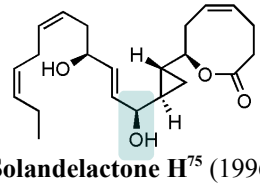 **Solandelactone H**[75] (1996)	Comparison *J*-based	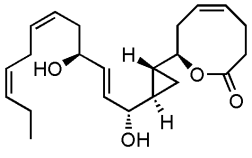	Total Synthesis[76]
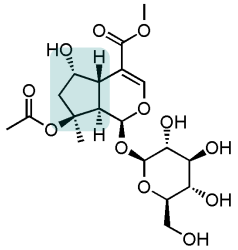 **Barlerin**[77] (2004)	NOESY NMR Comprison	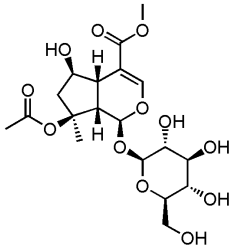	NOESY[78]

Table I.1 continued

Proposed Structure	Initial Structure Determination Method	Revised Structure	Structure Revision Method
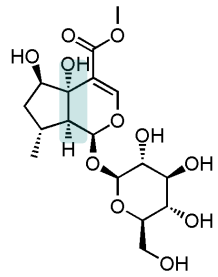 **Penstemoside**[77] (2004)	NOESY NMR Comprison	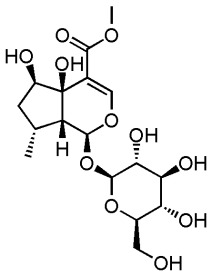	NOESY[78]
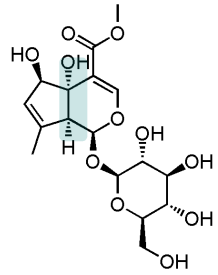 **Dehydropenstemoside**[77] (2004)	NOESY NMR Comprison	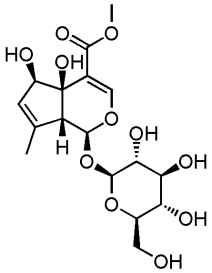	NOESY[78]
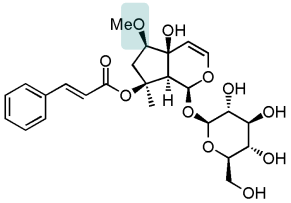 **Harpagoside**[79] (2003)	HR-MS NOESY HMBC	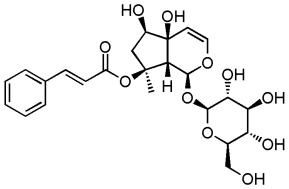	NMR Comparison[78]
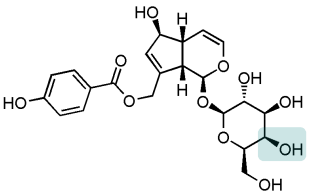 **Agnuside**[80] (2004)	Degradation GCMS OR	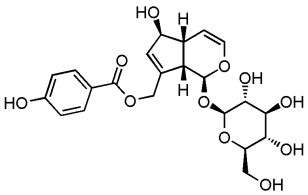	NOESY[78]

Table I.1 continued

Proposed Structure	Initial Structure Determination Method	Revised Structure	Structure Revision Method
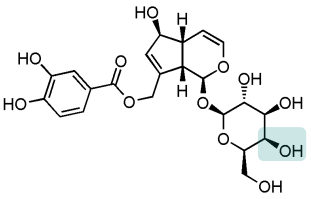 **3,4-hydroxybenzoylaucubin**[80] (2004)	NMR Comparison	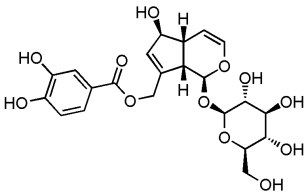	NOESY[78]
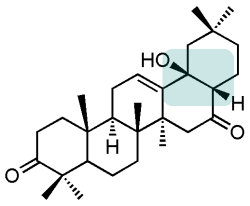 **Camellenodiol**[81] (1981)	^{1}H NMR CD	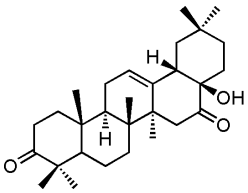	COSY HMBC X-ray[82]
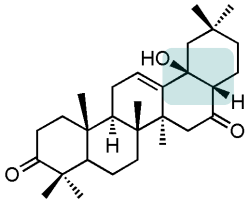 **Camelledionol**[81] (1981)	^{1}H NMR CD	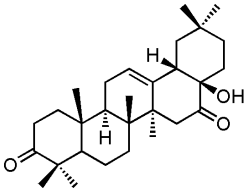	COSY HMBC[82]
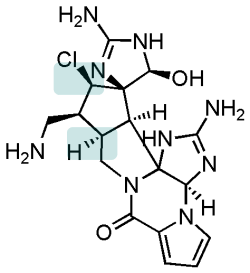 **Palau'amine**[83] (1993)	ROESY *J*-based	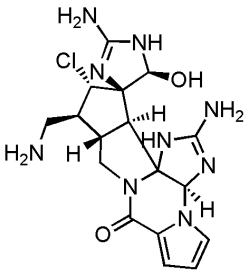	ROESY Mol. Mod. *J*-based[84]
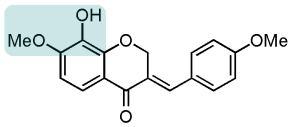 **Intricatin**[85] (1989)	D_2O Shift[86]	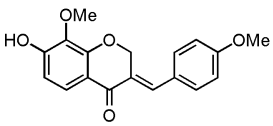	Total Synthesis[87]

Table I.1 continued

Proposed Structure	Initial Structure Determination Method	Revised Structure	Structure Revision Method
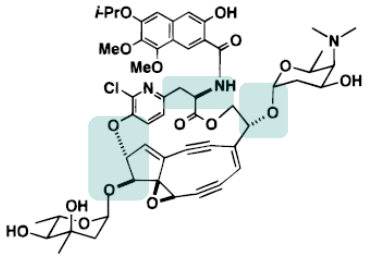 **Kedarcidin**[88] (1993)	Degradation 1 D & 2D NMR	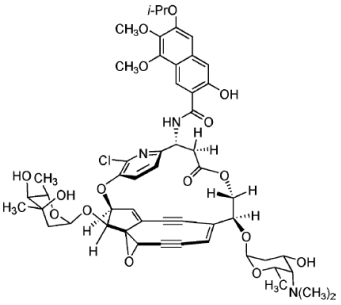	Total Synthesis[89] First partial synthesis had an error.[90]
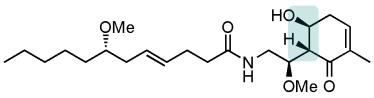 **Malyngamide U**[91] (2003)	*J*-based NOESY	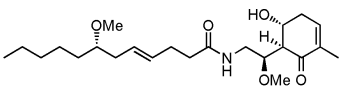	Total Synthesis[92]
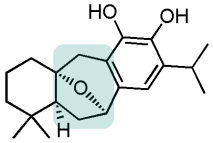 **Abrotandiol**[93] (2007)	1D & 2D NMR Comparison	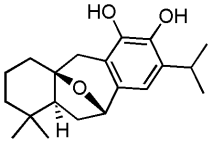	Total Synthesis[94]
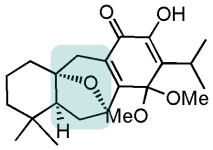 **Abrotanone**[93] (2007)	1D & 2D NMR Comparison	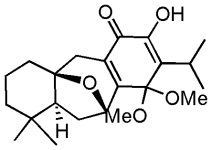	Total Synthesis[94]
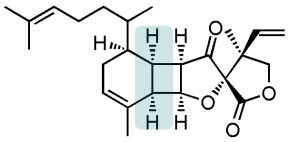 **Biyouyanagin**[95] (2005)	NOE	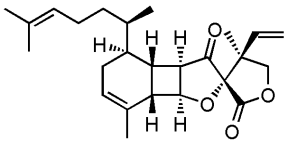	Total Synthesis[96]
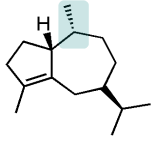 **Aciphyllene**[97] (1983)		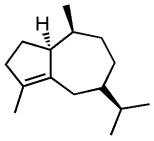	Total Synthesis[98]

Table I.1 continued

Proposed Structure	Initial Structure Determination Method	Revised Structure	Structure Revision Method
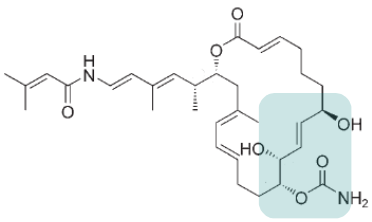 **Palmerolide A**[99] (2006)	Mosher *J*-based NOE	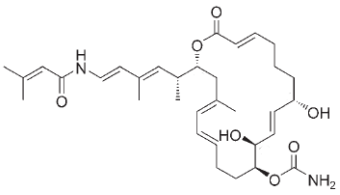	Total Synthesis[100]
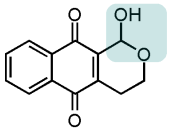 **Benz[g]isochromene-dione**[101] (1995)	EI-MS ^{1}H, ^{13}C NMR HETCOR	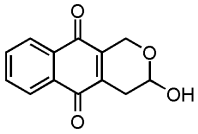	Total Synthesis[102]
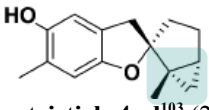 **Laurentristich-4-ol**[103] (2005)	NOE	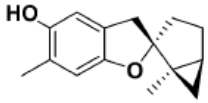	Total Synthesis[104]
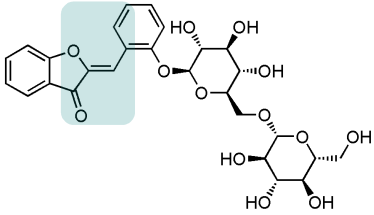 **Dalmaisione D**[105] (1972)	^{1}H, ^{13}C NMR	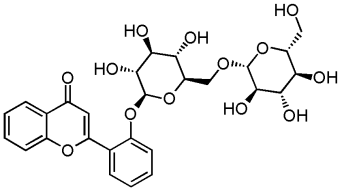	Total Synthesis[106]
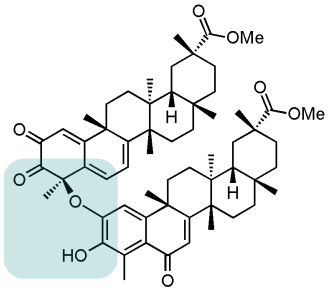 ***Rzedowskia*** **bistriterpenoid α**[107] (1996)		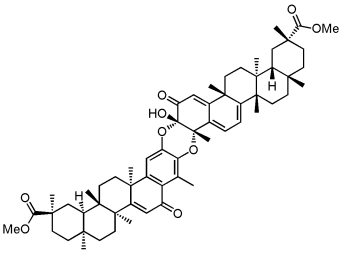 Xuxuarine Eα	Biomimetic Semi-synthesis[108]

Table I.1 continued

Proposed Structure	Initial Structure Determination Method	Revised Structure	Structure Revision Method
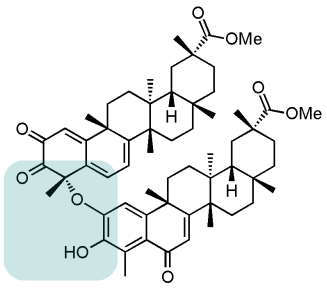 ***Rzedowskia* bistriterpenoid α[107]** (1996)		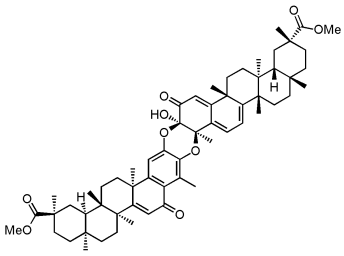 Xuxuarine Eα	Biomimetic Semi-synthesis[108]
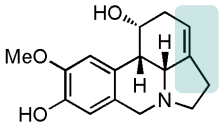 **Kirkine[109]** (1995)	1D & 2D NMR NOE	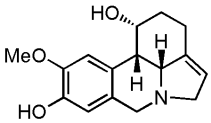	Total Synthesis[110]
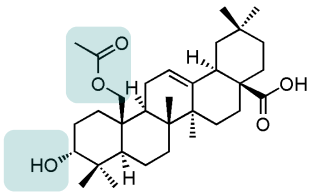 **25-acetoxy-3a-hydroxyolean-12-en-28-oic acid[111]** (2004)	1D & 2D NMR NOE	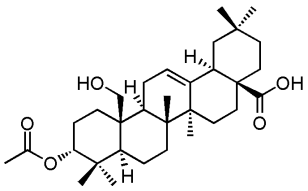	Semi-synthesis[112]
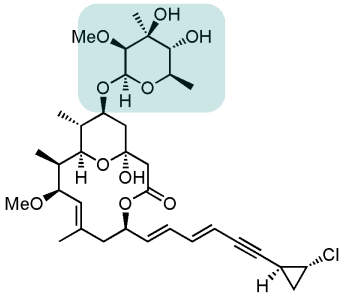 **Callipeltoside C[113]** (1996)	ROESY NOE	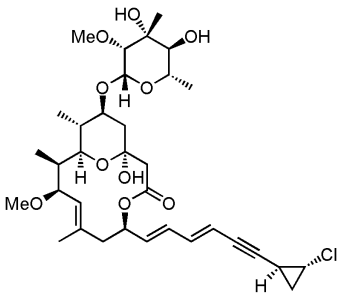	Total Synthesis[114]

Table I.1 continued

Proposed Structure	Initial Structure Determination Method	Revised Structure	Structure Revision Method
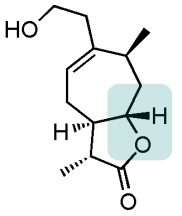 **Diversifolide**[115] (1999)	*J*-based	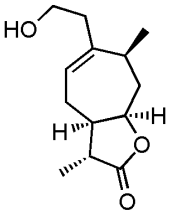	Total Synthesis[116]
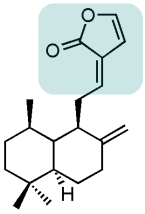 **Labdane diterpenoid**[117] (2006)	1D & 2D NMR IR HR EI-MS NOE	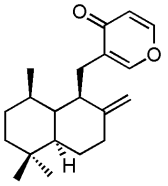	Total Synthesis[118]
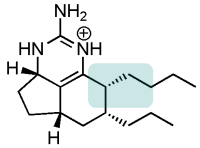 **Netamine E**[119] (2006)	NOE	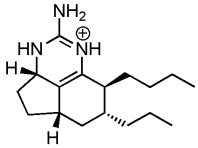	Total Synthesis[120]
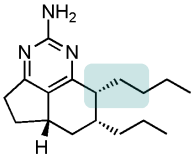 **Netamine G**[119] (2006)	NOE	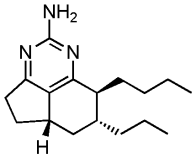	Total Synthesis[120]
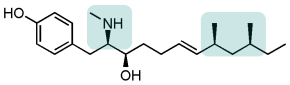 **Tyroscherin**[121] (2004)	*J*-based Mosher Derivatization Optical Rotation	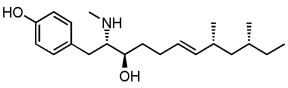	Total Synthesis[122]

Table I.1 continued

Proposed Structure	Initial Structure Determination Method	Revised Structure	Structure Revision Method
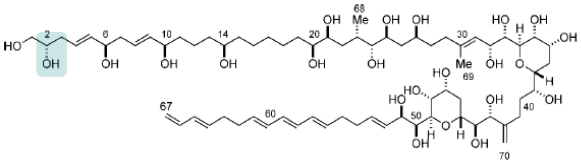 **Amphidinol 3**[123] (1999)			
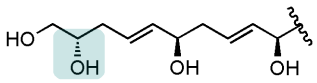 **Amphidinol 3 Fragment**[123]	Ozonolysis Derivatization Chiral HPLC	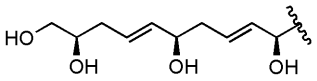	Combinatorial synthesis of fragments[124]
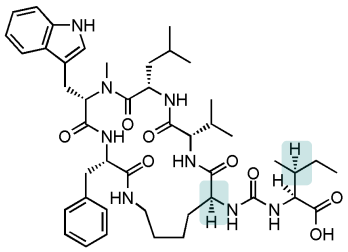 **Brunsvicamide A**[125] (2006)	Derivatization Chiral GCMS	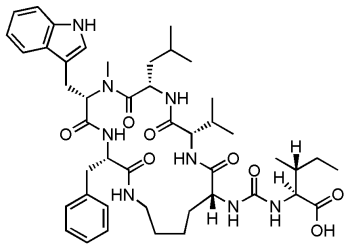	Total Synthesis[126]
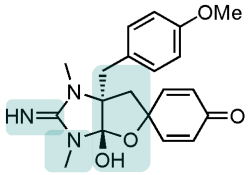 **Spiroleucettadine**[127] (2004)	HMBC ROESY	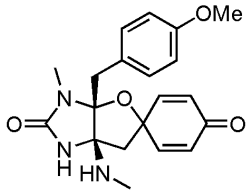	^{13}C Predict. X-ray[128]
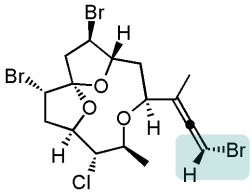 **Obtusallene V**[129] (2000)	Mol. Mod. NMR Comparison	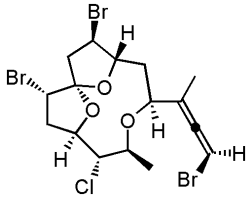	^{13}C Predict.[130]

Table I.1 continued

Proposed Structure	Initial Structure Determination Method	Revised Structure	Structure Revision Method
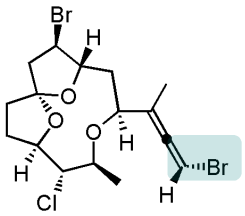 **Obtusallene VI**[129] (2000)	Mol. Mod. NMR Comparison	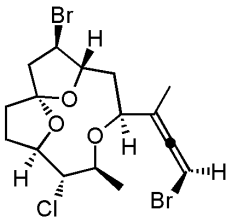	^{13}C Predict.[130]
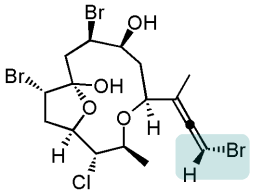 **Obtusallene VII**[129] (2000)	Mol. Mod. NMR Comparison	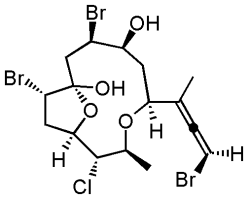	^{13}C Predict.[130]
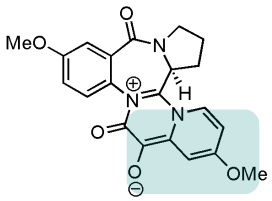 **Circumdatin A**[131] (1999)	INEPT2-INADEQUATE HMBC-INADEQUATE	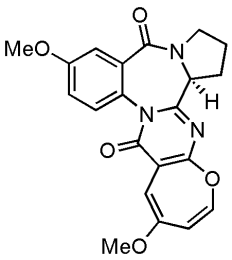	HMBC X-ray[132]
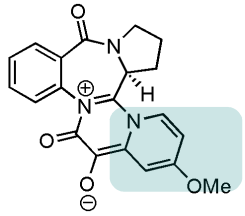 **Circumdatin B**[131] (1999)	INEPT2-INADEQUATE HMBC-INADEQUATE	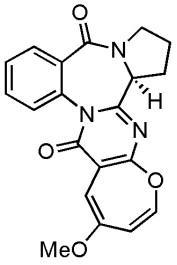	HMBC X-ray[132]

Table I.1 continued

Proposed Structure	Initial Structure Determination Method	Revised Structure	Structure Revision Method
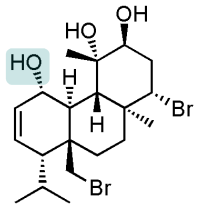 **Bromoditerpene**[133] (1987)	HR-MS ^{1}H NMR	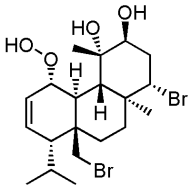	X-ray[134]
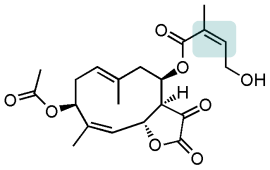 **Hiyodorilactone B**[135] (1978)	NOE NMR Comparison	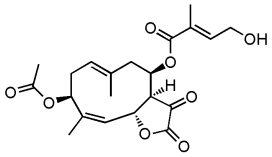	NOE[136]
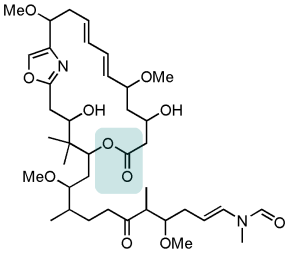 **Rhizopodin**[137] (1993)		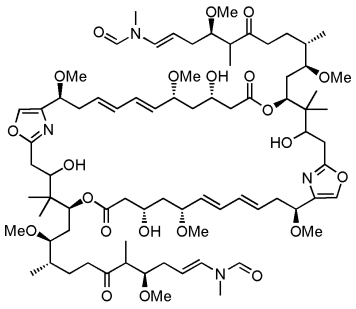	ESI-MS X-ray[138]
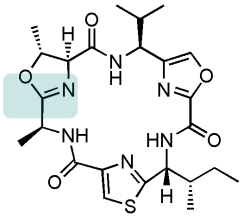 **Microcyclamide**[139] (2008)	ESI HR-MS HMBC Bioinformatics	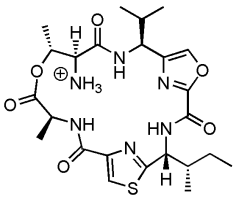	NMR Comparison Semi-synthesis ESI HR-MS[140]
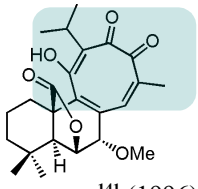 **Hassanane**[141] (1996)	HMBC Biosynthetic Prediction Mol. Mod.	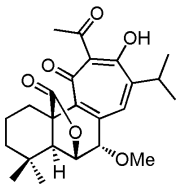	^{13}C Predict. UV Predict.[142]

Table I.1 continued

Proposed Structure	Initial Structure Determination Method	Revised Structure	Structure Revision Method
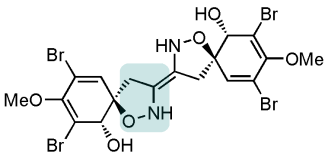 **Zamamistatin**[143] (2001)	NOESY ESI HR-MS	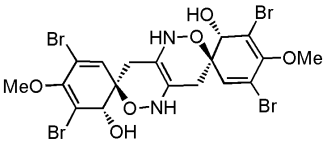 **See next entry**	Comparison with synthetic model compounds[144]
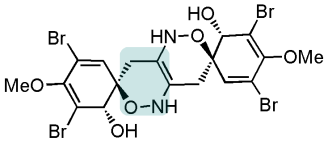 **Zamamistatin**[144] (2001)	Comparison with synthetic model compounds	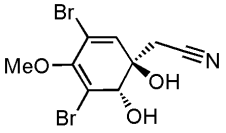	IR NMR and OR Comparison[145]

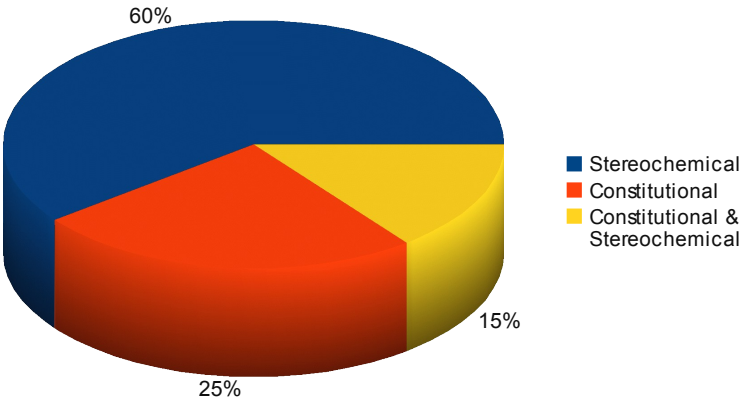

Figure I.2: Types of errors in natural product structure revisions

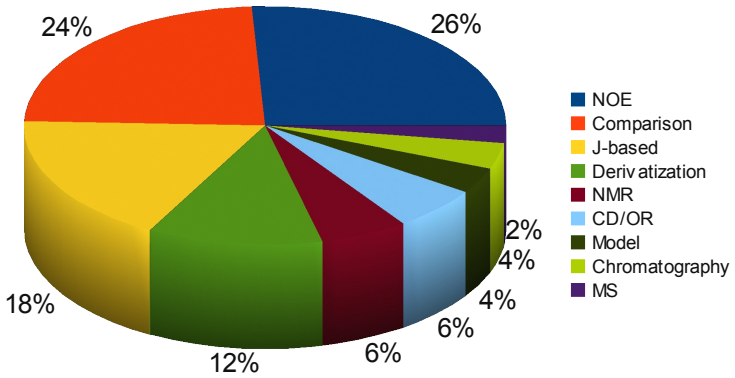

Figure I.3: Structure determination methods used in 2005-2008 for the erroneous cases

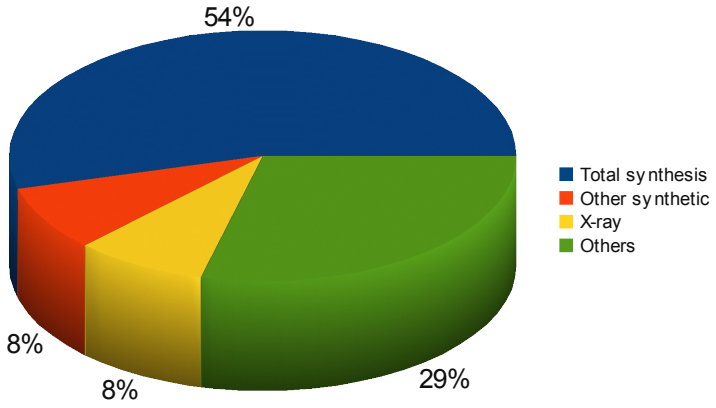

Figure I.4: Structure revision methods used in 2005-2008

Remarkably, a majority of these structures were elucidated in the very recent years (1990-2008). Of the 83 structure revisions, 40% had constitutional errors (Figure I.2). This statistic comes as a surprise in this century when NMR tools, such as HMBC, to connect elucidated substructures are readily available (Figure I.3). However, a close examination of these structures reveals a subtle problem. Unless all theoretically possible HMBC correlations are observed, some structures are indistinguishable from their alternatives on the basis of HMBC spectroscopy only. An example of this type of

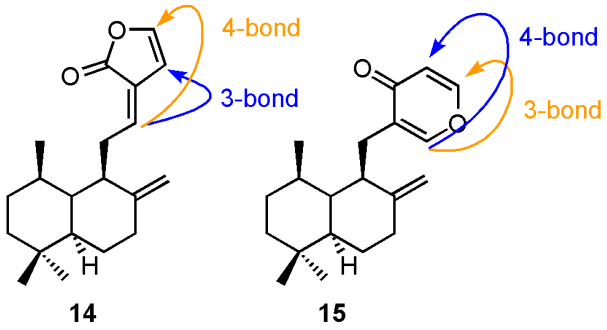

Figure I.5: Discrimination of possible structures by HMBC

The HMBC correlations necessary for distinction between the two possible structures are depicted as blue and orange arrows. If the blue correlation was only present, structure **14** would be correct. Likewise, if the orange correlation was only present, then structure **15** would be correct.

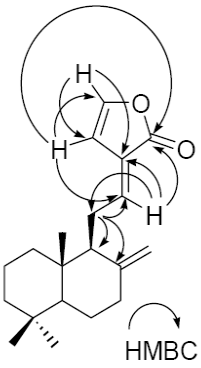

Figure I.6: HMBC correlations observed and recorded for the labdane diterpenoid[108]

The HMBC correlations necessary for discrimination of structures **14** and **15**, as noted in Figure I.5, were not recorded (or observed) for this natural product.

problem is shown in Figures I.5 and 6. This and other examples in Table I.2, particularly the structures with constitutional errors, illustrate how total synthesis is crucial for confirmation of structure (Figure I.4).

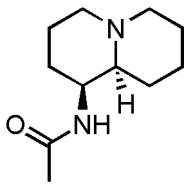

Epiquinamide
16

In addition to the mis-assignment of structures, there has been one case where total synthesis clarified the true identity of the bioactive metabolite. In 2003, Daly and coworkers isolated a novel quinolizidine alkaloid, epiquinamide (**16**) from a rainforest frog, *Epipedobates tricolor* in a sub-milligram quantity.[146] Initially, **16** was believed to be a subtype selective nicotinic receptor agonist and it attracted much attention from the synthetic community. By 2006, there had been several asymmetric total syntheses of epiquinamide enantiomers.[147] As a result of theses syntheses, it was found that structure **16** had no activity as a nicotinic receptor agonist.[147] Afterwards, evidence surfaced that the originally observed activity might have been due to a minor contamination of the sample with epibatidine.[148] Awareness of this error was made possible by the synthetic supply of **16** free of any other bioactive natural product contaminants. As technologies to elucidate the structures of minute quantities of natural products advance further, the need for supplying pure samples of natural products by total synthesis can be expected to increase.

I.3 Natural Products as Pharmaceuticals

Successful attempts have been made to present the case that natural products are a great resource for drug development.[149] Indeed, among all of the drugs that were approved between 1981 and 2006 for clinical use, 63% had their ultimate origin in

natural products (Figure I.7).[93] This recent success of natural products did not emerge from a vacuum, but it has been nurtured by the partnership with synthetic chemistry since the conception of organic chemistry. In the earliest era of organic chemistry, it was rarely taught as an independent discipline, but always in conjunction with medicine, geology, and other fields.[4,5] Even today, it is difficult to find an academic publication in organic synthesis that does not appeal to medical or ecological interests for a justification of the research.

A survey of the natural products discovered during the nineteenth century indicates that many are neurologically relevant compounds, such as caffeine, nicotine, codeine, and morphine (Table I.1).[5] It is disappointing, then, that the pool of clinically available natural products in neuropharmacology has not expanded significantly since this earliest era of natural product chemistry. In the last 25 years, only two neurologically relevant natural products, and an additional two compounds derived from natural

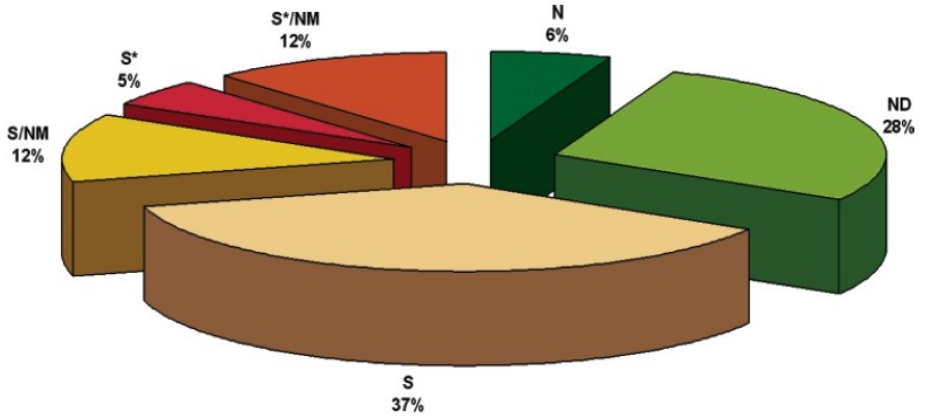

Figure I.7: All new small chemical entities that were approved for clinical use, 01/1981-06/2006, by source.[93]

N: Natural products. ND: Derived from a natural product and is usually a semisynthetic modification. S: Totally synthetic drug, often found by random screening/modification of an existing agent. S*: Made by total synthesis, but the pharmacophore is/was from a natural product. NM: Natural product mimic.

products, were approved for clinical use.[93] In contrast, 21 natural products and 99 compounds derived from natural products were approved for treatments of cancer and infectious diseases during the same period.[93] To respond to this challenge, current efforts are underway to discover novel neurotoxins from untapped natural sources.[150,151]

Despite more anti-cancer agents being approved for human treatment than any other pharmaceutical classes, there is still a great need for new drugs to treat cancer. For example, there are currently no effective chemotherapeutic treatments available for pancreatic cancer.[152] Even for the types of cancer that are known to be treatable by anti-cancer agents, severe side-effects and ineffectiveness towards metastasis still plague patients. With cancer being the second most common cause of death in the USA (23.1% of all deaths in 2004),[153] the search for new and more effective anti-cancer agents is still warranted indeed. Though outside the scope of this thesis, new anti-microbial agents are also urgently needed. In recent decades, infectious diseases have emerged as a substantial threat both in the USA and other countries.

In the past few years, the re-isolation of known compounds has become a hindrance to the productivity of natural products chemistry efforts.[154] Traditionally, terrestrial plants and microbes have been the major sources of natural products, and researchers have exhaustively studied those organisms.[5] Therefore, the current trend is to investigate organisms that have not been previously studied in detail. For example, investigation of poisonous frogs[155] and marine organisms[91] has enjoyed great productivity in recent years. Between 1968 and 1998, over 400 alkaloids of over 20 structural classes, most of which are neurologically relevant, were isolated from amphibians alone.[87] Considering the difficulty of obtaining extract samples from amphibian skin, this is a

remarkable achievement. From marine organisms, a relatively new source of secondary metabolites, a total of 812 new compounds were isolated in 2005 alone (716 for 2004), and this trend seems to continue.[93]

I.4 Organic Synthesis to Develop Natural Products as Drugs

With such an outstanding rate of discovery, one would expect to see more natural products being approved for clinical use. However, this is not the case. One cause for this unfortunate situation is the lack of follow-up investigation of bioactive natural products due to an insufficient supply of the compounds.[156] Consequently, many compounds with high potential are never tested *in vivo* in animals, which often requires more than hundreds of milligrams of material. Often times, the major barrier in drug development is this multi-hundred milligram (MHM) quantity, due to the frequent inability to produce more than several milligrams of a natural product in academic laboratories whether through synthesis or isolation. Once a compound performs favorably in *in vivo* assays and/or pre-clinical trials, pharmaceutical companies with sufficient financial resources may show interest in carrying out industrial-scale production of the compound for further testing (Figure I.8). Otherwise, due to financial difficulties, it is virtually impossible for non-commercial organizations to take a compound to clinical trial.

Figure I.8: Drug Development Process

Note that "identification of compound" in this figure refers to both lead compound discovery and medicinal chemistry (analog synthesis and evaluation) processes.

If the natural product is from a bacterium and/or fungus, culturing of the source organism is often possible at a scale large enough for isolation of the compound to meet the demands of *in vivo* assays. For most natural products isolated from animals, such as amphibians and marine invertebrates, neither large-scale collection or culturing of the source organism is realistic. Therefore, a scalable chemical synthesis is a necessary alternative to obtain a sufficient supply of the compound. Because large for-profit organizations would generally tend to avoid high risk projects, such as a compound at the *in vivo* testing stage, academic, non-profit institutions, and benevolent small businesses must face the challenge of realizing MHM-scale synthesis.

As Paul Wender has articulated, an ideal synthesis is "one in which the target molecule (natural or designed) is prepared from readily available, inexpensive starting materials in one simple, safe, environmentally acceptable, and resource-effective operation that proceeds quickly and in quantitative yield."[157] Employing these principles for achieving an efficient synthesis while applying creativity and utilizing the vast knowledge accumulated in the organic synthetic chemistry literature, it is possible to design and execute a large scale-amenable synthesis of the compound of interest.

Inspiring news hit the synthetic community in 2004 when Novartis disclosed their total synthesis of *60 g* of (+)-discodermolide (**17**).[158] Combining the strengths of the

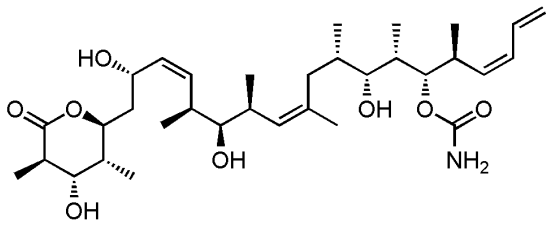

Discodermolide, **17**

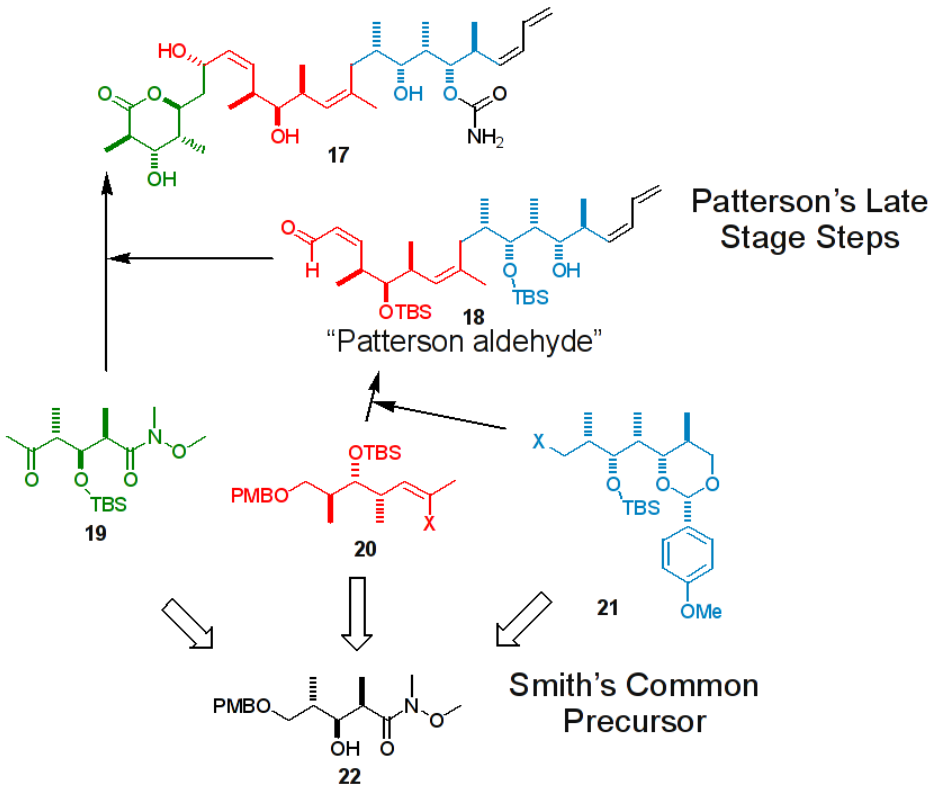

Scheme I.4: Novartis strategy for the synthesis of discodermolide (**17**)

synthetic routes developed by both Smith's and Patterson's laboratories (Scheme I.4),[159,160] Novartis pushed the scalability limit of total synthesis. Smith and coworkers devised a highly convergent and elegant synthesis, in which all three of the units (**19**, **20**, **21**) required for the discodermolide skeleton are derived from a single common precursor (**22**) with elaborate stereochemistry.[83] However, the preparation for the last coupling in Smith's synthesis involved a tranformation to a phosphonium salt that required 12.8 kbar of pressure, which would be too dangerous for an industrial scale synthesis. In the strategy developed by Patterson and coworkers, the last coupling proceeded with good

diastereoselectivity (21:4) and with excellent yield (87%), and it did not involve any potentially dangerous reaction conditions.[82]

> "Some 3,000 kg of the sponge--a quantity that probably does not exist--would have been needed to deliver 60 g of (+)-discodermolide. The large-scale total synthesis of such a complex natural product in such quantities was a first for Novartis and probably the entire pharmaceutical industry,"
> Stuart J. Mickel, Novartis[161]

> "It's [discodermolide synthesis by Novartis] probably the best piece of synthetic work to come out from an industrial company. The ability to make something at this level of complexity as opposed to extracting it from natural product sources illustrates the power of modern synthetic chemistry."
> Prof. Steven V. Ley, Univ. Cambridge[81]

Another obstacle to the development of drugs from natural products is the lack of comprehensive bioactivity profiling due to the limited number of in-house assays available. Without an extensive network of collaborations for bioassays, a number of important bioactivities can remain undetected. A marine cyanobacterial natural product, somocystinamide A's (**23**)[162] remarkable activity against angiogensis (IC_{50} of 500 fM against HUVEC and *in vivo* anti-angiogenic effect in zebrafish at 30 nM) was only revealed through a new collaborative relationship.[163] This promising compound represents only the tip of an iceberg of pharmacologically important marine natural

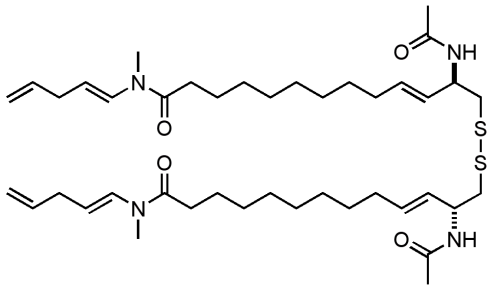

Somocystinamide, **23**

products. Yet, the discovery and development of these compounds as drugs will depend on collaborative efforts of chemists and biologists to identify bioactivities that are not yet known.

After a promising activity is discovered in a structurally defined natural product, there is usually still work to be done by synthetic chemists. In the example of **23**, the disulfide and enamide are of concerns with regards to human toxicity and compound stability. These functionalities may need to be replaced in order for the drug to be usable in clinical situations. Indeed, in Figure I.5, only 6% of the newly approved small molecule drugs are unmodified natural products, whereas 28% are modified natural products. This process of modification, medicinal chemistry, is as crucial as finding new compounds possessing new bioactivities.

I.5 Biosynthesis of Natural Products and Organic Synthesis

As demonstrated above, the organic synthesis of a natural product can have a multitude of benefits, namely, confirmation or clarification of structure, a solution to the supply issue, access to analogs, and detailed insights of the chemical properties of the compound. In addition, mechanistic insight derived from organic synthesis is indispensable to understanding the details of the biosynthetic processes in nature.[#] While working with secondary metabolites, the biosyntheses of such compounds naturally become of interest. The mechanism of an enzymatic reaction, in particular, is an intellectually satisfying problem for chemists to solve and can be useful for engineering of the biosynthetic pathway and *in vitro* application of the enzyme in chemical synthesis. Often, this is done by designing and synthesizing an isotope-labelled biosynthetic

intermediate and then analyzing the product of the enzymatic reaction that utilizes the intermediate.

Brevianamides and their related compounds are a family of natural products that are biosynthetically derived from tryptophan, proline, and one or two isoprene unit(s).[164] Many metabolites of this family share a core structure that appears to be derived from an intramolecular Diels-Alder reaction, and whether the producers of these metabolites, fungi *Penicilium* sp. and *Aspergillus* sp., possess a "Diels-Alderase," has been an exciting topic in the field of bioorganic chemistry.[78,165] Both brevianamide A (**33**) and brevianamide B (**34**) were found to be biosynthetically derived from a common precursor, deoxybrevianamide E (**30**) through a feeding experiment of tritium-labelled **30**, which was prepared through chemical synthesis.[166] When a synthetic precursor similar to **32** was allowed to undergo a Diels-Alder reaction, an epimer that is not analogous to any of the isolated natural products was the major product and an isomer that is analogous to **34** was the minor product (isomeric ratio = 2:1).[167] This result gives

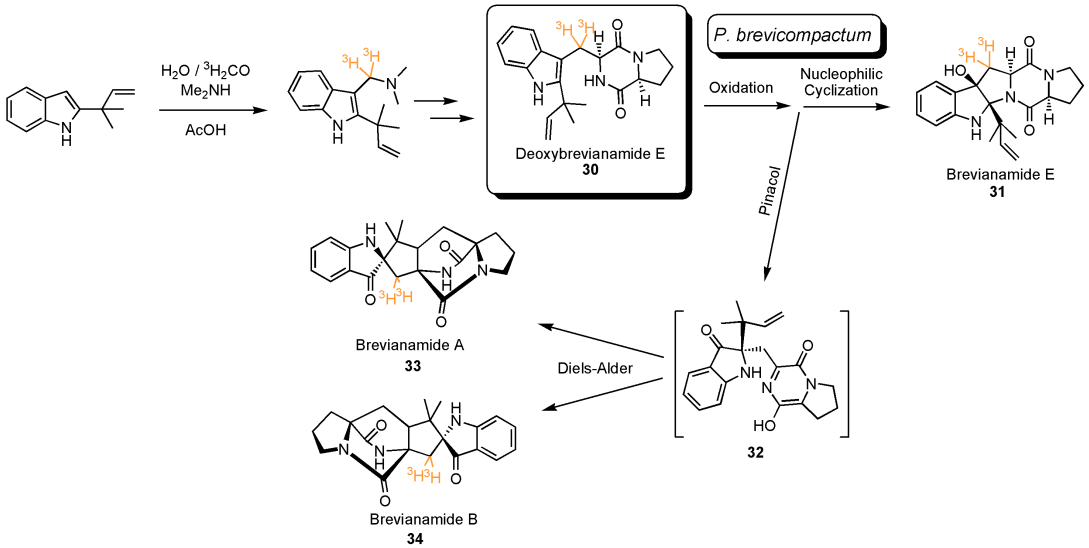

Scheme I.5: Synthetic contributions to the study of brevianamides biosynthesis

credence to the hypothesis that the Diels-Alder reaction in Schem I.5 is indeed enzyme-catalyzed and that **33** and **34** are not artifacts, but natural products.

Occasionally, it is possible for synthetic organic chemistry to more directly contribute to the biosynthetic study of natural products. By achieving total or partial synthesis of a natural product in a way that mimics the proposed biosynthetic pathway, one can gain direct chemical insight into the biochemical reactions of interest, as seen in the example above with brevianamides. Because a biomimetic synthesis relies upon the inherent nature of a key intermediate, a complex dimerization reaction of monomers and/ or an elaborate intramolecular reaction are often involved.[168] A recent and elegant example is the biomimetic total synthesis of grossularine-1 (**35**), a bisindole alkaloid isolated from a marine tunicate, *Dendrodoa grossularia*.[169] The dimeric nature of the molecule is not immediately apparent in the structure (**35**), but is clearly revealed in the elaborate sequence of transformations from the monomer **36** to **40**.

Another exceptionally elegant example in recent years is panepophenanthrin (**41**), whose total synthesis was reported simultaneously by Porco and Baldwin in 2003 (Scheme I.7).[170,171] Here the inherent propensity of the monomer (**42**) for dimerization is cleverly utilized to effect a stereoselective and hydrogen-bond-assisted Diels-Alder reaction to produce the natural product (**41**). Without this biomimetic step, the core tetracyclic skeleton would require a large number of synthetic steps to construct. Presumably, the exact same reaction can happen in nature with or without any assistance from an enzyme, which brings up the question about whether compounds like **41** are truly biosynthetic metabolites or not. Each case probably requires a separate consideration. In

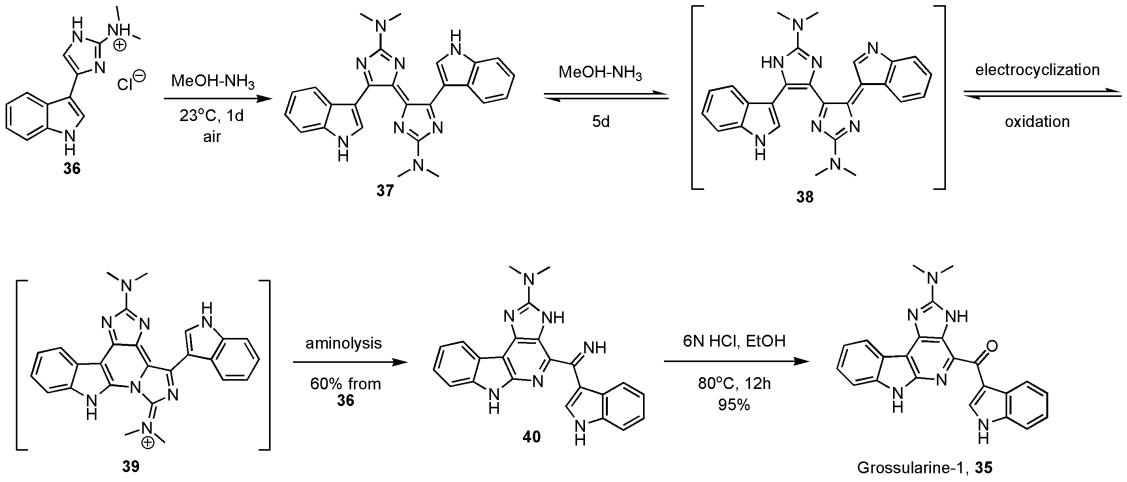

Scheme I.6: Biomimetic synthesis of grossularine-1 (**35**)

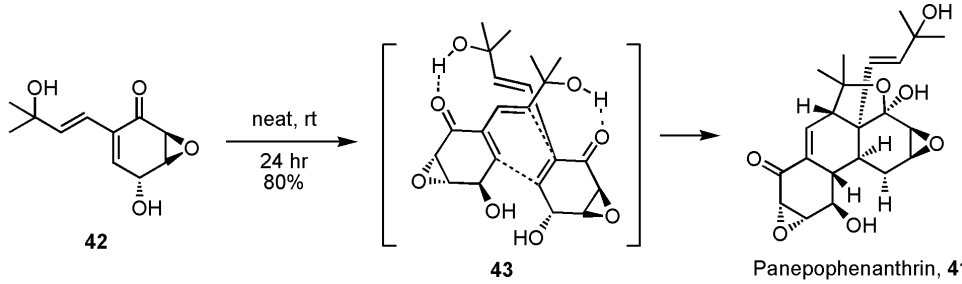

Scheme I.7: Biomimetic synthesis of panepophenanthrin (**41**) through a Diels-Alder reaction

this case, given that **42** requires an extremely high concentration (neat) for smooth dimerization, it is possible that the transformation to **41** is enzymatically catalyzed.

Finally, a cyanobacterial UV-screening natural product, scytonemin (**44**)[172] is an example of a dimeric metabolite that is now known to require enzymatic assistance for dimerization of the corresponding monomer.[173] Again, through chemical synthesis, a putative monomer **45** was prepared and subjected to various oxidizing conditions that could exist in nature. However, it was found that **45** does not dimerize under such conditions, thereby providing unique insights into the biosynthesis of scytonemin.

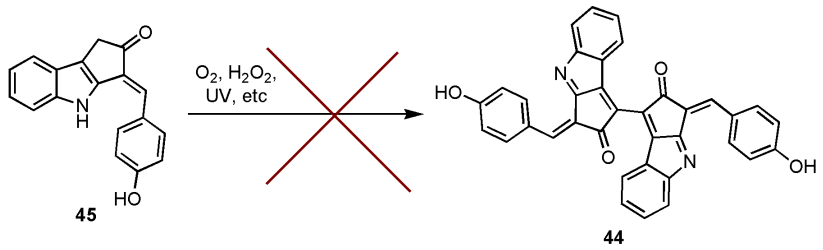

Scheme I.8: Scytonemin monomer does not dimerize under naturally occurring conditions

I.6 Rationale for Thesis Research

Three separate areas in which natural products chemistry has benefited from organic synthesis were discussed above; namely, structure elucidation and confirmation, pharmaceutical application, and biosynthetic study of natural products. Simultaneously, natural products have been the major driving force for the advancement of organic synthesis. Given this rich history, direct application of the power of organic synthesis to natural products should improve productivity in all three areas mentioned above. As an added significant benefit, new chemical transformations and synthetic strategies can be discovered in the process.

I.7 Overview of Thesis Chapters

Chapter II describes the isolation and characterization of two neurotoxic and ichthyotoxic polybrominated diphenyl ethers from a mixed assemblage of a red alga and cyanobacteria. Coauthors contributed the following: Z. Cao conducted the $[Ca^{2+}]_i$ assays; T. F. Murray oversaw the $[Ca^{2+}]_i$ assay work and contributed to the corresponding portion

of the article. The text of II, in whole, is the manuscript that has been submitted to *Toxicon* as it will appear: Takashi L. Suyama, Zhengyu Cao, Thomas F. Murray, and William H. Gerwick, Ichthyotoxic Brominated Diphenyl Ethers from a Mixed Assemblage of a Red Alga and Cyanobacterium: Structure Clarification and Biological Properties. The dissertation author was the primary investigator and author of the research which forms the basis of this chapter.

Chapter III describes the discovery of a novel fatty acid containing a vinylchloride functionality, credneric acid, from a marine cyanobacterium *Lyngbya* sp. The text of III, in part, will be used for a manuscript to be submitted to an academic journal. The dissertation author was the primary investigator and author of the research which forms the basis of this chapter.

Chapter IV describes the determination of the absolute configurations of a novel fatty acid containing cyclopropane moiety from a marine cyanobacterium *Lyngbya majuscula* through synthetic introduction of a stereochemical reference. A coauthor contributed the following: K. L. McPhail assisted with the purification of the natural product and acquisition and interpretation of the NMR data. The text of IV, in part, will be used for a manuscript to be submitted to an academic journal as it will appear: Takashi L. Suyama, Kerry L. McPhail, and William H. Gerwick, Absolute Stereochemistry by Synthetic Introduction of a Stereochemical Reference: Application to an Unusual Marine Cyanobacterial Lipid. The dissertation author was the primary investigator and author of the research which forms the basis of this chapter.

Chapter V describes the expedient, efficient and stereoselective total syntheses of a rainforest frog alkaloid epiquinamide and its enantiomer. The text of V, in part, is

published material as it appears: Takashi L. Suyama and William H. Gerwick, Practical Total Syntheses of Epiquinamide Enantiomers, *Organic Letters* **2006**, *8*, 4541-4543. The dissertation author was the primary investigator and author of the research which forms the basis of this chapter.

Chapter VI describes the stereoselective and stereospecific total synthesis of somocystinamide A. The text of VI, in part, is published material as it appears: Takashi L. Suyama and William H. Gerwick, Stereospecific Total Synthesis of Somocystinamide A, *Organic Letters* **2008**, *10,* 4449-4452. Another portion of the text of VI will be submitted to another academic journal. The dissertation author was the primary investigator and author of the research which forms the basis of this chapter.

Chapter VII describes the biomimetic total synthesis of a cyanobacterial UV-screening metabolite, scytonemin. The text of VII, in part, will be used for a manuscript to be submitted to an academic journal. The dissertation author was the primary investigator and author of the research which forms the basis of this chapter.

Chapter VIII summarizes my thesis research and provides conclusions based on the research.

The appendix describes my additional research activities that could not constitute thesis chapters by themselves.

References and footnotes

1 Kauffman, G. B.; Chooljian, S. H. Friedrich Wöhler (1800-1882), on the Bicentennial of His Birth. *Chem. Educator*, **2001**, *6*, 121-133.

2 Salzberg, H. W. *From Caveman to Chemist*, **1991**, American Chemical Society.

3 Wöhler, F. *Ann. Phys. Chem.* **1828**, *12*, 253.

4 Tarbell, D. S.; Tarbell, T. *Essays on the history of organic chemistry in the United States, 1875-1955.* **1986**, K & S Press, Nashville, TN. pp 5.

5 Mann, J. *Secondary Metabolism, 2nd Ed.*, **1987**, Oxford Science Publications.

6 Holy Bible, a) The Gospel according to John 19:40 b) Exodus 25:6

7 Indeed, the bioactivities of some of these compounds are still being discovered. For example, some of the health benefits of garlic are now attributed to the diallyl sulfide compounds found in it (Table I.1 and ref. 8).

8 Xiao, D.; Li, M.; Herman-Antosiewicz, A.; Antosiewicz, J.; Xiao, H.; Lew, K. L.; Zeng, Y.; Marynowski, S. W.; Singh, S. V. Diallyl Trisulfide Inhibits Angiogenic Features of Human Umbilical Vein Endothelial Cells by Causing Akt Inactivation and Down-Regulation of VEGF and VEGF-R2. *Nutr. Canc.* **2006**, *55*, 94-107.

9 Fischer, H.; Zeile, K. Synthese des Hämatoporphyrins, Protoporphyrins und Hämins. *Justus Liebigs Ann. Chem.* **1929**, *468*, 98-116.

10 Bachmann, W. E.; Cole, W.; Wilds, A. L. The total synthesis of sex hormone equilenin. *J. Am. Chem. Soc.* **1939**, *61*, 974.

11 Nicolaou, K. C.; Sorensen, E. J. *Classics in Total Synthesis*, **1996**, VCH publishers.

12 Nakanishi, K. *A Wandering Natural Products Chemist*, **1991**, American Chemical Society, pp 87.

13 Saraswathi, V.; Ramamoorthy, N.; Subramaniam, S.; Mathuram, V.; Gunasekaran, P.; Govindasamy, S. Inhibition of glycolysis and respiration of sarcoma-180 cells by echitamine chloride. *Chemotherapy* **1998**, *44*, 198-205.

14 Govindachari, T. R.; Rajappa, S. Echitamine. *Tetrahedron* **1961**, *15*, 132-143.

15 v. Group-Besanez *Ann. Chem.* **1875**, *176*, 88-89.

16 Nicolaou, K. C.; Snyder, S. A. Chasing Molecules That Were Never There: Misassigned Natural Products and the Role of Chemical Synthesis in Modern Structure Elucidation. *Angew. Chem. Int. Ed.* **2005**, *44*, 1012-1044.

17 To a somewhat lesser extent, compounds of biosynthetic and ecological interests have attracted natural products chemists' attention as well.

18 SciFinder Scholar search for “structure revision” and other related keywords

19 Gavagnin, M.; Mollo, E.; Cimino, G.; Ortea, J. A new γ-dihydropyrone-propionate from the caribbean sacoglossan *Tridachia crispata*. *Tetrahedron Lett.* **1996**, *37*, 4259–4262.

20 (a) Jeffery, D. W.; Perkins, M. V.; White, J. M. Synthesis of an Analogue of the Marine Polypropionate Tridachiahydropyrone. *Org. Lett.* **2005**, *7*, 407–409. (b) Jeffery, D. W.; Perkins, M. V.; White, J. M. Synthesis of the Putative Structure of Tridachiahydropyrone. *Org. Lett.* **2005**, *7*, 1581–1584.

21 Ireland, C.; Faulkner, D. J. The metabolites of the marine molluscs *tridachiella diomedea* and *tridachia crispata. Tetrahedron* **1981**, *37*, 233–240, Suppl. 1.

22 Fleming, I. *Pericyclic Reactions*, **1999**, Oxford University Press, pp 31-56.

23 Sharma, P.; Griffiths, N.; Moses, J. E. Biomimetic synthesis and structural revision of (±)-tridachiahydropyrone. *Org. Lett.* **2008**, *10*, 4025-4027.

24 Takashima, J.; Asano, S.; Ohsaki, A. *Tennen Yuki Kagobutsu Toronkai Koen Yoshishu* **2000**, *42*, 487.

25 Hu, G.; Liu, K.; Williams, L. J. The brosimum allene: a structural revision. *Org. Lett.* **2008**, *10*, 5493-5496.

26 Publications that merely claim that the original structures are incorrect, but do not give revised structures are omitted.

27 Encarnacion, R. D.; Sandoval, E.; Malmstrom, J.; Christophersen, C. Calafianin, a Bromotyrosine Derivative from the Marine Sponge *Aplysina gerardogreeni*. *J. Nat. Prod.* **2000**, *63*, 874–875.

28 (a) Ogamino, T.; Nishiyama, S. Synthesis and structural revision of calafianin, a member of the spiroisoxazole family isolated from the marine sponge, *Aplysina gerardogreeni. Tetrahedron Lett.* **2005**, *46,* 1083–1086. (b) Ogamino, T.; Obata, R.; Tomoda, H.; Nishiyama, S. Total Synthesis, Structural Revision, and Biological Evaluation of Calafianin, a Marine Spiroisoxazoline from the Sponge, *Aplysina gerardogreeni. Bull. Chem. Soc. Jpn.* **2006**, *79*, 134-139.

29 Wu, T.; Shi, L.; Kuo, S. Alkaloids and other constituents from Tribulus terrestris. *Phytochemistry* **1999**, *50*, 1411-1415.

30 Bremner, J.; Sengpracha, W.; Southwell, I.; Bourke, C.; Skelton, B.; White, A. The alkaloids of Tribulus terrestris: a revised structure for the alkaloid tribulusterine. *Acta Horticulturae* **2005**, *677*, 11-17.

31 Baetas, A. C. S.; Arruda, M. S. P.; Mu¨ller, A. H.; Arruda, A. C. *J. Braz. Chem. Soc.* **1999**, *10*, 181–183.

32 Maesa, D.; Vervischa, S.; Debenedettib, S.; Davioc, C.; Mangelinckxa, S.; Giubellinaa, N.; De Kimpe, N. Synthesis and structural revision of naturally occurring ayapin derivatives. *Tetrahedron* **2005**, *61*, 2505-2511.

33 Suzuki, K.; Yahara, S.; Maehata, K.; Uyeda, M. Isoaurostatin, a Novel Topoisomerase Inhibitor Produced by *Thermomonospora alba*. *J. Nat. Prod.* **2001**, *64*, 204–207.

34 Venkateswarlu, S.; Panchagnula, G. K.; Guraiah, M. B.; Subbaraju, G. V. Isoaurostatin: total synthesis and structural revision. *Tetrahedron* **2005**, *61*, 3013–3017.

35 Atta-Ur-Rahman; Choudhary, M. I.; Hayat, S.; Khan, A. M.; Ahmed, A. Two New Aurones from Marine Brown Alga Spatoglossum variabile. *Chem. Pharm*. *Bull*. **2001**, *49*, 105–107.

36 Venkateswarlu, S.; Panchagnula, G. K.; Gottumukkala, A. L.; Subbaraju, G. V. Synthesis, structural revision, and biological activities of 4'-chloroaurone, a metabolite of marine brown alga Spatoglossum variabile. *Tetrahedron* **2007**, *63*, 6909-6914.

37 Tang, Y.-Q.; Sattler, I.; Thiericke, R.; Grabley, S.; Feng, X.-Z. Feigrisolides A, B, C and D, New Lactones with Antibacterial Activities from Streptomyces griseus. *J. Antibiot*. **2000**, *53*, 934-943.

38 Alvarez-Bercedo, P.; Murga, J.; Carda, M.; Marco, J. A. Stereoselective Synthesis of the Published Structure of Feigrisolide A. Structural Revision of Feigrisolides A and B. *Org. Chem*. **2006**, *71*, 5766–5769.

39 Tang, Y.-Q.; Sattler, I.; Thiericke, R.; Grabley, S.; Feng, X.-Z. Feigrisolides A, B, C and D, New Lactones with Antibacterial Activities from *Streptomyces griseus*. *J. Antibiot.* **2000**, *53*, 934-943.

40 Kim, W. H.; Jung, J. H.; Lee, E. Feigrisolide C: Structural Revision and Synthesis. *J. Org. Chem*. **2005**, *70*, 8190-8192.

41 Graber, M. A.; Gerwick, W. H. *Tetrahedron Lett*. **1996**, *37*, 4635–4638.

42 Miyaoka, H.; Hara, Y.; Shinohara, I.; Kurokawa, T.; Yamada, Y. Synthesis and structural revision of marine eicosanoid agardhilactone. *Tetrahedron Lett*. **2005**, *46*, 7945–7949.

43 Snider, B. B.; Shi, B. Synthesis of pyrinodemins A and B. Assignment of the double bond position of pyrinodemin A. *Tetrahedron Lett.* **2001**, *42*, 1639–1642.

44 Ishiyama, H.; Tsuda, M.; Endo, T.; Kobayashi, J. Asymmetric Synthesis of Double Bond Isomers of the Structure Proposed for Pyrinodemin A and Indication of Its Structural Revision. *Molecules* **2005**, *10*, 312-316.

45 Nakamura, H.; Wu, H.; Ohizumi, Y.; Hirata, Y. Agelasine-A, -B, -C and -D, novel bicyclic diterpenoids with a 9-methyladeninium unit possessing inhibitory effects on na,K-atpase from the okinawa sea sponge *Agelas* sp. *Tetrahedron Lett.* **1984**, *25*, 2989-2992.

46 Marcos, I. S.; Garcia, N.; Sexmero, M. J.; Basabe, P.; Diez, D.; Urones, J. G. Synthesis of (+)-agelasine C. A structural revision. *Tetrahedron* **2005**, *61*, 11672-11678.

47 Rao, M. R.; Faulkner, D. J. Clavosolides A and B, Dimeric Macrolides from the Philippines Sponge *Myriastra clavosa*. *J. Nat. Prod*. **2002**, *65*, 386-388.

48 Son, J. B.; Kim, S. N.; Kim, N. Y.; Lee, D. H. Total Synthesis, Structural Revision, and Absolute Configuration of (+)-Clavosolide A. *Org. Lett.* **2006**, *8*, 661-664.

49 Hiort, J.; Maksimenka, K.; Reichert, M.; Perovi-Ottstadt, S.; Lin, W. H.; Wray, V.; Steube, K.; Schaumann, K.; Weber, H.; Proksch, P.; Ebel, R.; Mller, W. E. G.; Bringmann, G. New Natural Products from the Sponge-Derived Fungus Aspergillus niger. *J. Nat. Prod*. **2004**, *67*, 1532-1543.

50 Ye, Y. H.; Zhu, H. L.; Song, Y. C.; Liu, J. Y.; Tan, R. X. Structural Revision of Aspernigrin A, Reisolated from Cladosporium herbarum IFB-E002. *J. Nat. Prod*. **2005**, *68*, 1106-1108.

51 Subrahmanyam, C.; Kumar, S. R. A new polyoxygenated steroid from the gorgonian *Gorgonella. J. Chem. Res.* (S) **2000**, 182.

52 Zhang, W.; Guo, Y. W.; Gavagnin, M.; Mollo, E.; Cimino, G. Suberoretisteroids A-E, five new uncommon polyoxygenated steroid 24-ketals from the Hainan gorgonian Suberogorgia reticulata. *Helv. Chim. Acta* **2005**, *88*, 87-94.

53 Shimbo, K.; Tsuda, M.; Izui, N.; Kobayashi, J. Amphidinolide W, a New 12-Membered Macrolide from Dinoflagellate Amphidinium sp. *J. Org. Chem*. **2002**, *67*, 1020.

54 Ghosh, A. K.; Gong, G. Total Synthesis and Revision of C6 Stereochemistry of (+)-Amphidinolide W. *J. Org. Chem.* **2006**, *71*, 1085-1093.

55 Patil, A. D.; Freyer, A. J.; Taylor, P. B.; Carte´, B.; Zuber, G.; Johnson, R. K.; Faulkner, D. J. Batzelladines F−I, Novel Alkaloids from the Sponge *Batzella* sp.: Inducers of p56lck-CD4 Dissociation. *J. Org. Chem*. **1997**, *62*, 1814-1819.

56 Cohen, F.; Overman, L. E. Evolution of a Strategy for the Synthesis of Structurally Complex Batzelladine Alkaloids. Enantioselective Total Synthesis of the Proposed Structure of Batzelladine F and Structural Revision. *J. Am. Chem. Soc.* **2006**, *128*, 2594-2603.

57 Bourdelais, A. J.; Jacocks, H. M.; Wright, J. L. C.; Bigwarfe, P. M., Jr.; Baden, D. G. A New Polyether Ladder Compound Produced by the Dinoflagellate *Karenia brevis*. *J. Nat*. *Prod*. **2005**, *68*, 2-6.

58 Fuwa, H.; Ebine, M.; Bourdelais, A. J.; Baden, D. G.; Sasaki, M. Total Synthesis, Structure Revision, and Absolute Configuration of (-)-Brevenal. *J. Am. Chem. Soc.* **2006**, *128*, 16989-16999.

59 Ahmed, A. A.; Mahmoud, A. A. Jasonol, a rare tricyclic eudesmane sesquiterpene and six other new sesquiterpenoids from Jasonia candicans. *Tetrahedron* **1998**, *54*, 8141-52.

60 Fang, L.; Bi, F.; Zhang, C.; Zheng, G.; Li, Y. Total synthesis of 4a,5a,10b-trihydroxycadinane and its C4-isomer: structural revision of a natural sesquiterpenoid. *Synlett* **2006**, *16*, 2655-2657.

61 Lin, W.; Brauers, G.; Ebel, R.; Wray, V.; Berg, A.; Sudarsono; Proksch, P. Novel Chromone Derivatives from the Fungus *Aspergillus versicolor* Isolated from the Marine Sponge *Xestospongia exigua*. *J. Nat. Prod*. **2003**, *66*, 57–61.

62 Saito, F.; Kuramochi, K.; Nakazaki, A.; Mizushina, Y.; Sugawara, F.; Kobayashi, S. Synthesis and Absolute Configuration of (+)-Pseudodeflectusin: Structural Revision of Aspergione B. *Eur. J. Org. Chem.* **2006** *21*, 4796–4799.

63 Cutler, H. G.; Jacyno J. M.; Harwood J. S.; Dulik, D.; Goodrich, P. D.; Roberts, R. G. Botcinolide: A Biologically Active Natural Product from *Botrytis cinerea*. *Biosci. Biotech. Biochem.* **1993**, *57*, 1980-1982.

64 Tani, H.; Koshino, H.; Sakuno, E.; Cutler, H. G.; Nakajima, H. Botcinins E and F and Botcinolide from *Botrytis cinerea* and structural revision of botcinolides. *J. Nat. Prod.* **2006**, *69*, 722–725.

65 Cutler, H. G.; Parker, S. R.; Ross, S. A.; Crumley, F. G.; Schreiner, P. R. A Biologically Active Natural Homolog of Botcinolide from Botrytis cinerea. *Biosci. Biotech. Biochem.* **1996**, *60*, 656-658.

66 Collado, I. G.; Aleu, J.; Herna´ndez-Gala´n, R.; Hanson, J. R. Some metabolites of Botrytis cinerea related to botcinolide. *Phytochemistry* **1996**, *42*, 1621-1624.

67 Yamada, T.; Iritani, M.; Minomura, K.; Kawai, K.; Numata, A. Peribysins A–D, potent cell-adhesion inhibitors from a sea hare-derived culture of Periconia species. *Org. Biomol. Chem.* **2004**, *2*, 2131–2135.

68 Koshino, H.; Satoh, H.; Yamada, T.; Esumi, Y. Structural revision of peribysins C and D. *Tetrahedron Lett.* **2006**, *47*, 4623-26.

69 Hiort, J.; Maksimenka, K.; Reichert, M.; Perovic-Ottstadt, S.; Lin, W. H.; Wray, V.; Steube, K.; Schaumann, K.; Weber, H.; Proksch, P.; Ebel, R.; Mu¨ller, W. E. G.; Bringmann, G. New Natural Products from the Sponge-Derived Fungus Aspergillus niger. *J. Nat. Prod.* **2004**, *67*, 1532-1543.

70 Schlingmann, G.; Taniguchi, T.; He, H.; Bigelis, R.; Yang, H. Y.; Koehn, F. E.; Carter, G. T.; Berova, N. Reassessing the structure of pyranonigrin. *J. Nat. Prod*. **2007**, *70*, 1180-1187.

71 (a) Ravikumar, P. R.; Soman, R.; Chetty, G. L.; Pandey, R. C.; Sukh, D. Chemistry of Ayurvedic Crude Drugs: Part VI-(Shatavari-1): Structure of Shatavarin-IV. *Ind. J. Chem*. **1987**, *26B*, 1012–1017. (b) Joshi, J.; Sukh, D. Chemistry of Ayurvedic Crude Drugs: Part III-Shatavari-2: Structure Elucidation of Bioactive Shatavarin-I & Other Glycosides. *Ind. J. Chem*. **1988**, *27B*, 12–16.

72 Hayesa, P. Y.; Jahidina, A. H.; Lehmannb, R.; Penmanb, K.; Kitchinga, W.; De Voss, J. J. Structural revision of shatavarins I and IV, the major components from the roots of Asparagus racemosus. *Tetrahedron Lett.* **2006**, *47*, 6965-6969.

73 Evidente, A.; Conti, L.; Altomare, C.; Bottalico, A.; Sindona, G.; Segre, A. L.; Logrieco, A. Fusapyrone and deoxyfusapyrone, two antifungal a -pyrones from Fusarium semitectum. *Nat. Toxins* **1994**, *2,* 4–13

74 Hiramatsu, F.; Miyajima, T.; Murayama, T.; Takahashi, K.; Koseki, T.; Shiono, Y. Isolation and Structure Elucidation of Neofusapyrone from a Marine-derived Fusarium species, and Structural Revision of Fusapyrone and Deoxyfusapyrone. *The Journal of Antibiotics* **2006** *59*, 704–709.

75 Seo, Y.; Cho, K. W.; Rho, J.-R.; Shin, J.; Kwon, B.-M.; Bok, S.-H.; Song, J.-I. Solandelactones A-I, Lactonized Cyclopropyl Oxylipins Isolated from the Hydroid Solanderia secunda. *Tetrahedron* **1996**, *52*, 10583-96.

76 Pietruszka, J.; Rieche, A. C. M. Total synthesis of marine oxylipins solandelactones A-H. *Adv. Synth. Catal*. **2008**, *350*, 1407-1412.

77 Delazar, A.; Byres, M.; Gibbons, S.; Kumarasamy, Y.; Modarresi, M.; Nahar, L.; Shoeb, M.; Sarker, S. D. Iridoid Glycosides from Eremostachys glabra. *J. Nat. Prod*. **2004**, *67*, 1584-1587.

78 Jensen, S. R.; Çalış, I.; Gotfredsen, C. H.; Søtofte, I. Structural Revision of Some Recently Published Iridoid Glucosides. *J. Nat. Prod*. **2007**, *70,* 29–32.

79 Ahmed, B.; Al-Rehaily, A. J.; Al-Howiriny, T. A.; El-Sayed, K. A.; Ahmad, M. S. Scropolioside-D_2 and Harpagoside-B: Two New Iridoid Glycosides from Scrophularia deserti and Their Antidiabetic and Antiinflammatory Activity. *Biol. Pharm. Bull*. **2003**, *26*, 462-467.

80 Ahmad, I.; Afza, N.; Anis, I.; Malik, A.; Fatima, I.; ul-Haq, A.; Tareen, R. B. Iridoid glycosides and a benzofuran type sesquiterpene from *Buddleja crispa*. *Heterocycles* **2004**, *63*, 1875-1881.

81 Itokawa, H.; Nakajima, H.; Ikuta, A.; Iitaka, Y. Two triterpenes from the flowers of *Camellia japonica*. *Phytochemistry.* **1981**, *20*, 2539-2542.

82 Yoshikawa, M.; Morikawa, T.; Asao, Y.; Fujiwara, E.; Nakamura, S.; Matsuda, H. Medicinal flowers. XV. The structures of noroleanane- and oleanane-type triterpene oligoglycosides with gastroprotective and platelet aggregation activities from flower buds of Camellia japonica. *Chem. Pharmaceut. Bull.* **2007**, *55*, 606-612.

83 Kinnel, R. B.; Gehrken, H.-P.; Scheuer, P. J. Palau'amine: a cytotoxic and immunosuppressive hexacyclic bisguanidine antibiotic from the sponge *Stylotella agminata*. *J. Am. Chem. Soc.* **1993**, *115*, 3376 – 3377.

84 (a) Koeck, M.; Grube, A.; Seiple, I. B.; Baran, P. S. The pursuit of Palau'amine. *Angew. Chem. Int. Ed.* **2007**, *46*, 6586-6594. (b) Grube, A.; Köck, M. Structural Assignment of Tetrabromostyloguanidine: Does the Relative Configuration of the Palau'amines Need Revision? Angew. *Chem. Int. Ed*. **2007**, *46*, 2320 – 2324.

85 Wall, M. E.; Wani, M. C.; Manikumar, H. T.; Taylor, H.; McGivney, R. Plant Antimutagens, 6. Intricatin and Intricatinol, New Antimutagenic Homoisoflavonoids from *Hoffmanosseggia intricata*. *J. Nat. Prod*. **1989**, *52*, 774-778.

86 Peter, A.; Amenechi, P. I. Isoflavonoid and pterocarpinoid extractives of Lonchocarpus laxiflorus. *J. Chem. Soc. C* **1969**, 887-896.

87 Siddaiah, V.; Maheswara, M.; Rao, C. V.; Venkateswarlub, S.; Subbarajub, G. V. Synthesis, structural revision, and antioxidant activities of antimutagenic homoisoflavonoids from Hoffmanosseggia intricata. *Bioorg. Med. Chem. Lett.* **2007**, 17, 1288–1290.

88 (a) Leet, J. E.; Schroeder, D. R.; Hofstead, S. J.; Golik, J.; Colson, K. L.; Huang, S.; Klohr, S. E.; Doyle, T. W.; Matson, J. A. Kedarcidin, a new chromoprotein antitumor antibiotic: structure elucidation of kedarcidin chromophore. *J. Am. Chem. Soc.* **1992**, *114*, 7946-7948. (b) Leet, J. E.; Schroeder, D. R.; Langley, D. R.; Colson, K. L.; Huang, S.; Klohr, S. E.; Lee, M. S.; Golik, J.; Hofstead, S.J.; Doyle, T. W.; Matson, J. A. Chemistry and structure elucidation of the kedarcidin chromophore. *J. Am. Chem. Soc.* **1993**, *115*, 8432-8443.

89 Ren, F.; Hogan, P. C.; Anderson, A. J.; Myers, A. G. Kedarcidin chromophore: Synthesis of Its Proposed Structure and Evidence for a Stereochemical Revision. *J. Am. Chem. Soc*. **2007**, *129*, 5381–5383.

90 Kawata, S.; Ashizawa, S.; Hirama, M. Synthetic Study of Kedarcidin Chromophore: Revised Structure. *J. Am. Chem. Soc.* **1997**, *119*, 12012–12013.

91 McPhail, K. L.; Gerwick, W. H. Three New Malyngamides from a Papua New Guinea Collection of the Marine Cyanobacterium Lyngbya majuscula. *J. Nat. Prod*. **2003**, *66*, 132.

92 Li, Y.; Feng, J.-P.; Wang, W.-H.; Chen, J.; Cao, X.-P. Total Synthesis and Correct Absolute Configuration of Malyngamide U. *J. Org. Chem.* **2007**, *72*, 2344-2350.

93 Khaliq, S.; Volk, F.-J.; Frahm, A. W. Phytochemical Investigation of Perovskia abrotanoides. *Planta Med*. **2007**, *73*, 77-83.

94 Simmons, E. M.; Yen, J. R.; Sarpong, R. Reconciling Icetexane Biosynthetic Connections with Their Chemical Synthesis: Total Synthesis of (±)-5,6-Dihydro-6a-hydroxysalviasperanol, (±)-Brussonol, and (±)-Abrotanone. *Org. Lett.* **2007**, *9*, 2705-2708.

95 Tanaka, N.; Okasaka, M.; Ishimaru, Y.; Takaishi, Y.; Sato, M.; Okamoto, M.; Oshikawa, T.; Ahmed, S. U.; Consentino, L. M.; Lee, K.-H. Biyouyanagin A, an Anti-HIV Agent from Hypericum chinense L. var. salicifolium. *Org. Lett*. **2005**, *7*, 2997-2999.

96 Nicolaou, K. C.; Sarlah, D.; Shaw, D. M. Total synthesis and revised structure of biyouyanagin A. *Angew. Chem. Int. Ed.* **2007**, *46*, 4708-4711.

97 Nii, H.; Furukawa, K.; Iwakiri, M.; Kubota, T. *Nippon Nogeikagaku Kaishi* **1983**, *57*, 733–741; *Chem. Abstr.* **1983**, *99*, 200329.

98 Blay, G.; Garcia, B.; Molina, E.; Pedro, J. R. Synthesis of (+)-pechueloic acid and (+)-aciphyllene. Revision of the structure of (+)-aciphyllene. *Tetrahedron* **2007**, *63*, 9621-9626.

99 Diyabalanage, T.; Amsler, C. D.; McClintock, J. B.; Baker, B. J. Palmerolide A, a Cytotoxic Macrolide from the Antarctic Tunicate Synoicum adareanum. *J. Am. Chem. Soc*. **2006**, *128*, 5630 – 5631.

100(a) Nicolaou, K. C.; Guduru, R.; Sun, Y.-P.; Banerji, B.; Chen, D. Y.-K. Total synthesis of the originally proposed and revised structures of palmerolide A. *Angew. Chem. Int. Ed.* **2007**, *46*, 5896-5900. (b) Nicolaou, K. C.; Sun, Y.-P.; Guduru, R.; Banerji, B.; Chen, D. Y.-K. Total Synthesis of the Originally Proposed and Revised Structures of Palmerolide A and Isomers Thereof. *J. Am. Chem. Soc.* **2008**, *130*, 3633-3644.

101 Solis, P. N.; Lang'at, C.; Gupta, M. P.; Kirby, G. C.; Warhurst, D. C.; Phillipson, J. D. Bio-active Compounds from Psychotria camponutans. *Planta Med.* **1995**, *61*, 62-65.

102 Jacobs, J.; Claessens, S.; De Kimpe, N. First straightforward synthesis of 1-hydroxy-3,4-dihydro-1H-benz[g]isochromene-5,10-dione and structure revision of a bioactive benz[g]isochromene-5,10-dione from Psychotria camponutans. *Tetrahedron* **2008**, *64*, 412-418.

103 Sun, J.; Shi, D.; Ma, M.; Li, S.; Wang, S.; Han, L.; Yang, Y.; Fan, X.; Shi, J.; He, L. Sesquiterpenes from the Red Alga *Laurencia tristicha*. *J. Nat. Prod.* **2005**, *68*, 915-919.

104 Chen, P.; Wang, J.; Liu, K.; Li, C. Synthesis and Structural Revision of (±)-Laurentristich-4-ol. *J. Org. Chem*. **2008**, *73*, 339-341.

105 Hastings, J. S.; Heller, H. G. The stereochemistry of aurones [2-substituted benzylidenebenzofuran-3(2H)-ones] *J. Chem. Soc., Perkin Trans.* **1972**, *1*, 2128-2132.

106 Harkat, H.; Blanc, A.; Weibel, J.-M.; Pale, P. Versatile and Expeditious Synthesis of Aurones via AuI-Catalyzed Cyclization. *J. Org. Chem*. **2008**, *73*, 1620-1623.

107 Gunatilaka, A. A. L. In: Herz, W.;Kirby, G. W.; Moore, R. E.; Steglich, W.; Tamm,C. *Progress in the Chemistry of Organic Natural Products* vol.67, Springer-Verlag/Wien, New York **1996**, pp. 1–123.

108 Jacobsen, N. E.; Wijeratne, E. M. K.; Corsino, J.; Furlan, M.; Bolzani, V. S.; Gunatilaka, A. A. L. Biomimetic synthesis of xuxuarines Ea and Eb: Structure revision of Rzedowskia bistriterpenoids. *Bioorg. Med. Chem.* **2008**, *16*, 1884-1889.

109 Bastida, J.; Codina, C.; Peeters, P.; Rubiralta, M.; Orozco, M.; Luque, F. J.; Chharbra, S. C. Alkaloids from *Crinum kirkii*. *Phytochemistry* **1995**, *40*, 1291-1293.

110 Biechy, A.; Hachisu, S.; Quiclet-Sire, B.; Ricard, L.; Zard, S. Z. The total synthesis of (±)-fortucine and a revision of the structure of kirkine. *Angew. Chem. Int. Ed.* **2008**, *47*, 1436-1438.

111 Sakai, K.; Fukuda, Y.; Matsunaga, S.; Tanaka, R.; Yamort, T. New Cytotoxic Oleanane-Type Triterpenoids from the Cones of *Liquidamber styraciflua*. *J. Nat. Prod*. **2004**, *67*, 1088-1093.

112 Sun, H.; Fang, W.-S.; Hu, C. An efficient semi-synthesis and structure revision of a cytotoxic triterpenoid 25-acetoxy-3a-hydroxyolean-12-en-28-oic acid from *Liquidamber styraciflua*. *J. Asian Nat. Prod. Res*. **2008**, *10*, 271-276.

113 Zampella, A.; D'Auria, M.V.; Minale, L.; Debitus, C.; Roussakis, C. Callipeltoside A: A Cytotoxic Aminodeoxy Sugar-Containing Macrolide of a New Type from the Marine Lithistida Sponge *Callipelta* sp. *J. Am. Chem. Soc.* **1996**, *118*, 11085-11088.

114 Carpenter, J.; Northrup, A. B.; Chung, D.; Wiener, J. J. M.; Kim, S.-G.; MacMillan, D. W. C. Total synthesis and structural revision of callipeltoside C. *Angew. Chem. Int. Ed*. **2008**, 47, 3568-3572.

115 Kuo, Y.-H.; Lin, B.-Y. A New Dinorxanthane and Chromone from the Root of *Tithonia diversifolia*. *Chem. Pharm. Bull.* **1999**, 47, 428-429.

116 Matsuo, K.; Yokoe, H.; Shishido, K.; Shindo, M. Synthesis of diversifolide and structure revision. *Tetrahedron Lett.* **2008**, 49, 4279-4281.

117 Akiyama, K.; Kikuzaki, H.; Aoki, T.; Okuda, A.; Lajis, N. H.; Nakatani, N. Terpenoids and a Diarylheptanoid from *Zingiber ottensii*. *J. Nat. Prod.* **2006**, *69,* 1637-1640.

118 Boukouvalas, J.; Wang, J.-X. Structure Revision and Synthesis of a Novel Labdane Diterpenoid from Zingiber ottensii. *Org. Lett.* **2008**, 10, 3397-3399.

119 Sorek, H.; Rudi, A.; Gueta, S.; Reyes, F.; Martin, M. J.; Aknin, M.; Gaydou, E.; Vacelet, J.; Kashman, Y. Netamines A–G: seven new tricyclic guanidine alkaloids from the marine sponge *Biemna laboutei*. *Tetrahedron* **2006**, *62*, 8838–8843.

120 Yu, M.; Pochapsky, S. S.; Snider, B. B. Synthesis of 7-Epineoptilocaulin, Mirabilin B, and Isoptilocaulin. A Unified Biosynthetic Proposal for the Ptilocaulin and Batzelladine Alkaloids. Synthesis and Structure Revision of Netamines E and G. *J. Org. Chem.* **2008**, 73, 9065-9074.

121 Hayakawa, Y.; Yamashita, T.; Mori, T.; Nagai, K.; Shin-ya, K.; Watanabe, H. J. Structure of Tyroscherin, an Antitumor Antibiotic against IGF-1-dependent Cells from *Pseudallescheria* sp. *Antibiot.* **2004**, *57*, 634–638.

122 Katsuta, R.; Shibata, C.; Ishigami, K.; Watanabe, H.; Kitahara, T. Synthesis and structure revision of tyroscherin, a growth inhibitor of IGF-1-dependent tumor cells. *Tetrahedron Lett.* **2008**, 49, 7042-7045.

123 Murata, M.; Matsuoka, S.; Matsumori, N.; Paul, G. K.; Tachibana, K. Absolute Configuration of Amphidinol 3, the First Complete Structure Determination from Amphidinol Homologues: Application of a New Configuration Analysis Based on Carbon−Hydrogen Spin-Coupling Constants. *J. Am. Chem. Soc.* **1999**, *121*, 870–871.

124 Oishi, T.; Kanemoto, M.; Swasono, R.; Matsumori, N.; Murata, M. Synthesis of the 1,5-Polyol System Based on Cross Metathesis: Structure Revision of Amphidinol 3. *Org. Lett.* **2008**, 10, 5203-5206.

125 Mueller, D.; Krick, A.; Kehraus, S.; Mehner, C.; Hart, M.; Kuepper, F. C.; Saxena, K.; Prinz, H.; Schwalbe, H.; Janning, P.; Waldmann, H.; Koenig, G. M. Brunsvicamides A-C: sponge-related cyanobacterial peptides with Mycobacterium tuberculosis protein tyrosine phosphatase inhibitory activity. *J. Med. Chem.* **2006**, 49, 4871-4878.

126 Walther, T.; Arndt, H.-D.; Waldmann, H. Solid-support based total synthesis and stereochemical correction of brunsvicamide A. *Org. Lett.* **2008**, 10, 3199-3202.

127 Ralifo, P.; Crews, P. J. A New Structural Theme in the Imidazole-Containing Alkaloids from a *Calcareous Leucetta* Sponge. *Org. Chem*. **2004**, *69*, 9025–9029.

128 White, K. N.; Amagata, T.; Oliver, A. G.; Tenney, K.; Wenzel, P. J.; Crew, P. Structure Revision of Spiroleucettadine, a Sponge Alkaloid with a Bicyclic Core Meager in H-Atoms *J. Org. Chem*. **2008**, 73, 8719–8722.

129 Guella, G.; Mancini, I.; Öztunç, A.; Pietra, F. Conformational Bias in Macrocyclic Ethers and Observation of High Solvolytic Reactivity at a Masked Furfuryl (=2-Furylmethyl) C-Atom. *Helv. Chim. Acta* **2000**, *83*, 336–348.

130 Braddock, D. C.; Rzepa, H. S. Structural Reassignment of Obtusallenes V, VI, and VII by GIAO-Based Density Functional Prediction. *J. Nat. Prod.* **2008**, 71, 728-730.

131 Rahbæk, L.; Breinholt, J.; Frisvad, J. C.; Christophersen, C. Circumdatin A, B, and C: Three New Benzodiazepine Alkaloids Isolated from a Culture of the Fungus *Aspergillus ochraceus*. *J. Org. Chem*. **1999**, *64*, 1689-1692.

132 Ookura, R.; Kito, K.; Ooi, T.; Namikoshi, M.; Kusumi, T. Structure Revision of Circumdatins A and B, Benzodiazepine Alkaloids Produced by Marine Fungus *Aspergillus ostianus*, by X-ray Crystallography. *J. Org. Chem.* **2008**, 73, 4245-4247.

133 Cafieri, F.; De Napoli, L.; Fattorusso, E.; Santacroce, C. Diterpenes from the red alga *Sphaerococcus coronopifolius*. *Phytochemistry* **1987**, *26,* 471–473.

134 Smyrniotopoulos, V.; Quesada, A.; Vagias, C.; Moreau, D.; Roussakis, C.; Roussis, V. Cytotoxic bromoditerpenes from the red alga *Sphaerococcus coronopifolius*. *Tetrahedron* **2008**, 64, 5184-5190.

135 Takahashi, T.; Eto, H.; Ichimura, T.; Murae, T. Hiyodorilactones A and B, new tumor inhibitory germacradienolides from *Eupatorium sachalinense* makino. *Chem. Lett.* **1978**, 1345-1348.

136 Tori, M.; Morishita, N.; Hirota, N.; Saito, Y.; Nakashima, K.; Sono, M.; Tanaka, M.; Utagawa, A.; Hirota, H. Sesquiterpenoids isolated from *Eupatorium glehnii*. Isolation of guaiaglehnin A, structure revision of hiyodorilactone B, and genetic comparison. *Chem. Pharmaceut. Bull*. **2008**, 56, 677-681.

137 Sasse, F.; Steinmetz, H.; Höfle, G.; Reichenbach, H. Rhizopodin, a new compound from *Myxococcus stipitatus* (myxobacteria) causes formation of rhizopodia-like structures in animal cell cultures. *J. Antibiot.* **1993**, *46*, 741–748.

138 Jansen, R.; Steinmetz, H.; Sasse, F.; Schubert, W.-D.; Hagelueken, G.; Albrecht, S. C.; Mueller, R. Isolation and structure revision of the actin-binding macrolide rhizopodin from *Myxococcus stipitatus* (Myxobacteria). *Tetrahedron Lett.* **2008**, 49, 5796-5799.

139 Ziemert, N.; Ishida, K.; Quillardet, P.; Bouchier, C.; Hertweck, C.; Tandeau de Marsac, N.; Dittmann, E. Microcyclamide Biosynthesis in Two Strains of Microcystis aeruginosa: from Structure to Genes and Vice Versa. *Appl. EnViron. Microbiol.* **2008**, *74*, 1791-1797.

140 Portmann, C.; Blom, J. F.; Kaiser, M.; Brun, R.; Juttner, F.; Gademann, K. Isolation of aerucyclamides C and D and structure revision of microcyclamide 7806A: Heterocyclic ribosomal peptides from *Microcystis aeruginosa* PCC 7806 and their antiparasite evaluation. *J. Nat. Prod.* **2008**, 71, 1891-1896.

141 Luis, J. G.; Lahlou, E. H.; Andre´s, L. S. Hassananes: C23 terpenoids with a new type of skeleton from *Salvia apiana* Jeps. *Tetrahedron* **1996**, *52*, 12309-12312.

142 Yang, J.; Huang, S.-X.; Zhao, Q.-S. Structure Revision of Hassanane with Use of Quantum Mechanical 13C NMR Chemical Shifts and UV-Vis Absorption Spectra. *J. Phys. Chem.* **2008**, 112, 12132-12139.

143 Takada, N.; Watanabe, R.; Suenaga, K.; Yamada, K.; Ueda, K.; Kita, M. Uemura, Zamamistatin, a significant antibacterial bromotyrosine derivative, from the Okinawan sponge *Pseudoceratina purpurea*. *Tetrahedron Lett*. **2001**, *42*, 5265-5267.

144 Hayakawa, I.; Teruya, T.; Kigoshi, H. Revised structure of zamamistatin. *Tetrahedron Lett.* **2006**, *47*, 155-158.

145 Kita, M.; Tsunematsu, Y.; Hayakawa, I.; Kigoshi, H. Structure of zamamistatin - a correction. *Tetrahedron Lett.* **2008**, 49, 5383-5384.

146 Fitch, R. W.; Garraffo, H. M.; Spande, T. F.; Yeh, H. J. C.; Daly, J. W. Bioassay-guided isolation of epiquinamide, a novel quinolizidine alkaloid and nicotinic agonist from an Ecuadoran poison frog, *Epipedobates tricolor. J. Nat. Prod.* **2003**, *66*, 1345-1350.

147 (a) Wijdeven, M. A.; Botman, P. N. M.; Wijtmans, R.; Schoemaker, H. E.; Rutjes, F. P. J. T.; Blaauw, R. H. Total Synthesis of (+)- Epiquinamide. *Org. Lett.* **2005**, *7*, 4005-4007. (b) Suyama, T. L.; Gerwick, W. H. Practical Total Syntheses of Epiquinamide Enantiomers. *Org. Lett.* **2006**, *8*, 4541-4543. (c) Wijdeven, M. A.; Wijtmans, R.; van den Berg, R. J. F.; Noorduin, W.; Schoemaker, H. E.; Sonke, T.; van Delft, F. L.; Blaauw, R. H.; Fitch, R. W.; Spande, T. F.; Daly, J. W.; Rutjes, F. P. J. T. *N*,*N*-Acetals as *N*-Acyliminium Ion Precursors: Synthesis and Absolute Stereochemistry of Epiquinamide. *Org. Lett.* **2008**, *10*, 4001-4003. (d) Ghosh, S.; Shashidhar, J. Total synthesis of (+)- epiquinamide from -mannitol. *Tetrahedron Lett.* **2009**, *50*, 1177-1179. (e) Huang, P.-Q.; Guo, Z.-Q.; Ruan, Y.-P. A Versatile Approach for the Asymmetric Syntheses of (1*R*,9a*R*)- Epiquinamide and (1*R*,9a*R*)-Homopumiliotoxin 223G. *Org. Lett.* **2006**, *8*, 1435-1438. (f) Voituriez, A.; Ferreira, F.; Perez-Luna, A.; Chemla, F. Asymmetric synthesis of (-)-1-hydroxyquinolizidinone, a common intermediate for the syntheses of (-)-homopumiliotoxin 223G and (-)- epiquinamide. *Org. Lett.* **2007**, *9*, 4705-4708. (g) Tong, S.; Barker, D. A concise synthesis of (±) and a total synthesis of (+)-epiquinamide. *Tetrahedron Lett.* **2006**, *47*, 5017-5020. (h) Kanakubo, A.; Gray, D.; Innocent, N.; Wonnacott, S.; Gallagher, T. The synthesis and nicotinic binding activity of (±)-epiquinamide and (±)-C(1)-epiepiquinamide. *Bioorg. Med. Chem. Lett.* **2006**, *16*, 4648-4651.

148 Fitch, R. W.; Sturgeon, G. D.; Patel, S. R.; Spande, T. F.; Garraffo, H. M.; Daly, J. W.; Blaauw, R. H. Epiquinamide : A Poison That Wasn't from a Frog That Was. *J. Nat. Prod.* **2009**, *72*, 243-247.

149 Newman, D. J.; Cragg, G. M. Natural products as sources of new drugs over the last 25 years. *J. Nat. Prod.* **2007**, *70*, 461-477.

150 Füllbeck, M.; Michalsky, E.; Dunkel, M.; Preissner, R. Natural products: sources and databases. *Nat. Prod. Rep.* **2006**, *23*, 347-356.

151 Hill, R. A. *Annu. Rep. Prog. Chem. Sect. B*, **2003**, *99*, 183-207.

152 Ghaneh, P.; Costello, E. J P Neoptolemos Biology and management of pancreatic cancer. *J. Postgrad. Med*. **2008,** *84,* 478-497.

153 Heron, M. Deaths: Leading Causes for 2004 National Vital Statistics Reports **2007**, *56*, 1-96.

154 Sarker, S. D.; Latif, Z.; Gray, A. I. *Natural Products Isolation*, **2006**, Humana Press Inc.

155 Daly, J. W.; Spande, T. F.; Garraffo, H. M. Alkaloids from Amphibian Skin: A Tabulation of Over Eight-Hundred Compounds. *J. Nat. Prod.* **2005**, *68*, 1556-1575.

156 Moores Cancer Center Retreat, **2007**, San Diego, California.

157 Wender. P. A. Introduction: Frontiers in Organic Synthesis. *Chem. Rev.* **1996**, *96*, 1-2.

158 Mickel, S. J.; Sedelmeier, G. H.; Niederer, D.; Daeffler, R.; Osmani, A.; Schreiner, K.; Seeger-Weibel, M.; Bérod, B.; Schaer, K.; Chen, R. G.; Chen, W.; Jagoe, C. T.; Kinder, F. R., Jr.; Loo, M.; Prasad, K.; Repi, O.; Shieh, W.; Wang, R.; Waykole, L.; Xu, D. D.; Xue, S. Large-Scale Synthesis of the Anti-Cancer Marine Natural Product (+)-Discodermolide. Part 1: Synthetic Strategy and Preparation of a Common Precursor. *Org. Process Res. Dev*. **2004**, *8*, 92-100.

159 Smith, A.B.; Beauchamp, T. J.; LaMarche, M. J.; Kaufman, M. D.; Qiu, Y.; Arimoto, H.; Jones, D. R.; Kobayashi, K. Evolution of a Gram-Scale Synthesis of (+)-Discodermolide. *J. Am. Chem. Soc.* **2000**, *122*, 8654-8664.

160 Patterson, I.; Florence, G. J.; Gerlach, K.; Scott, J. P.; Sereinig, N. A Practical Synthesis of (+)-Discodermolide and Analogues: Fragment Union by Complex Aldol Reactions. *J. Am. Chem. Soc.* **2001**, *123*, 9535-9544.

161 Freemantle, M. Scaled-up synthesis of discodermolide. *Science & Technology* **2004**, *82*, 33-35.

162 Nogle, L. M.; Gerwick, W. H. Somocystinamide A, a Novel Cytotoxic Disulfide Dimer from a Fijian Marine Cyanobacterial Mixed Assemblage. *Org. Lett.* **2002**, *4,* 1095-1098.

163 Wrasidlo, W.; Mielgo, A.; Torres, V. A.; Barbero, S.; Stoletov, K.; Suyama, T. L.; Klemke, R. L.; Gerwick, W. H.; Carson, D. A.; Stupack, D. G. The marine lipopeptide somocystinamide A triggers apoptosis via caspase 8. *Proc. Natl. Acad. Sci.* **2008**, *105*, 2313-2318.

164 Williams, R. M.; Cox, R. J. Paraherquamides, brevianamides, and asperparalines: laboratory synthesis and biosynthesis. an interim report. *Acc. Chem. Res.* **2003**, *36*, 127-139.

165 Williams, R. M. Total synthesis and biosynthesis of the paraherquamides: an intriguing story of the biological Diels-Alder construction. *Chem. Pharm. Bull.* **2002**, *50*, 711-740.

166 Sanz-Cervera, J. F.; Glinka, T.; Williams, R. M. Biosynthesis of brevianamides A and B: in search of the biosynthetic diels-alder construction. *Tetrahedron*, **1993**, *49*, 8471-8482.

167 Williams, R. M.; Kwast, E. Carbanion-mediated Oxidative Deprotection of Non-enolizable Benzylated Amides. *Tetrahedron Lett.* **1989**, *30*, 451-454.

168 For example, see Paul G. Bulger,a Sharan K. Bagalb and Rodolfo Marquez, Recent advances in biomimetic natural product synthesis, *Nat. Prod. Rep.*, 2008, 25, 254–297 .

169 Miyake, F. Y.; Yakushijin, K.; Horne, D. A. Biomimetic synthesis of grossularines-1. *Angew. Chem. Int. Ed.* **2005**, *44*, 3280 –3282 .

170 Lei, X.; Johnson, R. P.; Porco Jr., J. A. Total Synthesis of the Ubiquitin-Activating Enzyme Inhibitor (+)-Panepophenanthrin. *Angew. Chem. Int. Ed.* **2003**, *42*, 3913-3917.

171 Moses, J. E.; Commeiras, L.; Baldwin, J. E.; Adlington, R. M. Total Synthesis of Panepophenanthrin. *Org. Lett.* **2003**, *5*, 2987–2988.

172 Proteau, P. J.; Gerwick, W. H.; Garcia-Pichel, F.; Castenholz, R. The structure of scytonemin, an ultraviolet sunscreen pigment from the sheaths of cyanobacteria . *Experientia* **1993**, *49*, 825-829.

173 See Chapter VII of this dissertation

Chapter II

Ichthyotoxic brominated diphenyl ethers from a mixed assemblage of a red alga and cyanobacterium: structure clarification and biological properties

Abstract

Primary fractions from the extract of a tropical red alga mixed with filamentous cyanobacteria, collected from Papua New Guinea, were active in a neurotoxicity assay. Bioassay guided isolation led to two natural products (**1**, **2**) with relatively potent calcium ion influx properties. The more prevalent of the neurotoxic compounds (**1**) was characterized by extensive NMR, mass spectrometry, and X-ray crystallography, and shown to be identical to a polybrominated diphenyl ether metabolite present in the literature, but reported with different NMR properties. To clarify this anomalous result, we synthesized a candidate isomeric polybrominated diphenyl ether (**3)**, but this clearly had different NMR shifts than the reported compound. We conclude that the original isolate of 3,4,5-tribromo-2-(2,4-dibromophenoxy)phenol was contaminated with a minor compound, giving rise to the observed anomalous NMR shifts. The second and more minor natural product (**2**) isolated in this study was a more highly brominated species. All three compounds showed a low micromolar ability to increase intracellular calcium ion concentrations in mouse neocortical neurons as well as toxicity to zebrafish. Because polybrominated diphenyl ethers have both natural as well as anthropomorphic origins, and accumulate in marine organisms at higher trophic level (mammals, fish, birds), these neurotoxic properties are of environmental significance and concern.

II.1 Introduction

Polybrominated diphenyl ethers (PBDEs) have recently attracted considerable attention due to an increasing awareness that these compounds accumulate in higher trophic level animals, including sperm whales,[1,2] sea gulls,[3] seals,[2] polar bears,[4] as well as in humans.[5,6] Some PBDEs are industrially produced in large quantities for use as flame retardants, and therefore their presence in animals has generally been assumed to be of anthropogenic origin.[7] Hydroxylated congeners of PBDEs (OH-PBDEs) have also been found in many of these same higher animals,[3,4,8] and recent studies have shown that the OH-PBDEs found in large marine-associated animals may be of mixed origins with some deriving from natural sources and the others being derivatives of anthropogenic PBDEs. Moreover, a variety of anthropogenic PBDEs have been shown to undergo hydroxylation in rats via oxidative metabolism, thereby producing OH-PBDE congeners.[9,10] Nevertheless, a number of OH-PBDEs are known to be natural products of various marine organisms, such as sponges, tunicates, and cyanobacteria.[11,12,13] Environmental concerns have been raised over the occurrence of PBDEs in higher animals because PBDEs have been linked to endocrine disruption.[2,14] Activities similar to those of chlorinated aromatic compounds have been observed with PBDEs, such as aryl hydrocarbon-receptor agonist and antagonist activities, thyroid toxicity, and effects on the immune system.[15] Neonatal exposure to PBDEs has been shown to cause neurotoxicity in adult animals.[14] OH-PBDEs have also been shown to disrupt thyroid hormone homeostasis presumably due to their structural similarity to the thyroxin-type endogenous thyroid hormones.[4] Recently, BDE-47 and 6-OH-BDE-47 have been shown to trigger an increase in cytosolic Ca^{2+} concentration as well as exocytosis of catecholamines in

neuronal cells within a few minutes.[16,17] These findings indicate that PBDEs and OH-PBDEs have the potential to acutely disrupt normal neuronal communication in animals.

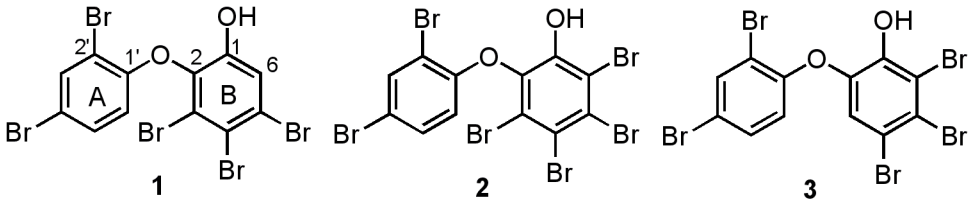

Figure II.1: OH-PBDE congeners isolated from the red alga/cyanobacteria assembly (**1** and **2**) and an alternative regioisomer of **1** (**3**).

Our program has been systematically screening marine algae and cyanobacteria for secondary metabolites with neuropharmacological properties, partially because of the environmental impacts these substances may impose, and partially to detect agents with potentially useful biomedical properties.[18,19,20,21] Because a variety of cellular events can trigger an increase in cytosolic Ca^{2+} levels in neuronal cells, we have employed a FLIPR-based fluorescence assay which detects Ca^{2+} modulation in mouse neocortical neurons. Herein, we describe the assay-guided isolation, structural determination and neurotoxicological evaluation of two OH-PBDE congeners (**1** and **2**, Figure II.1) from a mixed assemblage of marine cyanobacteria and a red alga. In the course of this work, we have also corrected the assignment of a ^{13}C NMR signal for **1** in the literature which could be a source of confusion in future efforts with OH-PBDE congeners.

II.2 Materials and Methods

II.2.1 Reagents and algal material

All solvents used were of HPLC grade from EMD and were used without purification. TLC grade silica gel from Sigma-Aldrich was used for vacuum liquid chromatography (VLC). Flash chromatography was performed using EMD silica gel (230-400 mesh). Trypsin, penicillin, streptomycin, heat-inactivated fetal bovine serum, horse serum and soybean trypsin inhibitor were obtained from Atlanta Biologicals. Minimum essential medium, deoxyribonuclease (DNase), poly-L-lysine, cytosine arabinoside, veratridine, aconitine, and deltamethrin were from Sigma-Aldrich. The fluorescent dye Fluo-3, and pluronic acid F-127 were obtained from Invitrogen Corporation.

Algal material was collected at Grabo reef in Papua New Guinea at 12-18 m depth by SCUBA. The algae was identified in the field as *Vidalia sp.*, but subsequent microscopic examination of the voucher sample identified it to likely be *Leptofaucia sp.* Additionally, a small abundance of cyanobacterial filaments similar to *Oscillatoria* were observed in the sample by light microscopy.

II.2.2 Bioassay-guided isolation of OH-PBDEs

A total of 2 L of the red algal and cyanobacterial assemblage (dry weight 128 g) was extracted with CH_2Cl_2 / MeOH (2:1). Upon removal of the solvents *in vacuo*, a portion (4.0 g) of the crude extract (4.6 g) was fractionated into nine fractions using silica gel vacuum liquid chromatography (hexanes to EtOAc to MeOH), one of which (308 mg, eluted with 2:3 EtOAc/hexanes) possessed Ca^{2+} modulating activity in mouse neocortical neurons. A portion (306 mg) of the active fraction was further fractionated by flash column chromatography[22] on silica gel (hexanes/Et_2O 1:9 to 1:8) to obtain seven sub-

fractions, of which two (2 mg and 77 mg) were associated with Ca^{2+} modulation activity. The larger sub-fraction was further purified by HPLC using a Jupiter 10µ C18 300A column (250 x 10 mm) with a gradient solvent system (2.5 mL/min, 3:2 MeCN/H_2O to 4:1 over 30 min, then to MeCN over 10 min) to obtain 15 mg (0.38% of extract) of compound **1** (R_t = 52 min) and ~0.5 mg (0.01% of extract) of compound **2** (R_t = 55 min), both of which were confirmed to have Ca^{2+} modulating activity.

II.2.3 Neocortical neuron cultures

Primary cultures of neocortical neurons were obtained from embryonic day 16 Swiss-Webster mice. Briefly, pregnant mice were euthanized by CO_2 asphyxiation and their neocortices were collected. Isolated neocortices were then removed of their meninges, minced by trituration using a Pasteur pipette, and treated with trypsin for 25 minutes at 37ºC. The cells were then dissociated by two successive trituration and sedimentation steps in soybean trypsin inhibitor and DNase containing isolation buffer, centrifuged and resuspended in Eagle's minimal essential medium (MEM) supplemented with 2 mM L-glutamine, 10% fetal bovine serum, 10% horse serum, 100 IU/mL penicillin and 0.10 mg/mL streptomycin, pH 7.4. Cells were plated onto poly-L-lysine-coated 96-well clear-bottomed black-well plate at a density of 1.5 x 10^5 cells/well. Plates were incubated at 37ºC with 5% CO_2 and 95% humidity. To prevent proliferation of nonneuronal cells, cytosine arabinoside (10 µM) was added to the culture medium on day 2 after plating. The culture media was changed both on days 5, 8 and 11 using a serum-free growth medium containing Neurobasal Medium supplemented with B-27, 100 I.U./ mL penicillin, 0.10 mg/mL streptomycin, and 0.2 mM L-glutamine. Neocortical neurons

were used between 11-13 days *in vitro* (DIV) for Ca^{2+} influx assay. All animal use protocols were approved by the Institutional Animal Care and Use Committee (IACUC).

II.2.4 Ca^{2+} modulation assay

Neocortical neurons cultured in 96-well plate were removed their medium and replaced with dye loading buffer (100 µL/well) containing 4 µM Fluo-3 and 0.04% Pluronic F-127 in Lock's buffer (in mM: 8.6 Hepes, 5.6 KCl, 154 NaCl, 5.6 Glucose, 1.0 $MgCl_2$, 2.3 $CaCl_2$, 0.0001 glycine, pH 7.4). After 1 h incubation in dye loading buffer, cells were washed five times with Locke's buffer using automated cell washer (Bioteck instrument Inc., VT, USA) leaving a final volume of 150 µL in each well. The plate was then transferred to Fluorescence Laser Plate Reader (FLIPR) (Molecular Devices, Sunnyvale, CA, USA) chamber. Cells were excited by the 488-nm line of argon laser and Ca^{2+} bound fluo-3 emission in the 500–600 nm range was recorded with the charge coupled device (CCD) camera. Fluorescence readings were taken once every 9 s for 3 min to establish the baseline and then 50 µL of test compound containing solution (4x) was added to each well from the compound plate, yielding a final volume of 200 µL/well. The cells were exposed to the testing compounds for another 42 min.

II.2.5 Assay data analysis

Concentration-response relationships were generated by non-linear regression analysis using GraphPad software (Version 4.0; San Diego, CA).

II.2.6 Structure elucidation

All NMR data were collected in $CDCl_3$ using Varian Inova 300 MHz and 500 MHz instruments. ^{1}H and ^{13}C NMR signals were referenced to the solvent peaks at 7.26 ppm and 77.0 ppm, respectively. High resolution mass spectra were recorded on a Thermo-Finnigan MAT900XL spectrometer. A crystal was grown from a CH_2Cl_2 solution of **1** by diffusional exchange with hexanes for X-ray crystallographic analysis on a Bruker APEX CCD detector.

II.2.7 Ichthyotoxicity assay

Various quantities of the natural product **1** in 174 μL of EtOH was added to 50 mL Erlenmeyer flasks containing 40 mL of aquarium water. For controls, 174 μL of EtOH was added to the water. Both treatments and controls were run in duplicate. Adult male zebra fish of approximately 4 cm length were randomly selected from aquaria and individually placed in the Erlenmeyer flasks. Time of death was determined by observing a lack of gill movement and no visible responses to swirling of the flask for one full minute.

II.3 Results and Discussion

Fractions from the crude lipid extract of a Papua New Guinea mixed collection of a red marine alga, tentatively identified as *Leptofauchea* sp. and a marine cyanobacterium *Oscillatoria* sp., showed an ability to increase the intracellular concentration of Ca^{+2} in mouse neocortical neurons. Bioassay guided isolation of the active compounds sequentially used flash column chromatography and HPLC, and yielded one more prevalent (**1**) and one minor compound (**3**).

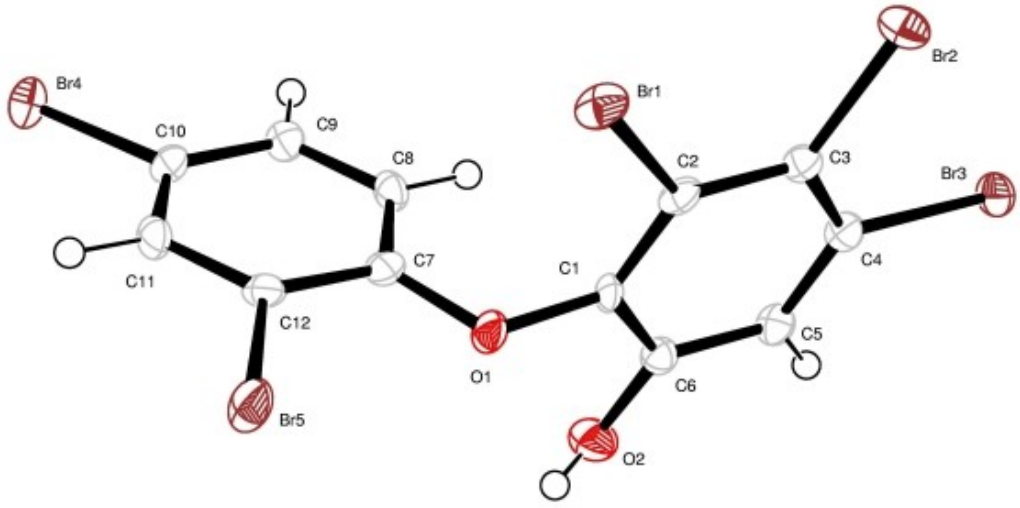

Figure II.2: X-ray crystal structure of **1**.

Analysis by ESI-LCMS (negative mode) revealed the polybrominated nature of compound **1** and indicated a molecular weight of 1160 (obs. [M^-] *m/z* 1159). Subsequent analysis by ^{13}C NMR showed 4 protonated and 8 quarternary ^{13}C signals, indicating that the compound was either a symmetric dimer having a molecular weight of 1160 or that it was a monomer with a molecular weight of 580 that easily dimerizes in the mass spectrometer. High resolution EIMS clarified that it was a monomer with an exact mass of *m/z* 575.6211, yielding a molecular formula of $C_{12}H_5O_2Br_5$ (calc. 575.6201). ^1H and ^{13}C NMR, COSY, HSQC, and HMBC data readily identified two benzenoid rings connected to one another by an ether linkage. By ^{13}C NMR chemical shifts and consideration of the molecular formula, one of the rings possessed 2 bromines while the other had 3 bromines and a hydroxyl group. Further analysis of the HMBC spectrum revealed the A ring to be a 2,4-dibromo-phenoxyl group. The regiochemical assignment of the B ring, however, could not be made confidently based on NMR data alone. Further, the ^{13}C NMR data for

Table II.1: Comparison of NMR data for two isolates of **1** and **3** ($CDCl_3$)

	1, ref 25		**1**, this study		**3**	
Position	^{13}C	^{1}H	^{13}C	^{1}H	^{13}C	^{1}H
1	148.9		148.9		144.5	
2	139.9		139.4		143.1	
3	**113.6**		**121.1**		120.7	7.00
4	119.3		119.2		114.9	
5	122.9		122.9		122.4	
6	120.8	7.42	120.7	7.44	121.6	
1'	151.8		151.6		151.3	
2'	112.8		112.7		115.6	
3'	136.4	7.79	136.2	7.79	136.5	7.81
4'	116.3		116.2		118.2	
5'	131.6	7.29	131.6	7.30	132.1	7.45
6'	115.8	6.41	115.7	6.41	121.5	6.89

1 did not match that reported for any known OH-PBDE. Because **1** deposited well-formed crystals from CH_2Cl_2/hexanes, an X-ray crystallographic analysis was conducted to give an excellent quality crystal structure (Figure II.2). Comparison of this structure with the literature for naturally occurring OH-PBDEs showed it to be identical to one previously reported from *Dysidea herbacea*.[25,23]

In comparing our ^{13}C NMR data to those reported in the literature for compound **1**, a significant discrepancy was noted in the chemical shift for C3 (Table II.1). Only the Bowden data are included in this table because the only other ^{13}C NMR data available were recorded in DMSO and not in $CDCl_3$,[24] but they were similar to our data. One hypothesis for this anomalous NMR data was that previous workers had mis-assigned structure **1** to their material, and that it was in fact the data for another structure. Of the 59 possible regioisomers of **1**, 50 could be eliminated based on the fact that the A ring of Bowden's isolation of **1** had three protons and the HMBC and COSY correlations were sufficient to confidently assign this sub-structure. Of the remaining 9 structural possibilities, two could be disregarded based on HMBC correlations observed by Bowden. Specifically, the lone proton on the B ring showed HMBC correlations to 4 carbons,[25] and thus, the only carbon for which there was not an HMBC correlation should be *para* to the carbon bearing this proton. Based on the predicted chemical shifts of the oxygen bearing carbons, six other isomers could be disregarded, leaving only a single regioisomer that required consideration (**3**). Regioisomer **3** is also a known naturally occurring compound having also been isolated from the marine sponge *Dysidea herbacea*.[11]

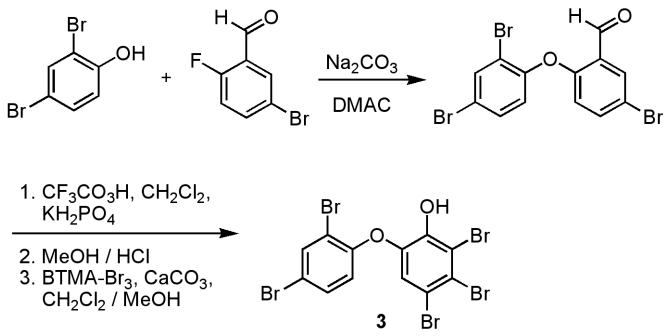

Scheme II.1: Synthesis of **3** by Marsh's route.

Because the ^{13}C NMR data for **3** in $CDCl_3$ has not been published,[11] this compound was synthesized by Marsh's route (Scheme II.1).[26] However, comparison of the ^{13}C NMR shifts of synthetic **3** with those reported by Bowden revealed that they were considerably different (Table II.1). Subsequently, a close inspection of the ^{13}C NMR spectrum from the Bowden material revealed a small peak at 121.1 ppm (B. F. Bowden, personal communication), which corresponds well with our data for C-3 in compound **1**. Because C-3 is *para* to the only protonated carbon in ring B, this ^{13}C atom is predicted to relax slowly such that its detection may require longer delay times.[27] Moreover, during our purification of **1**-**3**, it was difficult to remove minor contaminants that had similar NMR signatures to these OH-PBDEs. In this regard, it is possible that the 113.6 ppm signal reported for C3 by Bowden et al. was actually the quickly relaxing (e.g. protonated) resonance of a minor contaminant in the sample.

Having unequivocally established the structure of **1**, a minor compound was also characterized that eluted very closely to **1** by RP-HPLC and showed Ca^{2+} modulating activity. A molecular formula of $C_{12}H_4O_2Br_6$ was determined for compound **2** based on low resolution negative ion ESI-LCMS (obs. $[M-H]^-$ *m/z* 658.74). The isotopic pattern

observed for the molecular ion was consistent with the presence of 6 bromine atoms. Although NMR characterization of this compound was challenging due to the small quantity isolated (~0.5 mg) and the presence of chromatographically similar impurities, ^{1}H NMR and ^{1}H-^{1}H COSY analysis revealed a three proton spin system consisting of a vicinally coupled pair (7.29 ppm and 6.39 ppm) and a third (7.79 ppm) which was *meta* coupled to δ 7.29. These shifts and coupling pattern matched those reported for synthetic **2** and thus, this material was identified as 3,4,5,6-tetrabromo-2-(2',4'-dibromo-phenoxy)-phenol (**2**).

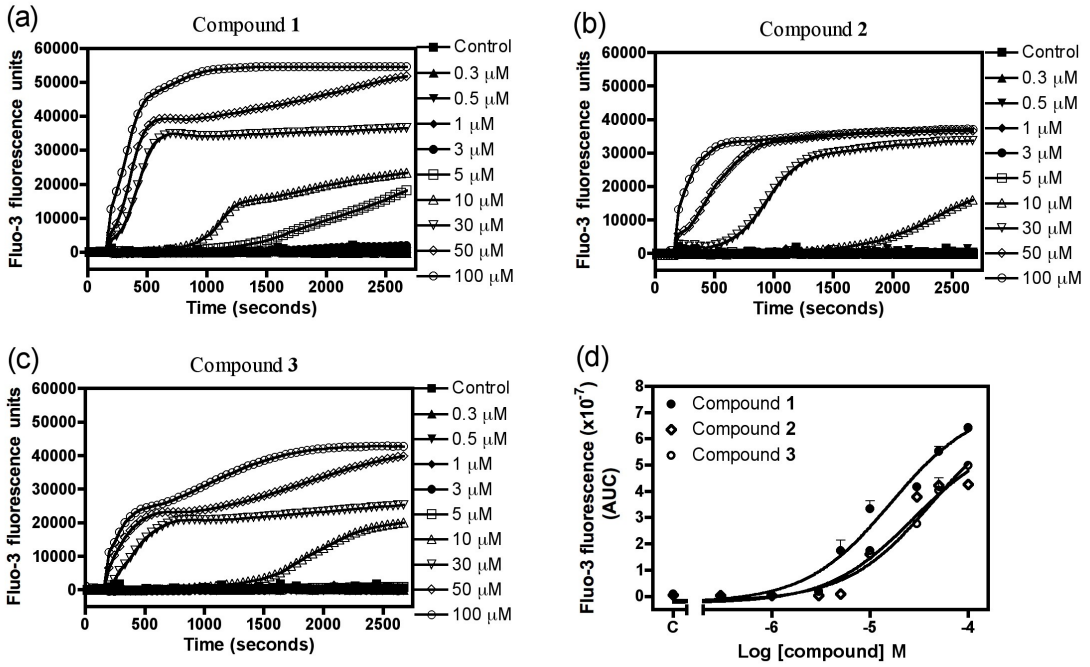

Figure II.3: Ca^{2+} modulation assay in mouse neocortical neurons for compounds **1**-**3**.

Compounds **1**-**3** were tested in the Ca^{2+} modulation assay in mouse neocortical neurons at various concentrations and their EC_{50} values were determined to be 16.4 μM

(9.8 μM- 27.2 μM, 95% Confidence Intervals), 27.2 μM (12.3 μM- 59.8 μM, 95% Confidence Intervals) and 42.4 μM (23.2 μM- 77.5 μM, 95% Confidence Intervals), respectively (Figure II.3). In light of the finding that **1** may act as an environmental neurotoxin,[16] its toxicity to zebrafish was also evaluated. At 5 μg/mL (8.6 μM) media concentration, the fish immediately attempted to escape out of the container and its apparent rate of respiration visibly increased; such behaviors were not observed for the control group. Within 5 minutes, the treated fish appeared to have difficulty maintaining their proper orientation, and within 20 minutes, both died. Similar effects were seen at 1 μg/mL (1.7 μM), but it took 50 min for the fish to expire. At 0.5 μg/mL (0.86 μM), the fish appeared to be unaffected for the duration of the 3 hour assay. Regioisomer **3** had the same effect but was less potent (8.6 μM, death at 25 min; no effect at 1.7 μM), suggesting that many congeners of OH-PBDEs may display ichthyotoxicity.

Both the long term and the short term neurotoxic effects of polychlorinated biphenyls (PCBs) have been studied extensively. Notably, PCBs disrupt the intracellular Ca^{2+} homeostasis, which is critical for a variety of cell functions, including release of neurotransmitters.[14] As for the longer term effects, PCBs can modulate muscarinic and nicotinic receptors and also disrupt neurological development.[14] Similarly, PBDEs have been shown to have detrimental effects to learning and memory functions in mice. These behavioral effects are likely related to the observation that PBDEs reduced the densities of nicotinic receptors in the hippocampus of mice.[28] Given the ability of **1**, **2**, and **3** to alter cytoplasmic concentrations of Ca^{+2} ions, the observed ichthyotoxicity of **1** and **2** may involve calcium ion induced neurotoxicity.

These findings are significant in light of recent reports that OH-PBDEs have wide-spread occurrence in the marine environment.[3,4,8] In *Disdea herbacea*, at least 1~6% of the dry weight of the organism is composed of OH-PBDEs and visible crystals of these compounds have been observed in the sponge tissue.[13] In addition to sponges, tunicates, and blue-green algae, we report here that a red alga and/or cyanobacterium living in association with the red alga as a source of OH-PBDEs.[29] Since most of the world's seaweeds are red algae[30] and many invertebrates feed on these algae, the presence of OH-PBDEs in marine invertebrates may actually reflect the natural occurrence and bioaccumulation of these compounds into higher trophic levels. Among PBDEs, pentabrominated congeners are known to be environmentally more mobile due to their greater water solubility, volatility, K_{ow} (octanol/water partition coefficient), and lipophilicity.[7] OH-PBDEs are expected to be reasonably lipophilic and yet more water soluble than PBDEs. Therefore, they may be even more prone to bioaccumulation due to their increased mobility in the environment.

The possibility raised by these findings is that many OH-PBDEs are of natural occurrence yet possess neurotoxic properties of environmental significance. In this regard, it is possible that human populations have been exposed to these materials through seafood consumption for a lengthy period and that this exposure may have had historical as well as current health implications. PCBs and brominated flame retardants other than PBDEs are suspected to be responsible for abnormal behavior phenomena such as the 'beaching of cetaceans.'[31,32] Because of their structurally related nature, it is possible that OH-PBDEs of natural or anthropogenic origins may contribute to such events. Thus, it is important to both characterize the origin and occurrence of OH-PBDEs

as well as details of their molecular neurotoxicology.

Acknowledgment

The text of II, in whole, has been submitted for publication to Toxicon at the time of writing. The dissertation author was the primary author and directed and carried out the research, which forms the basis for this chapter.

X-ray crystallographic analysis by A. Rhinegold and A. DiPasquale at UCSD is acknowledged. We thank L. Tan and D. Sherman for help with collection of the algal material, B. F. Bowden for providing copies of their ^{13}C NMR spectra of **1**, and L. Gerwick for providing zebrafish. We further thank the government of Papua New Guinea for scientific collection permits and funding from NIH Grant 053398 is acknowledged.

Appendix

Table of Contents of Appendix

1.Photographs of The Red Algal Voucher Sample

2.X-ray Crystallographic Analysis

3.Isolation Scheme for **1** and **2**

4.^{1}H NMR Spectrum of **1** in $CDCl_3$

5.^{13}C NMR Spectrum of **1** in $CDCl_3$

6.^{1}H-^{1}H COSY Spectrum of **1** in $CDCl_3$

7.^{1}H-^{13}C HSQC Spectrum of **1** in $CDCl_3$

8.^{1}H-^{13}C HMBC Spectrum of **1** in $CDCl_3$

9.^{1}H NMR Spectrum of **3** in $CDCl_3$

10.^{13}C NMR Spectrum of **3** in $CDCl_3$

11.^{1}H-^{1}H COSY Spectrum of **3** in $CDCl_3$

12.^{1}H-^{13}C HSQC Spectrum of **3**

13.^{1}H-^{13}C HMBC Spectrum of **3** in $CDCl_3$

14.^{1}H NMR Spectrum of **2** in $CDCl_3$

15.^{1}H-^{1}H COSY Spectrum of **2** in $CDCl_3$

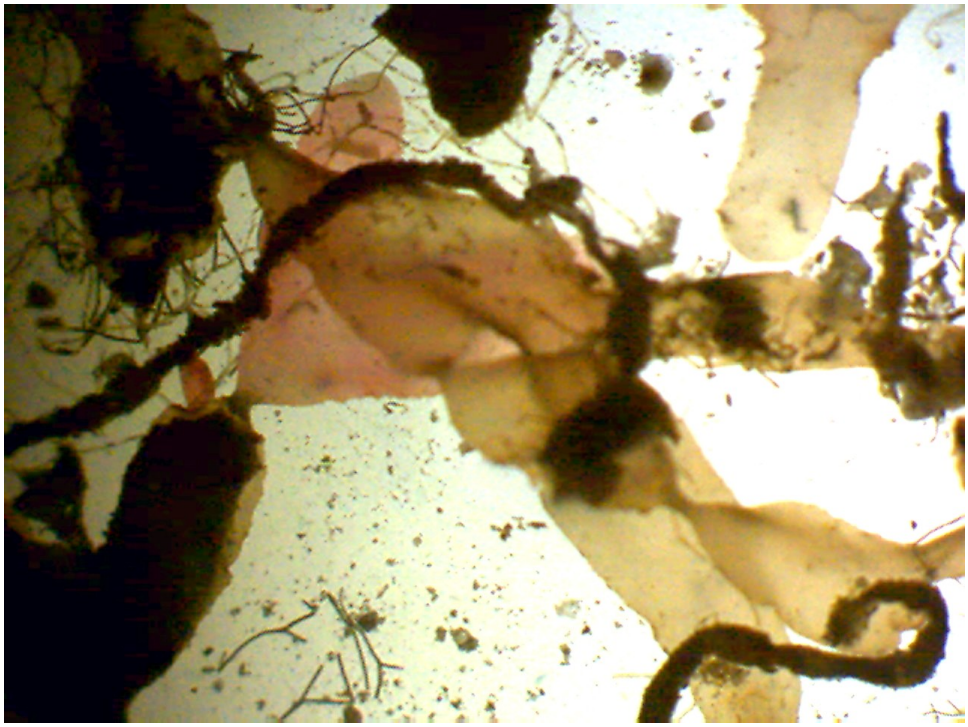

Figure II.4: Photographs of the red algal voucher sample

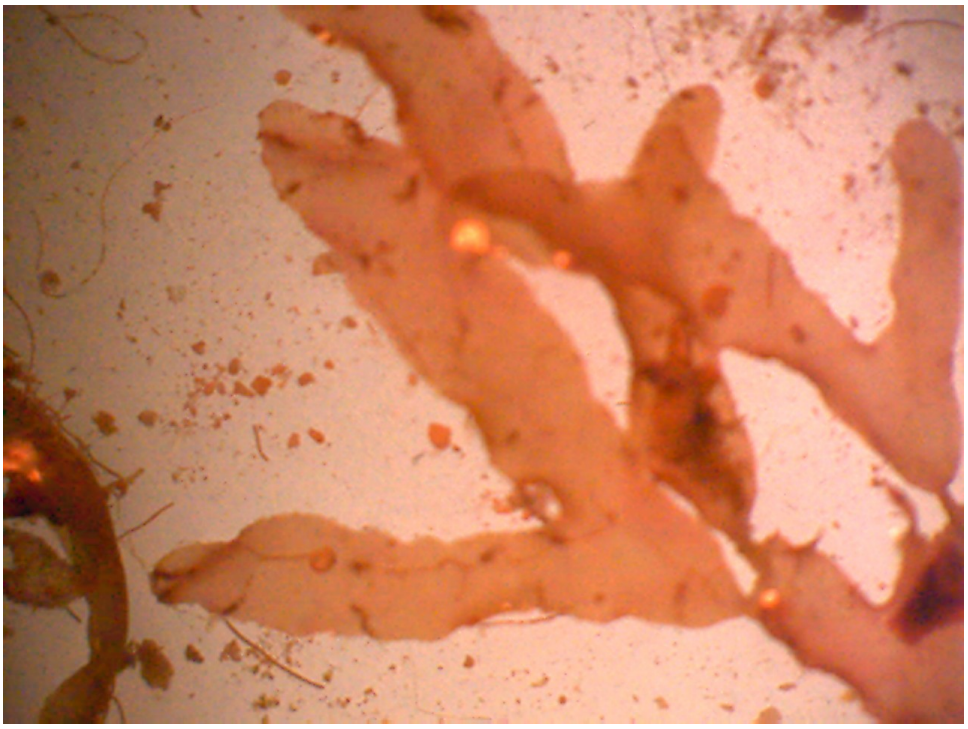

Figure II.5: Photograph of the red algal voucher sample

X-ray Crystallographic Analysis

A colorless block 0.12 x 0.08 x 0.08 mm in size was mounted on a Cryoloop with Paratone oil. Data were collected in a nitrogen gas stream at 100(2) K using phi and omega scans. Crystal-to-detector distance was 60 mm and exposure time was 5 seconds per frame using a scan width of 0.5°. Data collection was 98.7% complete to 67.00° in θ. A total of 8115 reflections were collected covering the indices, -9<=*h*<=9, -10<=*k*<=10, -25<=*l*<=24. 2597 reflections were found to be symmetry independent, with an R_{int} of 0.0280. Indexing and unit cell refinement indicated a primitive, monoclinic lattice. The space group was found to be P2(1)/c (No. 14). The data were integrated using the Bruker SAINT software program and scaled using the SADABS software program. Solution by direct methods (SIR-2004) produced a complete heavy-atom phasing model consistent with the proposed structure. All non-hydrogen atoms were refined anisotropically by full-matrix least-squares (SHELXL-97). All hydrogen atoms were placed using a riding model. Their positions were constrained relative to their parent atom using the appropriate HFIX command in SHELXL-97.

Table II.2: Crystal data and structure refinement for **1**.

X-ray ID	gerw02	
Sample/notebook ID	1572D2C	
Empirical formula	C12 H5 Br5 O2	
Formula weight	580.71	
Temperature	100(2) K	
Wavelength	1.54178 Å	
Crystal system	Monoclinic	
Space group	P2(1)/c	
Unit cell dimensions	a = 7.7959(5) Å	▪ = 90°.
	b = 8.8184(5) Å	▪ = 92.671(2)°.
	c = 21.0376(12) Å	▪ = 90°.
Volume	1444.71(15) $Å^3$	
Z	4	
Density (calculated)	2.670 Mg/m^3	
Absorption coefficient	16.803 mm^{-1}	
F(000)	1072	
Crystal size	0.12 x 0.08 x 0.08 mm^3	
Crystal color/habit	colorless block	
Theta range for data collection	4.21 to 68.08°.	
Index ranges	-9<=h<=9, -10<=k<=10, -25<=l<=24	
Reflections collected	8115	
Independent reflections	2597 [R(int) = 0.0280]	
Completeness to theta = 67.00°	98.7 %	
Absorption correction	Analytical	
Max. and min. transmission	0.3467 and 0.2377	
Refinement method	Full-matrix least-squares on F^2	
Data / restraints / parameters	2597 / 0 / 174	
Goodness-of-fit on F^2	1.159	
Final R indices [I>2sigma(I)]	R1 = 0.0391, wR2 = 0.1018	
R indices (all data)	R1 = 0.0394, wR2 = 0.1021	
Extinction coefficient	0.00126(9)	
Largest diff. peak and hole	1.337 and -1.007 $e.Å^{-3}$	

Table II.3: Atomic coordinates (x 10^4) and equivalent isotropic displacement parameters ($Å^2$x 10^3) for **1**. U(eq) is defined as one third of the trace of the orthogonalized U^{ij} tensor.

	x	y	z	U(eq)
C(1)	1442(6)	2778(6)	4601(2)	17(1)
C(2)	1873(6)	4251(6)	4435(2)	18(1)
C(3)	2477(6)	5284(6)	4901(2)	17(1)
C(4)	2615(6)	4782(6)	5531(2)	18(1)
C(5)	2167(7)	3329(6)	5701(2)	19(1)
C(6)	1584(6)	2306(6)	5237(2)	18(1)
C(7)	1886(7)	904(6)	3823(2)	19(1)
C(8)	3595(7)	721(6)	3994(2)	19(1)
C(9)	4599(7)	-253(6)	3651(2)	19(1)
C(10)	3873(7)	-1037(6)	3133(2)	21(1)
C(11)	2171(7)	-826(6)	2941(2)	21(1)
C(12)	1183(6)	146(6)	3285(2)	19(1)
O(1)	756(4)	1782(4)	4149(2)	21(1)
O(2)	1203(5)	875(4)	5391(2)	30(1)
Br(1)	1606(1)	4788(1)	3572(1)	23(1)
Br(2)	3061(1)	7263(1)	4676(1)	23(1)
Br(3)	3451(1)	6077(1)	6189(1)	22(1)
Br(4)	5202(1)	-2438(1)	2681(1)	24(1)
Br(5)	-1156(1)	448(1)	3038(1)	31(1)

Table II.4: Bond lengths [Å] and angles [°] for **1**.

C(1)-O(1)	1.383(6)	C(7)-O(1)	1.378(6)
C(1)-C(2)	1.389(7)	C(7)-C(12)	1.405(7)
C(1)-C(6)	1.401(7)	C(8)-C(9)	1.387(8)
C(2)-C(3)	1.403(7)	C(8)-H(8)	0.9500
C(2)-Br(1)	1.879(5)	C(9)-C(10)	1.388(7)
C(3)-C(4)	1.397(7)	C(9)-H(9)	0.9500
C(3)-Br(2)	1.870(5)	C(10)-C(11)	1.382(8)
C(4)-C(5)	1.380(7)	C(10)-Br(4)	1.896(5)
C(4)-Br(3)	1.888(5)	C(11)-C(12)	1.380(8)
C(5)-C(6)	1.390(7)	C(11)-H(11)	0.9500
C(5)-H(5)	0.9500	C(12)-Br(5)	1.891(5)
C(6)-O(2)	1.340(6)	O(2)-H(2)	0.8400
C(7)-C(8)	1.373(8)		
O(1)-C(1)-C(2)	120.8(5)	C(8)-C(7)-C(12)	119.5(5)
O(1)-C(1)-C(6)	118.6(4)	O(1)-C(7)-C(12)	115.7(5)
C(2)-C(1)-C(6)	120.5(5)	C(7)-C(8)-C(9)	120.1(5)
C(1)-C(2)-C(3)	120.6(5)	C(7)-C(8)-H(8)	119.9
C(1)-C(2)-Br(1)	117.4(4)	C(9)-C(8)-H(8)	119.9
C(3)-C(2)-Br(1)	122.0(4)	C(10)-C(9)-C(8)	119.8(5)
C(4)-C(3)-C(2)	117.7(5)	C(10)-C(9)-H(9)	120.1
C(4)-C(3)-Br(2)	121.8(4)	C(8)-C(9)-H(9)	120.1
C(2)-C(3)-Br(2)	120.5(4)	C(11)-C(10)-C(9)	120.9(5)
C(5)-C(4)-C(3)	122.1(5)	C(11)-C(10)-Br(4)	118.7(4)
C(5)-C(4)-Br(3)	117.0(4)	C(9)-C(10)-Br(4)	120.4(4)
C(3)-C(4)-Br(3)	120.9(4)	C(12)-C(11)-C(10)	118.8(5)
C(4)-C(5)-C(6)	119.9(5)	C(12)-C(11)-H(11)	120.6
C(4)-C(5)-H(5)	120.0	C(10)-C(11)-H(11)	120.6
C(6)-C(5)-H(5)	120.0	C(11)-C(12)-C(7)	120.8(5)
O(2)-C(6)-C(5)	120.7(5)	C(11)-C(12)-Br(5)	119.9(4)
O(2)-C(6)-C(1)	120.2(5)	C(7)-C(12)-Br(5)	119.3(4)
C(5)-C(6)-C(1)	119.1(5)	C(7)-O(1)-C(1)	117.5(4)
C(8)-C(7)-O(1)	124.9(5)	C(6)-O(2)-H(2)	109.5

Table II.5: Anisotropic displacement parameters ($Å^2 x\ 10^3$)for **1**. The anisotropic displacement factor exponent takes the form: $-2 \pi^2 [h^2 a^{*2} U^{11} + ... + 2 h k a^* b^* U^{12}]$

	U^{11}	U^{22}	U^{33}	U^{23}	U^{13}	U^{12}
C(1)	16(2)	20(2)	14(2)	-8(2)	1(2)	-3(2)
C(2)	17(2)	26(3)	10(2)	1(2)	2(2)	0(2)
C(3)	16(2)	19(2)	15(2)	0(2)	1(2)	0(2)
C(4)	15(2)	24(2)	15(2)	-3(2)	-2(2)	-1(2)
C(5)	23(2)	22(3)	12(2)	1(2)	0(2)	1(2)
C(6)	16(2)	19(2)	18(3)	-1(2)	2(2)	1(2)
C(7)	23(2)	22(2)	12(2)	1(2)	4(2)	-5(2)
C(8)	25(3)	18(2)	13(2)	-1(2)	-2(2)	-5(2)
C(9)	23(2)	20(2)	14(2)	2(2)	-2(2)	0(2)
C(10)	27(3)	23(3)	13(2)	0(2)	5(2)	-3(2)
C(11)	30(3)	21(2)	12(2)	-2(2)	0(2)	-5(2)
C(12)	17(2)	29(3)	12(2)	1(2)	0(2)	-9(2)
O(1)	17(2)	30(2)	16(2)	-10(2)	1(1)	-4(2)
O(2)	31(2)	22(2)	37(2)	2(2)	7(2)	-4(2)
Br(1)	22(1)	34(1)	12(1)	4(1)	-1(1)	-2(1)
Br(2)	24(1)	20(1)	25(1)	5(1)	-1(1)	-4(1)
Br(3)	25(1)	24(1)	17(1)	-6(1)	-2(1)	-5(1)
Br(4)	28(1)	26(1)	18(1)	-4(1)	-1(1)	6(1)
Br(5)	16(1)	53(1)	23(1)	-18(1)	-1(1)	-3(1)

Table II.6: Hydrogen coordinates (x 10^4) and isotropic displacement parameters ($Å^2$x 10^3) for **1**.

	x	y	z	U(eq)
H(5)	2255	3028	6135	23
H(8)	4090	1261	4347	23
H(9)	5781	-384	3770	23
H(11)	1689	-1341	2578	25
H(2)	320	595	5179	45

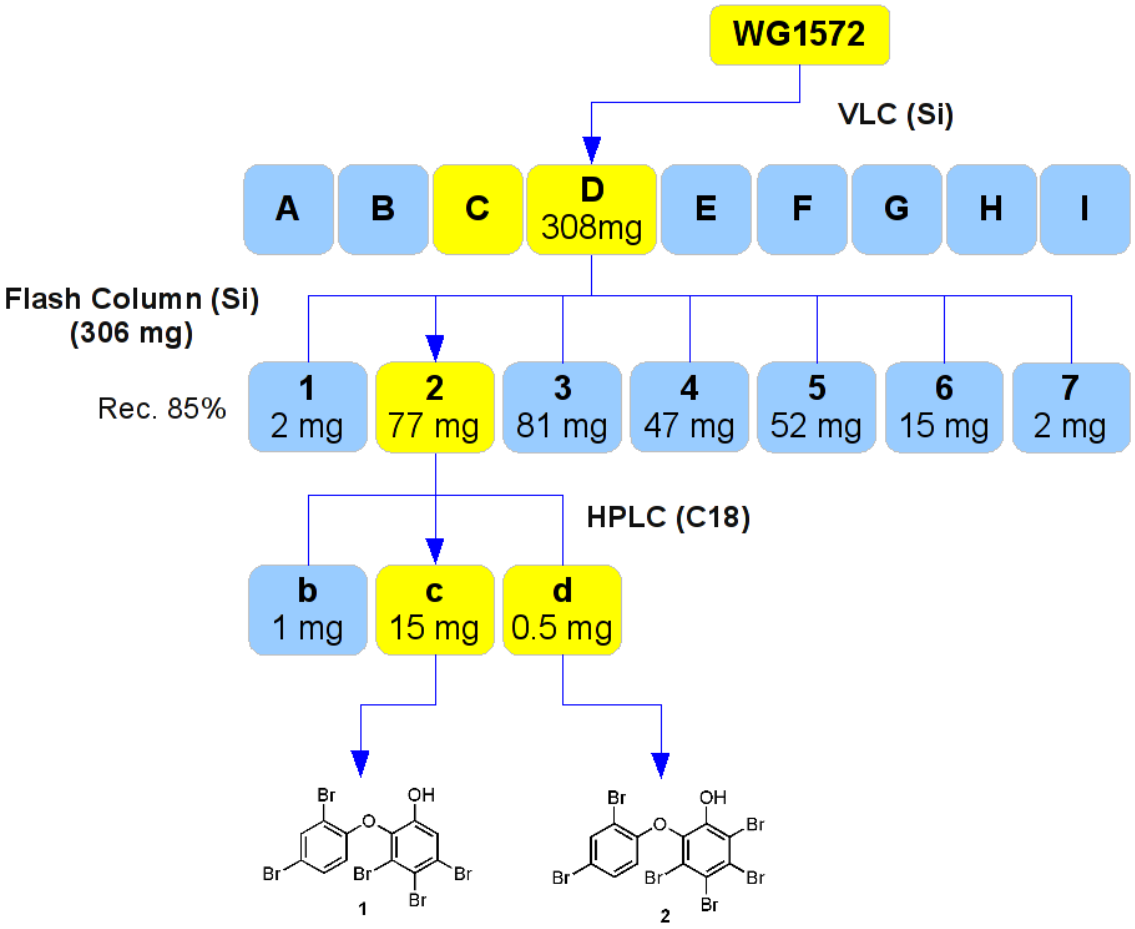

Figure II.6: Isolation scheme for **1** and **3**

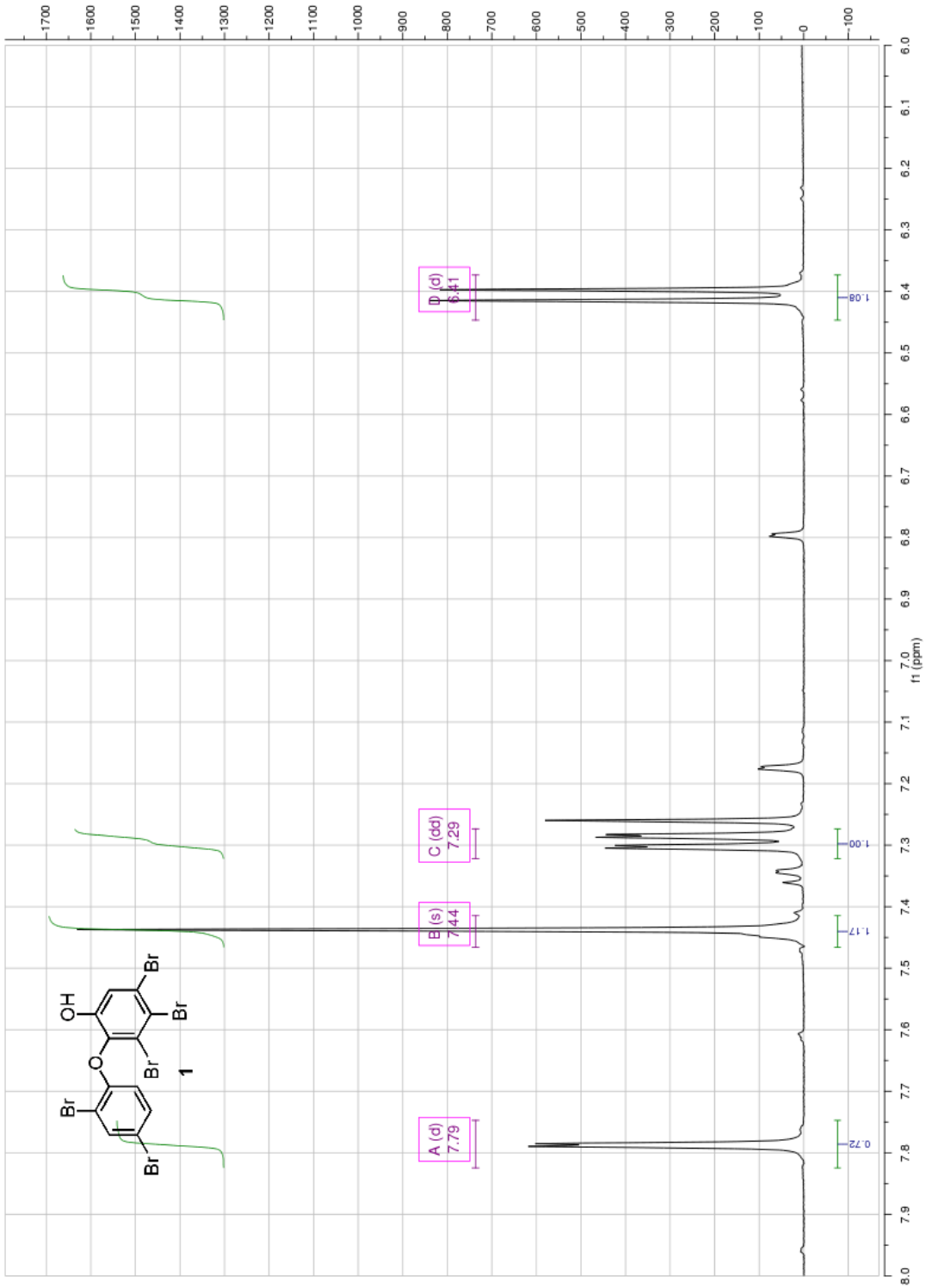

Figure II.7: ^{1}H NMR Spectrum of **1** in $CDCl_3$

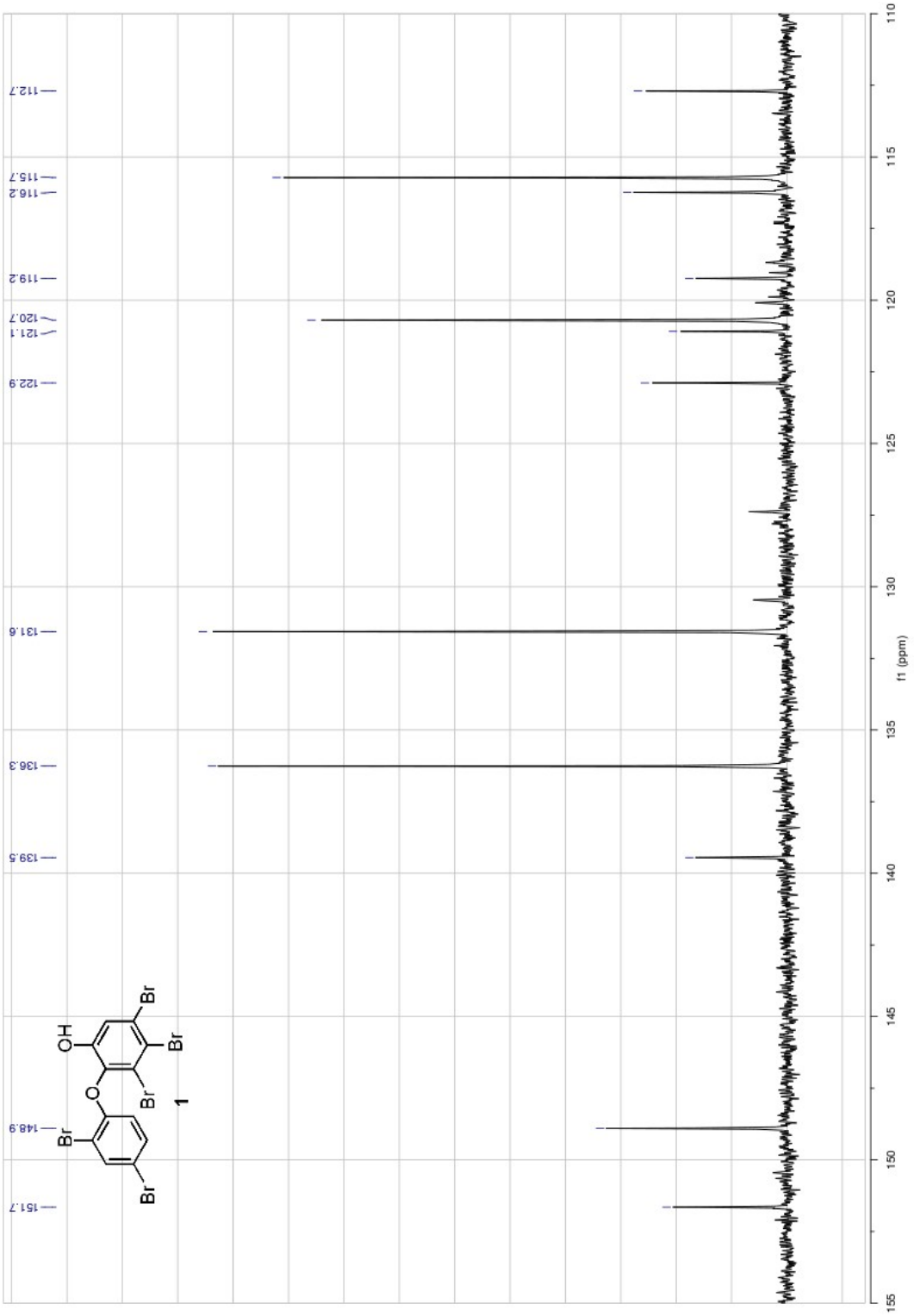

Figure II.8: ^{13}C NMR Spectrum of **1** in $CDCl_3$

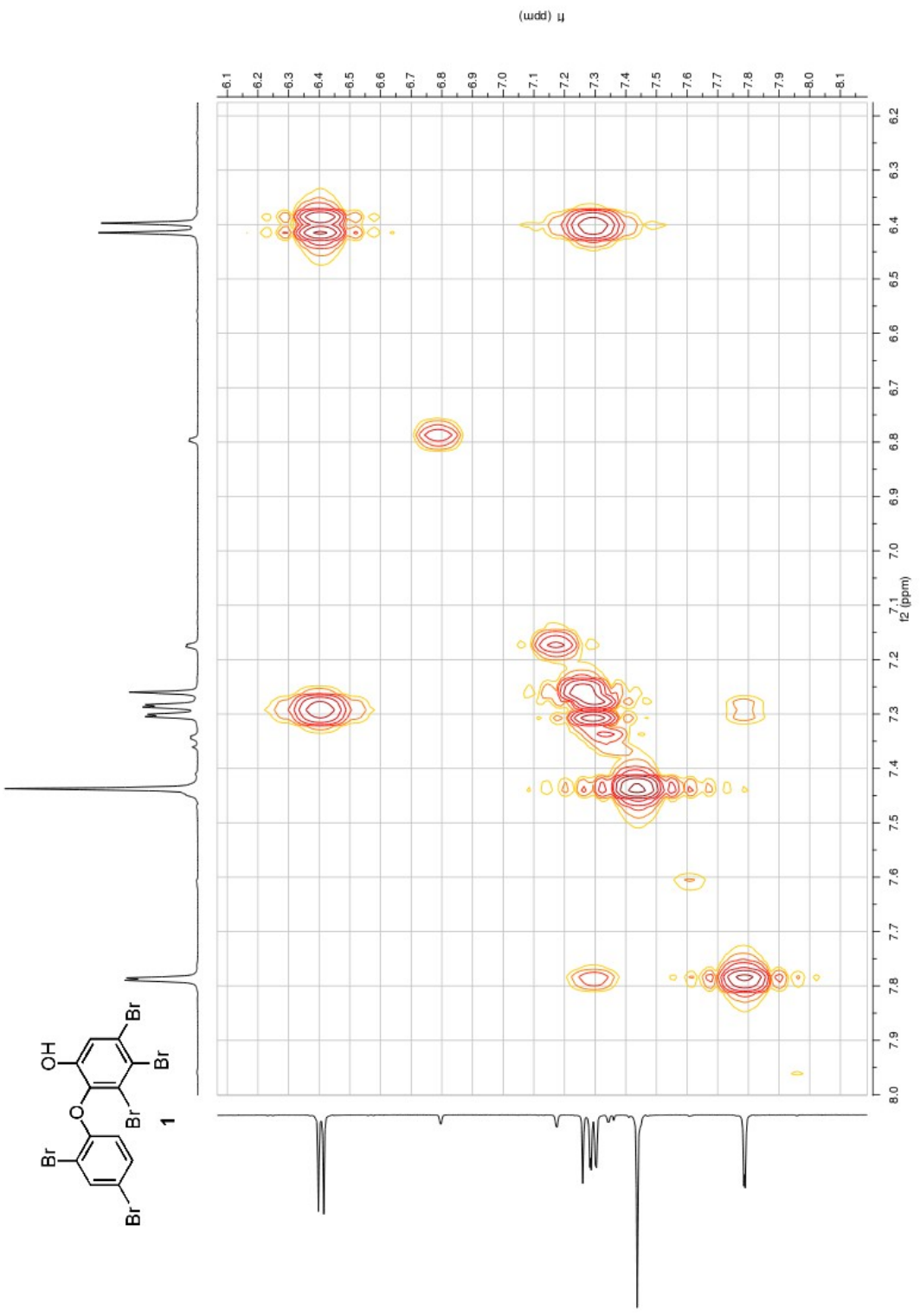

Figure II.9: ^{1}H-^{1}H COSY Spectrum of **1** in $CDCl_3$

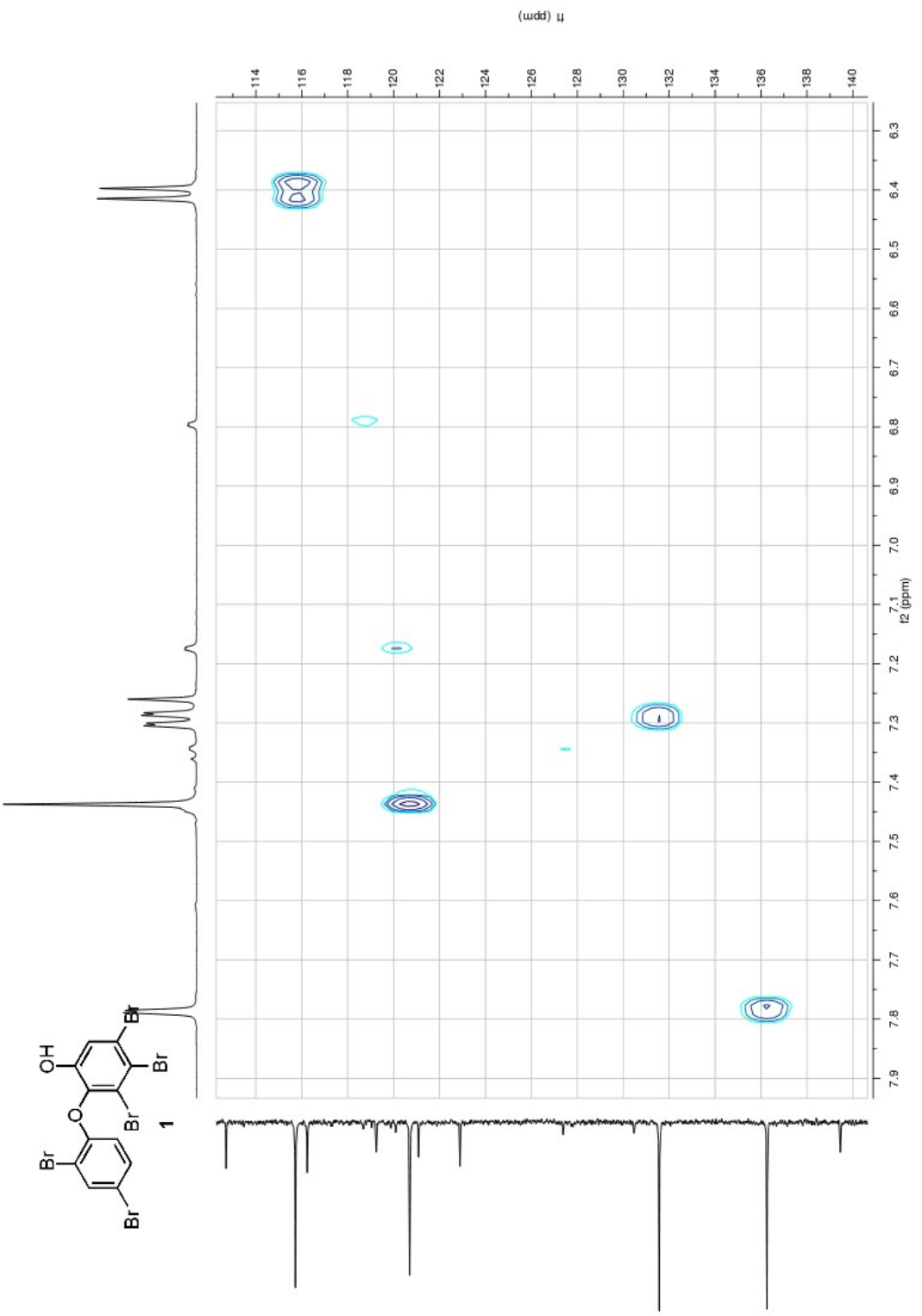

Figure II.10: ^{1}H-^{13}C HSQC Spectrum of **1** in $CDCl_3$

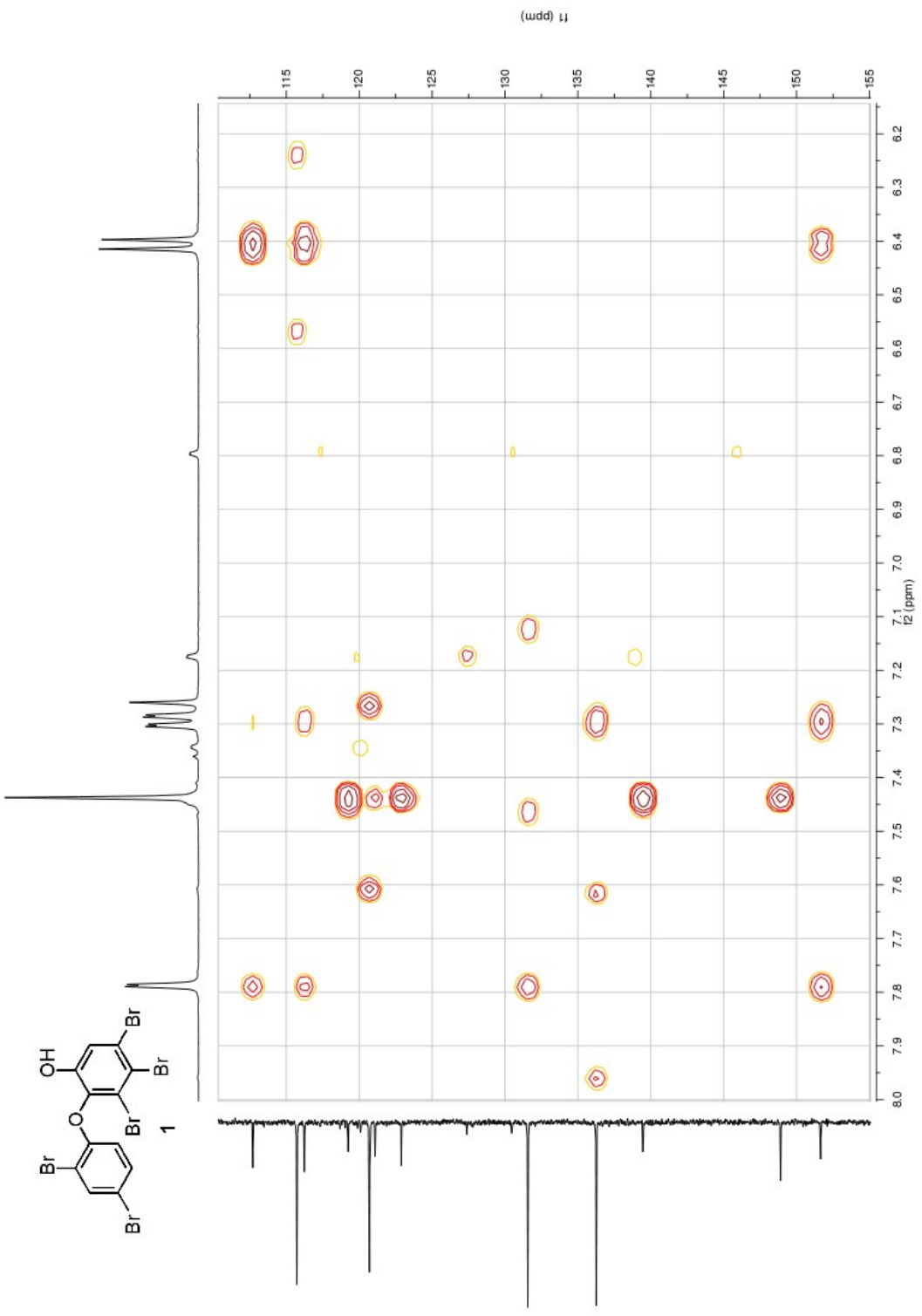

Figure II.11: ^{1}H-^{13}C HMBC Spectrum of **1** in $CDCl_3$

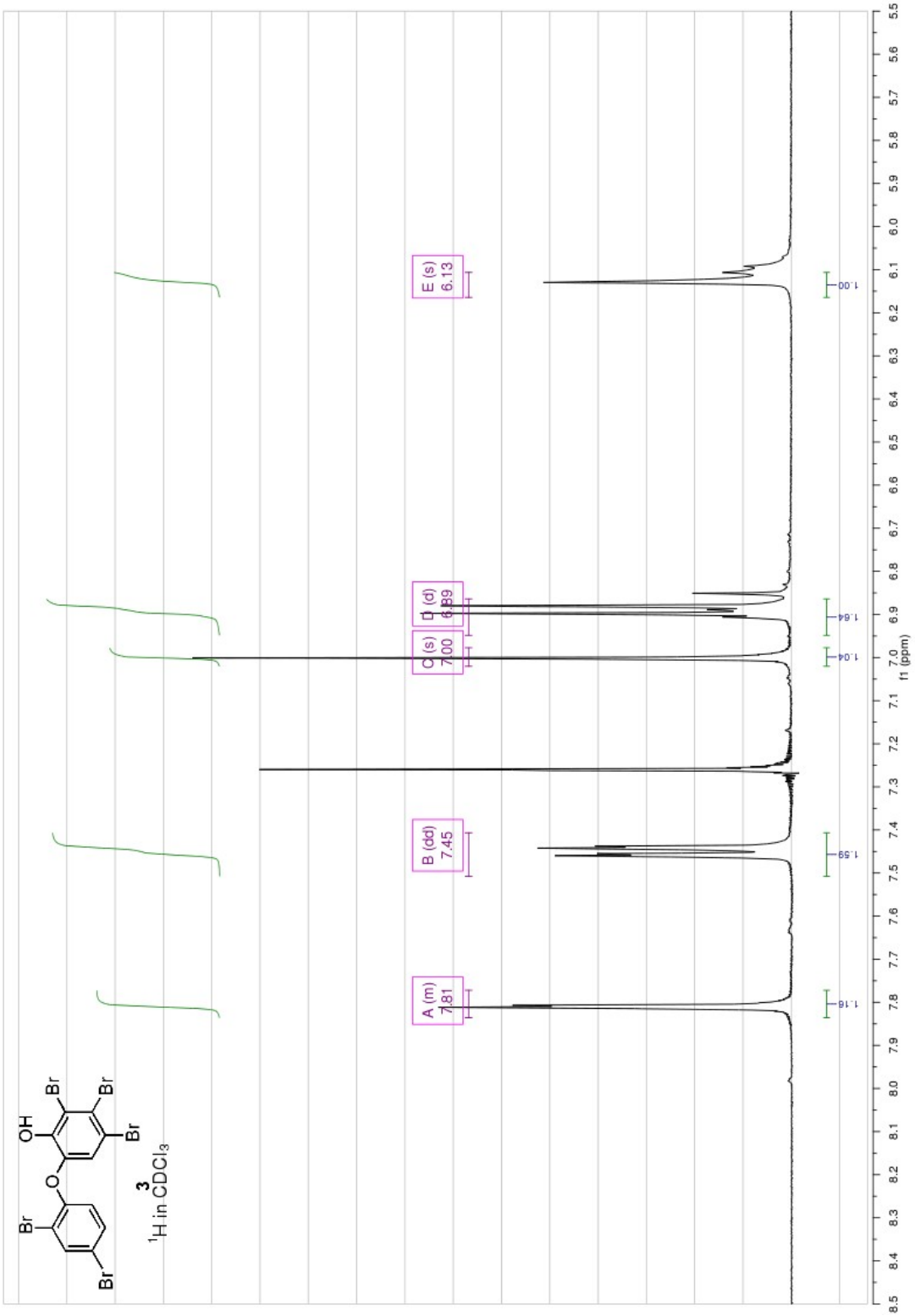

Figure II.12: ^{1}H NMR Spectrum of **1** in $CDCl_3$

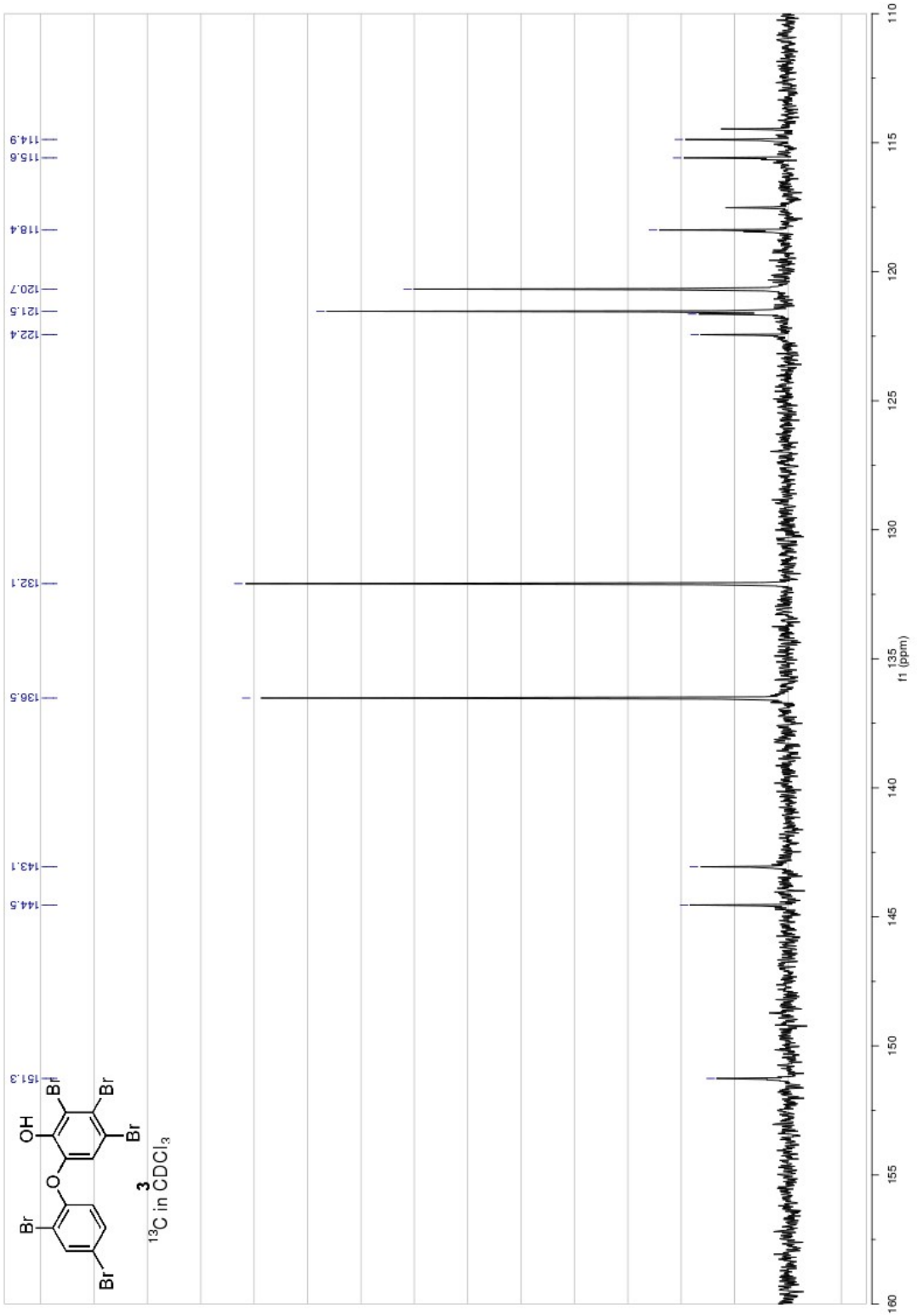

Figure II.13: ^{13}C NMR Spectrum of **3** in $CDCl_3$

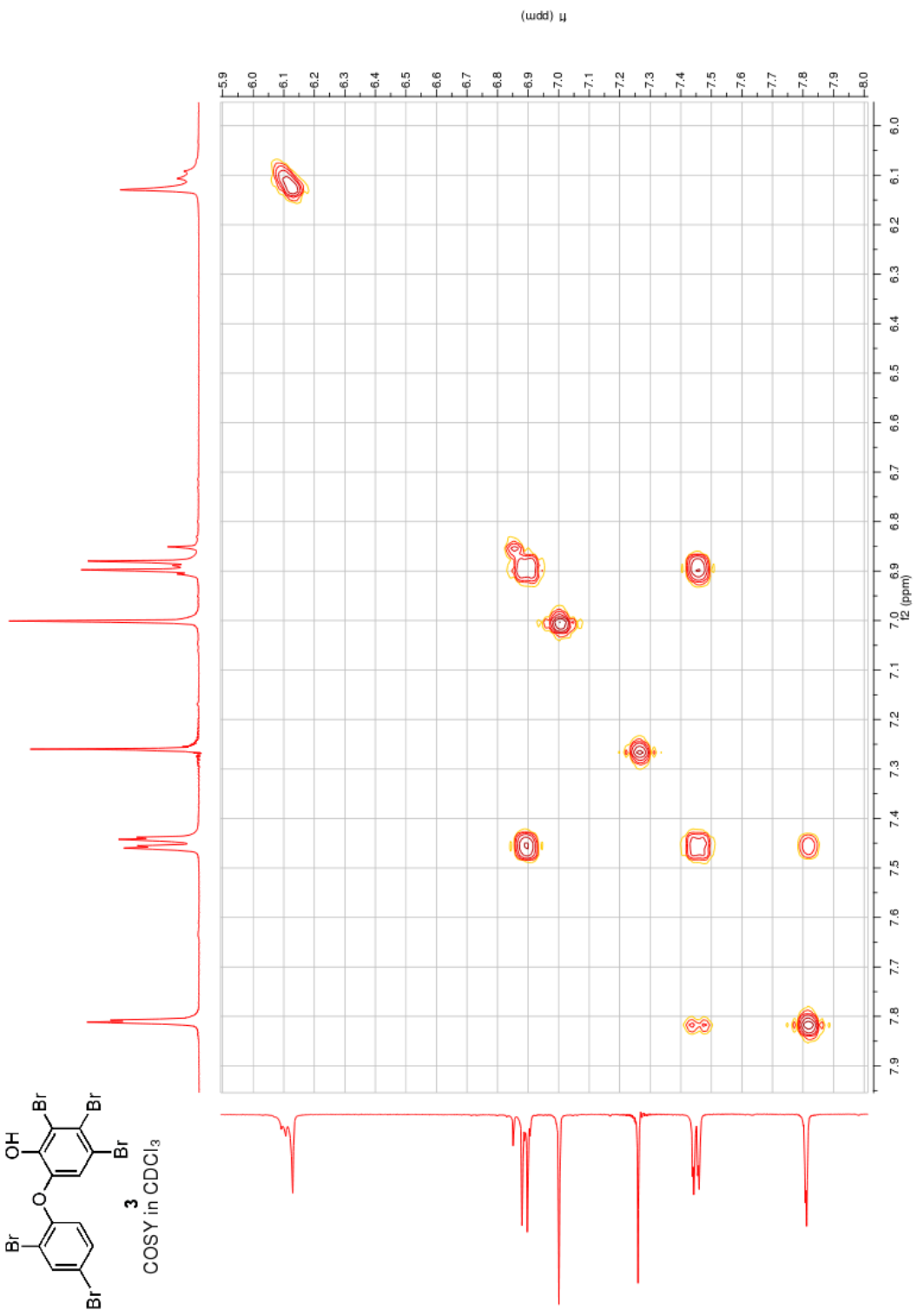

Figure II.14: ^{1}H-^{1}H COSY Spectrum of **3** in $CDCl_3$

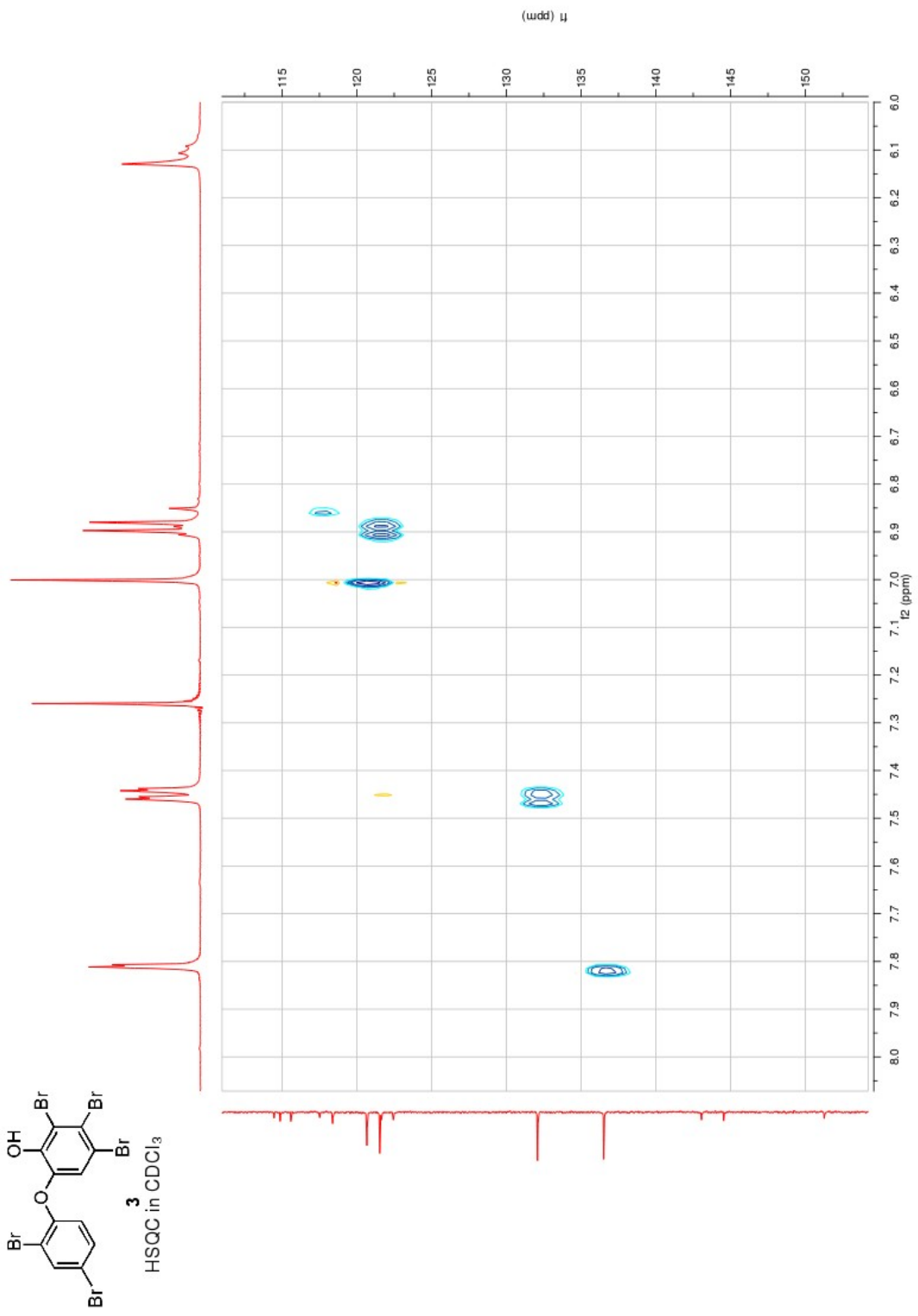

Figure II.15: ^{1}H-^{13}C HSQC Spectrum of **3** in $CDCl_3$

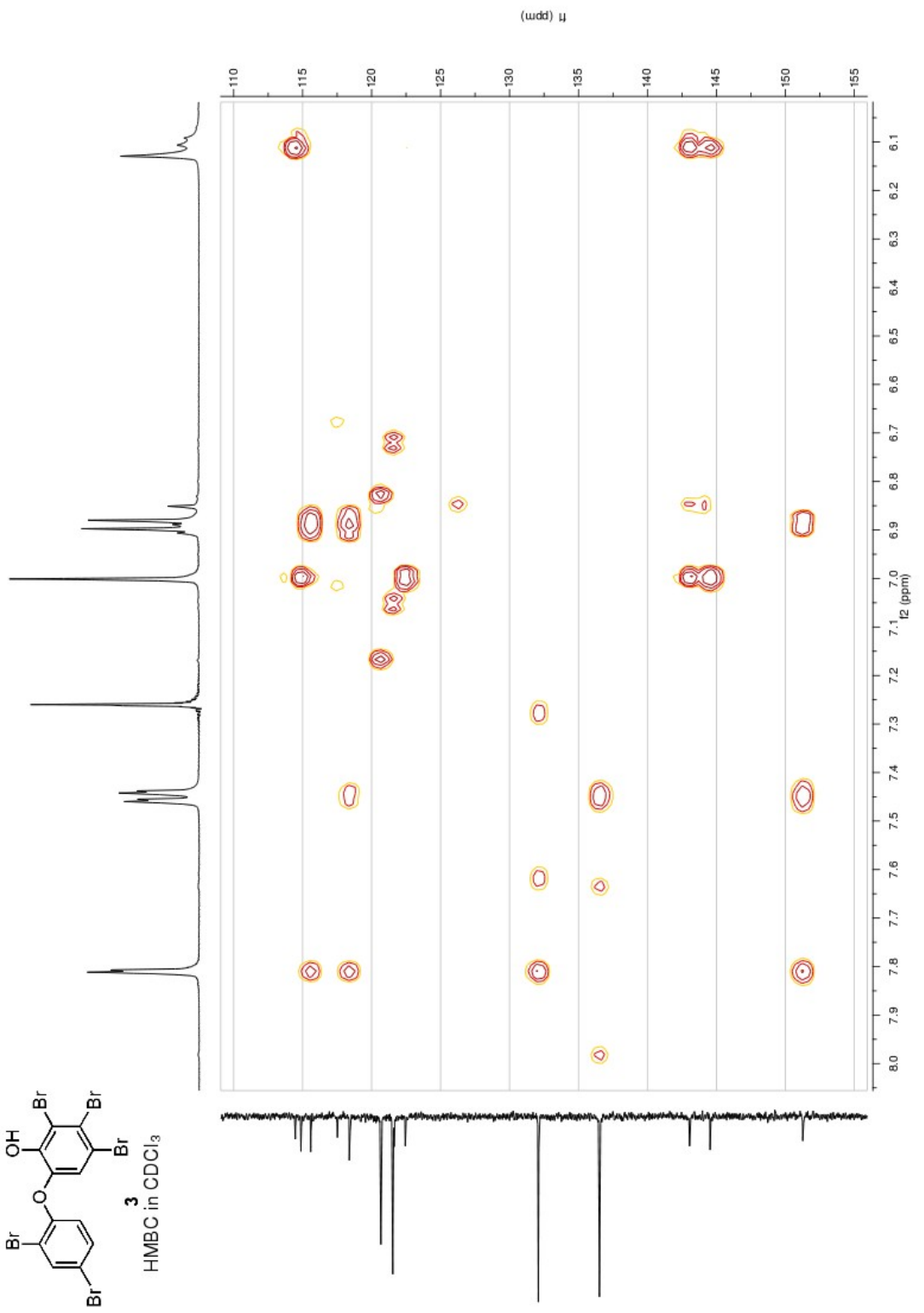

Figure II.16: ^{1}H-^{13}C HMBC Spectrum of **3** in $CDCl_3$

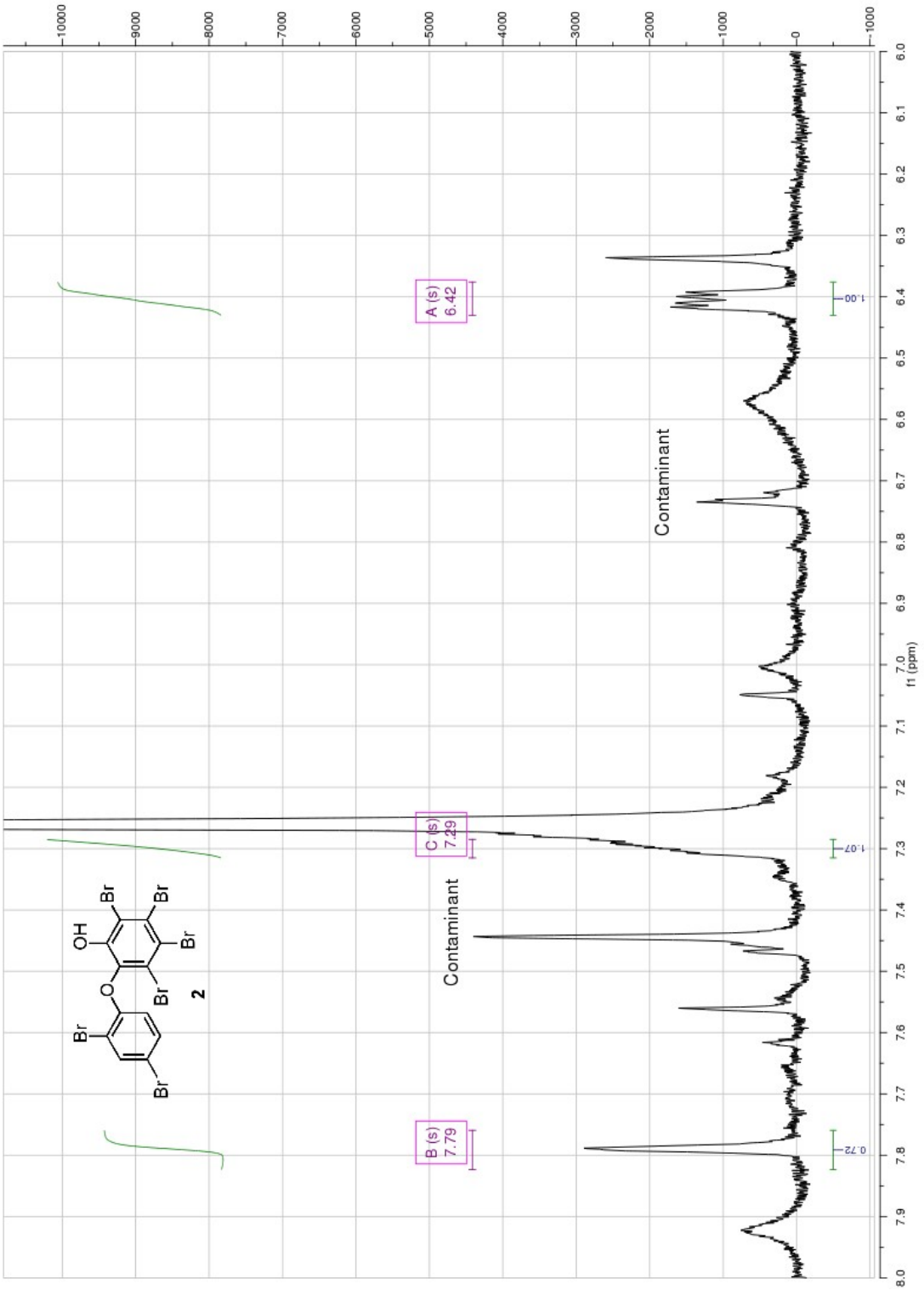

Figure II.17: ^{1}H NMR Spectrum of **2** in $CDCl_3$

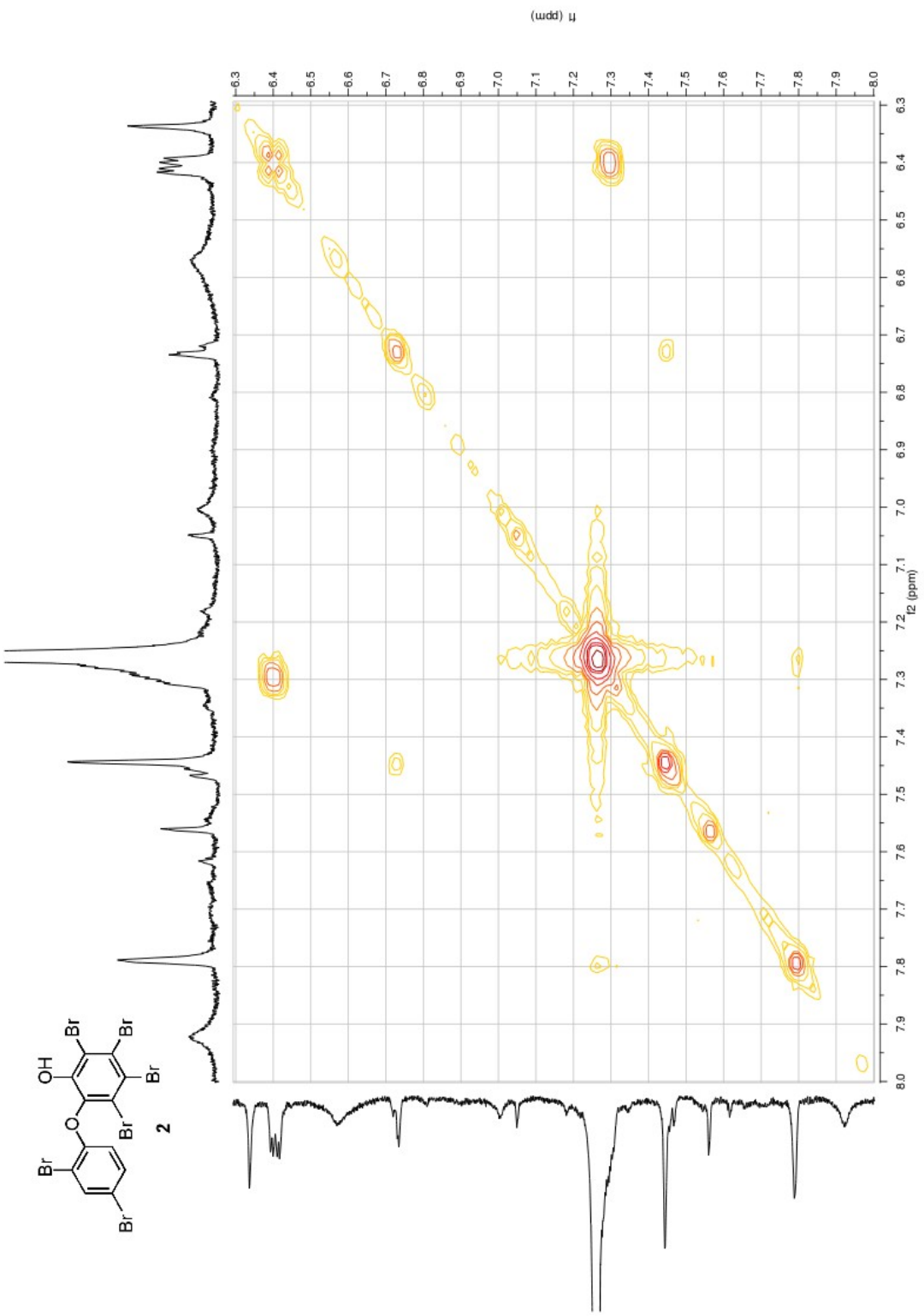

Figure II.18: ^{1}H-^{1}H COSY Spectrum of **2** in $CDCl_3$

References and footnotes

1 Marsh, G.; Athanasiadou, M.; Athanassiadis, I.; Bergman, Å.; Endo, T.; Haraguchi, K. Identification, quantification, and synthesis of a novel dimethoxylated polybrominated biphenyl in marine mammals caught off the coast of Japan. *Environ. Sci. Technol.* **2005**, *39*, 8684-8690.

2 Vos, J. G.; Becher, G.; van den Berg, M.; de Boer, J.; Leonards, P. E. G. Brominated flame retardants and endocrine disruption. *Pure Appl. Chem.* **2003**, *75*, 2039-2046.

3 Verreault, J.; Gebbink, W. A.; Gauthier, L. T.; Gabrielsen, G. W.; Letcher, R. J. Brominated flame retardants in glaucous gulls from the Norwegian Arctic: more than just an issue of polybrominated diphenyl ethers. *Environ. Sci. Technol.* **2007**, *41*, 4925-4931.

4 Kelly, B. C.; Ikonomou, M. G.; Blair, J. D.; Gobas, F. A. P. C. Hydroxylated and methoxylated polybrominated diphenyl ethers in a Canadian arctic marine food web. *Environ. Sci. Technol.* **2008**, *42*, 7069-7077.

5 Betts, K. S. Science news: rapidly rising PBDE levels in North America. *Environ. Sci. Technol.* **2002**, *36*, 50A-2A.

6 Athanasiadou, M.; Cuadra, S. N.; Marsh, G.; Bergman, Å.; Jakobsson, K. Polybrominated diphenyl ethers (PBDEs) and hydroxylated PBDE metabolites in young humans from Managua, Nicaragua. *Environ. Health Perspect.* **2008**, *116*, 400-408.

7 Hale, R. C.; Alaee, M.; Manchester-Neesvig, J. B.; Stapleton, H. M.; Ikonomou, M. G. Polybrominated diphenyl ether flame retardants in the North American environment. *Environ. Int.* **2003**, *29*, 771-779.

8 McKinney, M. A.; Cesh, L. S.; Elliott, J. E.; Williams, T. D.; Garcelon, D. K.; Letcher, R. J. Brominated flame retardants and halogenated phenolic compounds in North American West Coast bald eaglet (Haliaeetus leucocephalus) plasma. *Environ. Sci. Technol.* **2006**, *40*, 6275-6281.

9 Malmberg, T.; Athanasiadou, M.; Marsh, G.; Brandt, I.; Bergman, Å. Identification of hydroxylated polybrominated diphenyl ether metabolites in blood plasma from polybrominated diphenyl ether exposed rats. *Environ. Sci. Technol.* **2005**, *39*, 5342-5348.

10 Marsh, G.; Athanasiadou, M.; Athanassiadis, I.; Sandholm, S. Identification of hydroxylated metabolites in 2,2',4,4'-tetrabromodiphenyl ether exposed rats. *Chemosphere* **2006**, *63*, 690-697.

11 Carte, B.; Faulkner, D. J. Polybrominated diphenyl ethers from *Dysidea herbacea*, *Dysidea chlorea* and *Phyllospongia foliascens*. *Tetrahedron* **1981**, *37*, 2335-2339.

12 Carte, B.; Kernan, M. R.; Barrabee, E. B.; Faulkner, D. J.; Matsumoto, G. K.; Clardy, J. Metabolites of the nudibranch *Chromodoris funerea* and the singlet oxygen oxidation products of furodysin and furodysinin. *J. Org. Chem.* **1986**, *51*, 3528-3532.

13 Unson, M. D.; Holland, N. D.; Faulkner, D. J. A brominated secondary metabolite synthesized

by the cyanobacterial symbiont of a marine sponge and accumulation of the crystalline metabolite in the sponge tissue. *Mar. Biol.* **1994**, *119*, 1-11.

14 Mariussen, E.; Fonnum, F. Neurochemical targets and behavioral effects of organohalogen compounds: an update. *Crit. Rev. Toxicol.* **2006**, *36*, 253–289.

15 Hwang, H.; Park, E.; Young, T. M.; Hammock, B. D. Occurrence of endocrine-disrupting chemicals in indoor dust. *Sci. Total Environ.* **2008**, *404*, 26-35.

16 Dingemans, M. M. L.; de Groot, A.; van Kleef, R. G. D. M.; Bergman, Å.; van den Berg, M.; Henk P.M. Vijverberg, H. P. M.; Westerink , R. H. S. Hydroxylation increases the neurotoxic potential of BDE-47 to affect exocytosis and calcium homeostasis in PC12 cells. *Environ. Health Perspect.* **2008**, *116*, 637-643.

17 Dingemans, M. M. L.; Ramakers, G. M. J.; Gardoni, F.; van Kleef, R. G. D. M.; Bergman, Å; Di Luca, M.; van den Berg, M.; Westerink, R. H. S.; Vijverberg, H. P. M. Neonatal exposure to brominated flame retardant BDE-47 reduces long-term potentiation and postsynaptic protein levels in mouse hippocampus. *Environ. Health Perspect.* **2007**, *115,* 865–870.

18 Berman, F. W.; Murray, T. F. Brevetoxin-induced autocrine excitotoxicity is associated with manifold routes of Ca^{2+} influx. *J. Neurochem.* **2000**, 74, 1443-1451.

19 Li, W. I.; Berman, F. W.; Okino, T.; Yokokawa, F.; Shioiri, T.; Gerwick, W. H.; Murray, T. F., 2001. Antillatoxin is a novel marine cyanobacterial toxin that potently activates voltage-gated sodium channels. *Proc. Natl. Acad. Sci.* **2001**, *98*, 7599-7604.

20 Rogers, K. L.; Fong, W. F.; Redburn, J.; Griffiths, L. R. Fluorescence detection of plant extracts that affect neuronal voltage-gated Ca^{2+} channels. *Eur J Pharm Sci.* **2002**, *15*, 321-330.

21 Dravid, S. M.; Murray, T. F. Fluorescent detection of Ca^{2+}-permeable AMPA/kainate receptor activation in murine neocortical neurons. *Neurosci. Lett.* **2003**, *351*, 145-148.

22 Still, W. C.; Khan, M.; Mitra, A. Rapid chromatographic technique for preparative separations with moderate resolution. *J. Org. Chem.* **1978**, *43*, 2923-2925.

23 Agrawal, M. S.; Bowden, B. F. Marine sponge *Dysidea herbacea* revisited: another brominated diphenyl ether. *Mar. Drugs* **2005**, *3*, 9-14.

24 Fu, X.; Schmitz, F. J. New brominated diphenyl ether from an unindentified species of *Dysidea* sponge. *13*C NMR data for some brominated diphenyl ethers. *J. Nat. Prod.* **1996**, *59*, 1102-1103.

25 Bowden, B. F.; Towerzey, L.; Junk, P. C. A new brominated diphenyl ether from the marine sponge *Dysidea herbacea*. *Aust. J. Chem.* **2000**, *53*, 299-301.

26 Marsh, G.; Stenutz, R.; Bergman, Å. Synthesis of hydroxylated and methoxylated polybrominated diphenyl ethers – natural products and potential polybrominated diphenyl ether metabolites. *Eur. J. Org. Chem.* **2003**, 2566-2576.

27 Crews, P.; Rodríguez, J.; Jaspars, M. *Organic Structure Analysis*, Oxford, **1998**, pp. 169-181.

28 Viberg, H.; Fredriksson, A.; Eriksson, P. Neonatal exposure to polybrominated diphenyl ether (PBDE 153) disrupts spontaneous behaviour, impairs learning and memory, and decreases hippocampal cholinergic receptors in adult mice. *Toxicol. Appl. Pharmacol.* **2003**, *192*, 95-106.

29 Malmvärn, A.; Marsh, G.; Kautsky, L.; Athanasiadou, M.; Bergman, Å.; Asplund, L. Hydroxylated and methoxylated brominated diphenyl ethers in the red algae *Ceramium tenuicorne* and blue mussels from the Baltic Sea. *Environ. Sci. Technol.* **2005**, *39*, 2990-2997.

30 Garrison, T., *Oceanography 5th Ed.* Brooks/Cole publisher, **2005**, pp 349-350.

31 Symons, R. K.; Burniston, D.; Jaber, R.; Piro, N.; Trout, M.; Yates, A.; Gales, R.; Terauds, A.; Pemberton, D.; Robertson, D. Southern hemisphere cetaceans. A study of the POPs PCDDs/PCDFs and dioxin-like PCBs in stranded animals from the Tasmanian coast. *Organohalogen Compounds* **2003**, *62*, 257-260.

32 Law, R. J.; Allchin, C. R.; deBoer, J.; Covaci, A.; Herzke, D.; Lepom, P.; Morris, S.; Tronczynski, J.; de Wit, C. A. Levels and trends of brominated flame retardants in the European environment. *Chemosphere* **2006**, *64*, 187–208.

Chapter III

Discovery of a novel vinylchloride containing fatty acid from a marine cyanobacterium *Lyngbya* sp.

Abstract

A novel fatty acid containing a vinyl chloride moiety was discovered through NMR-guided fractionations of an aqueous extract of a marine cyanobacterium, *Lyngbya* sp. collected in Papua New Guinea. While no bioactivity has yet been found to be associated with this natural product, its biogenesis is of significance in light of other important cyanobacterial compounds containing a similar vinylchloride functional group.

III.1 Introduction

It has been exceptionally productive to search for novel natural products in marine cyanobacteria, particularly species of *Lyngbya*.[1] For example, jamaicamides A-C and malyngamides A-X have been found from marine cyanobacteria and nudibranchs (Figure III.1, III.2),[2,3] and nudibranchs probably obtain these compounds from feeding on cyanobacteria.[4] All of these natural products have a common biosynthetic theme in that they possess a PKS-derived long lipid chain and an NRPS-derived peptidic portion.[5] Furthermore, all three jamaicamides and 20 of the 27 malyngamides contain a rather unusual functionality, a vinylchloride group.[2,3] Pyrrolone rings seen in all three jamaicamides and malyngamides A, Q, R, and X further add to the overall striking resemblance of these metabolites.

The apparent rule for the construction of malyngamides is that if two acetate units and a glycine unit are used for the "head group," then the final product will contain a linear "head group" that is attached to either a pyrrolone or a pyrrolidinone with the exception of malyngamide P (**19**). Alternatively, if three acetate units and a glycine unit are used, then a cyclohexane with various oxidation states will be the biosynthetic product for the "head group." Moreover, the vinylchloride unit resides on the C-1 of the glycine unit, suggesting that the sp^2 carbon bearing the chloride is not derived from *S*-adenosyl-methionine (SAM), but from the C-2 carbon of another acetate unit.[6] In HMG-CoA biosynthesis, an intermediate to the 5-carbon unit of terpenes, the same strategy is employed, where an aldol reaction between an acetoacetyl CoA and an acetyl CoA is catalyzed by HMG-CoA synthase. Likewise, in jamaicamides,[7] the vinlychloride carbon

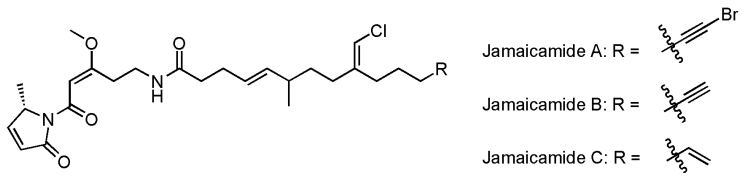

Figure III.1: Jamaicamides A-C

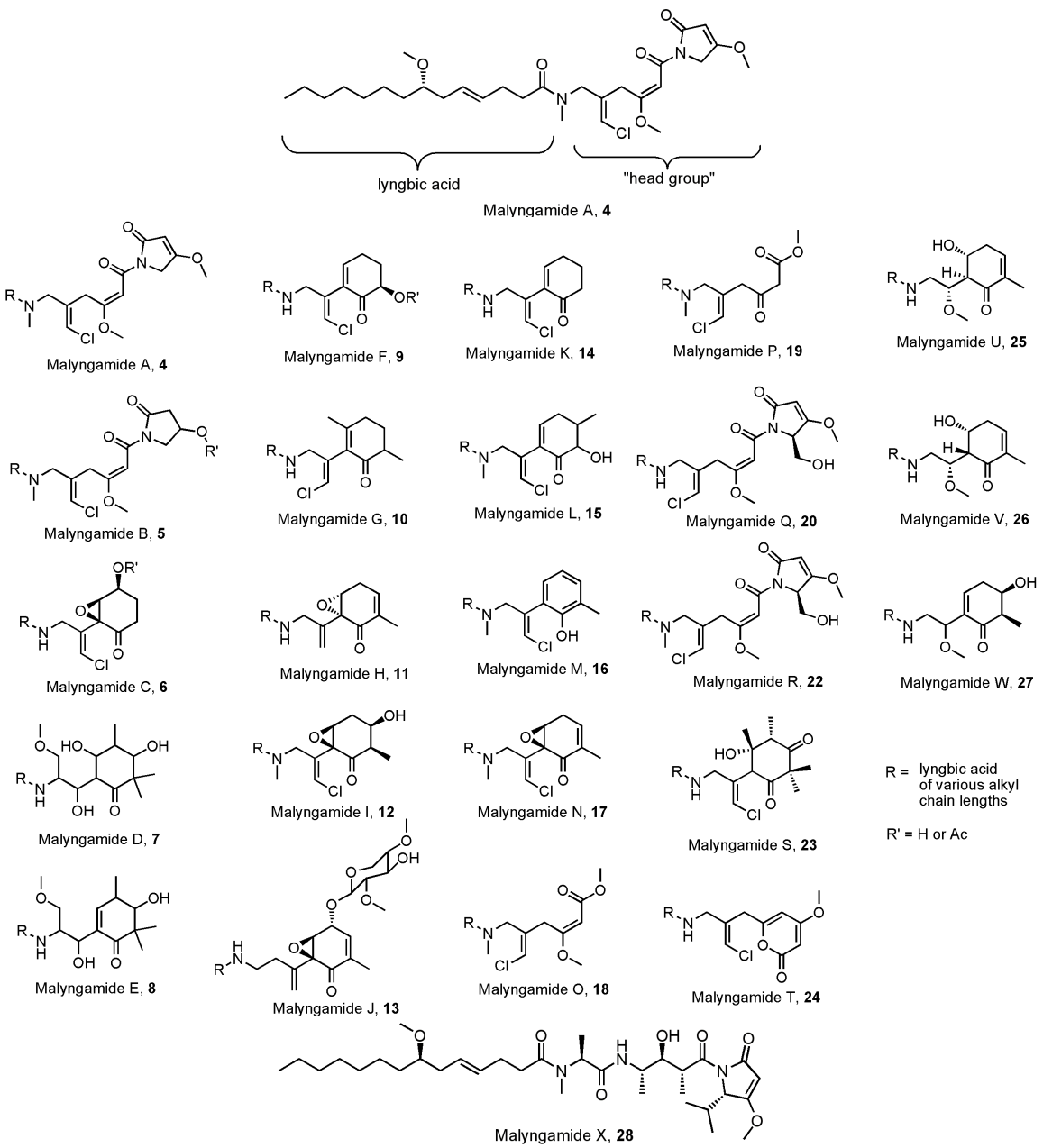

Figure III.2: Malyngamides A-X

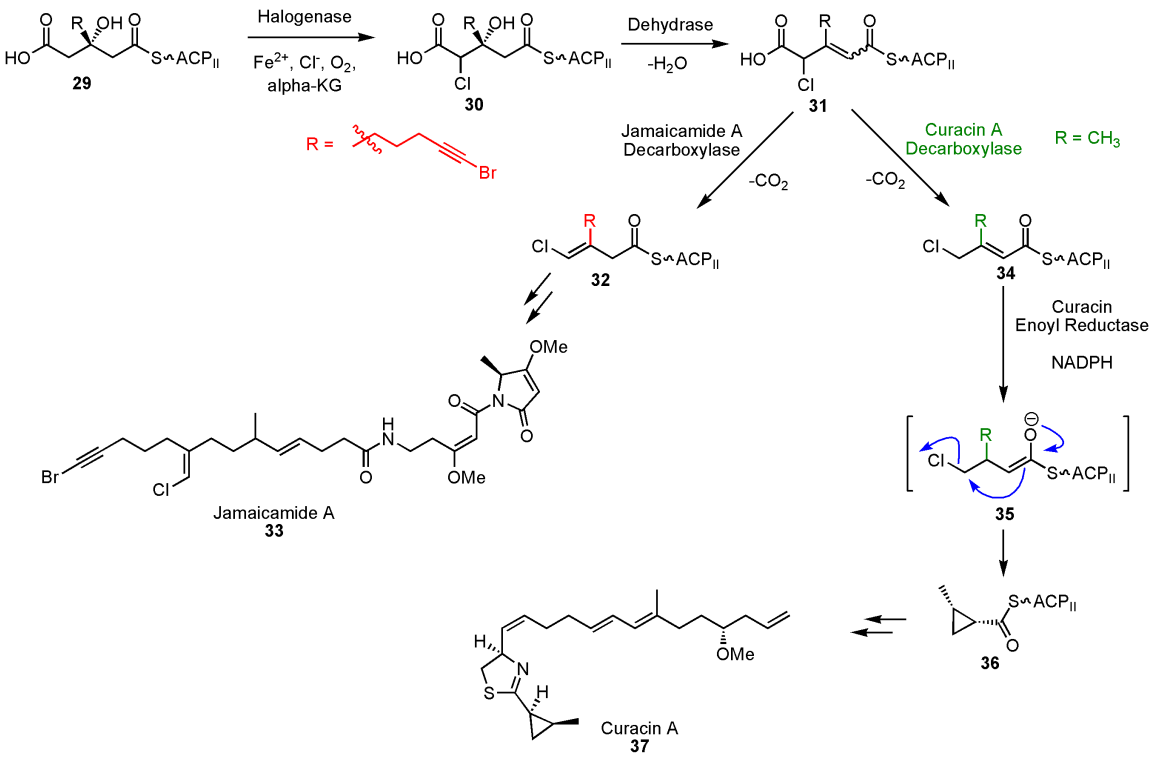

Scheme III.1: Divergent biosyntheses of jamaicamide A and curacin A

The two different biosynthetic pathways leading to **33** and **37** utilize the same chemistry until the chlorinated intermediate **31**, after which the corresponding decarboxylases distinguish the pathways (**32** for jamaicamide A; **34** for curacin A).

has been shown to be derived from the C-2 of acetate.[2] Recently, the biosynthesis of jamaicamides was found to be closely related to that of curacins, where the two different pathways share a common intermediate (**31**) as shown in Scheme III.1.[8] Herein described is a novel natural product isolated from *Lyngbya* that also possesses a vinylchloride group.

III.2 Collection of the Cyanobacterial Material

Tropical areas are biologically very diverse environments in which many species compete for space and nutritional resources. Therefore, organisms in such environments

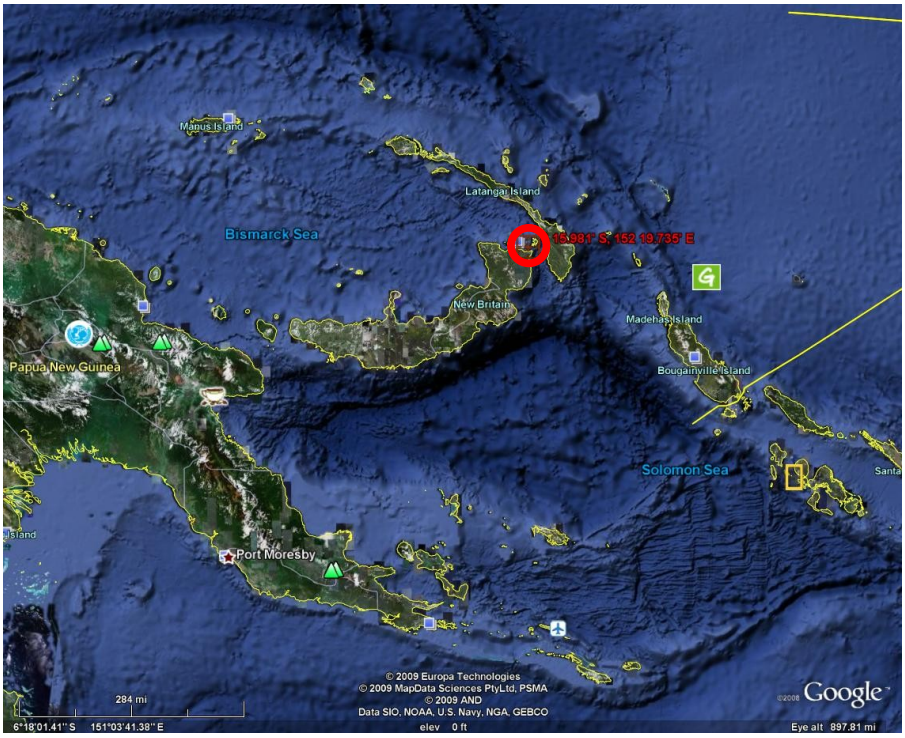

Figure III.3: Satellite Image of Algae Collection Site

The satellite image was obtained through Google Earth™. The site of collection is indicated by the red circle.

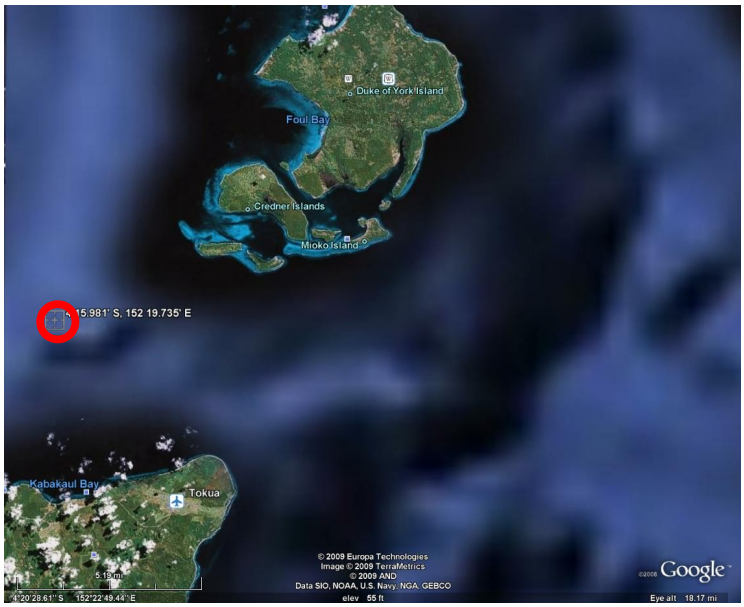

Figure III.4: Zoom-up of the Satelite Image of the *Lyngbya* Collection Site

The satellite image was obtained through Google Earth™. The site of collection is indicated by the red circle.

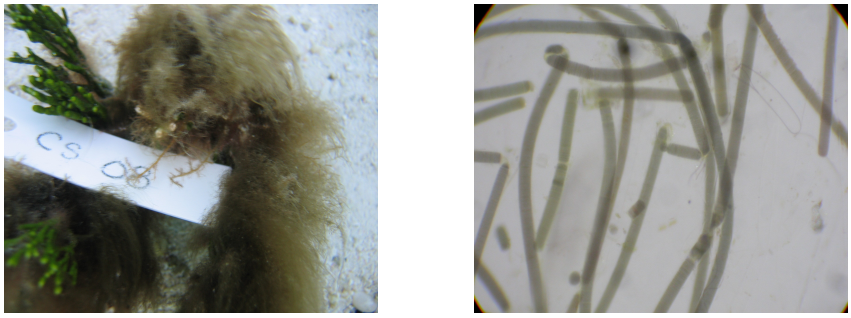

Figure III.5: "Green *Lyngbya*" collected in Papua New Guinea

are expected to possess a rich collection of secondary metabolites suited for competition. In order to acquire such metabolites, a sample of *Lyngbya sp.* was collected in Papua New Guinea (PNG). The cyanobacterial material was collected at a site between the northeast coast of New Britain Island and the southwest coast of Credner Island by snorkeling (S 4º 15.981'; E 152º 19.735'; Figure III.3 and III.4) at the depth of 1 m.[9] The alga had the typical hair-like morphology of *Lyngbya*, but had a greenish color unlike typical *Lyngbya* (Figure III.5).

III-3 Isolation of the Novel Fatty Acid

Since water-soluble organic natural products are very difficult to handle, they are not as well studied as other organic compounds. Therefore, it is a better likelihood to find a novel compound in aqueous soluble materials. One of the aims of this study was to develop a methodology to purify natural products from the aqueous extract. The cyanobacterial material (WG-1560) was extracted exhaustively with CH_2Cl_2 and MeOH (2:1) for the isolation of lipid contents.[10] The remaining aqueous layers and the EtOH used for preservation of the alga were combined and the volatiles were removed under vacuum. The residues were resuspended in EtOH and the insolubles were filtered off

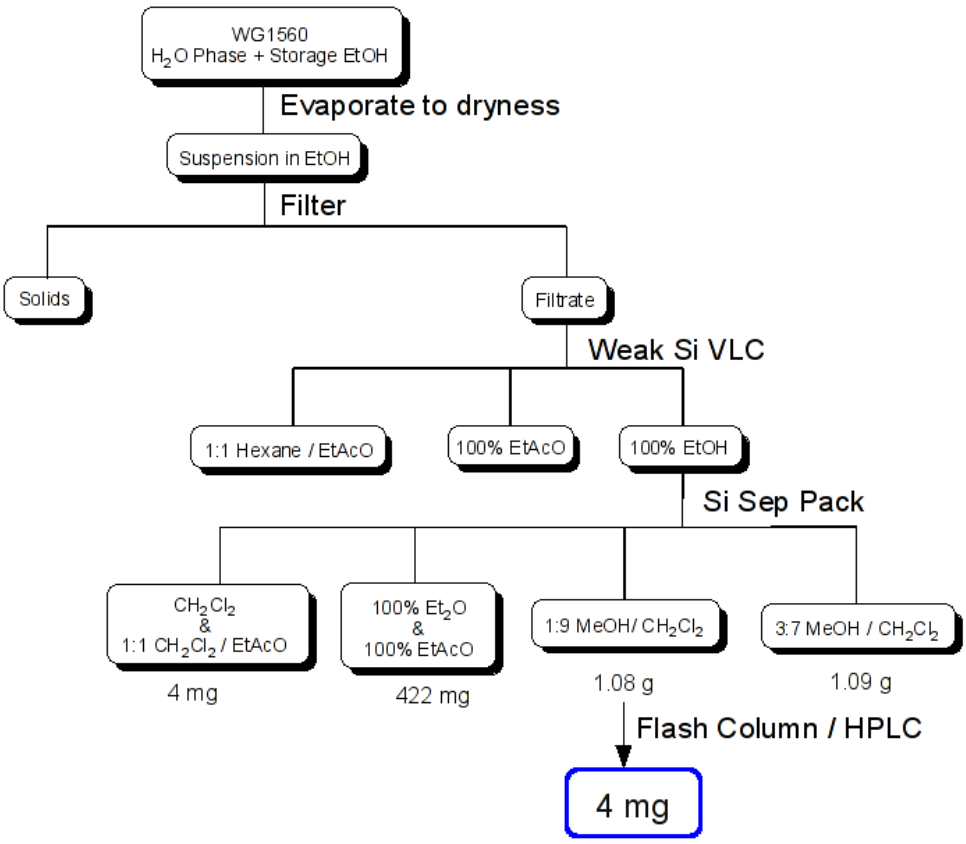

Scheme III.2: Isolation process for credneric acid (**38**)

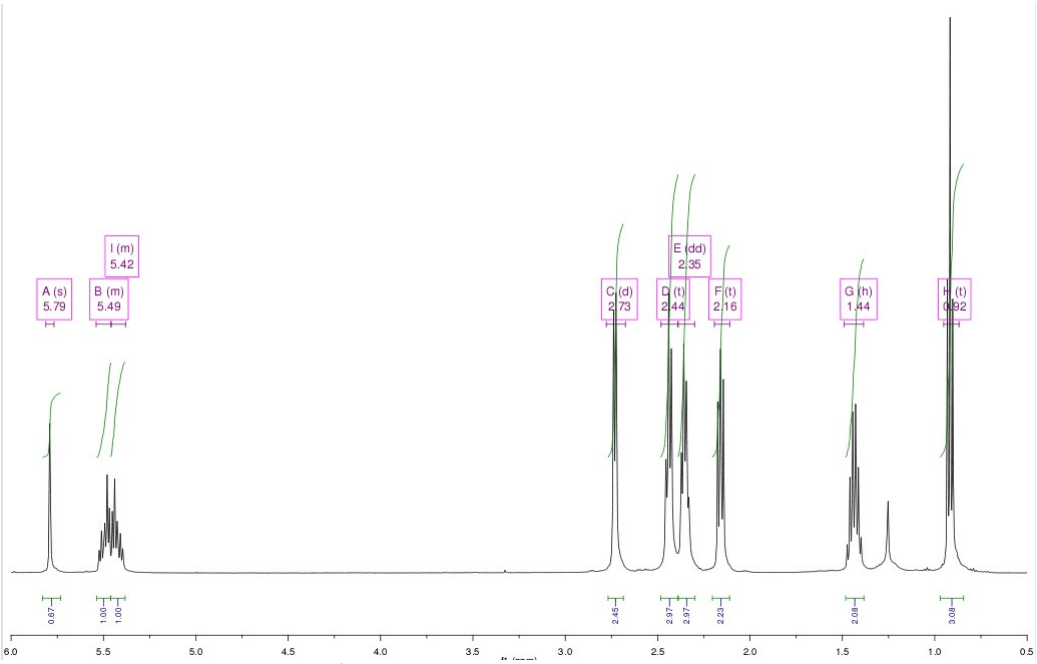

Figure III.6: ^{1}H NMR Spectrum of Credneric Acid (**38**)

(Scheme III.2). The filtrate was then subjected to two steps of rough normal phase chromatgraphy to generate a few fractions. The fraction that contained compounds separable by TLC was subjected to flash column chromatography with silica gel as the stationary phase and a gradient mixture of MeOH and CH_2Cl_2 as the mobile phase to obtain several fractions. One of the fractions contained a fairly pure compound and it was further purified by semi-prep reverse phase HPLC to obtain 4 mg of a colorless oil. The compound was named "credneric acid," after the nearby island where the cyanobacterial material was collected.

III.4 Structure Elucidation of Credneric Acid

The purified material was first analyzed by ^{1}H NMR (Figure III.6), which revealed that the compound was a short chain fatty acid. However, one unusual singlet signal was observed at 5.79 ppm. Further analysis by ^{13}C NMR, COSY, and HSQC (Table III.1) led to substructures as shown in Scheme III.3. Finally, the two and three bond heteronuclear coupling information obtained by HMBC analysis allowed connection of the three substructures (Table III.1). The unknown "R" group was determined to be a chlorine atom based on the high resolution mass spectroscopy analysis (*m/z* 217.0990 expected for $C_{11}H_{18}O_2Cl$ [M+H]; observed *m/z* 217.0995) and the NMR chemical shift (^{1}H 5.79 ppm; ^{13}C 113.1). The stereochemical assignment of the two olefins were made by the coupling constant between the two vinyl protons (5.42 ppm and 5.49 ppm; J = 15.4 Hz) and 1D ROESY correlations of key protons on and around the olefins (Scheme III.4).

Table III.1: ^{1}H and ^{13}C NMR, COSY, HSQC, and HMBC data for credneric acid (**38**)

The HSQC data are reflected in the assignment of the ^{1}H NMR signals to their respective ^{13}C NMR signals.

Position	^{13}C	^{1}H	COSY	HMBC
1	178.9			2.44, 2.35
2	33.7	2.44	2.35	2.35
3	27.4	2.35	5.48, 2.44	5.42, 2.44
4	130.5	5.48	2.35	2.73, 2.44, 2.36
5	128.1	5.42	2.73	2.73, 2.36
6	37.9	2.73	5.42	5.79, 5.48, 5.42, 2.16
7	141.4			5.79, 2.73, 2.16, 1.44
8	32.2	2.16	1.44	5.79, 2.73, 1.44, 0.92
9	20.2	1.44	2.16, 2.16, 0.92	2.16, 0.92
10	13.9	0.92	1.44	2.16, 1.44
11	113.1	5.79		2.73, 2.16

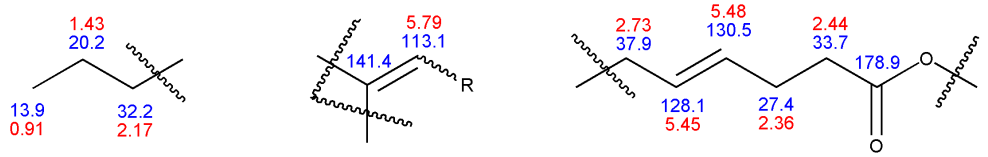

Scheme III.3: Substructures of Credneric Acid by ^{1}H NMR, COSY, and HSQC

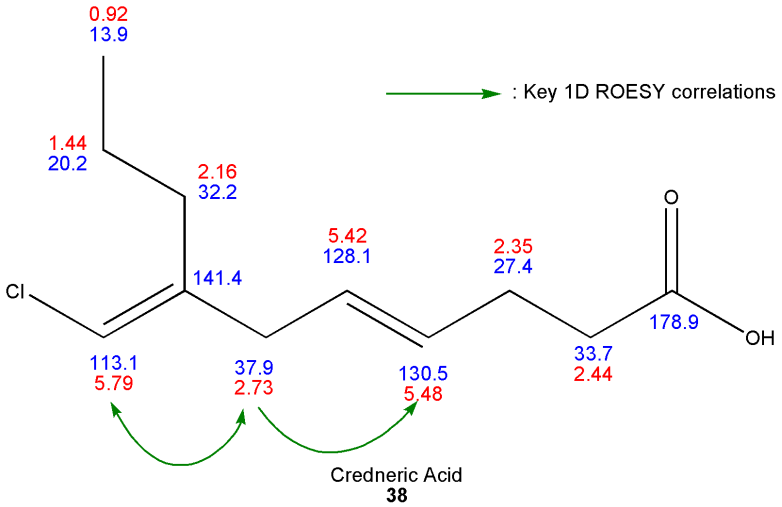

Scheme III.4: Stereochemical Assignments of Credneric Acid by 1D ROESY Correlations

III.5 Significance of Crendneric Acid

While the gene cluster responsible for the biosynthesis of jamaicamides has been identified already,[2] the biosynthetic process for this halogenation step is only speculative and largely based on other related natural products.[7] Since there is remarkable resemblance between credneric acid (**38**) and the middle portion of the jamaicamides, it may be advantageous to study the biosynthesis of simpler compounds like **38** to gain insights into the halogenation process for the jamaicamides and the malyngamides. For example, biosynthetic precursors necessary for enzymatic reactions with a putative halogenating enzyme would be easier to synthesize for credneric acid than for the jamaicamides.

Credneric acid was tested in H-460 cytotoxicity and Na^+ channel activation and blocking assays, but it was found to be inactive (data not shown). It is possible that the compound is not able to cross cell membranes due to its polar carboxylic acid group.

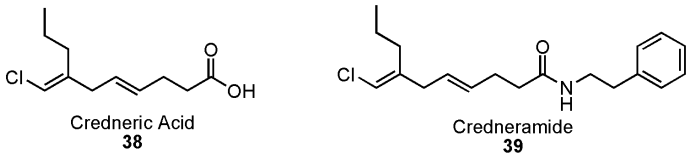

Figure III.7: Credneric Acid and Credneramide

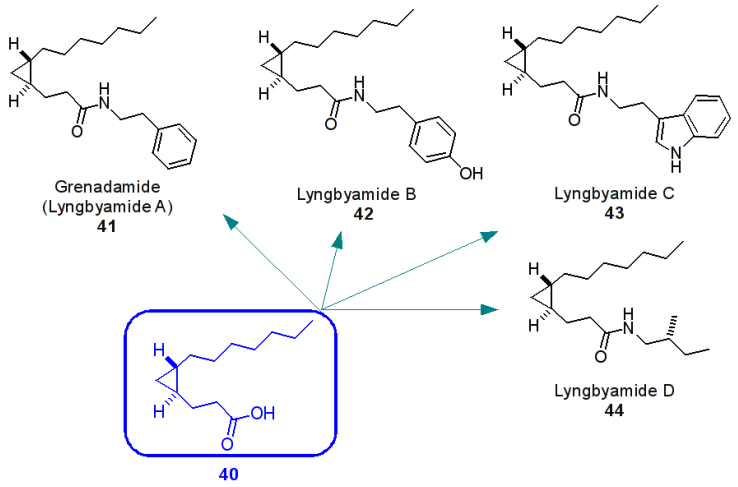

Scheme III.5: Cyclopropane Fatty Acid and Lyngbyamides

Alternatively, it is possible that this natural product lacks functional groups necessary for bioactivity. After the discovery of **38**, a related natural product, credneramide (**39**, Figure III.7), was isolated from the CH_2Cl_2 / MeOH extract of the same collection of *Lyngbya* in our laboratory.[11] This amide derivative of **38** was found to be only moderately active in anti-parasitic assays against malaria, chagas, and leishmania and Na^+ channel blocking assay in Neuro-2a cells. It may be that **38** is merely a biosynthetic precursor for amides,

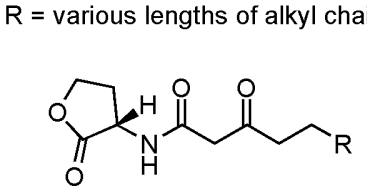

N-Acyl Homoserine Lactones (AHL)

Figure III.8: N-Acyl Homoserine Lactones (AHLs)

such as **39**, and it is not produced as a secondary metabolite with its own biological or ecological significance.

Cyanobacteria appear to produce various natural products based on some common foundational biosynthetic units. For example, malyngamides all have lyngbic acid in common, with minor variations (Figure III.2). Furthermore, grenadamide (lyngbyamide A), and lyngbyamides B-D have the same cyclopropane fatty acid in common (Scheme III.5).[12] All of these amides have some structural resemblance to bacterial quorum sensing molecules such as AHLs (*N*-acyl homoserine lactones; Figure III.8).[13] This resemblance may be related to the biological roles that these amide natural products have in nature. Likewise, **38** appears to be a foundational biosynthetic unit on which *Lyngbya* builds other compounds, such as **39**. Given the precedence with lyngbyamides and malyngamides, discovery of other credneric acid derivatives are expected in the future.

III.6 Conclusion

A novel fatty acid containing a vinylchloride functionality was discovered and characterized from a PNG collection of *Lyngbya*. Despite its inactivity in the few bioassays tested thus far, this natural product may play an important role as a template for synthesizing bioactive amide derivatives. Credneric acid may also be useful for the study of the biosynthetic chlorination processes in cyanobacteria.

III.7 Experimental Section

General

Unless noted otherwise, all materials were purchased from commercially available sources and were used without further purification. Flash chromatorgraphy[14] and vacuum liquid chromatography were performed using EM Science silica gel (230-400 mesh). TLC was performed using EM Science pre-coated silica gel plates (Merck 60 F_{254}). IR spectra were recorded on a Nicolet Magna-IR 550. ^{1}H NMR and ^{13}C NMR spectra were recorded on a Varian Inova spectrometer (500MHz) or on a Varian Inova spectrometer (300 MHz and 75 MHz, respectively). ^{1}H and ^{13}C spectra recorded in $CDCl_3$ were referenced to the residual solvent peaks at 7.26 ppm and 77.0 ppm, respectively. High resolution mass spectra were recorded on a ThermoFinnigan MAT900XL spectrometer.

Isolation and Characterization of Credneric Acid

The cyanobacterial material (41 g, dry weight) was extracted exhaustively with CH_2Cl_2 and MeOH (2:1) for the isolation of lipid contents. The remaining aqueous layers and the EtOH used for preservation of the alga were combined and the volatiles were removed under vacuum. The residues were resuspended in EtOH and the insolubles were filtered off (Scheme III.1). By using vacuum, the filtrate was pulled through a pad of water-treated silica gel with differing solvents (vacuum liquid chromatography, VLC). Most of the organic content was eluted with EtOH, but not with other solvents (Scheme III.1). Upon concentration under vacuum, the residues were subjected to solid phase extraction (SPE) with silica gel. By eluting with different solvents (1:1 CH_2Cl_2/EtOAc; EtAcO; 1:9 MeOH/CH_2Cl_2; 3:7 MeOH/CH_2Cl_2), four fractions (4 mg, 422 mg, 1.08 g, and 1.09 g, respectively) were obtained (Scheme III.1). Only the third fraction (1:9 MeOH/CH_2Cl_2 elution) had a TLC profile that appeared suitable for normal phase

separation of compounds. The material in the third SPE fraction was subjected to flash column chromatography with silica gel as the stationary phase and a gradient mixture of MeOH and CH_2Cl_2 as the mobile phase to obtain several fractions. One of the fractions contained a fairly pure compound (7 mg) and it was further purified by semi-prep reverse phase HPLC (250 x10.00 mm Synergi 4μ Hydro-RP 80A column, MeCN/H_2O gradient) to obtain 4 mg of a colorless oil. IR (film on KBr) 3428 (br), 2965, 2930, 2873, 1711, 1632, 1431, 1410, 1284, 1252, 1212, 1158, 968, 795 cm^{-1}. ^1H NMR (500 MHz, $CDCl_3$) δ 5.79 (s, 1H), 5.49 (dt, *J* = 15.4, 6.2 Hz, 1H), 5.42 (dt, *J* = 15.4, 6.4 Hz, 1H), 2.73 (d, 6.2 Hz, 2H), 2.44 (t, *J* = 7.4 Hz, 2H), 2.35 (dt, *J* = 6.4, 7.0 Hz, 2H), 2.16 (t, *J* = 7.7 Hz, 2H), 1.44 (h, *J* = 7.5 Hz, 2H), 0.92 (t, *J* = 7.3 Hz, 3H). ^{13}C NMR (75 MHz, $CDCl_3$) δ 178.9, 141.4, 130.5, 128.1, 113.1, 37.9, 33.7, 32.2, 27.4, 20.2, 13.9. HRMS (EI): calcd for $C_{11}H_{18}O_2Cl$ (M+H): 217.0990, found 217.0995.

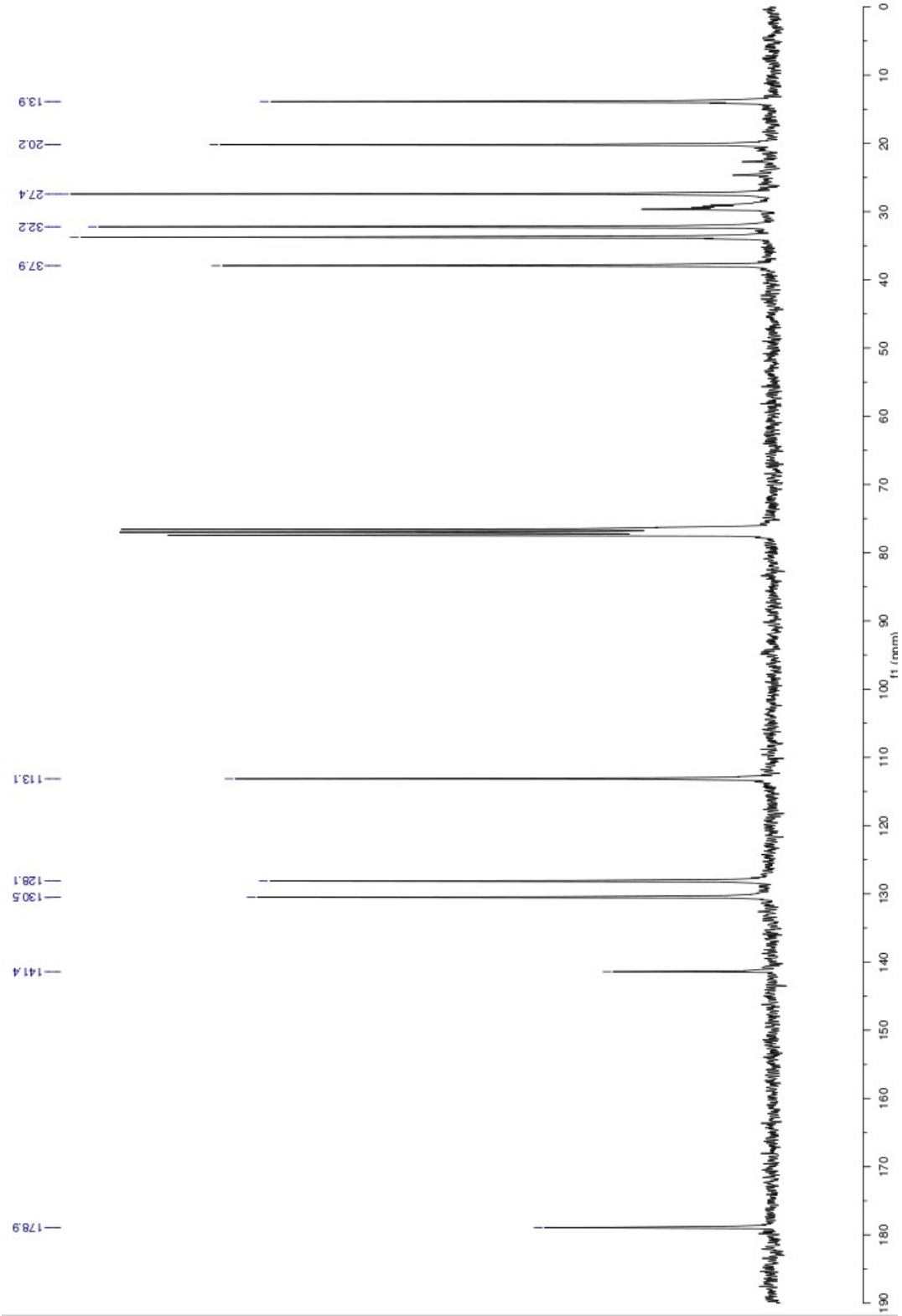

Figure III.9: Credneric Acid (38) ^{13}C NMR Spectrum in $CDCl_3$

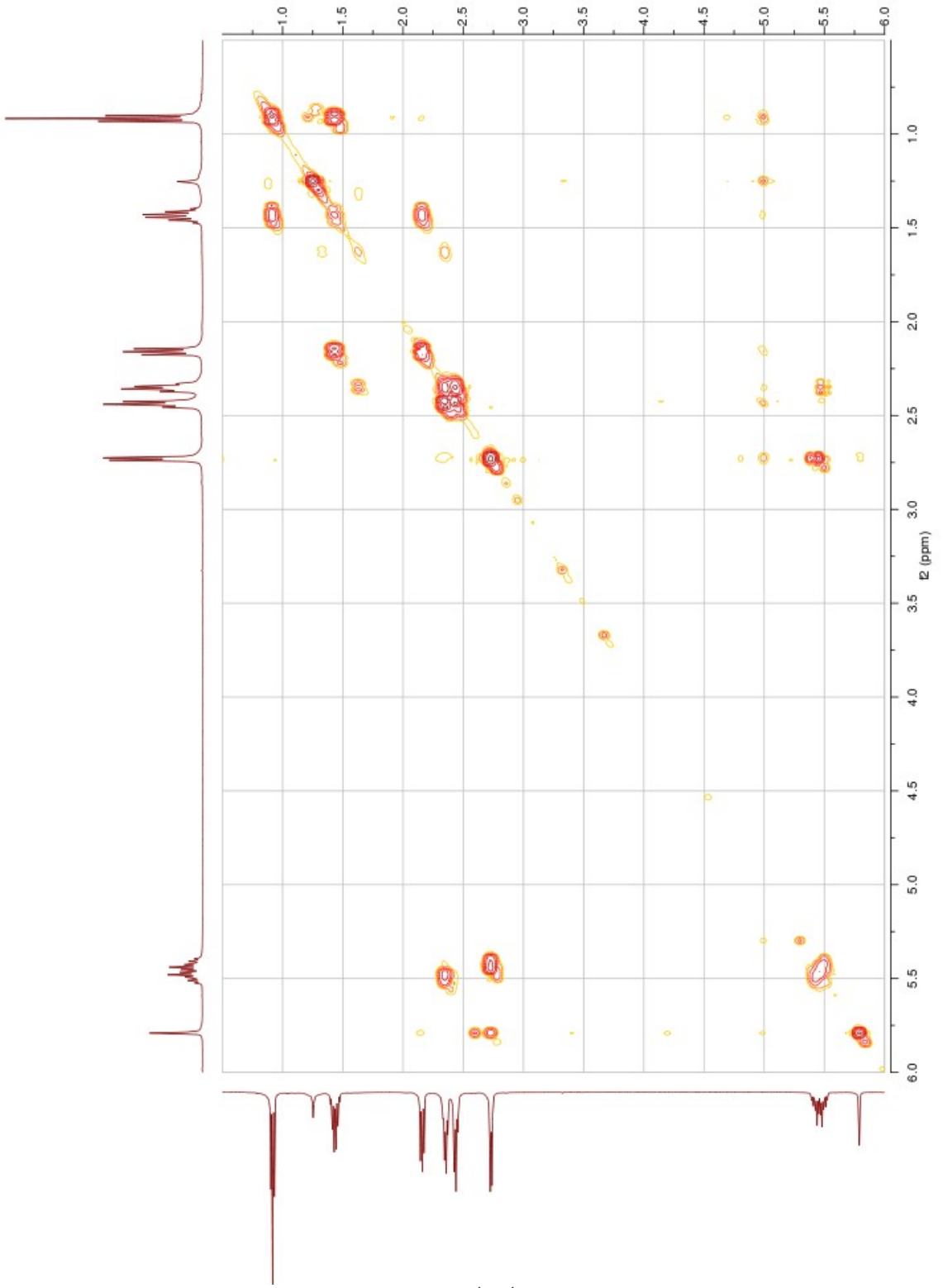

Figure III.10: Credneric Acid (38) ^{1}H-^{1}H COSY Spectrum in $CDCl_3$

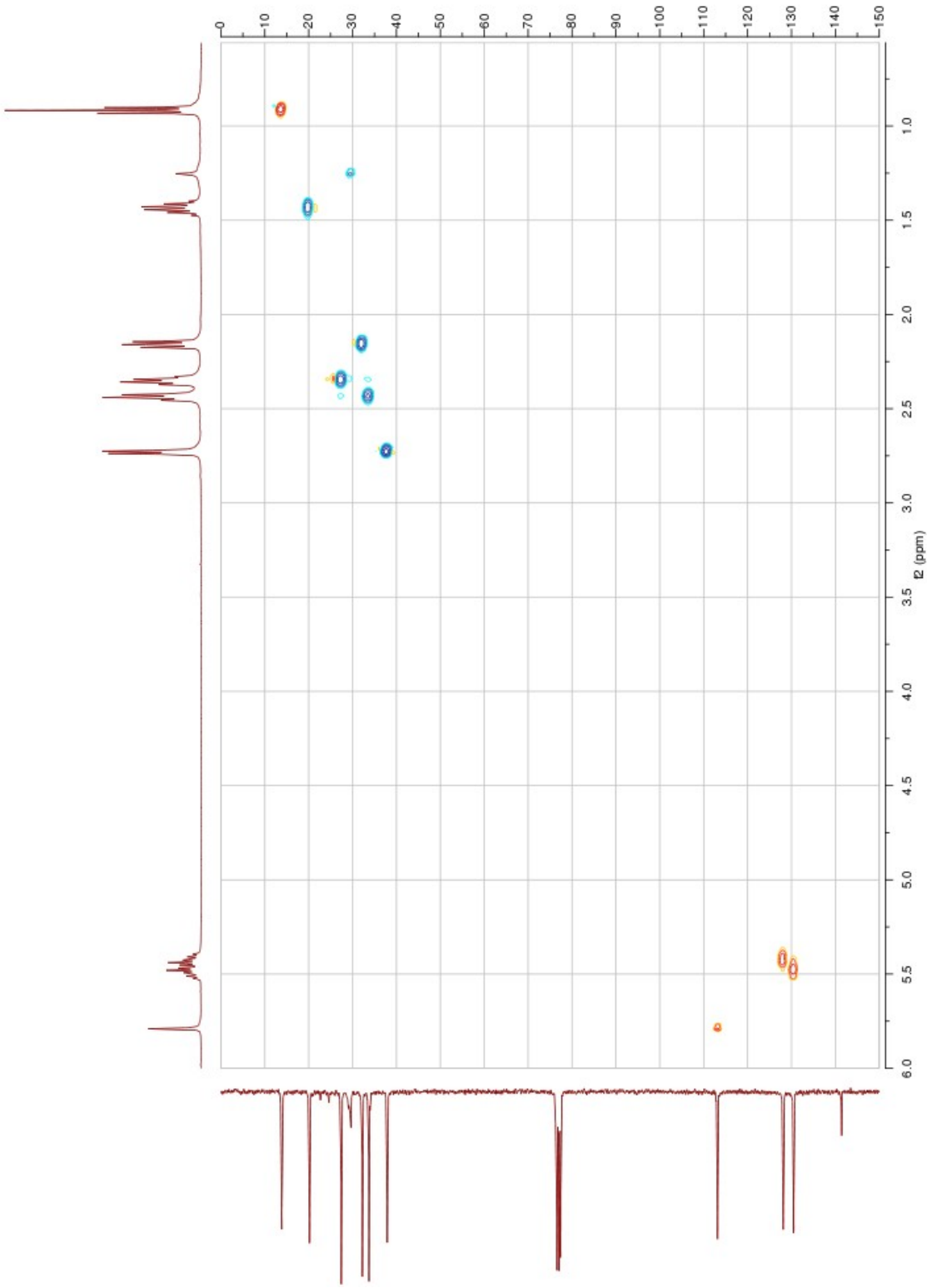

Figure III.11: Credneric Acid (**38**) ^{1}H-^{13}C HSQC Spectrum in $CDCl_3$

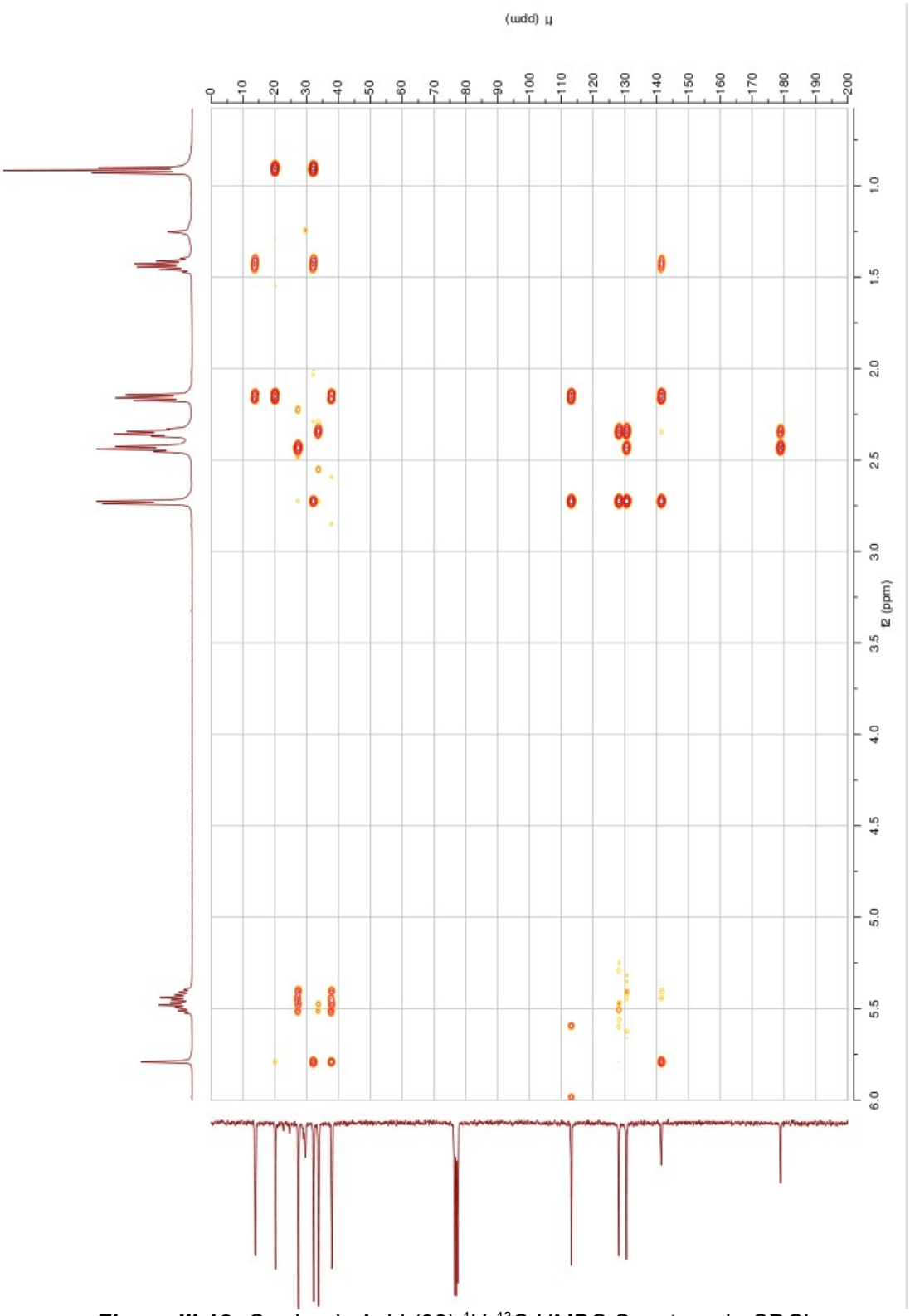

Figure III.12: Credneric Acid (**38**) ^{1}H-^{13}C HMBC Spectrum in $CDCl_3$

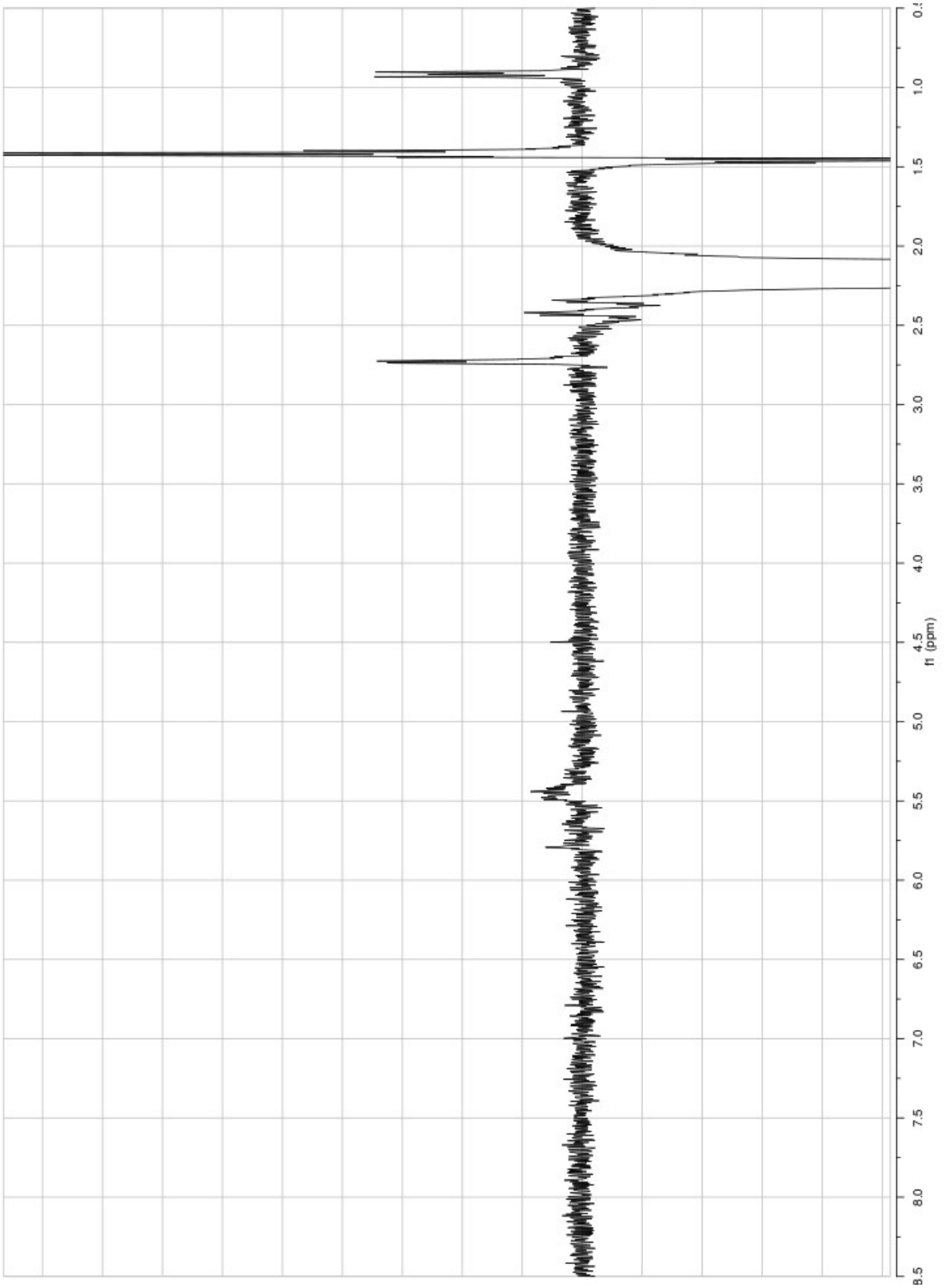

Figure III.13: Credneric Acid (**38**) 1D ROESY Spectrum: Irradiated at 2.73 ppm in $CDCl_3$

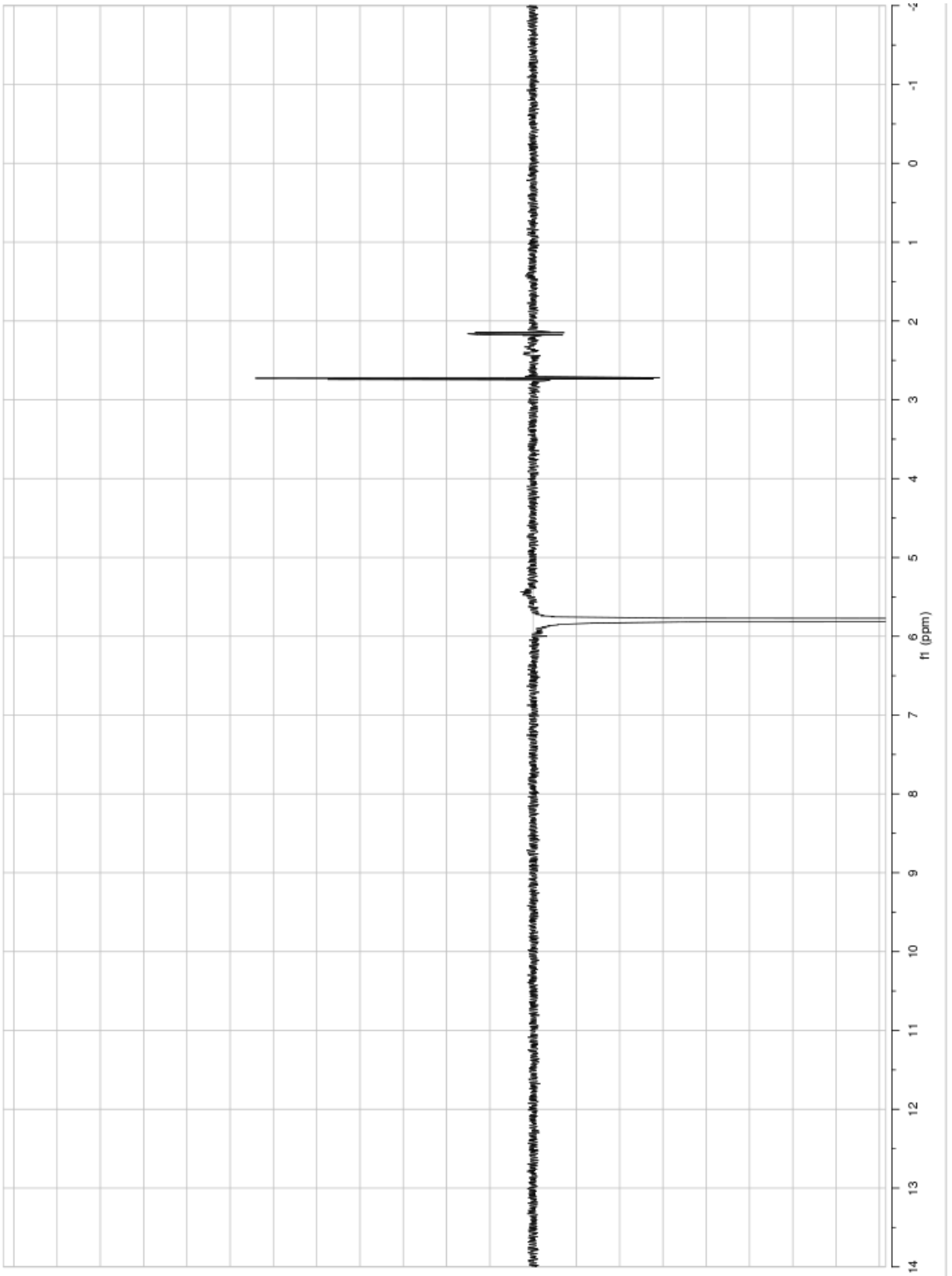

Figure III.14: Credneric Acid (**38**) 1D ROESY Spectrum: Irradiated at 5.79 ppm in $CDCl_3$

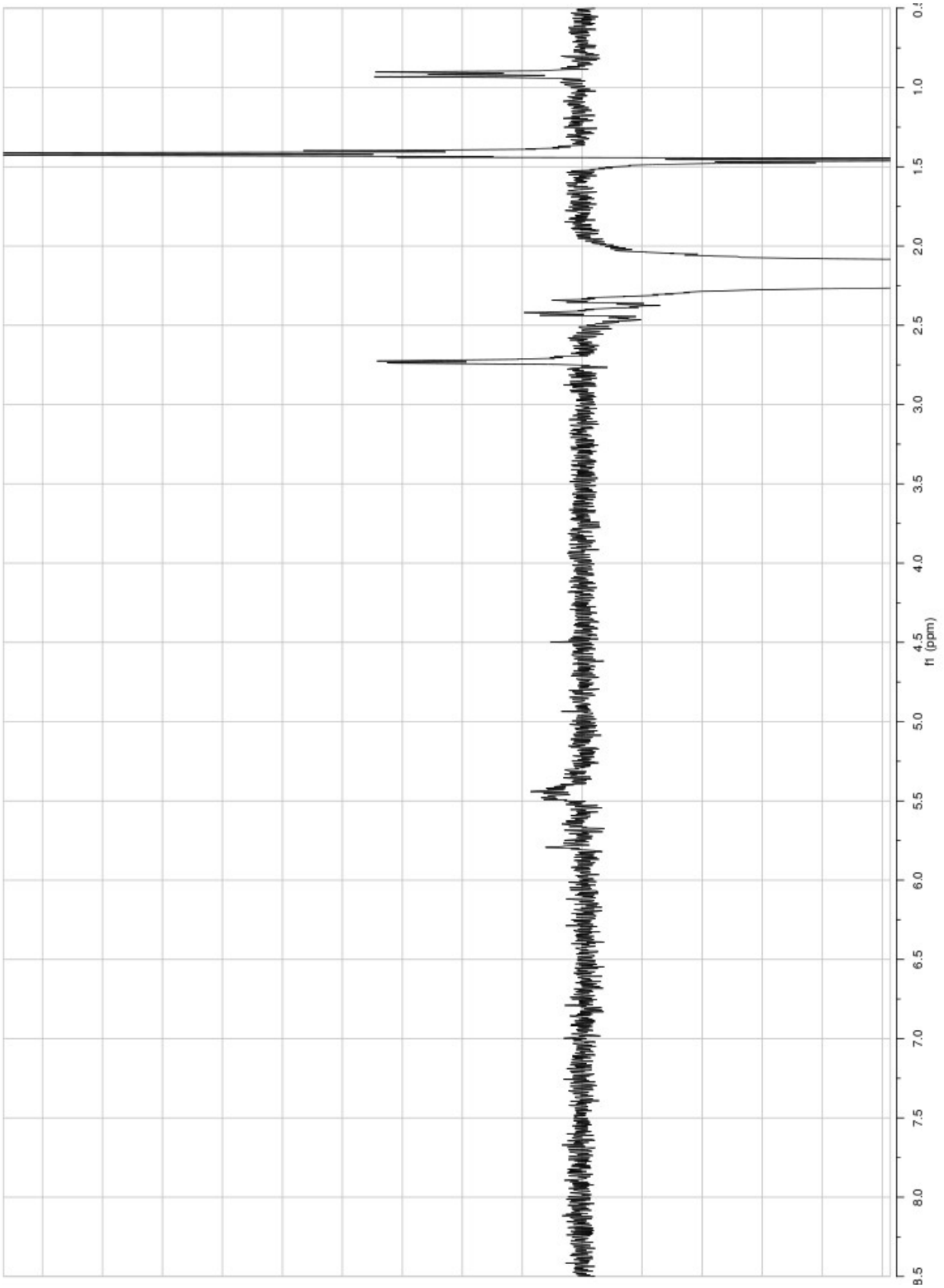

Figure III.15: Credneric Acid (**38**) 1D ROESY Spectrum: Irradiated at 2.16 ppm in $CDCl_3$

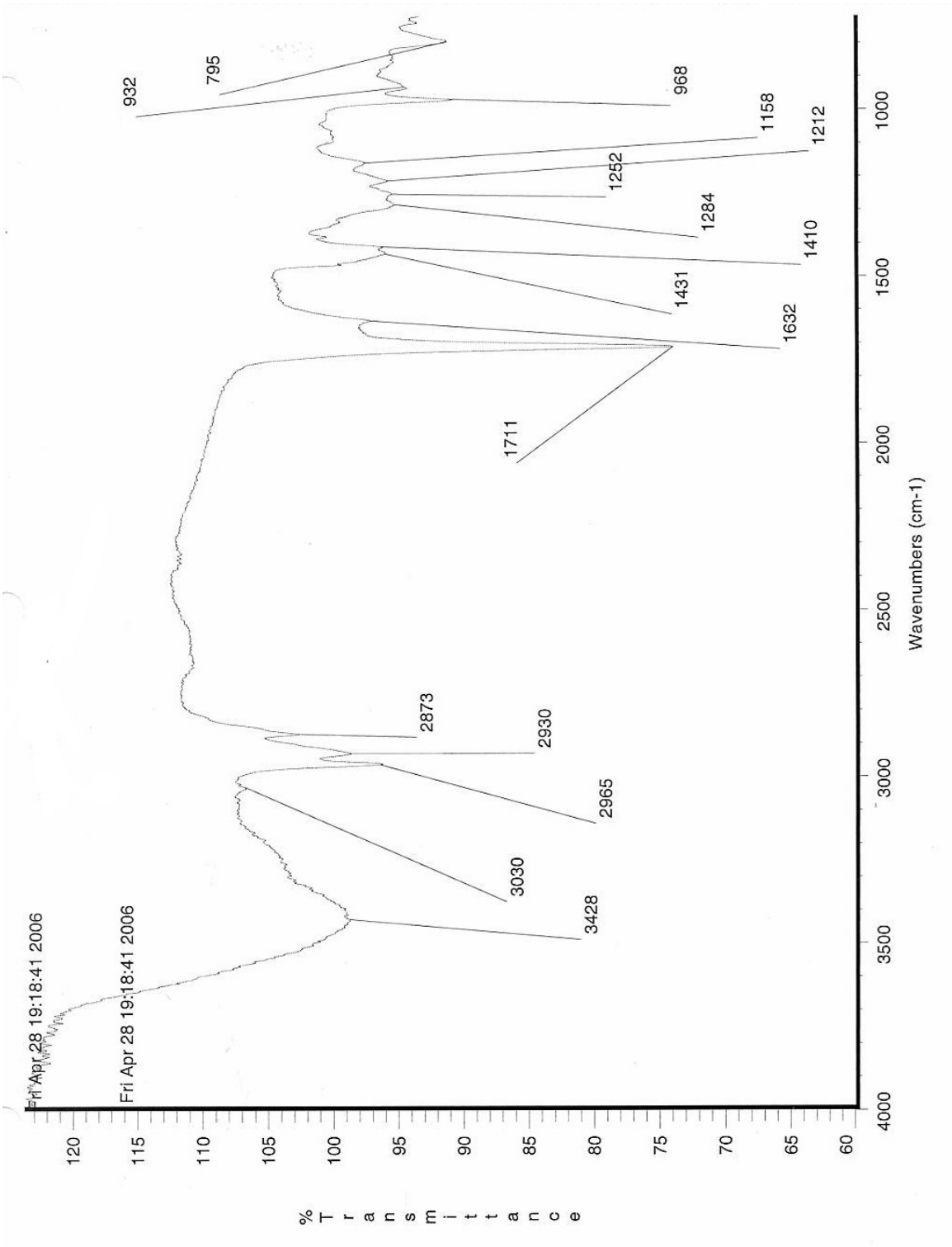

Figure III.16: IR spectrum of **38**

References and Footnotes

1 Gerwick, W. H.; Tan, L. T.; Sitachitta, N. *The Alkaloids*; Cordell, G. A., Ed.; Academic Press; San Diego, CA **2001**; Vol. 57, pp 75-184.

2 Edwards, D. J.; Marquez, B. L.; Nogle, L. M.; McPhail, K.; Goeger, D. E.; Roberts, M. A.; Gerwick , W. H. Structure and biosynthesis of the jamaicamides, new mixed polyketide-peptide neurotoxins from the marine cyanobacterium *Lyngbya majuscula*. *Chemistry & Biology* **2004**, *11*, 817–833.

3 (a) Appleton, D. R.; Sewell, M. A.; Berridge, M. V.; Copp, B. R. A new biologically active malyngamide from a New Zealand collection of the sea hare *Bursatella leachii*. *J. Nat. Prod.* **2002**, *65*, 630-631. (b) Kan, Y.; Sakamoto, B.; Fujita, T.; Nagai, H. New malyngamides from the Hawaiian cyanobacterium *Lyngbya majuscula*. *J. Nat. Prod.* **2000**, *63*, 1599-1602. (c) Gallimore, W. A.; Scheuer, P. J. Malyngamides O and P from the sea hare *Stylocheilus longicauda*. *J. Nat. Prod.* **2000**, *63*, 1422-1424. (d) Milligan, K. E.; Marquez, B.; Williamson, R. T.; Davies-Coleman, M.; Gerwick, W. H. Two New Malyngamides from a Madagascan *Lyngbya majuscula*. *J. Nat. Prod.* **2000**, *63*, 965-968. (e) Kan, Y.; Fujita, T.; Nagai, H.; Sakamoto, B.; Hokama, Y. Malyngamides M and N from the Hawaiian red alga *Gracilaria coronopifolia*. *J. Nat. Prod.* **1998**, *61*, 152-155. (f) Wu, M.; Milligan, K. E.; Gerwick, W. H. Three new malyngamides from the marine cyanobacterium *Lyngbya majuscula*. *Tetrahedron* **1997**, *53*, 15983-15990. (g) Todd, J. S.; Gerwick, W. H. Malyngamide I from the tropical marine cyanobacterium *Lyngbya majuscula* and the probable structure revision of stylocheilamide. *Tetrahedron Lett.* **1995**, *36*, 7837-40. (h) Praud, A.; Valls, R.; Piovetti, L.; Banaigs, B. Malyngamide G: structure of a new chlorinated amide from a blue-green alga epiphytic on *Cystoseira crinita*. *Tetrahedron Lett.* **1993**, *34*, 5437-40. (i) Gerwick, W. H.; Reyes, S.; Alvarado, B. Two malyngamides from the Caribbean cyanobacterium *Lyngbya majuscula*. *Phytochem.* **1987**, *26*, 1701-4. (j) Ainslie, R. D.; Barchi, J. J., Jr.; Kuniyoshi, M.; Moore, R. E.; Mynderse, J. S. Structure of malyngamide C. *J. Org. Chem.* **1985**, *50*, 2859-62. (k) Cardellina, J. H., II; Marner, F. J.; Moore, R. E. Malyngamide A, a novel chlorinated metabolite of the marine cyanophyte *Lyngbya majuscula*. J. Am. Chem. Soc. **1979**, *101*, 240-2. (l) Cardellina, J. H., II; Dalietos, D.; Marner, F. J.; Mynderse, J. S.; Moore, R. E. (-)-trans-7(S)-Methoxytetradec-4-enoic acid and related amides from the marine cyanophyte *Lyngbya majuscula*. *Phytochem.* **1978**, *17*, 2091-5.

4 Garson M. J. Marine mollusks from Australia and New Zealand: chemical and ecological studies. *Prog. Mol. Subcell. Biol.* **2006**, *43,* 159-74.

5 Fischbach, M. A.; Walsh, C. T. Assembly-line enzymology for polyketide and nonribosomal peptide antibiotics: Logic, machinery, and mechanisms. *Chem. Rev.* **2006**, *106*, 3468-3496.

6 Dewick, P. M. *Medicinal natural products; a biosynthetic approach, 2nd Ed*. John Wiley & Sons Ltd. **2001**, pp 169-170.

7 Vaillancourt, F. H.; Yeh, E.; Vosburg, D. A.; Garneau-Tsodikova, S.; Walsh, C. T. Nature's inventory of halogenation catalysts: oxidative strategies predominate. *Chem. Rev.* **2006**, *106*, 3364–3378.

8 Gu, L.; Wang, B.; Kulkarni, A.; Geders, T. W.; Grindberg, R. V.; Gerwick, L.; Håkansson, K.; Wipf, P.; Smith, J. L.; Gerwick, W. H.; Sherman, D. H. Metamorphic enzyme assembly in polyketide diversification. Submitted for peer review.

9 This collection was made by Dr. Carla Sorrels.

10 The extracted alga was numbered as "WG-1560" for tracking purposes in the lab.

11 This work was done by Ms. Karla Malloy.

12 Nannini, C. J., "Novel secondary metabolites from a Madagascar collection of Lyngbya majuscula" (MS thesis, Oregon State University, 2002), Chapter II.

13 Uroz, S.; Dessaux, Y.; Oger, P. Quorum sensing and quorum quenching: the Yin and Yang of bacterial communication. *ChemBioChem* **2009**, *10*, 205-216.

14 Still, W. C.; Khan, M.; Mitra, A. Rapid chromatographic technique for preparative separations with moderate resolution. *J. Org. Chem.* **1978**, *43*, 2923-2925.

Chapter IV

Absolute stereochemistry of novel fatty acids by synthetic introduction of a stereochemical reference

Abstract

A combined synthetic and spectroscopic method was developed to determine the absolute stereochemistry of an enatiomeric pair of novel fatty acids isolated from two collections of a marine cyanobacterium. Use of an oxazolidinone chiral auxiliary to transport stereochemical information over three bonds is described. However, a subsequent report of a total synthesis of a related natural product was in conflict with the results of this approach. There may have been an error in the NMR analysis of the cyclopropane fatty acid derivative or in the optical rotation measurement of the fatty acids themselves.

IV.1 Introduction

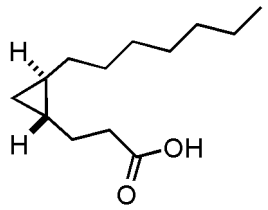

Cyclopropane containing fatty acid (**1**)

A Madagascar collection of the marine cyanobacterium *Lyngbya majuscula* yielded a series of novel cyclopropyl-ring containing fatty acid derivatives which possessed antifungal, neurotoxic and cannabinomimetic activities.[1] Co-occurring with these derivatives was significant quantities of the parent fatty acid (**1**). Subsequently, we isolated what appeared to be the identical fatty acid, based on ^{1}H, ^{13}C NMR, and FAB-MS data, from the same genus of cyanobacterium collected in Curaçao. However, the optical rotation values of these two samples were found to be opposite one another ($[\alpha]_D^{25}$ +19.3° for the Madagascar sample **1-m** and $[\alpha]_D^{25}$ –9.8° for the Curaçao sample **1-c**), a finding confirmed by converting both to their corresponding 4-bromobenzyl esters (**2**), purification, and measurement of the rotation value for these derivatives.[2] The Madagascar-derived 4-bromobenzyl ester gave an $[\alpha]_D^{25}$ +8.8° whereas the Curaçao fatty acid derivative showed $[\alpha]_D^{25}$ –7.9°.

The finding of two enantiomeric forms of **1** from two different collections of the same marine cyanobacterium motivated us to determine the absolute stereochemistry of each in order to gain insight into the biological properties of the two series as well as the

biogenesis of the cyclopropyl ring. However, no enantiospecific synthesis of this class of fatty acids had been reported at the outset of this project. Initial attempts to crystallize the 4-bromobenzyl-esterified fatty acids for crystallographic analysis failed, and hence, we were inspired to develop a new strategy for their stereochemical determination. The use of a Mosher ester was discounted because this technique is limited to the configurational assignment of a chiral center immediately adjacent to the derivatizable site.[3] However, it was realized that the carboxyl functionality in **1** provided an opportunity for the addition of a chiral auxiliary which could then be used through a diastereospecific reaction to introduce a chiral appendage at C-2. We then envisioned that this latter appendage could be related to chiral centers present in the natural product using a variety of NMR techniques (nOe and *J* values). To our knowledge, this strategy which interfaces the power of chirally-induced chemical synthesis with NMR spectroscopy has never been applied to a natural product structure elucidation.

IV.2 Synthetic introduction of stereochemical reference (SISTER) method

Both enantiomers of the cyclopropyl fatty acid (**1**) were isolated from the Madagascar and Curaçao collections of *L. majuscula* by a combination of silica gel VLC and flash column chromatography. The chiral auxiliary, (*S*)-(+)-4-benzyl-2-oxazolidinone (**3**), was condensed with each acid to produce imide derivatives **4** and **5** (Scheme IV.1). The same reaction was repeated with (*R*)-(+)-4-benzyl-2-oxazolidinone as the chiral auxiliary and the Madagascar-derived cyclopropyl fatty acid (**1-m**) to produce imide derivative **6**. Each of these imides was methylated under standard conditions to produce

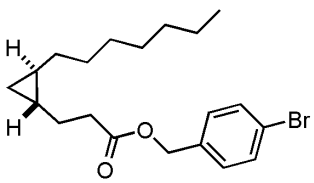

4-bromobenzyl ester of cyclopropane fatty acid **1** (**2**)

α-methyl derivatives **7** (from **4**), **8** (from **5**) and **9** (from **6**). For all three synthetic sequences, only a single stereoisomer was observed as the final reaction product (**7**-**9**).

The ^{1}H NMR of **7** and **8** showed distinctive chemical shifts and splitting patterns for the cyclopropane ring protons, confirming that they were indeed diasteriomeric to one other, and thus **1-m** and **1-c** were indeed enantiomers. However, the ^{1}H NMR spectrum of **8** was identical to that of **9**, indicating that these derivatives were enantiomeric. This was substantiated by measuring similar rotations of opposite sign for **8** (+48°) and **9** (-25°). Since **8** and **9** have opposite absolute stereo-configurations of both the oxazolidinone (*S* and *R*, respectively) and the cyclopropane ring (+ and -), the stereochemistry of the α-methyl carbon in these two derivatives must be opposite to each other as well. Because **7** and **9** possess different relative stereochemistries between the cyclopropyl ring and the α-methyl group, as evidenced by their different NMR spectra, we conclude that the asymmetric alkylation was exclusively controlled by the oxazolidinone stereochemistry and not the cyclopropyl ring stereochemistry. The overriding influence of the auxiliary during the conversion of **6** to **9** was predicted based on the rationale that the long alkyl chain would be as far away from ionic lithium-chelated six-membered ring as possible during the alkylation transition state, thus overcoming any mismatching effects during

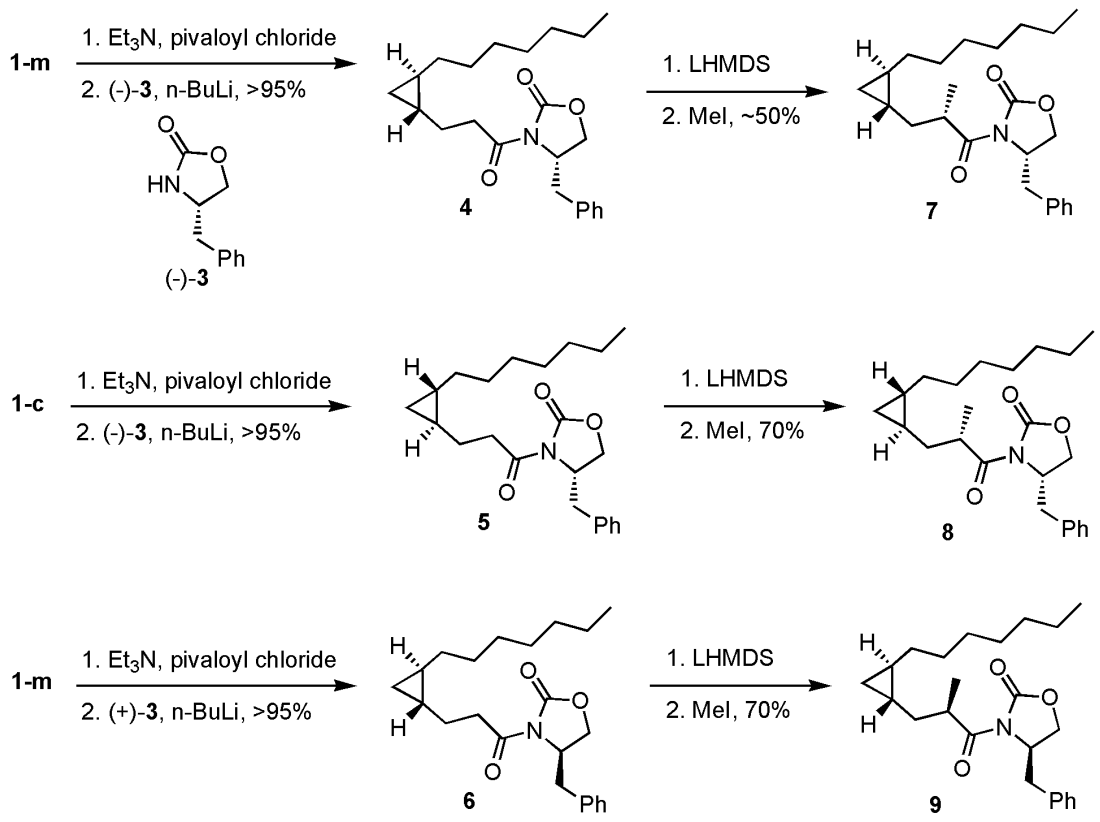

Scheme IV.1: Derivatization of cyclopropane fatty acids **1-m** and **1-c**

Note that the depicted absolute stereochemistry is according to the findings obtained through this SISTER method (*vide infra*).

this reaction (Figure IV.1). Hence, the stereochemistry of the α-methyl group in **7** and **8** was *S* whereas it was *R* in derivative **9**.

A variety of NMR techniques (^{1}H-COSY, homonuclear decoupled ^{1}H NMR, iterative spin simulation, phase-sensitive E.COSY, and 2D ROESY) were applied to relate the stereochemistry of the α-methyl group to that of the cyclopropyl bridgehead stereocenters in derivatives **7** and **8**. First, all proton chemical shifts were assigned for all three derivatives (**7**-**9**) using ^{1}H-^{1}H COSY data. The values of the key ^{1}H-^{1}H coupling constants for **7** and **8** were determined by a combination of ^{1}H NMR, homonuclear

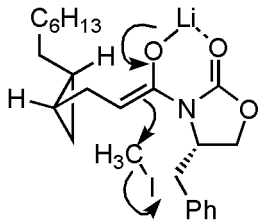

Figure IV.1: Proposed transition state of alkylation of the enolate of **5** guided by oxazolidinone auxiliary

decoupled ^{1}H NMR, and X-WIN NMR spin simulation program. These were in good agreement with those obtained from the phase-sensitive E.COSY experiment.

Using the Karplus-type equation proposed by Altona,[4] the dihedral angles between the key bonds were estimated (Figure IV.2). Alternatively, the Karplus-type equation proposed by Barfield and Smith,[5] which takes into consideration the bond angles, did not yield reasonable dihedral angles (Table IV.1). Despite the fact that the key coupling constants are all similar to each other (around 7 Hz), a qualitative trend was seen in the calculated dihedral angles. For example, the dihedral angle predicted from the ROESY analyses for $H^{3\alpha}$-C^{3}-$C^{1'}$-$H^{1'}$ is larger (60°) than that for $H^{3\beta}$-C^{3}-$C^{1'}$-$H^{1'}$ and the coupling constant is indeed larger for $H^{3\beta}$-$H^{1'}$ than for $H^{3\alpha}$-$H^{1'}$ (Figure IV.2). Detailed analysis of ROESY experiments led to the identification of 13 relevant dipolar interactions for derivative **7** and 17 for derivative **8**. The relative stereochemistry predicted between the α-methyl center and cyclopropyl ring centers by these two approaches were in excellent agreement (Figure IV.2). Finally, the energy minimized structures of both **7** and **8** were simulated through conformer distribution (molecular mechanics) and geometry optimization (Hartree-Fock) calculations and compared with those obtained from the Altona calculations and the ROESY data.[6] All three lines of evidence converge to

establish compound **7** as having 1*R*, 2*R*, 2´S stereochemistry and compound **8** to have 1*S*, 2*S*, 2´*S* stereochemistry (Figure IV.2).

Table IV.1: Dihedral angles calculated or simulated by different methods for **7** and **8**

Dihedral angles from Spartan were calculated with semi-empirical PM3; those from ROESY were estimated manually using a molecular model kit; those from Altona & Barfield equations were calculated from experimental coupling constants.

	7					**8**				
Protons	Altona	Barfield	Model	ROESY	Actual *J*	Actual *J*	ROESY	Model	Barfield	**Altona**
H^{2a}-H^{3a}	67°or171°	NA	89°	~60°	6.4	6.0	~60°	66°	NA	**169°or69°**
H^{2a}-H^{3b}	64°or173° or1.0°	NA	156°	~150°	7.2	7.3	~160°	177°	NA	**1.1°or64° or174**
H^{3a}-H^{4}	68°or172°	131°or34°	45°	~30°	6.5	6.9	~170°	163°	130°or36°	**173°or66°**
H^{3b}-H^{4}	**65°or174° or0.9°**	**133°or33°**	**67°**	**~70°**	**7.2**	**7.1**	**~70°**	**81°**	**131°or34°**	**66°or174°**

However, as this work was concluding, Baird and coworkers reported their total synthesis of (+)-grenadamide, which assigned the absolute configurations of this cyclopropyl fatty acid to be 1*R*, 2*R* (Scheme IV.2).[7] This result directly contradicted our work because (+)-**1** was assigned 1*S*, 2*S* in our hands whereas (+)-**1**, one of the intermediates in Baird's synthesis, was assigned 1*R*, 2*R*.[8] A number of possible explanations were considered: 1) Our stereochemical assignement was erroneous, 2) The optical rotation measured by us or Baid et al. had the wrong sign, 3) The stereochemical assignment of the chiral starting material that Baird et al. used was erroneous. It should be noted that the only other asymmetric synthesis of grenadamide was reported by Taylor and coworkers who simply correlated their absolute stereochemical assignments of their synthetic products with those of Baird's.[9] Therefore, Baird's work is the only source of contention with the results of our SISTER analysis.

After careful re-examination of our own assignments,[10] the third possibility mentioned above was evaluated through a literature search. The history of absolute stereochemistry assignment of the chiral cyclopropane fatty acid starting material is remarkably complex (Figure IV.3). It is interesting that the stereoconfiguration was never independently determined throughout the chain of citations. Instead, the absolute stereochemical assignments were correlated to previous literature through chemical transformations to reference compounds or through comparison of CD spectra. In fact, it is unclear how the original compound's absolute configuration was assigned in 1927 (Figure IV.3) because the first absolute stereochemical assignments (tartaric acid) were made in 1951 by Bijvöt et al. through X-ray crystallography.[11]

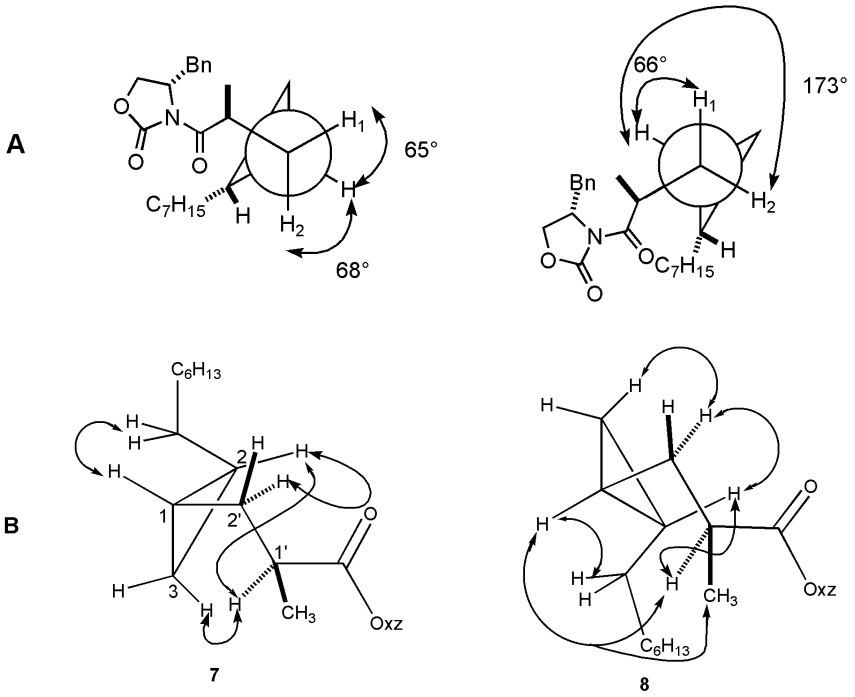

Figure IV.2: Dihedral angles predicted from the ^{1}H-^{1}H coupling constants and Altona equation (A) and select ROESY correlations for **7** and **8** (B).

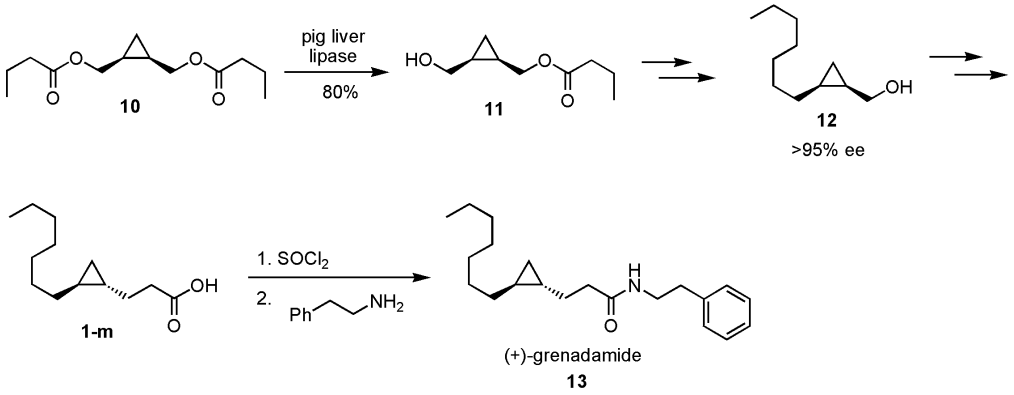

Scheme IV.2: Total synthesis of (+)-grenadamide (**13**) by Baird et al.

Here lies the weakness of the modern scientific research; so much of our work relies heavily on the previous work, but often without any verification due to time constraints. It is therefore admirable that so many natural product chemists have re-visited the structures of natural products that were previously characterized and have

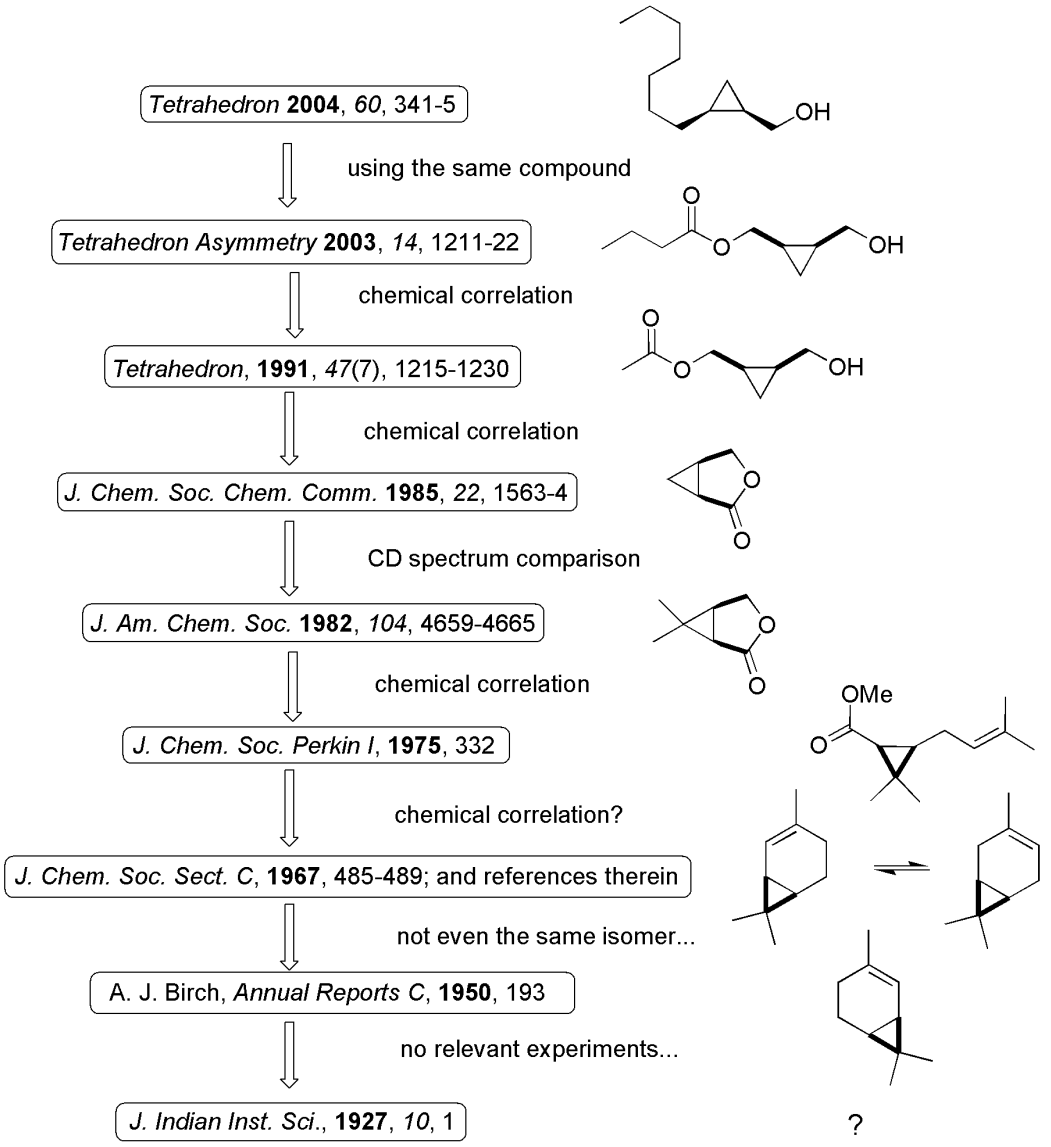

Figure IV.3: History of the absolute stereochemical assignment of cyclopropane derivative **11**

found a significant number of them to be incorrect through more or less independent means.[12] Synthetic chemists, by default, synthesize the reported structures and are able to discover errors in the structure assignment as an additional benefit of the synthetic work. However, re-visiting a natural product's structure is not an activity that natural product chemists often perform as it requires much diligence and rigor.

Although it would be difficult to determine at what point in the chain of citations any erroneous stereochemical assignments may have occurred, it is relatively trivial to independently verify the absolute configurations of the cyclopropane starting material **11** used by Baird et al. Thus, the synthesis of **11** was performed according to literature.[13] X-ray crystallography was considered the best choice of stereochemical assignment due to its unequivocal nature. However, various derivatives of **11** could not be crystallized in a suitable form for crystallographic work.

Subsequently, **11** was converted to **15** for modified Mosher's analysis (Scheme IV.3). Careful 1D and 2D NMR analysis of **15** and **16** indicated that the C-2 position had *S* configuration, which is consistent with Baird's assignment. However, an NOE correlation was observed between H-1 and H-4, which suggested that the cyclopropane ring had a *trans* relative stereochemistry (Figure IV.4). Considering that α-epimerization of **14** was possible during chromium oxidation to the carboxylic acid (Scheme IV.3), the C-2 stereocenter was assigned to be *S*, contradicting Baird's work. To independently verify or discount this assignment, a suitable crystal of **15** was obtained for X-ray crystallographic analysis. To our grief, the crystal structure revealed that the

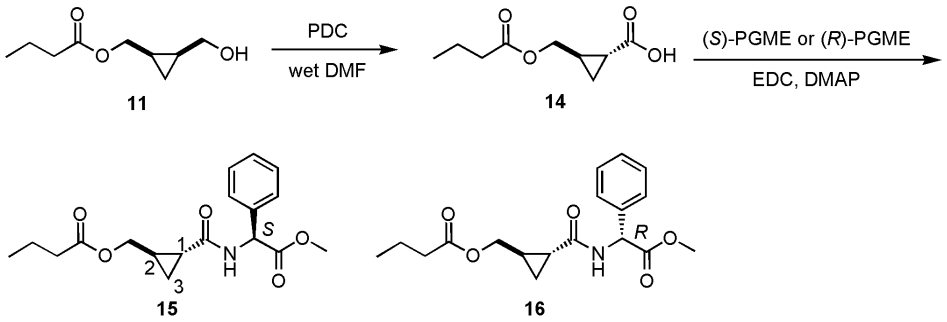

Scheme IV.3: Synthesis of PGME derivatives from **11**

Note that the stereochemistry of **14** is drawn as *trans*. However, it was later discovered to be *cis* (vide infra).

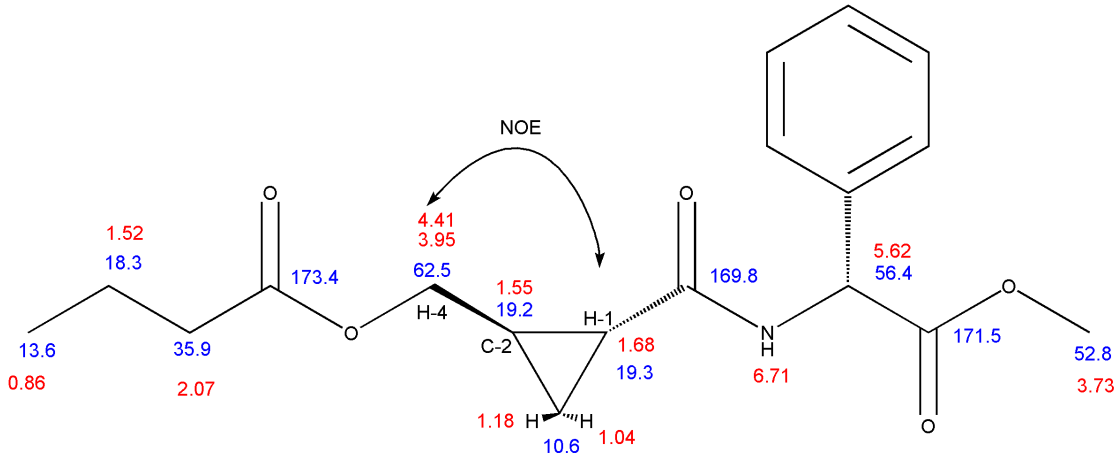

Figure IV.4: ^{1}H and ^{13}C NMR assignments and an NOE correlation of **16** in $CDCl_3$

The structure is shown as *trans* due to the NOE correlation observed between H-1 and H-4. However, the relative sterechemistry was later shown to be *cis* based on an X-ray crystal structure of **15** (Figure IV.5). The ^{1}H and ^{13}C assignments were made through the use of COSY, HSQC, and HMBC spectra in conjunction with the ^{1}H and ^{13}C NMR spectra. The ^{1}H chemical shifts are shown in red and the ^{13}C chemical shifts are shown in blue.

cyclopropane ring retained its *cis* configuration (Figure IV.5). This result unequivocally assigns the absolute configurations of **1-m** to be 1*S*, 2*S* (Figure IV.6), thereby re-affirming Baird's assignment of grenadamide.

The final explanation to be evaluated for reconciling our work and Baird's work was to ascertain the validity of optical rotation values obtained for **1-m** and **1-c**. Of the many structure determination tools utilized by natural product chemists today, the polarimeter is perhaps the most error-prone instrument. It is extremely sensitive to chiral contamination, and depending on the condition of the light source, different values can be obtained for the same sample. Moreover, unlike spectra obtained from NMR or MS, optical rotation values usually do not leave substantial records of their measurement. The optical rotation value obtained by C. Nannini ($[\alpha]_D$ –7.6° for **1-c**)[1] was consistent with

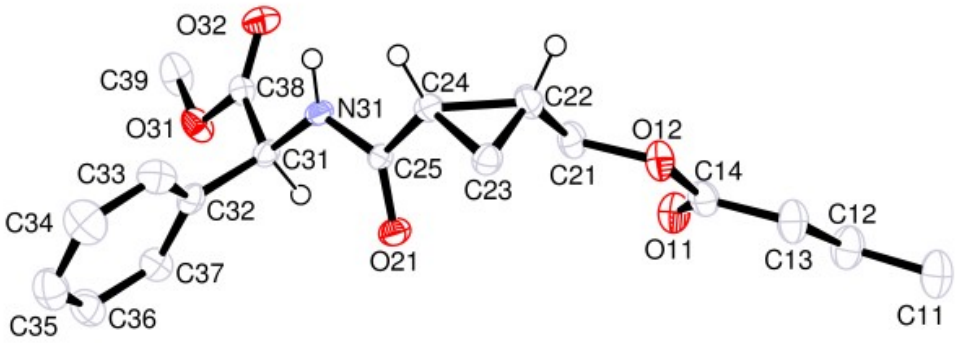

Figure IV.5: X-ray crystal structure of **15**

This crystal structure unequivocally showed that the stereochemistry of the carboxylic acid **14** is *cis*. The NOE correlation between the proton on C24 and C21 (Figure IV.4) could not be explained.

this work ($[\alpha]_D$ –9.8° for 1-c). Therefore, it is unlikely that any human error, such as mislabeling of the samples, was introduced.

IV.4 Conclusions

A pair of enantiomeric natural products were isolated from the same genus collected from different locations. We developed a new concept for determining absolute stereochemistry of natural products (i.e. the SISTER method, Figure IV.7). However, X-ray crystallographic investigation indicated that either our ROESY and *J*-based analysis was incorrect or one of the optical rotation values was wrong. It may require a re-collection of the algal material to resolve the confusion that has plagued this project.

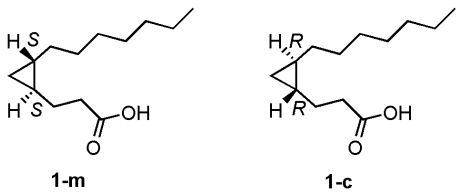

1-m **1-c**

Figure IV.6: Corrected stereochemistry of **1-m** and **1-c**

However, as shown in Figure IV.3, the ultimate origin of the absolute stereochemical assignment of the cyclopropane derivative **11** is unclear. Therefore, it is possible that the absolute configurations of **11** were never fully determined, but that its arbitrary assignments happened to be the correct ones. After all, there is always a fifty-fifty chance in the art of assigning absolute stereochemistry.

IV.5 Experimental Section

General

UV and IR spectra were recorded on a Beckman DU 640B UV spectrophotometer and a Nicolet 510 spectrophotometer, respectively. NMR spectra were recorded either at a ^{1}H resonance frequency of 600.04 MHz (Bruker DRX 600) or 400.13 MHz (Bruker DPX 400). The Bruker DRX 600 was equipped with a Bruker Q-Switch TXI probe and the DPX 400 was equipped with a Bruker BBO probe. All chemical shifts are reported relative to residual $CHCl_3$ (δ_H 7.27, δ_C 77.23) or C_6HD_5 (δ_H 7.16) as internal standard. HRMS were obtained on a Kratos MS 50 TC mass spectrometer. Optical rotations were measured with a Perkin-Elmer model 243 polarimeter. HPLC was performed using Waters 515 pumps and a Waters 996 photodiode array spectrophotometer. TLC grade (10-40 mesh) silica gel was used for vacuum chromatography, and Merck aluminum-backed TLC sheets (Silica gel 60 F_{254}) were used for TLC. All solvents were purchased as HPLC grade. THF and triethylamine were freshly distilled before they were used (from Na-benzophenone and CaH_2, respectively). (*R*)-and-(*S*)-4-benzyl-2-oxazolidinones, fatty acids (**1-m** and **1-c**), and the amide derivatives (**7**, **8**, and **9**) were dried with a

vacuum pump before use in synthetic reactions. Other reagents were used without any purification unless specified. All reagents, except for the natural fatty acids **1-m** and **1-c** and the solvents were purchased from Sigma-Aldrich. All reactions were carried out under argon.

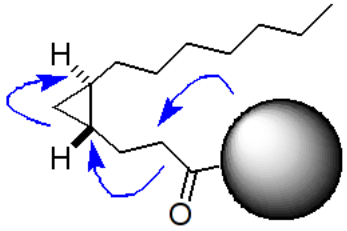

Figure IV.7: Synthetic Introduction of a Stereochemical Reference (SISTER) method conceptual figure

The blue arrows indicate the flow of stereochemical information from a synthetically introduced chiral group (gray ball).

Isolation of (1'*S*, 2'*S*)-3'-(2-heptyl-cyclopropyl)-propionic acid (1-m) and (1*R*, 2*R*)-3´-(2-heptyl-cyclopropyl)-propionic acid (1-c). Metabolite **1-m** was isolated from the crude extract of a Madagascar collection of *L. majuscula* by silica gel flash chromatography. The eluent composition was gradually changed from CH_2Cl_2 to acetonitrile/CH_2Cl_2 (1:9). The same procedure was used to purify **1-c** from a Curaçao collection of this cyanobacterium. A total of 42.7 mg of crude **1-m** and 23.3 mg of crude **1-c** were isolated. Due to the inherently poor chromatographic properties of these fatty acids, these crude materials with relatively low purity were used for subsequent reactions without additional purification.

Synthesis of (1′*R*, 2′*R*, 4′′′*S)*-4′-Benzyl-3′′′-[3-(2′-heptyl-cyclopropyl)-propionyl]-oxazolidin-2′′′-one (5). In 300 μL of THF were dissolved 23.3 mg crude **1-c** which was cooled to -78°C. To this solution were added pivaloyl chloride (17 μL, 0.14 mmol) and triethylamine (16 μL, 0.11 mmol). The reaction mixture was stirred and allowed to warm to RT from -78°C over a period of 1 hour. Meanwhile, (*S*)-(-)-4-benzyl-2-oxazolidinone (58.7 mg, 0.331 mmol) was dissolved in 300 μL of THF and cooled to -78°C. To this solution was added 185 μL of 2.0 M n-butyllithium solution in cyclohexane (0.37 mmol) and the reaction mixture was stirred for 20 minutes. The lithiated oxazolidinone solution was transferred to the solution of the mixed anhydride at -78°C. This reaction was stirred and allowed to warm up to RT over 24 hours, and then quenched with 5 mL of aqueous 1 M NH_4Cl solution and the aqueous layer extracted with CH_2Cl_2 (3 × 5 mL). The organic layer was subsequently washed with 5 mL of H_2O and dried with $MgSO_4$. The concentrated mixture was analyzed by TLC (MeOH/CH_2Cl_2, 1:19) which showed that no starting material (**2**) was present, thus indicating a yield >95%. The resultant mixture was purified by silica gel flash chromatography with CH_2Cl_2 as eluent to yield 36.2 mg of a pale-yellow oil. This was used for subsequent reactions without further purification. ^{1}H NMR ($CDCl_3$; 400MHz) δ 0.23 (2H, m, 3′-CH_2), 0.49 (2H, m, 1′-CH and 2′-CH), 0.88 (3H, t, J = 6.9 Hz, 7′′-CH_3), 1.26 (12H, m, alkyl chain), 1.60 (2H, m, 3-CH_2), 2.75 (1H, dd, J = 13.2 Hz, 9.7 Hz, Bn-CH_2), 3.02 (2H, m, 5′′′-CH_2), 3.31 (1H, dd, J = 13.3 Hz, 3.0 Hz, Bn-CH_2), 4.18 (2H, m, 2-CH), 4.67 (1H, m, 4′′′-CH), 7.19-7.36 (5H, m, phenyl); MS (FAB) 372.1 (M+1). Likewise, semi-purified compound **4** (111.4 mg, crude weight) was synthesized in the same manner starting with 42.7 mg of crude **1-m**.

Synthesis of (1′*R*, 2′*R*, 2*S*, 4‴*S*)-4‴Benzyl-3‴-[3-(2′-heptyl-cyclopropyl)-2-methyl-propionyl]-oxazolidin-2´´´-one (7). The amide **5** (31.2 mg, 84 μmol) was dissolved in 400 μL of THF and the solution was cooled to -78°C. Lithium hexamethyldisilazide (95 μL, 1.0 M solution in THF, 95 μmol) was added dropwise and the mixture was stirred for 20 minutes. Excess methyl iodide (55 μL) was added dropwise at -78°C and the reaction mixture was allowed to warm to RT over 6 hours. The reaction was then quenched with 4 mL of NH_4Cl aqueous solution and extracted with CH_2Cl_2 (3 ×5 mL). The combined organic layers were washed with 2 mL of H_2O and then dried with $MgSO_4$. The resulting mixture was concentrated under reduced pressure and passed through a short silica gel column followed by a C18 column (eluents were CH_2Cl_2 and MeOH, respectively). After evaporation of solvents under reduced pressure, 27.7 mg of crude material was recovered, and this was purified by HPLC using a reverse phase semi-preparative column (YMC, ODS-AQ, 250 × 10 mm I.D., 5 μm, 120 Å; H_2O/MeOH, 0.7:99.3). The major compound in the reaction mixture was the by-product, pivaloyl oxazolidinone; however, 2.1 mg of **7** were isolated. Based on the HPLC peak integration of **4** and **7** in the reaction mixture, the yield of **7** was estimated to be 70%. Only one isomer of the methylated product was observed. **8** and **9** were synthesized in the same manner and only one diastereomer was observed in each synthesis (50% and 60% yields, resepectively). Colorless oil; UV λ max 255 nm; IR υ 2923cm^{-1}, 1776 cm^{-1}, 1697cm^{-1}; ^{1}H NMR (C_6D_6; 400MHz) δ 0.27 (2H, m, 3′-CH_2), 0.58 (1H, m, 1′-CH), 0.62 (1H, m, 2′-CH), 0.91 (3H, t, J = 6.8 Hz, 7″-CH_3), 1.29 (12H, m, alkyl chain), 1.34 (3H, d, J = 7.0 Hz, 2-CCH_3), 1.46 (1H, ddd, J = 13.6 Hz, 6.5 Hz, 6.4 Hz, pro-*S*-3-CH_2), 1.84 (1H, ddd, J = 13.6 Hz, 7.2 Hz, 7.2 Hz, pro-*R*-3-CH_2), 2.29 (1H, dd, J = 13.4 Hz, 9.3 Hz, Bn-CH_2), 2.97 (1H, dd, J = 13.4 Hz, 3.0 Hz, Bn-CH_2), 3.20

(1H, dd, 5‴-CH_2), 3.46 (1H, dd, J = 9.1 Hz, 2.6 Hz, 5‴-CH_2), 4.14 (1H, ddt, J = 7.2 Hz, 7.0 Hz, 6.4 Hz, 2-CH), 4.25 (1H, m, 4‴-CH), 6.90-7.10 (5H, m, phenyl); ^{13}C NMR ($CDCl_3$; 100 MHz) δ 12.4, 14.3, 16.7, 17.5, 18.9, 22.9, 29.6, 29.7, 29.8, 32.1, 34.4, 38.1, 38.3, 38.4, 55.6, 66.2, 127.6, 129.2, 129.7, 135.6, 153.3, 177.5. $[\alpha]_D^{28}$ = + 48° (c = 1.2, $CHCl_3$).

(1′*R*, 2′*R*, 2*S*, 4‴*S*)-4‴-Benzyl-3‴-[3-(2′-heptyl-cyclopropyl)-2′-methyl-propionyl]-oxazolidin-2‴-one (8). Colorless oil; UV λ max 257 nm, IR υ 2918cm^{-1}, 1776 cm^{-1}, 1692cm^{-1} ; ^{1}H NMR (C_6D_6; 400MHz) δ 0.23 (1H, m, 3′-CH_2), 0.39 (1H, m, 3′-CH_2), 0.45 (1H, m, 2′-CH), 0.59 (1H, m, 1′-CH), 0.92 (3H, t, J = 6.9Hz, 7″-CH_3), 1.29 (12H, m, alkyl chain), 1.33 (3H, d, J = 7.0 Hz, 2-CCH_3), 1.43 (1H, ddd, J = 13.7 Hz, 6.9 Hz, 6.0 Hz, pro-*S*-3-CH_2), 1.84 (1H, ddd, J = 13.7 Hz, 7.3 Hz, 7.1 Hz, pro-*R*-3-CH_2), 2.30 (1H, dd, J = 13.4 Hz, 9.7 Hz, Bn-CH_2), 2.98 (1H, dd, J = 13.5 Hz, 2.7 Hz, Bn-CH_2), 3.22 (1H, dd, 5‴-CH_2), 3.47 (1H, dd, J = 9.0 Hz, 2.5 Hz, 5‴-CH_2), 4.16 (1H, ddq, 7.3 Hz, 7.0 Hz, 6.0 Hz, 2-CH), 4.23 (1H, m, 4‴-CH), (5H, m, phenyl); ^{13}C NMR ($CDCl_3$, 100MHz) δ 11.9, 14.3, 16.7, 17.4, 19.3, 22.9, 29.6, 29.7, 29.8, 32.1, 34.1, 38.1, 38.2, 55.7, 66.2, 127.5, 129.1, 129.7, 135.6, 153.3, 177.6. $[\alpha]_D^{28}$ = + 42° (c = 2.5, $CHCl_3$).

(1′*S*, 2′*S*, 2*R*, 4‴*R*)-4‴-Benzyl-3‴-[3-(2′-heptyl-cyclopropyl)-2′-methyl-propionyl]-oxazolidin-2‴-one (9). Colorless oil; IR υ 2924cm^{-1}, 1782 cm^{-1}, 1693cm^{-1} ; ^{1}H NMR (C_6D_6; 400MHz) δ 0.23 (1H, m, 3′-CH_2), 0.39 (1H, m, 3′-CH_2), 0.45 (1H, m, 2′-CH), 0.59 (1H, m, 1′-CH), 0.92 (3H, t, J = 6.9Hz, 7″-CH_3), 1.29 (12H, m, alkyl chain), 1.33 (3H, d,

J = 7.0 Hz, 2′-CCH_3), 1.43 (1H, ddd, J = 13.7 Hz, 6.9 Hz, 6.0 Hz, pro-*S*-3′-CH_2), 1.84 (1H, ddd, J = 13.7 Hz, 7.3 Hz, 7.1 Hz, pro-*R*-3′-CH_2), 2.30 (1H, dd, J = 13.4 Hz, 9.7 Hz, Bn-CH_2), 2.98 (1H, dd, J = 13.5 Hz, 2.7 Hz, Bn-CH_2), 3.22 (1H, dd, 5′′-CH_2), 3.47 (1H, dd, J = 9.0 Hz, 2.5 Hz, 5′′-CH_2), 4.16 (1H, ddq, 7.3 Hz, 7.0 Hz, 6.0 Hz, 2′-CH), 4.23 (1H, m, 4′′-CH); $[\alpha]_D^{28} = -25°$ (c = 9.5, $CHCl_3$).

Acknowledgement. We gratefully acknowledge helpful discussions with R. Kohnhert, the OSU Biochemistry and Biophysics NMR facility for use of the Bruker DRX600 NMR instrument (V. Hsu), the OSU Mass Spectrometry Facility (J. Moore).

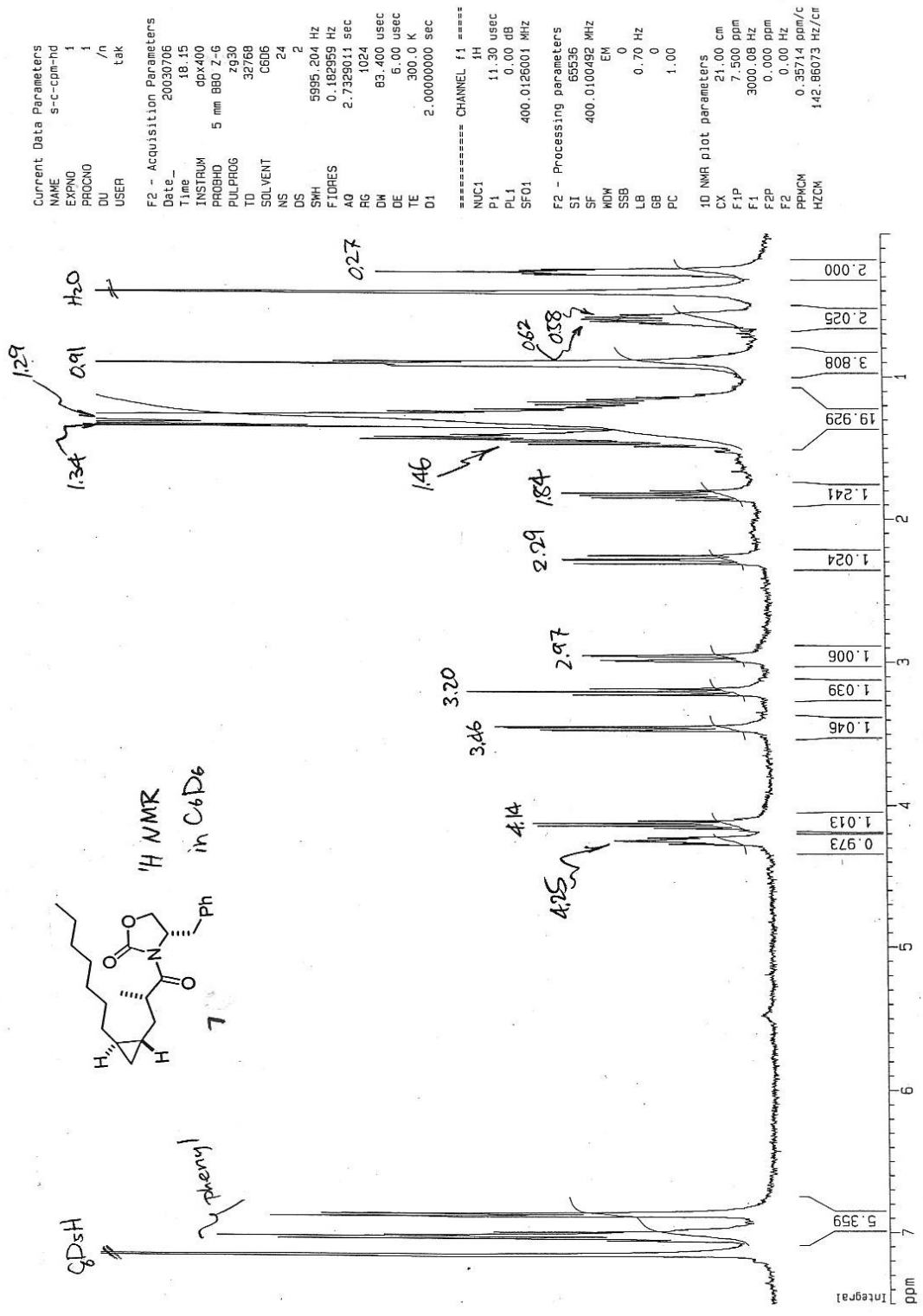

Figure IV.8: ^{1}H NMR spectrum of **7** in C_6D_6

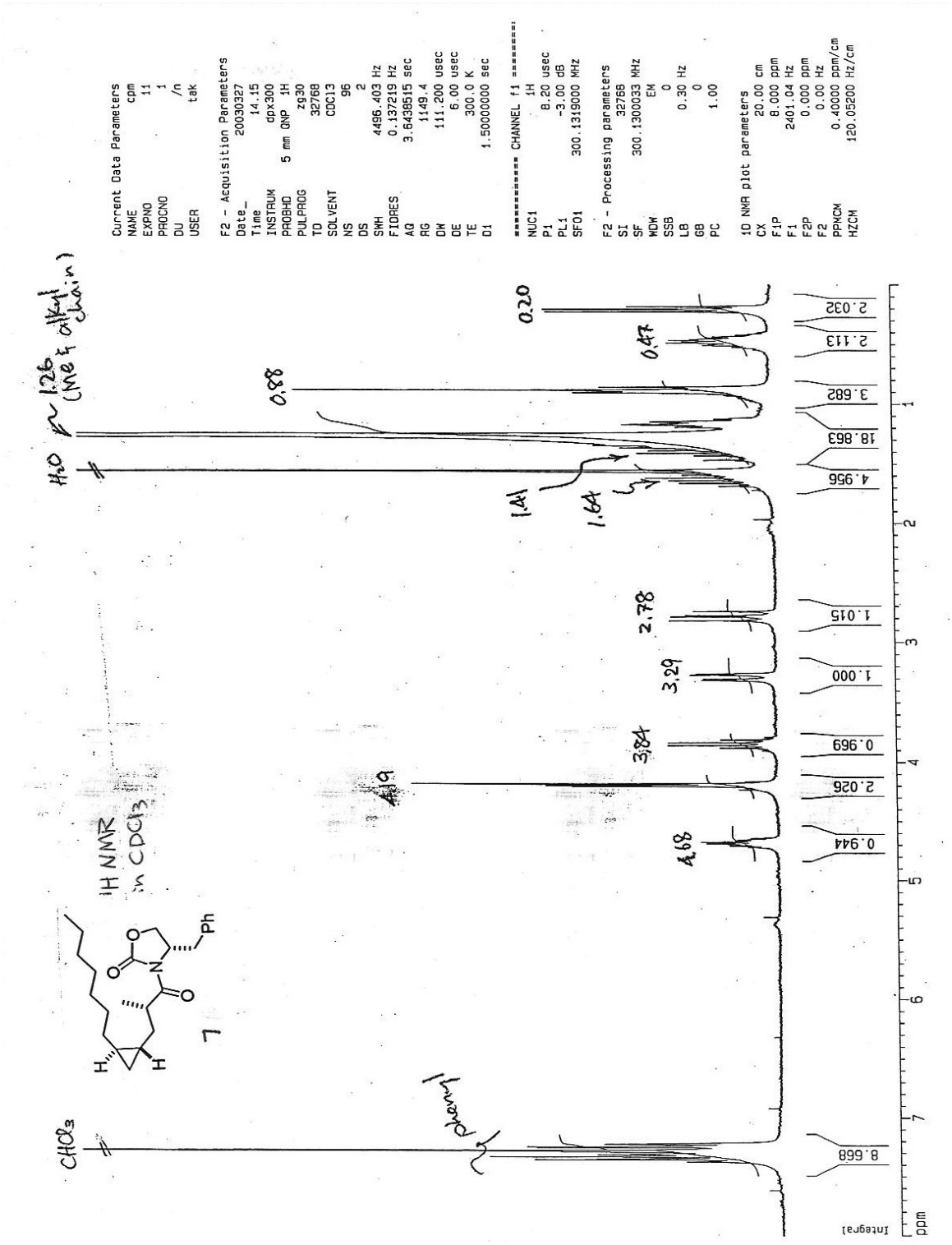

Figure IV.9: ^{1}H NMR spectrum of **7** in $CDCl_3$

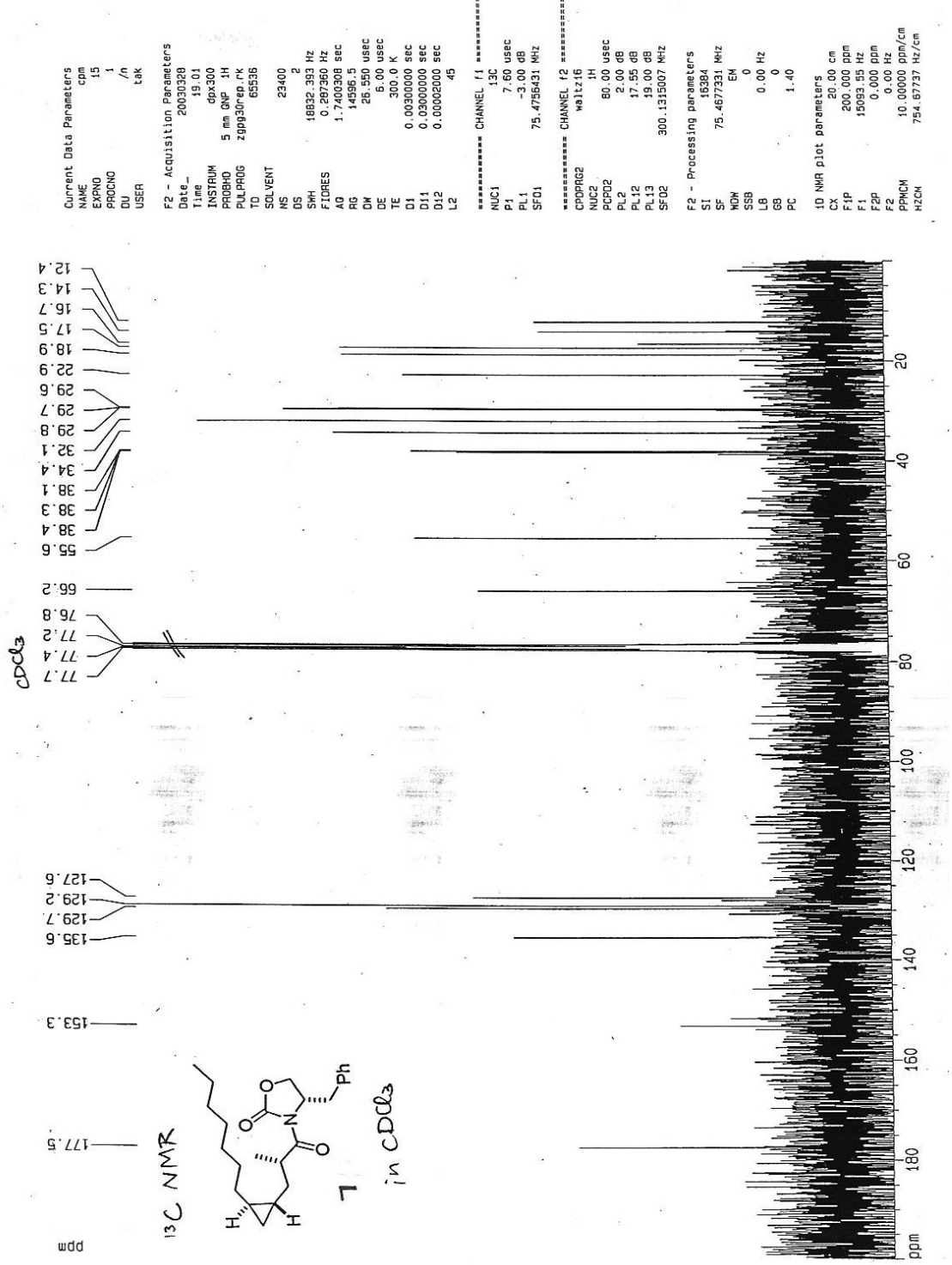

Figure IV.10: ^{13}C NMR spectrum of **7** in $CDCl_3$

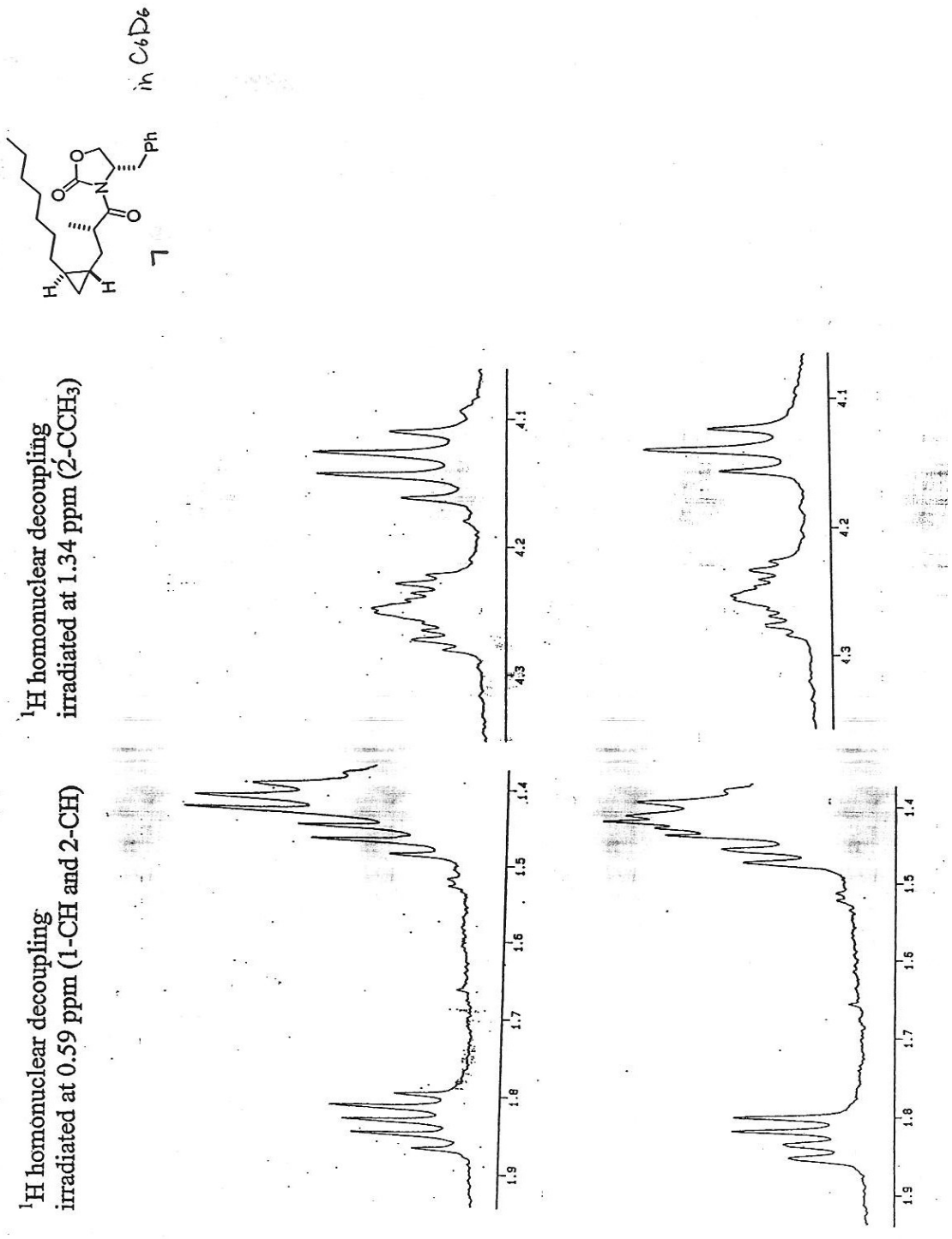

Figure IV.11: ^{1}H-^{1}H Homonuclear decoupling experiment for **7** in C_6D_6 – Part 1

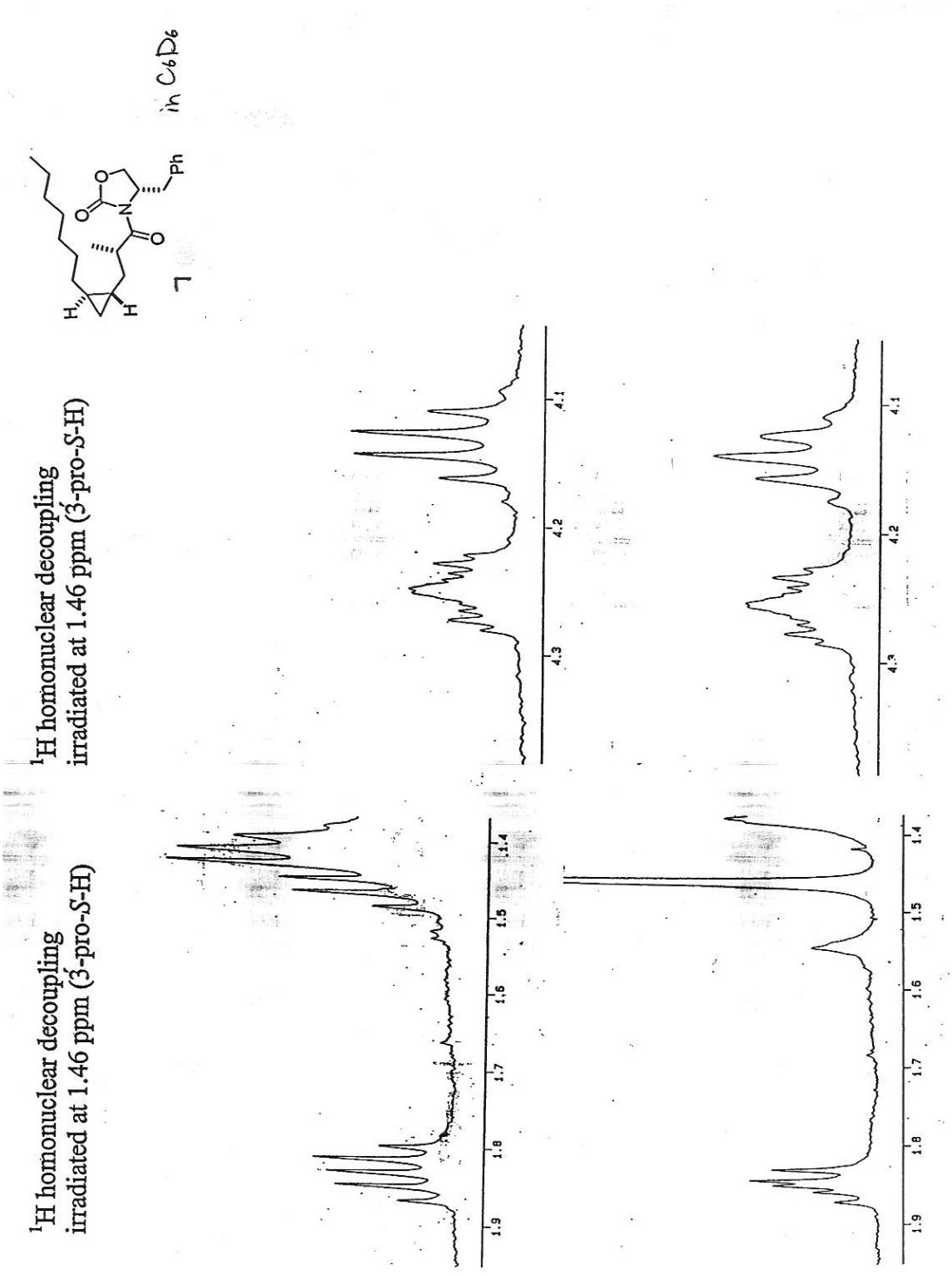

Figure IV.12: ^{1}H-^{1}H Homonuclear decoupling for **7** in C_6D_6 – Part 2

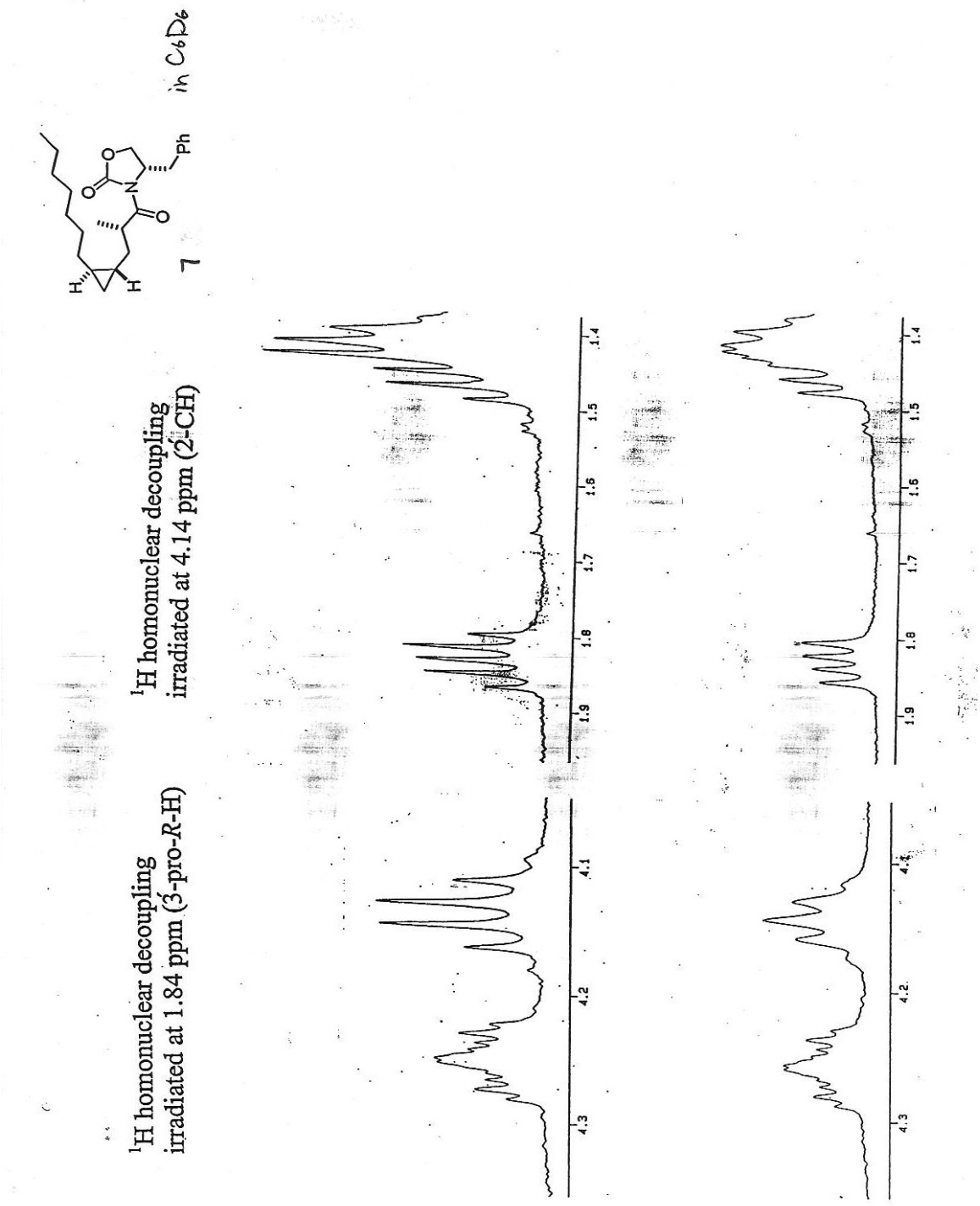

Figure IV.13: ^{1}H-^{1}H Homonuclear decoupling experiment for **7** in C_6D_6 – Part 3

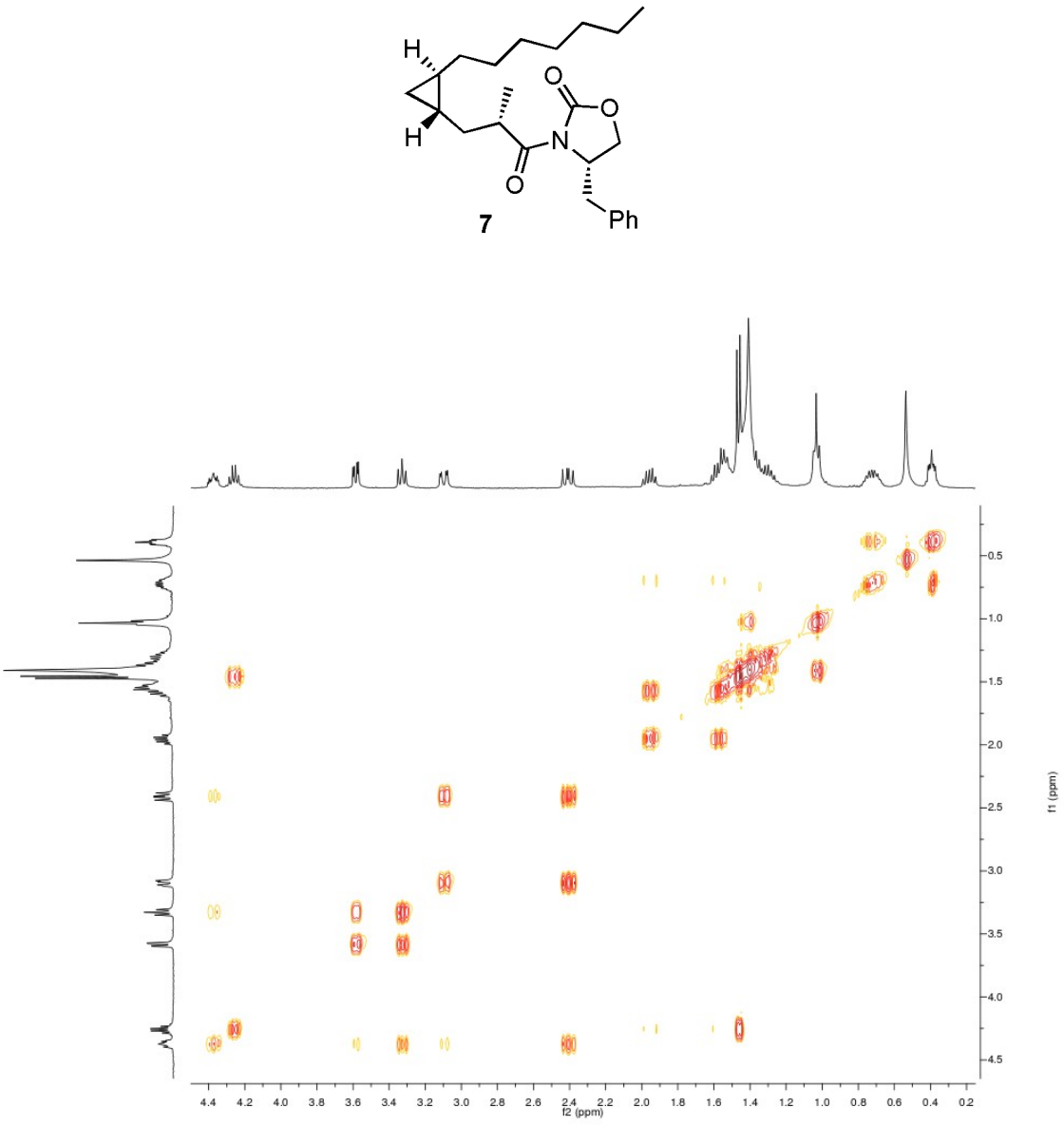

Figure IV.14: ^{1}H-^{1}H COSY spectrum of **7** in C_6D_6

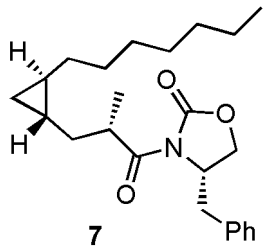

7

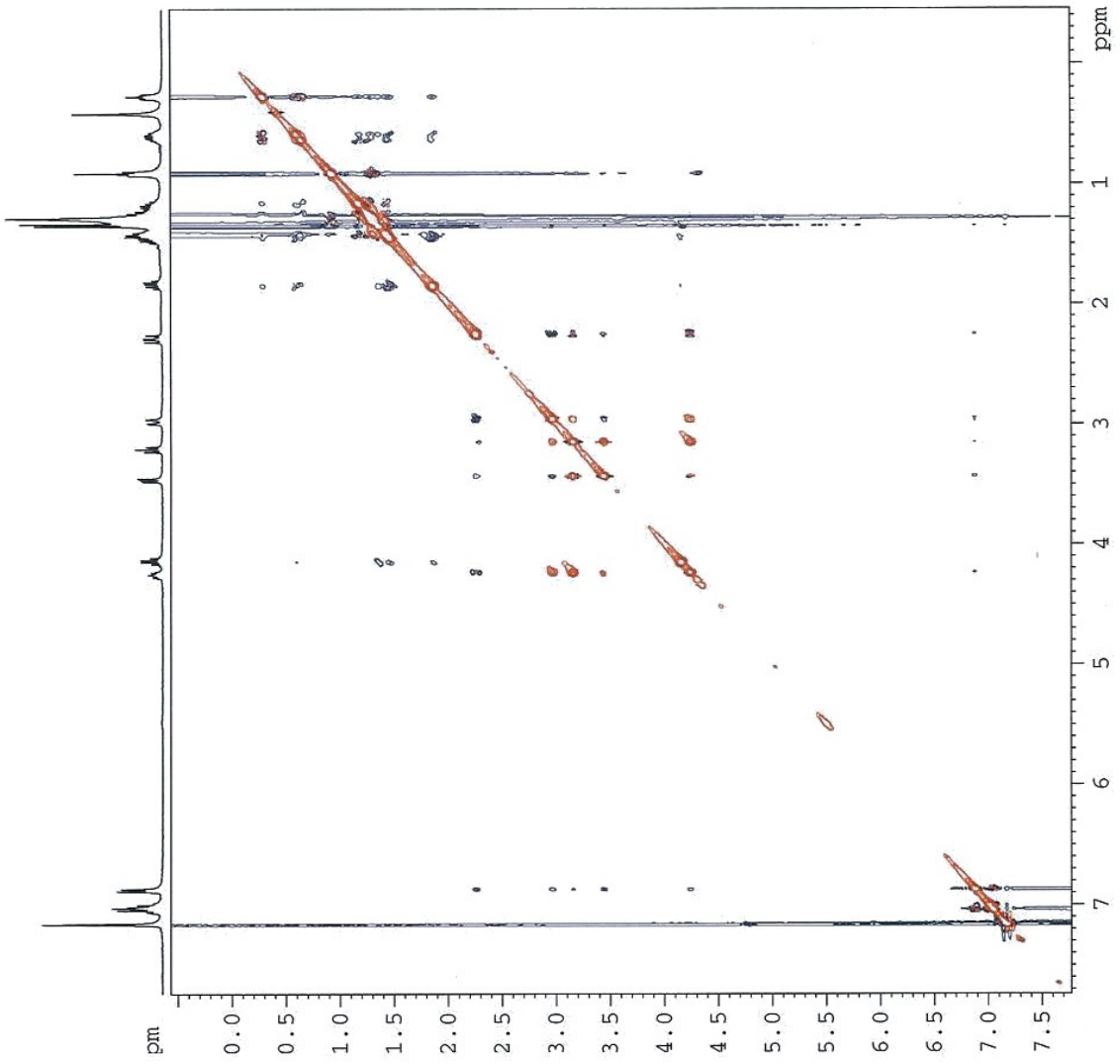

Figure IV.15: ROESY spectrum of **7** in C_6D_6

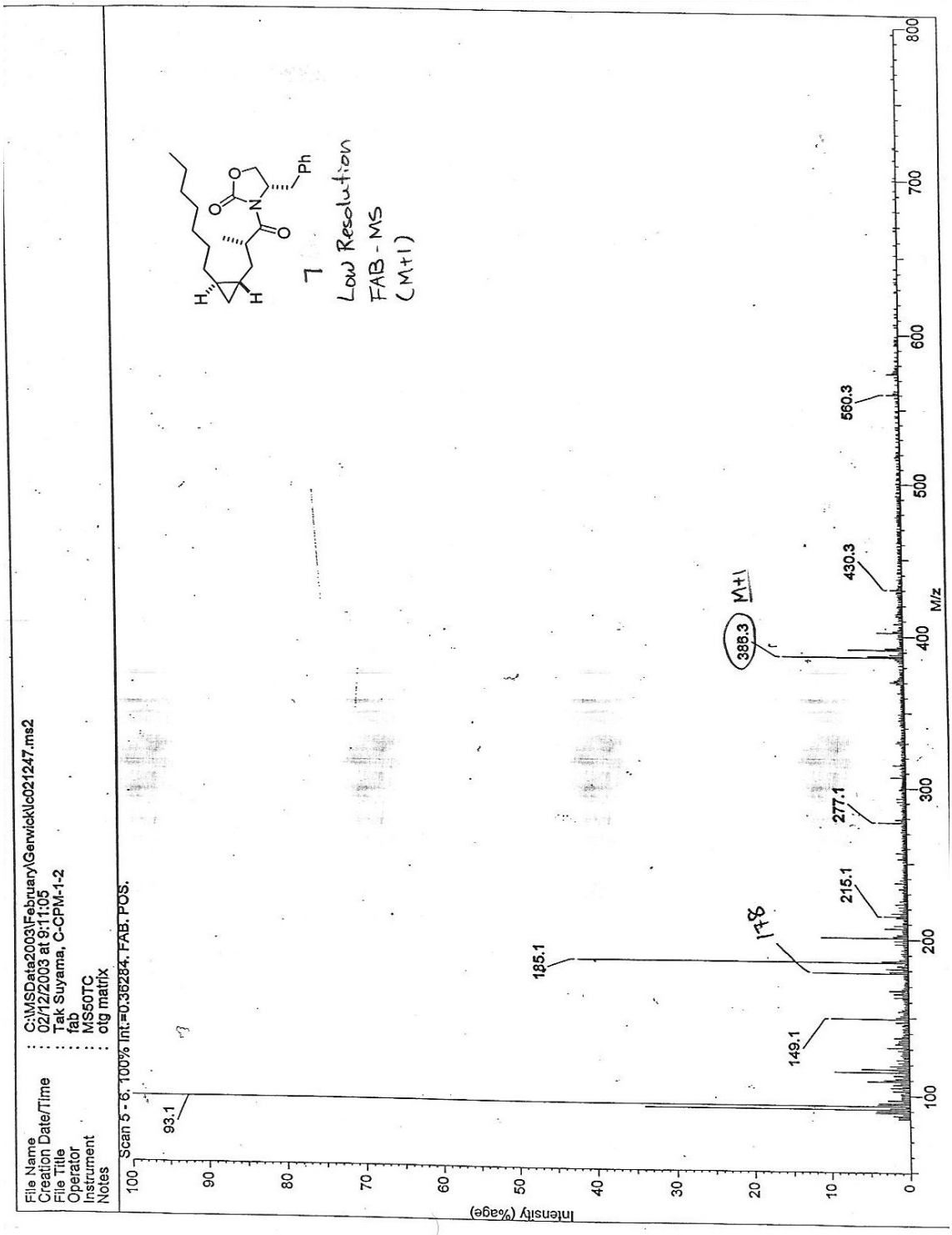

Figure IV.16: LR FAB MS spectrum of **7**

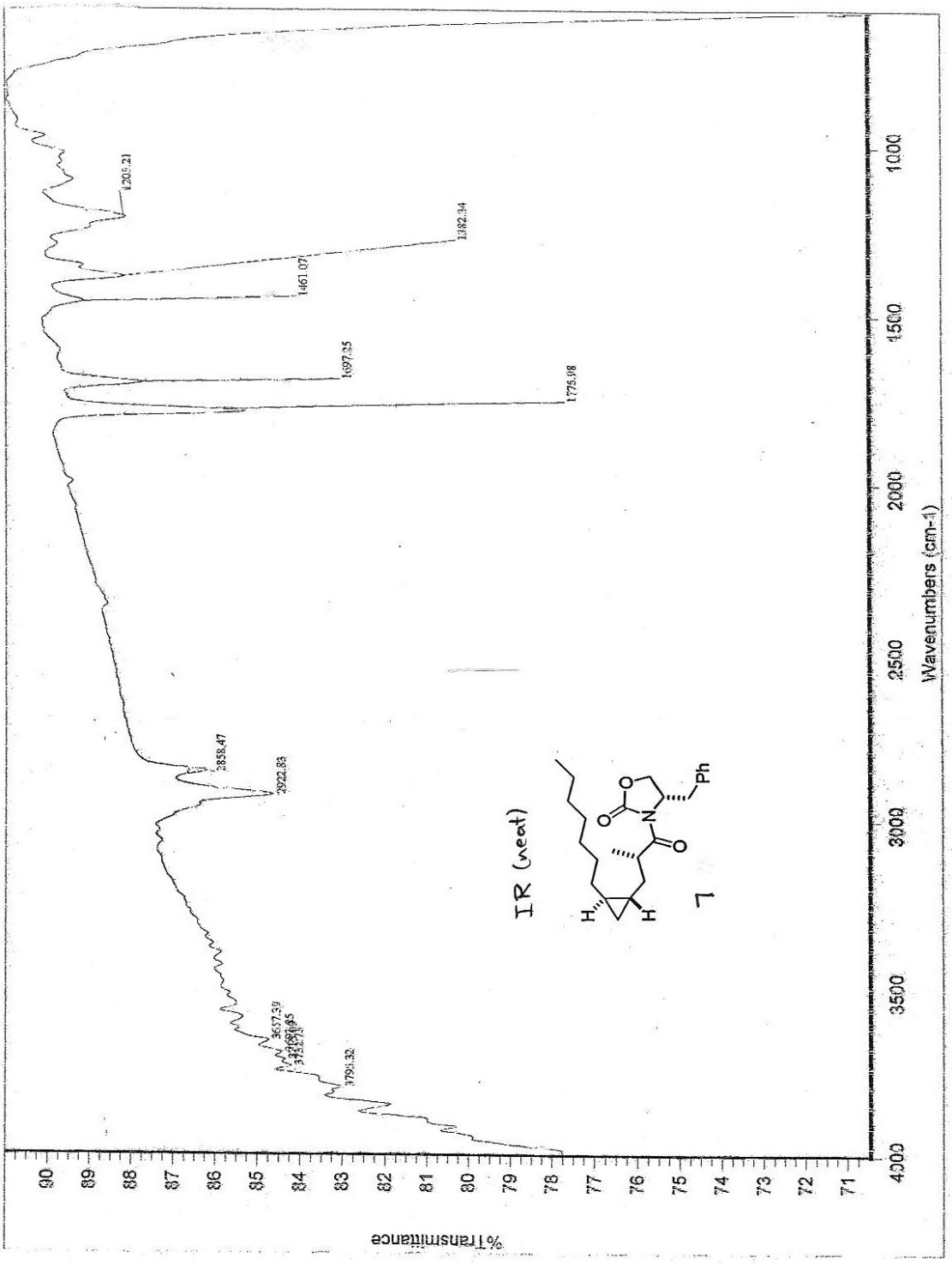

Figure IV.17: IR spectrum of **7**

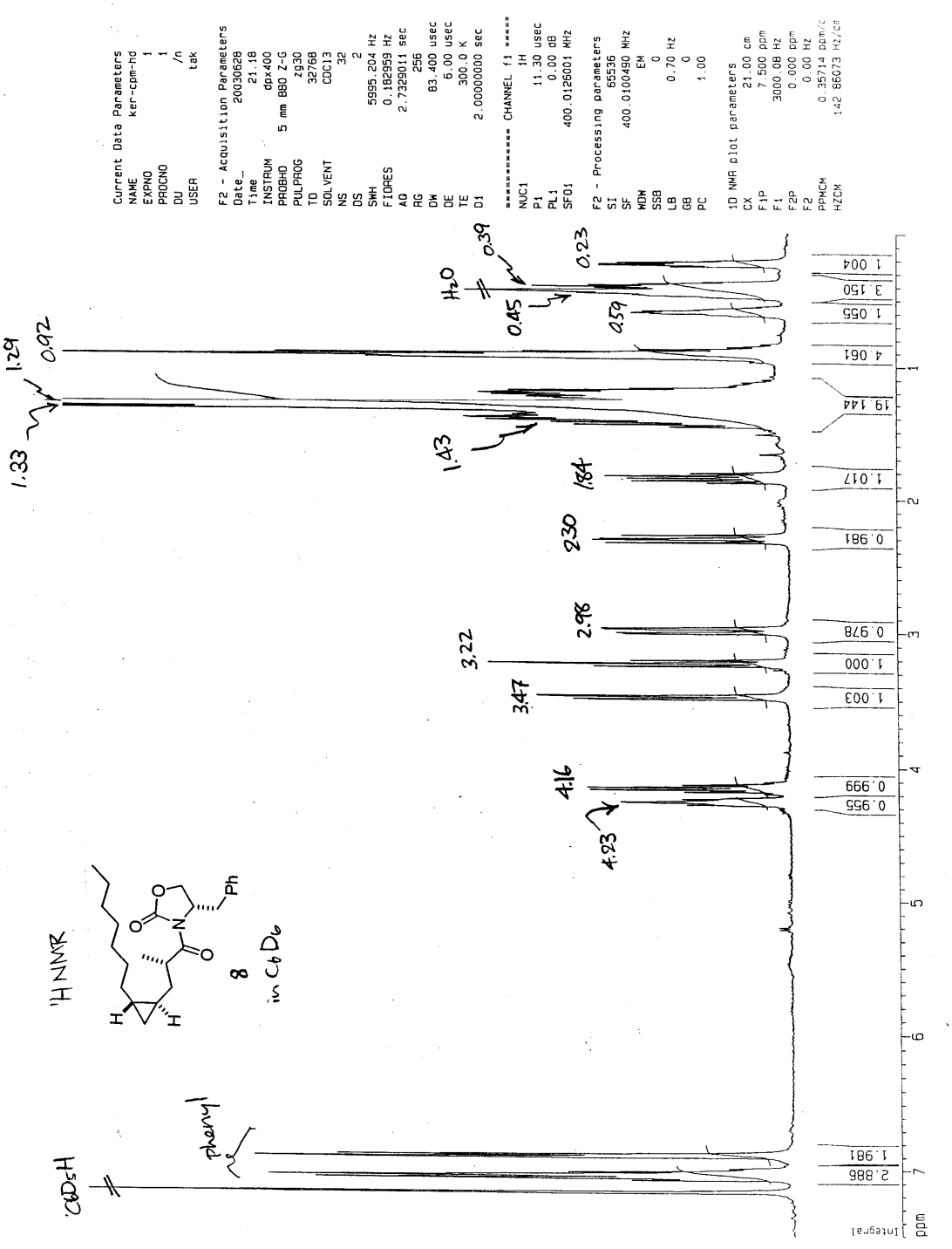

Figure IV.18: ^{1}H NMR spectrum of **8** in C_6D_6

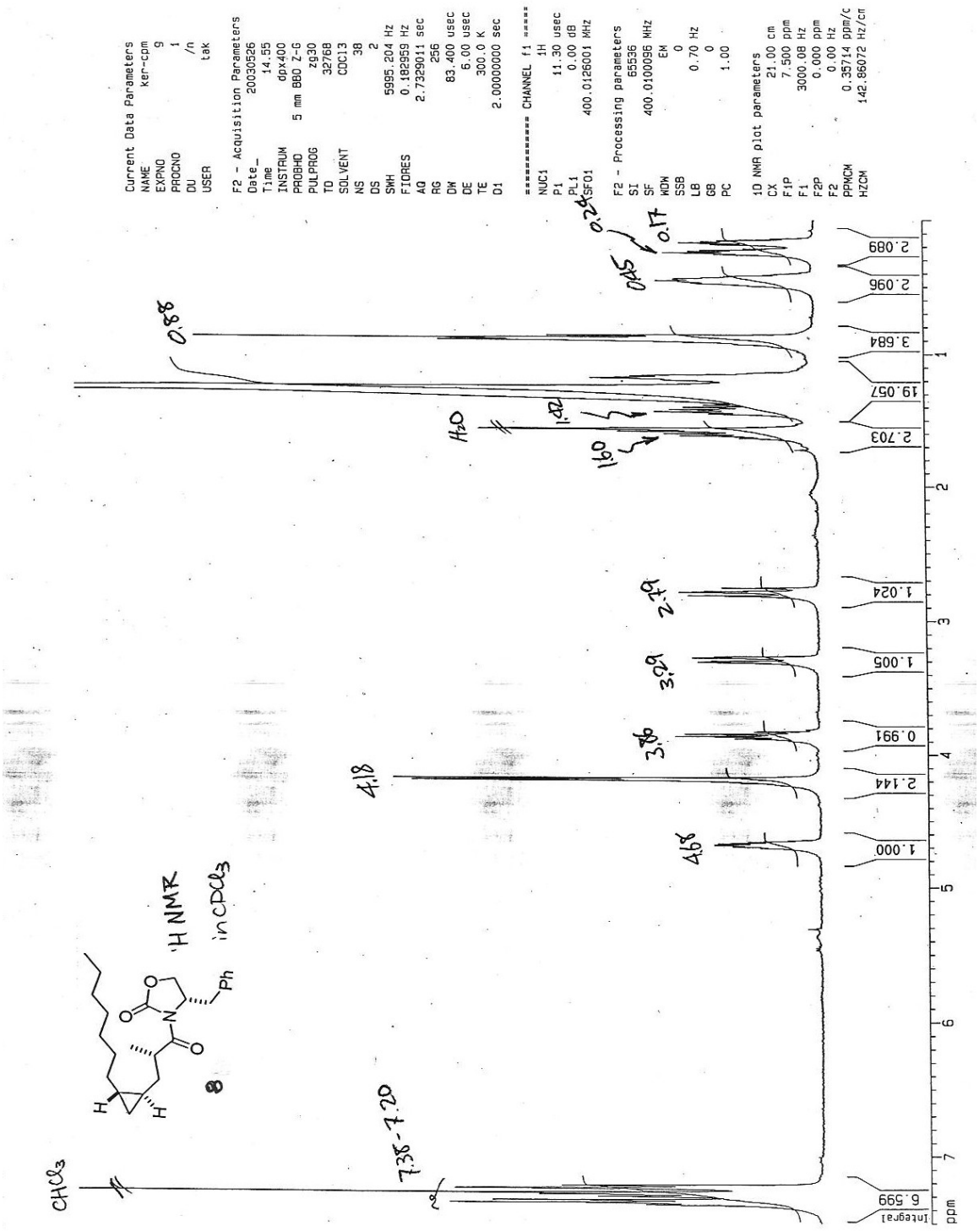

Figure IV.19: ^{1}H NMR spectrum of **8** in $CDCl_3$

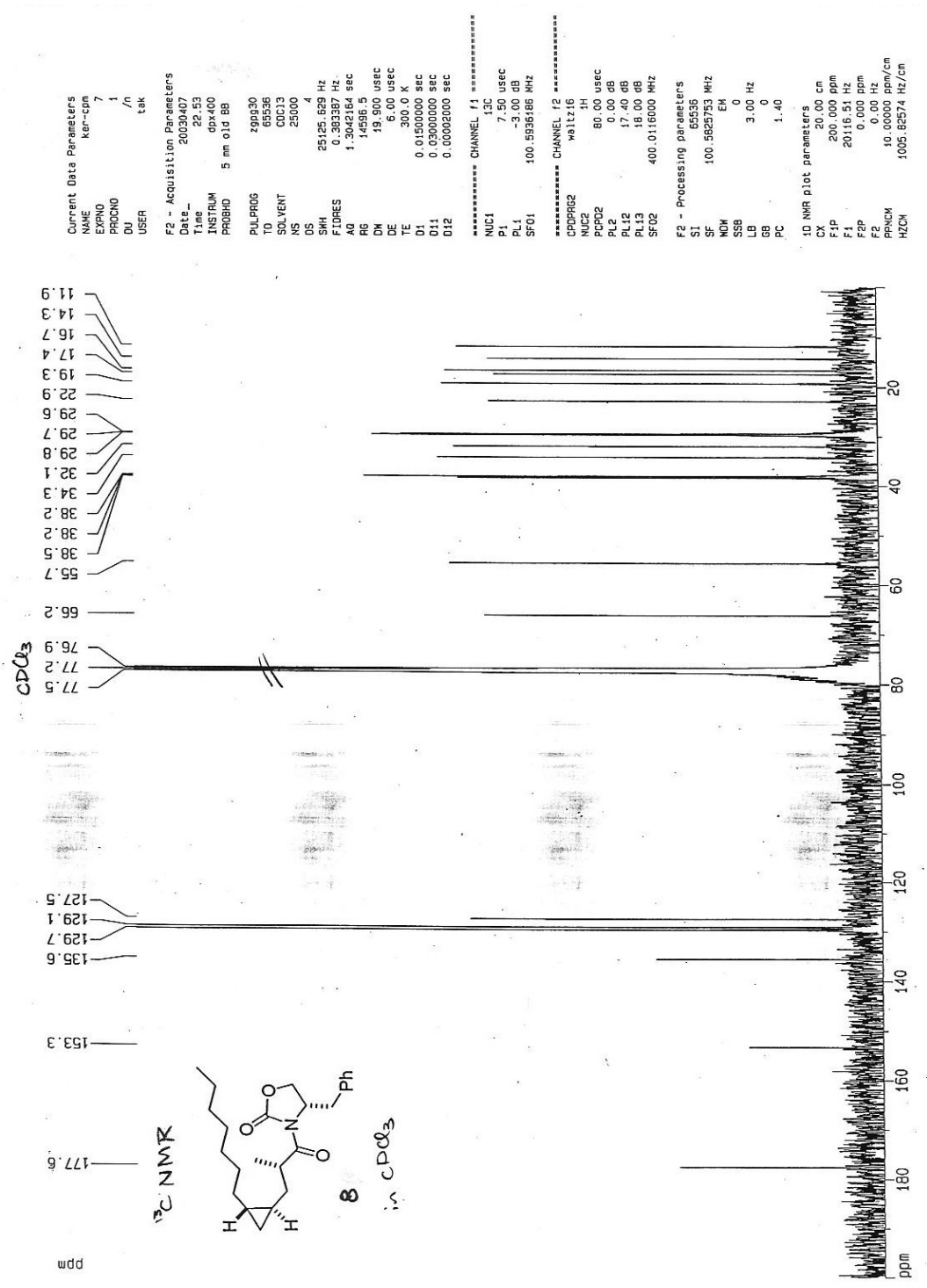

Figure IV.20: ^{13}C NMR spectrum of **8** in $CDCl_3$

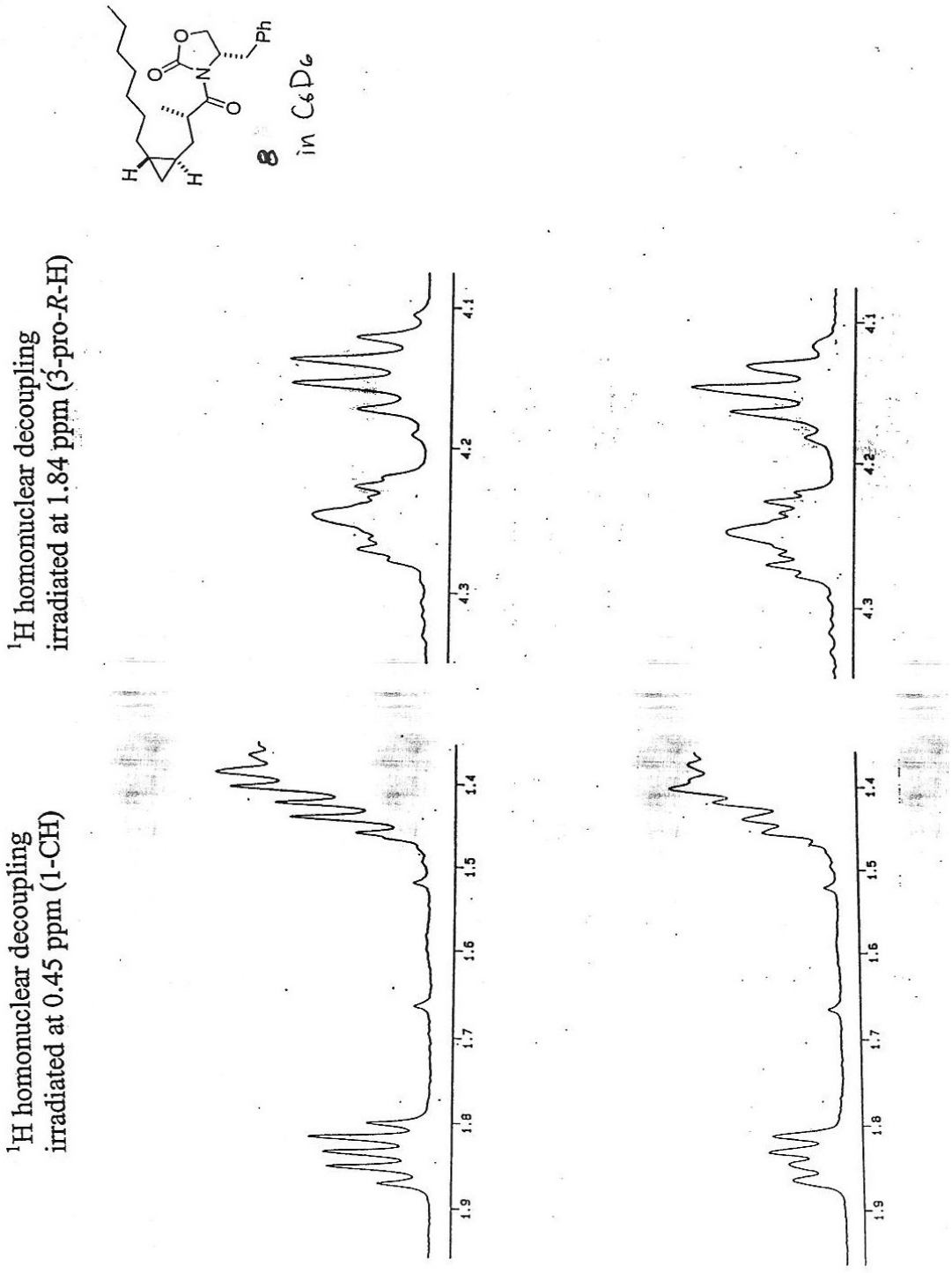

Figure IV.21: ^{1}H-^{1}H Homonuclear decoupling experiment for **8** in C_6D_6 – Part 1

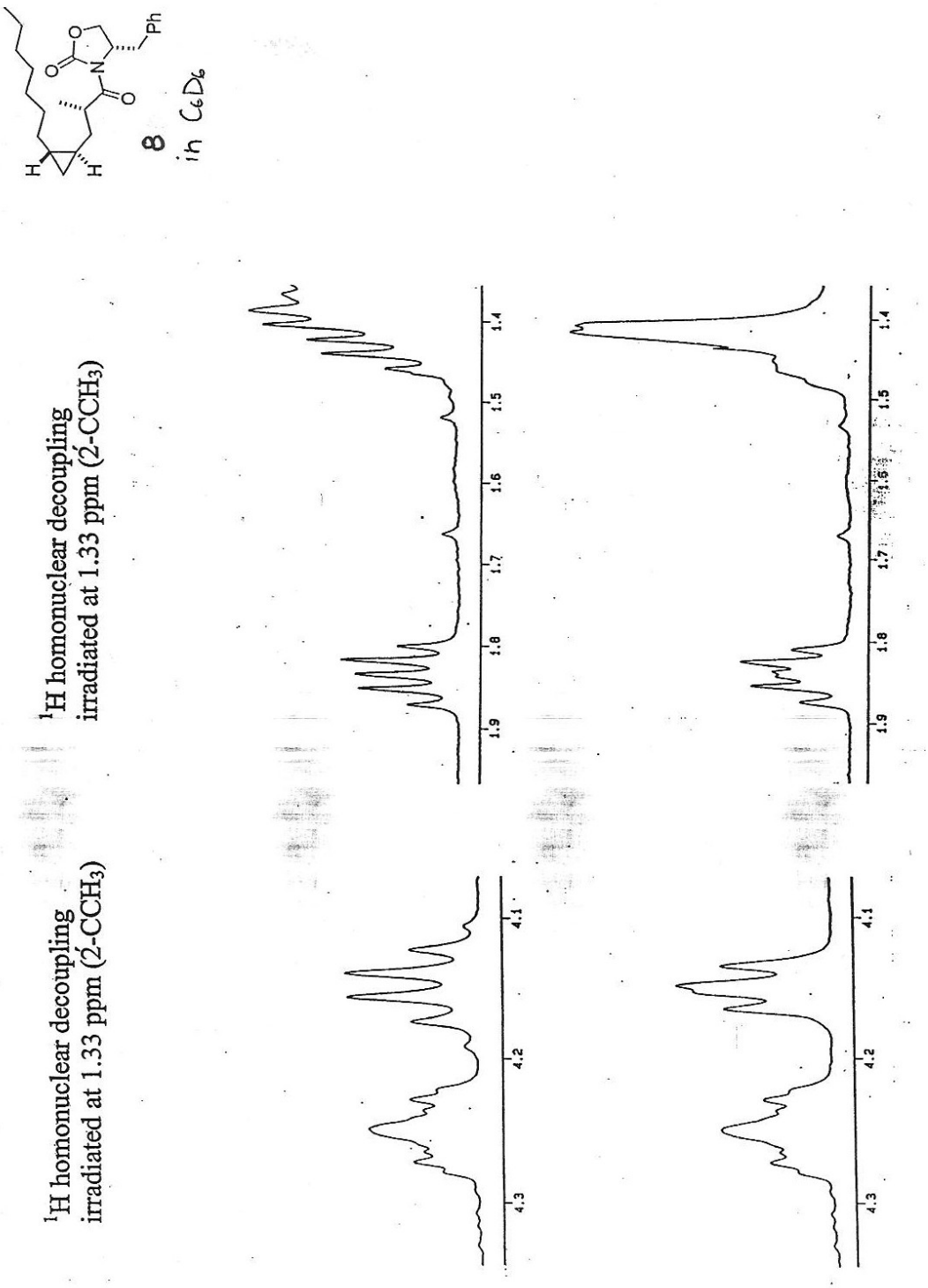

Figure IV.22: ^{1}H-^{1}H Homonuclear decoupling experiment for **8** in C_6D_6 – Part 2

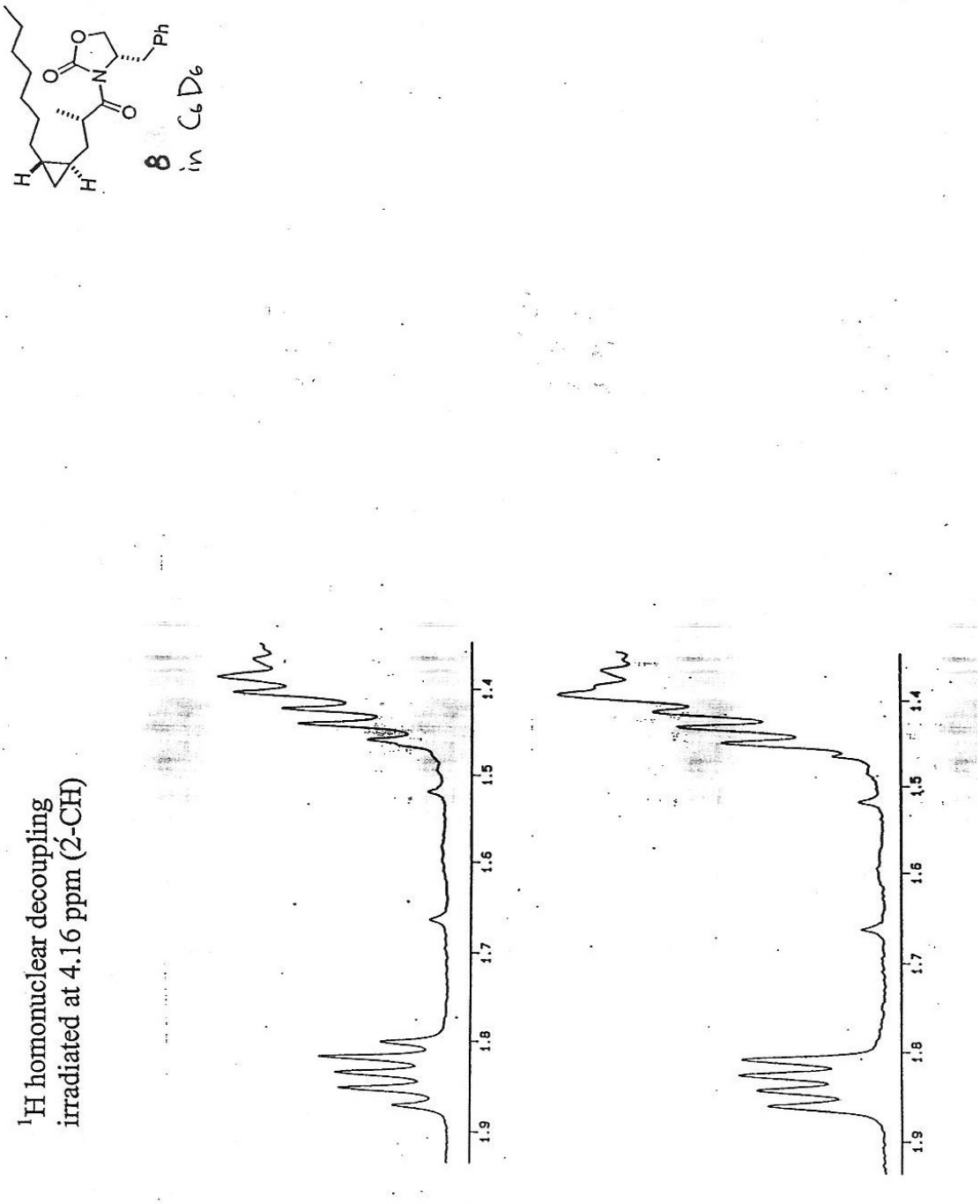

Figure IV.23: ^{1}H-^{1}H Homonulcear decoupling experiment for **8** in C_6D_6 – Part 3

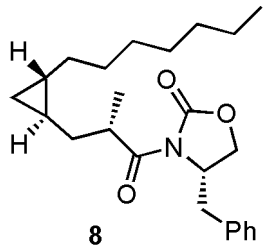

8

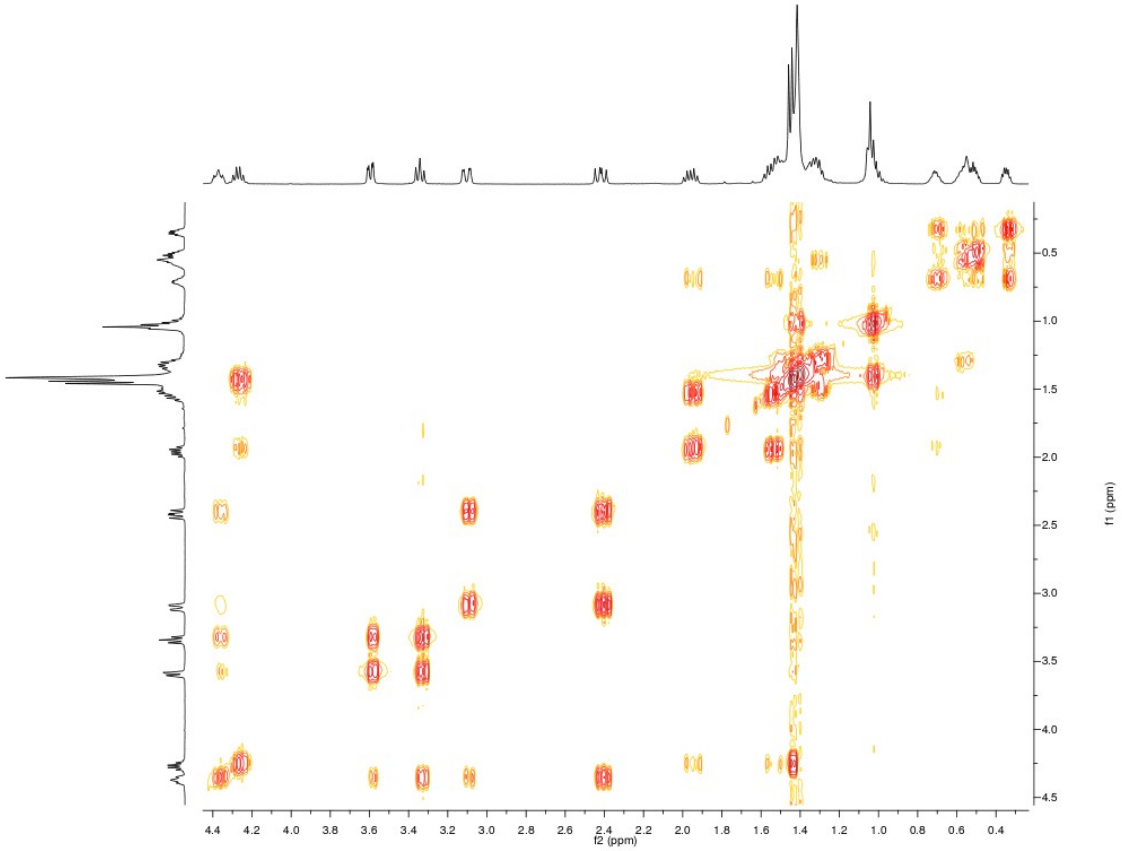

Figure IV.24: ^{1}H-^{1}H COSY spectrum of **8** in C_6D_6

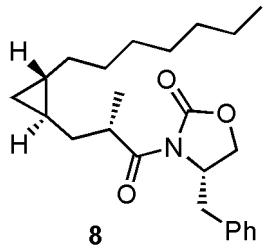

8

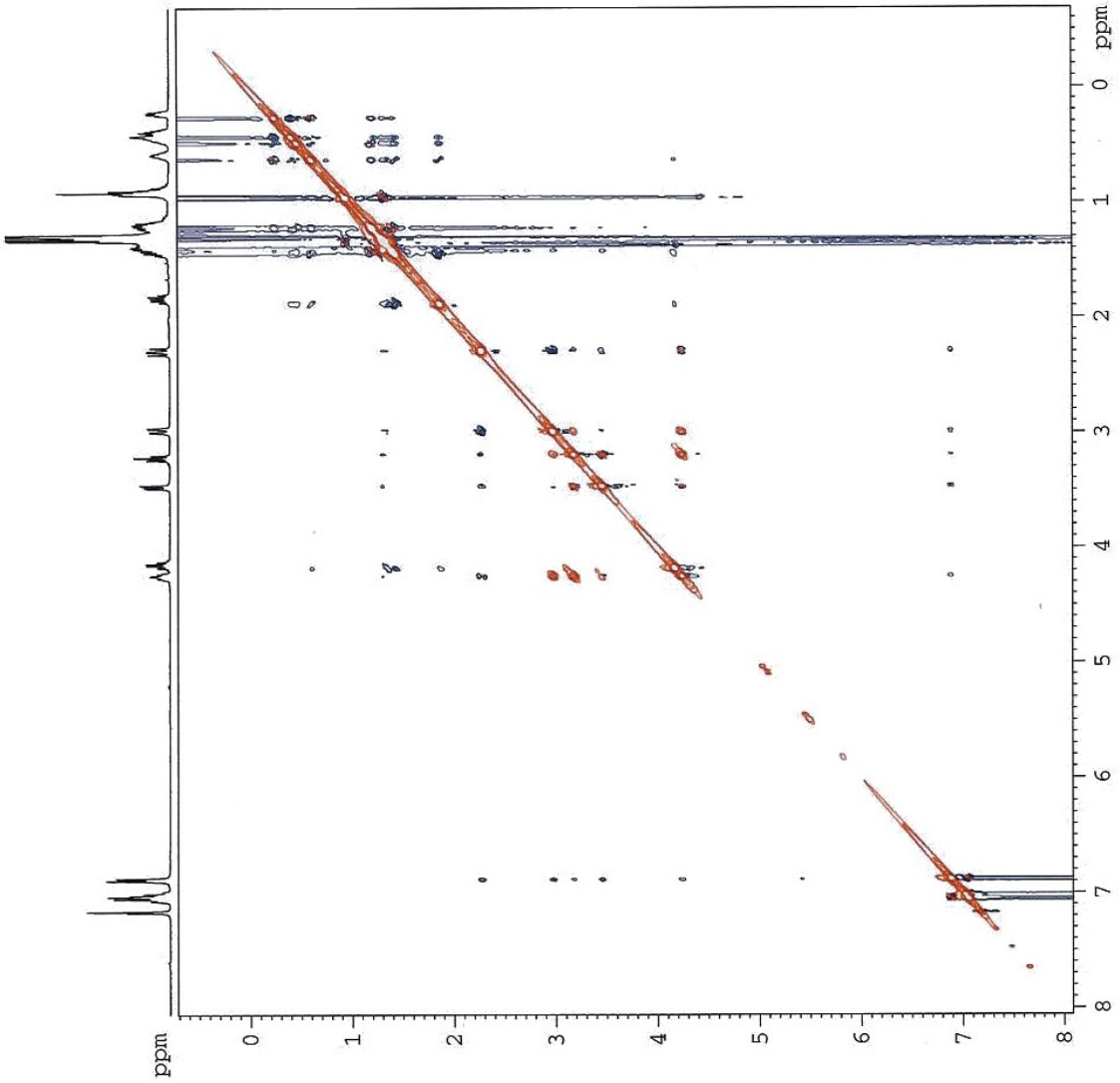

Figure IV.25: ROESY spectrum of **8** in C_6D_6

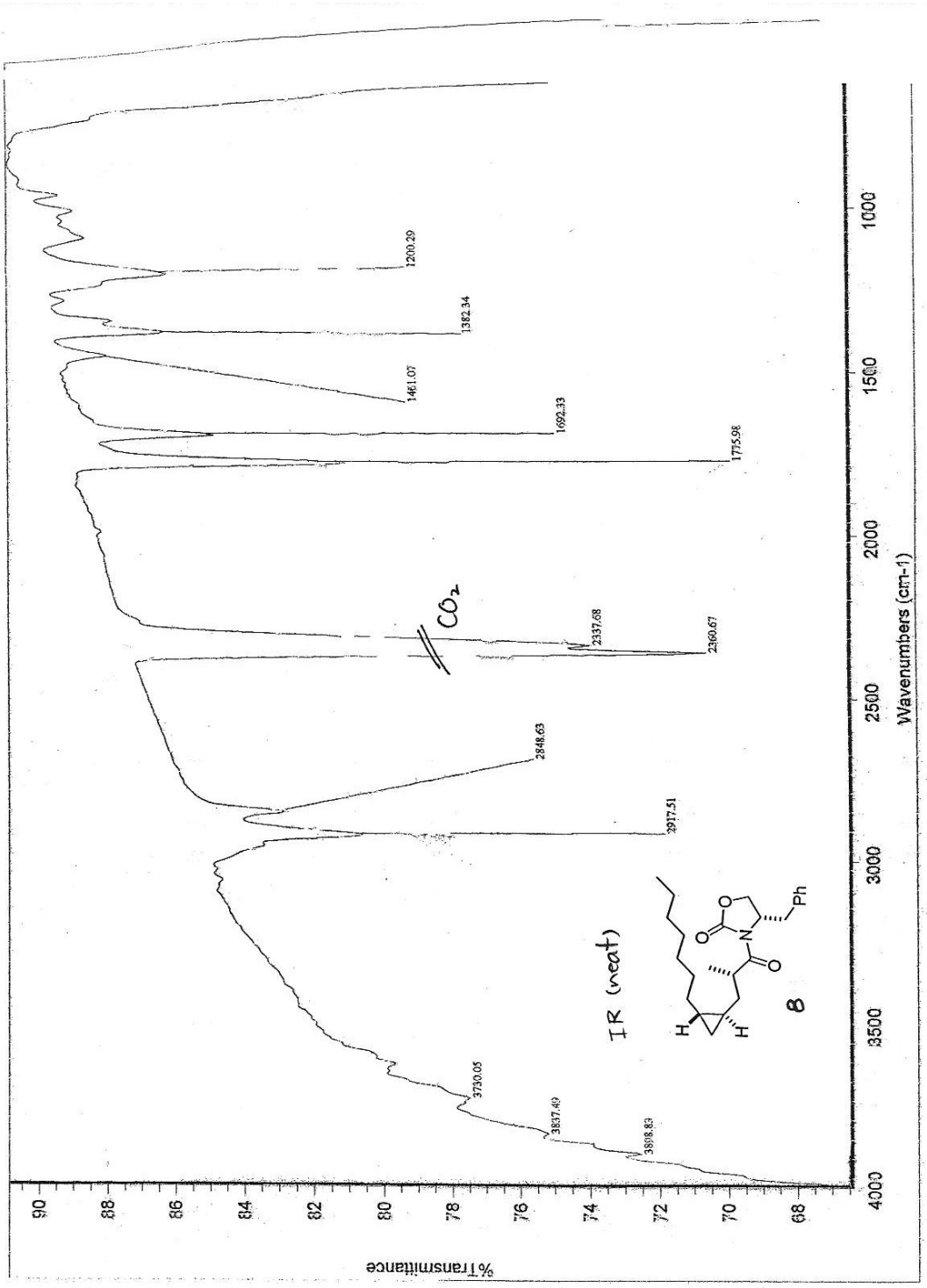

Figure IV.26: IR spectrum of **8**

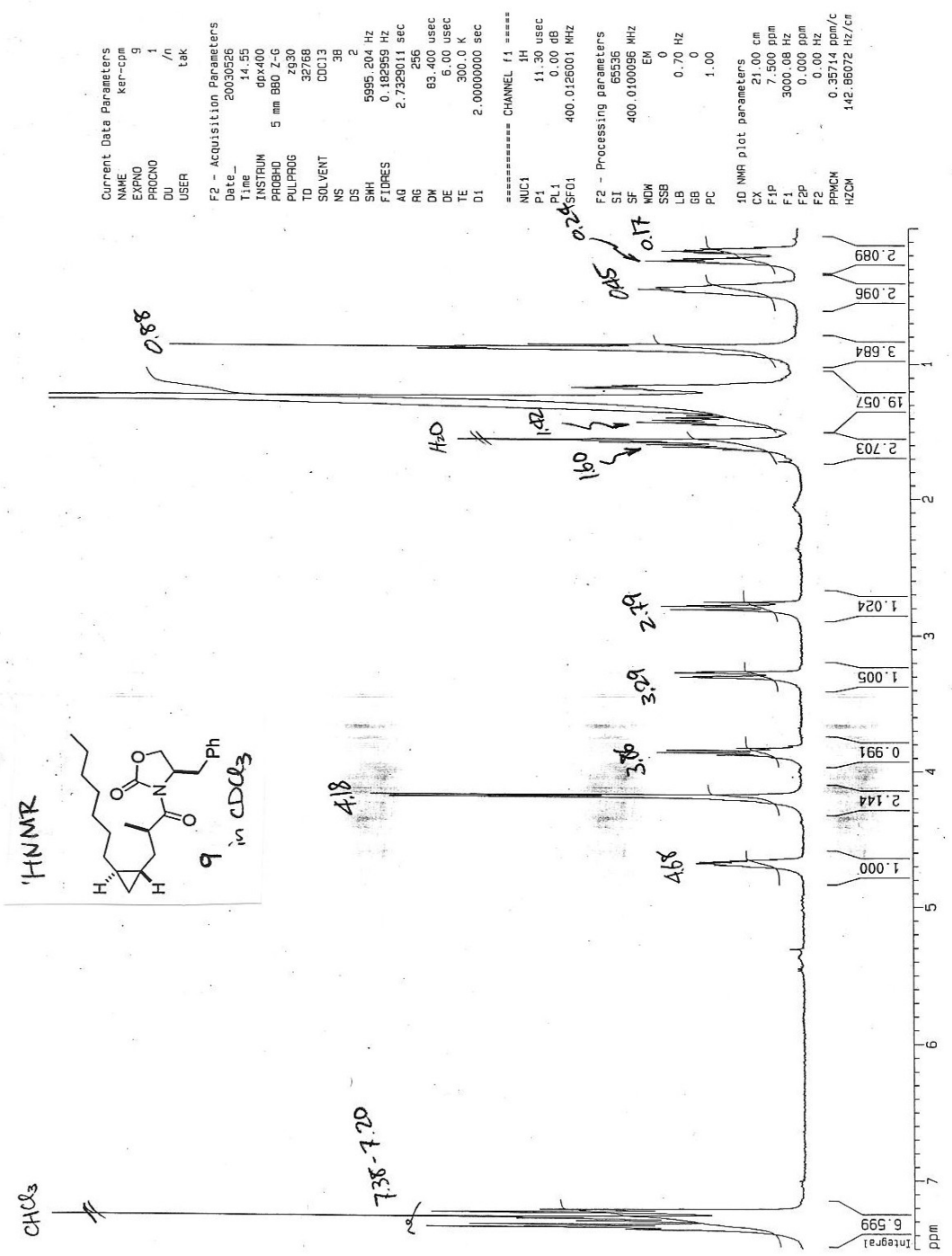

Figure IV.27: ^{1}H NMR spectrum of **9** in $CDCl_3$

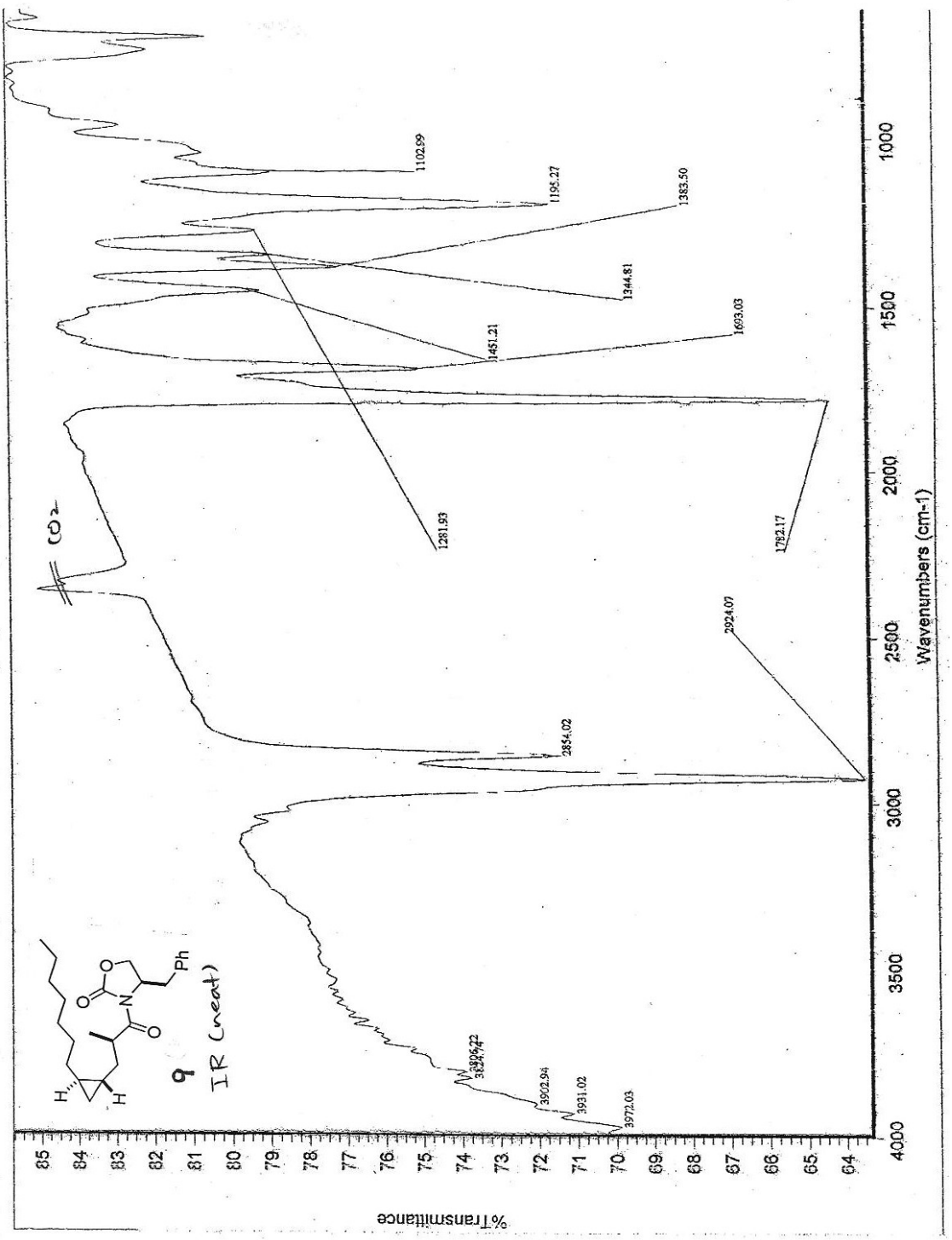

Figure IV.28: IR spectrum of **9**

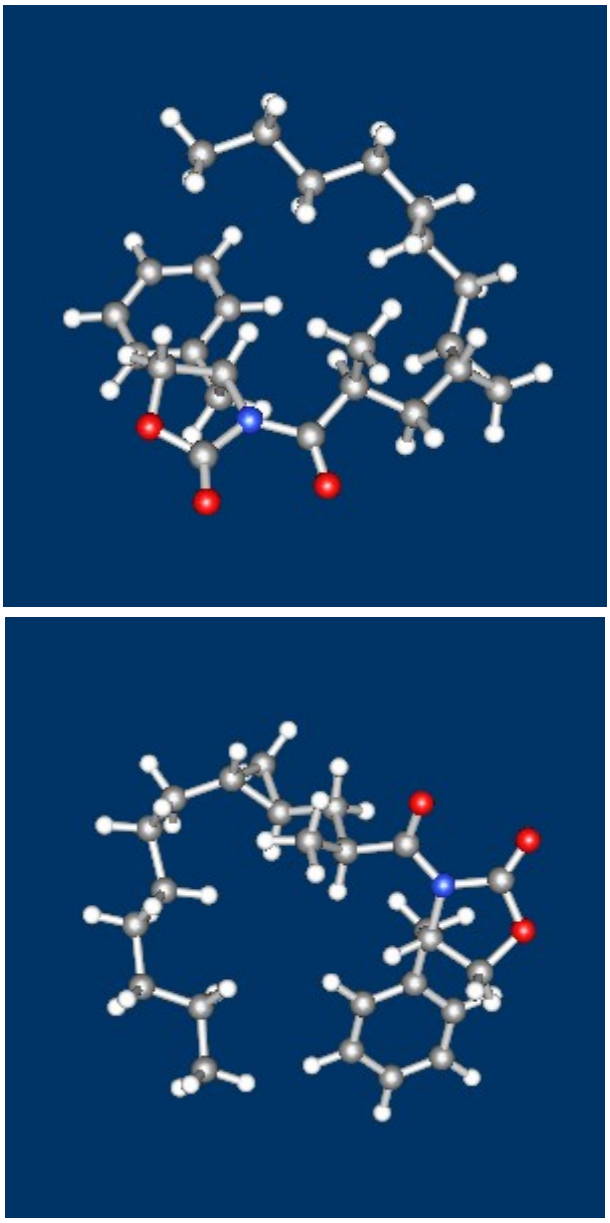

Figure IV.29: Geometry optimized 3D structures of **7** (above) and **8** (below)

The best conformers were obtained through conformer distribution calculation (molecular mechianics) and their geometry was optimized using *ab initio* calculations (HF 3-21G*). The stereoisomistry depicted here are what was predicted based on the SISTER method. However, the stereochemistry of the cyclpropanes were later determined to be the opposite of what is depicted here (see the text above).

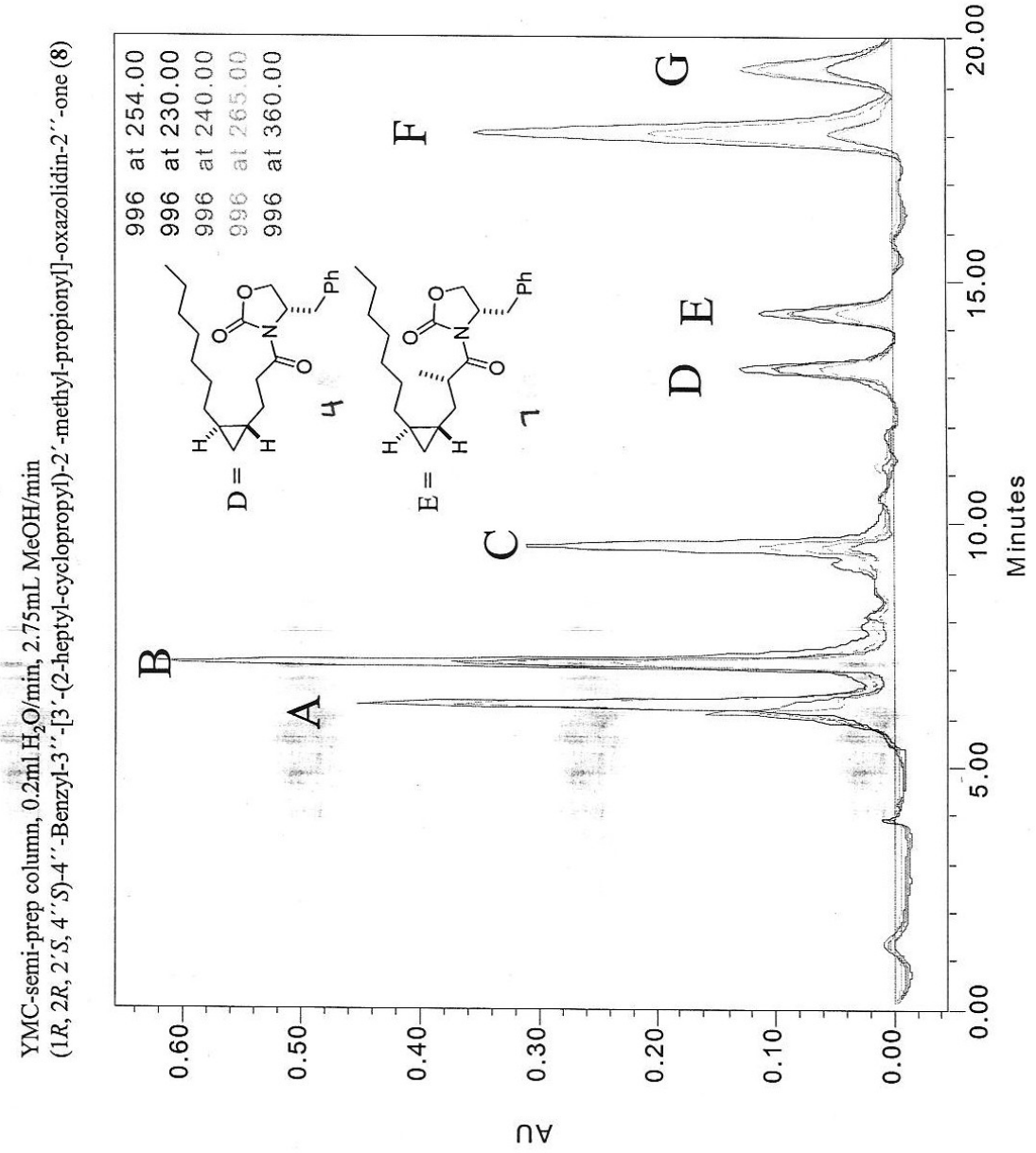

Figure IV.30: HPLC chromatogram for **4** and **7**

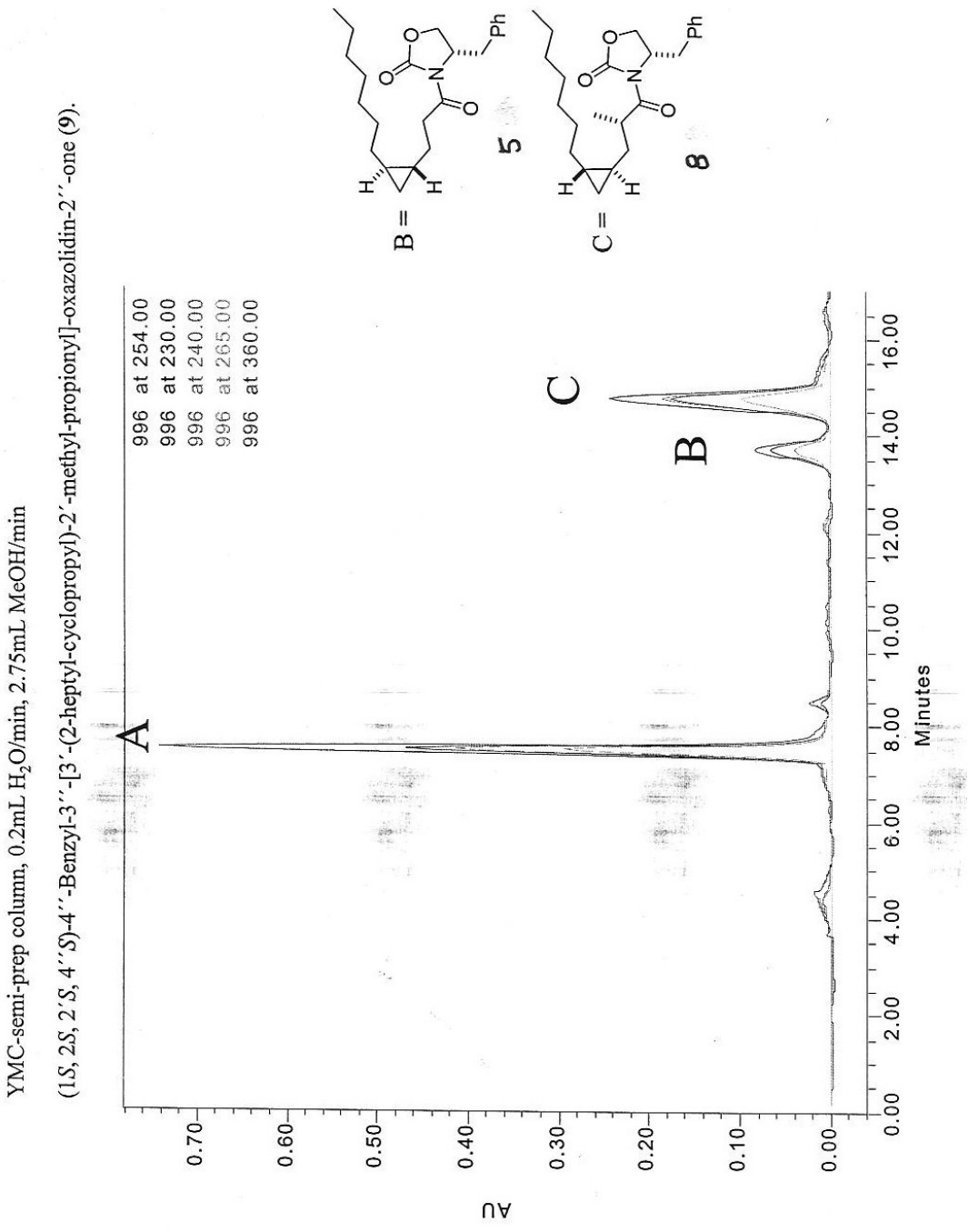

Figure IV.31: HPLC chromatogram for **5** and **8**

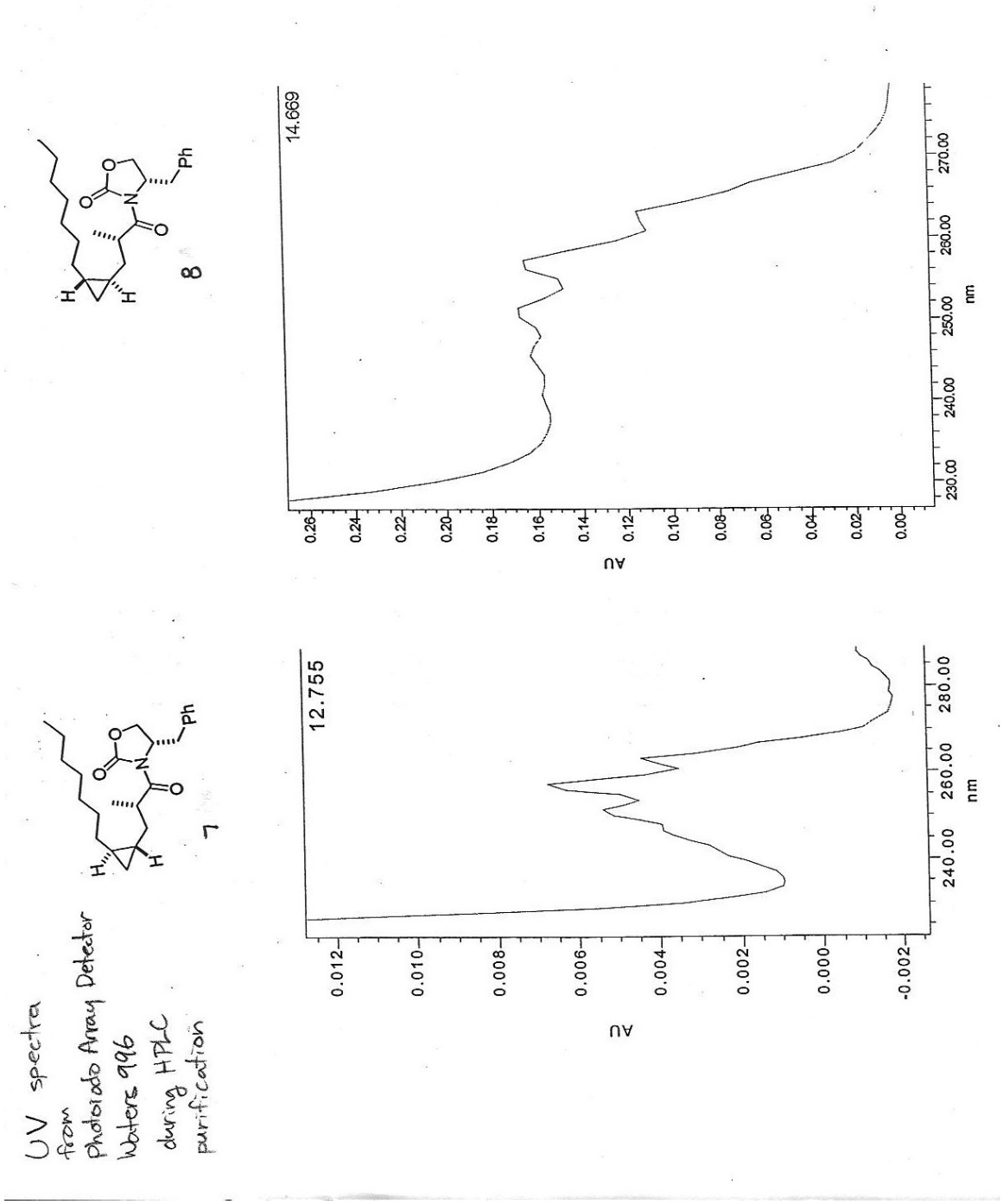

Figure IV.32: UV spectra of **7** and **8**

References and footnotes

1 Nannini, C. J. Novel secondary metabolites from a Madagascar collection of *Lyngbya majuscula*. **2002**, M.S. Thesis.

2 Complete purification of the fatty acids themselves were not possible by normal means.

3 (a) Teng, Rong-Wei; Shen, Ping; Wang, De-Zu; Yang, Chong-Ren., *Bopuxue Zazhi*, **2002**, *19*(2), 203-223. (b) Harada, Nobuyuki; Watanabe, Masataka; Kosaka, Masashi; Kuwahara, Shunsuke., *Yuki Gosei Kagaku Kyokaishi*, **2001**, *59*(10), 985-995. (c) Kusumi, Takenori; Ohtani, Ikuko I., *Biology-Chemistry Interface*, **1999**, 103-137

4 Haasnoot, C. A.; De Leeuw, F. A. A. M.; Altona, C. The relationship between proton-proton NMR coupling constants and substituent electronegativities—I : An empirical generalization of the Karplus equation. *Tetrahedron.* **1980**, *36*, 2783-2792.

5 Barfield, M; Smith, W. B. Internal H-C-C angle dependence of vicinal ^{1}H-^{1}H coupling constants. *J. Am. Chem. Soc.* **1992**, *114*, 1574-1581

6 See the experimental section for the geometry optimized 3D structures of **7** and **8**.

7 Al Dulayymi, J. R.; Baird, M. S.; Jones, K. The absolute stereochemistry of grenadamide. *Tetrahedron* **2004**, *60*, 341-345.

8 Coxon, G. D.; Al-Dulayymi, J. R.; Baird, M. S.; Knobl, S.; Robertsa, E.; Minnikin , D. E. The synthesis of (11*R*,12*S*)-lactobacillic acid and its enantiomer. *Tetrahedron Asymm.* **2003**, *14*, 1211-1222.

9 Avery, T. D.; Culbert, J. A.; Taylor, D. K. The first total synthesis of natural grenadamide. *Org. Biomol. Chem.* **2006**, *4*, 323-330.

10 Alternative interpretations of the ROESY correlations were considered. However, the original interpretations were more consistent with the molecular modeling results.

11 Bijvöt, J. M.; Peerdeman, A. F.; van Bommel, A. J. Determination of the absolute configuration of optically active compounds by means of X-rays. *Nature* **1951**, *168*, 271-272.

12 See Chapter I of this dissertation

13 Grandjean, D.; Pale, P.; Chuche, J. Enzymatic hydrolysis of cyclopropanes. Total synthesis of optically pure dictyopterenes A and C. *Tetrahedron* **1991**, *47*, 1215-1230.

Chapter V

Use of biomimetic starting materials for expedient total synthesis of epiquinamide enantiomers: true identity of bioactive metabolite

Abstract

A quinolizidine alkaloid isolated from a rainforest frog, *Epipedobates tricolor*, epiquinamide was initially regarded as a neuropharmacologically important compound due to its apparent selectivity for a nicotinic acetylcholine receptor subtype. In order to facilitate pharmacological and absolute stereochemical investigation of the molecule, concise and scalable syntheses of epiquinamide enantiomers were accomplished with high overall yields and high stereoselectivity from readily commercially available materials. However, it was found that none of the stereoisomers of epiquinamide was responsible for the observed bioactivity. Through this error, the importance of total synthesis of a natural product is clearly highlighted.

V.1 Introduction

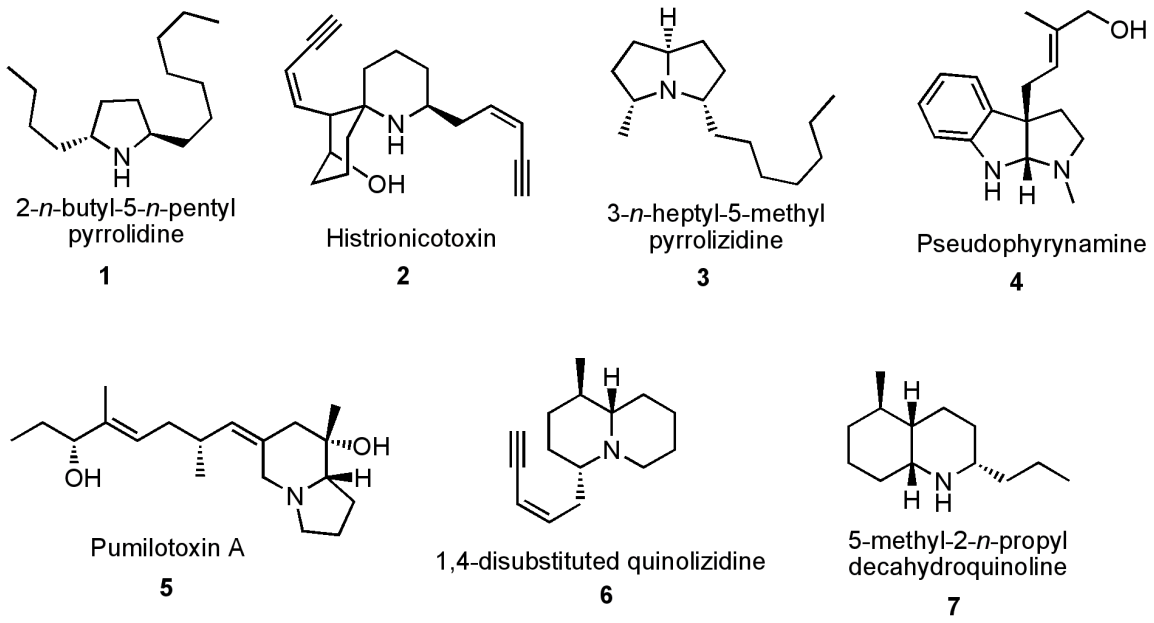

Figure V.1: Frog skin alkaloids of various core skeletons

In order to discover novel natural products with biomedically relevant bioactivities, relatively untapped sources including amphibian skin have been investigated in the recent decades.[1,2,3] In particular, rainforest frogs have proven to be a rich source of bioactive and structurally complex alkaloids (Figure V.1).[1,2] Typically, these alkaloids have pyrrolidine (**1**), piperidine (**2**), pyrrolizidine (**3**), indole (**4**), indolizidine (**5**), quinolizidine (**6**), or decahydroquinoline (**7**) core structures with relatively low degrees of unsaturation.[1,2] Having stereoelectronics similar to endogenous alkaloidal compounds essential to neurological functions in higher animals, these secondary metabolites can have a variety of neurological activities both in vitro and in vivo.[3] Many of the frog skin natural products have been traced back to the amphibian's dietary sources, such as insects and other arthropods.[1] However, the ultimate source may

be of microbial origin in some cases.[4] This is an ecological theme parallel to that seen with microbial natural products isolated from marine invertebrates.[4,5]

Epipedobates tricolor
Photograph from reference 3

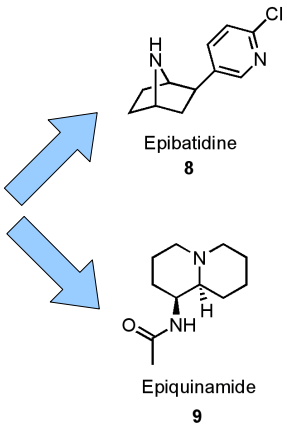

Figure V.2: Skin of *Epipedobates tricolor* contains epibatidine and epiquinamide

Epibatidine (**8**) was isolated from an Ecuadorian frog *Epipedobates tricolor* (Figure V.2) in 1992 by Daly and co-workers and has become one of the cornerstone compounds in the field of nicotinic acetylcholine receptor (nAChR) studies.[2,3,6] Epiquinamide (**9**) was isolated along with **8** from the same frog species in 2003[7] and has attracted much attention due to its potent and selective agonistic activities against β2 nicotinic receptors.[2,3,7] Its potential to be a lead compound in the development of pharmacological agents seemed promising, following the history of epibatidine.[6,8]

Although a plethora of nicotinic receptor agonists have been discovered, none of them are known to be sufficiently selective for subtypes of the nicotinic acetylcholine receptors (nAChR).[9] There are varying abundances of nAChR subtypes in different tissues of the human body, and it is conceivable that by selectively targeting a certain tissue, the possibility of side effects could be reduced.[9] However, the major limiting factor in testing this compound was its low availability from nature (240 μg from the

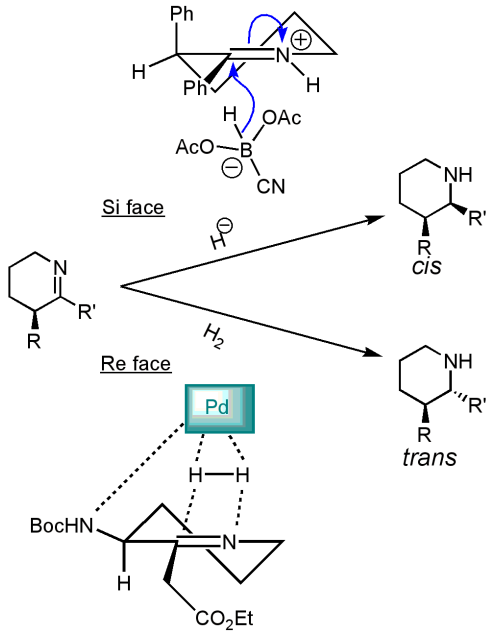

Scheme V.1: Reduction of dehydropiperidine: two stereochemical outcomes

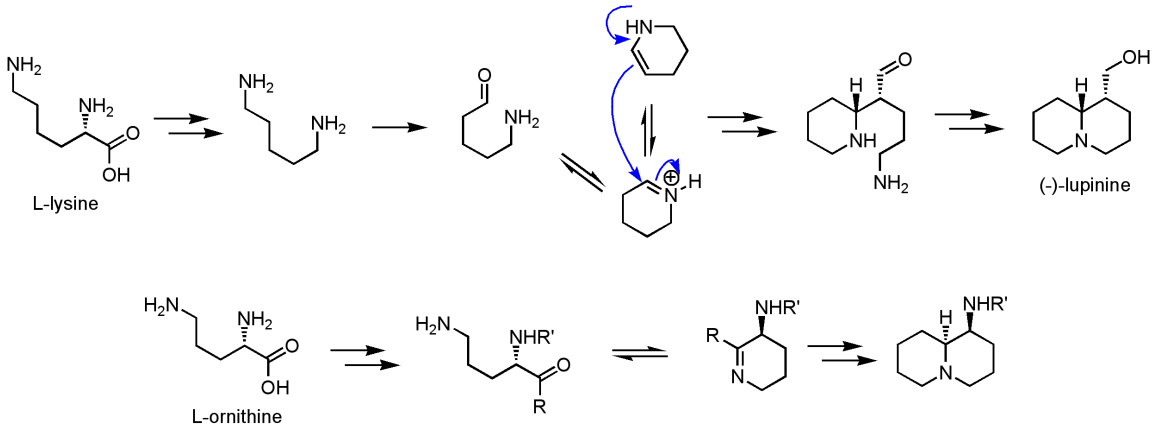

Scheme V.2: Applying the synthetic logic of quinolizidine biosynthesis to the synthesis of epiquinamide skeleton

skins of 183 frogs).[7] To meet this need and to explore new chemistry for the construction of the novel quinolizidine skeleton, a number of research groups have undertaken the total synthesis of **9**.[10] To date, there have been four[11,12,13,14] enantiospecific total syntheses of (+)-**9** and three[12,15,16] enantiospecific total synthesis of (−)-**9**, respectively. In addition, there have been two racemic syntheses of **9**[17,18] and two syntheses of the epimer of **9**

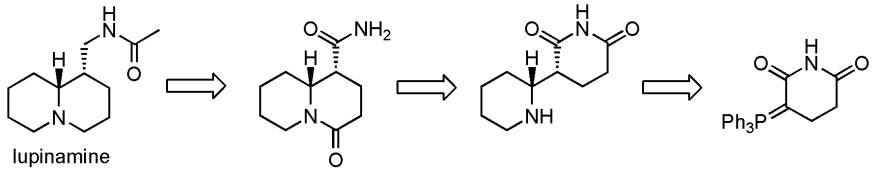

Scheme V.3: Biomimetic synthesis of lupinamine by Wanner and Koomen

(**15**).[12,19] In the literature on epiquinamide, the optical rotation value of the natural product was never reported due to its low availability.[7] Access to both enantiomers was therefore of great importance.

V.2 Rationale for epiquinamide synthesis strategy

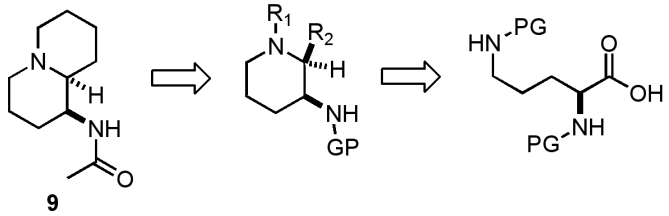

Scheme V.4: Initial Retrosynthetic Analysis of Epiquinamide

The quinolizidine system could be derived from a piperidine with appropriate appendages that could be cyclized to give the second ring. The initial synthetic strategy was formed around the reductive amination reaction to furnish the bicyclic tertiary amine (Schemes IV.1 through IV.3). This idea was inspired by the observation that there had been little effort to synthesize *cis*-2,3-disubstituted piperidines.[20,21,22] Some precedence exists in the literature that suggested that such reductive amination using H_2 would give *trans* stereochemistry via chelation control[22] (Scheme V.2; H_2 reaction) while *cis* stereochemistry would be achieved if hydride was used[20] via a Felkin-Anh type transition state (Scheme V.2; hydride reaction).[23] This latter stereochemical outcome was expected[24]

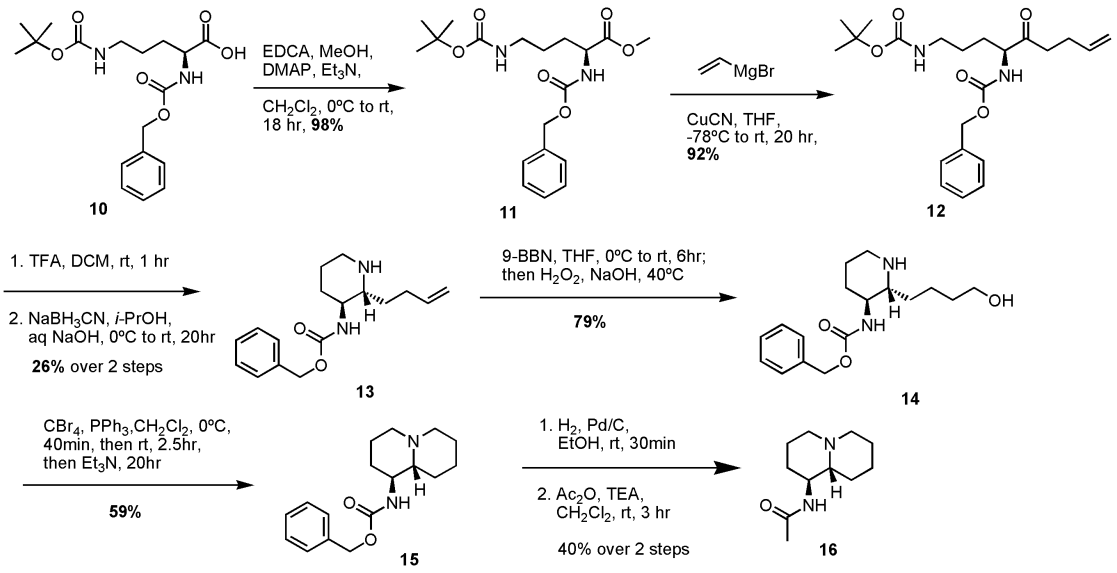

Scheme V.5: Total synthesis of (1*R*,9*S*)-epi-epiquinamide (**16**)

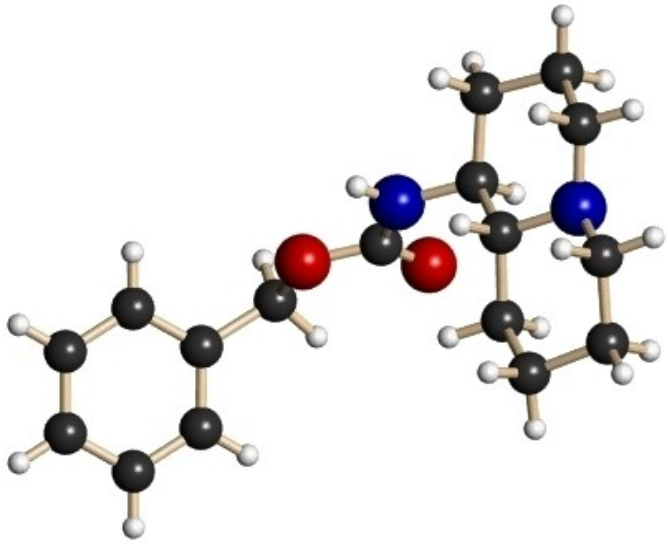

Figure V.3: X-ray crystal structure of epi-epiquinamide (**15**)

for the stereoselective reduction of **2** based on the assumption that the protecting group would not chelate to the boron atom of $NaBH_3CN$ under acidic conditions.

The biosythesis of quinolizidine is generally thought to involve a lysine residue (Scheme V.3).[25] Being inspired by nature's strategy, it was realized that utilization of ornithine could result in retention of the chiral amine group and stereochemical guidance

by the same group (Scheme V.4). This strategy eliminates the need for introducing chirality at any point in the synthesis. In order to maximize the flexibility of the synthesis, a biomimetic approach can be utilized without strictly adhering to a synthetic route that employs the exact chemistry used in the biosynthesis. For example, Koomen and Wanner have achieved biomimetic synthesis of quinolizidine alkaloids including lupinamine (Scheme V.5).[26] If the same strictly biosynthetic approach was applied to epiquinamide, it would be difficult to exert enantioselectivity. By starting out with a naturally occurring chiral molecule and using it in a biomimetic manner, the synthesis can be both expedient and cost-effective.

V.3 Attempts to synthesize epiquinamide

The cyclization via reductive amination, however, yielded *trans*-piperidine in excellent de (**13**). The relative stereochemistry of this product was confirmed by an X-ray crystal structure of the Cbz-protected quinolizidine after the second cyclization (Figure V.3). This result may be explained by an exchange of ligands on the boron atom; *i.e.*, the chelation model. If the oxygen atom of the Boc group becomes one of the ligands, the tethered cyanoborohydride would transfer its hydride from the *Si* face (when R and R' are those of **9** in Scheme V.2) rather than the *Re* face.

Subsequently, two alternative routes that utilize an acyliminium ion as a key intermediate were devised (Schemes IV.6 and IV.7). One route features addition of vinyl borylate to the acyliminium ion[27] (from **13**) and the other route centers around a hetero Diels-Alder reaction[28] with the acyliminum ion (from **22**) as the dienophile. Despite some

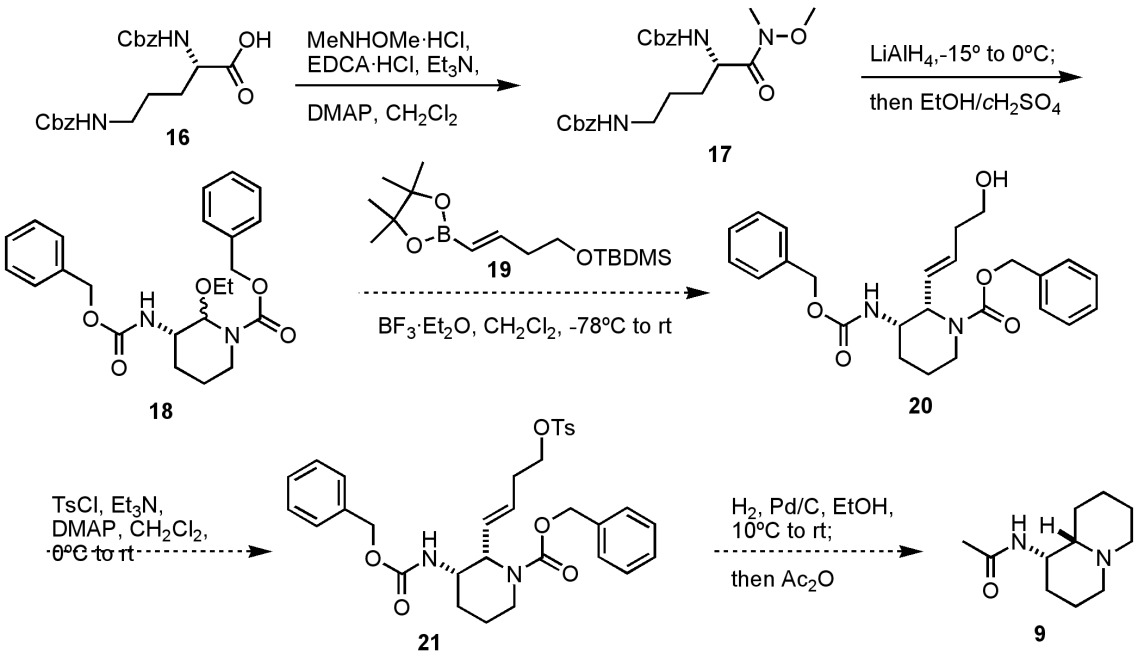

Scheme V.6: Proposed total synthesis of (+)-epiquinamide via boron nucleophilic addition to acyl imminium ion

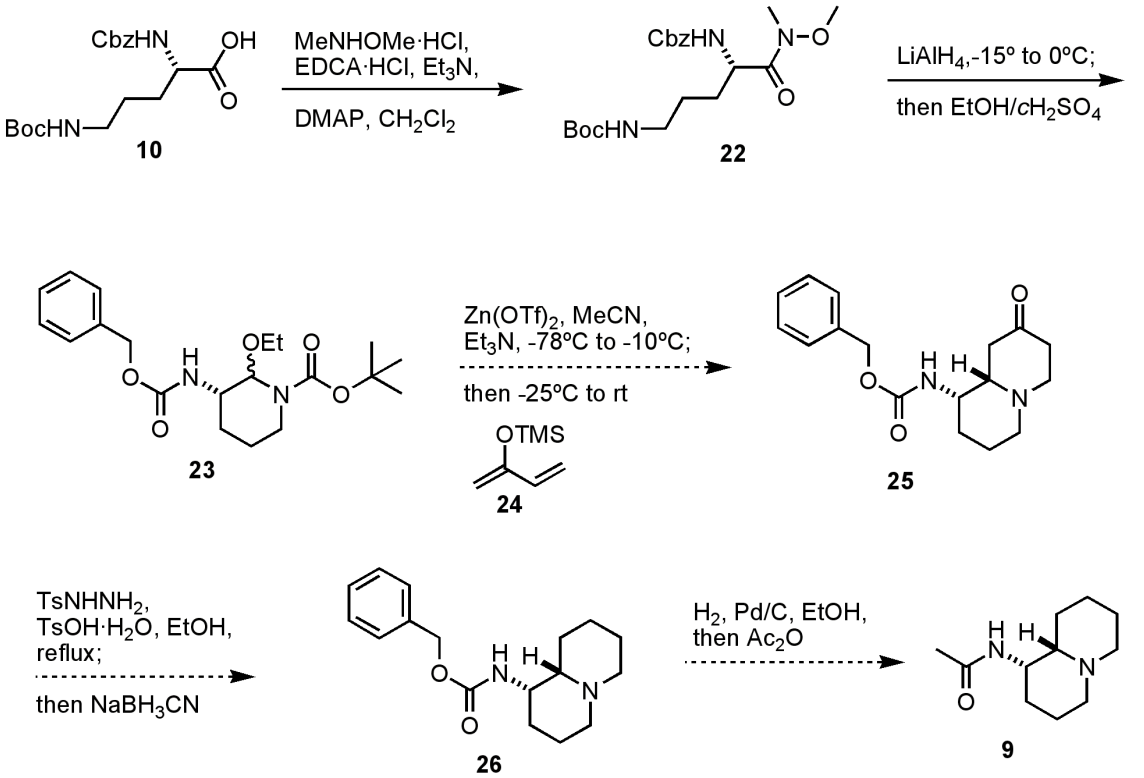

Scheme V.7: Proposed total synthesis of (+)-epiquinamide via hetero Diels-Alder

of the promising precedents in the literature, these approaches proved unsuccessful due to complications with the unstable acyliminium ion.

V.4 Total synthesis of epiquinamide

According to the chelation model, borohydride reduction of the ketone **29** should give the anti configuration.[29,30] Using a similar synthetic logic as applied to the first attempted synthesis (Scheme V.1), the first piperidine ring can be synthesized via cyclization through S_N2 displacement as shown in Scheme V.7. The substrate for the S_N2 reaction can be easily derived from a corresponding amino alcohol, such as **30**, which could be synthesized from ornithine.

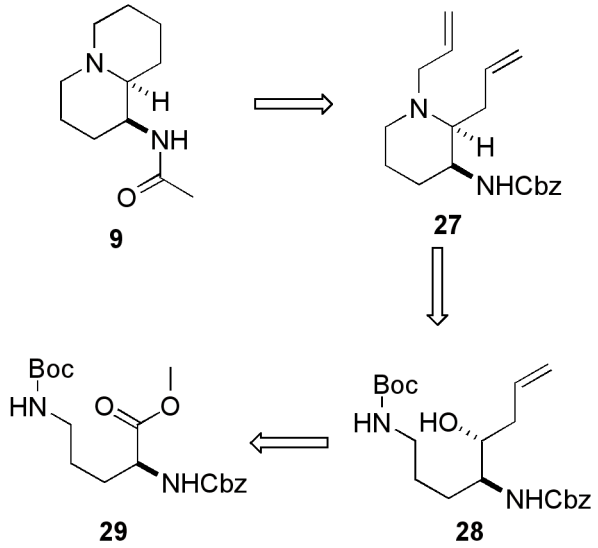

Scheme V.8: Retrosynthetic analysis of (+)-epiquinamide

The synthesis of the intramolecular S_N2 substrate began with a commercially available ornithine derivative **10**, which was first converted smoothly to the Weinreb amide **29** using a common coupling condition (Scheme V.8).[31,32] After simple washings, the product was fairly pure and required no further purification. Upon treatment with an

allyl Grignard reagent,[33] we obtained the ketone **30** as white crystals. Chelation-controlled hydride reduction of **30** yielded a highly crystalline alcohol, **28** (Scheme V.10).[30,34] By ^{1}H and ^{13}C NMR, none of the other diastereomer was observed in the crystallized product, whose stereochemistry was ultimately proven by completion of the total synthesis and comparison to epi-epiquinamide (**15**).[35] Mesylation of the amino alcohol proceeded smoothly with an excellent yield, and again the product was crystalline. Therefore, the synthesis of the S_N2 substrate **31** was accomplished very conveniently and without chromatographic purification unless recovery of the residual amount of the product in the filtrate was desired.

Transformation of the mesylate **31** to the title compound was accomplished as shown in Scheme V.8. Removal of the Boc group in TFA/CH_2Cl_2 followed by intramolecular S_N2 cyclization induced by K_2CO_3 and subsequent *N*-alkylation in acetonitrile yielded the diallyl piperidine **27** in good yield.[36,37,38,39,40] The synthesis of the

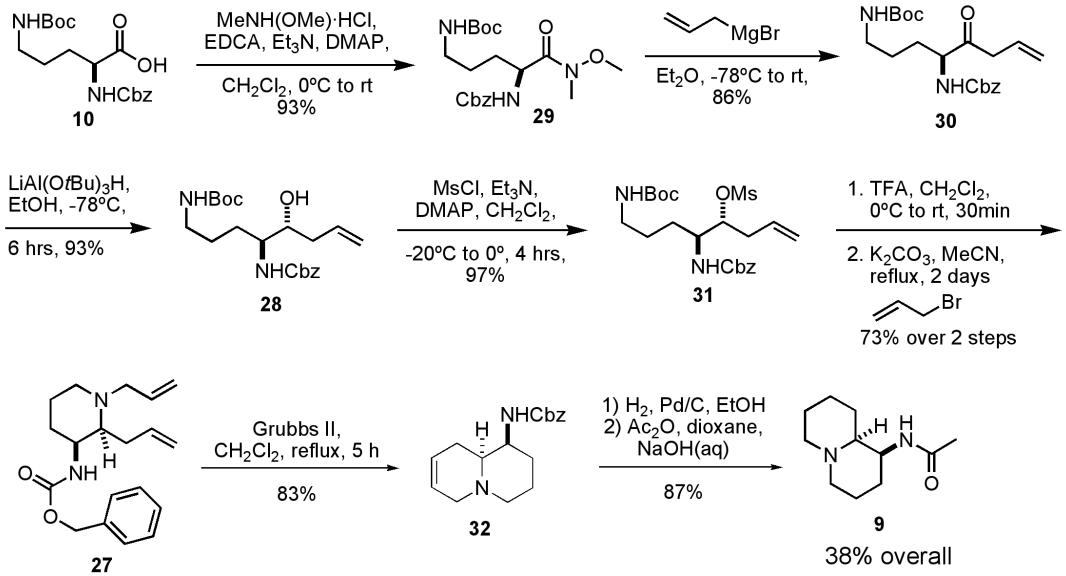

Scheme V.9: Total synthesis of (+)-epiquinamide

epiquinamide skeleton was concluded by ring-closing metathesis (RCM) reaction on **27** using the Grubbs second-generation catalyst.[41,42] It is noteworthy that this was one of the earlier examples of a basic and relatively unhindered *N*-allyl group undergoing ruthenium-catalyzed RCM.[43,44] The scope of functional group tolerance by the Grubbs second-generation catalyst seems to be greater than the consensus at the time.[42,43,44] However, the purification of this rather polar RCM product presented difficulties.[45] The problem was overcome when Cho and Kim's method was employed with a small modification.[46] Since then, a phosphine-free ruthenium catalyst (second-generation Hoveyda-Grubbs catalyst) became commercially available, thereby making some of the purification issues obsolete.[47,48]

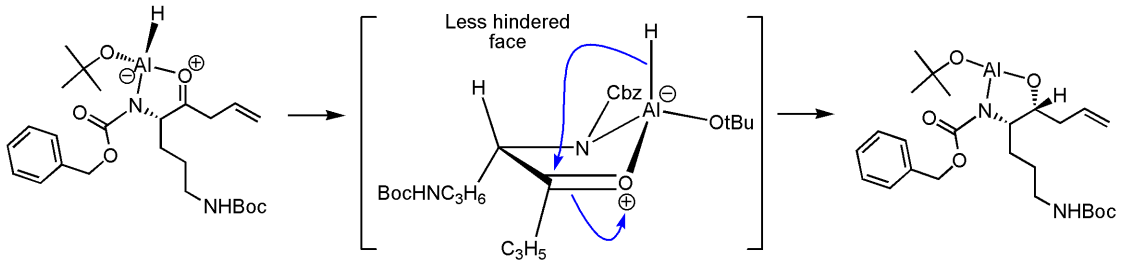

Scheme V.10: Chelation-controlled hydride reduction of ketone (**30**)

After the aluminum hydride source chelates with both the ketone oxygen and the carbamate nitrogen, it transfers the hydride onto the less hindered face of the ketone. Subsequent hydrolysis yields the reduced product **28**.

Deprotection, alkene reduction, and acetylation were accomplished in one pot by hydrogenation of **32** in ethanol with acetic anhydride (8 steps overall).[49] A better yield was observed when this process was separated into two steps as shown in Scheme V.8 (9 steps overall).[11] By ^{1}H and ^{13}C NMR, a single isomer was observed. This material had the identical ^{1}H and ^{13}C NMR and IR spectra and HR mass (EI) to those of the authentic material.[7] The reproducible overall yields of (+)-**9** beginning from **10** were 38% and 28%

for the longer and shorter sequences, respectively. The specific optical rotation value also matched that of the material from the previous total synthesis ((+)-**9** $[\alpha]^{22}_{D}$ = +24° (*c* 0.10, $CHCl_3$)).[50] Only three chromatographic purification steps were required throughout the synthesis. The synthesis of the other enantiomer was performed in the same manner starting with commercially available δ*N*-Boc-α*N*-Cbz-D-ornithine. This latter synthesis was accomplished in two weeks, demonstrating the practicality of this synthetic route (**(-)-9** $[\alpha]^{22}_{D}$ = –22º, *c* 0.13, $CHCl_3$).[51] In comparison to other enantiospecific syntheses of **9** (12-15 steps),[11-17] efficiency of this synthesis is outstanding. This is largely due to the choice of a biomimetic starting material as mentioned earlier.

V.5 Bioactivity and absolute stereochemistry of epiquinamide

With both of the enantiomers of epiquinamide in hand, the next goal was to determine the absolute stereochemistry of natural epiquinamide. Neither the optical rotation value nor the circular

dichroism spectrum of the authentic natural product was ever reported.[7] In the absence of access to the natural sample for comparison in chiral chromatography with the two synthetic enantiomers, the only plausible method of stereochemistry determination was to compare the biological activity of the two isomers. If one was as active as the reported natural product, but not the other stereoisomer, then it can be concluded that the former isomer possesses the natural stereo-configuration.

However, neither of the compounds were active in the in-house Na^+ channel activation and blocking activity assays using neuroblastoma cells (Neuro 2a),[52] the cytotoxicity assays using human lung cancer cells (H460), or the brine shrimp assay.

Furthermore, Gallagher and coworkers independently reported that racemic epiquinamide was inactive in their competitive binding assays using [^{3}H]epibatidine.[53] With all of these results combined, it was considered highly likely that the active compound in the original sample from the frogs was not epiquinamide, but some other exceptionally bioactive contaminant.

Two years later, Rutjes and coworkers compared their synthetic standards of both enantiomers of epiquinamide with the authentic sample and determined that the natural compound is the dextrorotatory isomer ((1*S*,9*S*)-(+)-epiquinamide).[13] Subsequently, Fitch and coworkers reported GCMS evidence that the observed bioactivity of epiquinamide was due to a trace amount of cross-contamination of epibatidine (**8**).[19] This rather unfortunate finding demonstrates yet another benefit of total synthesis of a natural product; the total synthesis helps to confirm the identity of the bioactive metabolite.

> "While these data are somewhat embarrassing to report, they are not entirely unusual in the isolation of natural products. Further, the results are a reminder that the presence of multiple active substances in an extract (in this case compounded by small amounts of sample available) can sometimes lead to erroneous results from cross-contamination that are not always evident *a priori*. This underscores the importance of obtaining synthetic material whenever possible to corroborate both structure and pharmacology. In this case, we were able to produce a correct structure, but were misled by contamination in the pharmacology. Often with more complex structures, the converse occurs. Thus,it is important that the pharmacognosist work in collaboration with the synthetic/medicinal chemist to produce data that are unequivocal."
> Fitch et al, 2009[19]

V.6 Conclusion

Epiquinamide, a trace natural product isolated from amphibian skin in an effort to discover a subtype selective nAChR agonists, was enantioselectively synthesized from a

biomimetic starting material in an extremely concise and efficient manner. The unfortunate realization that the structure **9** does not possess the reported bioactivity further confirms the contemporary need for total synthesis of novel natural products.

V.7 Experimental Section

General

Unless noted otherwise, all materials were purchased from commercially available sources and were used without further purification. Anhydrous dichloromethane and diethyl ether were purchased from VWR. All reactions were carried out under dry argon atmosphere unless otherwise noted. Flash chromatorgraphy was performed using Fisher silica gel (230-400 mesh). TLC was performed using EM Science pre-coated silica gel plates (Merck 60 F_{254}). Melting points were determined on an Electrothermal Mel-Temp device and are uncorrected. Optical rotations were measured on a Rudolph Research Autopol III polarimeter and a Jasco P1010 polarimeter. IR spectra were recorded on a Nicolet Magna-IR 550. For **11-16**, ^{1}H NMR and ^{13}C NMR spectra were recorded on a Bruker spectrometer (300 MHz and 75 MHz, respectively). For **27-32** and **9**, ^{1}H NMR and ^{13}C NMR spectra were recorded on a Varian Inova spectrometer (500MHz) or on a Varian Inova spectrometer (300 MHz and 75 MHz, respectively). ^{1}H and ^{13}C spectra recorded in $CDCl_3$ were referenced to the residual solvent peaks at 7.26 ppm and 77.0 ppm, respectively. High resolution mass spectra were recorded on a ThermoFinnigan MAT900XL spectrometer.

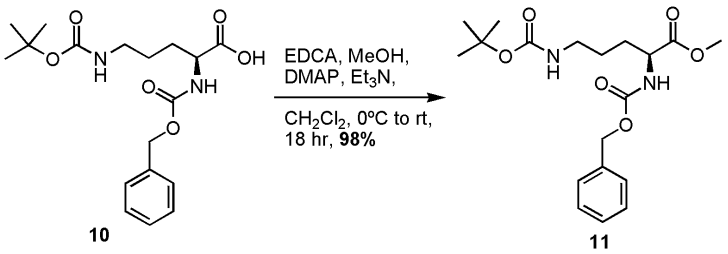

(*S*)-methyl 12,12-dimethyl-3,10-dioxo-1-phenyl-2,11-dioxa-4,9-diazatridecane-5-carboxylate (11). To *αN*,*δN*-protected ornithine **10** (718 mg, 1.96 mmol) in CH_2Cl_2 (10 mL) at 0 ºC were added anhydrous MeOH (300 µL, 7.4 mmol), DMAP (43 mg, 0.35 mmol), EDC·HCl (403 mg, 2.10 mmol), and Et_3N (280 µL, 2.0 mmol) successively. After the reaction mixture was warmed to rt over night under stirring, the volatiles were removed under vacuum. The residues were resuspended in Et_2O. The solution was washed with 0.5 M HCl, 1M $NaHCO_3$, and brine successively. Upon drying over Na2SO4, the solution was passed through a silica gel plug (1:1 EtOAc / Hex) and the solvents were removed under vacuum. Colorless gummy substance (**11**; 703 mg, 1.85 mmol, 94%) was obtained, and it was pure enough for the subsequent reactions. TLC Rf = 0.43 (1:1 EtOAc / Hex). ^{1}H and ^{13}C NMR spectra: see Figures V.4 and 5.

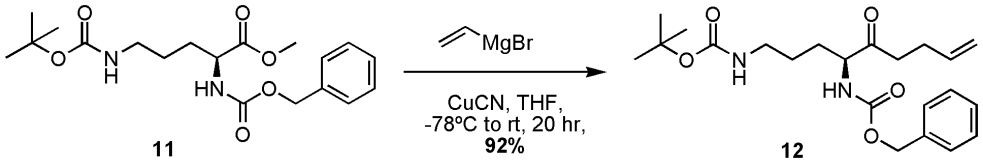

(*S*)-*αN*-Cbz, *δN*-Boc 6,9-diaminonon-1-en-5-one (12). To the suspension of CuCN (330 mg, 3.68 mmol) in THF (7 mL) at −78 ºC was added 1.0 M vinyl magnesium bromide solution in THF (50 mL) over ~7 min. The solution of **11** (3.14 g, 8.25 mmol) in THF (30 mL) was cannulated in over 5 min. The reaction mixture was gradually warmed to rt over

night under stirring. The mixture turned black. After cooling to 0 ºC, the reaction was quenched by addition of 1M HCl (200 mL) and the mixture was stirred for 15 min. Then the mixture was extracted with Et_2O thrice. The combined organic layer was washed with 1M $NaHCO_3$, water, and brine successively. Upon drying over Na2SO4, the solution was concentrated under vacuum and the residues were subjected to flash column chromatography to obtain off-white solid (**12**; 3.056 g, 7.56 mmol, 92%). TLC Rf = 0.57 (1:1 EtOAc / Hex). ^1H and ^{13}C NMR spectra: see Figures V.6 and 7.

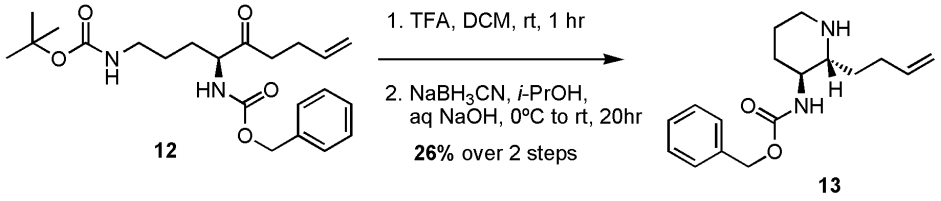

(2*R*,3*S*) benzyl-2-(but-3-enyl)piperidin-3-ylcarbamate (13). To the solution of the ketone **12** (1.72 g, 4.27 mmol) in CH_2Cl_2 (25 mL) at rt was added TFA (25 mL). The solution was stirred at rt for 1 hr and the volatiles were removed under vacuum. The oily residues were dissolved in *i*-PrOH (40 mL) and the solution was cooled to 0 ºC. NaOH solution in EtOH was added to adjust the pH to ~3. NaBH3CN (1.38 g, 22.0 mmol) was added in two portions and the solution was warmed to rt over night under stirring. Then 1M HCl (30 mL) was added to quench the reaction. Evolution of H_2 gas was observed. The volatiles were removed under vacuum. To the residues were added saturated $NaHCO_3$ and the aqueous layer was extracted with CH_2Cl_2 twice and $CHCl_3$ twice. The combined organic layer was dried over Na_2SO_4. Upon removal of the solvents under vacuum, the residues were subjected to flash column chromatography using silica gel

(0.5% Et_3N buffer, 1:49 MeOH / CH_2Cl_2 to 1:4 MeOH / CH_2Cl_2) to obtain the product (**13**; 325 mg, 1.13 mmol, 26% over two steps). ^1H and ^{13}C NMR spectra: see Figures V.8 and 9.

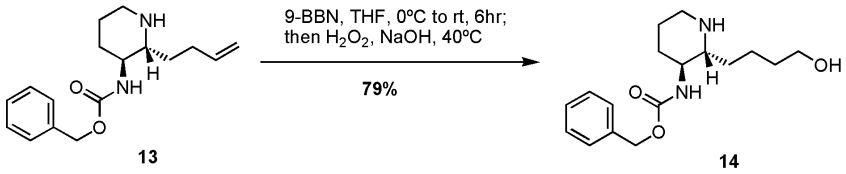

(2*R*,3*S*) benzyl-2-(4-hydroxybutyl)piperidin-3-ylcarbamate (14). No experimental details. ^1H and ^{13}C NMR spectra: see pages Figures V.10 and 11.

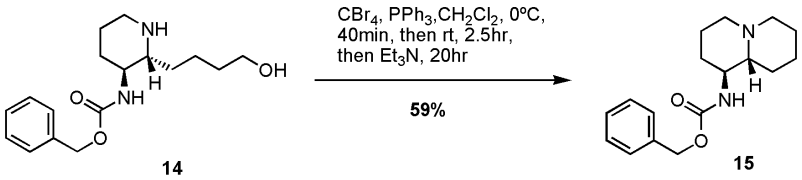

(1*S*,9a*R*) benzyl-octahydro-1H-quinolizin-1-ylcarbamate (15). To the solution of the amino alcohol **14** (56 mg, 0.183 mmol) in CH_2Cl_2 were added CBr_4 (91 mg, 0.27 mmol) and PPh_3 (120 mg, 0.46 mmol) successively at 0 ºC under stirring. The solution was warmed to rt quickly after 30 min, and it was kept at rt for 2.5 hrs. Then Et_3N (64 μL, 0.46 mmol) was added, which made the solution turn yellow. The solution was left stirring at rt for over night. Upon quenching the reaction with 1M HCl (30 mL), the organic phase was washed with 1M HCl (20 mL x 3). The combined aqueous phase was basified with solid NaOH, and it was extracted with CH_2Cl_2 (30 mL x 4). Upon drying over K_2CO_3 and removal of the solvent under vacuum, the residues were subjected to

flash column chromatography using silica gel (1:9 MeOH / CH_2Cl_2). However, the product was still contaminated with phosphine compounds and it was further purified by semi-prep HPLC using a Synergi 4μ Hydro-RP 80A (250 x 10 mm) column (1.2 mL / min H_2O to 1.5 mL / min 5:3 MeCN / H_2O) with acetic acid buffer (0.1%). The product (**15**) had a retention time of 6.02 min (31 mg, 0.11 mmol, 59%). ^1H and ^{13}C NMR spectra: see Figures V.12 and 13.

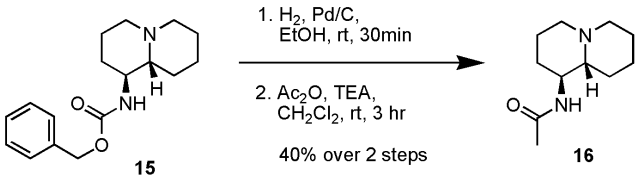

9-epi-epiquinamide (16). No experimental details. ^1H and ^{13}C NMR spectra: see Figures V.14 and 15. GCMS data: see Figure V.16.

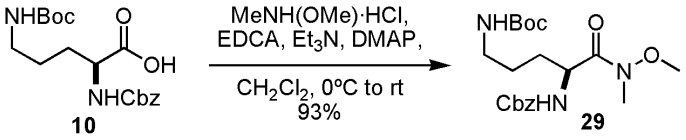

(2*S*)-2-benzyloxycarbonylamino-5-*tert*-butyloxycarbonylamino-(*N*-methoxy-*N*-methyl)pentanoyl amide (29). To *αN*,*δN*-protected ornithine **10** (7.285 g, 19.88 mmol) in CH_2Cl_2 (80 mL) stirring vigorously at 0 ºC was added *N*,*O*-dimethylhydroxylamine hydrochloride (2.180 g, 22.35 mmol), Et_3N (3.78 mL, 26.90 mmol), (3-dimethylamino-propyl)-ethyl-carbodiimide hydrochloride (4.216 g, 21.99 mmol), and 4-dimethylamino pyridine (240 mg, 1.96 mmol) sequentially. The resulting solution was left stirring to warm up to room temperature over night (18 hours). The volatiles were removed on a

rotary evaporator and the residue was suspended in ethyl acetate (200 mL). The insoluble solids were filtered off and rinsed with EtAcO. The filtrate was sequentially washed with 0.2 M HCl, water, 1.0 M $NaHCO_3$, water, and brine and was dried over $MgSO_4$. After filtration using Celite®, the solvents were removed under vacuum and a colorless glass (**29**) was obtained and was used without purification for the next step. (7.564 g, 18.47 mmol, 93%). TLC Rf = 0.30 EtAcO/hexane (3:2). $[\alpha]_D^{24}$ –6.3º (*c* 1.20, $CHCl_3$). IR (film) 3332, 3080, 3024, 2975, 2936, 1709, 1654, 1530, 1450, 1398, 1367, 1250, 1160 cm^{-1}. ^1H NMR (500 MHz, $CDCl_3$) δ 7.26-7.36 (m, 5H), 5.53 (d, *J* = 9.0 Hz, 1H), 5.08 (m, 2H), 4.73 (m, 1H), 4.57 (m, 1H), 3.77 (s, 3H), 3.20 (s, 3H), 3.12 (m, 2H), 1.70-1.80 (m, 2H), 1.49-1.61 (m, 2H), 1.41 (s, 3H). ^{13}C NMR (75 MHz, $CDCl_3$) δ 172.3, 156.1, 155.8, 136.2, 128.4, 128.0, 127.9, 79.0, 66.8, 61.5, 50.6, 40.0, 30.0, 28.3, 25.8. HRMS (EI): calcd for $C_{20}H_{32}N_3O_6$ (M + H): 410.2286, found: 410.2287.

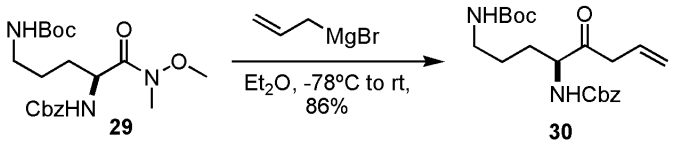

(5*S*)-2-benzyloxycarbonylamino-5-*tert*-butyloxycarbonylamino-4-oxo-1-octene (30). To the solution of allylmagnesium bromide in Et_2O (1.0 M, 100 mL, 100 mmol) at -78 ºC was added the solution of the Weinreb amide **29** (9.060 g, 22.13 mmol) in Et_2O (135 mL) dropwise over 1 hour while vigorously stirring. The resulting slurry mixture was warmed to room temperature and stirred for 30 min. Upon cooling to -10 ºC, aqueous HCl solution (1.0 M, 125 mL) was added carefully and the mixture was stirred for 5 min at -10 ºC. After partitioning, the aqueous layer was extracted with Et_2O (30 mL × 3) and the

combined organic layer was washed sequentially with cold 0.1 M HCl, cold water, cold 1.0 M $NaHCO_3$, and brine, and then was dried over $MgSO_4$. Upon filtration through Celite®, the solvents were removed under vacuum. The residue was dissolved in a mixture of Et_2O and CH_2Cl_2, and hexane was added and the product was re-crystallized (7.138 g, white needles). The filtrate was concentrated under vacuum and was purified by flash chromatography (EtAcO / hexane 1:9 to 1:4). The separation of the double bond-isomerized products from the desired product was difficult. The product (**30**) was a white solid (total 7,420 g, 19.00 mmol, 86%). TLC Rf = 0.46 EtAcO / hexane (2:3). Mp 85~86 ºC. $[\alpha]_D^{24}$ +46º (*c* 0.34, $CHCl_3$). IR (film) 3332, 3080, 3025, 2975, 2936, 1693, 1639, 1525, 1452, 1250, 1168 cm^{-1}. ^1H NMR (500MHz, CDCl3) δ 7.29-7.37 (m, 5H), 5.82-5.96 (m, 1H), 5.55 (d, *J* = 7.2 Hz, 1H), 5.23-5.19 (m, *J* =11.0 Hz, 1H), 5.13-5.09 (m, *J* = 11.0 Hz, 1H), 5.09 (s, 2H), 4.57 (bs, 2H), 4.44-4.50 (m, 1H), 3.28 (d, *J* = 6.6 Hz, 2H), 3.09-3.17 (m, 2H), 1.86-1.97 (m, 2H), 1.46-1.59 (m, 2H), 1.43 (s, 9H). ^{13}C NMR (75 MHz, $CDCl_3$) δ 206.5, 156.0,156.0, 136.2, 129.5, 128.5, 128.2, 128.1, 119.5, 79.3, 67.0, 59.1, 59.0, 44.5, 39.9, 28.6, 28.4, 25.8. HRMS (EI): calcd for $C_{21}H_{31}N_2O_5$ (M + H): 391.2227, found: 391.2221.

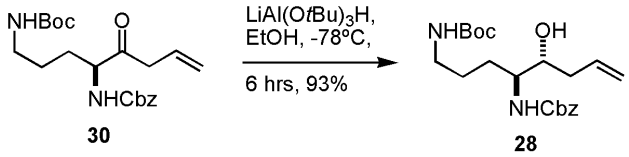

30 **28**

(4*R*,5*S*)-5-benzyloxycarbonylamino-8-*tert*-butyloxycarbonylamino-4-hydroxy-1-octene (28). To the suspension of LiAl(O*t*-Bu)$_3$H (10.25 g, 40.31 mmol) in EtOH (70 mL) stirring at -78 ºC was added ketone **30** (3.952 g, 10.12 mmol) in EtOH (70 mL)

dropwise over 30 min. After stirring for 5 hours at -70 to -78º C, 10% citric acid (100 mL) was added, and the mixture was stirred for 20 min. This mixture was extracted with CH_2Cl_2 four times, and the combined organics were washed with water, saturated $NaHCO_3$, brine and dried over Na_2SO_4. Upon concentration under vacuum, the mixture was dissolved in minimal amount of CH_2Cl_2 / Et_2O (1:2) and small amount of hexane was added. After slow cooling to -20 ºC, crystals were washed with Et_2O / hexane (1:1) and then dried under vacuum (3.516 g). The filtrate containing the product was purified by flash chromatography (EtAcO / hexane 1:9 to 1:1) after concentration under vacuum (**28**; total 3.703g, 9.435 mmol, 93%). TLC Rf = 0.33 EtAcO / hexane (1:1). Mp 106 ºC. $[\alpha]_D^{24}$ +22º (*c* 0.37, $CHCl_3$). IR (film) 3348, 3317, 3068, 2944, 1689, 1538, 1452, 1260, 1160. ^{1}H NMR (300 MHz, $CDCl_3$) δ 7.26-7.38 (m, 5H), 5.74-5.88 (m, 1H), 5.16 (m, 2H), 5.05-5.12 (m, 2H), 5.09 (s, 2H), 4.57 (m, 1H), 3.67 (m, 2H), 3.11 (m, 2H), 2.11-2.32 (m, 2H), 1.51-1.70 (m, 2H), 1.28-1.51 (m, 11H). ^{13}C NMR (300 MHz, $CDCl_3$) δ 156.6, 156.1, 136.4, 134.4, 128.5, 128.1, 128.1, 118.3, 79.2, 73.2, 66.8, 55.0, 40.3, 38.3, 28.4, 26.8, 26.2. HRMS (EI): calcd for $C_{21}H_{33}N_2O_5$ (M + H): 393.2384, found 393.2375.

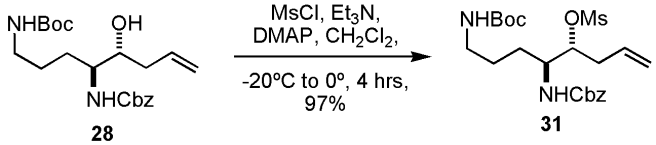

(4*R*,5*S*)-5-benzyloxycarbonylamino-8-*tert*-butyloxycarbonylamino-4-methanesulfonyloxy-1-octene (31). To the solution of the amino alcohol **28** (4.2807 g, 10.91 mmol) in CH_2Cl_2 (320 mL) stirring at -15 ºC was added Et_3N (3.13 mL, 22.3 mmol). Methanesulfonyl chloride (1.27 mL, 16.4 mmol) was added dropwise, and then 4-

dimethylaminopyridine (702 mg, 5.75 mmol) was added. The solution was left stirring at temperature ranging from -15 ºC to 0 ºC for 4 hours. Cold water (100 mL) was then added rapidly at 0 ºC. The mixture was extracted with CH_2Cl_2 three times and the combined organics were washed with cold 1.0 M HCl, cold water, cold $NaHCO_3$, and dried over Na_2SO_4. Upon removal of the solvents under vacuum, the product was recrystallized from CH_2Cl_2 / Et_2O / hexane system as white crystals (4.838 g, 10.28 mmol). The residual product in the filtrate was purified by flash chromatography (EtAcO / hexane 1:9 to 2:3) and white solid (**31**) was obtained (total 4.978 g, 10.58 mmol, 97 % yield). TLC Rf = 0.70 EtAcO / hexane 1:1. Mp 67ºC. $[\alpha]_D^{24}$ –27º (*c* 0.50, $CHCl_3$). IR (film) 3402, 2983, 2944, 1689, 1639, 1525, 1452, 1365, 1339, 1254, 1173, 913 cm^{-1}. ^1H NMR (500 MHz, $CDCl_3$) δ 7.26-7.36 (m, 5H), 5.74-5.85 (m, 1H), 5.25 (m, 1H), 5.18 (d, *J* = 9.5 Hz, 1H), 5.16 (m, 1H), 5.10 (s, 2H), 4.83 (m, 1H), 4.58 (m, 1H), 3.88 (m, 1H), 3.11 (m, 2H), 2.98 (s, 3H), 2.46-2.54 (m, 1H), 2.37-45 (m, 1H), 1.54-1.66 (m, 2H), 1.27-1.49 (m, 11). ^{13}C NMR (75 MHz, $CDCl_3$) δ 156.1, 156.0, 136.4, 132.3, 128.4, 128.0, 127.9, 119.2, 83.5, 79.2, 66.8, 53.0, 39.9, 38.5, 36.1, 28.3, 26.7, 25.4. HRMS (EI): calcd for $C_{22}H_{34}N_2O_7S$: 470.2081, found 470.2083.

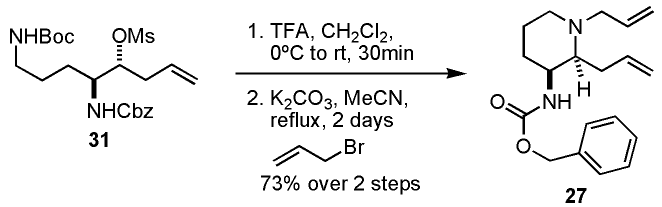

(2*S*, 3*S*)-2-allyl-3-benzyloxycarbonylaminopiperidine (27). To the solution solution of the mesylate **31** (2.734 g, 5.809 mmol) in CH_2Cl_2 (43 mL) at 0ºC was added

trifluoroacetic acid (11 mL) dropwise over 5 min while stirring. Immediately the reaction mixture was warmed to room temperature and was stirred for 45 min. Upon cooling the reaction mixture to 0ºC again and diluting the mixture with CH_2Cl_2 (100 mL), 2M K_2CO_3 solution (100 mL) was added carefully. This mixture was partitioned and the aqueous phase was extracted with CH_2Cl_2 (50 mL × 4). The combined organic phase was dried over anhydrous K_2CO_3 and was filtered through celite. The solvents were removed on a rotary evaporator. The residues were then dissolved in CH_3CN (450 mL), and K_2CO_3 (4.20 g, 30.4 mmol) was added in two portions over 3 hours. After stirring the mixture for 24 hours, the mixture was gradually heated up to 70ºC over 1.5 hours. The consumption of the primary amine was confirmed on TLC, and the mixture was filtered through celite and was concentrated in vacuum to ca. 90 mL. After the addition of K_2CO_3 (1.78g, 12.9 mmol), the mixture was stirred for 30 min at room temperature. Then allylbromide (800µL, 9.19 mmol) and additional K_2CO_3 (0.98 g, 7.1 mmol) were added and the mixture was left stirring at room temperature for 30 hours. Additional allylbromide (200µL, 2.30 mmol) and K_2CO_3 (0.54 g, 3.9 mmol) was added and the mixture was stirred at room temperature for 4 hours. Upon filtration of the mixture, the solvents were removed on a rotary evaporator. To the residues were added Et_2O (200 mL) and saturated $NaHCO_3$ (150 mL). After partitioning the phases, the aqueous phase was extracted with Et_2O (50 mL × 4). The combined organic phases were dried over Na_2SO_4, and filtered through Celite®. After the removal of the solvents under vacuum, the residue was purified by flash chromatography (EtAcO / hexane, 1:19 to 1:4), yielding a colorless oil (**27**; 1.382 g, 4.395 mmol, 76 % over 2 steps). TLC Rf = 0.45 EtAcO / hexane 1:1. $[\alpha]_D^{24}$ = +16º (*c* 0.23, $CHCl_3$). IR (film) 3427, 3078, 3029, 2942, 2864, 2811,1720, 1640, 1500,

1456, 1341, 1214, 919 cm^{-1}. ^{1}H NMR (300 MHz, $CDCl_3$) δ 7.28-7.38 (m, 5H), 5.86-5.71 (m, 2H), 5.48 (m, 1H), 5.16-4.96 (m, 7H), 3.84 (m, 1H), 3.29 (m, 1H), 2.92 (m, 1H), 2.80 (m, 1H), 2.35-2.46 (m, 2H), 2.15-2.03 (m, 2H), 1.84 (m, 1H), 1.64 (m, 1H), 1.47 (m, 1H), 1.39 (m, 1H). ^{13}C NMR (75 MHz, $CDCl_3$) δ 155.5, 136.7, 134.9, 134.4, 128.3, 127.9, 127.9, 117.6, 117.2, 66.3, 63.0, 56.3, 52.6, 48.1, 33.9, 29.5, 20.8. Both ^{1}H and ^{13}C NMR spectra contain rotamer signals.[55] HRMS (EI): calcd for $C_{19}H_{26}N_2O_2$ (M): 314.1989, found 314.1994.

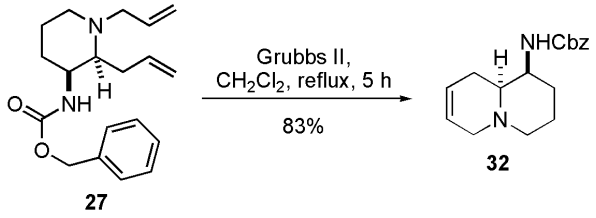

27 32

(1*S*, 10*S*)-1-benzyloxycarbonylamine-7,8-dehydroquinolizidine (31). To the solution of the 1,2-diallyl piperazine **27** (1.131 g, 3.597 mmol) in CH_2Cl_2 (360 mL) was added Grubb's 2nd generation catalyst (269 mg, 0.360 mmol) in two portions over 2 hours. The mixture was brought to reflux slowly and the temperature was reduced to room temperature after 2 hours for the second addition of the catalyst. Then the mixture was refluxed again for 5 hours (while monitoring by TLC) and cooled again to room temperature. Silica gel (3.0 g) was added and the mixture was stirred for 10 min. The solids were filtered through Celite® and rinsed with CH_2Cl_2 thoroughly. To the filtrate was added activated charcoal (ca. 20 g) and the mixture was left stirring at room temperature over night. Upon filtration through Celite®, the filtrate was concentrated on a rotary evaporator. The residue was purified by flash chromatography on silica gel twice to yield

transparent brown oil still contaminated with a miniscule amount of the ruthenium catalyst (**32**; 855 mg, 2.986 mmol,). TLC Rf = 0.24 CH_2Cl_2 / MeOH 49:1. $[\alpha]_D^{24}$ –40º (*c* 0.33 $CHCl_3$). IR (film) 3431, 3055, 2960, 2807, 2758, 1718, 1644, 1500, 1337, 1217, 1095 cm^{-1}. ^1H NMR (500 MHz, $CDCl_3$) δ 7.28-7.35 (m, 5H), 5.68-5.71 (m, 1H), 5.57 (m, 1H), 5.10 (s, 2H), 3.77 (dd, *J* = 9.2, 2.5 Hz, 1H), 3.19 (m, *J* = 16.4 Hz, 1H), 2.89 (dd, *J* = 11.2, 2.2 Hz, 1H), 2.68 (m, *J* = 16.4 Hz, 1H), 2.35 (m, *J* = 8.3 Hz, 1H), 2.19-2.26 (m, 1H), 2.03 (td, *J* = 12.2, 3.1 Hz, 1H), 1.93 (m, 1H), 1.90 (m, 1H), 1.75 (m, *J* = 12.9, 3.8 Hz, 1H), 1.54 (m, *J* = 14.6 Hz, 1H), 1.49 (dt, *J* = 13.3, 3.7 Hz, 1H). ^{13}C NMR (75 MHz, $CDCl_3$) δ 156.2, 136.7, 128.4, 127.9, 127.8, 124.2, 123.4, 66.4, 58.9, 56.1, 54.3, 49.1, 29.8, 27.8, 20.3. Both ^1H and ^{13}C NMR spectra contain rotamer signals.[54] HRMS (EI): calcd for $C_{17}H_{22}N_2O_2$ (M): 286.1676, found 286.1677.

32 **9**

38% overall

(+)-epiquinamide (9). Method A. To the solution of the dehydroquinolizidine **32** (200 mg, 0.698 mmol) in EtOH (3.7 mL) was added Pd/C (10% wt, 180 mg) carefully. Argon was evacuated and H_2 was bubbled into the mixture for 5 min. Then the reaction mixture was left stirring under H_2 atmosphere over night using balloon pressure. Acetic anhydride (170 μL, 1.80 mmol) was added in three portions over 1 hour. The reaction mixture was left stirring again over night and then was filtered through Celite® and the filter case was rinsed with ethanol. Upon concentration, the residue was purified by flash chromatography on silica gel (CH_2Cl_2 / MeOH / 28% NH_4OH(aq) 99:0.9:0.1 to 90:9:1) to

yield pale yellow solid (**9**; 87 mg, 0.44 mmol, 63 % yield). Rf = 0.39 CH_2Cl_2 / MeOH / 28% NH_4OH(aq) 90:9:1. Mp 130ºC. $[\alpha]_D^{24}$ +24º (*c* 0.10, $CDCl_3$). IR (film) 3427, 2949, 2862, 2814, 2766, 1637, 1540, 1376, 1295, 1211 cm^{-1}. ^1H NMR (300 MHz, $CDCl_3$) δ 6.24 (bs, 1H), 3.92 (m, *J* = 8.8, 2.0 Hz, 1H), 2.78 (m, 2H), 2.01 (s, 3H), 1.94 (m, 3H), 1.85 (m, *J* = 13.4 Hz, 1H), 1.72 (m, *J* = 13.2 Hz, 2H), 1.19-1.63 (m, 7H). ^{13}C NMR (75 MHz, $CDCl_3$) δ 169.6, 64.4, 56.7, 56.6, 48.0, 29.5, 28.9, 25.4, 23.9, 23.4, 20.4. HRMS (EI): calcd for $C_{11}H_{21}N_2O_1$ (M + H): 197.1648, found 197.1650.

(+)-epiquinamide. Method B. To the solution of the dehydroquinolizidine **32** (290 mg, 1.01 mmol) in EtOH (3.0 mL) was added Pd/C (10% wt, 100 mg) carefully. Argon was evacuated and H_2 was bubbled into the mixture for 5 min. Then the reaction mixture was left stirring under H_2 atmosphere over night using balloon pressure. The reaction mixture was left stirring again over night and then was filtered through Celite® and the filter cake was rinsed with ethanol. The solvent was removed under vacuum, and the residues were dissolved in dioxane (10 mL). While stirring, aqueous solution of NaOH (1.0 M, 10 mL) was added slowly at room temperature. After 2 hours, the reaction mixture was extracted with CH_2Cl_2 (20 mL × 4). The organic layer was dried over Na_2SO_4 and was concentrated under vacuum. The residue was purified by flash chromatography on silica gel (CH_2Cl_2 / MeOH / 28% NH_4OH(aq) 99:0.9:0.1 to 90:9:1) to yield pale yellow solid (**9**; 173 mg, 0.881 mmol, 87 % yield).

(-)-epiquinamide. TLC Rf = 0.39 CH_2Cl_2 / MeOH / 28% NH_4OH(aq) 90:9:1. $[\alpha]_D^{24}$ –22º (*c* 0.13, $CHCl_3$). . ^1H and ^{13}C NMR: identical to **(+)-9**. HRMS (EI): calcd for $C_{11}H_{21}N_2O_1$ (M + H): 197.1648, found 197.1648.

NMR Spectra

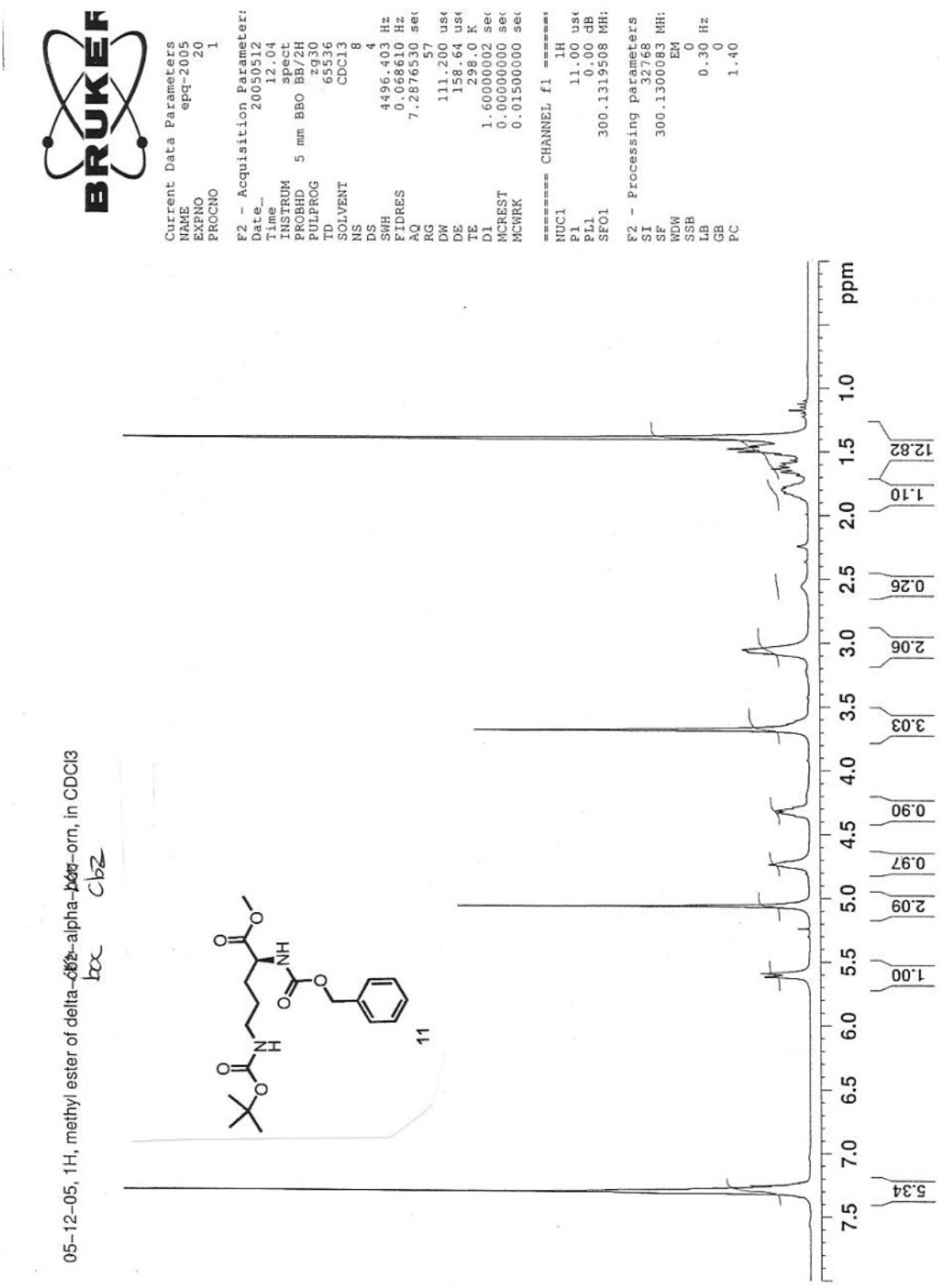

Figure V.4: ^{1}H NMR Spectrum of **11** in $CDCl_3$

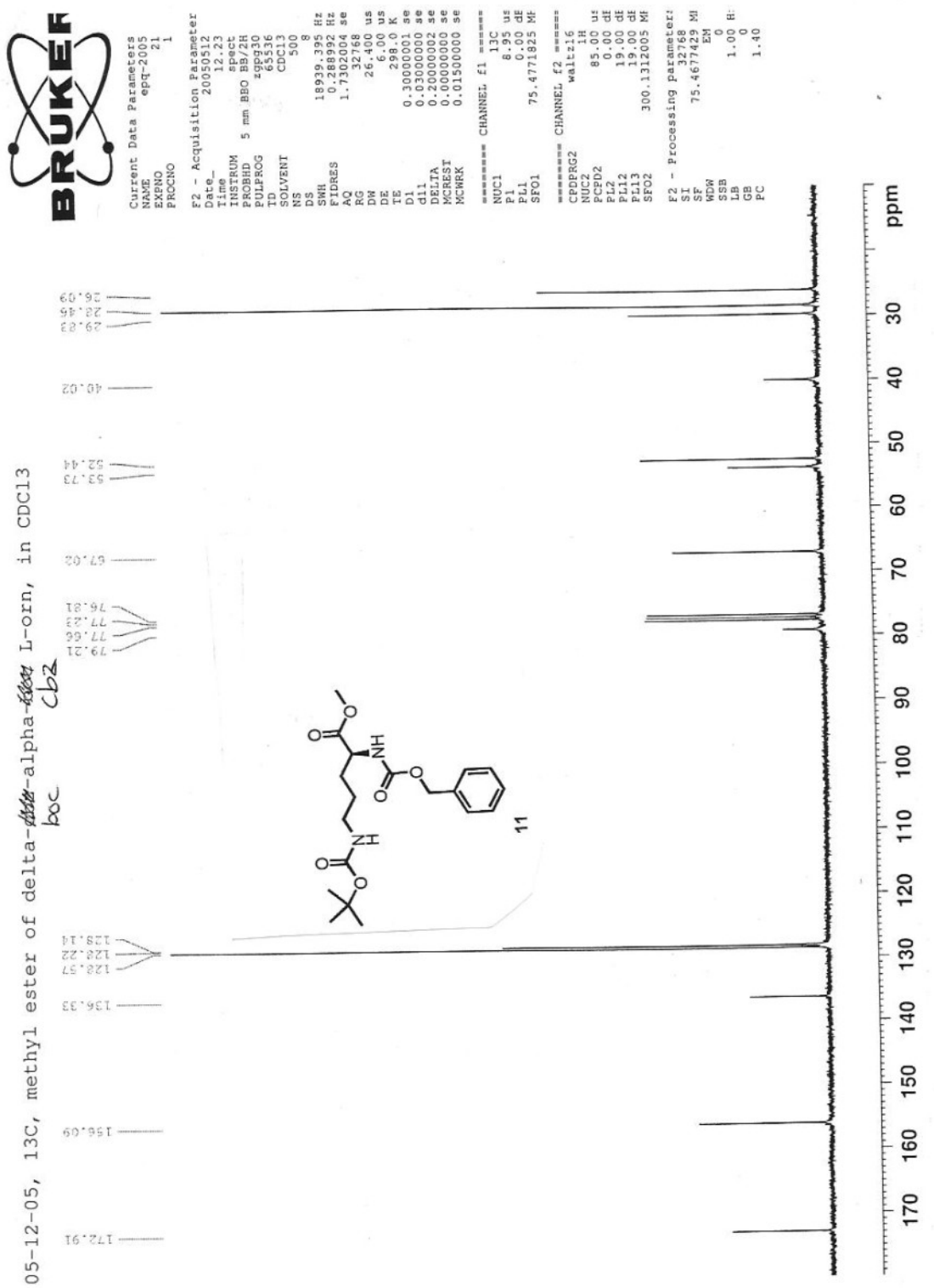

Figure V.5: ^{13}C NMR Spectrum of **11** in $CDCl_3$

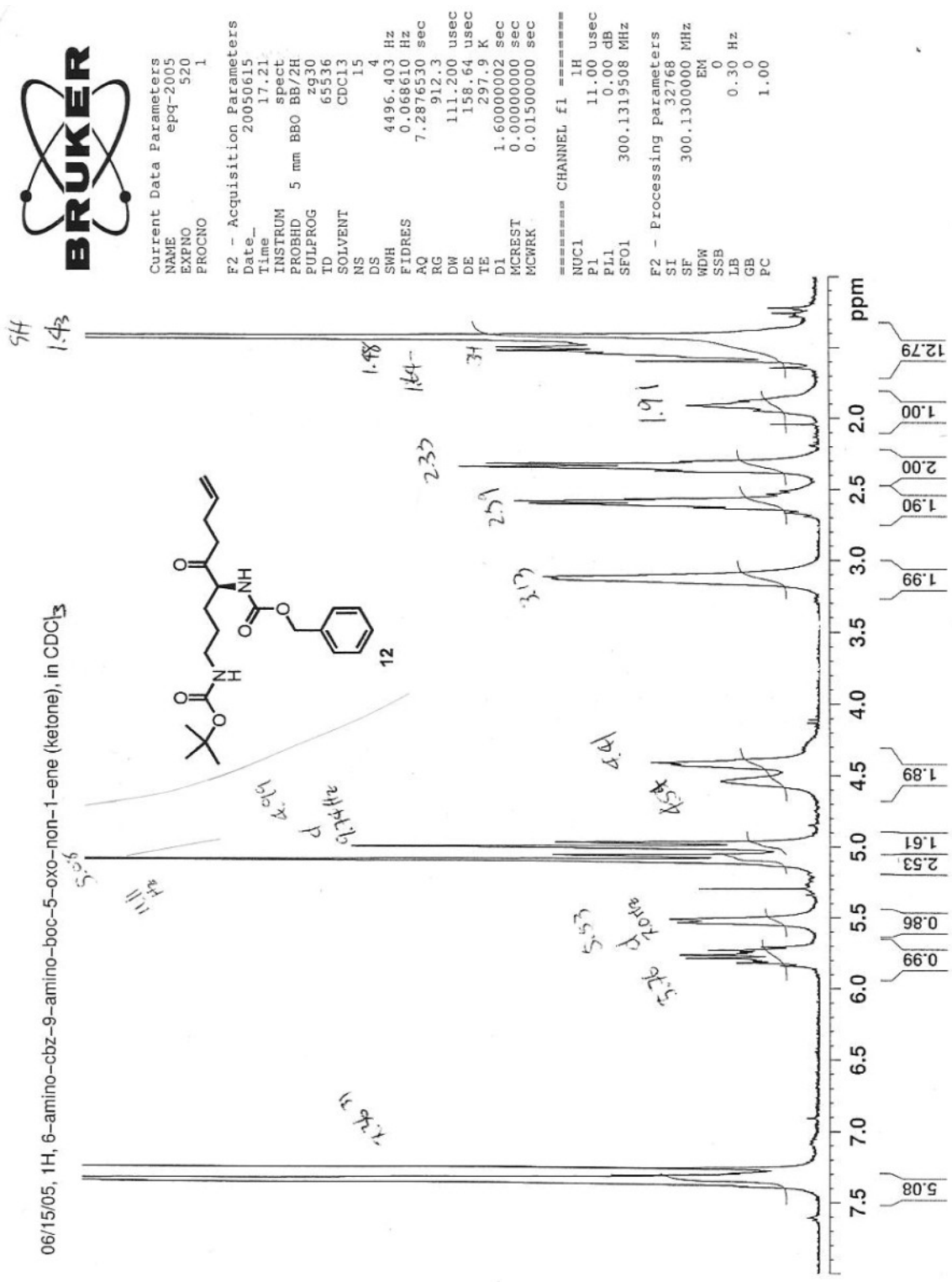

Figure V.6: ^{1}H NMR Spectrum of **12** in $CDCl_3$

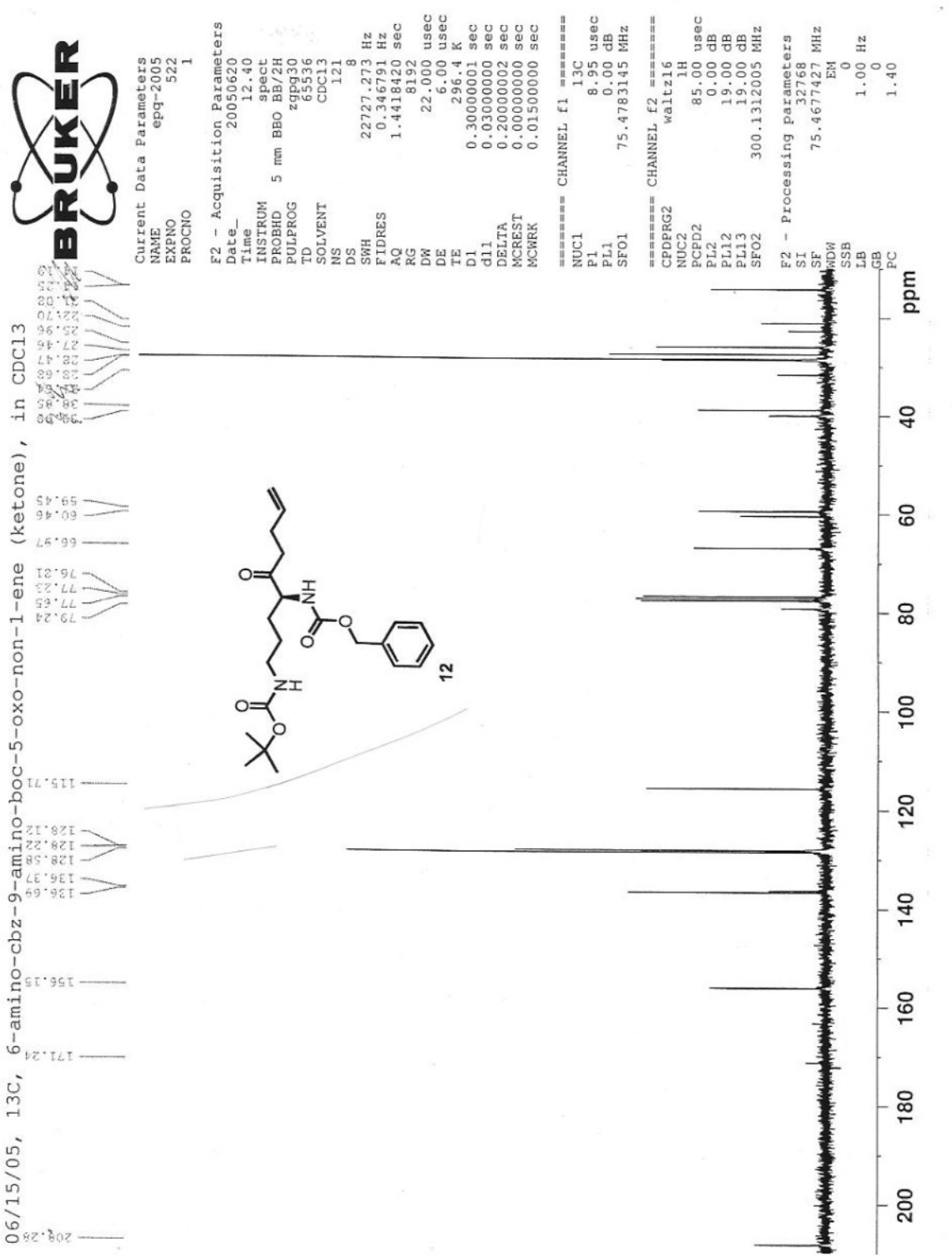

Figure V.7: ^{13}C NMR Spectrum of **12** in $CDCl_3$

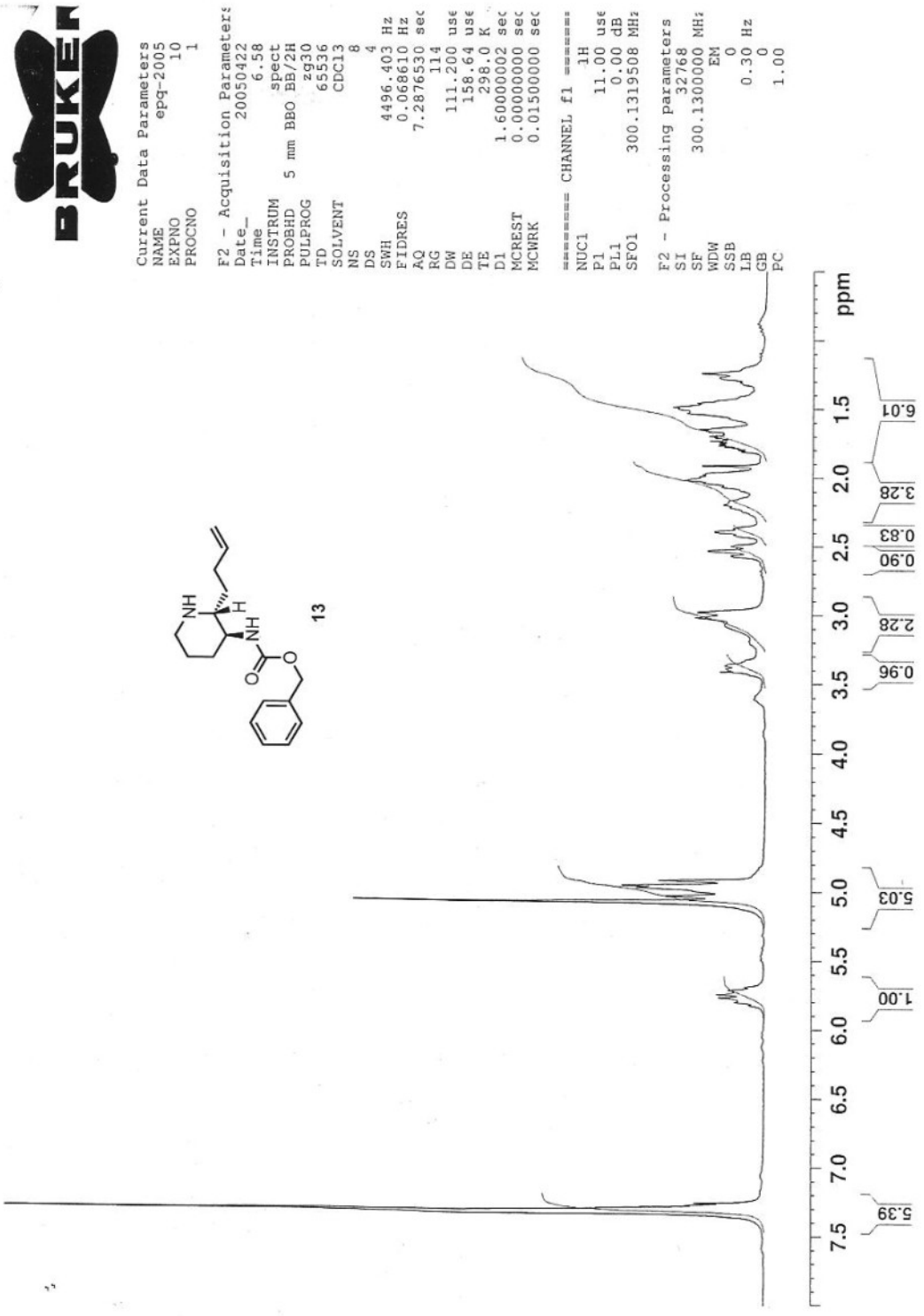

Figure V.8: ^{1}H NMR Spectrum of **13** in $CDCl_3$

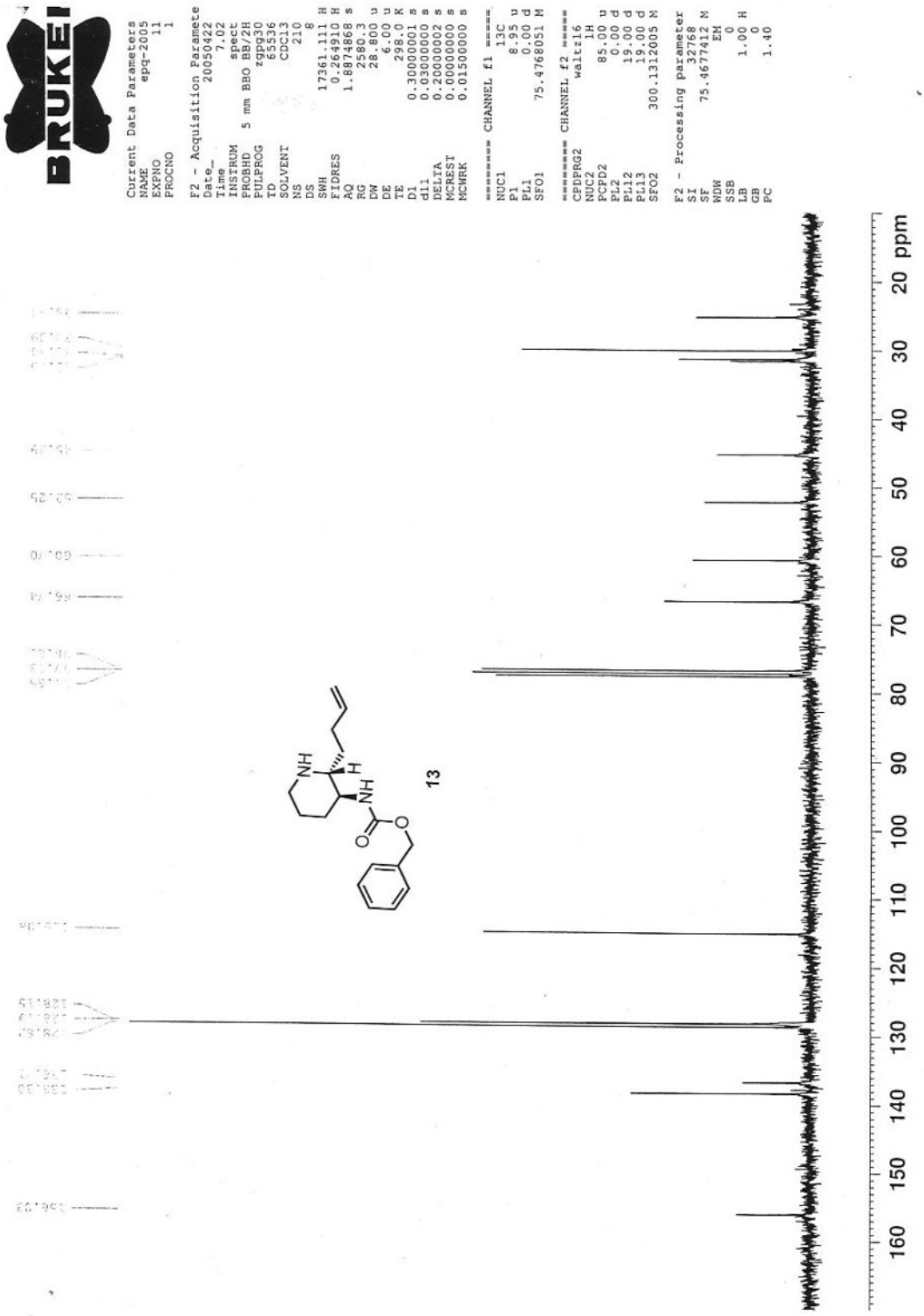

Figure V.9: ^{13}C NMR Spectrum of **13** in $CDCl_3$

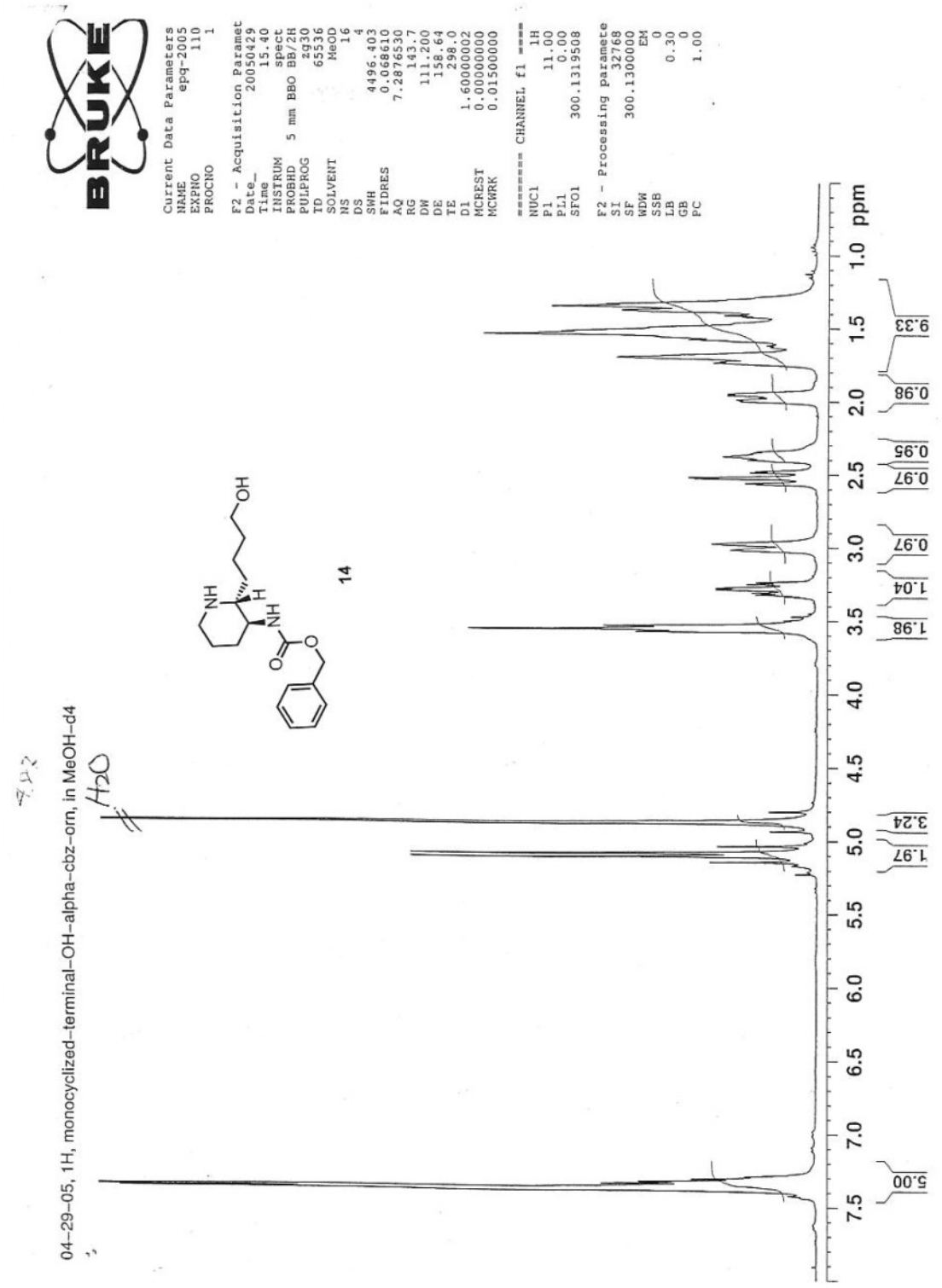

Figure V.10: ^{1}H NMR Spectrum of **14** in $CDCl_3$

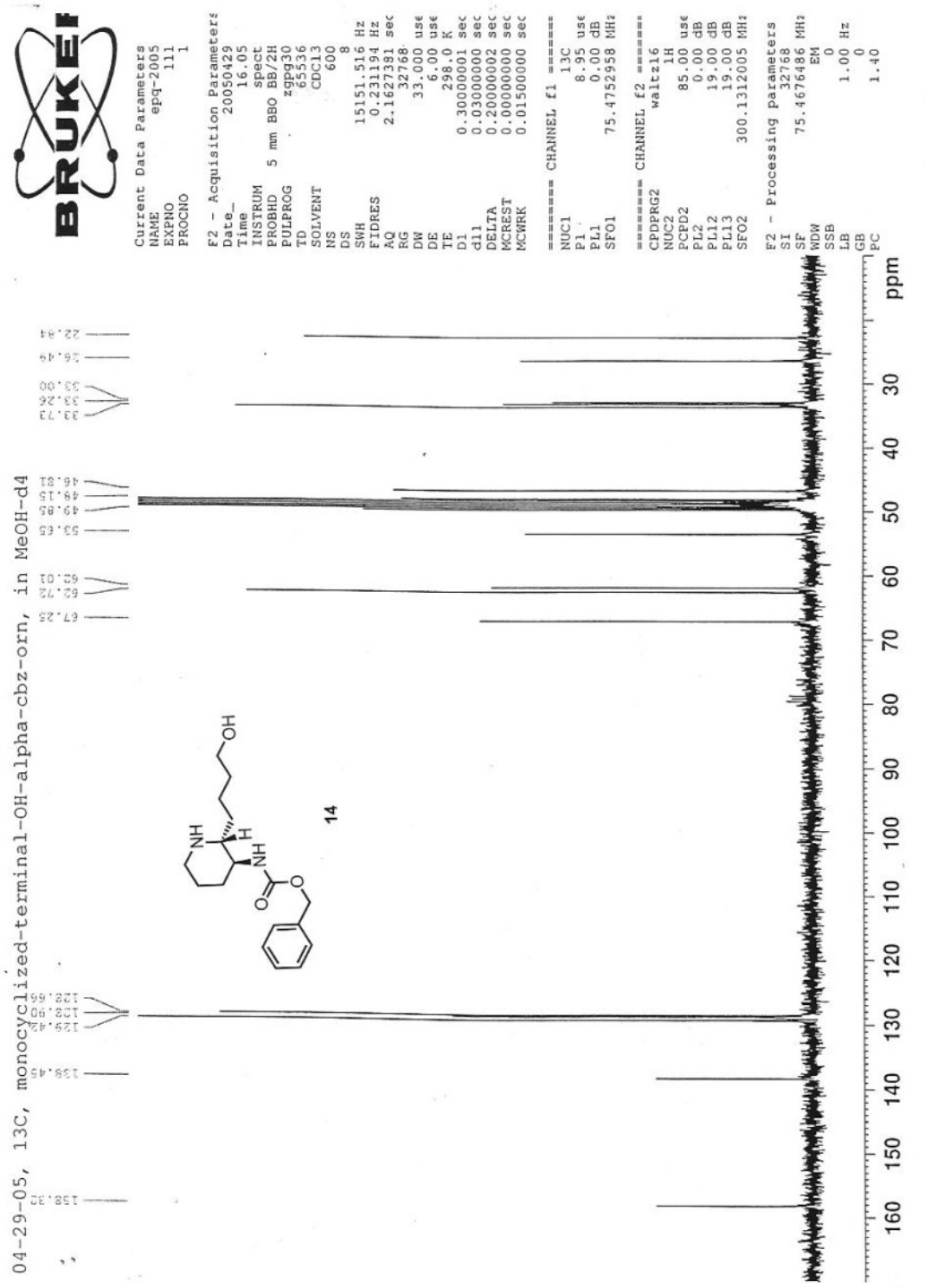

Figure V.11: ^{13}C NMR Spectrum of **14** in $CDCl_3$

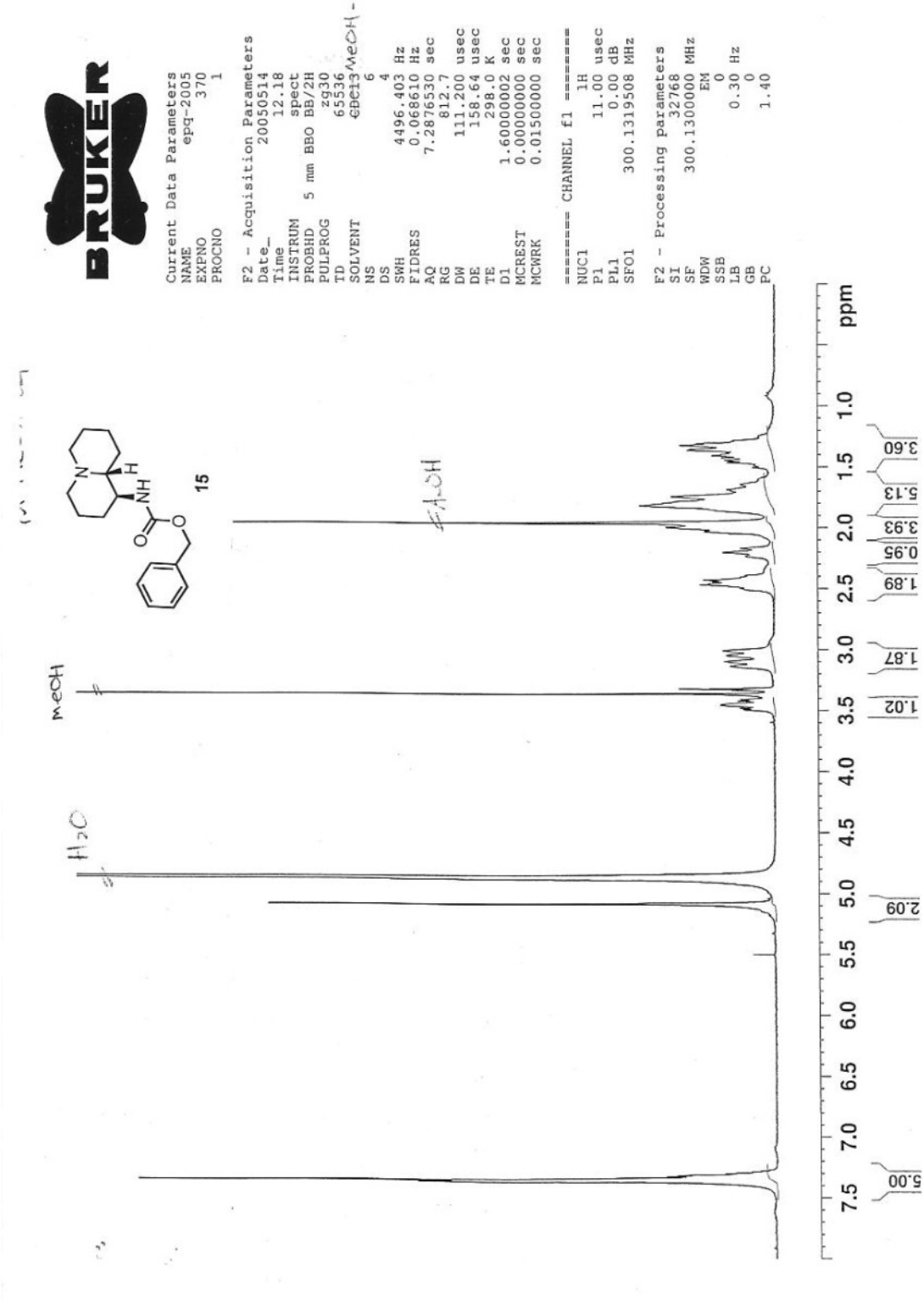

Figure V.12: ^{1}H NMR Spectrum of **15** in MeOH-d_4

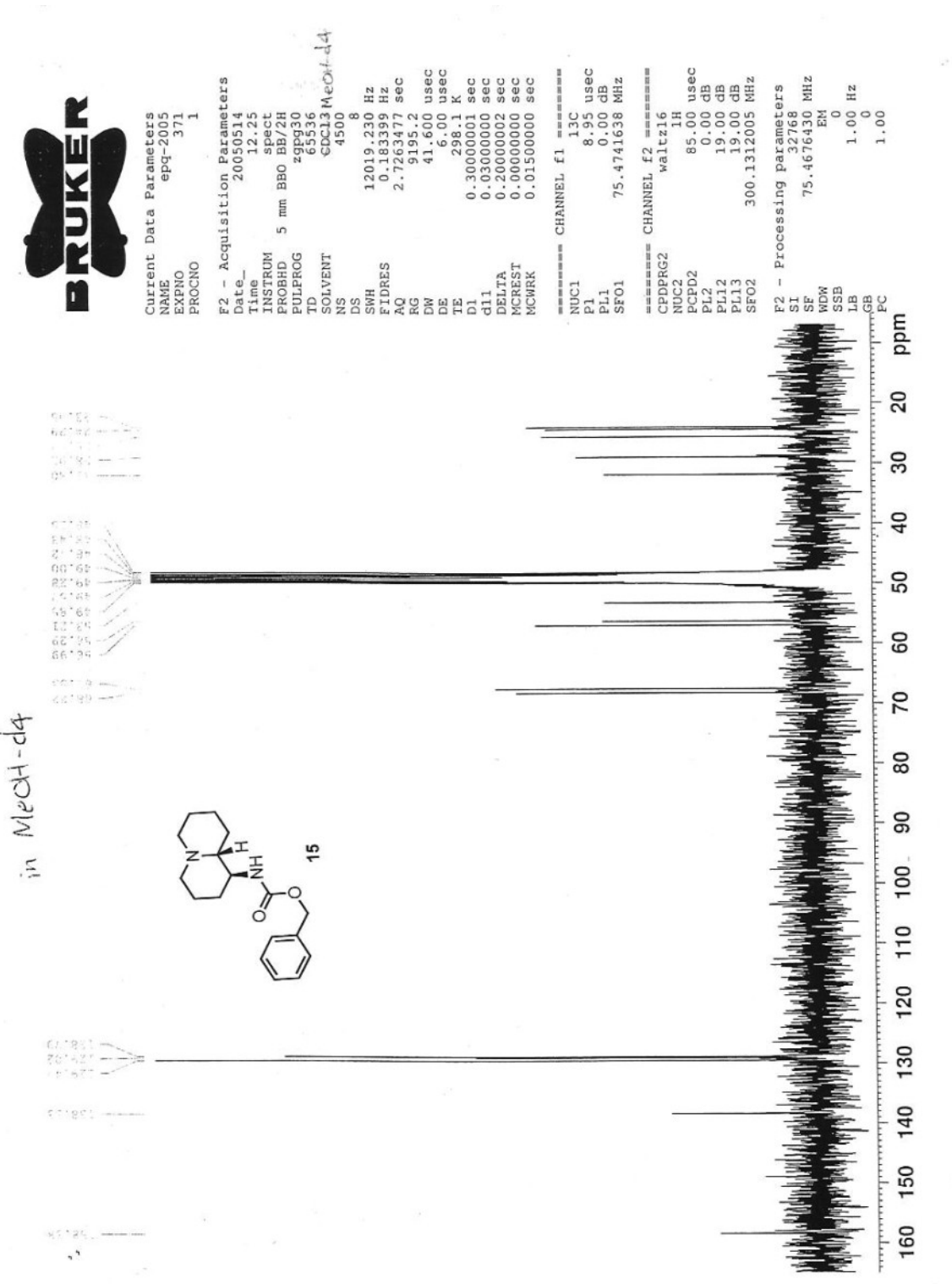

Figure V.13: ^{13}C NMR Spectrum of **15** in MeOH-d_4

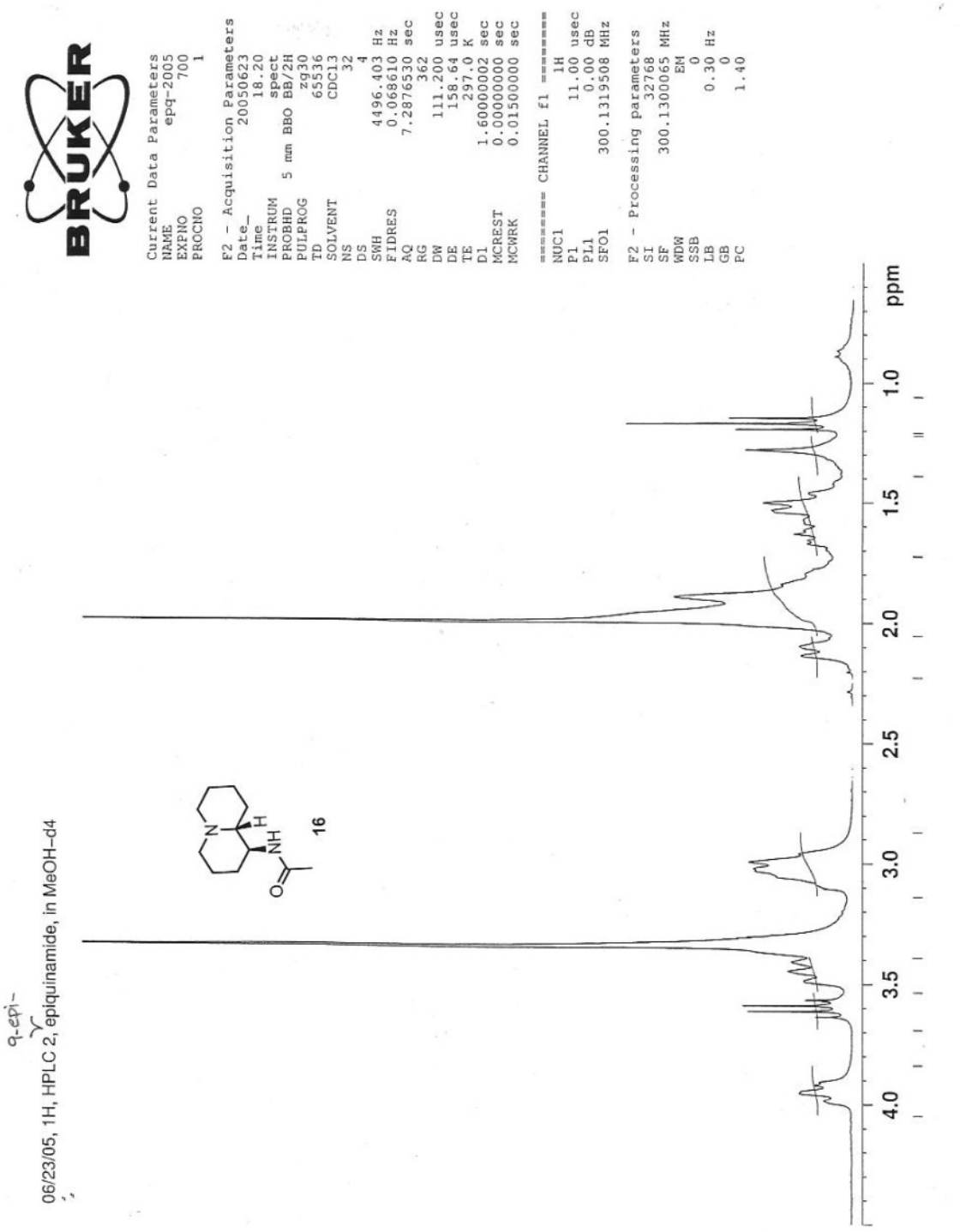

Figure V.14: ^{1}H NMR Spctrum of **16** in $CDCl_3$

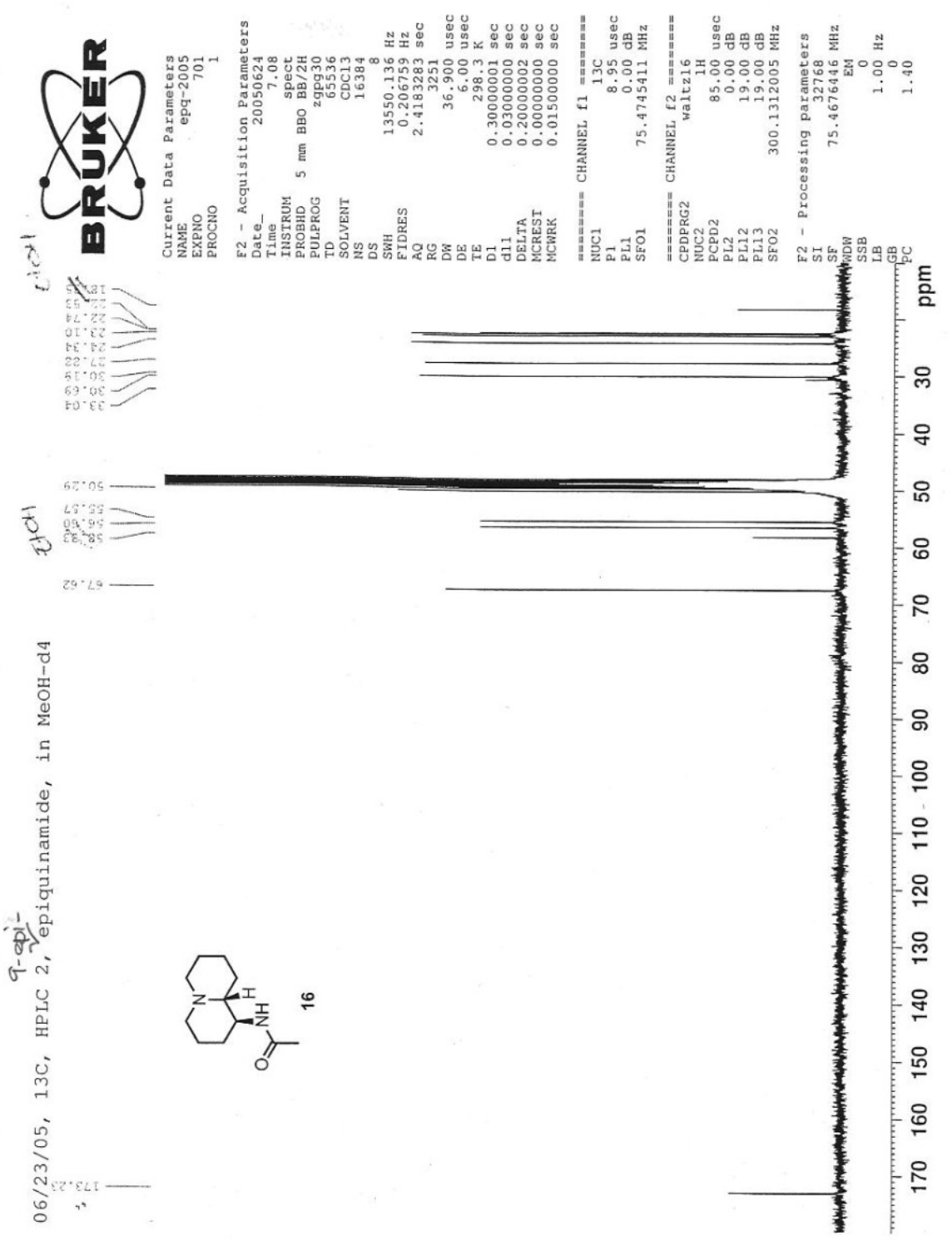

Figure V.15: ^{13}C NMR Spectrum of **16** in $CDCl_3$

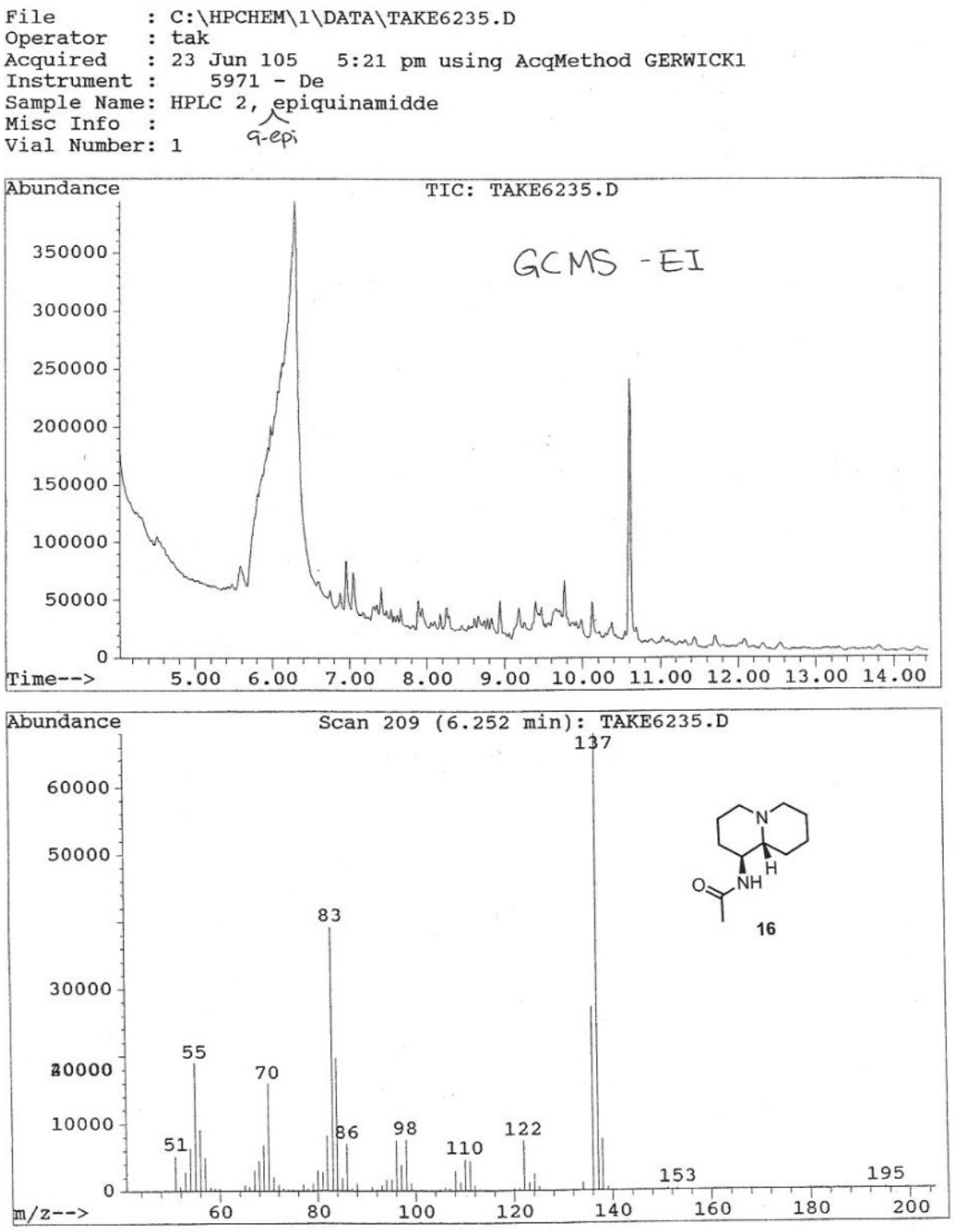

Figure V.16: EI-GCMS Chromatogram and Mass Spectrum of **16**

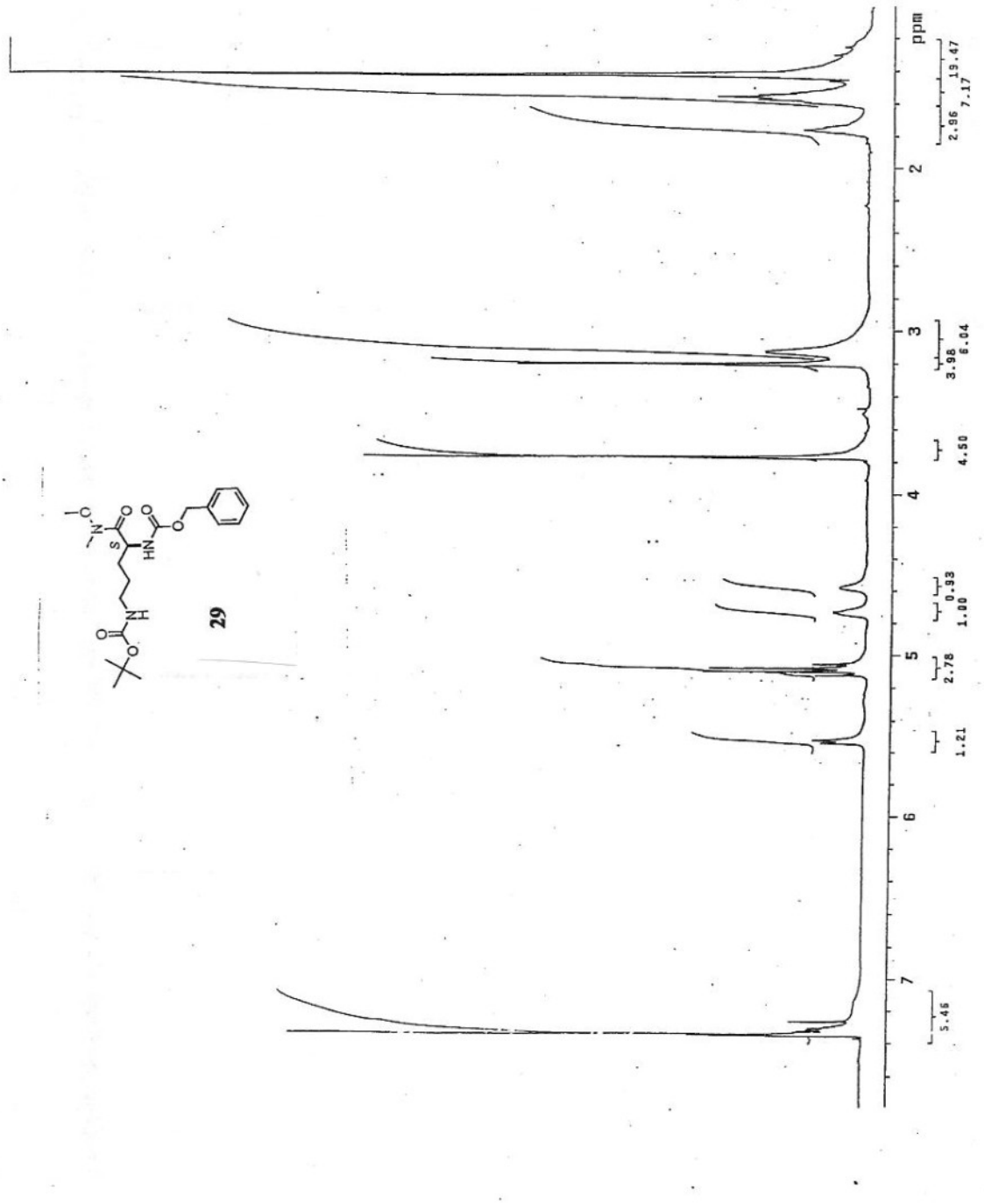

Figure V.17: ^{1}H NMR spectrum **29** in $CDCl_3$

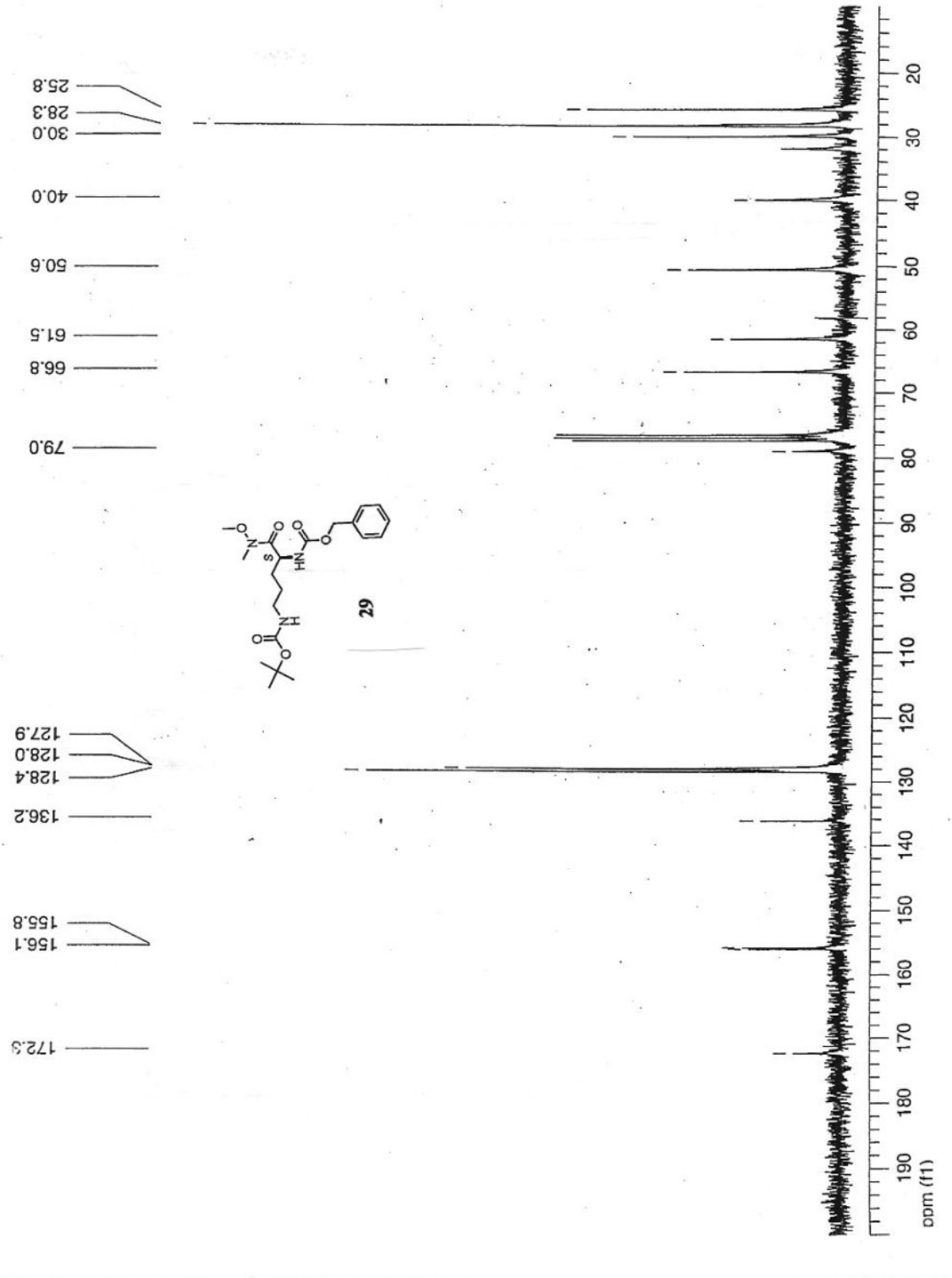

Figure V.18: ^{13}C NMR spectrum of **29** in $CDCl_3$

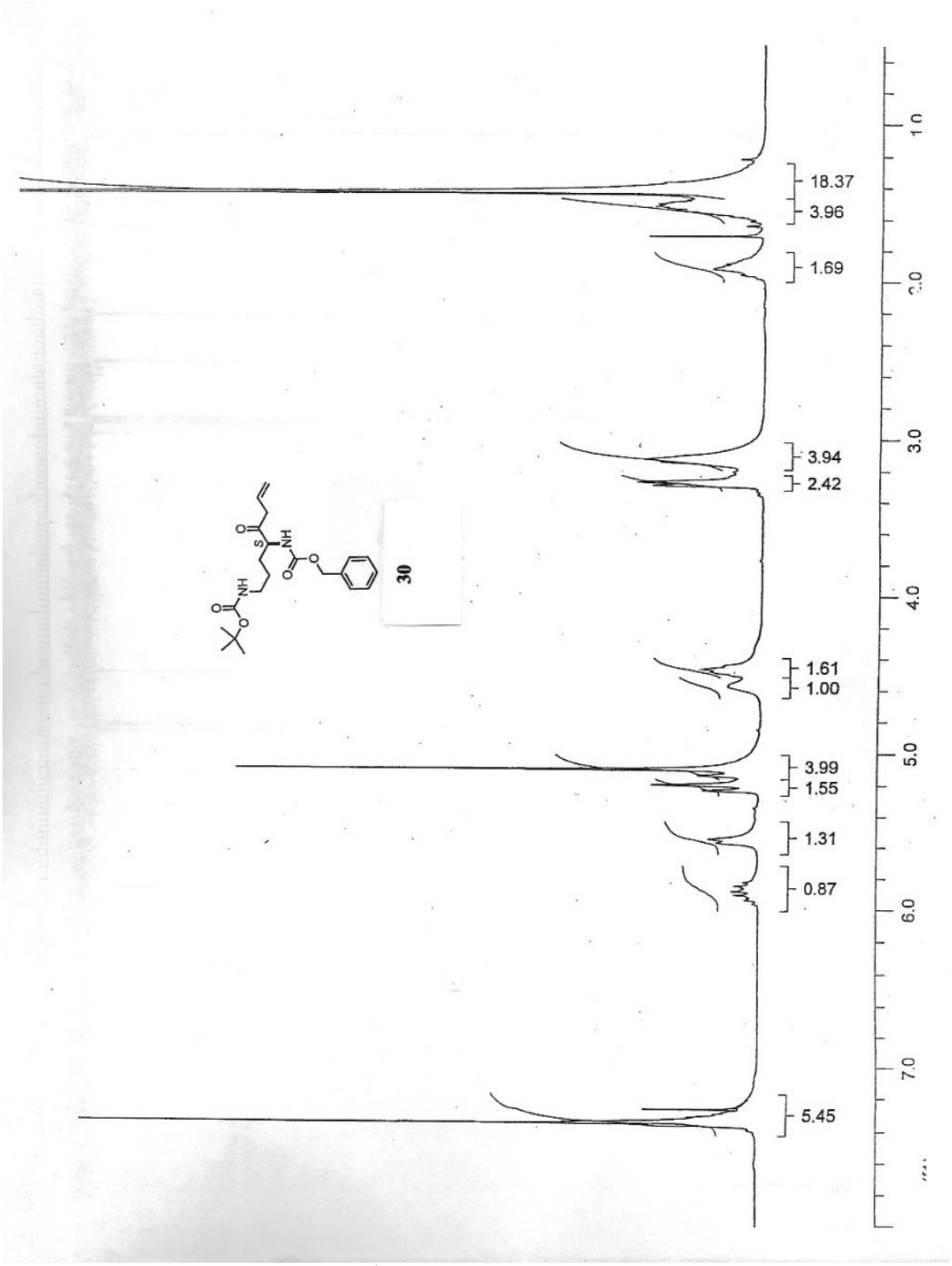

Figure V.19: ^{1}H NMR spectrum of **30** in $CDCl_3$

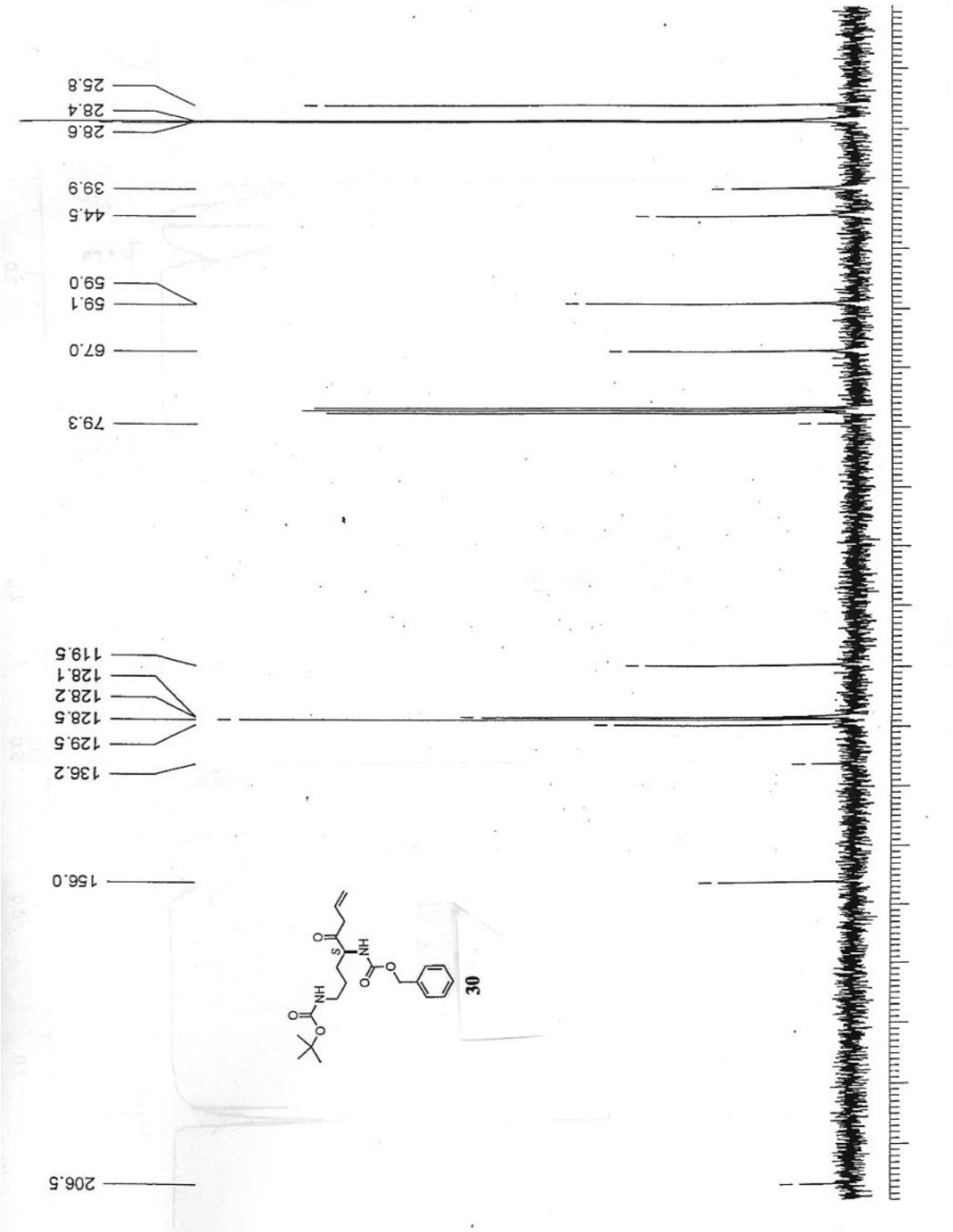

Figure V.20: ^{13}C NMR spectrum of **30** in $CDCl_3$

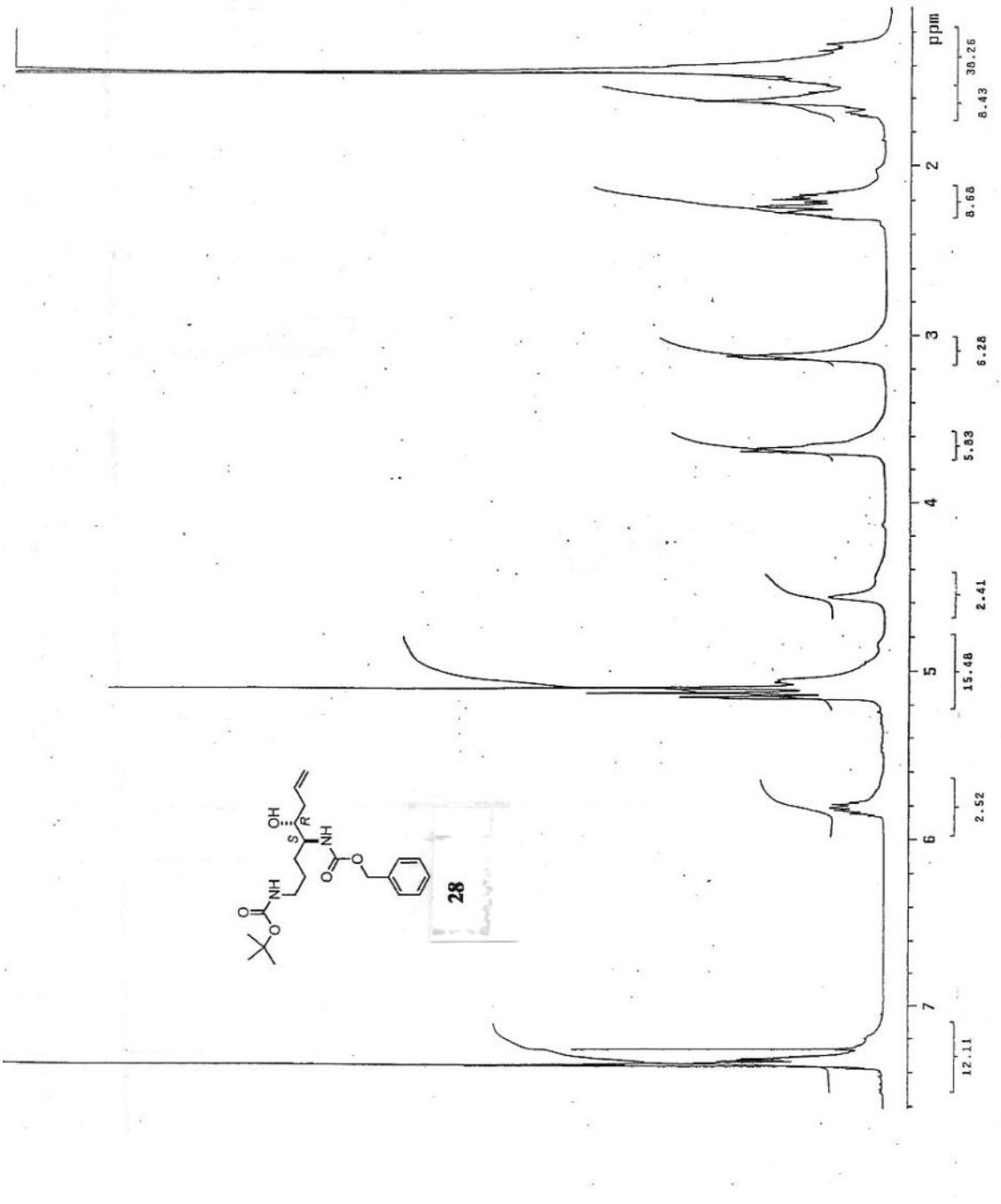

Figure V.21: ^{1}H NMR spectrum of **28** in $CDCl_3$

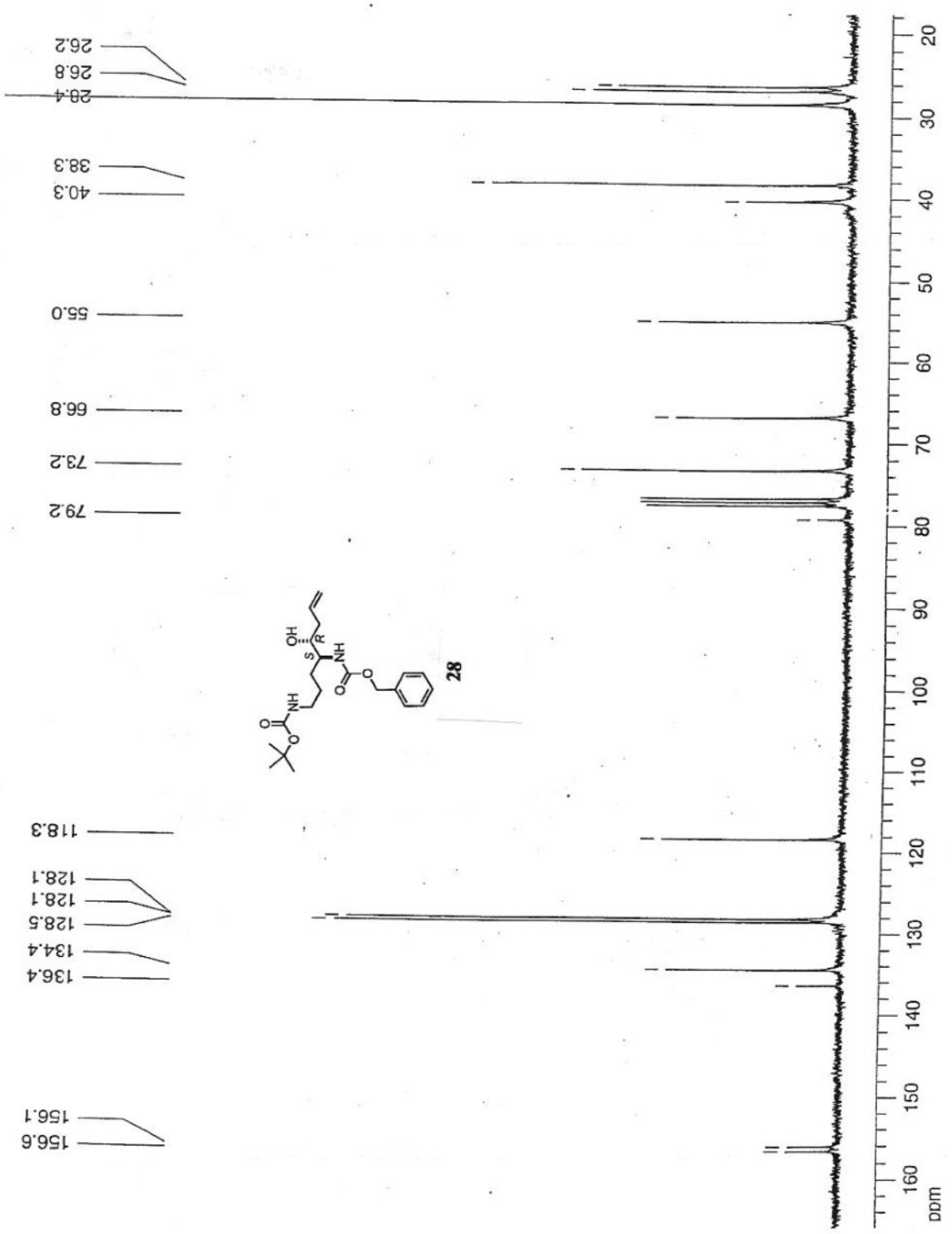

Figure V.22: ^{13}C NMR spectrum of **28** in $CDCl_3$

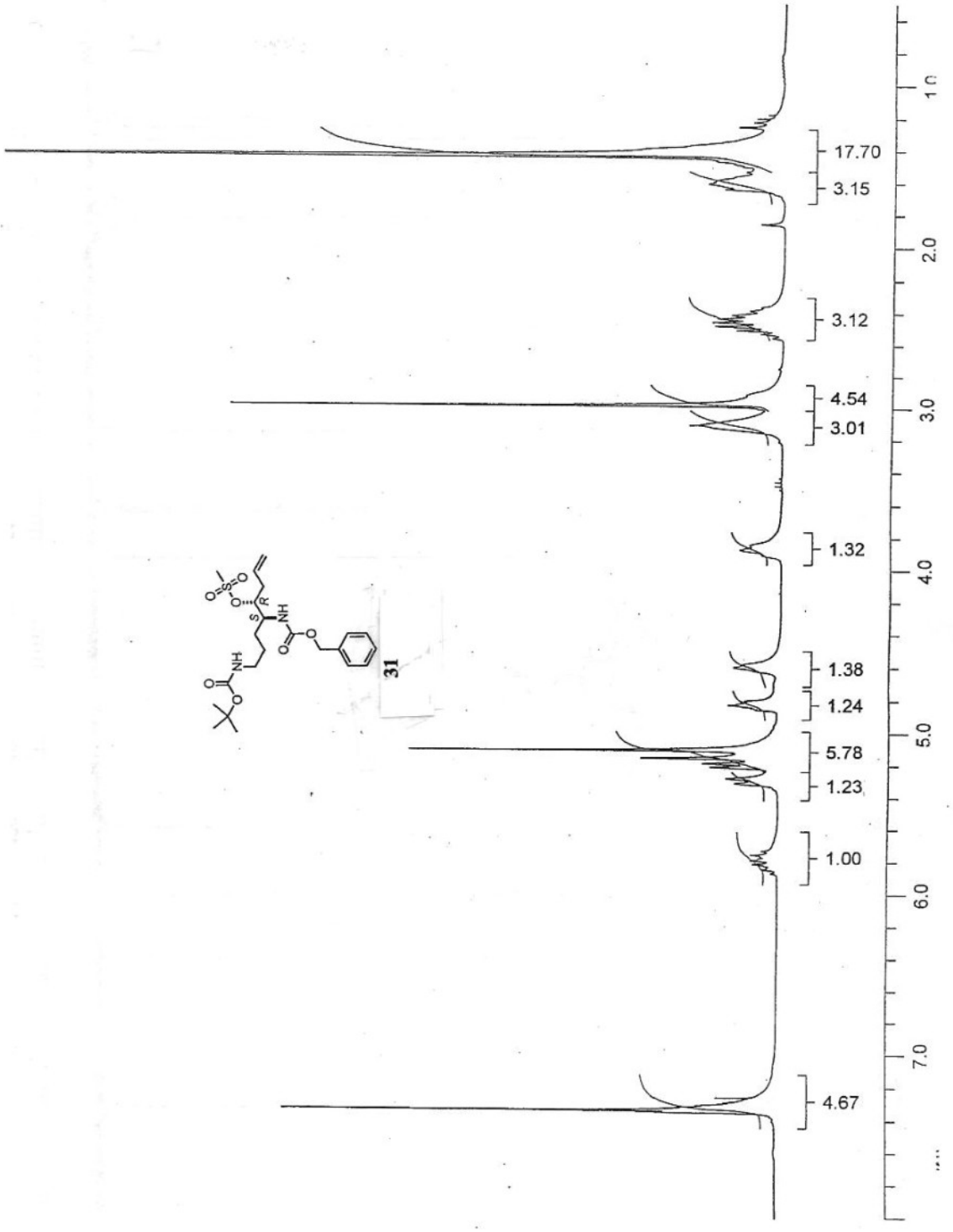

Figure V.23: ^{1}H NMR spectrum of **31** in $CDCl_3$

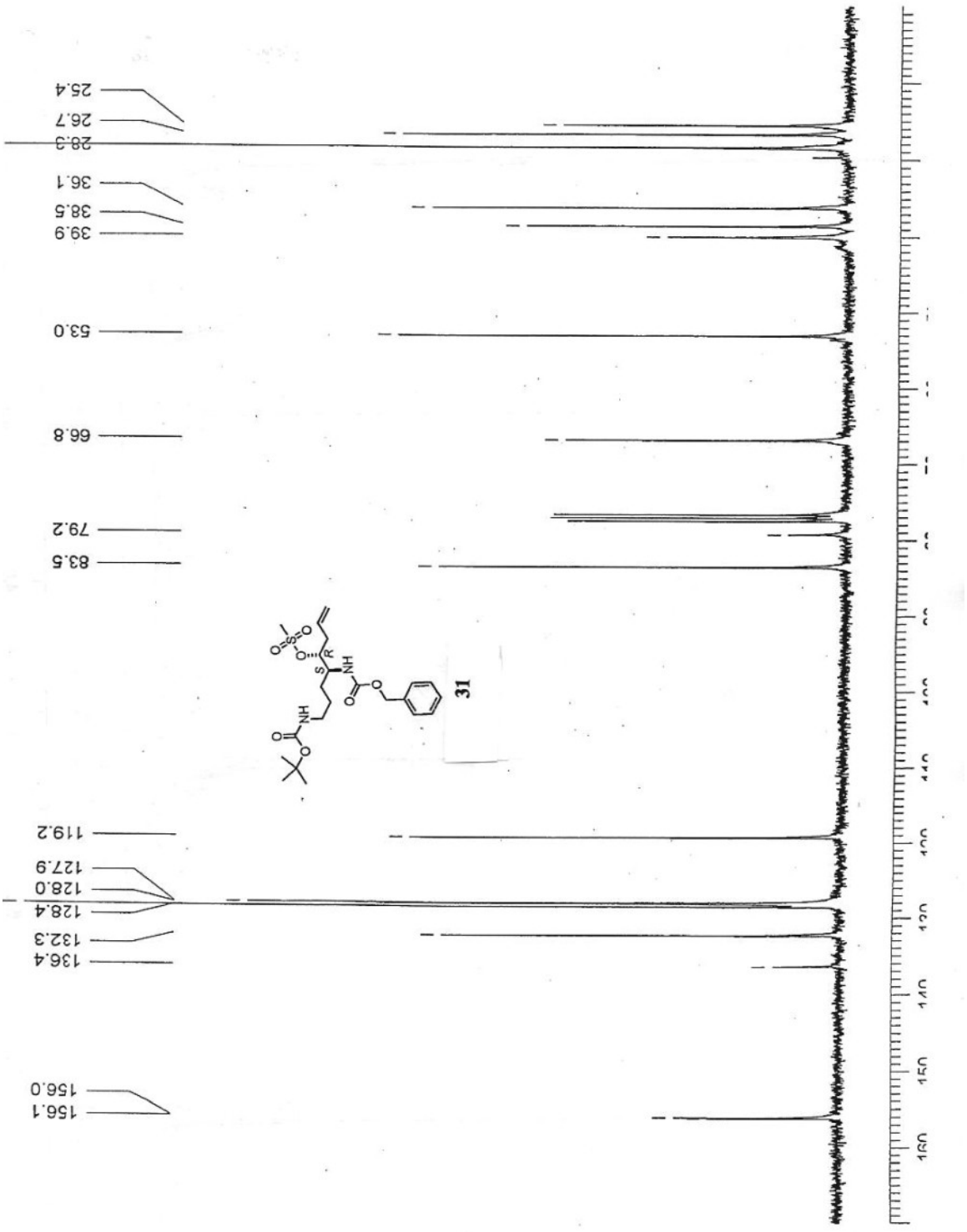

Figure V.24: ^{13}C NMR spectrum of **31** in $CDCl_3$

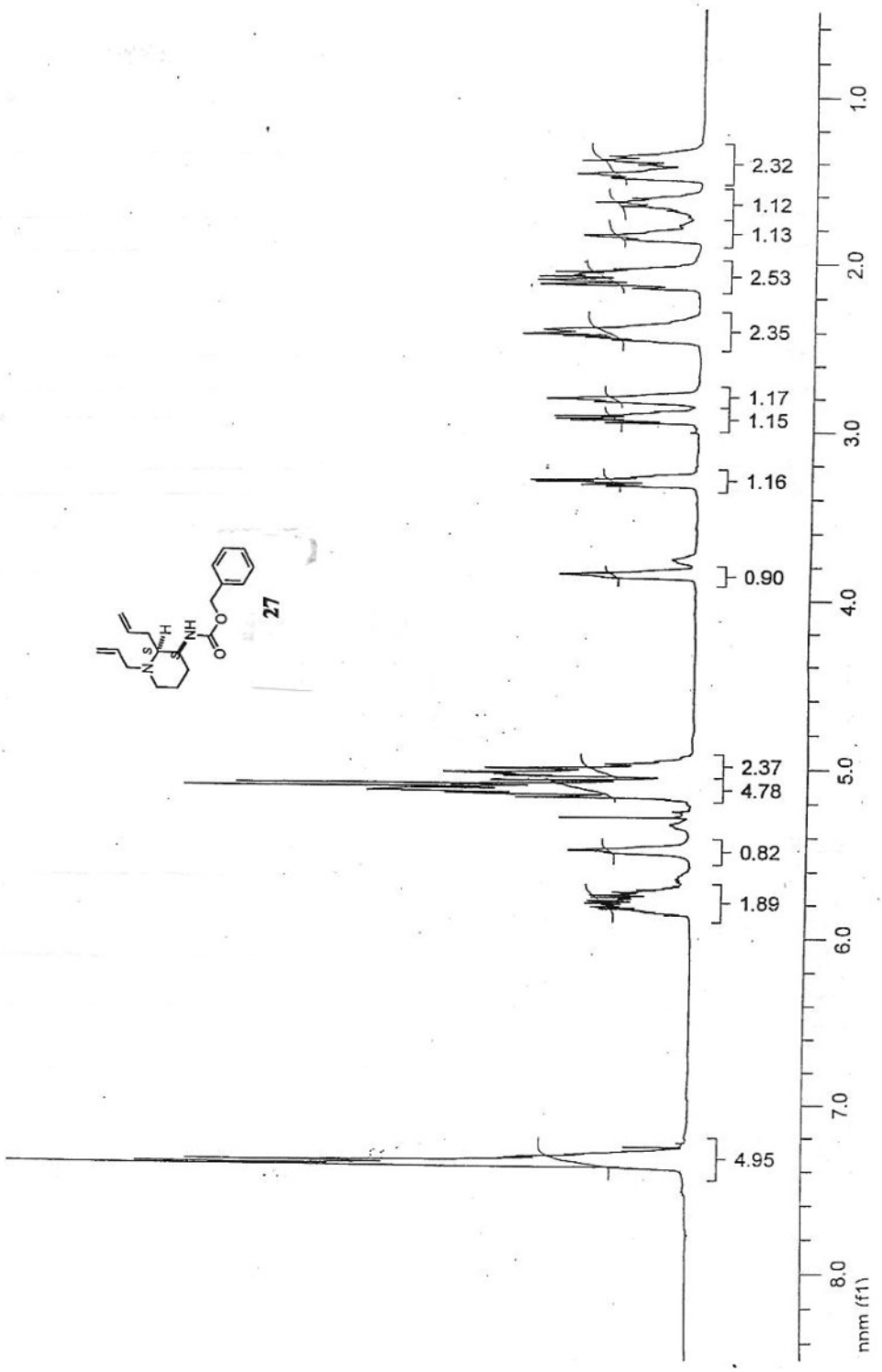

Figure V.25: ^{1}H NMR spectrum of **27** in $CDCl_3$

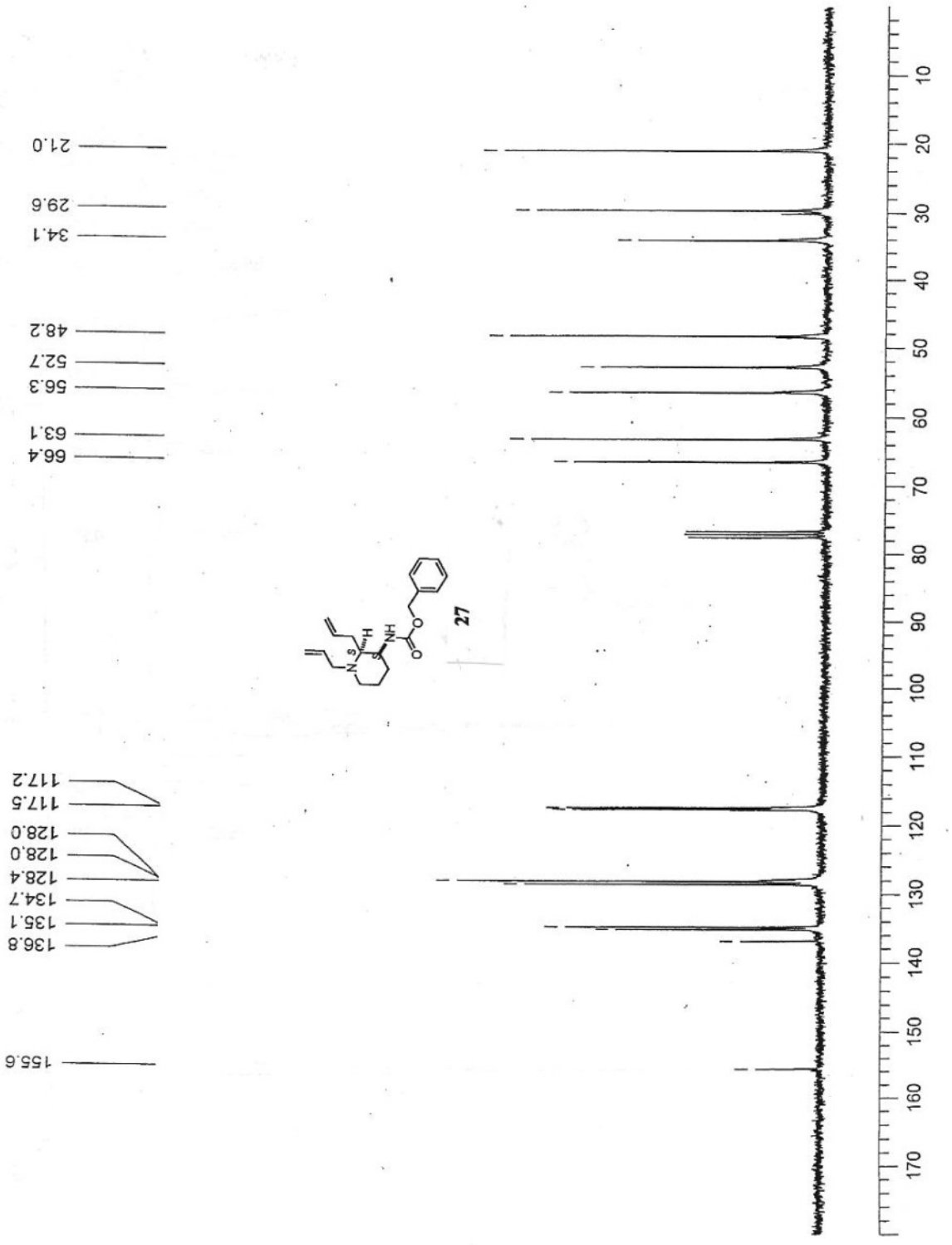

Figure V.26: ^{13}C NMR spectrum of **27** in $CDCl_3$

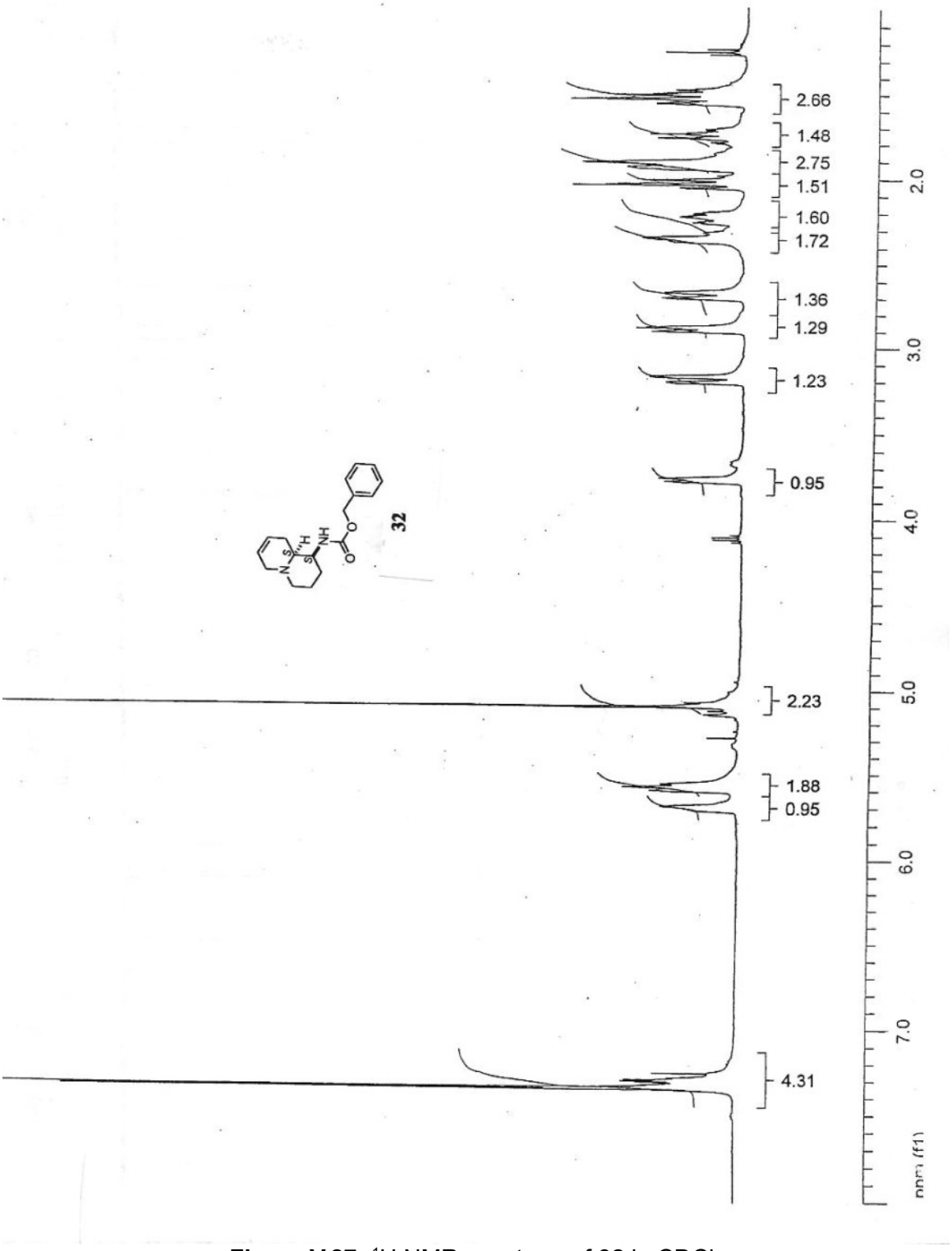

Figure V.27: ^{1}H NMR spectrum of **32** in $CDCl_3$

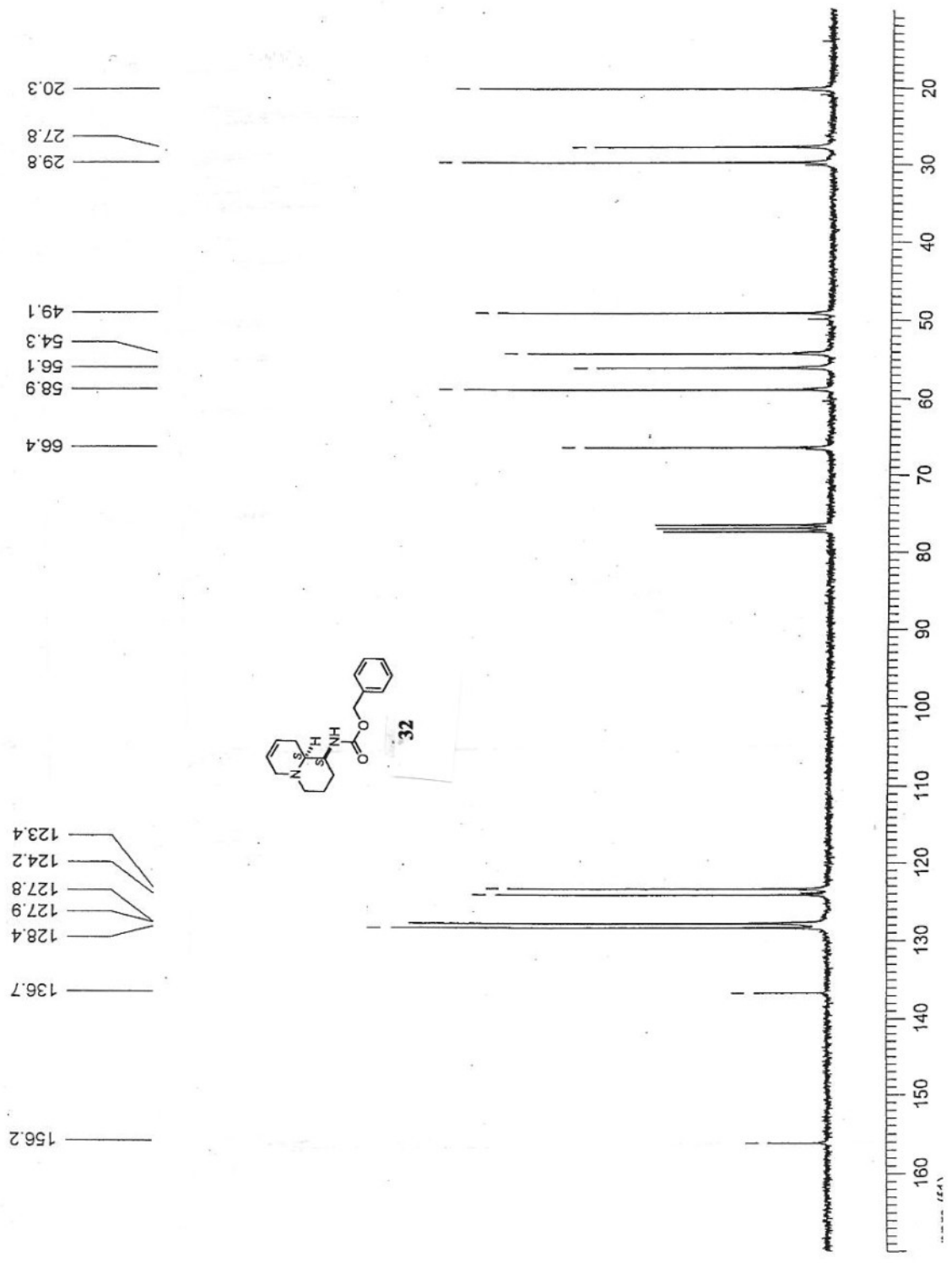

Figure V.28: ^{13}C NMR spectrum of **32** in $CDCl_3$

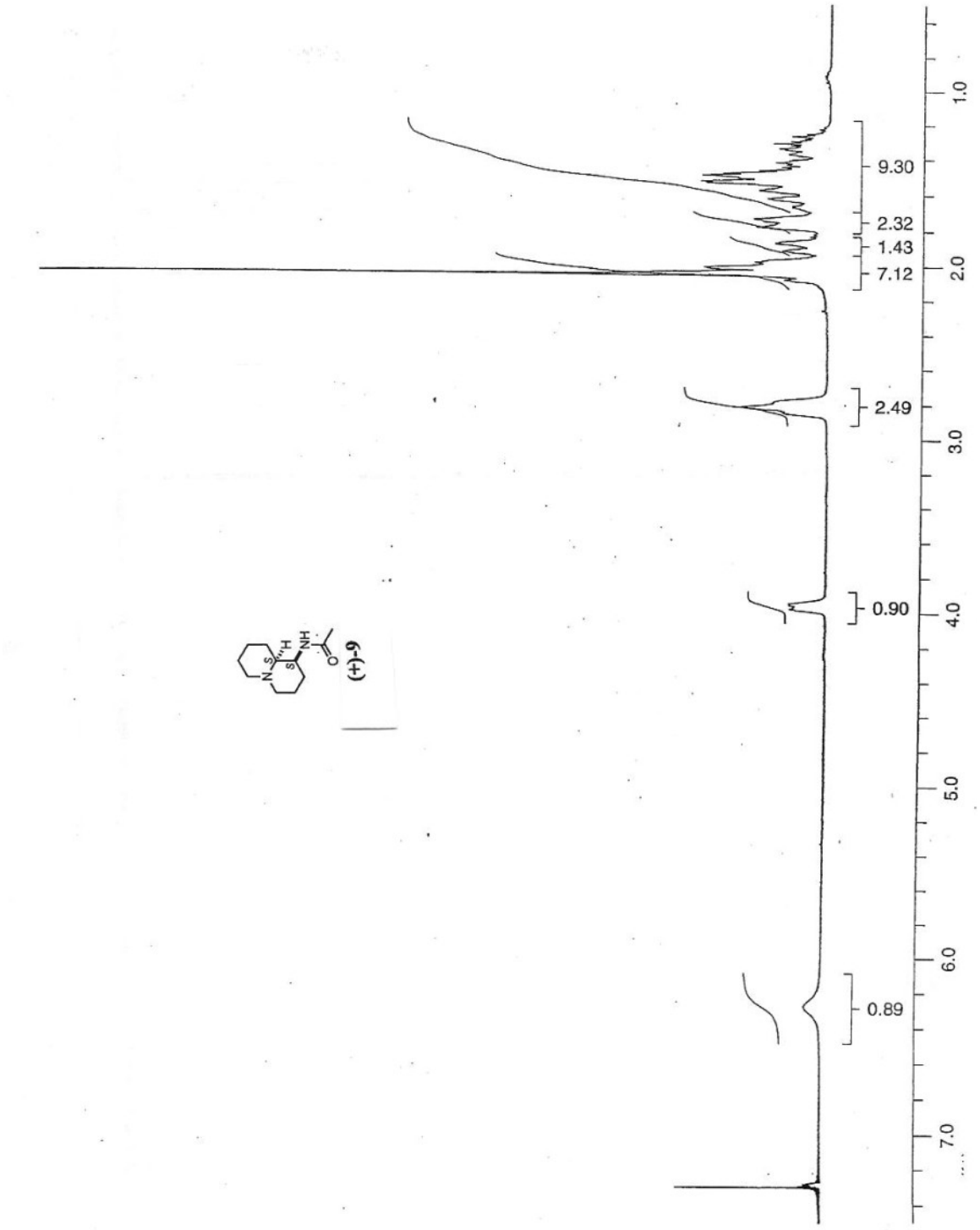

Figure V.29: ^{1}H NMR spectrum of **(+)-9** in $CDCl_3$

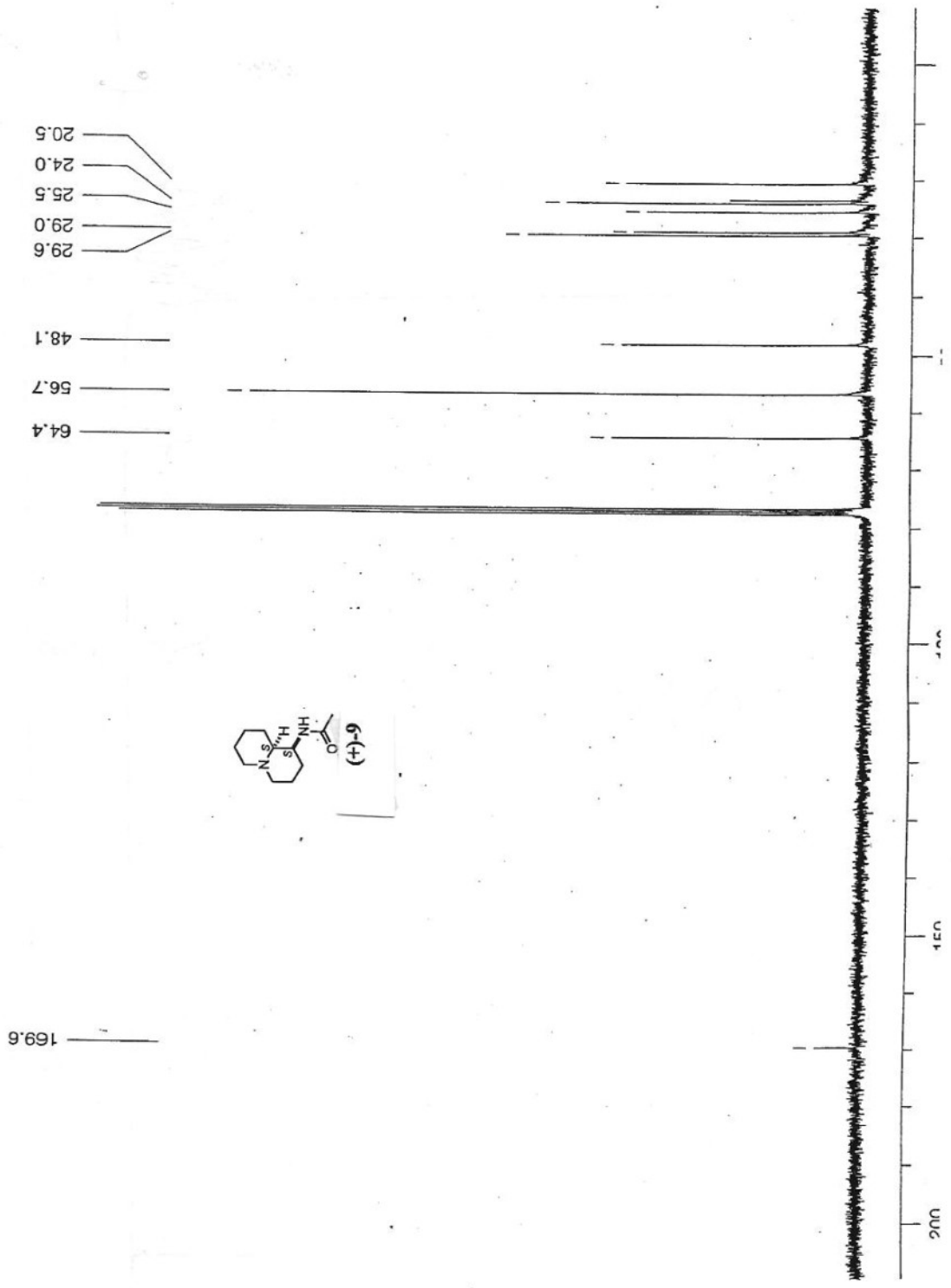

Figure V.30: ^{13}C NMR spectrum of **(+)-9** in $CDCl_3$

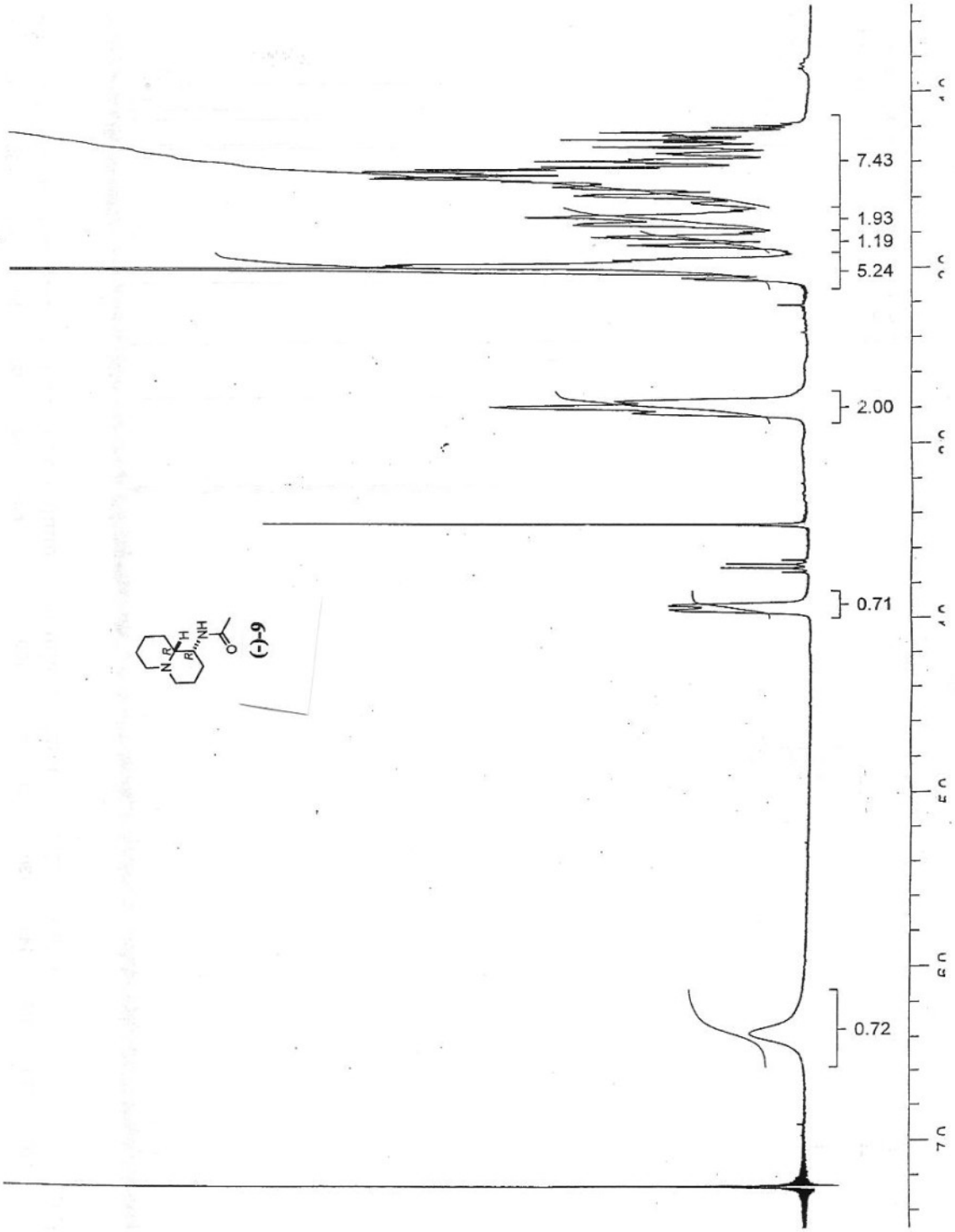

Figure V.31: ^{1}H NMR spectrum of **(-)-9** in $CDCl_3$

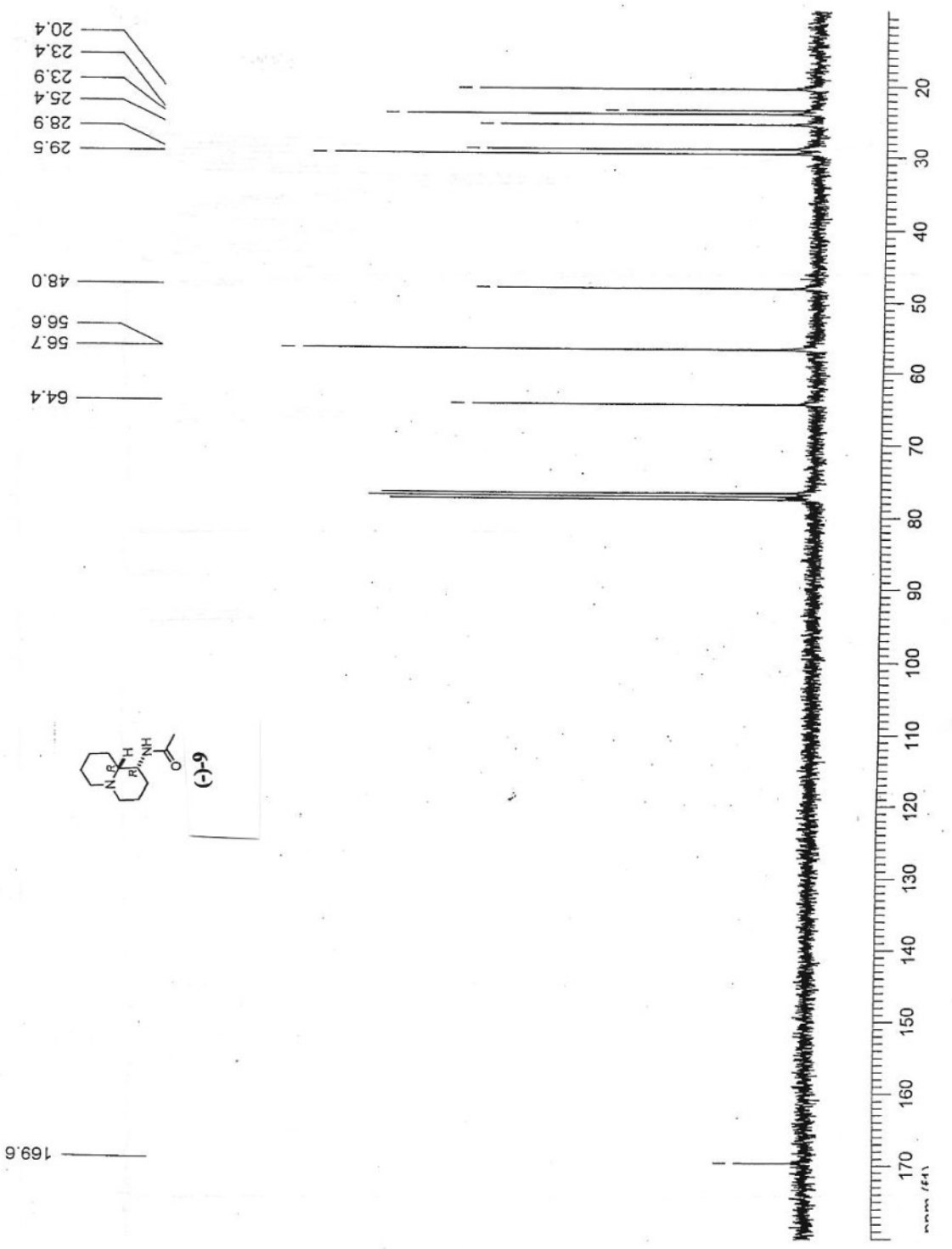

Figure V.32: ^{13}C NMR spectrum of **(-)-9** in $CDCl_3$

References and footnotes

1 Daly, J. W. Ernest Guenther award in chemistry of natural products. amphibian skin: a remarkable source of biologically active arthropod alkaloids. *J. Med. Chem.* **2003**, *46*, 445-452.

2 Daly, J. W.; Spande, T. F.; Garraffo, H. M. Alkaloids from amphibian skin: a tabulation of over eight-hundred compounds. *J. Nat. Prod.* **2005**, *68*, 1556-1575.

3 Daly, J. W. Nicotinic agonists, antagonists, and modulators from natural sources. *Cell. Mol. Neurobiol.* **2005**, *25*, 513-552.

4 Daly, J. W. Marine toxins and nonmarine toxins: convergence or symbiotic organisms? *J. Nat. Prod.* **2004**, *67*, 1211-1215.

5 Simmons, T. L.; Coates, R. C.; Clark, B. R.; Engene, N.; Gonzalez, D.; Esquenazi, E.; Dorrestein, P. C.; Gerwick, W. H. Biosynthetic origin of natural products isolated from marine microorganism–invertebrate assemblages. *Proc. Natl. Acad. Sci.* **2008**, *105*, 4587–4594.

6 Spande, T. F.; Garraffo, H. M.; Edwards, M. W.; Yeh, H. J. C.; Pannell, L.; Daly, J. W. Epibatidine: a novel (chloropyridyl)azabicycloheptane with potent analgesic activity from an Ecuadoran poison frog. *J. Am. Chem. Soc.* **1992**, *114*, 3475-3478.

7 Fitch, R. W.; Garraffo, H. M.; Spande, T. F.; Yeh, H. J. C.; Daly, J. W. Bioassay-guided isolation of epiquinamide, a novel quinolizidine alkaloid and nicotinic agonist from an Ecuadoran poison frog, *Epipedobates tricolor*. *J. Nat. Prod.* **2003**, *66*, 1345-1350.

8 Baker, D. D.; Alvi, K. A. Small-molecule natural products: new structures, new activities. *Curr. Opin. Biotechnol.* **2004**, *15*, 576-583.

9 Gotti, C.; Riganti, L.; Vailati, S.; Clementi, F. Brain Neuronal Nicotinic Receptors as New Targets for Drug Discovery. *Curr. Pharm.Design* **2006**, *12*, 407-428.

10 12 groups in total, 11 of which have published their work so far.

11 Wijdeven, M. A.; Botman, P. N. M.; Wijtmans, R.; Schoemaker, H. E.; Rutjes, F. P. J. T.; Blaauw, R. H. Total Synthesis of (+)- Epiquinamide. *Org. Lett.* **2005**, *7*, 4005-4007.

12 Suyama, T. L.; Gerwick, W. H. Practical Total Syntheses of Epiquinamide Enantiomers. *Org. Lett.* **2006**, *8*, 4541-4543.

13 Wijdeven, M. A.; Wijtmans, R.; van den Berg, R. J. F.; Noorduin, W.; Schoemaker, H. E.; Sonke, T.; van Delft, F. L.; Blaauw, R. H.; Fitch, R. W.; Spande, T. F.; Daly, J. W.; Rutjes, F. P. J. T. *N*,*N*-Acetals as *N*-Acyliminium Ion Precursors: Synthesis and Absolute Stereochemistry of Epiquinamide. *Org. Lett.* **2008**, *10*, 4001-4003.

14 Ghosh, S.; Shashidhar, J. Total synthesis of (+)- epiquinamide from -mannitol. *Tetrahedron Lett.* **2009**, *50*, 1177-1179.

15 Huang, P.-Q.; Guo, Z.-Q.; Ruan, Y.-P. A Versatile Approach for the Asymmetric Syntheses of (1*R*,9a*R*)- Epiquinamide and (1*R*,9a*R*)-Homopumiliotoxin 223G. *Org. Lett.* **2006**, *8*, 1435-1438.

16 Voituriez, A.; Ferreira, F.; Perez-Luna, A.; Chemla, F. Asymmetric synthesis of (-)-1-hydroxyquinolizidinone, a common intermediate for the syntheses of (-)-homopumiliotoxin 223G and (-)- epiquinamide. *Org. Lett.* **2007**, *9*, 4705-4708.

17 Tong, S.; Barker, D. A concise synthesis of (±) and a total synthesis of (+)- epiquinamide. *Tetrahedron Lett.* **2006**, *47*, 5017-5020.

18 Kanakubo, A.; Gray, D.; Innocent, N.; Wonnacott, S.; Gallagher, T. The synthesis and nicotinic binding activity of (±)- epiquinamide and (±)-C(1)-epiepiquinamide. *Bioorg. Med. Chem. Lett.* **2006**, *16*, 4648-4651.

19 Fitch, R. W.; Sturgeon, G. D.; Patel, S. R.; Spande, T. F.; Garraffo, H. M.; Daly, J. W.; Blaauw, R. H. Epiquinamide : A Poison That Wasn't from a Frog That Was. *J. Nat. Prod.* **2009**, *72*, 243-247.

20 Pal, K.; Behnke, M. L.; Tong, L. A general stereocontrolled synthesis of *cis*-2,3 disubstituted pyrrolidines and piperidines. *Tetrahedron Lett.* **1993**, *34*, 6205-6208.

21 Singh, R.; Ghosh, S. K. Synthesis of enantiomerically pure all cis-2,3,6-trisubstituted piperidine: a silicon mediated total synthesis of (+)-carpamic acid. *Tetrahedron Lett.* **2002**, *43*, 7711-7715.

22 (a) Gómez-Monterrey, I.; González-Muniz, R.; Herranz, R.; García-López, M. T. Stereospecific synthesis of (2R,3S)-3-amino-2-piperidineacetic acid derivatives for use as conformational constraint in peptides. *Tetrahedron Lett.* **1993**, *34*, 3593-3594. (b) Jefford, C. W.; Wang, J. B. An enantiospecific synthesis of solenopsin A. *Tetrahedron Lett.* **1993**, *34*, 2911-2914.

23 (a) Anh, N. T.; Eisenstein, O. *Nouv. J. Chim.* **1977**, *1*, 61-70. (b) Lodge, E. P.; Heathcock, C. H. Acyclic stereoselection. 40. Steric effects, as well as .sigma.*-orbital energies, are important in diastereoface differentiation in additions to chiral aldehydes. *J. Am. Chem. Soc.* **1987**, *109*, 3353-3361.

24 The corresponding transition states were modeled at semi-empirical (PM3) level and the relative energy difference between the two transition states leading to the two stereoisomers was calculated. Based on this result, Si-face addition of hydride was predicted (data not shown).

25 Rana, Jatinder; Robins, David J. Quinolizidine alkaloid biosynthesis : incorporation of cadaverine-1-amino-^{15}N,1-^{13}C into lupinine. *J. Chem. Soc. Chem. Comm.* **1984**, *2*, 81-2.

26 Wanner, M. J.; Koomen, G. Biomimetic synthesis of quinolizidine alkaloids. *Tetrahedron* **1991**, *47*, 8431-8442.

27 Batey, R. A.; MacKay, D. B.; Santhakumar, V. Alkenyl and aryl boronates – mild nucleophiles for the stereoselective formation of functionalized N-heterocycles. *J. Am. Chem. Soc.* **1999**, 121, 5075-5076.

28 Speckamp, W. N.; Moolenaar, M. J. New developments in the chemistry of *N*-acyliminium ions and related intermediates. *Tetrahedron* **2000**, *56*, 3817-3856.

29 Guarna, A.; Occhiato, E. G.; Machetti, F.; Scarpi, D. A Concise route to 19-nor-10-azasteroids, a new class of steroid 5α-reductase Inhibitors. Synthesis of (+)-19-nor-10-azatestosterone and (+)-17β-(acetyloxy)-(5β)-10-azaestr-1-en-3-one. *J. Org. Chem.* **1998**, 4111-4115.

30 So, R. C.; Ndonye, R.; Izmirian, D. P.; Richardson, S. K.; Guerrera, R. L.; Howell, A. R. Straightforward synthesis of sphinganines via a serine-derived Weinreb amide. *J. Org. Chem.* **2004**, *69*, 3233-3235.

31 Nahm, S.; Weinreb, S. M. *N*-methoxy-*N*-methylamides as effective acylating agents. *Tetrahedron Lett.* **1981**, *22*, 3815-3818.

32 Mentzel, M.; Hoffmann, H. M. R. *N*-Methoxy-*N*-methylamides (Weinreb amides) in modern organic synthesis. *J. Prakt. Chem.* **1997**, *339*, 517-524.

33 Grignard, V. Sur quelques nouvelles combinaisons organométaliques du magnésium et leur application à des synthèses d'alcools et d'hydrocabures. *Compt. Rend.* **1900**, *130*, 1322–1325.

34 Haug, B. E.; Rich, D. H. Synthesis of a Gln-Phe hydroxy-ethylene dipeptide isostere. *Org. Lett.* **2004**, *6*, 4783-4786.

35 The bridgehead proton of **9** has a chemical shift of δ 3.91 ppm, and that of **15** has a shift of δ 3.95 ppm in MeOH-d_4. Otherwise, the two compounds have exactly the same carbon framework and molecular weight by NMR and LRMS.

36 Abe, H.; Aoyagi, S.; Kibayashi, C. Total synthesis of the tricyclic marine alkaloids (-)-lepadiformine, (+)-cylindricine C, and (-)-fasicularin via a common intermediate formed by formic acid-induced intramolecular conjugate azaspirocyclization. *J. Am. Chem. Soc.* **2005**, *127*, 1473-1480.

37 Wang, Q.; Sasaki, N. A. Versatile approach to enantiopure 2,6-disubstituted piperidin-3-ol framework: application to the total synthesis of (+)-deoxoprosopinine. *J. Org. Chem.* **2004**, *69*, 4767-4773.

38 Cyclization was extremely slow in the absence of base.

39 Sundberg, R. J.; Amat, M.; Fernando, A. M. Analogs of the iboga alkaloids. Synthesis and reactions of (.+-.)-15-oxo-20-deethylcoronaridine derivatives. *J. Org. Chem.* **1987**, *52*, 3151-3159.

40 Kinderman, S. S.; Wekking, M. M. T.; van Maarseveen, J. H.; Schoemaker, H. E.; Hiemstra, H.; Rutjes, F. P. J. T. A stereodivergent approach to substituted 4-hydroxypiperidines. *J. Org.*

Chem. **2005**, *70*, 5519-5527.

41 Scholl, M.; Ding, S.; Lee, C. W.; Grubbs, R. H. Synthesis and activity of a new generation of ruthenium-based olefin metathesis catalysts coordinated with 1,3-dimesityl-4,5-dihydroimidazol-2-ylidene ligands. *Org. Lett.* **1999**, *1*, 953-956.

42 Nicolaou, K. C.; Bulger, P. G.; Sarlah, D. Metathesis reactions in organic synthesis. *Angew. Chem. Int. Ed.* **2005**, *44*, 4490-4527.

43 Hong, S. H.; Grubbs, R. H. Highly active water-soluble olefin metathesis catalyst. *J. Am. Chem. Soc.* **2006**, *128*, 3508-3509.

44 Vernall, A. J.; Abell, A. D. Cross metathesis of nitrogen-containing systems. *Aldrichimica Acta* **2003**, *36*, 93-105.

45 Compain, P. Olefin metathesis of amine-containing systems: beyond the current consensus. *Adv. Synth. Catal.* **2007**, *349*, 1829 – 1846.

46 Published methods for the removal of the ruthenium catalyst are better suited for nonpolar compounds. For examples, see: (a) Maynard, H. D.; Grubbs, R. H. Purification technique for the removal of ruthenium from olefin metathesis reaction products. *Tetrahedron Lett.* **1999**, *40*, 4137-4140. (b) Haack, K. L.; Ahn, Y. M.; Georg, G. I. A convenient method to remove ruthenium byproducts from olefin metathesis reactions using polymer-bound triphenylphosphine oxide (TPPO). *Mol. Diversity* **2005**, *9*, 301-303.

47 Amir H. Hoveyda, Dennis G. Gillingham, Joshua J. Van Veldhuizen, Osamu Kataoka, Steven B. Garber, Jason S. Kingsbury and Joseph P. A. Harrity Ru complexes bearing bidentate carbenes: from innocent curiosity to uniquely effective catalysts for olefin metathesis. *Org. Biolmol. Chem.* **2004**, *2*, 8-23.

48 Michrowska, A; Grela, K. Quest for the ideal olefin metathesis catalyst. *Pure Appl. Chem.* **2008,** *80*, 31–43.

49 Shinada, T.; Hayashi, K.; Yoshida, Y.; Ohfune, Y. Squaric acid derivatives prevent the removal of N-Cbz and N-Fmoc groups under catalytic hydrogenation reaction. *Synlett* **2000**, *10*, 1506-1508.

50 The literature value of **(+)-9** was $[\alpha]^{20}_{D}$ = +28° (*c* 0.23, $CHCl_3$) (see ref 11) and $[\alpha]^{22}_{D}$ = +26.2° (*c* 0.23, $CHCl_3$) (see ref 17).

51 The literature value of **(-)-9** was $[\alpha]^{20}_{D}$ = - 25° (*c* 0.26, $CHCl_3$) (see ref 15).

52 LePage, K. T.; Dickey, R. W.; Gerwick, W. H.; Jester, E. L.; Murray, T. F. On the use of neuro-2a neuroblastoma cells versus intact neurons in primary culture for neurotoxicity studies. *Critical Reviews in Neurobiology* **2005**, *17*, 27-50.

53 Kanakubo, A.; Gray, D.; Innocent, N.; Wonnacott, S.; Gallagher, T. The synthesis and nicotinic binding activity of (±)-epiquinamide and (±)-C(1)-epiepiquinamide. *Bioorg. Med. Chem. Lett.*

2006, *16*, 4648-4651.

54 Moraczewski, A. L.; Banazsynski, L. A.; From, A. M.; White, C. E.; Smith, B. D. Using hydrogen bonding to control carbamate C−N rotamer equilibria. *J. Org. Chem.* **1998**, *63*, 7258-7262.

Chapter VI

Stereospecific total synthesis of somocystinamide A; an extremely potent antiangiogenic marine natural product containing synthetically challenging functional groups.

Abstract

A marine cyanobacterial metabolite, somocystinamide A, has been shown to have exceptional anti-angiogenic activities through caspase-8-mediated apoptosis of endothelial cells. Due to its promising bioactivity profile, total synthesis of this natural product was accomplished despite synthetically challenging features including an enamide and disulfide. After an initial successful route was developed, the total synthesis was revised to be suitable for larger-scale synthesis to provide for *in vivo* evaluations and analog production.

VI.1 Introduction

Over the last few decades, natural products have been directly or indirectly responsible for over 60% of the new small molecule drugs tested in clinical trials.[1] Of various sources of natural products, marine organisms represent a relatively new frontier.[1,2] Marine cyanobacteria of the genus *Lyngbya* have been an exceptionally rich source of biologically significant natural products.[2] Somocystinamide A (**1**) was isolated from a mixed assemblage of *Schizothrix* and *Lyngbya majuscula* collected in Somo Somo, Fiji.[3] The initial report by Nogle and Gerwick cited its activity against Neuro-2a neuroblastoma cells with an IC_{50} value of 1.8 μM.[3]

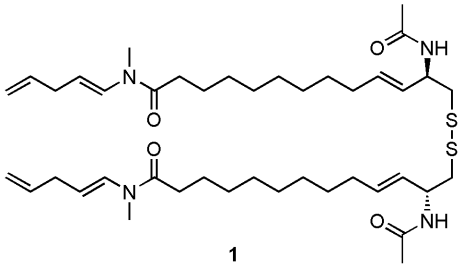

Somocystinamide A

Subsequently, **1** was found to have extremely potent cytotoxic activity against *h*uman *u*mbilical *v*ein *e*ndothelial *c*ells (HUVEC) with an IC_{50} of 500 fM.[4] HUVEC cells

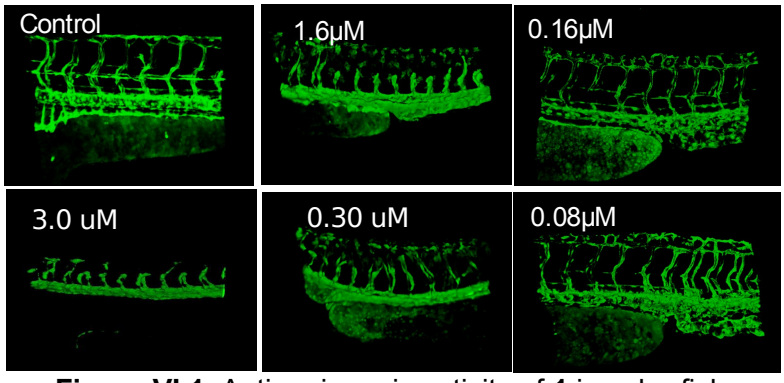

Figure VI.1: Antiangiogenic activity of **1** in zebrafish

Transgenic Tg(fli1:EGFP) zebrafish embryos in which GFP is expressed in endothelial cells were incubated without (control) or with increasing concentrations of 1: 3 μM, 1.6 μM, 300 nM, 160 nM, or 80 nM. The GFP gene was coupled to the VEGF gene so that fluorescence would be observed at sites where angiognesis (promoted by VEGF) was occurring. Blood vessel morphology was recorded by fluorescence microscopy.

are primary endothelial cells derived from human tissues and are a good model for studying angiogenesis.[5] In cancer therapy, it is crucial to have control over angiogenesis in the tissues surrounding a tumor. Growing tumors need an even greater supply of nutrients from the blood than normal tissue. Therefore, a compound that inhibits the growth of HUVEC cells would be expected to be advantageous against cancer through anti-angiogenic effects. Furthermore, **1** was shown to be cytotoxic against A549 (human lung carcinoma) cells with an IC_{50} value of 46 nM.[4]

*V*ascular *e*ndothelial *g*rowth *f*actor (VEGF) is a key growth factor that is involved in angiogenesis.[5] In rapidly developing organisms, the presence of this protein in a particular area indicates active formation of blood vessels. The use of transgenic zebrafish embryos, which are transparent, allows direct observation of a drug's effects on angiogensis through the visualization of *g*reen *f*luorescent *p*rotein (GFP) that is placed under the control of a VEGF promotor.[6] In such a study by our collaborators at the Moores Cancer Center, somocystinamide A (**1**) was found to significantly reduce the level of GFP, and thus indicate a reduced level of VEGF activity present in zebrafish embryos even at low drug concentrations (<0.1 μM, the media concentration).[4] Equally significant, the zebrafish were not adversely affected by the compound even at 1.6 μM,[4] providing a large potential therapeutic window (Figure VI.1).

Of the various mechanisms by which a cell can be killed by a chemical agent, apoptosis is the most effective mechanism. This is because certain forms of apoptotic processes can be initiated, in principle, by as little as a single molecule coming into contact with the corresponding receptor on the cell surface.[7] Therefore, when extremely potent cytotoxicity is observed, it is reasonable to hypothesize that the cytotoxicity is

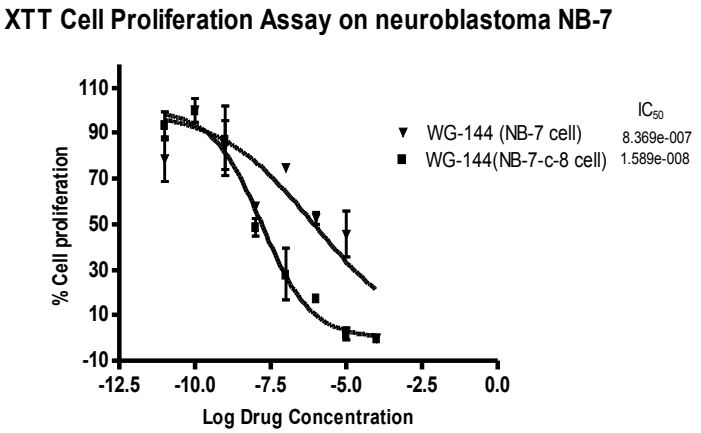

Figure VI.2: Impact of somocystinamide A (**1**) on proliferation of paired neuroblastoma cells lacking caspase 8 expression (triangles) or expressing caspase 8 (squares)[4]

Caspase-8 potentiates the activity of **1** by 50 fold.

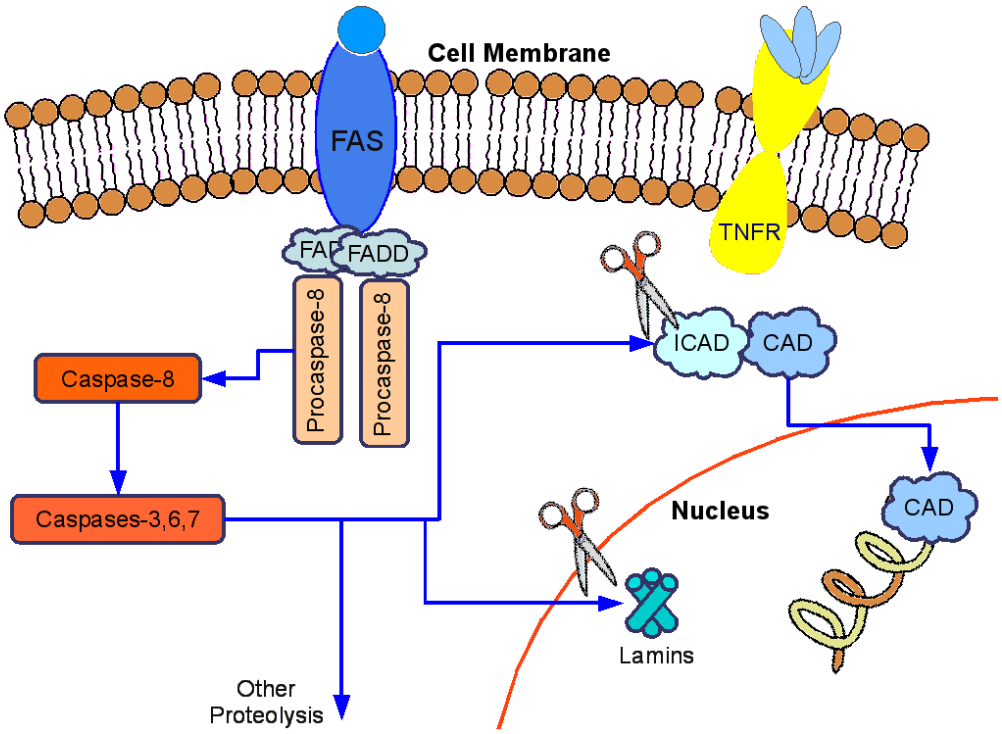

Figure VI.3: Extrinsic pathway via activation of caspase-8 leading to apoptosis

FAS: Fas death receptor, TNFR: tumor necrosis factor receptor, FADD: Fas-associated protein with death domain, CAD: caspase activated DNase, ICAD: inhibitor of CAD. Scissors indicate proteolytic activities.

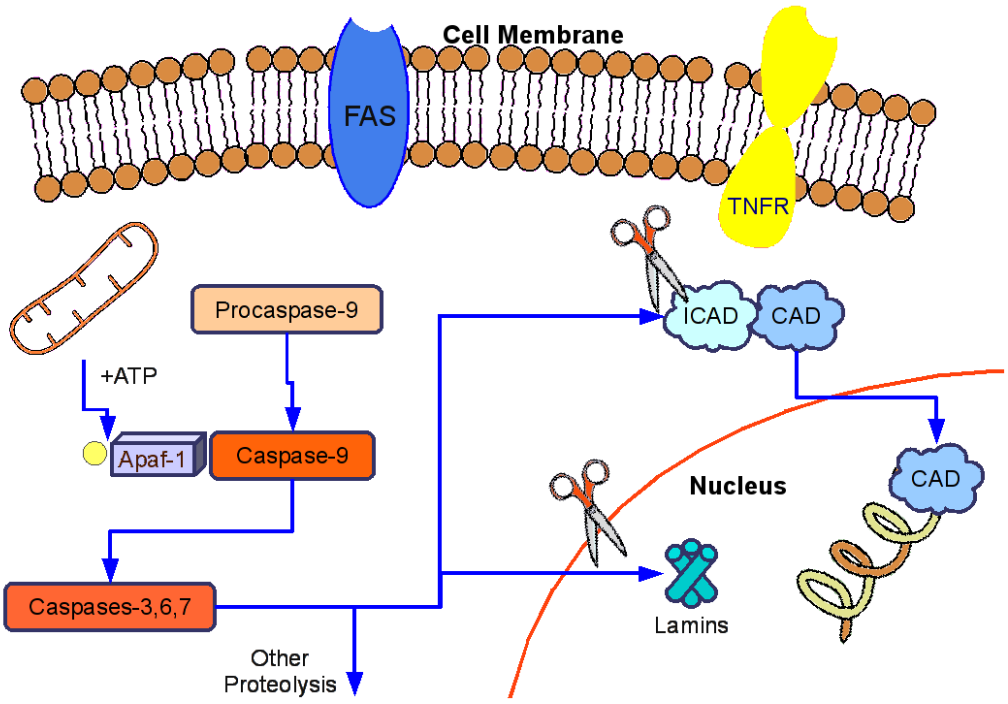

Figure VI.4: Intrinsic pathway via activation of caspase-9 leading to apoptosis

Upon binding of cytochrome c and dATP, Apaf-1 (apoptotic peptidase activating factor 1) recruits procaspase-9 through its caspase recruitment domain (CARD) and releases the active form of caspase-9. The rest of the apoptotic events are essentially identical to those of the extrinsic pathway (Figure VI.3).

caused via an apoptotic mechanism. A study conducted using two neuroblastoma-7 cell lines, one with caspase 8 expression and the other without it, lends further evidence to the hypothesis that somocystinamide A is an apoptosis inducer.[8] The former cell line was found to be 50-fold more susceptible to the effects of **1** than the latter (Figure VI.2).[4] Caspase 8 is normally an inactive protease, but once activated through recruitment by FADD proteins at the death receptor and subsequent self-proteolysis of the pro-domain, it can activate executioner caspases (caspases-3,6,7), which will exercise their destructive proteolytic ability and cause apoptosis (Figure VI.3).[7] Because the initial recruitment of

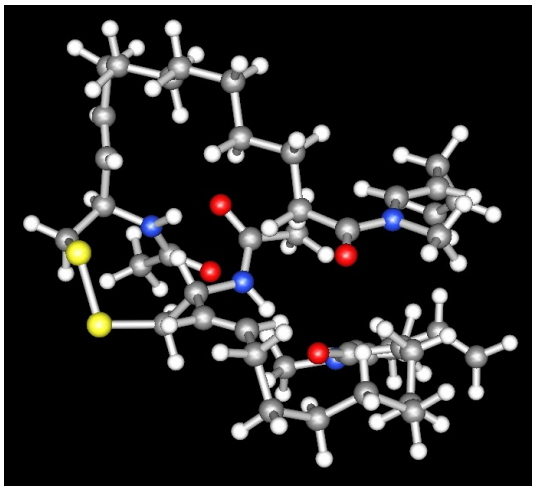

Figure VI.5: Most stable conformer of somocystinamide A found through molecular modeling

Molecular mechanics-level calculation was used for conformer search. The distance between the amide NH proton and the amide oxygen in the center of the figure is only 2.2 Å.

the pro-caspase 8 is induced through an extracellular signal, this process is called an extrinsic pathway.[7] Interestingly, **1** was also found to intrinsically trigger apoptosis through the caspase-9 pathway (Figure VI.4), but to a lesser extent.[4] Moreover, when **1** was reduced to the corresponding monomeric thiol, its bioactivity was lost, suggesting that either the dimeric nature or the disulfide functionality of **1** is necessary for the activity.[4] Conformer distribution calculation of **1** revealed evidence for intramolecular hydrogen bonding between the acetamide groups, which would hold the molecule in a pair-of-forceps fashion (Figure VI.5). Given that the enamide functionality appears to be necessary for the bioactivity, it is possible that each enamide functionality in **1** is responsible for recruitment of a pro-caspase-8 protein and that a pair of pro-caspase-8 proteins are brought together through the virtue of the aforementioned conformation.

Furthermore, examination of A549 cells stained with DAPI, anti-ceramide, and anti-caspase-8 suggested that the mechanism of somocystinamide A-mediated apoptosis

involved structural alterations to the plasma membrane.[4] To determine whether the observed activity was simply due to the lipophilic nature of the natural product, an analog of **1** that lacks any functionalization in the middle of the chain was tested (**2**).[9] This analog (**2**) was found to be completely inactive. Likewise, the hydrolysis product of **1**, bis-methylamide **3** was also inactive.[10] Therefore, the enamide as well as some or all of the other functional groups present in **1** seem to be necessary for induction of apoptosis.

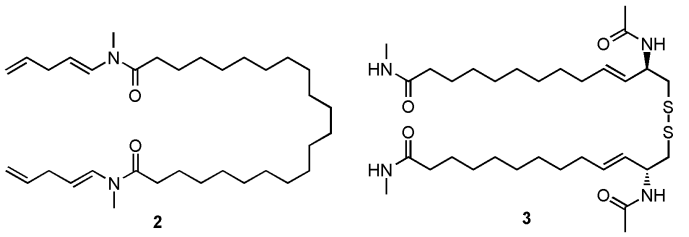

Docosanedioic *bis*-enamide analog (**2**) and hydrolyzed analog of **1** (**3**).

Somocystinamide A (**1**) completely and readily intercalates within liposomes and it retains potent anti-proliferative activity when administered as such.[4] Therefore, if the solubility of **1** or its analogs prove to be an issue in the course of development, use of liposomes would be a potentially viable mechanism for delivery of the drug. The combination of the anti-proliferative activities and the ability to induce apoptosis in endothelial cells is an excellent biological profile for potential treatment of cancer.[11] An endogenous protein, angiostatin,[12] has a similar bioactivity profile, and it has advanced to phase II clinical trial as of 2008 for treatment of lung cancer.[13] Given its bioactivity profile, somocystinamide A (**1**) presents itself as a promising cancer therapeutic.

VI.2 Synthetically challenging features of somocystinamide A

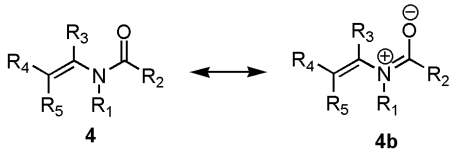

Scheme VI.1: Enamide

When an olefin is introduced immediately adjacent to an amide, the characteristics of the compound changes more drastically compared to the alkylamide analog. One of the most noticeable changes is the shift in UV absorption spectrum. Enamide, by which is meant a vinyl amide herein, possesses conjugation of the carbonyl double bond and the alkenyl group. This conjugated system absorbs UV at 230-240 nm,[14] which can be a useful physical property when the presence of an enamide compound is sought by HPLC techniques. Easily accessible enamides will almost always have a proton at R_3 position (Scheme VI.1). The proton is also very diagnostic for an enamide moiety in that it gives rise to a unique doublet ^{1}H NMR signal at 7.0-7.2 ppm.[15]

Chemically, enamides can be significantly more unstable than amides due to the possible tautomerism to become an acyl imine or an acyl iminium ion that is further activated by the adjacent carbonyl group. For example, pronounced instability of somocystinamide A (**1**) was noted when it underwent complete hydrolysis in $CDCl_3$ in an NMR tube due to the residual moisture and acid (HCl) present in $CDCl_3$ (Scheme VI.2).[3] Given this precedence, it is possible that some natural products, as we know them, are actually artifacts of hydrolytic decomposition of enamides.

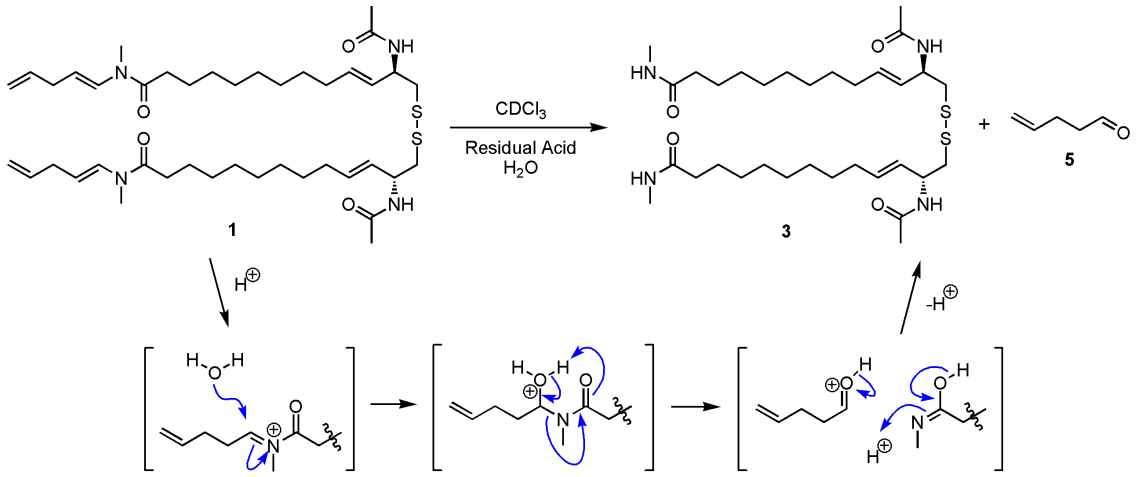

Scheme VI.2: Instability of enamide as seen in the facile decomposition of somocystinamide A

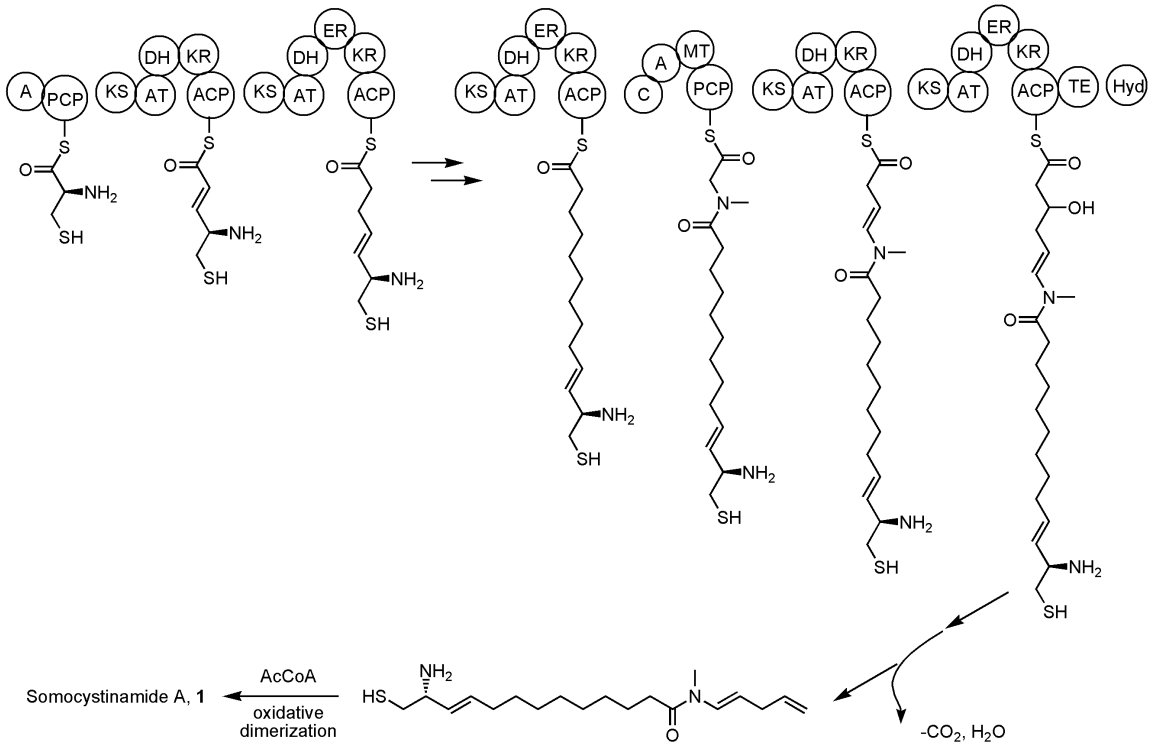

Figure VI.6: Proposed biosynthesis of somocystinamide A (**1**)

The depicted mechanism of the terminal olefin formation is reminiscent of the predicted biosynthesis of curacin A, which also contains a terminal olefin.[18]

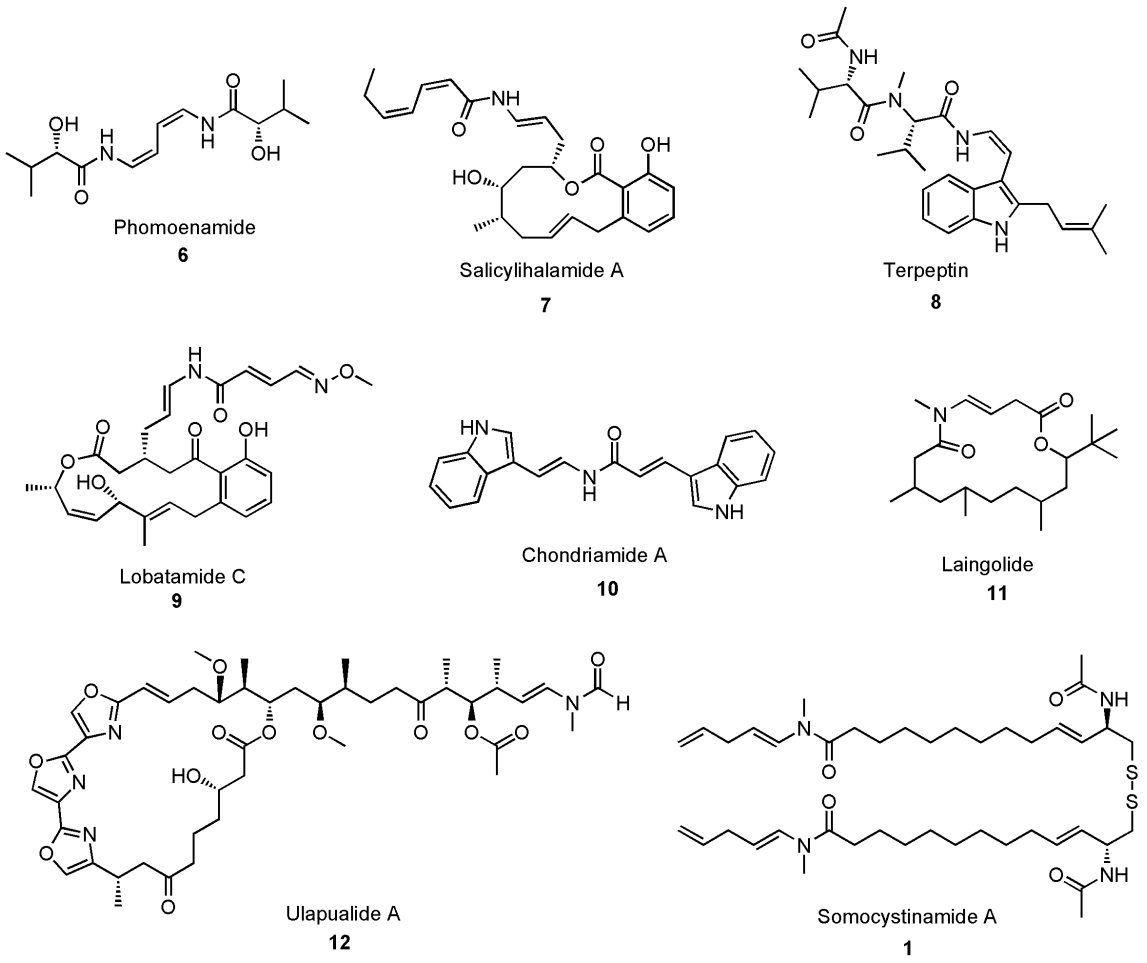

Figure VI.7: Enamide containing natural products

The enamide functional group comes in different forms: a secondary enamide, where R_1 is a proton, or a tertiary enamide, where R_1 is an alkyl group (Scheme VI.1). As will be discussed later, this distinction becomes significant for devising a strategy to introduce the enamide functionality. In fact, most of the accomplishments in enamide synthesis have been for secondary enamides, and the same approaches have been found ineffective for tertiary enamides.[16]

As discussed earlier, the enamide is a labile functional group and therefore care must be taken to avoid inadvertent decomposition during handling of the compound. Growing sophistication in natural product isolation techniques have no doubt contributed to the increasing number of enamide-containing secondary metabolites that have been isolated in recent years (Figure VI.7). All of these natural products appear to have been assembled through hybrid PKS-NRPS systems (except for **10**, a peptide derivative),[17] where the bulk of the carbon skeletons are constructed through PKS catalytic activities and amino acid residues are embedded via NRPS catalytic activities to provide the nitrogen of the enamide moieties. In particular, the biosynthesis of somocystinamide A (**1**) was proposed as shown in Figure VI.6.[18] Most of these natural products have been shown to possess strong bioactivity. Enamide-containing natural products can be categorized into secondary enamides (**6**-**10**) and tertiary enamides (**11**, **12**, **1**). The latter group generally has a methyl group on the enamide nitrogen that is most likely derived from *S*-methy-adenosylmethionine.[19,20]

Phomoenamide (**6**), for example, was shown to have a minimum inhibitory concentration (MIC) value of 6.25 μg/mL against *Mycobacterium tuberculosis* H37Ra.[21] Salicylihalamide A (**7**) is strongly cytotoxic against NCI melanoma cell line (GI_{50} = 7 nM)[22] and is a very potent inhibitor of vacuolar H^+-ATPases (IC_{50} < 1 nM),[23] whose involvement is implicated in diseases such as osteoporosis and cancer (Figure VI.7).[24] Likewise, lobatamides, which are structurally related to the salicylihalamides, also possesses cytotoxicity against human cancer cell lines and inhibitory activity against vacuolar H^+-ATP ases.[25] The peptidic compounds terpeptin (**8**) and chondriamide A (**10**) have cell-cycle inhibition activity and cytotoxicity against colon cancer cells (LOVO

cells), respectively.[26,27] Ulapualides, isolated from sponges and nudibranchs, have been shown to have antifungal and ichthyotoxic properties, as well as cytotoxicity against leukemia cells.[28] Interestingly, almost all of the recently isolated enamide natural products are of marine origin. These newly discovered and bioactive enamide natural products should drive innovation in the synthesis of enamides.

There have been extensive studies on enamide chemistry in the context of heterocycle and asymmetric synthesis, where enamides are used as synthons.[29,30] There is one review on the preparation of this labile, yet crucial functional group.[15] In Scheme VI.3, four major types of approaches for synthesizing enamides are summarized.

In devising a strategy for the synthesis of **1**, the stabilities of both the disulfide and the enamide became of concern. Since the installment of the enamide was envisioned to be performed at a very late stage, if not at the last step, it was desirable to assess the difficulty of synthesizing a tertiary enamide as part of a model system. The most straightforward and expeditious approach to the desired enamide is to acylate the corresponding carboxylic acid with the fully furnished imine (Scheme VI.3).[31] This approach was successful with simple substrates bearing carboxylic acids and no other functional groups (Scheme VI.4).

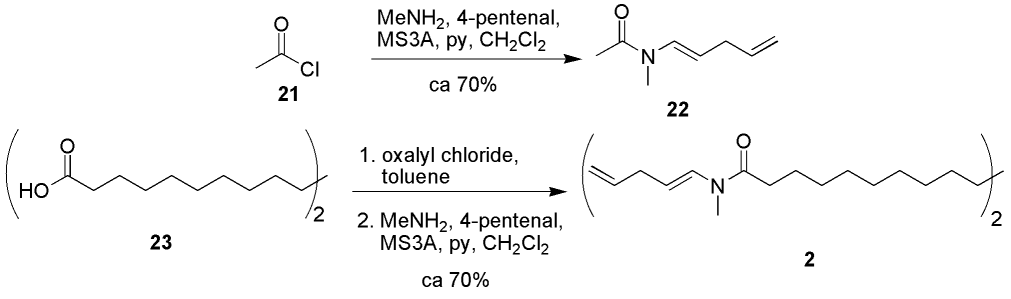

Scheme VI.3: Enamide synthesis on model systems through acylation of imine

Furthermore, the presence of the disulfide group in **1** requires great care and consideration during the course of synthesis.[32] For example, synthetic investigation of epidithiapiperazine-dione natural products (such as **24** in Figure VI.8) has met with much difficulty in the installation of the disulfide (Scheme VI.6).[32,33] To date, only one complete total synthesis of a compound of this class has been reported.[34] Another case in point is

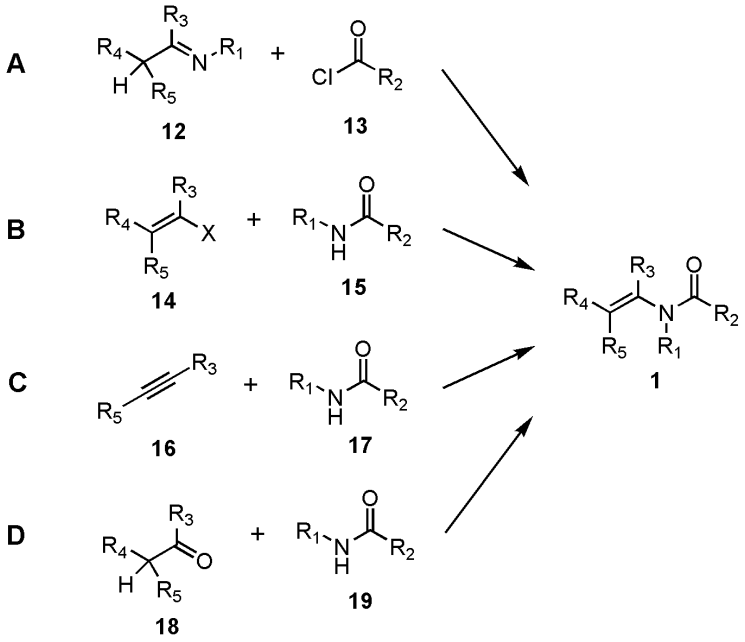

Scheme VI.4: Different approaches to enamide functional group

A: direct acylation of imine, B: vinylation of amide, C: amide addition to alkyne, D: condensation of aldehyde to amide. Curtius rearrangement of α,β-unsaturated acyl azides was excluded due to its rarity. Typically, other approaches also utilize one of these reactions to prepare the starting enamide material.

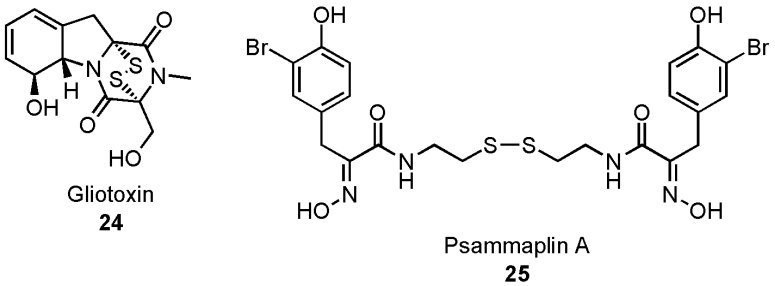

Figure VI.8: Examples of disulfide-containing natural products

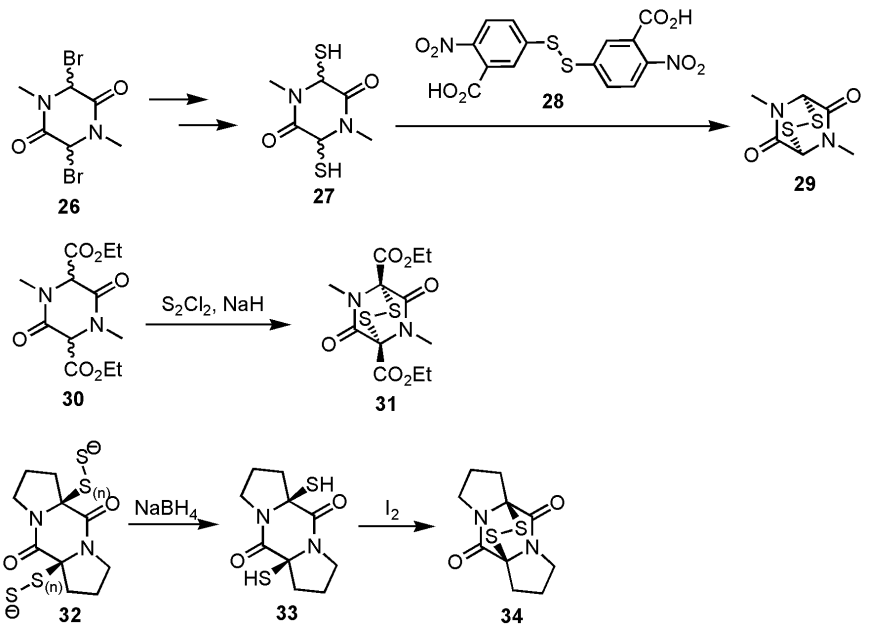

Scheme VI.5: Approaches to install disulfide of the epidithiapiperazinedione core

In the first and the third case, a multi-step maneuver of functional groups is required to install disulfide. In the second case, a very harsh condition (S_2Cl_2 and NaH) is required. None of these approaches would be ideal for a total synthesis of a natural product with labile functional groups.[34]

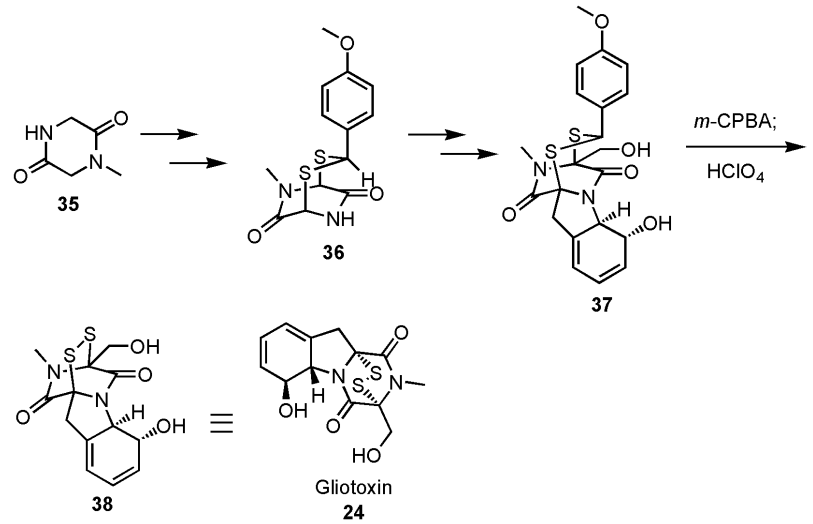

Scheme VI.6: Total synthesis of glyotoxin involving sensitive installation of disulfide

After a lengthy investigation, a strategy was devised in which the disulfide is only formed in the last step. Any attempts to install it in earlier stages were not successful.[34]

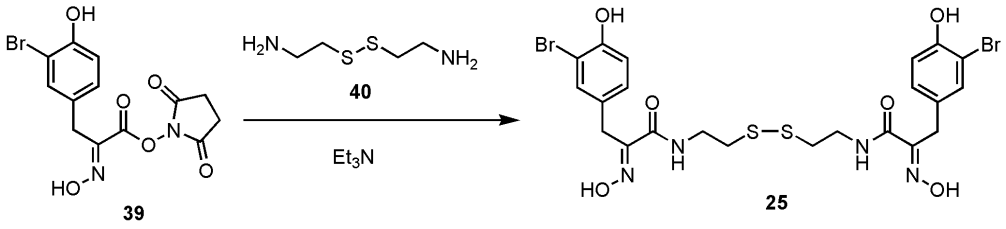

Scheme VI.7: Synthesis of psammaplin A

The installation of the labile disulfide had to be reserved until the last step.[35]

psammaplin A (**25**); in all three of the published syntheses of **25**, the sulfur atoms were introduced as a disulfide in the final step so as to avoid side reactions (Scheme VI.7).[35]

VI.3 Attempted synthesis of somocystinamide A through Suzuki coupling

With a method to construct a simple enamide in hand, retrosynthetic analysis of the natural product led to the proposed synthetic approach shown in red in Scheme VI.8. Suzuki coupling is well known as a robust reaction to connect a vinyl or aryl halide to a vinyl or aryl borylate.[36] The reaction is somewhat less reliable if the boron is on an sp^3

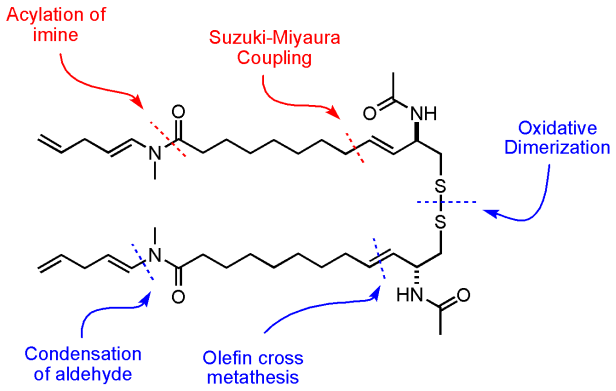

Scheme VI.8: Retrosynthetic analysis of somocystinamide A

The initial strategy is shown in red while the successful approach is shown in blue.

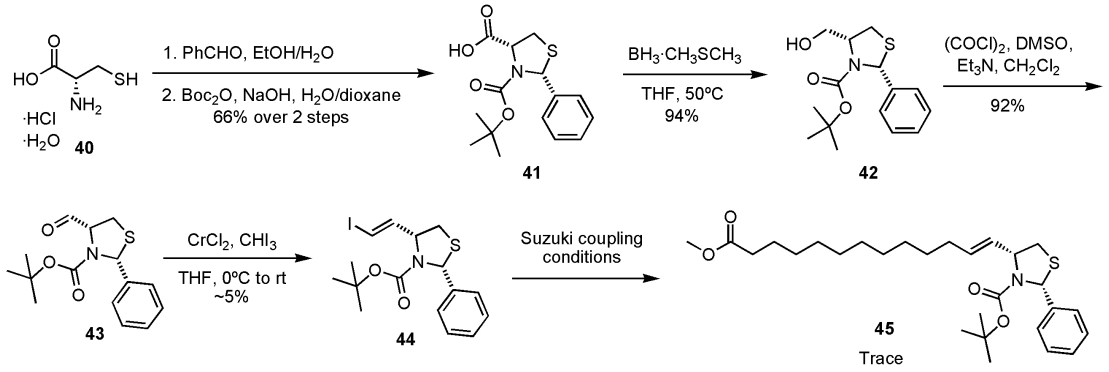

Scheme VI.9: Synthesis of vinyl iodide for Suzuki coupling (Scheme VI.10)

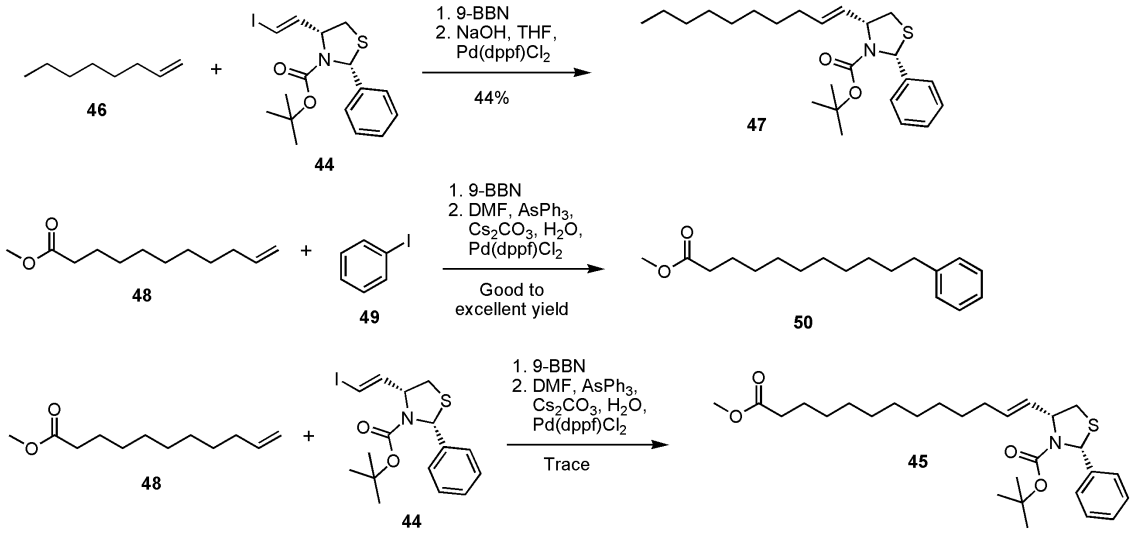

Scheme VI.10: Suzuki coupling with varying coupling partners

For convenience, a commercially available olefin **48** was used despite the wrong length of the alkyl chain.

carbon.[36,37] Thus, besides the enamide synthesis, other steps of concern in the proposed synthesis were the Takai vinyl iodide synthesis[38] and the Suzuki coupling. The Takai reaction was tested on a commercially available aldehyde derived from proline, which is structurally very similar to the actual substrate except for the absence of sulfur. This

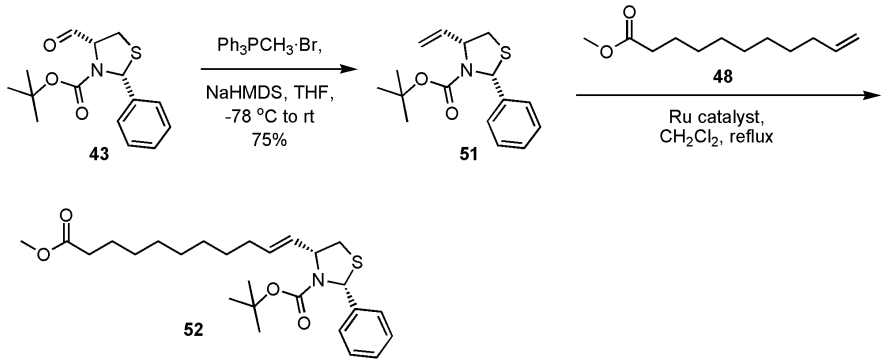

Scheme VI.11: Ruthenium catalyzed cross metathesis approach

reaction proceeded with good yield (70%). The necessary vinyl halide for the Suzuki coupling could be synthesized via the Takai protocol from the corresponding aldehyde.[38] Finally late-stage dimerization at the sulfur atom via air oxidation and installation of the enamide moiety were planned to complete the synthesis of **1**.

The synthesis of **1** began with the putative biosynthetic precursor, L-cysteine, whose stereochemistry translates into the final product. The cysteine was then protected as a Boc-thiazolidine **41** with the use of benzaldehyde and Boc anhydride.[39] Following reduction of the carboxylic acid **41** to an alcohol **42** and oxidization back up to the aldehyde **43** via a Swern reaction,[39,40] the aldehyde was treated with chromium (II) chloride and iodoform (Takai protocol).[38] The Takai reaction seemed to give a good yield by direct TLC analysis of the reaction mixture. However, after work-up and chromatography, only a minute amount of the desired product was recovered, possibly due to the presence of excess iodoform (elutes closely with the product) and decomposition of the vinyl iodide. Brief efforts at optimizing this reaction were not successful.

The vinyl iodide **44** was tested for the Suzuki coupling reaction and only a trace amount of the desired product was formed. The difficulty of this reaction was attributed to the combination of functional group incompatibility and, possibly, the excess 9-BBN that could have reduced the palladium-vinyl complex to the terminal alkene.[41] To examine the latter possibility, the same Suzuki coupling reaction was carried out with a trifluoroboronate substrate, which is a solid that can be isolated.[42] However, this approach also proved unfruitful.

VI.4 Cross metathesis approach to somocystinamide A skeleton

To circumvent the Suzuki coupling problem, a cross metathesis approach was employed.[43] Conveniently, commercially available methyl 10-undecenoate (**48**) would give the correct chain length for the natural product because the terminal sp^2 carbon would be cleaved off in the process. The metathesis reaction was carried out using **48** and the vinyl thiazolidine **51**, which was synthesized from the aldehyde **43** via a simple Wittig reaction.[44] Different Ruthenium catalysts and various amounts of each substrate and the catalyst were screened to find an optimum condition for this coupling reaction (Table VI.1).

The production of the dimeric ester **53** seemed much faster than the desired product by TLC analysis. This observation seemingly implied that the dimerization of the ester happens first and then the dimeric ester is used in the actual metathesis. Therefore it was hypothesized that the yield could be improved by utilizing pre-prepared dimeric ester for the metathesis, which would presumably reduce the work load for the catalyst. However, this hypothesis was discounted because the use of **12** as one of the

coupling partners did not improve the yield and apparently opened another reaction pathway for the starting material (entry 5, Table VI.1). In any case, the second generation Hoveyda catalyst was found to be the best catalyst for this purpose.[45]

Table VI.1: Optimization of ruthenium-catalyzed cross metathesis.

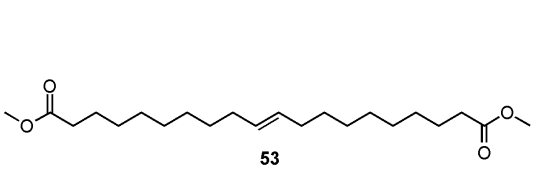

53

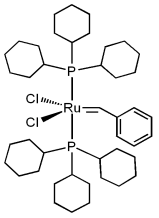

Grubbs I

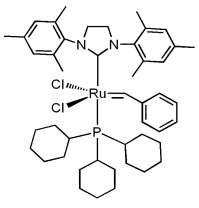

Grubbs II

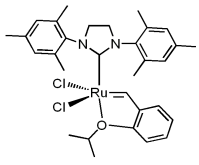

Hoveyda II

	catalyst	conc.[a]	ester[b]	yield of **52** [c]
1	Grubbs I, 20 mol %	0.04	**48**, 10 equiv	0%
2	Grubbs II, 20 mol %	0.04	**48**, 10 equiv	26% (na)
3	Grubbs II, 4 mol %	0.04	**48**, 3 equiv	23% (57%)
4	Hoveyda II, 5 mol %	0.03	**48**, 3 equiv	81% (94%)
5	Hoveyda II, 5 mol %	0.03	**53**, 1.5 equiv	53% (55%)
6	Hoveyda II, 2.5 mol %	0.03	**48**, 3 equiv	44% (na)
7[d]	Hoveyda II, 5 mol %	0.04	**48**, 3 equiv	73% (83%)
8[e]	Hoveyda II, 5 mol %	0.2	**48**, 2.2 equiv	82% (82%)

(a) Concentration of **9** (M); (b) Equivalents of **48** or **53** with respect to **51**; (c) Isolated yields. Yields in parentheses are based on recovered starting material; (d) 3.2 g scale (*ca*. 10 times more than entries 1~6); (e) 5.5 g scale. The E/Z ratio was 18:1.

VI.5 Total synthesis of somocystinamide A

With a reliable coupling protocol in hand, a new synthetic route was devised, as shown in Scheme VI.12. The deprotection of the cysteine residue was effected by reduction of the benzylic carbon with sodium in liquid ammonia in excellent yield (**54**).[13] Upon methylation with diazomethane, the resulting thiol (**55**) was treated with TFA and subsequently with acetic anhydride and triethylamine to replace the Boc protecting group with acetate, which results in acylation of the thiol group as well (**56**). Both the removal of the unwanted acetate on the thiol and hydrolysis of the methyl ester were achieved in one step by treatment with lithium hydroxide in aqueous THF, which also causes the oxidative dimerization of the thiol if performed in air (somocystinoic acid, **57**).[46] This air oxidation only occurred with small scale reactions (<100 mg). Attempts to effect the

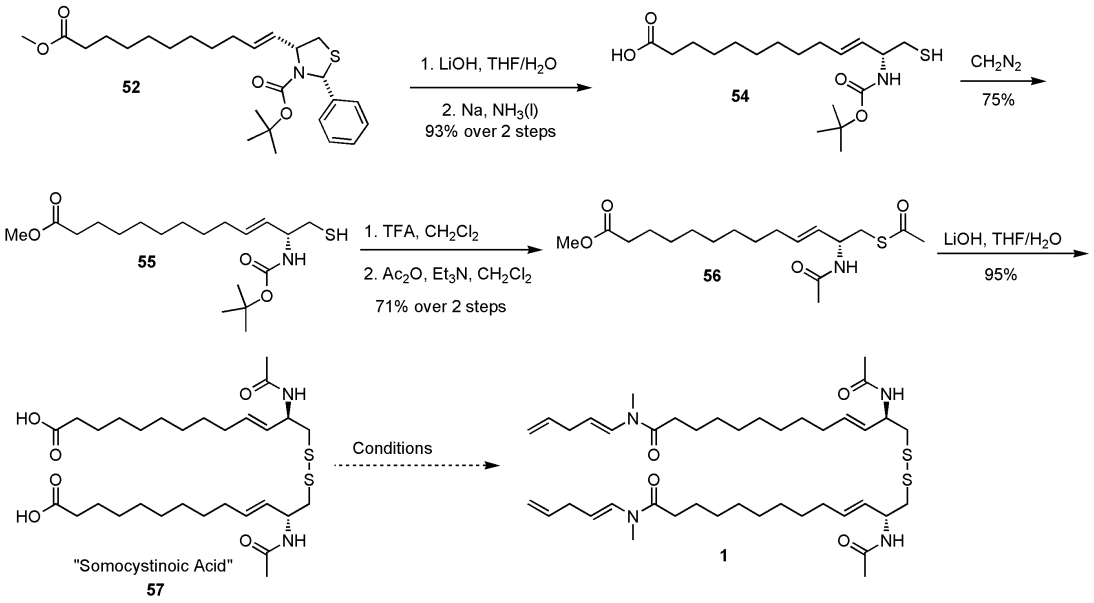

Scheme VI.12: Initially planned final steps to Somocystinamide (**1**)

dimerization with conventional means, such as treatment with I_2, did not give good yields.

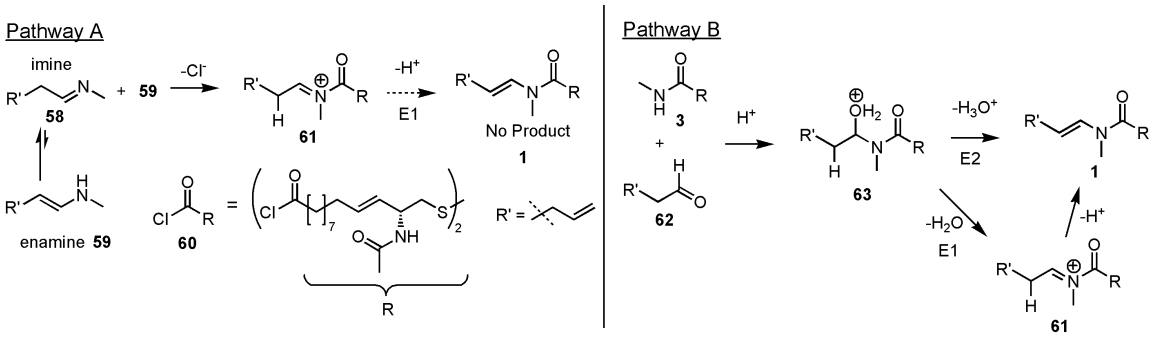

Scheme VI.13: Possible mechanism of enamide formation

The method developed from the model study was used to effect the acylation with the corresponding imine. Various conditions were investigated to couple the *in situ* generated imine **58** to the corresponding di-acyl chloride **60**, whose formation was verified by the reaction with methylamine to produce **3** (Scheme VI.13, Table VI.2). Model compounds (**63-65**) were also tested in this investigation for enamide formation (Figure VI.9, Table VI.2). In most cases, the starting material decomposed while in some cases a trace amount of **1** was observed (Table VI.2). This result was curious because, in

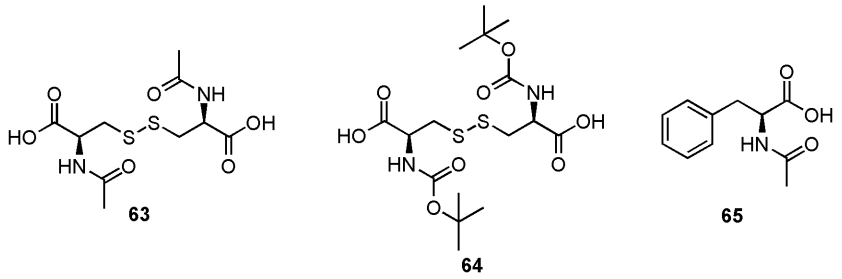

Figure VI.9: Model compounds used in the study of enamide formation

Table VI.2: Enamide formation via acyl chloride

	Substrate	Conditions	Result
1	**63**	1. $SOCl_2$ (excess), CH_2Cl_2 2. $MeNH_2$, 4-pentenal, MS3Å	Decomp.
2	**63**	1. $(COCl)_2$, DMF, CH_2Cl_2 2. $MeNH_2$, 4-pentenal, MS3Å	Decomp.
3	**64**	1. $SOCl_2$ (excess), CH_2Cl_2 2. $MeNH_2$, 4-pentenal, MS3Å	Decomp.
4	**64**	1. $(COCl)_2$, DMF, CH_2Cl_2 2. $MeNH_2$, 4-pentenal, MS3Å	Decomp.
5	**64**	1. $(COCl)_2$, DMF, CH_2Cl_2 2. MeOH, Et_3N	Methyl Ester, low yield
6	**65**	1. $SOCl_2$ (excess), CH_2Cl_2 2. $MeNH_2$, 4-pentenal, MS3Å	Decomp.
7	**65**	1. $SOCl_2$ (1.5 eq), CH_2Cl_2 2. MeOH, Et_3N	Methyl ester, moderate yield
8	**57**	1. $(COCl)_2$ (excess), CH_2Cl_2 2. $MeNH_2$, 4-pentenal, MS3Å	Trace of **1**
9	**57**	1. $SOCl_2$ (excess), CH_2Cl_2 2. $MeNH_2$, 4-pentenal, MS3Å	Decomp.
10	**57**	1. $(COCl)_2$, DMF, CH_2Cl_2 2. MeOH, Et_3N	Methyl Ester, low yield
11	**57**	1. $(COCl)_2$, DMF, CH_2Cl_2 2. $MeNH_2$, 4-pentenal, MS3Å	Trace of **1**
12	**23**	1. $EtCO_2Cl$, Et_3N, CH_2Cl_2 2. $MeNH_2$, 4-pentenal, MS3Å	No Acylation
13	**64**	1. $EtCO_2Cl$, Et_3N, CH_2Cl_2 2. $MeNH_2$, 4-pentenal, MS3Å	No Acylation
14	**65**	1. $EtCO_2Cl$, Et_3N, CH_2Cl_2 2. $MeNH_2$, 4-pentenal, MS3Å	No Acylation
15	**21**	1. EDCA·HCl, Et_3N, CH_2Cl_2 2. $MeNH_2$, 4-pentenal, MS3Å	No Acylation
16	**21**	$MeNH_2$, 4-pentenal, MS3Å	~70% yield
17	**23**	1. $(COCl)_2$ (excess), CH_2Cl_2 2. $MeNH_2$, 4-pentenal, MS3Å	~70% yield

addition to the model study, there are reports of synthesis of simple enamides via acylation of the corresponding acid chloride with imine.[47] It is possible that the putative acyl iminium ion intermediate **61** is intercepted intramolecularly due to the dimeric nature of the substrate (Scheme VI.13).[48] In support of this hypothesis, the tautomer **59** was not observed at all by ^{1}H or ^{13}C NMR in CD_2Cl_2.[49]

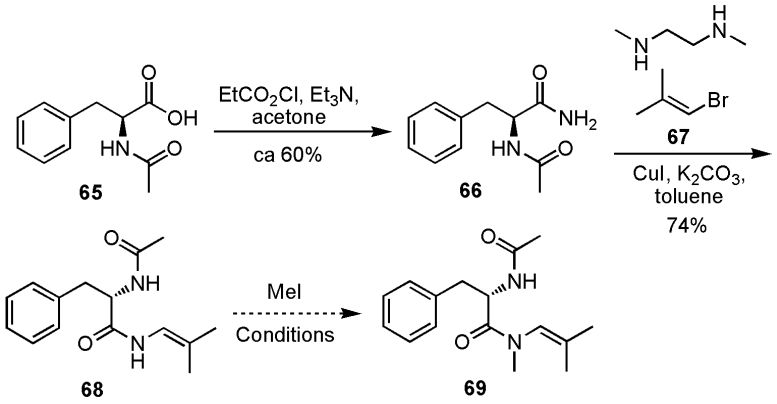

Scheme VI.14: Copper-mediated vinylation of a primary amide model compound (**65**) and attempted chemoselective methylation

For the methylation step, the investigated conditions are the following: K_2CO_3 in EtOH, MeCN, and dioxane; NaHMDS in THF, NaH in THF.

Conventionally, protocols for enamide formation include, in addition to acylation of imines, direct addition of amides to alkynes, condensation of aldehyde with amide, and the olefination of amides (Scheme VI.3). Most of these protocols suffer from low yields and/or lack of stereocontrol on the double bond geometry. The most recent collective effort in enamide synthesis has been on the development of amide vinylation methodology. In 1991, Suzuki and coworkers first reported successful vinylation of amides with vinyl halide in the presence of copper (I) iodide.[50] At the time when there were only a few methods to regiospecifically and stereospecifically produce enamides,

this noble method guaranteed both aspects of reaction specificity. Since the regiospecificity and stereospecificity are solely dictated by the position of the halide on the olefin, this methodology could be universally applied to any enamide systems as long as all the functional groups are tolerated. In the past decade, Buchwald and coworkers have improved this reaction through identification of a more suitable ligand for the copper catalyst.[16a] As such, a Cu-mediated vinylation approach was explored. However, as expected from the literature,[16a] direct vinylation of acyclic secondary amide was not possible. While it was possible to vinylate a primary amide model compound, the required chemoselective methylation of the enamide moiety was not successful (Scheme VI.14).

The observation that the hydrolytic decomposition of **1** to **3** seems to have relatively low activiation energy[3] inspired us to carry out the opposite reaction, namely condensation of the aldehyde **5**[51] with **3** (Scheme VI.15). Because of the need to remove water during the course of reaction, the use of a Soxhlet extraction apparatus was more

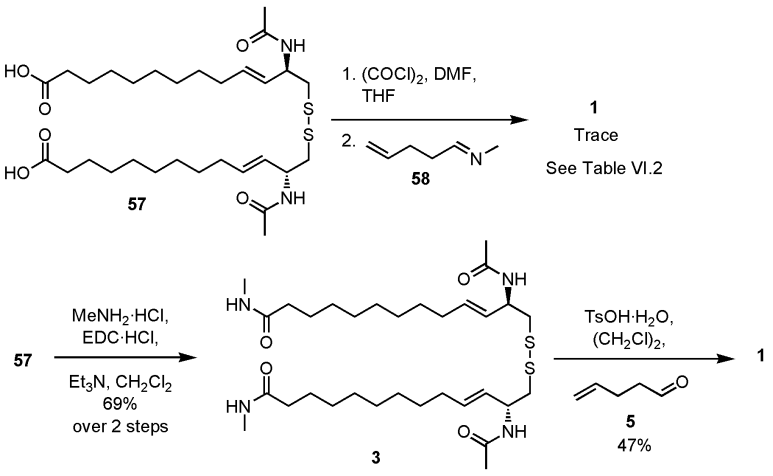

Scheme VI.15: Final steps to somocystinamide A (**1**)

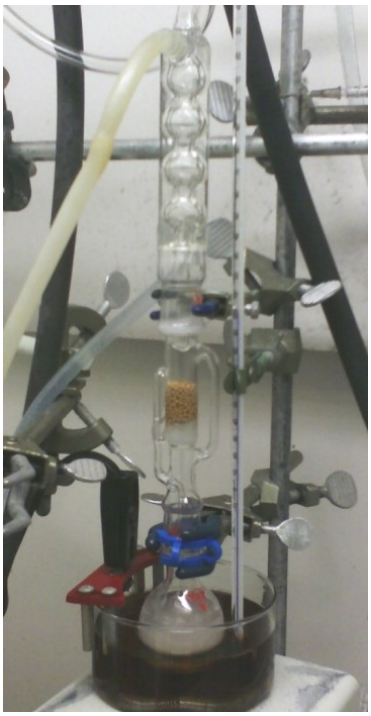

Figure VI.10: Reaction setup for enamide formation using molecular sieves and glass wool in a Soxhlet extractor

convenient for small scale reactions and it also allowed for use of solvents heavier than water (Figure VI.10).[52] Observing that the putative intermediate **21** did not yield **1**, we hypothesized that the E1 path way was not viable (Scheme VI.13). In support of this hypothesis, use of a more polar solvent, THF, had an adverse effect in comparison to 1,2-dichloroethane, a more non-polar solvent.[53] The best result was obtained when TsOH was used as the catalyst, which gave a 47% yield (Scheme VI.15).[54] Thus, a total synthesis of **1** was completed. This synthesis is fairly robust for all steps but the last two such that >1 g of **57** was prepared. However, scale-up for the production of **3** proved difficult due to complications in the purification procedure as a consequence of the extremely poor

solubility of **3**. Therefore, a modified synthetic route or improved purification protocols are necessary for larger-scale production of **1** and its analogs.

VI.6 Bioassays of the synthetic sample of somocystinamide A

Upon the completion of a total synthesis of somocystinamide A (**1**), its in vivo activity was investigated in brine shrimp. While **1** was not lethal to the brine shrimp even at 130 μM (media concentration) after 24 hours of exposure, their motility was significantly impaired even at 1.3 μM. A much decreased quantity of intestinal contents were found in the treated group. Thus, **1** seems to possess biological properties not yet understood.

In an A549 (human lung carcinoma) cytotoxicity assay, the synthetic sample of somocystinamide A (**1**) possessed anti-proliferative activity, but to a lesser extent than the natural sample. Initially there was concern about the possibility that **1** was not the extremely bioactive metabolite in the earlier investigation.[55] To investigate the cause of this decreased activity, a hypothesis was formed and examined; synthetic **1** is purer than natural **1** and the natural sample contained contaminants that assisted in solubilizing **1**, whereas the synthetic sample had poor solubility. While much better than **3**, the solubility of **1** is not satisfactory for many purposes. Indeed, in the brine shrimp assays, the samples at 100 μM were cloudy with incompletely dissolved **1**. In 96-well plate cytotoxicity assays, serial dilutions are made from the highest concentration solution. Therefore, if any portion of **1** precipitates in the highest concentration solution, all of the wells containing solutions of **1** also have decreased concentrations of **1**.

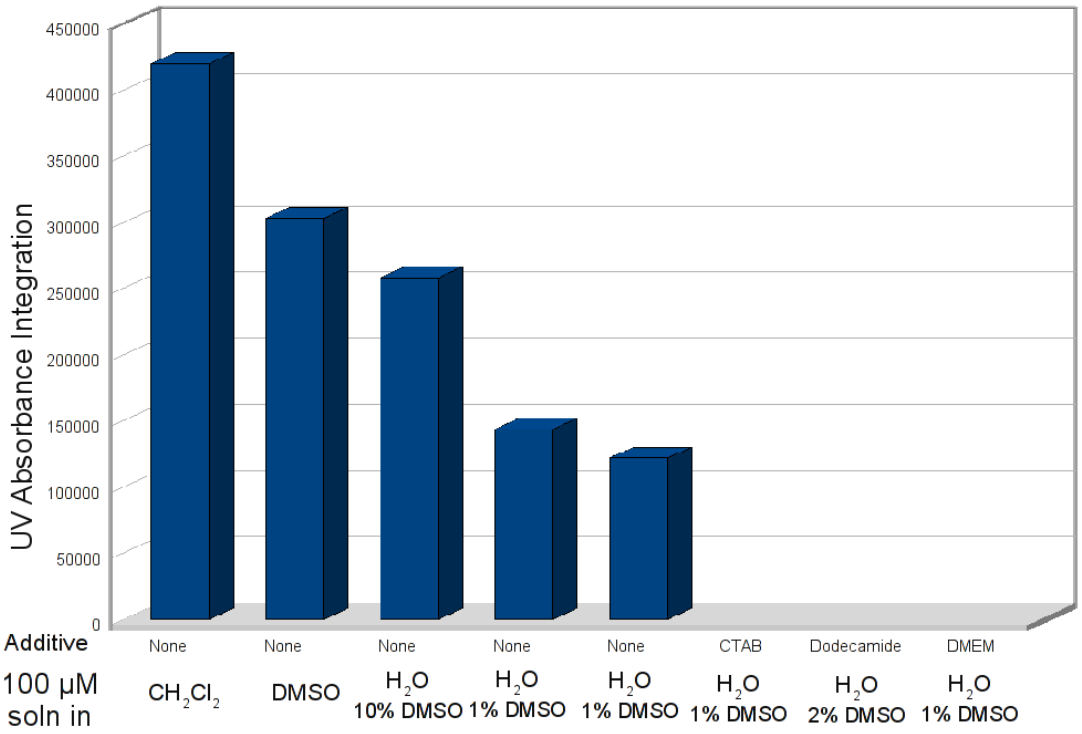

Figure VI.11: Solubility of somocystinamide A (1) in various media

The solubility was measured by the UV absorbance (Y-axis) of RP-HPLC PDA dectector. For each run, 10 µL of a 100 µM solution was injected. The X-axis denotes the presence or absence of additives. The 4th and 5th runs were duplicates.

Because all the in vitro bioassays are done in aqueous environments, the solubility of somocytinamide A (**1**) in various types of aqueous solutions were examined (Figure VI.11). The solubility was determined by injecting a sample of **1** onto a RP-HPLC column and measuring the PDA-detected UV-absorbance of **1**. As expected, more of the compound was detected when only organic solvents were used (the first two entries in Figure VI.9). However, when a solution of **1** was diluted with H_2O, the measured solubility decreased significantly. Phase-transfer catalyst-like additives (CTAB, dodecamide, DMEM) eliminated the solubility of **1**. Given these results, any future

bioassay of **1** must be carried out with care. It is recommended that the maximum amount of organic solvents tolerated by the cells be used in the sample solutions.

VI.7 Scalable synthesis of somocystinamide A

While the above synthetic route is sufficient for small-scale synthesis in a laboratory, it has three main bottlenecks in terms of scaling-up.

1.The conversion of **52** to **56** requires 5 steps for what is essentially a deprotection-reprotection maneuver.

2.The conversion of **57** to **3** cannot be readily scaled-up due to the insolubility of **3**. If **3** readily dissolved in solvents such as EtOAc, the workup and purification would be simply a matter of aqueous acid/base washings for this amine coupling step.

3.The final step of introducing the enamide moiety has not been optimized beyond 41% yield.

In order to remedy all three of these issues, an efficient alternative method must be first developed for the production of **3**, which would enable optimization studies on the finals step from **3** to **1**. When investigating the enamide formation reaction with simpler substrates, such as undecanoic acid, it was observed that the resulting tertiary enamide had excellent solubility in common solvents such as CH_2Cl_2 and MeOH. However, the dimeric equivalent of this compound, **2**, had extremely poor solubility in these same solvents. Suspecting that the insolubility of bis-amide **3** was at least partially due to its dimeric nature and the methyl amide functionality, a synthetic route for **3** was devised in which the intermediates remain as monomers until the enamide formation step as shown in Scheme VI.16.

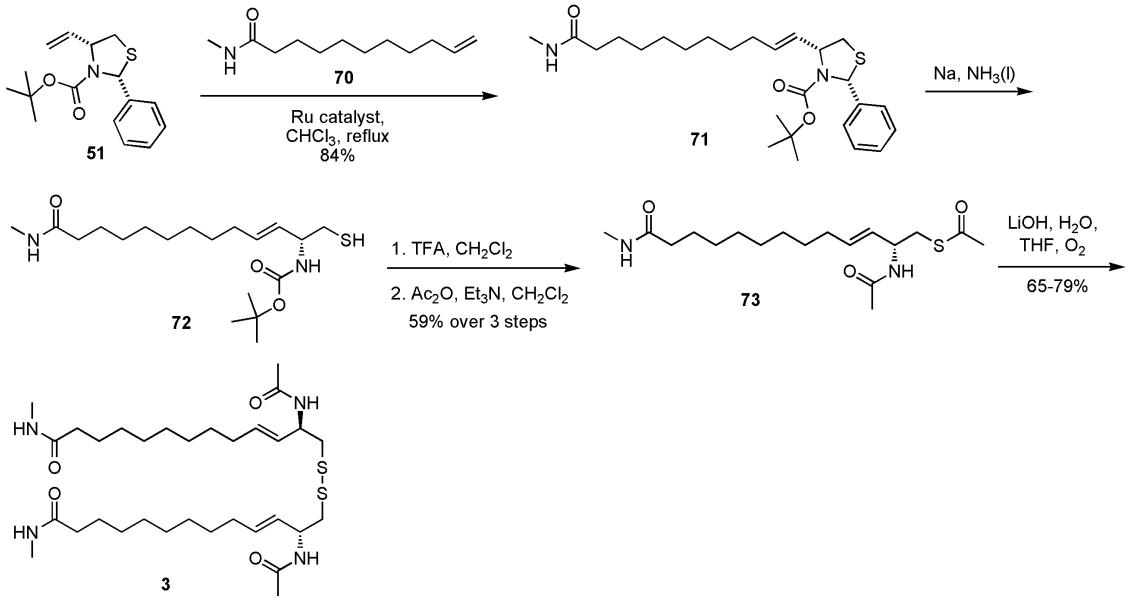

Scheme VI.16: Revised synthesis of the bis-methylamide **3**

This scheme shortened the synthesis by two steps. However, the cross metathesis step suffered low yields (~40%) under the same condition as the previous synthesis. After examination of the reaction by-products, a large amount of dimer **74** was found as an insoluble solid. In the previous reaction (**51** to **52**), the dimeric ester by-product was able to be recycled in the reaction (Table IV.1, entry 5), which was probably a large contributing factor to the excellent yield (82%) despite the faster formation of **53** than **52**. Therefore, it was hypothesized that if a solvent system that solubilize **74** was utilized, the yield would increase due to recycling of **74**. When 9:1 CH_2Cl_2 / MeOH was used, the yield decreased and most of the starting material (**51**) was left intact. When $CHCl_3$ was used, the cross metathesis proceeded smoothly with excellent yield (81-84%). It was

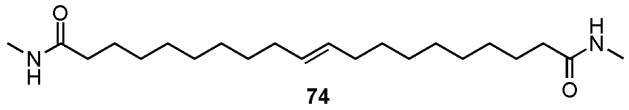

noted, however, that the purification of the product (**71**) was more troublesome than **52** due to the increased polarity of **71**.

Afterwards, the conversion of **71** to **73** was straightforward. As a result of this revised synthesis, the use of a potentially dangerous and toxic reagent, diazomethane was also eliminated.[56] The hydrolysis/oxidation step from **73** to **3** only required washing of the precipitated product, **3**, thereby taking advantage of its insolubility. However, the yield was somewhat less than ideal (65%). Purification methods such as washing of a solid is well-suited for future adaptation to industrial scale production should the compound become a pharmaceutical product.[57] All of these steps were done at fairly large scales and >1 g of **73** and >500 mg of **3** were obtained, the latter of which would not have been reasonable without this revision of the synthesis. Finally, the penultimate natural product **3** (301 mg) could be converted to somocystinamide A (**1**, 119 mg, 33% yield) through the previously established method (Scheme VI.15), thereby completing a sufficiently large-scale synthesis[58] required for future *in vivo* investigations. The overall yield of this revised synthetic route was 11% over 7 steps from the known aldehyde **43**, whereas the overall yield of the earlier synthesis was 9% over 10 steps from **43**. Despite a small difference in the overall yield, the smaller number of steps required for the revised route makes it significant improvement.

VI.8 Conclusions

A stereoselective and stereospecific total synthesis of a promising anti-angiogenic marine natural product, somocystinamide A (**1**) was accomplished through ruthenium-catalyzed olefin cross metathesis, molecular oxygen and base-promoted dimerization of

the thiol, and enamide formation through condensation of aldehyde with amide. This synthesis provided material for further bioassays and helped to identify the solubility problem of this natural product. Furthermore, the synthesis was successfully revised to suit the future needs for synthesis of analogs and a large supply of the compound for *in vivo* evaluations.

VI.9 Experimental section

General Experimental Procedures and Materials

Unless noted otherwise, all materials were purchased from commercial sources and were used without further purification. Anhydrous benzene was purchased from EMD. Tetrahydrofuran (THF) was distilled from sodium / benzophenone. Et_3N and CH_2Cl_2 were distilled from CaH. Ac_2O was distilled from quinone. Dimethyl sulfoxide (DMSO), oxalyl chloride, and trifluoroacetic acid (TFA) were distilled without desiccant. All reactions were carried out under dry argon atmosphere unless otherwise noted. Reaction temperatures herein recorded are external temperatures unless otherwise noted. Flash chromatorgraphy was performed using EMD silica gel (230-400 mesh) in all cases.[59] Thin layer chromatographic (TLC) analysis was performed using EM Science pre-coated silica gel plates (Merck 60 F_{254}). Melting points were determined on an Electrothermal Mel-Temp device and are uncorrected. Optical rotations were measured on a Jasco P-2000 polarimeter. IR spectra were recorded on a Nicolet Magna-IR 550. ^1H NMR and ^{13}C NMR spectra were recorded on a Varian Inova spectrometer (500 MHz and 125 MHz, respectively) or on a Varian Inova spectrometer (300 MHz and 75 MHz, respectively). ^1H and ^{13}C spectra recorded in $CDCl_3$ (or in $CD_3OD/CDCl_3$) were referenced to the residual solvent peaks at 7.26 ppm ($CHCl_3$) and 77.0 ppm ($CDCl_3$), respectively. High resolution mass spectra were recorded on a ThermoFinnigan MAT900XL spectrometer.

Preparation of Known Aldehyde 43

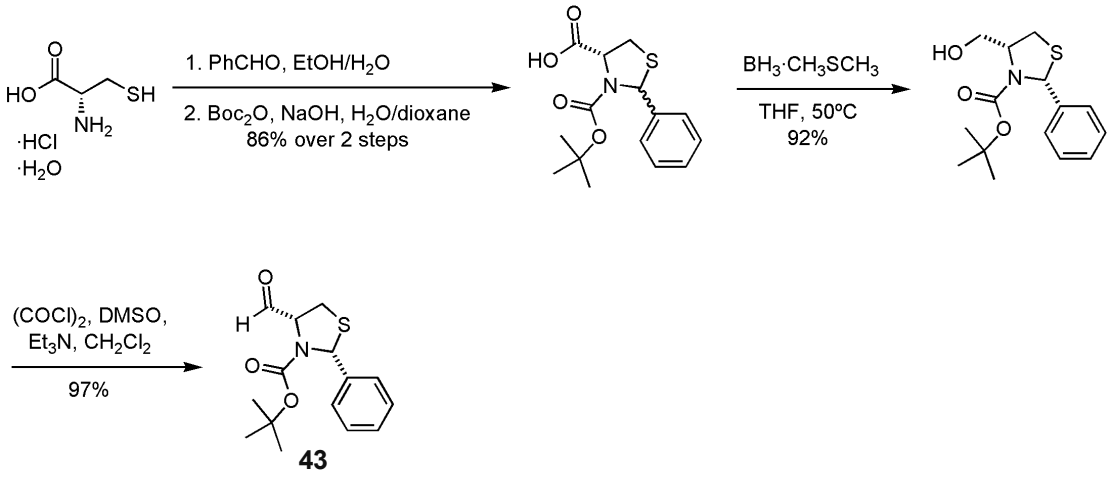

The first step was done according to reference 59.[60] The rest of the steps to the aldehyde (**43**) were carried out according to reference 38.[39]

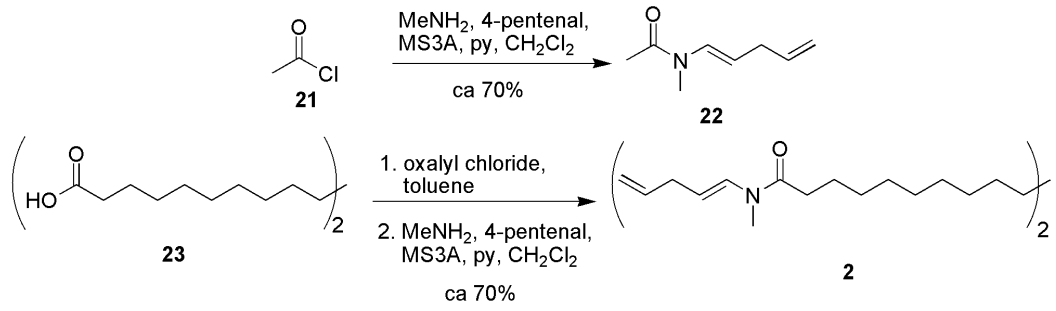

Synthesis of enamides 22 and 2. To a solution of the aldehyde **5** (97 μL, 0.98 mmol) in CH_2Cl_2 (5 mL) was added a 2M solution of $MeNH_2$ in THF (0.49 mL, 0.98 mmol) and $MgSO_4$ (710 mg) at 0˚C. Immediately, the mixture was warmed to rt and left stirring for 1.5 hrs. Then neat acetylchloride (70 μL, 0.98 mmol) was added. After 10 min, pyridine (95 μL, 1.18 mmol) was added, and the mixture was left stirring for 3 hrs at rt. The reaction mixture was filtered and was poured into a cold saturated solution of $NaHCO_3$. Upon phase separation, the organic layer was washed with saturated $NaHCO_3$ and was dried over Na_2SO_4. The volatiles were removed *in vacuo* and a brown oil was obtained, which was mostly pure by TLC and ^{1}H NMR (96 mg, ~70% yield). In order to obtain an analytically pure sample, the brown oil was subjected to flash column chromatography using silica gel (1:6 EtOAc / Hexanes to 1:5 EtOAc / Hexanes). A colorless oil (51 mg, 0.37 mmol, 37%) was obtained. TLC Rf = 0.41 (3:7 EtOAc/Hexanes). The bis-enamide **2** was synthesized in the same manner except that two equivalents of **5** and $MeNH_2$ were used. ^{1}H and ^{13}C NMR spectra: see Figures VI.10-13.

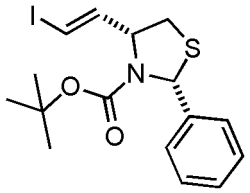

(2*R*,4*R*)-tert-butyl 4-((*E*)-2-iodovinyl)-2-phenylthiazolidine-3-carboxylate (44). $CrCl_2$ (5.189 g, 42.22 mmol) was flame-dried in a flask under vacuum. Upon cooling to rt, THF (31 mL) was added and the suspension was stirred at rt for 25 min. Then the mixture was cooled to 0°C. A solution of the aldehyde **43** (1.972 g, 6.693 mmol) and CHI_3 (5.270 g, 13.38 mmol) in THF (30 mL) was cannulated dropwise into the $CrCl_2$ suspension over 20 min. An additional amount of THF (10 mL) was used to rinse the flask containing **43** and CHI_3, which was cannulated again into the $CrCl_2$ suspension. At this point, TLC analysis showed that there was little starting material left, and that a significant amount of the desired product had formed. This mixture was taken out of the ice bath immediately and was stirred at rt for 4 hrs. The mixture was diluted with Et_2O (30 mL), and it was poured into brine, which was extracted with Et_2O (20 mL x 2). The organic layer was washed with brine, and was dried over Na_2SO_4. Upon removal of the solvents, the residues were subjected to flash column chromatography (hexanes to 1:4 EtOAc/hexanes) to obtain 124 mg of the product (**44**) as a pale yellow solid (4.4% yield). TLC Rf = 0.30 (1:4 EtOAc / hexanes). ^1H and ^{13}C NMR spectra: see Figures VI.15 and 16.

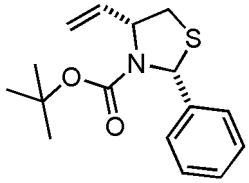

(2*R*,4*R*)-2-phenyl-4-vinylthiazolidine-3-*tert*-butyl carboxylate (51). To the suspension of $MePPh_3 \cdot Br$ (13.37 g, 37.43 mmol) in THF (150 mL) at –78°C (dry ice bath) was added 1.0 M NaHMDS (43 mL, 43 mmol) dropwise under vigorous stirring, which resulted in a yellow solution. The dry ice bath was removed and the solution stirred for 45 min at rt.

The solution was cooled again to –78°C and a solution of the aldehyde (8.302 g, 28.30 mmol, synthesized according to literature[2]) in THF (100 mL) was added dropwise. Then the solution was warmed to rt over night under stirring. Consumption of the aldehyde was confirmed by TLC analysis. Then 1.0 M aqueous NH_4Cl (100 mL) and Et_2O (100 mL) were added successively. The aqueous phase was extracted with Et_2O (100 mL x 2). The combined organic phase was washed with brine, dried over Na_2SO_4, and was filtered through a plug of silica gel. Upon evaporation of solvents, the residue was purified by flash column chromatography (3:97 to 1:9 Et_2O / hexane) and a white solid (6.04 g, 20.7 mmol) was obtained (74% yield). Mp 44-45 ºC**.** TLC Rf 0.39 Et_2O / hexane (1:4). $[\alpha]_D^{23}$ +136.2º (*c* 6.50, $CHCl_3$). IR (film, KBr) ν_{max} 2977, 1698, 1367, 1164 cm^{-1}. ^1H NMR (300 MHz, $CDCl_3$) δ 7.22-7.39 (m, 5H), 6.10 (s, 1H), 6.03 (m, 1H), 5.37, (d, 17.1 Hz, 1H), 5.25 (dt, *J*=10.2, 0.9 Hz, 1H), 4.83 (m, 1H), 3.27 (dd, *J*=11.7, 6.6 Hz, 1H), 2.85 (dd, *J*=11.7, 5.1 Hz, 1H), 1.33 (s, 9H). ^{13}C NMR (75 MHz, $CDCl_3$) δ 153.7, 141.6, 137.8, 128.2, 127.5, 126.3, 117.2, 80.7, 66.3, 64.5, 36.1, 28.2. HRMS (EI): calcd for $C_{16}H_{21}O_2N_1S_1$: 291.1288, found 291.1284.

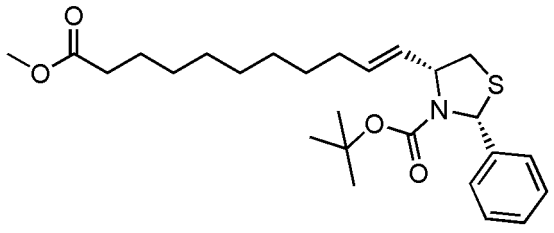

(2*R*,4*R*)-3-*tert*-butoxycarbonyl-4-((*E*)-11-methoxy-11-oxoundec-1-enyl)-2-phenylthiazolidine (52). To the solution of the thiazolidine olefin **51** (5.500 g, 18.87 mmol) in CH_2Cl_2 (95 mL) was added methyl undecenoate (9.2 mL, 41 mmol) at rt. The

solution was then subjected to vacuum-sonication-Ar introduction cycle three times for degassing. Then second generation Hoveyda-Grubbs catalyst (592 mg, 0.944 mmol) was addedin one portion. After 20 min of stirring at rt, the solution was refluxed for 16 hrs. Then the solvents were removed under vacuum and the residue was subjected to flash column chromatography (hexane to 1:9 Et_2O / hexane) to obtain colorless oil (7.174 g, 15.54 mmol, 82% yield). Along with the desired product was isolated the *cis* isomer (TLC Rf=0.52 Et_2O / hexane 3:7, 539 mg, 1.17 mmol, 6% yield *cis*). TLC Rf 0.47 Et_2O / hexane (3:7). $[\alpha]_D^{23}$ –81.7º (*c* 1.85, $CHCl_3$). IR (film, KBr) ν_{max} 2978, 2928, 2853, 1740, 1696, 1367, 1166 cm^{-1}. ^1H NMR (300 MHz, $CDCl_3$) δ 7.21-7.38 (m, 5H), 6.08 (s, 1H), 5.78 (dt, *J* = 15.3 Hz, 6.6 Hz, 1H), 5.63 (dd, *J* = 15.3 Hz, 7.6 Hz, 1H), 4.81 (ddd, *J* = 7.6, 6.5, 4.6 Hz, 1H), 3.65 (s, 3H), 3.24 (dd, *J*=11.7, 6.5 Hz, 1H), 2.79 (dd, *J* = 11.7, 4.6 Hz, 1H), 2.29 (t, *J* = 7.6 Hz, 2H), 2.06 (q, *J* = 6.8 Hz, 2H), 1.61 (m, 2H), 1.28-1.41 (m, 20H). ^{13}C NMR (75 MHz, $CDCl_3$) δ 174.2, 153.5, 141.8, 133.9, 129.4, 128.1, 127.3, 126.2, 80.4, 66.0, 63.8, 51.3, 36.5, 34.0, 32.1, 29.2, 29.1, 29.1, 29.0, 29.0, 28.2, 24.9. HRMS (EI): calcd for $C_{26}H_{39}O_4N_1S_1$: 461.2594, found 461.2592.

52-cis. ^1H NMR (500 MHz, $CDCl_3$) δ 7.40 – 7.16 (m, 5H), 6.13 (s, 1H), 5.63 (t, *J* = 9.7 Hz, 1H), 5.58 – 5.45 (m, 1H), 5.13 (d, *J* = 6.1 Hz, 1H), 3.65 (d, *J* = 1.7 Hz, 3H), 3.20 (dd, *J* = 11.6, 6.4 Hz, 1H), 2.72 (dd, *J* = 11.6, 5.5 Hz, 1H), 2.29 (t, *J* = 7.5 Hz, 2H), 2.25 – 2.10 (m, 2H), 1.60 (dd, J = 13.6, 6.8 Hz, 2H), 1.51 – 1.14 (m, 20H). ^{13}C NMR (125 MHz, $CDCl_3$) δ 174.15, 153.59, 141.92, 132.08, 129.72, 128.11, 127.30, 126.01, 80.46, 66.05, 59.14, 51.33, 36.75, 33.99, 29.58, 29.24, 29.19, 29.11, 29.02, 28.17, 27.60, 24.84.

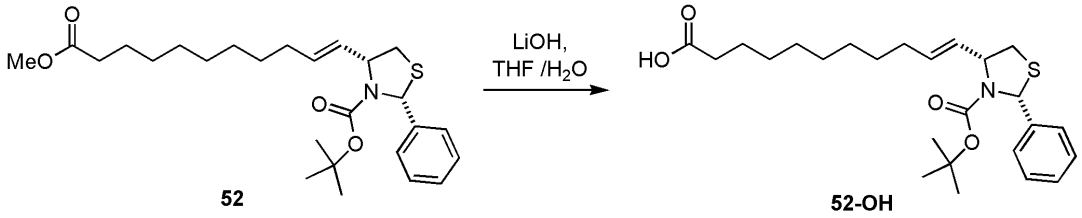

(*E*)-11-((2*R*,4*R*)-3-(*tert*-butoxycarbonyl)-2-phenylthiazolidin-4-yl)undec-10-enoic acid (52-OH). The solution of the methyl ester **52** (11.40 g, 24.70 mmol) in THF (240 mL) was cooled to 0°C. A solution of $LiOH \cdot H_2O$ (10.07 g, 240.2 mmol) in H_2O (120 mL) was added in one portion. Then the reaction mixture was stirred and warmed gradually over night to rt. Upon seeing some intact starting material on TLC, MeOH (25 mL) was added at rt. 6 hrs later, the solution was cooled to 0°C and Et_2O (200 mL) and 1M $NaHSO_4$ solution (300 mL) were added, after which the pH was *ca* 2~3. Upon phase separation, the aqueous layer was extracted with Et_2O (150 mL x 3). The combined organic layer was washed with brine (250 mL), dried over $MgSO_4$, and was filtered. Upon removal of the solvents, a gummy oil (11.27 g) was obtained, which was used in the next step without further purification. TLC Rf 0.70 EtAcO / hexane (3:2). $[\alpha]_D^{23}$ +69.5º (*c* 4.4, $CHCl_3$). IR (film, KBr) ν_{max} 2975, 2928, 2855, 1701, 1369, 1164 cm^{-1}. ^1H NMR (300MHz, $CDCl_3$) δ 7.21-7.38 (m, 5H), 6.08 (s, 1H), 5.78 (dt, *J* = 15.3, 6.6 Hz, 1H), 5.63 (dd, *J* = 15.3, 7.6 Hz, 1H), 4.82 (ddd, *J* = 7.6, 6.4, 4.7 Hz, 1H), 3.24 (dd, *J* = 12.2, 6.4 Hz, 1H), 2.80 (dd, *J* = 12.2, 4.7 Hz, 1H), 2.34 (t, *J* = 7.5 Hz, 2H), 2.07 (q, *J* = 6.7 Hz, 2H), 1.63 (m, 2H), 1.30-1.43 (m, 19H). ^{13}C NMR δ 179.5, 153.6, 141.8, 134.0, 129.4, 128.1, 127.4, 126.3, 80.5, 66.1, 63.9, 36.6, 34.2, 32.2, 29.21, 29.15, 29.04, 28.99 (3 C's), 28.2, 24.6. HRMS (EI): calcd for $C_{25}H_{37}O_4N_1S_1$: 447.2438, found 447.2441.

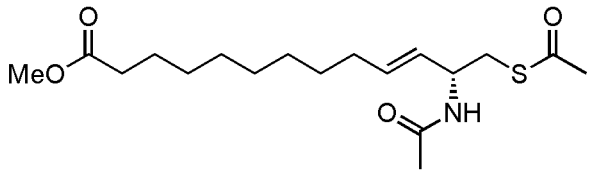

(*R,E*)-methyl 12-acetamido-13-(acetylthio)tridec-10-enoate (56). To the solution of the thiazolidine **52-OH** (11.145 g from the previous step) in THF (10 mL) was added $NH_3(l)$ (350 mL) that was distilled over Na. To this mixture was added cubic pieces (5~7 mm) of Na under vigorous stirring until dark blue color persisted. The mixture was kept refluxing at rt and Na pieces were added as necessary to keep the color for a total of 2 hrs. Then NH_4Cl was carefully added until the color disappeared. NH_3 was removed under gentle stream of N_2 to obtain a colorless oil (8.260 g).

The carboxylic acid (8.030 g, from the previous step) was dissolved in Et_2O (50 mL) and was cooled to 0°C. Ethereal solution of CH_2N_2 (0.14 M, 170 mL, 24 mmol) was added dropwise over 30 min. Then N_2 was bubbled in for 45 min to remove excess CH_2N_2. Upon removal of the solvent *in vacuo*, white crystals were obtained (8.74 g).

These crystals were dissolved in CH_2Cl_2 (200 mL) and was cooled to 0°C. Then TFA (50 mL) was added dropwise over 30 min. Upon further stirring at 0°C for 30 min, the volatiles were removed *in vacuo* to yield orange oil. Residual TFA was removed under hi-vacuum for 1 hr. This TFA salt was dissolved in CH_2Cl_2 (220 mL) and the solution was cooled to 0°C. Then Et_3N (30.6 mL, 220 mmol) and Ac_2O (10.4 mL, 110 mmol) were added slowly under stirring. The solution was let warm to rt over night under stirring. Then the volatiles were removed *in vacuo*. The residues were dissolved in Et_2O (200 mL) and 0.5 M HCl solution (200 mL) was added. Upon phase separation, the aqueous phase was extracted with Et_2O (200 mL x 2). The combined organic phase was

washed with H_2O (150 mL), saturated $NaHCO_3$ solution (100 mL), H_2O (100 mL), and brine (100 mL) successively. After flash column chromatography (15:85 EtAcO / hexane to 1:1 EtAcO / hexane), the desired product was obtained as a white solid (~4.2 g, 12 mmol, 50% yield over 5 steps). The disulfide methyl ester was also isolated as a colorless oil (173 mg, 0.275 mmol, 1% yield). Mp 70-71 ºC. TLC Rf 0.38 EtAcO / hexane (3:2). $[\alpha]_D^{23}$ –13.2º (*c* 6.10, $CHCl_3$). IR (film, KBr) ν_{max} 3278, 3081, 2985, 2926, 2852, 1737, 1691, 1647, 1547, 1434, 1373, 1186, 1139, 968, 630 cm^{-1}. ^1H NMR (500MHz, $CDCl_3$) δ 5.97 (d, *J* = 8.1 Hz, 1H), 5.57 (dtd, *J* = 15.5, 6.6, 1.2 Hz, 1H), 5.29 (ddt, *J* = 15.5, 6.4, 1.2 Hz, 1H), 4.50 (quin, *J* = 6.8 Hz, 1H), 3.60 (s, 3H), 3.01 (d, *J* = 6.6 Hz, 2H), 2.28 (s, 3H), 2.24 (t, *J* = 7.7 Hz, 2H), 1.94 (q, *J* = 7.8 Hz, 2H), 1.90 (s, 3H), 1.55 (quin, *J* = 7.4 Hz, 2H), 1.21-1.30 (m, 12H). ^{13}C NMR (125MHz, $CDCl_3$) δ 195.9, 174.1, 169.3, 133.1, 127.1, 51.3, 50.9, 33.9, 33.4, 32.0, 30.4, 29.0, 29.0, 28.9, 28.8, 28.8, 24.7, 23.1. HRMS (EI): calcd for $C_{18}H_{32}O_4N_1S_1$ (M+H): 358.2047, found 358.2045.

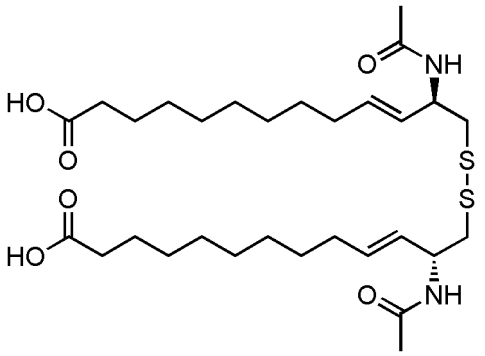

Somocystinoic acid (57). To the solution of the methyl ester (487 mg, 1.36 mmol) in THF (40 mL) was added 1M NaOH solution (20 mL) at rt under stirring. O_2 was continuously bubbled into the mixture while stirring at rt until the consumption of the

thiol was observed by TLC (20 hrs). The reaction mixture was diluted with Et_2O (30 mL) and 1M $KHSO_4$ solution (40 mL) was added at 0°C. Upon phase separation, the aqueous layer was extracted with Et_2O (30 mL) and EtAcO (30 mL x 2). The combined organic layer was dried over $MgSO_4$ and was filtered. Removal of the solvents *in vacuo* yielded pale yellow oil (458 mg), which was used without further purification for the next step. TLC Rf 0.41 AcOH / MeCN / EtAcO (1:9:90). $[\alpha]_D^{23}$ +41.6º (*c* 0.66, $CHCl_3$). IR (film, KBr) ν_{max} 3272(br), 3079(br), 2927, 2855, 1712, 1648, 1550, 1374, 969 cm^{-1}. ^1H NMR (300 MHz, $CDCl_3$) δ 6.23 (d, *J* = 8.1 Hz, 2H), 5.66 (dtd, *J* = 15.5, 6.8, 0.7 Hz, 2H), 5.43 (dd, *J* = 15.5, 6.2 Hz, 2H), 4.70 (quin, *J* = 6.5 Hz, 2H), 3.06 (dd, *J* = 13.5, 6.0 Hz, 2H), 2.85 (dd, *J* = 13.5, 6.2 Hz, 2H), 2.35 (t, *J* = 7.1 Hz, 4H), 2.04 (m, 4H), 2.03, (s, 6H), 1.64 (quin, *J* = 7.4 Hz, 4H), 1.26-1.43 (m, 20H). ^{13}C NMR (75 MHz, $CDCl_3$) δ 178.7, 170.1, 133.7, 127.6, 50.8, 44.5, 33.9, 32.0, 28.7, 28.7, 28.6, 28.5, 28.3, 24.6, 23.3. HRMS (FAB): calcd for $C_{30}H_{52}O_6N_2S_2$ (M+H): 601.3340, found 601.3337.

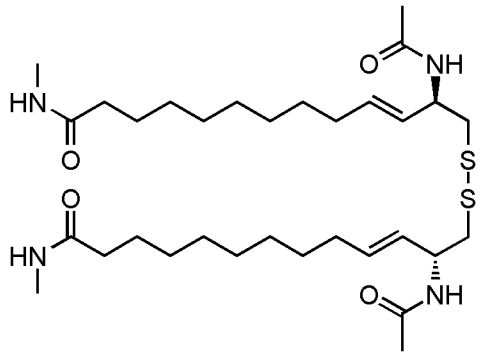

Somocystinoic acid di-*N,N*-methyl amide (17). To the suspension of somocystinoic acid (72 mg, 0.1198 mmol) in CH_2Cl_2 (8 mL) was added $MeNH_3Cl$ (24 mg, 0.36 mmol), Et_3N (84 μL, 0.60 mmol), and EDC·HCl (50 mg, 0.26 mmol), and DMAP (5 mg) successively

at 0°C under stirring. The reaction was immediately warmed to rt and was stirred at rt for 5 hrs. After 3 hrs into the reaction, white precipitates appeared. The solvents were removed under vacuum. The residues were taken up in CH_2Cl_2 / MeOH (2:1) and the mixture was washed with 0.5 M HCl solution and saturated $NaHCO_3$ solution and was dried over Na_2SO_4. Upon removal of the solvents, sufficiently pure material for the next step was obtained as a white solid (52 mg, 0.083 mmol, 69% yield over 2 steps). Mp 154-155 ºC. TLC Rf 0.36 MeOH / CH_2Cl_2 (1:9). $[\alpha]_D^{23}$ –17.8º (*c* 1.4, $CHCl_3$/MeOH 1:1). IR (film, KBr) ν_{max} 3306, 3276, 2918, 2849, 1642, 1540 cm^{-1}. ^1H NMR (300 MHz, $CD_3OD/CDCl_3$ 1:1, rotamers) δ 7.55 (d, *J* =8.3 Hz, 2H), 7.25 (bs, 2H), 5.31 (dt, *J* = 15.5, 6.7 Hz, 2H), 5.06 (dd, *J* = 15.5, 6.6 Hz, 2H), 4,24 (m, 2H), 2.53 (d, *J* = 7.1 Hz, 4H), 2.38 & 2.39 (s, 6H), 1.83 (t, *J* = 7.8 Hz, 4H), 1.68 (q, *J* = 6.5 Hz, 4H), 1.64 (s, 6H), 1.25 (quin, *J* = 7.4 Hz, 4H), 0.95-1.05 (m, 20H). ^{13}C NMR (75 MHz, $CD_3OD/CDCl_3$ 1:1, rotamers) δ 175.2, 175.1, 170.7, 170.6, 132.7, 127.2, 50.1, 43.3, 35.6, 35.5, 31.6, 28.6, 28.5, 28.5, 28.4, 28.3, 25.2, 25.1, 21.7,. 21.6. HRMS (EI): calcd for $C_{32}H_{59}O_4N_4S_2$ (M+H): 627.3972, found 627.3973.

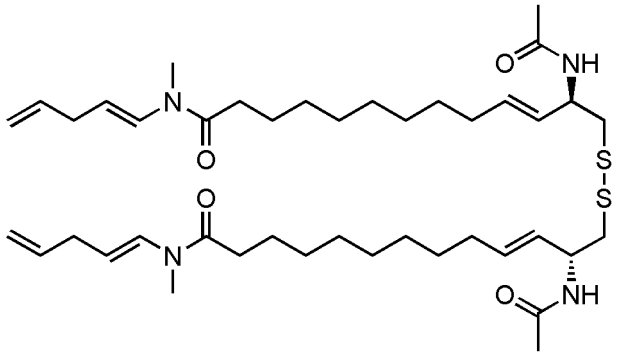

Somocystinamide A (1). The suspension of the methyl amide (42 mg, 0.0670 mmol) in 1,2-dichloroethane (20 mL) was degassed three times by vacuum-sonication-Ar introduction cycle. Then 4-pentenal (100 μL, 1.01 mmol, synthesized according to literature)[51] and $TsOH{\cdot}H_2O$ (3 mg, 0.015 mmol) were added successively at rt. The reaction mixture was refluxed for 14 hours under stirring in a Soxhlet apparatus that is equipped with glass wool and molecular sieves 4Å so as to remove residual H_2O. Then another batch of 4-pentenal (100 μL, 1.01 mmo) and $TsOH{\cdot}H_2O$ (3 mg, 0.015 mmol) were added. After 1.5 hours, 4-pentenal (100 μL, 1.01 mmol) was added again. Upon further refluxing and stirring for 1.5 hours, the reaction mixture was cooled to 0°C, and Et_3N (100 μL) was added. Most of the solvent was removed *in vacuo*, but *ca.* 1 mL of solvent was retained, which was directly subjected to flash column chromatography (EtAcO to 1:1:8 MeOH / CH_2Cl_2 / EtAcO) to obtain somocystinamide A (21 mg, 0.0277 mmol, 41% yield) as an off-white amorphous solid. Mp 93-95 ºC. TLC Rf 0.56 MeOH / CH_2Cl_2 / EtAcO (1:1:8). $[\alpha]_D^{22}$ +19.1º (*c* 0.59, $CHCl_3$). IR (film, KBr) ν_{max} 3286(br), 2926, 2854, 1645, 1541, 1395, 1289, 1087, 968 cm^{-1}. ^1H NMR (300 MHz, $CDCl_3$, rotamers) δ 7.35 (d, *J* = 14.4 Hz 0.6H), 6.67 (dt, J = 13.7, 1.3 Hz, 1.4H), 6.28 (d, *J* = 7.8 Hz, 2H), 5.84 (m, 2H), 5.65 (dtd, *J* = 15.5, 6.7, 1.1 Hz, 2H), 5.43 (dd, *J* = 15.5, 6.2 Hz, 2H), 4.91-5.11 (m, 4H), 4.67 (quin, *J* = 6.5 Hz, 2H), 3.07 and 3.08 (s, 6H), 3.06 (m, 2H), 2.82 (m, 6H), 2.42 (m, 4H), 2.03 (m, 4H), 2.01 (s, 6H), 1.64 (quin, *J* = 7.5 Hz, 4H), 1.25-1.38 (m, 20H). ^{13}C NMR (75 MHz, $CDCl_3$, rotamers) δ 171.7, 169.1, 137.4, 137.0, 133.7, 129.2, 128.1, 127.6, 115.4, 115.0, 109.0, 108.4, 50.8, 44.7, 34.5, 34.5, 34.4, 33.8, 32.3, 32.2, 29.7, 29.7, 29.3, 29.2, 29.0, 28.9, 25.0, 23.4. UV (MeOH) λ_{max} 234 nm (ε 3.2×10^5). HRMS (EI): calcd for $C_{42}H_{70}O_4N_4S_2$ (M^+): 758.4833, found 758.4823.

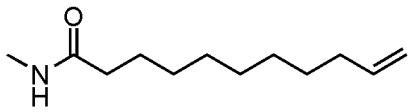

***N*-methylundec-10-enamide (70)**. To a solution of 10-undecenoic acid (25.136 g, 136.40 mmol) in CH_2Cl_2 (350 mL) was added $MeNH_2$·HCl (18.45 g, 273.3 mmol) at rt. This mixture was cooled to –15ºC and Et_3N (57.0 mL, 408 mmol) was added. Then EDC·HCl (27.29 g, 142.4 mmol) and DMAP (238 mg, 1.95 mmol) were added successively under vigorous stirring. The mixture was very cloud at this point. The mixture was gradually warmed to rt, and was stirred over night. The mixture appeared milky. Upon removal of the volatiles *in vacuo*, the solid residues were triturated with EtOAc (500 mL). This mixture was filtered, and the solids were rinsed with EtOAc. Then the EtOAc solution was poured into 1M HCl (250 mL), and the phases were separated. The organic layer was washed with H_2O (150 mL), saturated $NaHCO_3$ (150 mL), H_2O (100 mL), and brine (100 mL) successively. After the solution was dried over Na_2SO_4 and the solvent was removed, a white solid (**70**) resulted, which was sufficiently pure for the subsequent step. ^{1}H NMR (300 MHz, $CDCl_3$) δ 5.80 (ddt, *J* = 16.9, 10.2, 6.7 Hz, 1H), 5.50 (s, 1H), 5.05 – 4.86 (m, 2H), 2.80 (d, *J* = 4.9 Hz, 3H), 2.15 (t, *J* = 7.6 Hz, 2H), 2.02 (dd, *J* = 14.1, 6.9 Hz, 2H), 1.70 – 1.53 (m, 3H), 1.45 – 1.18 (m, 15H). ^{13}C NMR (75 MHz, $CDCl_3$) δ 173.80, 139.15, 114.10, 58.15, 36.71, 33.75, 29.28, 29.03, 28.86, 26.24, 25.75.

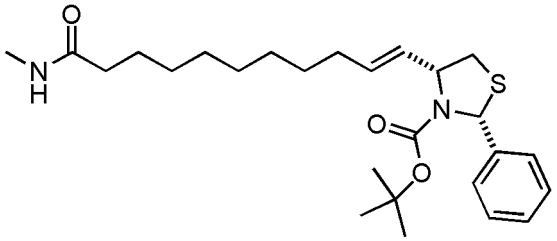

(2R,4R)-tert-butyl 4-((E)-11-(methylamino)-11-oxoundec-1-enyl)-2-phenyl thiazolidine -3-carboxylate (71). To the thiazolidine (**51**) (2.063 g, 7.079 mmol) and the methylamide (**70**) (2.270 g, 11.50 mmol) was added $CHCl_3$ (45 mL) that was passed through basic alumina (activity I). Then the reaction mixture was degassed in vacuum with ultrasonic assistance three times. Grubbs-Hoveyda II catalyst (95 mg, 0.152 mmol) was added. After stirring at rt for 30 min, the reaction mixture was refluxed (bath temperature = 80ºC). Over the course of 18 hrs, additional amounts of **70** (1.932 g, 9.791 mmol) and Grubbs-Hoveyda II catalyst (354 mg, 0.564 mmol, 5.8 mol%) were added in four portions. Then the mixture was cooled to rt, concentrated under vacuum, and subjected to silica gel flash column chromatography (1:9 EtOAc / Hex to 2:9:9 acetone / EtOAc / Hex). Some of the colored impurities were not completely removed. A dark-brown thick oil (2.752 g, 5.974 mmol, 84%) was obtained. TLC Rf = 0.47 (2:9:9 MeOH/ EtOAc/hexanes). $[\alpha]^{22}_D$ +58.6º (*c* 3.6, $CHCl_3$). IR (film, KBr) ν_{max} 3298(br), 2927, 2854, 1696, 1650, 1554, 1368, 1163, 1109, 697 cm^{-1}. ^1H NMR (400 MHz, $CDCl_3$) δ 7.37 – 7.19 (m, 5H), 6.05 (s, 1H), 5.83 – 5.70 (m, 1H), 5.61 (dd, *J* = 15.3, 7.4 Hz, 1H), 4.79 (s, 1H), 3.22 (dd, *J* = 11.7, 6.5 Hz, 1H), 2.81 – 2.75 (m, 1H), 2.75 (d, *J* = 4.9 Hz, 3H), 2.17 – 2.08 (m, 1H), 2.08 – 1.99 (m, 2H), 1.64 – 1.53 (m, 2H), 1.41 – 1.20 (m, 21H). ^{13}C NMR (100 MHz, $CDCl_3$) δ 173.8, 153.5, 141.7, 134.0, 129.3, 128.1, 127.4, 126.2, 80.4, 66.0, 63.8, 36.6, 36.5, 32.1, 29.2, 29.2, 29.1, 29.0, 28.9, 28.1, 26.1, 25.7. HRMS (ESI): calcd for $C_{26}H_{40}N_2O_3SNa$ $[M+Na^+]$: 483.2652, found 483.2654.

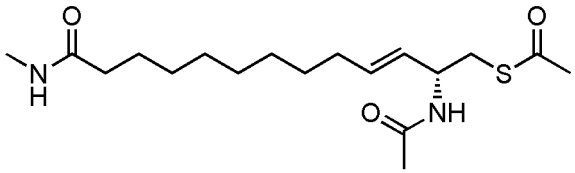

(*R*,*E*)-*S*-2-acetamido-13-(methylamino)-13-oxotridec-3-enyl ethanethioate (73). Liquid NH_3 (150 mL) was distilled from Na onto a solution of **71** (3.098 g, 6.725 mmol) in THF (10 mL). Then Na pieces (~ 5 mm cubes) were added to keep the color of the solution dark blue for 2 hrs under reflux (at rt) and vigorous stirring. Solid NH_4Cl was added carefully until the blue color disappeared. NH_3 was evaporated under a stream of N_2. Then 1M $NaHSO_4$ (300 mL) was added, which was extracted with EtOAc (200 mL x 3). The organic layer was washed with brine and dried over Na_2SO_4. Upon removal of the solvent in vacuo, amorphous pale brown solid (2.531 g) resulted, which was used in the next step without purification. This solid (2.531 g) was dissolved in CH_2Cl_2 (75 mL) and freshly distilled TFA (18 mL) was added at 0ºC under stirring. After the solution was kept at 0ºC under stirring for 30 min, the volatiles were removed in vacuo. The residues were placed under high vacuum for 2 hours, which resulted in a thick orange oil. This oil was dissolved in CH_2Cl_2 (100 mL) and the solution was cooled to 0ºC. Et_3N (15.8 mL, 113.2 mmol) and acetic anhydride (5.3 mL, 56.6 mmol) were added successively at 0ºC under stirring. The solution was gradually allowed to warm to rt. After 16 hrs of stirring at rt, the volatiles were removed in vacuo. The residues were treated with 1M $NaHSO_4$ (250 mL), which was extracted with EtOAc (200 mL x 3). The combined organic layer was washed with brine (150 mL) and dried over Na_2SO_4. Most of the solvent was removed under vacuum, and the crude solution was let stand in a -20ºC freezer over night. Pale brown solids were precipitated and filtered, which was rinsed with hexanes. Upon drying

under high vacuum, **73** was obtained as a pale brown solid (1.112 g). The filtrate contained some of the product, and it was purified by flash column chromatography (1:1 EtOAc/hexanes to 2:9:9 MeOH/EtOAc/hexanes). A total of 1.406 g of **73** was obtained (59% yield). Mp 95-97ºC. TLC Rf = 0.22 (2:9:9 MeOH/EtOAc/hexanes). $[\alpha]^{22}_{D}$ –8.0º (*c* 0.90, $CHCl_3$). IR (film, KBr) ν_{max} 3314, 3286, 3089(br), 2925, 2853, 1693, 1646, 1553, 1412, 1373, 1133, 968 cm^{-1}. ^1H NMR (300 MHz, $CDCl_3$) δ 6.03 (d, *J* = 8.3 Hz, 1H), 5.90 (s, 1H), 5.59 (ddd, *J* = 7.9, 7.3, 4.0 Hz, 1H), 5.43 – 5.21 (m, 1H), 4.52 (p, *J* = 6.3 Hz, 1H), 3.04 (d, *J* = 6.6 Hz, 2H), 2.76 (d, *J* = 4.8 Hz, 3H), 2.32 (s, 3H), 2.13 (t, *J* = 7.6 Hz, 2H), 2.00 – 1.95 (m, 2H), 1.93 (s, 3H), 1.72 – 1.42 (m, 2H), 1.26 (m, 10H). ^{13}C NMR (75 MHz, $CDCl_3$) δ 196.2, 173.9, 169.5, 133.1, 127.8, 58.1, 51.0, 36.5, 33.5, 32.0, 30.5, 29.1, 29.0, 29.0, 28.7, 26.2, 25.6, 23.2. HRMS (ESI): calcd for $C_{18}H_{32}N_2O_3SNa$ $[M+Na^+]$: 379.2026, found 379.2029.

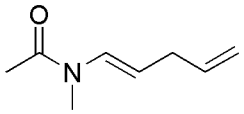

22

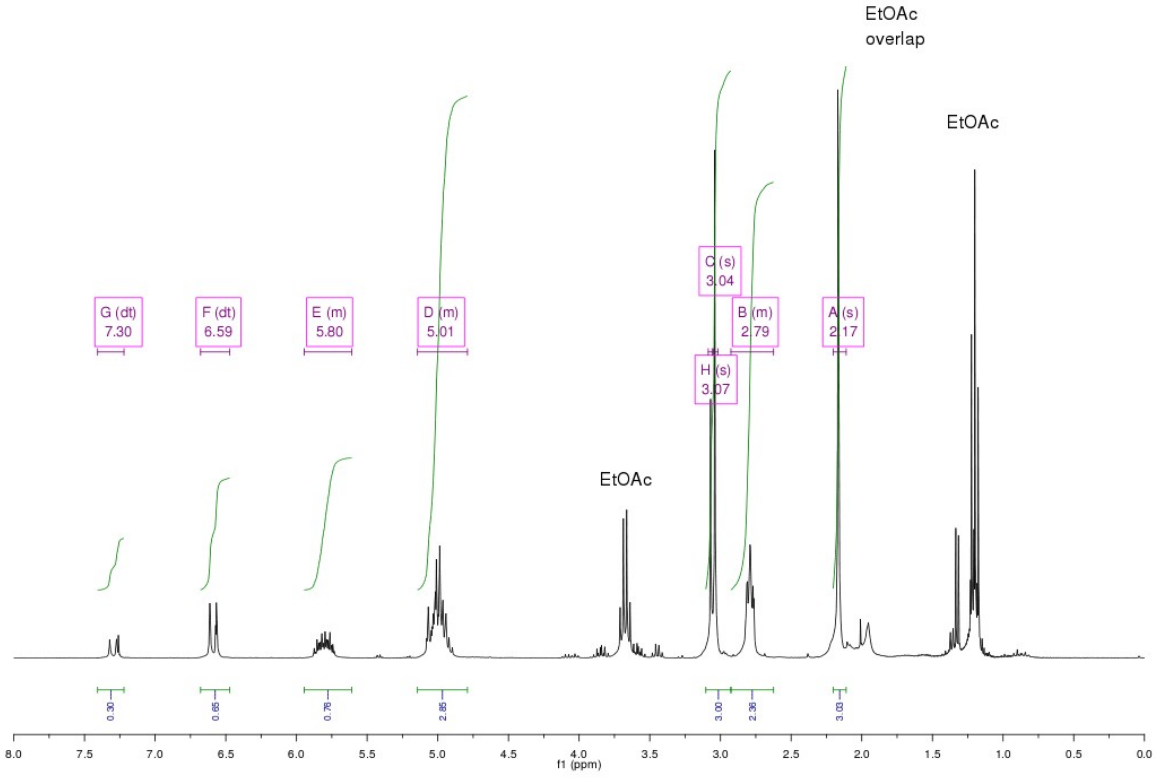

Figure VI.12: ^{1}H NMR spectrum of **22** in $CDCl_3$

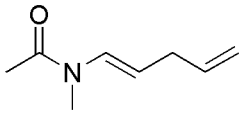

22

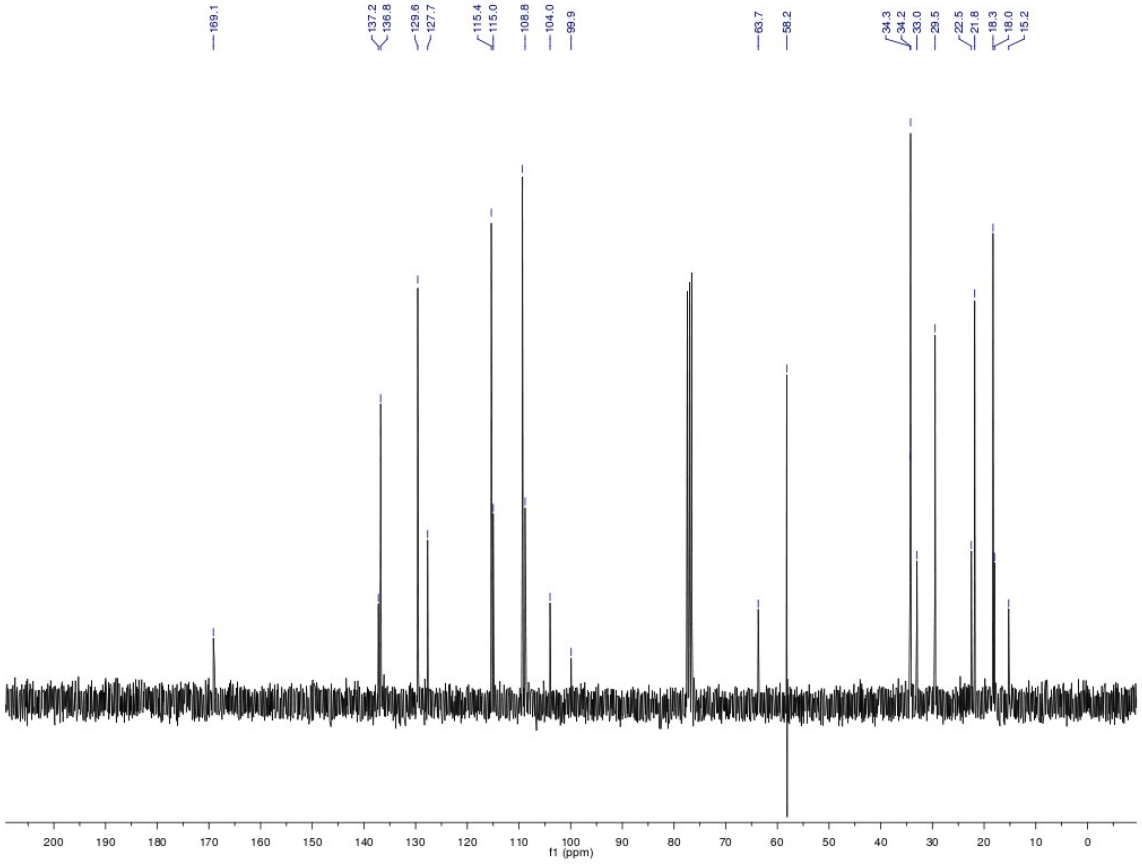

Figure VI.13: ^{13}C NMR spectrum of **22** in $CDCl_3$

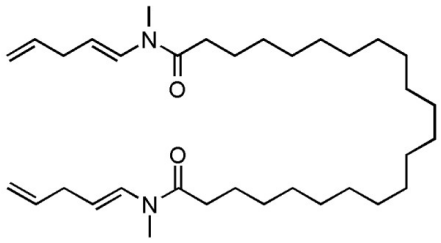

2

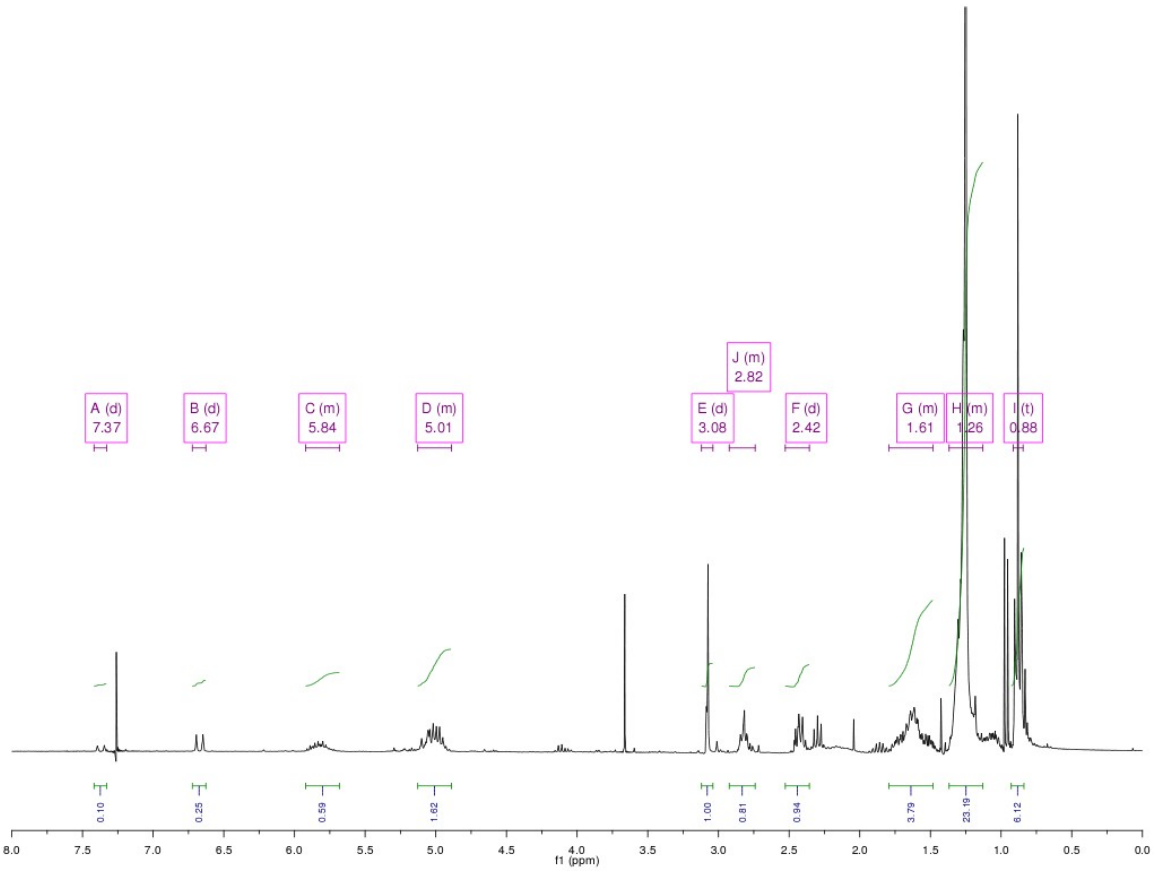

Figure VI.14: ^{1}H NMR spectrum of **2** in $CDCl_3$

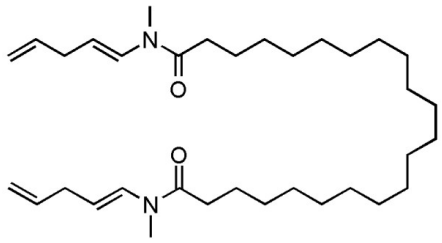

2

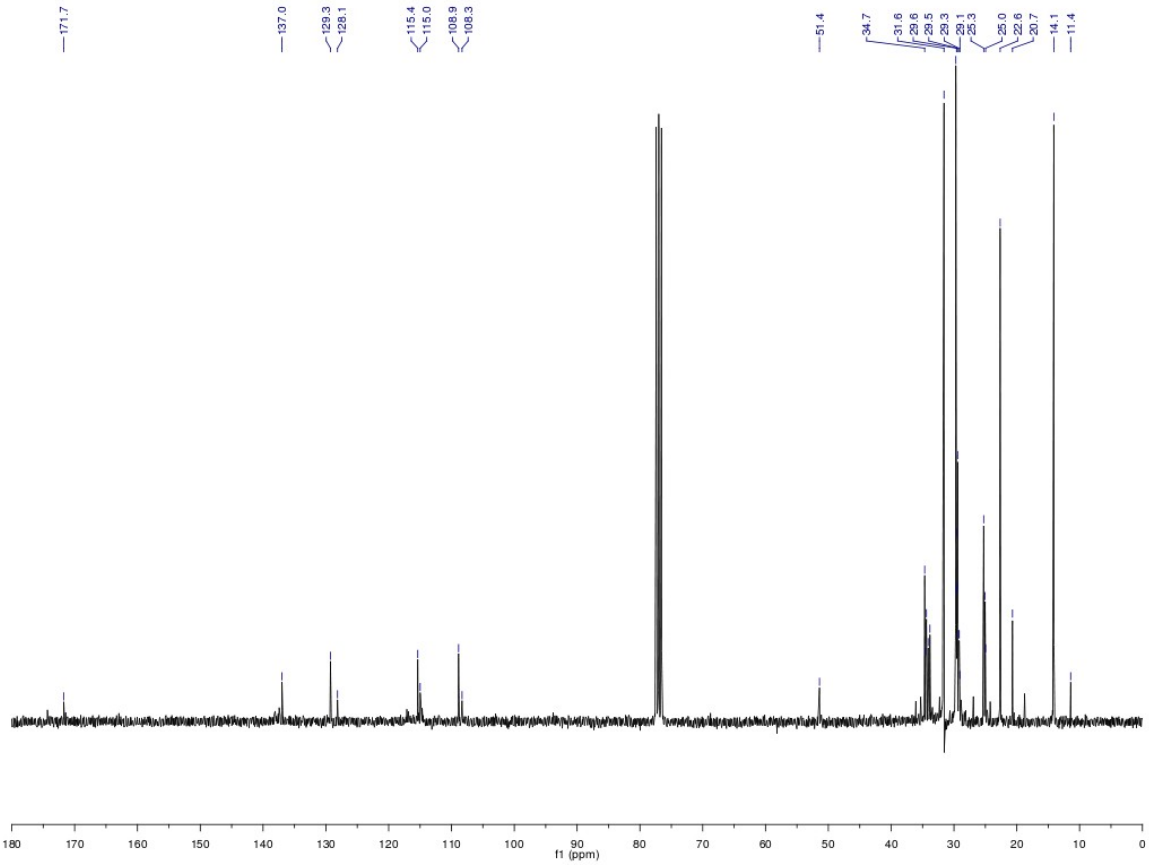

Figure VI.15: ^{13}C NMR spectrum of **2** in $CDCl_3$

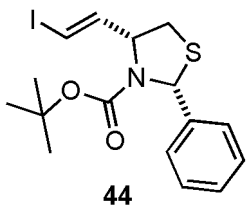

44

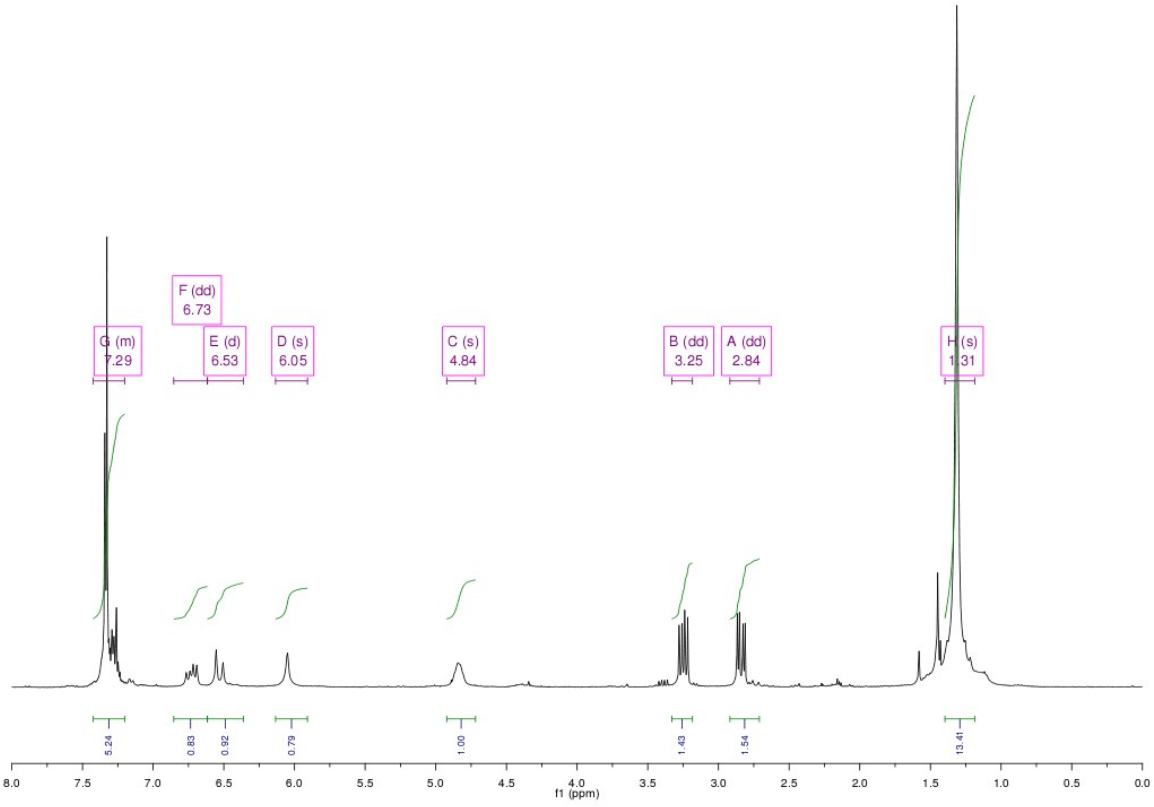

Figure VI.16: ^{1}H NMR spectrum of **44** in $CDCl_3$

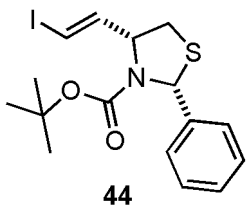

44

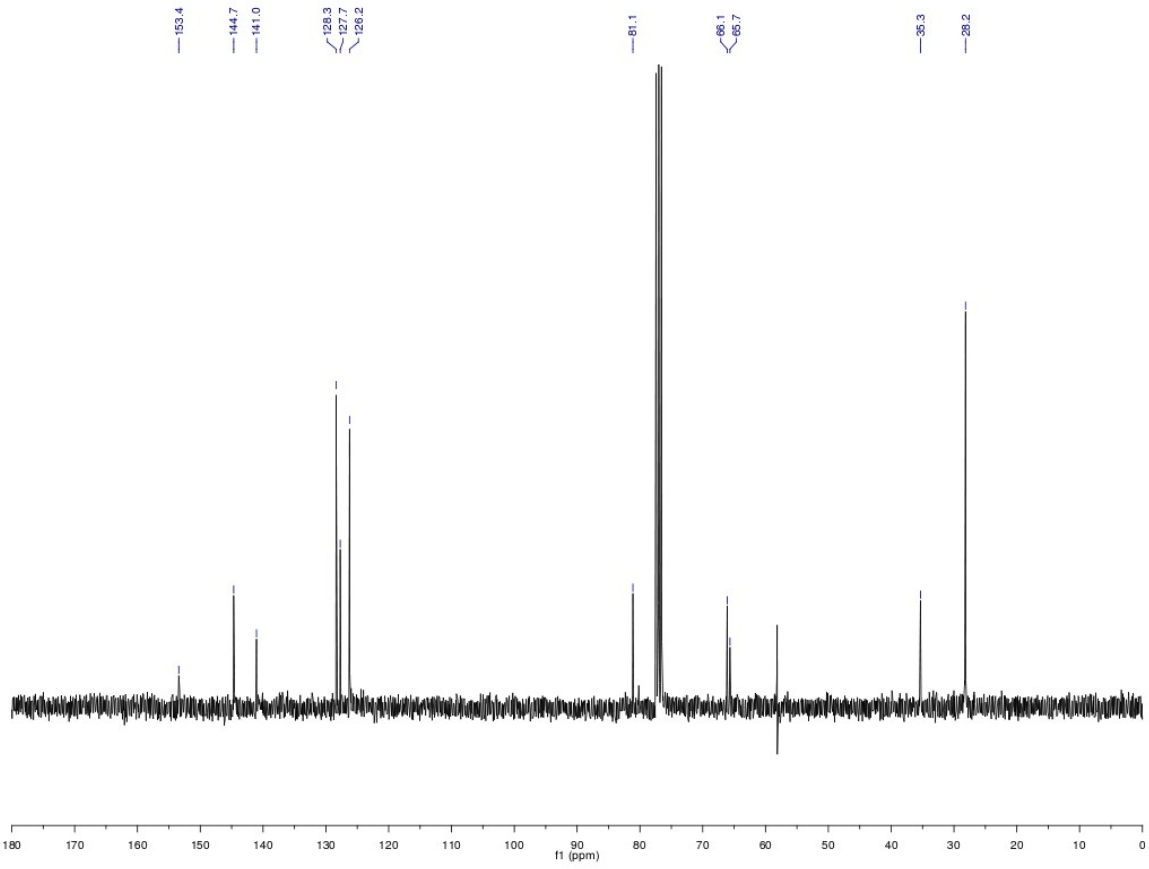

Figure VI.17: ^{13}C NMR spectrum of **44** in $CDCl_3$

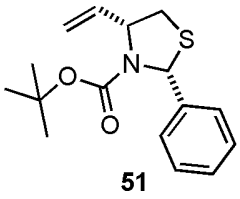

51

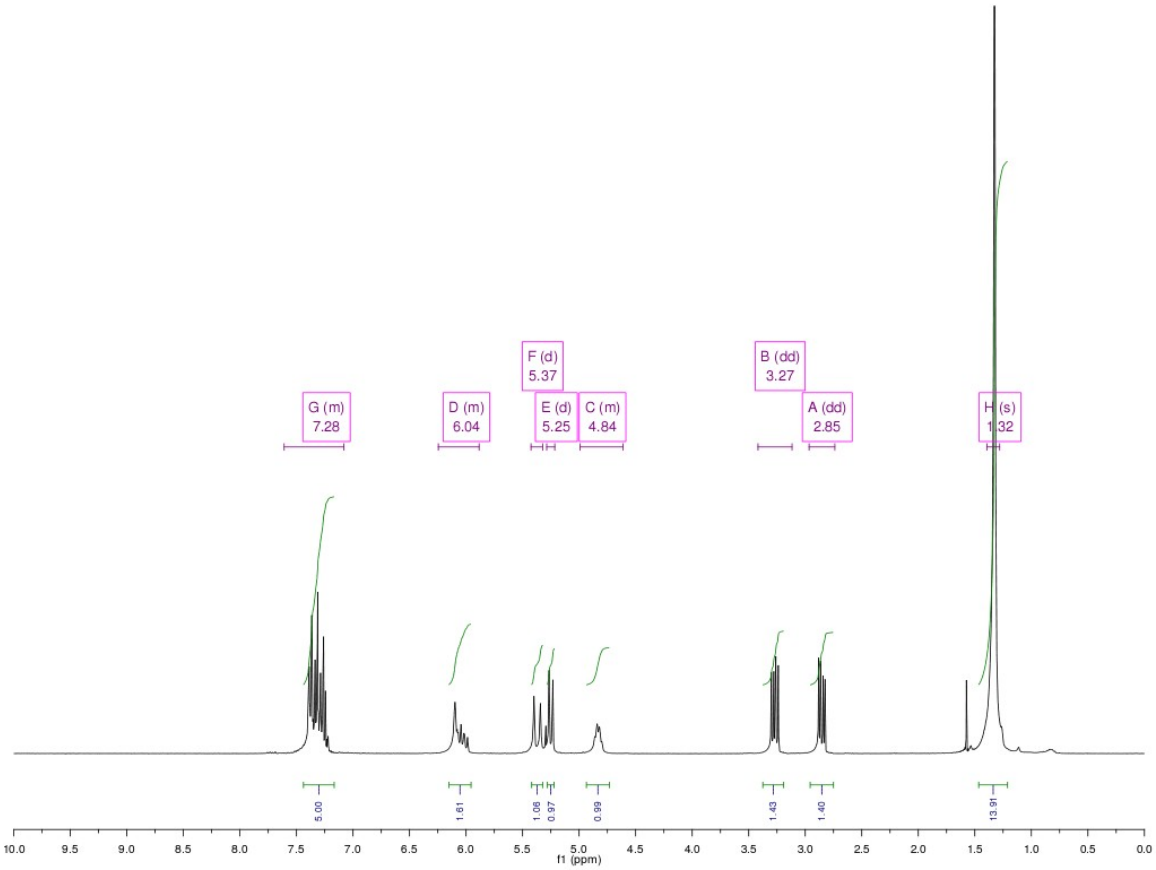

Figure VI.18: ^{1}H NMR spectrum of **51** in $CDCl_3$

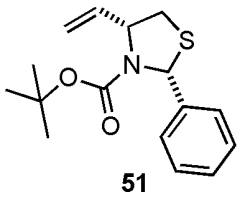

51

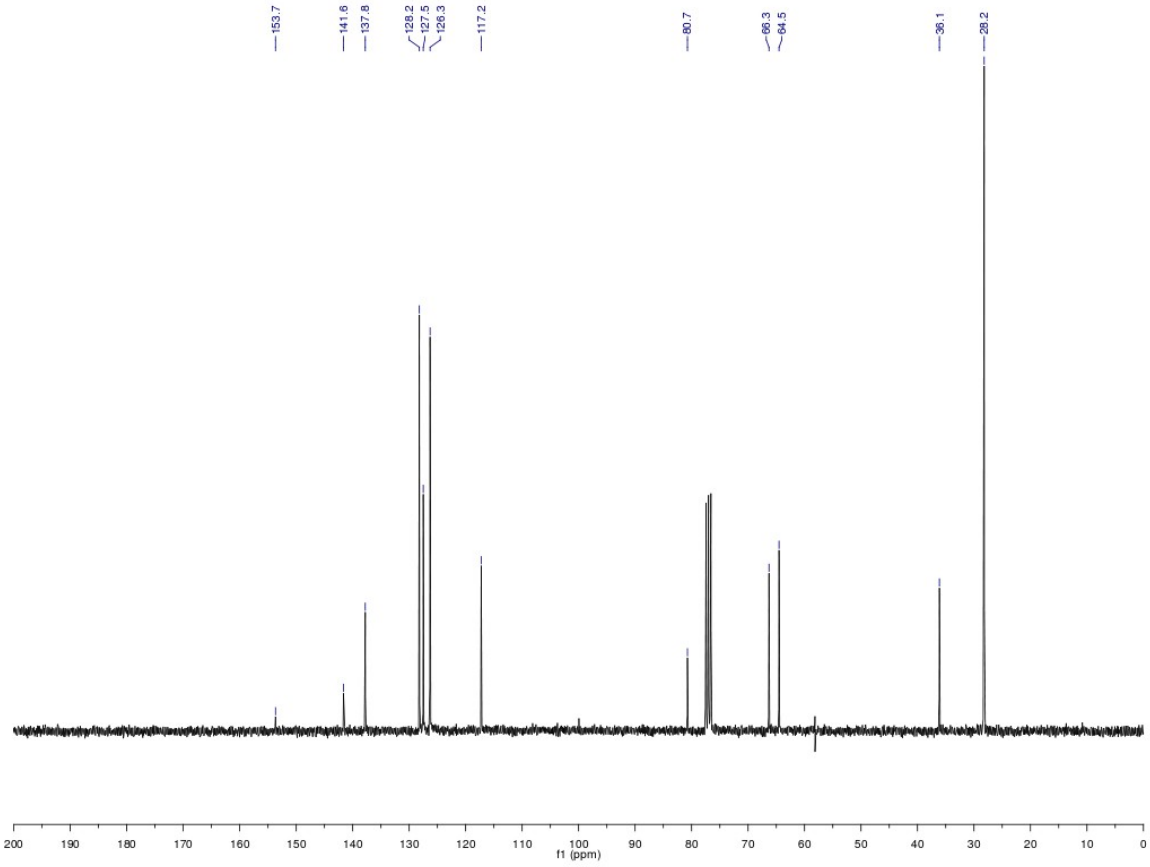

Figure VI.19: ^{13}C NMR spectrum of **51** in $CDCl_3$

Figure VI.20: ^{1}H NMR spectrum of **52** in $CDCl_3$

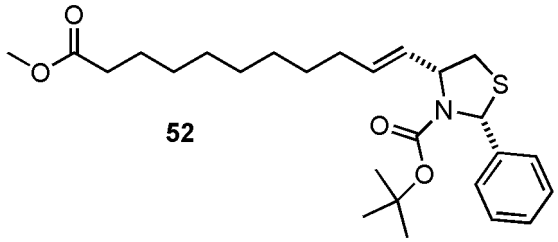

52

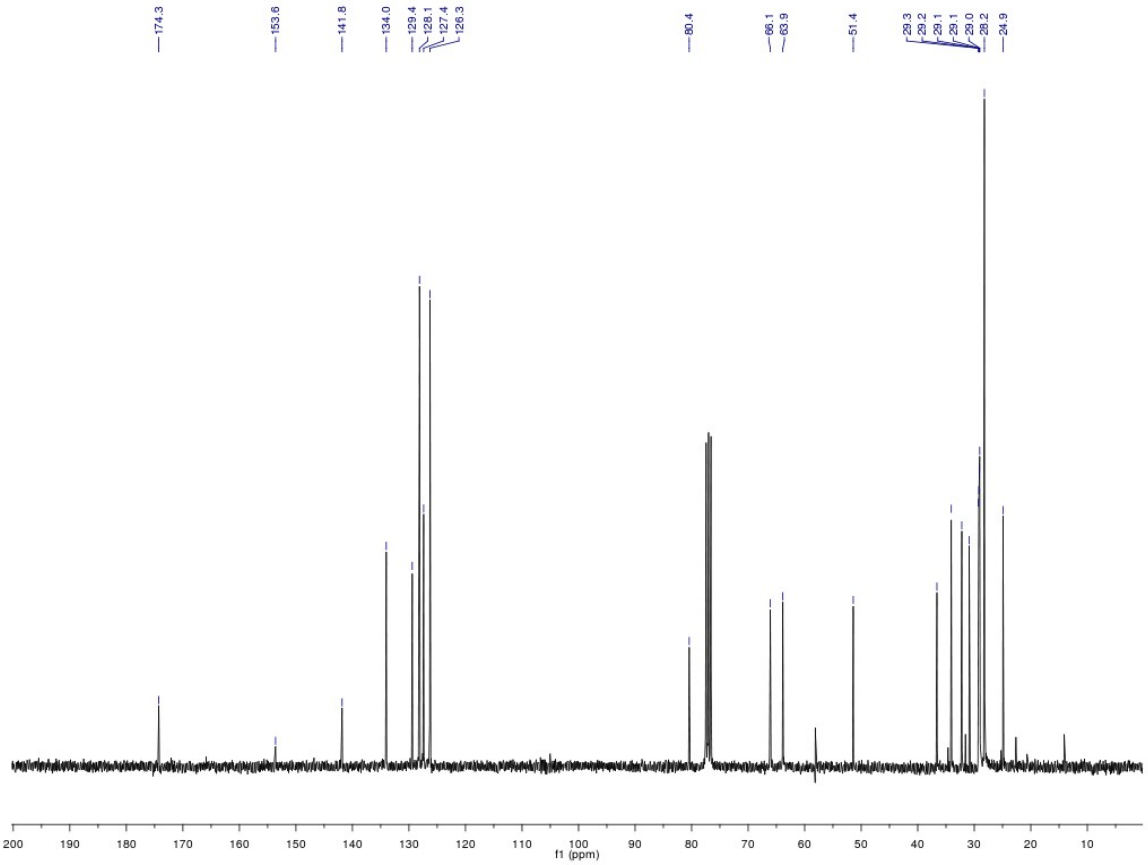

Figure VI.21: ^{13}C NMR spectrum of **52 in** $CDCl_3$

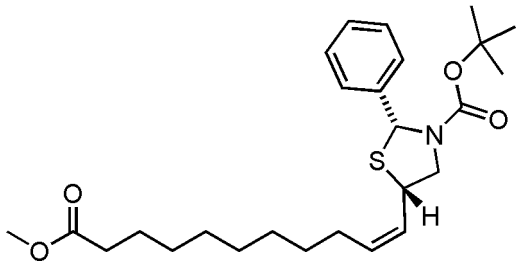

52-*cis*

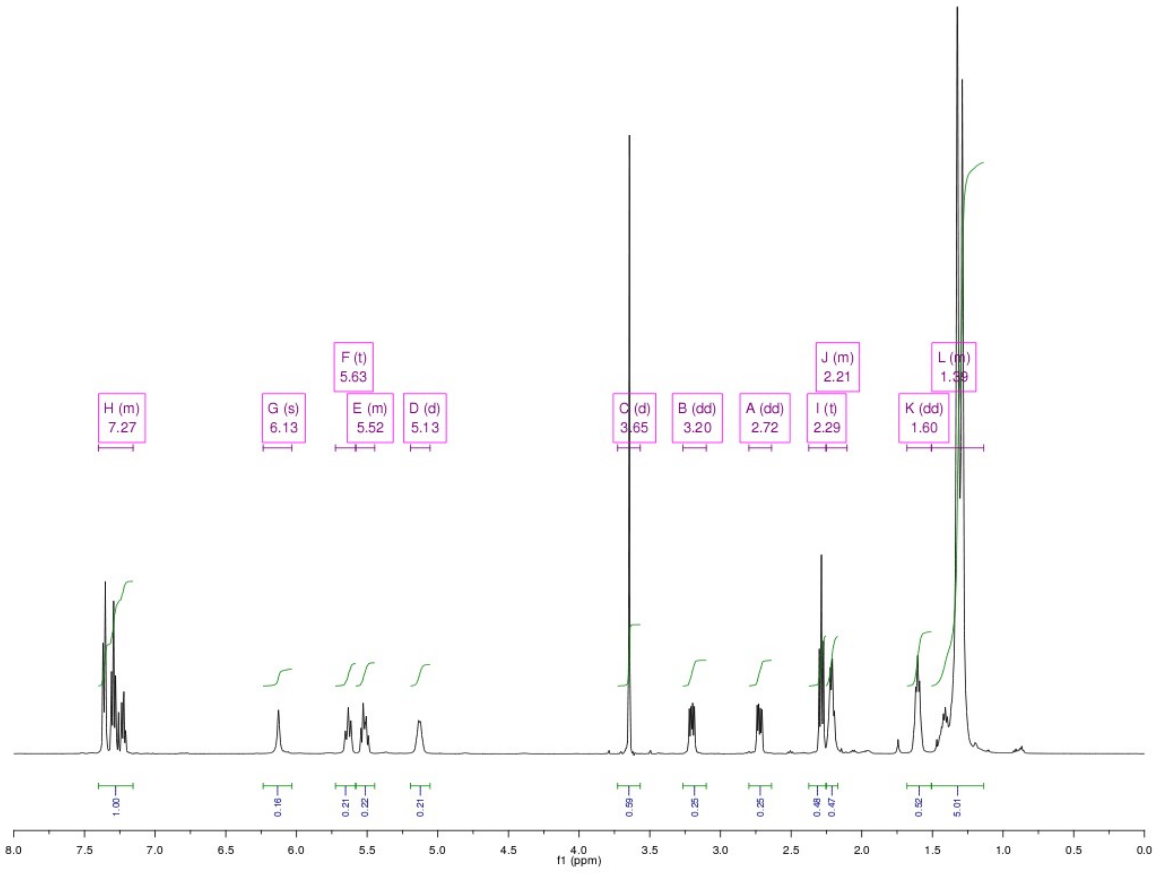

Figure VI.22: ^{1}H NMR spectrum of **52-cis** in $CDCl_3$

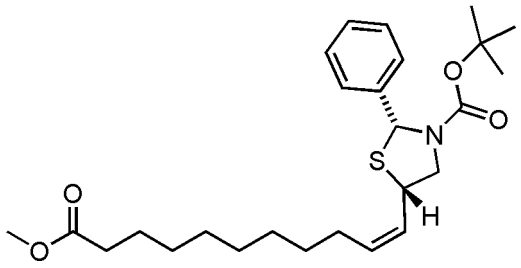

52-*cis*

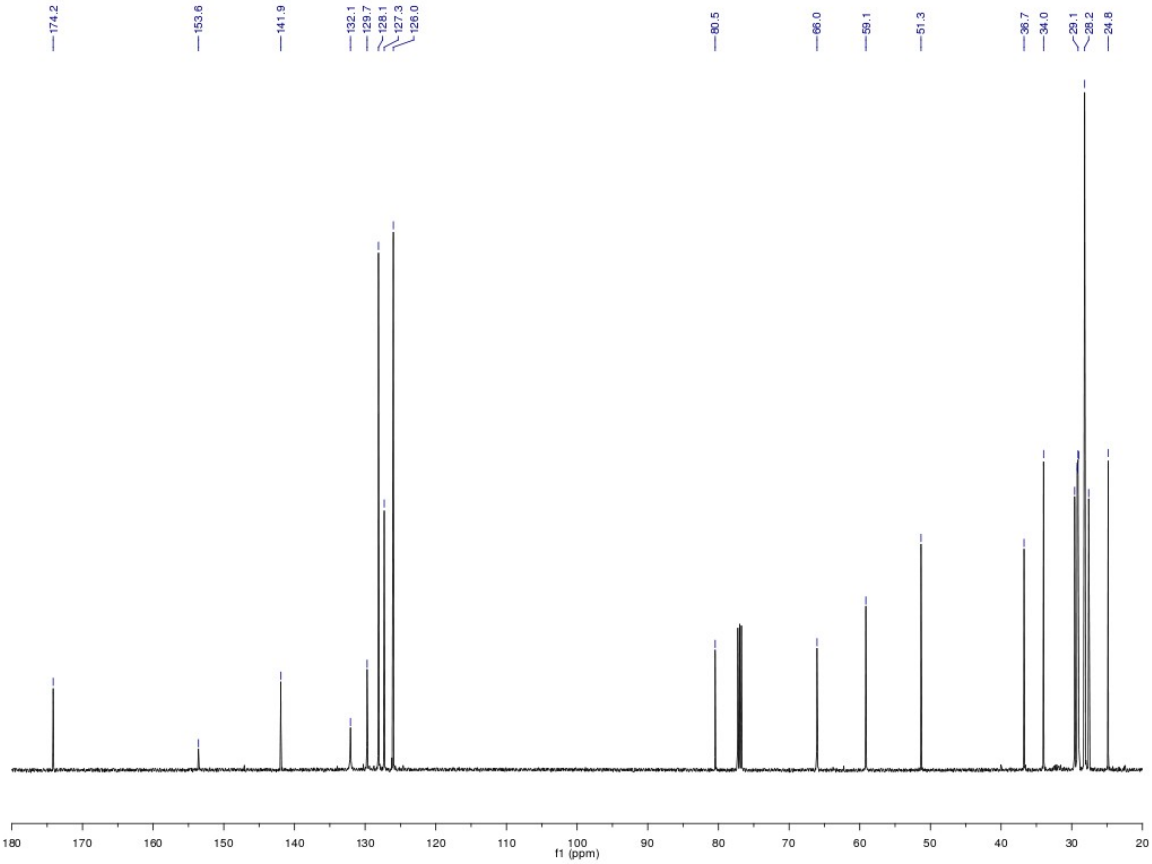

Figure VI.23: ^{13}C NMR spectrum of **52-cis** in $CDCl_3$

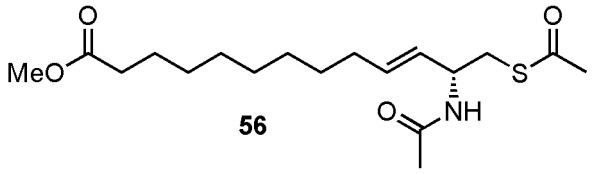

56

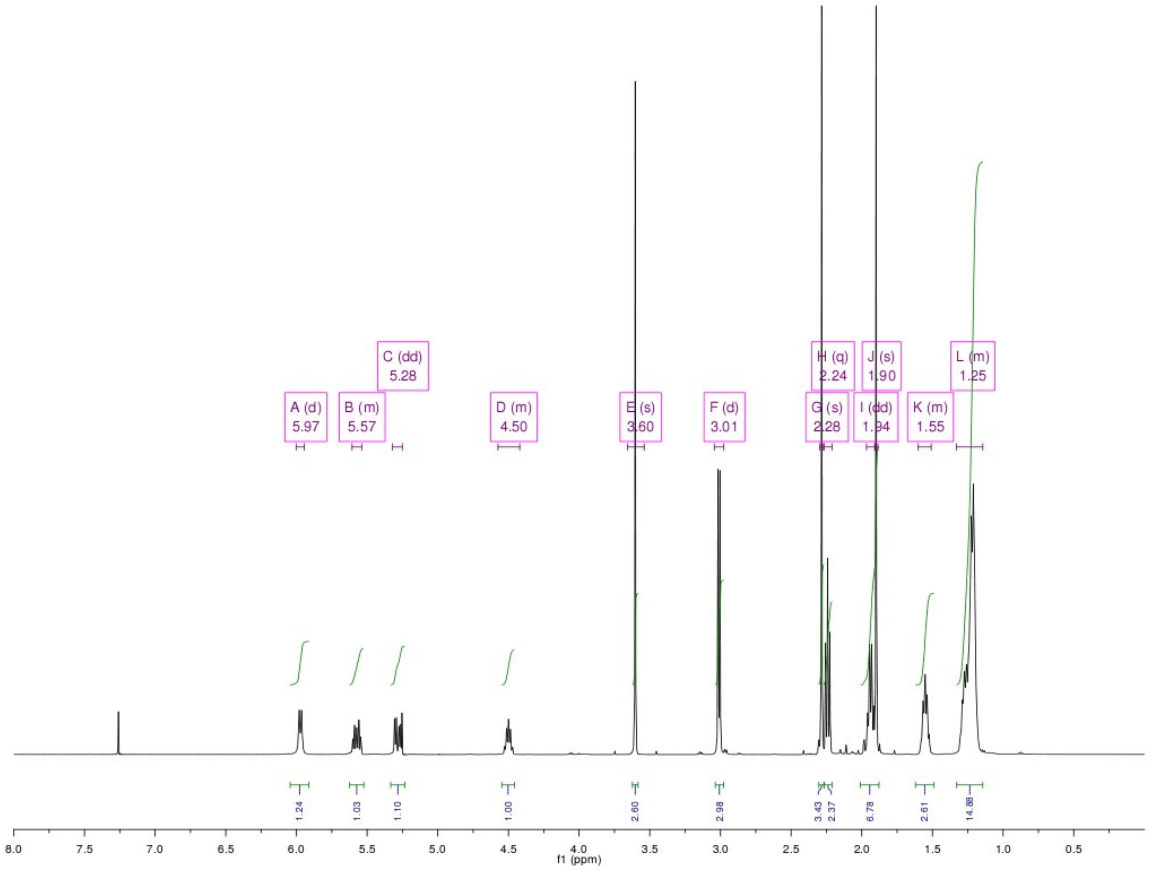

Figure VI.24: ^{1}H NMR spectrum of **56** in $CDCl_3$

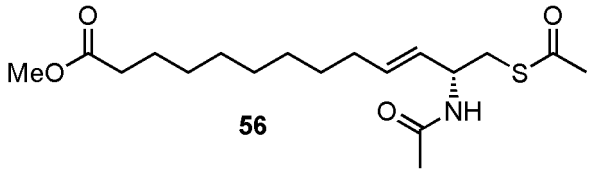

56

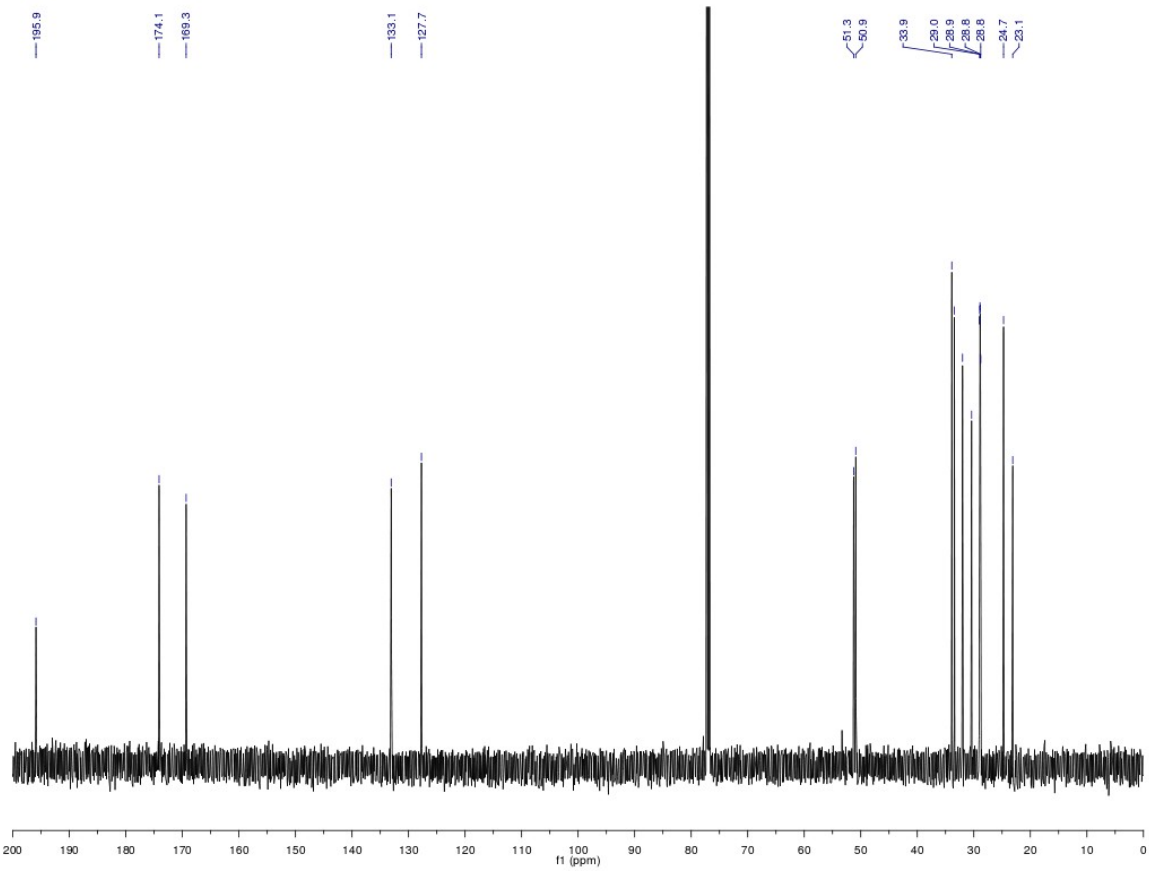

Figure VI.25: ^{13}C NMR spectrum of **56** in $CDCl_3$

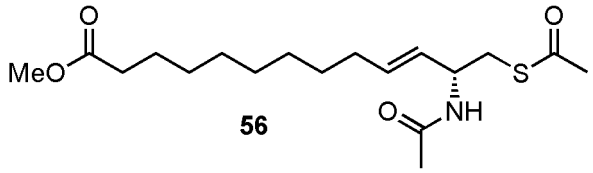

56

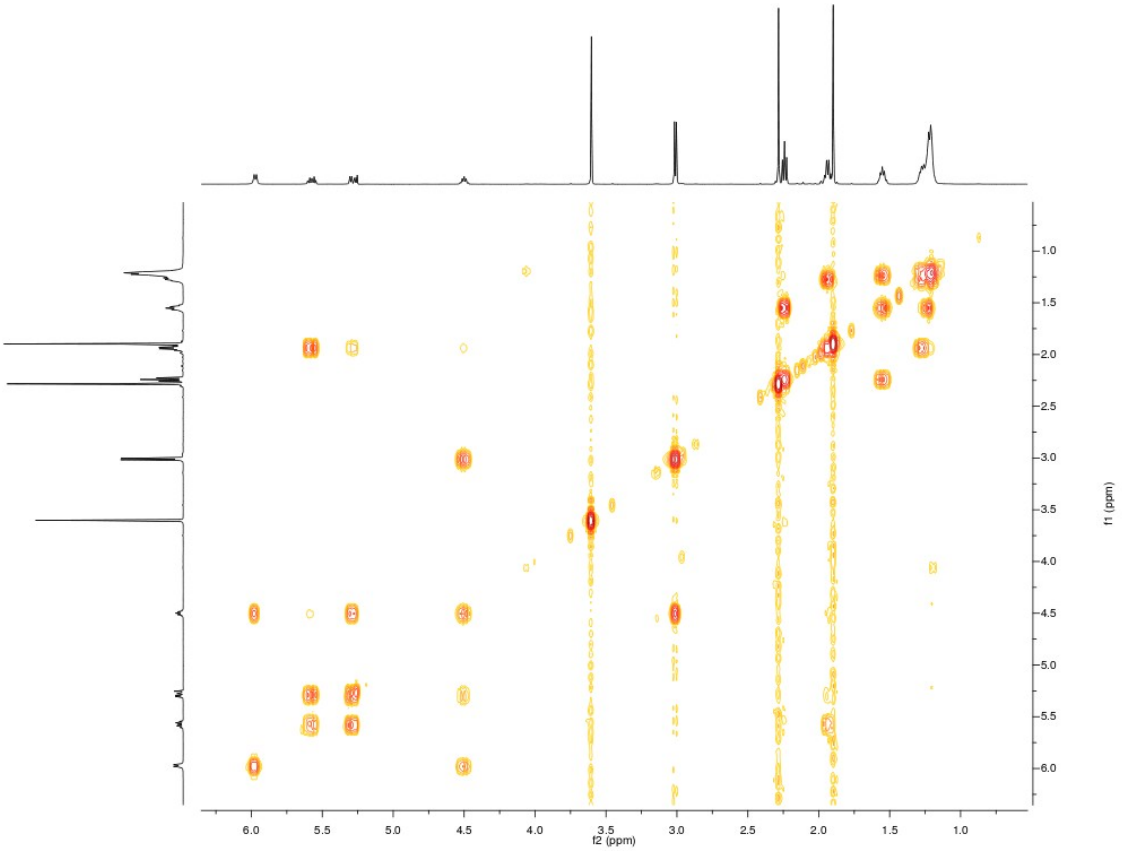

Figure VI.26: COSY spectrum of **56** in $CDCl_3$

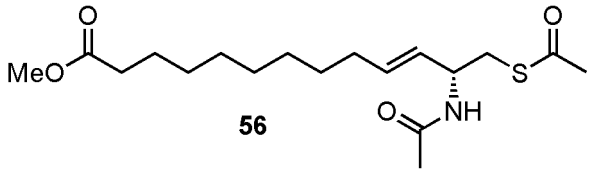

56

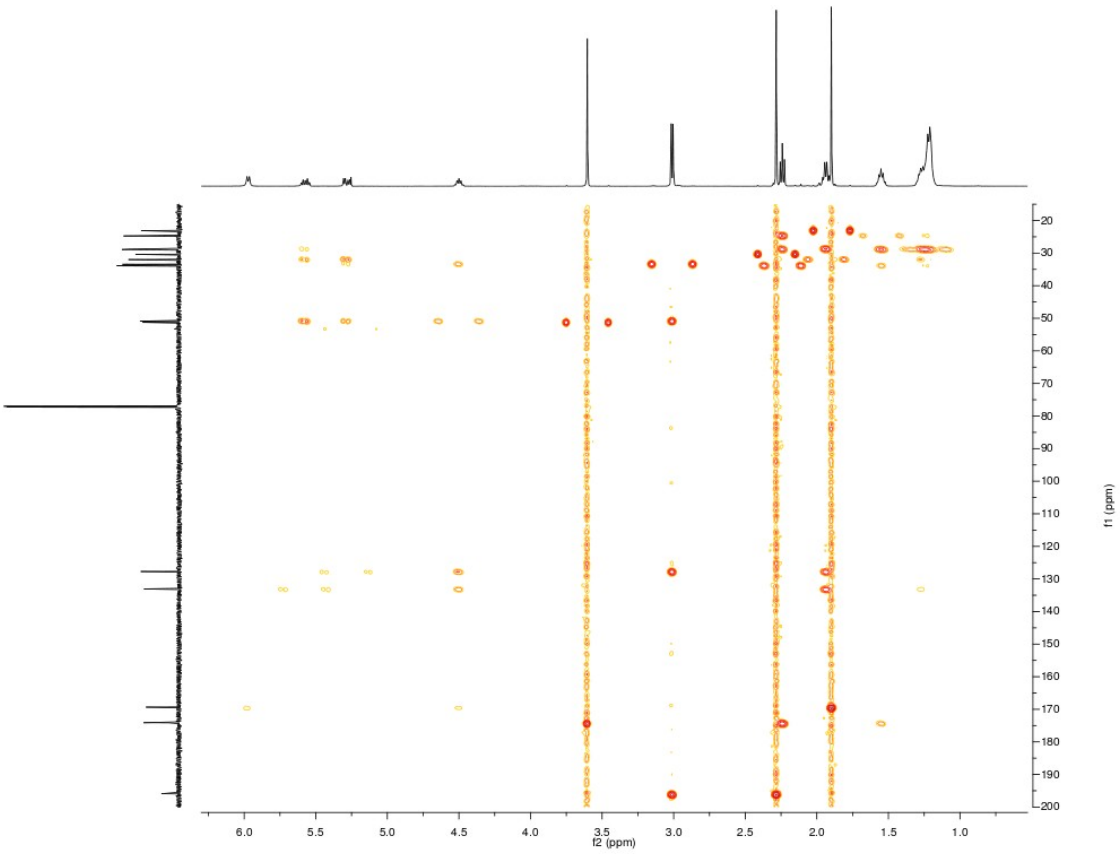

Figure VI.27: HMBC spectrum of **56** in $CDCl_3$

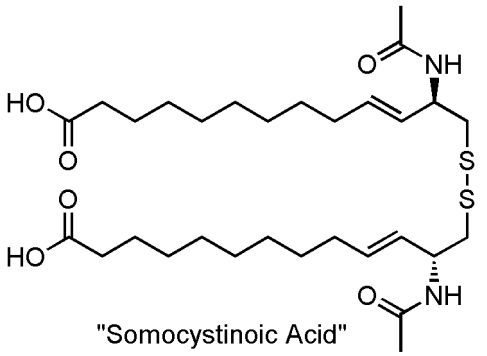

"Somocystinoic Acid"
57

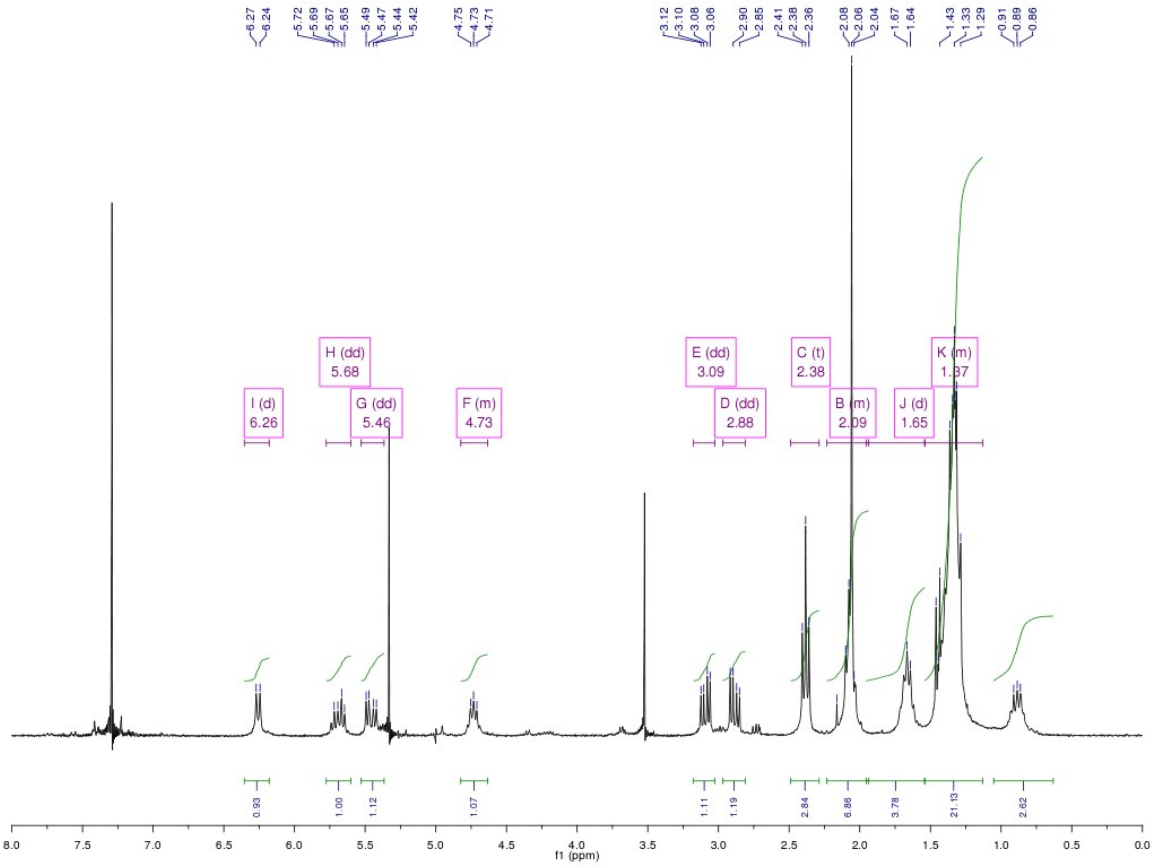

Figure VI.28: ^{1}H NMR spectrum of **57** in $CDCl_3$

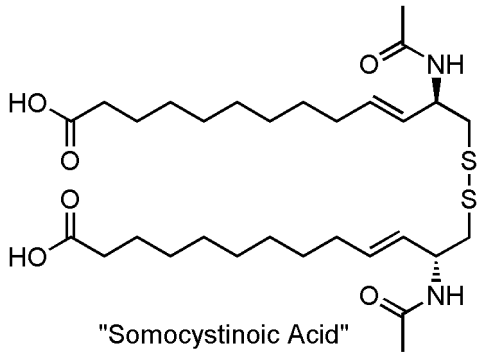

"Somocystinoic Acid"
57

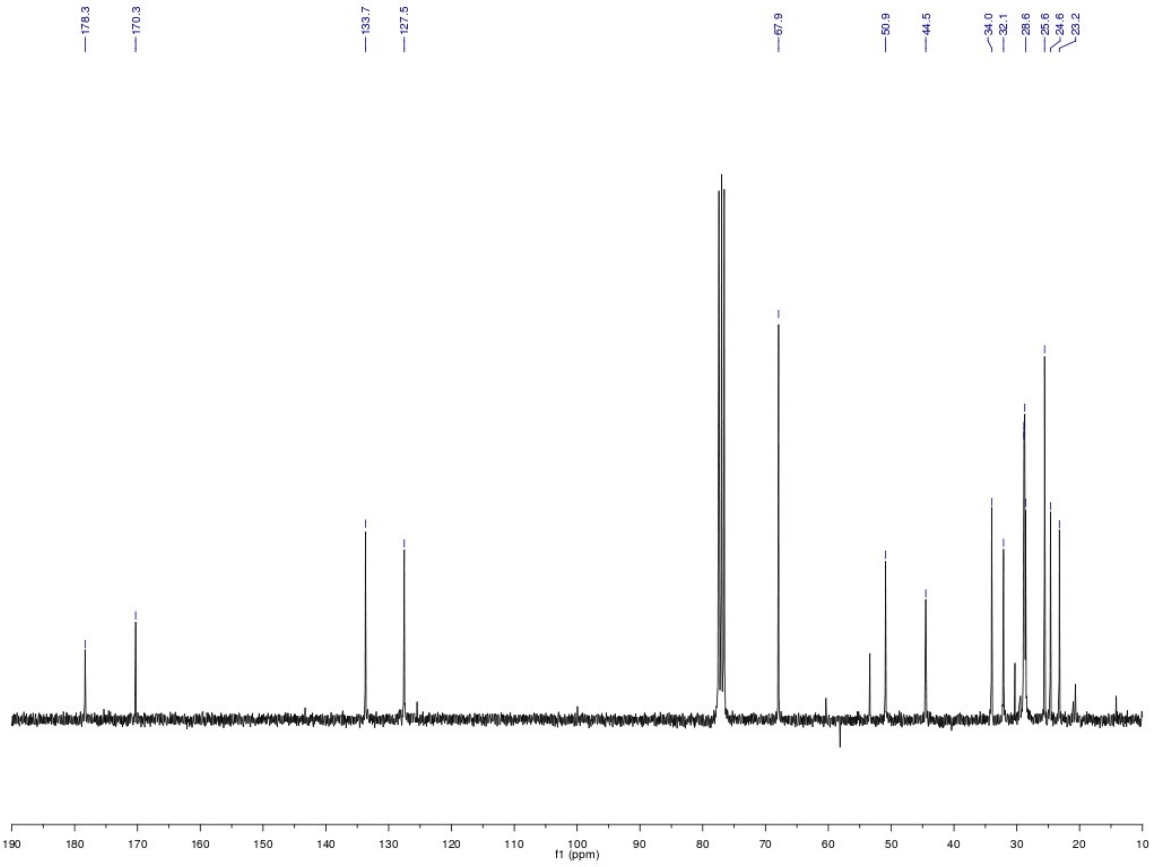

Figure VI.29: ^{13}C NMR spectrum of **57** in $CDCl_3$

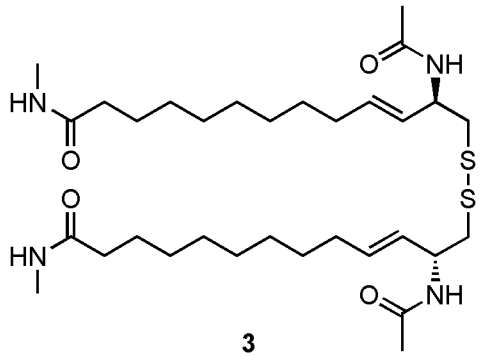

3

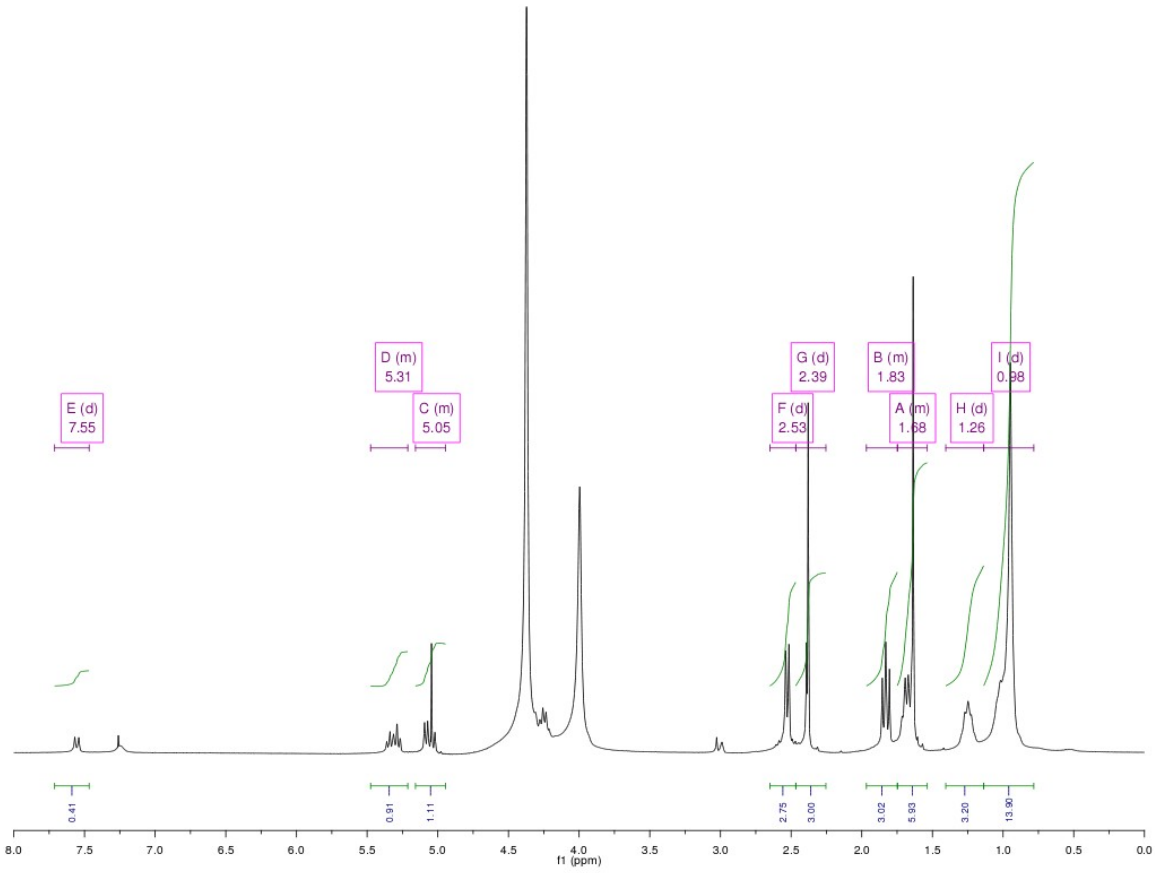

Figure VI.30: ^{1}H NMR spectrum of **3** in 1:1 $CDCl_3/CD_3OD$

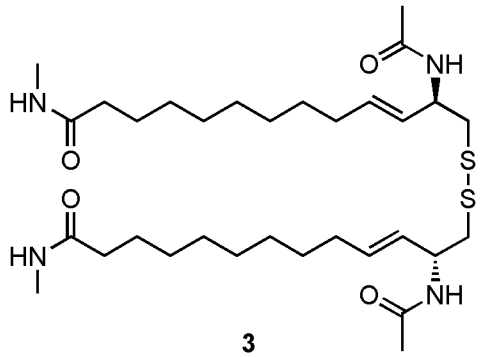

3

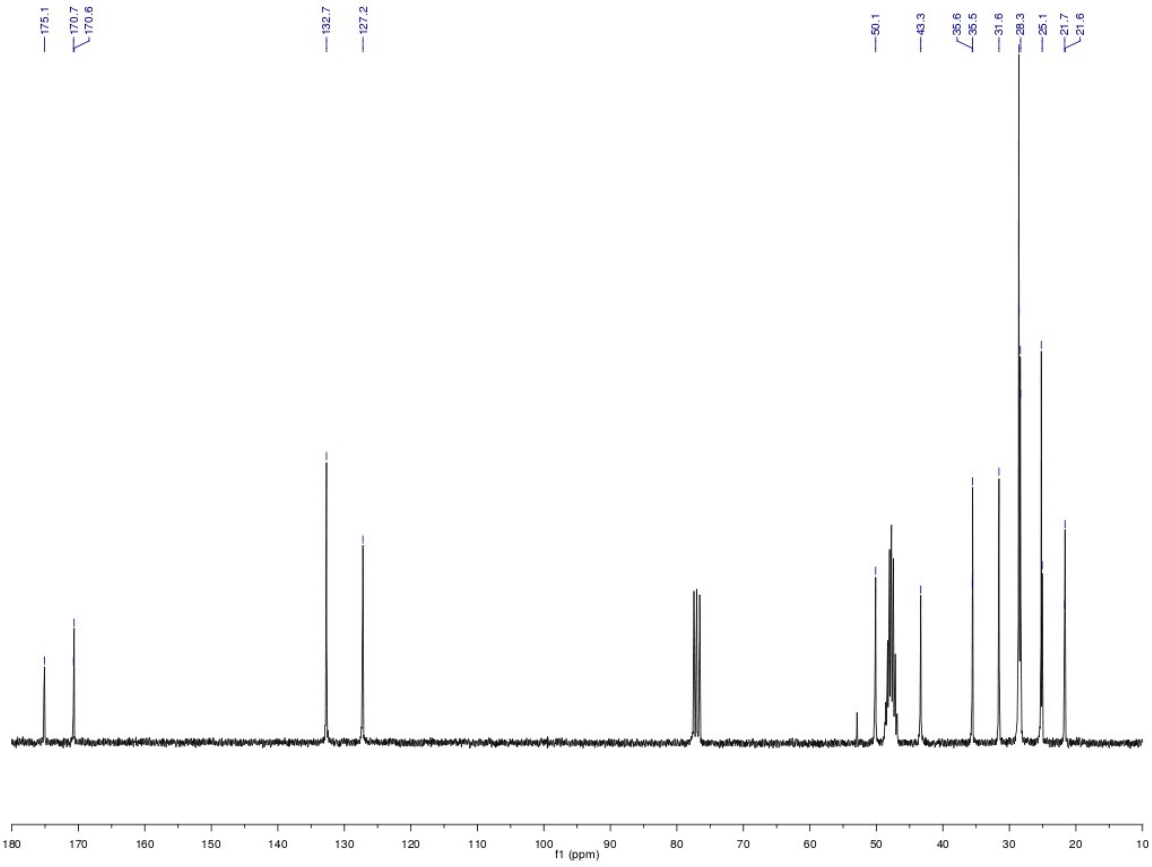

Figure VI.31: ^{13}C NMR spectrum of **3** in 1:1 $CDCl_3/CD_3OD$

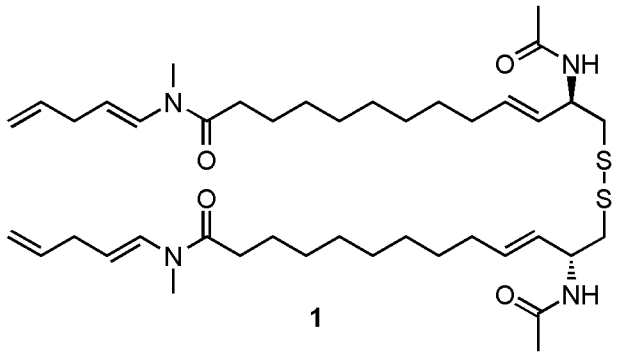

1

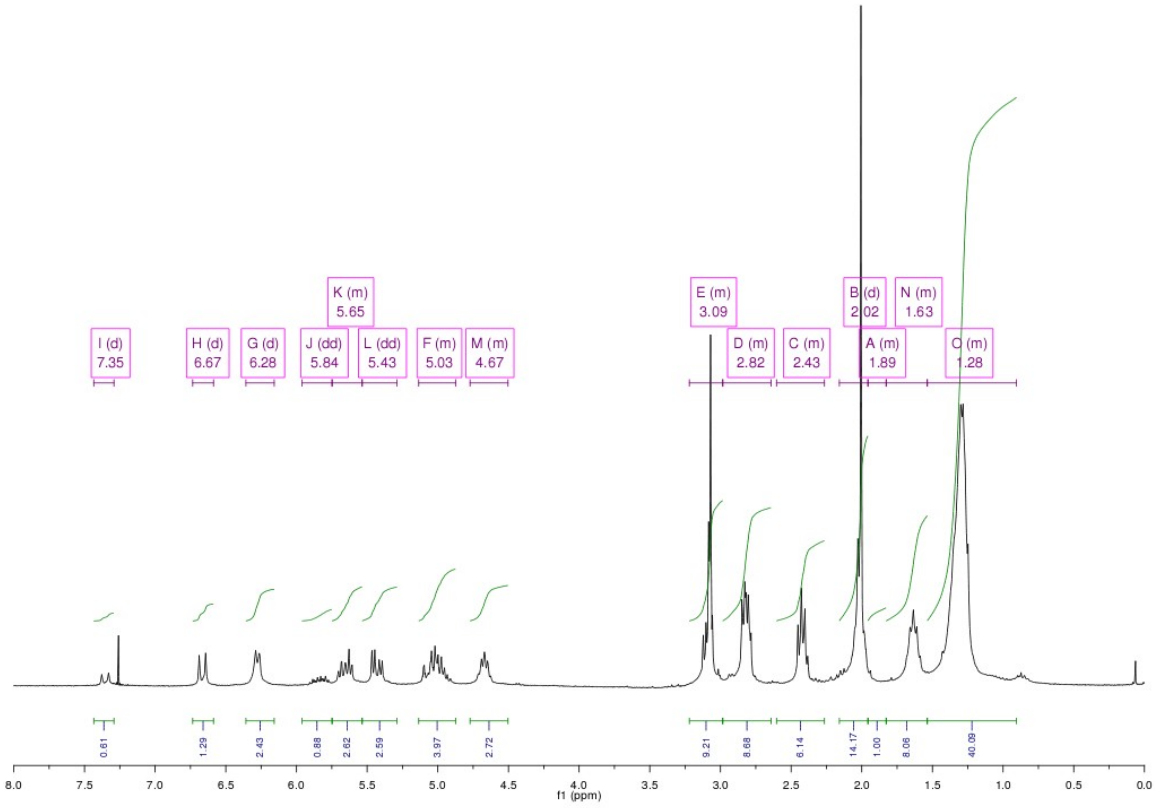

Figure VI.32: ^{1}H NMR spectrum of **1** in $CDCl_3$

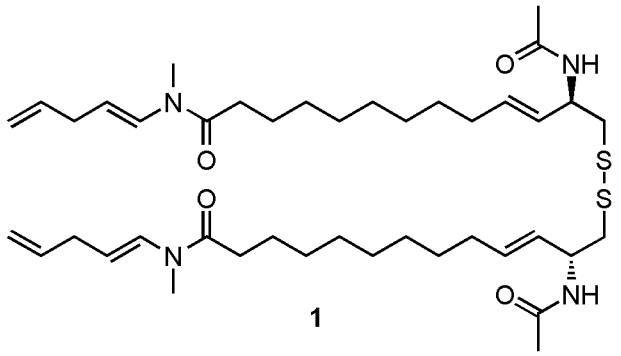

1

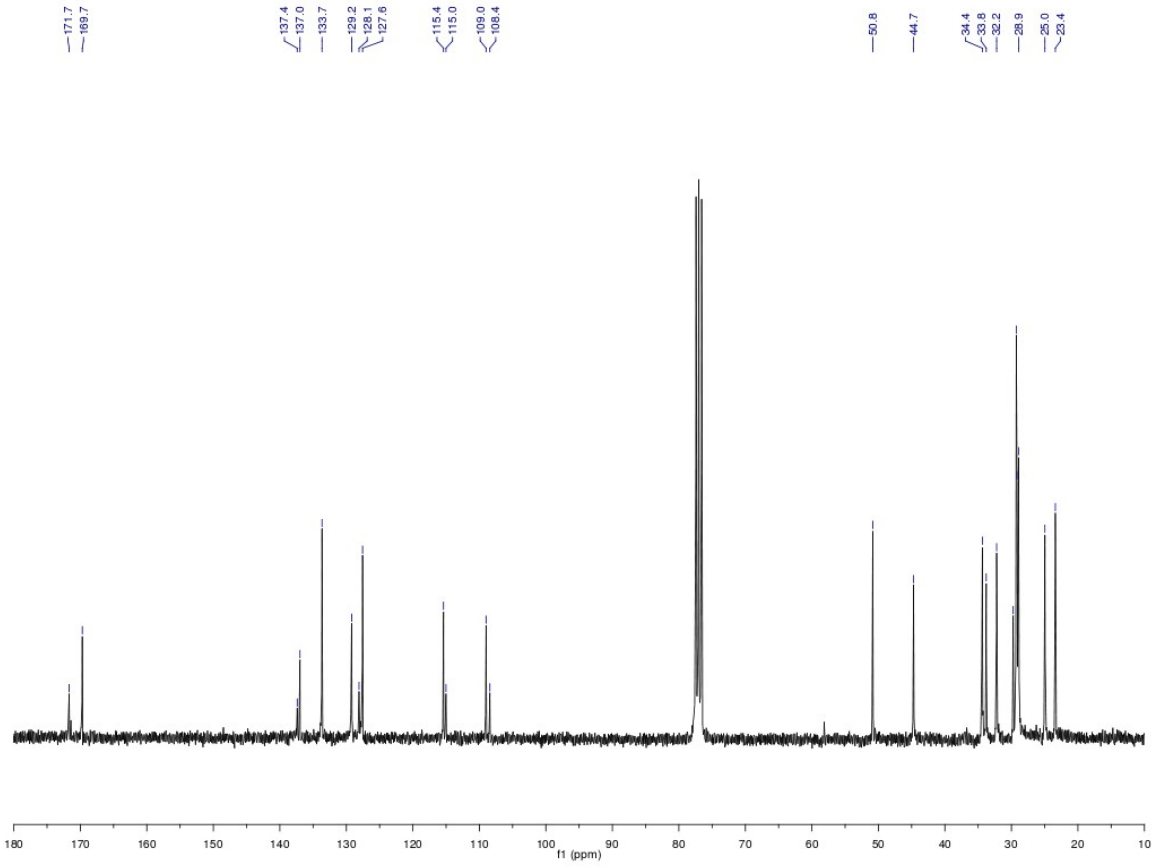

Figure VI.33: ^{13}C NMR spectrum of **1** in $CDCl_3$

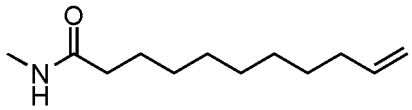

70

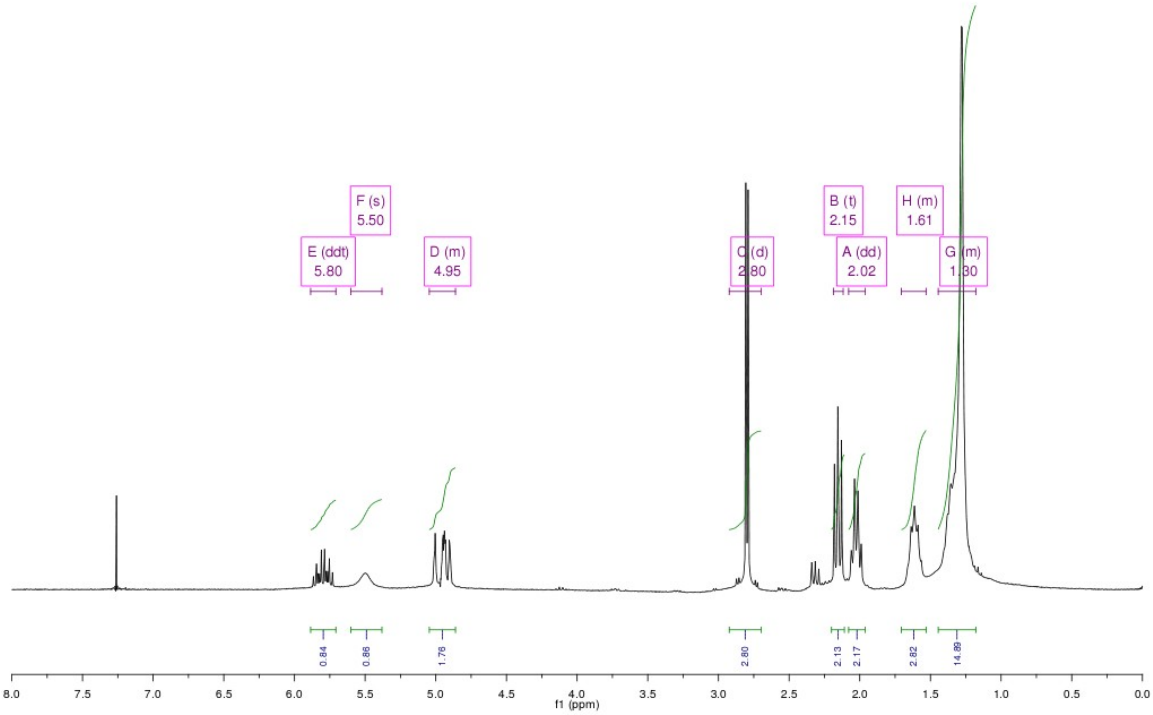

Figure VI.34: ^{1}H NMR spectrum of **70** in $CDCl_3$

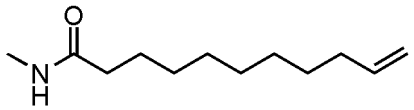

70

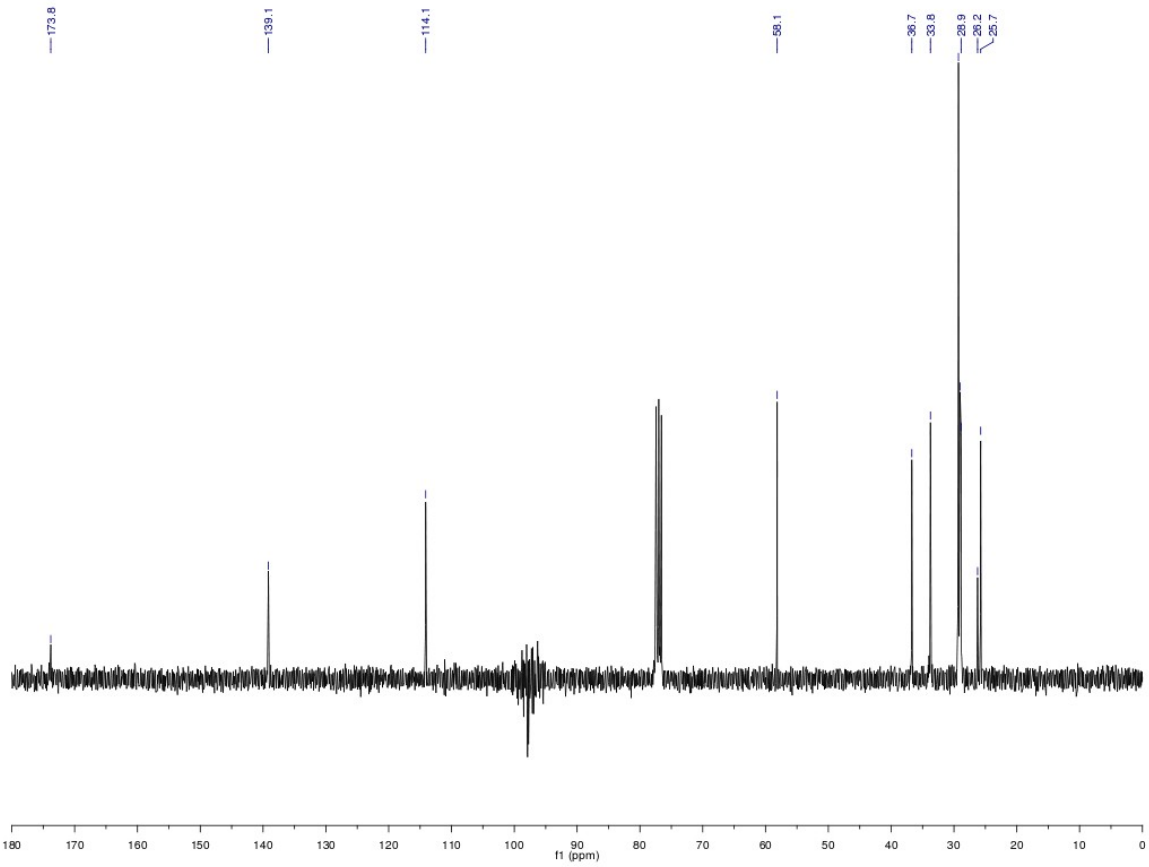

Figure VI.35: ^{13}C NMR spectrum of **70** in $CDCl_3$

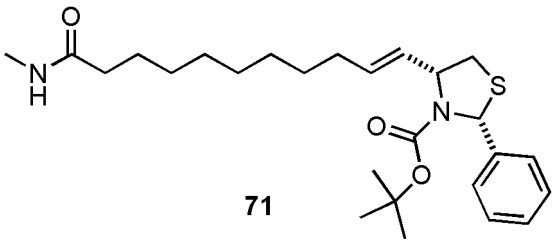

71

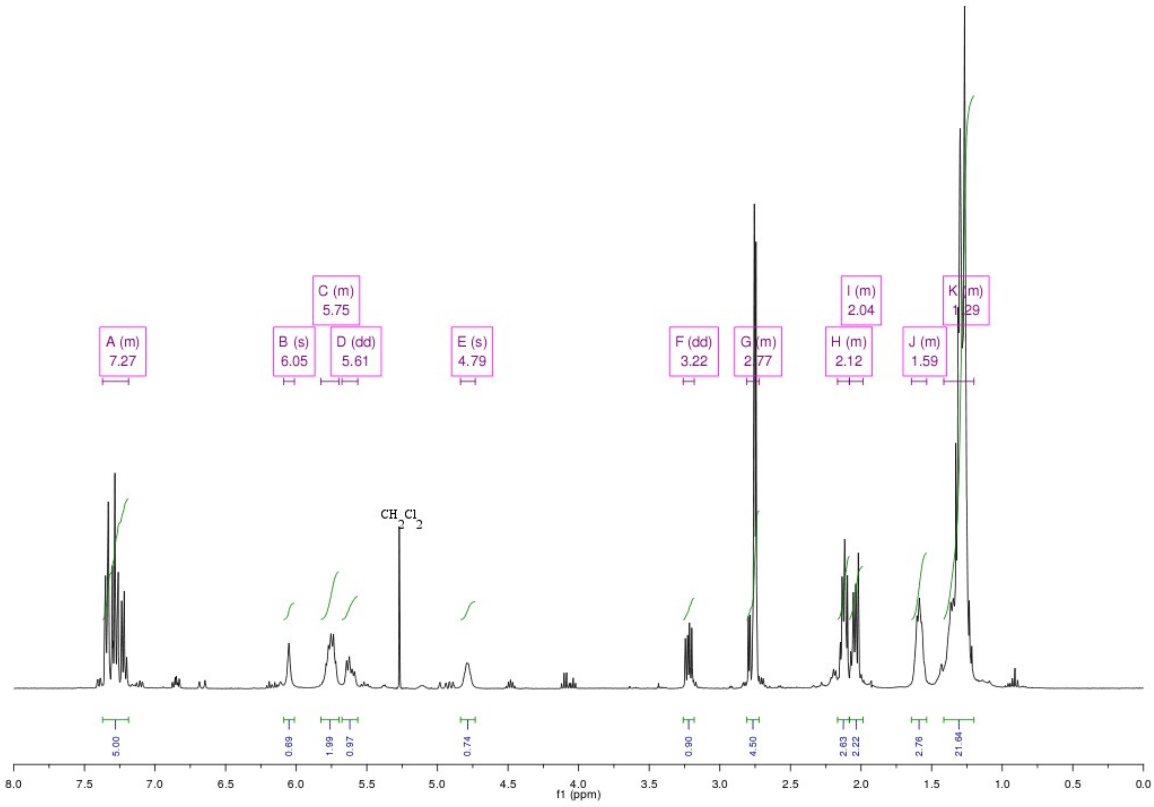

Figure VI.36: ^{1}H NMR spectrum of **71** in $CDCl_3$

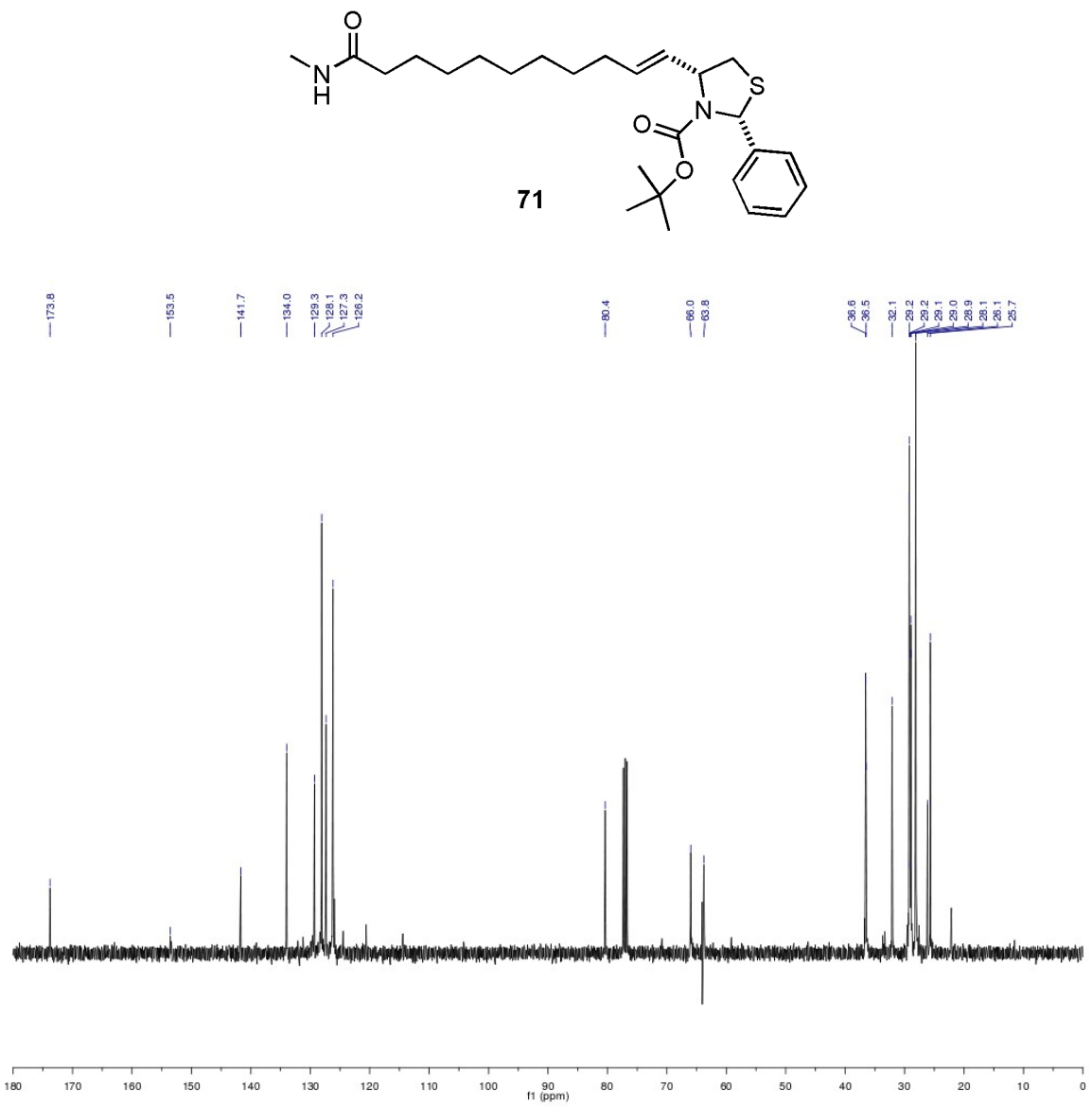

Figure VI.37: ^{13}C NMR spectrum of **71** in $CDCl_3$

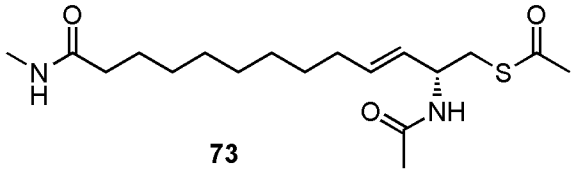

73

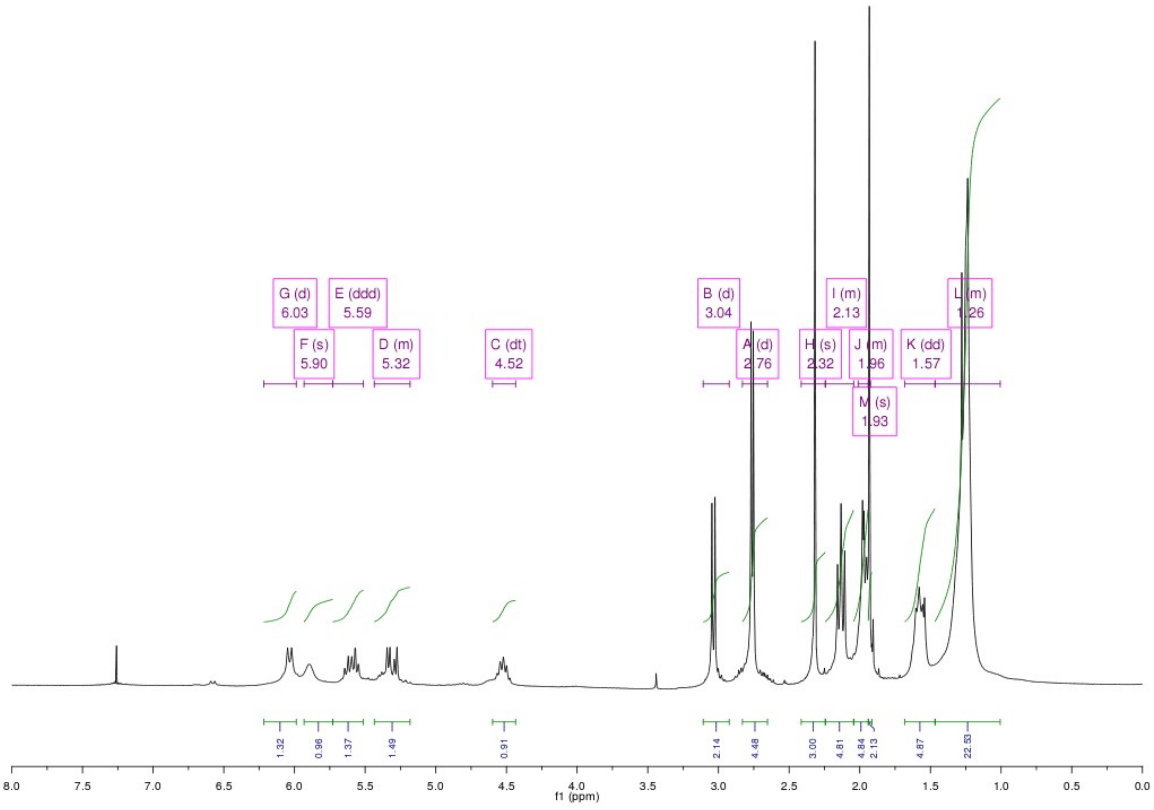

Figure VI.38: ^{1}H NMR spectrum of **73** in $CDCl_3$

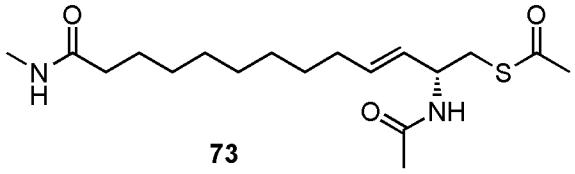

73

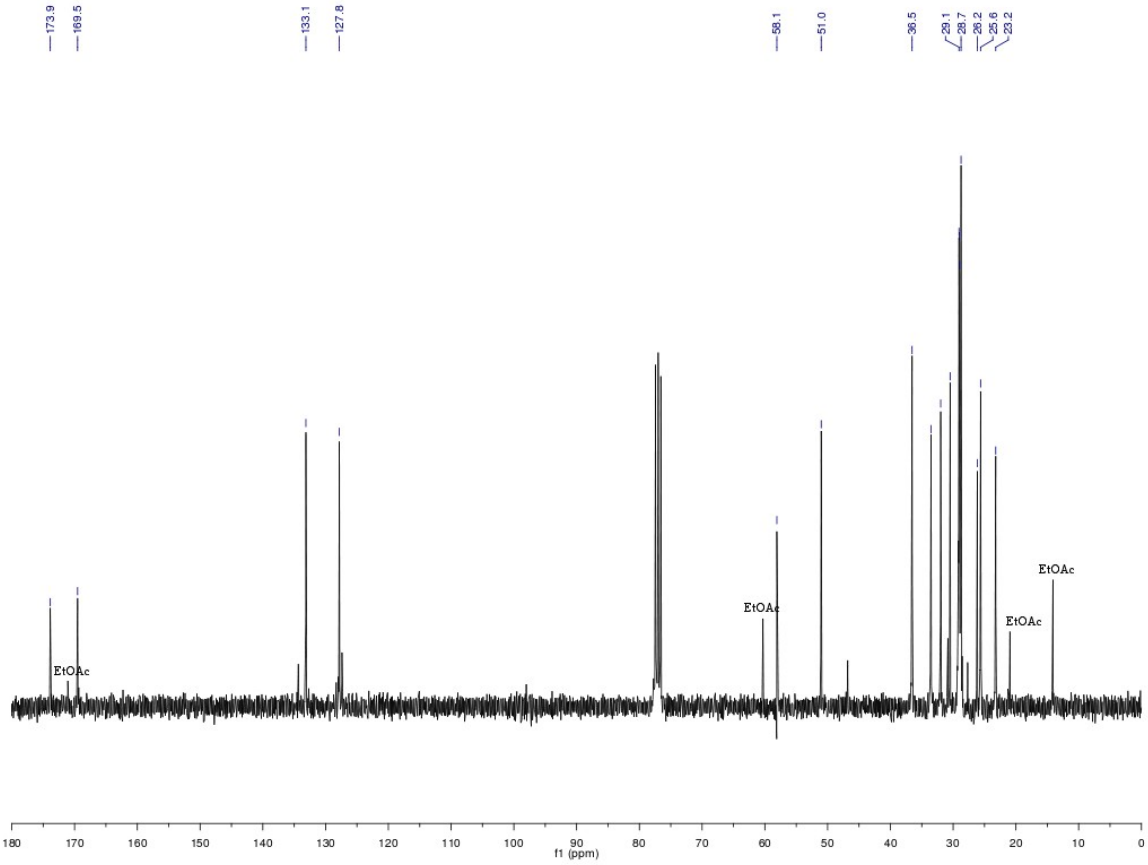

Figure VI.39: ^{13}C NMR spectrum of **73** in $CDCl_3$

References and footnotes

1 Newman, D. J.; Cragg, G. M. Natural products as sources of new drugs over the last 25 years. *J. Nat. Prod.* **2007**, *70*, 461-477.

2 Gerwick, W. H.; Tan, L. T.; Sitachitta, N. *The Alkaloids*; Cordell, G. A., Ed.; Academic Press; San Diego, CA **2001**; *Vol. 57*, pp 75-184.

3 Nogle, L. M.; Gerwick, W. H. Somocystinamide a, a novel cytotoxic disulfide dimer from a fijian marine cyanobacterial mixed assemblage. *Org. Lett.* **2002**, *4*(7), 1095-8.

4 Wrasidlo, W.; Mielgo, A.; Torres, V. A.; Barbero, S.; Stoletov, K.; Suyama, T. L.; Klemke, R. L.; Gerwick, W. H.; Carson, D. A.; Stupack, D. G. The marine lipopeptide somocystinamide A triggers apoptosis via caspase 8. *Proc. Natl. Acad. Sci.* **2008**, *105*, 2313-2318.

5 Park, H.-J.; Zhang, Y.; Georgescu, S. P.; Johnson, K. L.; Kong, D.; Galper, J. B. Human umbilical vein endothelial cells and human dermal microvascular endothelial cells offer new insights into the relationship between lipid metabolism and angiogenesis. *Stem Cell Reviews and Reports* **2006**, *2*, 93-101.

6 Goishi, K.; Klagsbrun, M. Vascular endothelial growth factor and its receptors in embryonic zebrafish blood vessel development. Current Topics in Developmental Biology **2004**, *62*, 127-152.

7 EarnShaw, W. C.; Martins, L. M.; Kaufmann, S. H. mammalian caspases: structure, activation, substrates, and functions during apoptosis. *Annu. Rev. Biochem*. **1999**, *68*, 383-424.

8 There is some evidence that **1** also induces intrinsic apoptosis, which involves caspase-9, in addition to the extrinsic apoptotic pathway involving caspase-8 (see ref. 4).

9 This compound was synthesized as shown in Scheme VI.4.

10 This compound was obtained through unintentional hydrolysis of **1** (see Scheme VI.2).

11 Bukowski, R. M. AE-941, a multifunctional antiangiogenic compound: trials in renal cell carcinoma. *Expert Opin. Investig. Drugs* **2003**, *12*, 1403-1411.

12 Wahl, M. L.; Kenan, D. J.; Gonzalez-Gronow, M.; PizzoMore, S. V. Angiostatin's Molecular Mechanism: Aspects of Specificity and Regulation Elucidated . *J. Cell. Biochem.* **2005**, *96*, 242-261.

13 National Instituted of Health. Safety and Efficacy Study of rhAngiostatin Administered in Combination With Paclitaxel and Carboplatin to Patients With Non-Small-Cell Lung Cancer. http://www.clinicaltrials.gov/ct/gui/show/NCT00049790;jsessionid=91EE48B7C2F7D935B96F12E31D5609E3?order=1 (accessed on 05/19/2009).

14 Crews, P.; Rodrĭguez, J.; Jaspars, M. Optical and chiroptical techniques: Ultraviolet spectroscopy. In *Organic Structure Analysis*; Oxford University Press: Oxford, 1998, pp 349-373.

15 Tracey, M. R.; Hsung, R. P.; Antoline, J.; Kurtz, K. C. M.; Shen, L.; Slafer, B. W.; Zhang, Y. Product class 4: *N*-Arylalkanamides, ynamides, enamides, dienamides, and allenamides. *Science of Synthesis* **2005**, *21*, 387-475.

16 (a) Jiang, L.; Job, G. E.; Klapars, A.; Buchwald, S. L. Copper-Catalyzed Coupling of Amides and Carbamates with Vinyl Halides . Org. Lett. 2003, 5, 3667–3669. (b) Dehli, J. R.; Legros, J.; Bolm, C. Synthesis of enamines, enol ethers and related compounds by cross-coupling reactions . *Chem. Commun.* **2005**, 973–986. (c) Han, C.; Shen, R.; Su, S.; Porco, J. A., Jr. Copper-Mediated Synthesis of N-Acyl Vinylogous Carbamic Acids and Derivatives: Synthesis of the Antibiotic CJ-15,801. *Org. Lett.* **2004**, *6*, 27–30.

17 (a) Ramaswamy, A. V.; Flatt, P. M.; Edwards, D. J.; Simmons, T. L.; Han, B.; Gerwick, W. H. The secondary metabolites and biosynthetic gene clusters of marine cyanobacteria. Applications in biotechnology. *Frontiers Mar. Biotech.* **2006**, 175-224. (b) Moore, Bradley S. Biosynthesis of marine natural products: macroorganisms (Part B). *Nat. Prod. Rep*, **2006**, *23*, 615-629.

18 Chang, Z.; Sitachitta, N.; Rossi, J. V.; Roberts, M. A.; Flatt, P. M.; Jia, J.; Sherman, D, H.; Gerwick, W. H. Biosynthetic Pathway and Gene Cluster Analysis of Curacin A, an Antitubulin Natural Product from the Tropical Marine Cyanobacterium *Lyngbya majuscula*. *J. Nat. Prod.* **2004**, *67*, 1356-1367.

19 Cantoni, G. L. The Nature of the Active Methyl Donor Formed Enzymatically from L-Methionine and Adenosinetriphosphate. *J. Am. Chem. Soc.* **1952**, *74*, 2942-2943.

20 Dewick, P. M. Secondary metabolism: The building blocks and construction mechanisms. In *Medicinal natural products: A biosynthetic approach*; 2nd Ed. John Wiley & Sons, LTD: London, **2001**, pp 7-34.

21 Rukachaisirikul, V.; Sommart, U.; Phongpaichit, S.; Sakayaroj, J.; Kirtikara, K. Metabolites from the endophytic fungus *Phomopsis* sp. PSU-D15. *Phytochem.* **2008**, *69*, 783-787.

22 (a) Erickson, K. L.; Beutler, J. A.; Cardellina, J. H., II; Boyd, M. R. Salicylihalamide A and B, novel cytotoxic macrolides from the marine sponge *Haliclona* sp. *J. Org. Chem.* **1997**, *62*, 8188–8192. (b) Erickson, K. L.; Beutler, J. A.; Cardellina, J. H., II; Boyd, M. R. Salicylihalamides A and B, Novel Cytotoxic Macrolides from the Marine Sponge *Haliclona* sp. [Erratum]. *J. Org. Chem.* **2001**, *66*, 1532.

23 Boyd, M. R.; Farina, C.; Belfiore, P.; Gagliardi, S.; Kim, J. W.; Hayakawa, Y.; Beutler, J. A.; McKee, T. C.; Bowman, B. J.; Bowman, E. J. Discovery of a novel antitumor benzolactone enamide class that selectively inhibits mammalian vacuolar-type (H+)-ATPases. *J. Pharmacol. Exp. Ther.* **2001**, *297*, 114–120.

24 Sun-Wada, G.-H.; Wada, Y.; Futai, M. Diverse and essential roles of mammalian vacuolar-type proton pump ATPase: toward the physiological understanding of inside acidic compartments. *Biochim. Biophys. Acta* **2004**, *1658*, 106–114.

25 Huss, M.; Wieczorek, H.; Inhibitors of V-ATPases: old and new players. *J. Exp. Biol.* **2009**, *212*, 341-346.

26 Palermoa, J. A.; Flowera, P. B.; Seldes, A. M. Chondriamides A and B, new indolic metabolites from the red alga *Chondria* sp. *Tetrahedron Lett.* **1992**, *33*, 3097-3100.

27 Jorge A. Palermo, Patricia Blanch Flower and Alicia M. Seldes. Chondriamides A and B, New Indolic Metabolites Red Alga *Chondria* sp. *Tetrahedron Lett.* **1992**, *33*, 3097-3100.

28 Pattenden, G.; Ashweek, N. J.; Baker-Glenn, C. A. G.; Kempson, J.; Walker, G. M.; Yee , J. G. K. Total synthesis of (−)-ulapualide A, a novel tris-oxazole macrolide from marine nudibranchs, based on some biosynthesis speculation . *Org. Biolmol. Chem.* **2008**, *6*, 1478-1497.

29 Su, S.; Kakeya, H.; Osada, H.; Porco, J. A. Jr. Synthesis and cell cycle inhibition of the peptide enamide natural products terpeptin and the aspergillamides . *Tetrahedron* **2003**, *59*, 8931-8946.

30 (a) Ninomiya, I. Applications of enamide chemistry to the synthesis of heterocyclic compounds. *Heterocycles* **1980**, *14*, 1567–1579. (b) Davies, D. T.; Kapur, N.; Parsons, A. F. Preparation of N-Heterocycles by Radical Cyclisation of Enamides Mediated by Manganese(III) or Copper(I). A Comparison of Cyclisation Methods. *Tetrahedron* **2000**, *56*, 3941–3949. (c) Baker, S. R.; Burton, K. I.; Parsons, A. F.; Pons, J.; Wilson, M. Tandem radical cyclisation of enamides mediated by tin hydride; pyrrolizidinone or indolizidinone ring formation. *J. Chem. Soc., Perkin Trans. 1* **1999**, *4*, 427–436. (d) Brodney, M. A.; Padwa, A. Generation and Trapping of N-Acyliminium Ions Derived from Isomünchnone Cycloadducts. A Versatile Route to Functionalized Heterocycles. *J. Org. Chem.* **1999**, *64*, 556–565. (e) Okano, T.; Sakaida, T.; Eguchi, S. Generation of 6-(Trifluoromethyl)-4,5-dihydro-2(3H)-pyridone and the Application to Synthesis of Some Fused Nitrogen Heterocycles Carrying a Trifluoromethyl Group on the Bridgehead Position via Radical Cyclization of Dihydropyridones. *J. Org. Chem.* **1996**, *61*, 8826–8830. (f) Schultz, A. G.; Guzzo, P. R.; Nowak, D. M. Asymmetric Organic Synthesis. Radical Cyclizations of Chiral Enamides. *J. Org. Chem.* **1995**, *60*, 8044–8050.

31 a) Cook, G. R.; Stille, J. R. Stereochemical consequences of the lewis acid-promoted 3-aza-cope rearrangement of N-alkyl-N-allyl enamines. *Tetrahedron* **1994**, *50*, 4105-4124. b) Padwa, A.; Heidelbaugh, T. M.; Kuethe, J. T.; McClure, M. S.; Want, Q. Tandem pummerer/mannich cyclization cascade of α-sulfinylamides as a method to prepare aza-heterocycles. *J. Org. Chem.* **2002**, *67*, 5928-5937.

32 Overman, L. E.; Sato, T. Construction of Epidithiodioxopiperazines by Directed Oxidation of Hydroxyproline-Derived Dioxopiperazines. *Org. Lett.* **2007**, *9*, 5267-5270.

33 Middleton, M. D.; Peppers, B. P.; Diver, S. T. Studies directed toward the synthesis of the scabrosins: validation of a tandem enyne metathesis approach . *Tetrahedron* **2006**, *62*, 10528-10540.

34 Fukuyama, T.; Nakatsuka, S.; Kishi, Y. Total synthesis of gliotoxin, dehydrogliotoxin, and hyalodendrin. *Tetrahedron* **1981**, *37*, 2045-2078.

35 (a) Nicolaou, K. C.; Hughes, R.; Pfefferkorn, J. A.; Barluenga, S.; Roecker, A. J. Combinatorial Synthesis through Disulfide Exchange: Discovery of Potent Psammaplin A Type Antibacterial Agents Active against Methicillin-Resistant *Staphylococcus aureus* (MRSA) . *Chem. Eur. J.* **2001**, *7*, 4280-4295. (b) Hoshino, O.; Murakata, M.; Yamada, K. An improved synthesis of psammaplin A. *Bioorg. Med. Chem. Lett.* **1992**, *2*, 1561-1562. (c) Hoshino, O.; Murakata, M.; Yamada, K. A convenient synthesis of a bromotyrosine derived metabolite, psammaplin A, from *Psammaplysilla* sp. *Bioorg. Med. Chem. Lett.* **1992**, *12*, 1561-1562.

36 Chemler, S. R.; Trauner, D.; Danishefsky, S. J. The B-alkyl Suzuki-Miyaura cross-coupling reaction: development, mechanistic study, and applications in natural product synthesis. *Angew. Chem. Int. Ed.* **2001**, *40*, 4544-4568.

37 Nicolau, K. C.; Bulger, P. G.; Sarlah, D. Palladium-catalyzed cross-coupling reactions in total synthesis. *ibid.* **2005**, *44*, 4442-4489.

38 a) Takai, K.; Nitta, K.; Utimoto, K. Simple and selective method for aldehydes (RCHO) .fwdarw. (E)-haloalkenes (RCH:CHX) conversion by means of a haloform-chromous chloride system. *J. Am. Chem. Soc.* **1986**, *108*, 7408-7410. b) Concellon, J. M.; Bernad, P. L.; Mejica, C. Synthesis of enantiopure (*S*)-(*E*)-1-haloalk-1-ene-3-amines with total or very high diastereoselectivity by halomethylenation of α-amino aldehydes promoted by $CrCl_2$**.** *Tetrahedron Lett.* **2005**, *46*, 569-571.

39 Deroose, F. D.; De Clercq, P. J. Novel enantioselective syntheses of (+)-biotin. *J. Org. Chem.* **1995**, *60*, 321-330.

40 Mancuso, A. J.; Huang, S. L.; Swern, D. Oxidation of long-chain and related alcohols to carbonyls by dimethyl sulfoxide "activated" by oxalyl chloride. *J. Org. Chem.* **1978**, *43*, 2480-2482.

41 There is evidence that **1** also induces intrinsic apoptosis in addition to the extrinsic apoptotic pathway involving caspase-8. However, initiation of the extrinsic pathway, which is more sensitive, appears to be the predominant mechanism of action.

42 Molander, G. A.; Ito, T. Cross-Coupling Reactions of Potassium Alkyltrifluoroborates with Aryl and 1-Alkenyl Trifluoromethanesulfonates. *Org. Lett.* **2001**, *3*, 393-396.

43 Nicolaou, K. C.; Bulger, P. G.; Sarlah, D. Metathesis reactions in total synthesis. *Angew. Chem. Int. Ed.* **2005**, *44*, 4490-4527.

44 Wittig, G.; Schöllkopf, U. Über Triphenyl-phosphin-methylene als olefinbildende Reagenzien. *Ber.* **1954**, *87*, 1318.

45 Garber, S. B.; Kingsbury, J. S.; Gray, B. L.; Hoveyda, A. H. Efficient and Recyclable Monomeric and Dendritic Ru-Based Metathesis Catalysts. *J. Am. Chem. Soc.* **2000**, *122*,

8168-8179.

46 I took the liberty to name this compound (**57**) somocystinoic acid because it is a new compound.

47 (a) Cook, G. R.; Stille, J. R. Stereochemical consequences of the lewis acid-promoted 3-aza-cope rearrangement of N-alkyl-N-allyl enamines. *Tetrahedron* **1994**, *50*, 4105–4124. (b) Gangadasu, B.; Narender, P.; Kumar, S. B.; Ravinder, M.; Rao, B. A.; Ramesh, C.; Raju, B. C.; Rao, V. J. Facile and selective synthesis of chloronicotinaldehydes by the Vilsmeier reaction. *Tetrahedron* **2006**, *62*, 8398–8403. (c) Cook, G. R.; Barta, N. S.; Stille, J. R. Lewis acid-promoted 3-aza-Cope rearrangement of N-alkyl-N-allyl enamines. *J. Org. Chem.* **1992**, *57*, 461–467. (d) Couture, A.; Dubiez, R.; Lablache-Combier, A. Secondary enamide and thioenamide photochemistry. A new spiroannulation method. *J. Org. Chem.* **1984**, *49*, 714–717. (e) Pattenden, G.; Ashweek, N. J.; Baker-Glenn, C. A. G.; Kempson, J.; Walker, G. M.; Yee, J. G. K. Total synthesis of (-)-ulapualide A, a novel tris-oxazole macrolide from marine nudibranchs, based on some biosynthesis speculation. *Org. Biomol. Chem.* **2008**, *6*, 1478–1497. (f) Morales, O.; Seide, W.; Watson, S. E. Synthesis of 7,6-fused bicyclic lactams for use as beta-turn mimics. *Synth. Commun.* **2006**, *36*, 965–973.

48 The acetamide, disulfide, or already formed enamide of the other half of the dimeric intermediate may act as a nucleophile to attack the iminium ion. For examples of nucleohilic additions to iminium ions, see: Moonen, K.; Stevens, C. V. *Synthesis* **2005**, *20*, 3603–3612.

49 In separate studies, reaction of **17** with simple unfunctionalized acid chlorides formed enamides, thus indicating the presence of an acyliminium ion intermediate like **21**. Because **19** was not observed by NMR, an acylenaminium intermediate is not likely

50 Ogawa, T.; Kiji, T.; Hayami, K.; Suzuki, H. Stereospecific one-pot synthesis of enamides and enimides by the copper iodide promoted vinylic substitution. *Chem. Lett.* **1991**, 1443-1446.

51 4-pentenal (**5**) was synthesized according to the following paper: Griffith, G. A.; Percy, J. M.; Pintat, S.; Smith, C. A.; Spencer, N.; Uneyama, E. Towards novel difluorinated sugar mimetics; syntheses and conformational analyses of highly-functionalised difluorinated cyclooctenones. *Org. Biomol. Chem.* **2005**, *3*, 2701–2712.

52 Instead of a thimble, glass wool and molecular sieves were used to capture any moisture distilled as an azeotrope.

53 (a) Saunders, W. H. Jr. *Acc. Chem. Res.* **1976**, *9*, 19-25. (b) Carey, F. A.; Sundberg, R. J. *Advanced Organic Chemistry Part A 4th Ed*, Kluwer Academic / Pleunum Publishers; New York, **2000**, 378-383.

54 Since the publication of this synthesis, the condition for enamide formation was slightly modified (higher concentration and more equivalents of the aldehyd) to increase the yield from 41 to 47%.

55 If this is the case, it would not be the first time. See Chapter V for the bioactivity of the synthetic sample of epiquinamide.

56 de Boer, T. J.; Backer, H. J. Diazomethane. *Org. Synth.* **1963**, *4*, 250-253.

57 Lee, S. *Process development : fine chemicals from grams to kilograms.* Oxford ; New York : Oxford University Press, **1995**.

58 Unfortunately, the 200 mg mark was not met for technically being a multi-hundred-milligram (MHM) scale synthesis. See Chapter I of this dissertation for the discussion on MHM synthesis.

59 Still, W. C.; Khan, M.; Mitra, A. Rapid chromatographic technique for preparative separations with moderate resolution. *J. Org. Chem.* **1978**, *43*, 2923-2925.

60 Chavan, S. P.; Chittiboyina, A. G.; Ramakrishna, G.; Tejwani, R. B.; Ravindranathan, T.; Kamat, S. K.; Rai, B.; Sivadasan, L.; Balakrishnan, K.; Rmalingam, S.; Deshpande, V. H. An unusual stereochemical outcome of radical cyclization: synthesis of (C)-biotin . *Tetrahedron*, **2005**, *61*, 9273-9280.

Chapter VII

Biomimetic total synthesis of a cyanobacterial UV-blocking natural product, scytonemin and insights into its biogenesis

Abstract

Scytonemin is a cyanobacterial alkaloid that has UV-screening properties. In order to gain insights into the biogenesis of the unique structure and to produce a chelation-free sample, synthetic studies were conducted on scytonemin. Through a successful synthesis of the proposed monomeric precursor of scytonemin, its spontaneous dimerization was shown to be impossible under ambient conditions. Various attempts to oxidatively dimerize this monomer and explanations for their failure are described herein. As a result, an alternative structure for the monomeric precursor of scytonemin was proposed.

VII.1 Introduction

Cyanobacteria can be commonly found in environments that are exposed to harmful levels of UV radation as well as sun light necessary for photosynthesis.[1] In order to avoid the deleterious effects of UVA (320-400 nm), UVB (280-320 nm), and UVC (190-280 nm) radiations, pigmented metabolites, including scytonemin (**1**),[2] are stored in the extracellular sheaths of many cyanobacteria.[1,3] Indeed, this dark-greenish brown indole alkaloid is particularly well suited for absorbing UV light in the blue wavelengths (Figure VIII.1).[4]

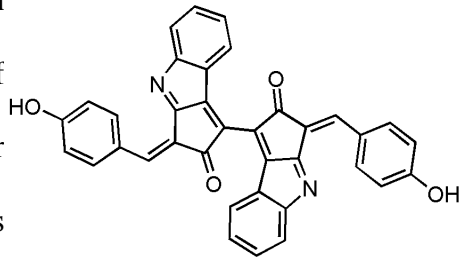

Scytonemin, **1**

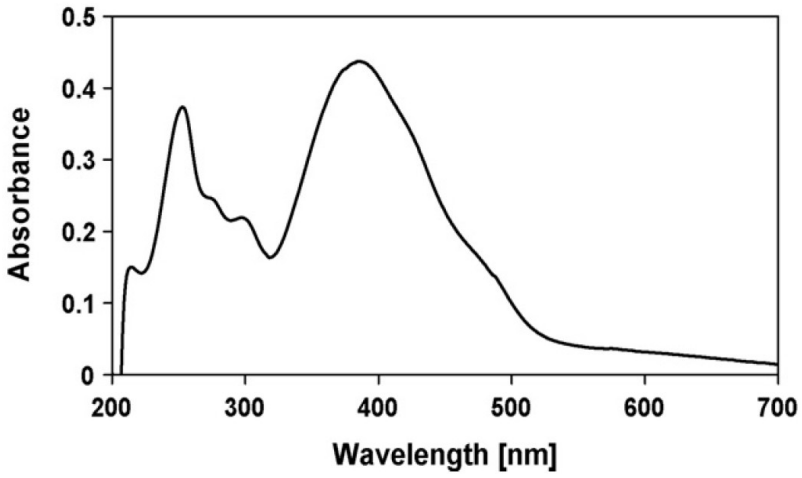

Figure VII.1: Light absorption spectrum of scytonemin (**1**) (taken from ref. 4)

This natural product is a dimer of a unit that appears to be derived from L-tryptophan and chorismate.[5] Under anaerobic conditions, scytonemin can exist in a reduced form (**2**) as shown in Scheme VII.1.[2] Almost 150 years after the initial report of the compound,[6] the structure of **1** was finally elucidated in 1993 by Gerwick and

coworkers through NMR and MS analysis of **1**, as well as those of the ozonolysis product of **2** (Scheme VII.1).[2] Incidentally, **3** is also a natural product (nostodione) isolated from a terrestrial cyanobacteria, *Nostoc commune*, and it is known to disrupt mitotic spindle formation in sea-urchin eggs.[7]

Due to the unique carbon skeleton and ecological significance of this metabolite, there is a considerable interest in its biosynthesis.[8] The first study in this regard by

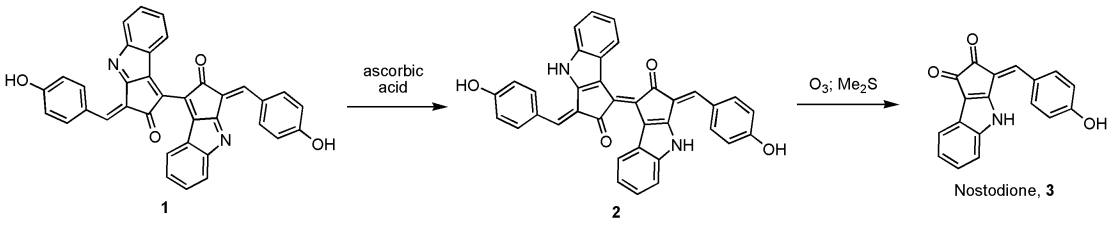

Scheme VII.1: Fragmentation of the reduced form of scytonemin (**2**) through ozonolysis in its structure elucidation (Gerwick et al. 1993)

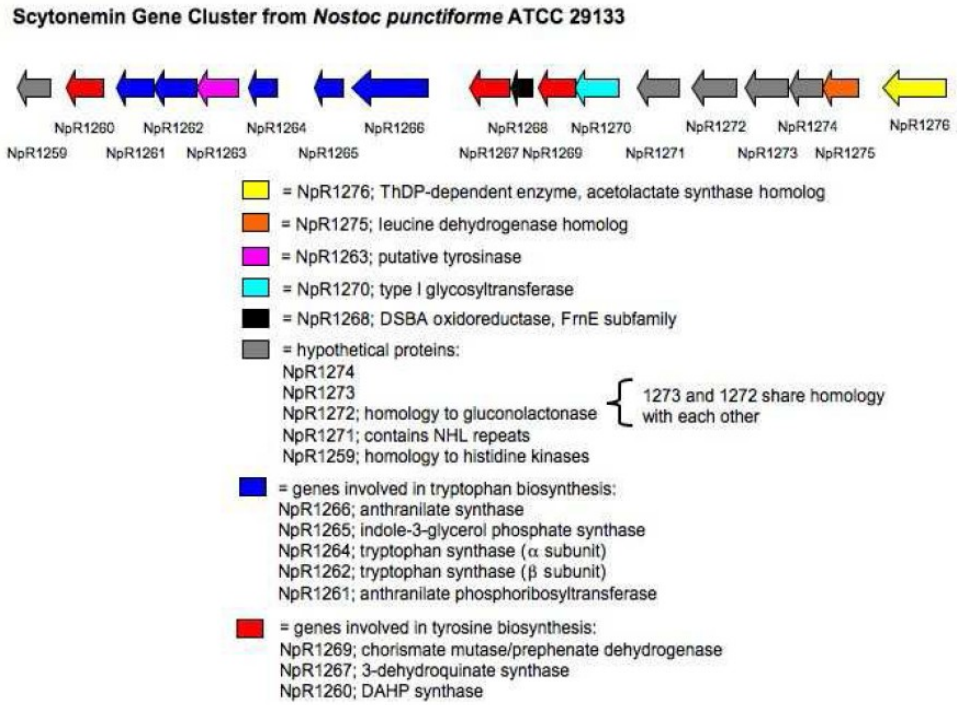

Scheme VII.2: Biosynthetic gene cluster for scytonemin in *Nostoc punctiforme*[5,6]

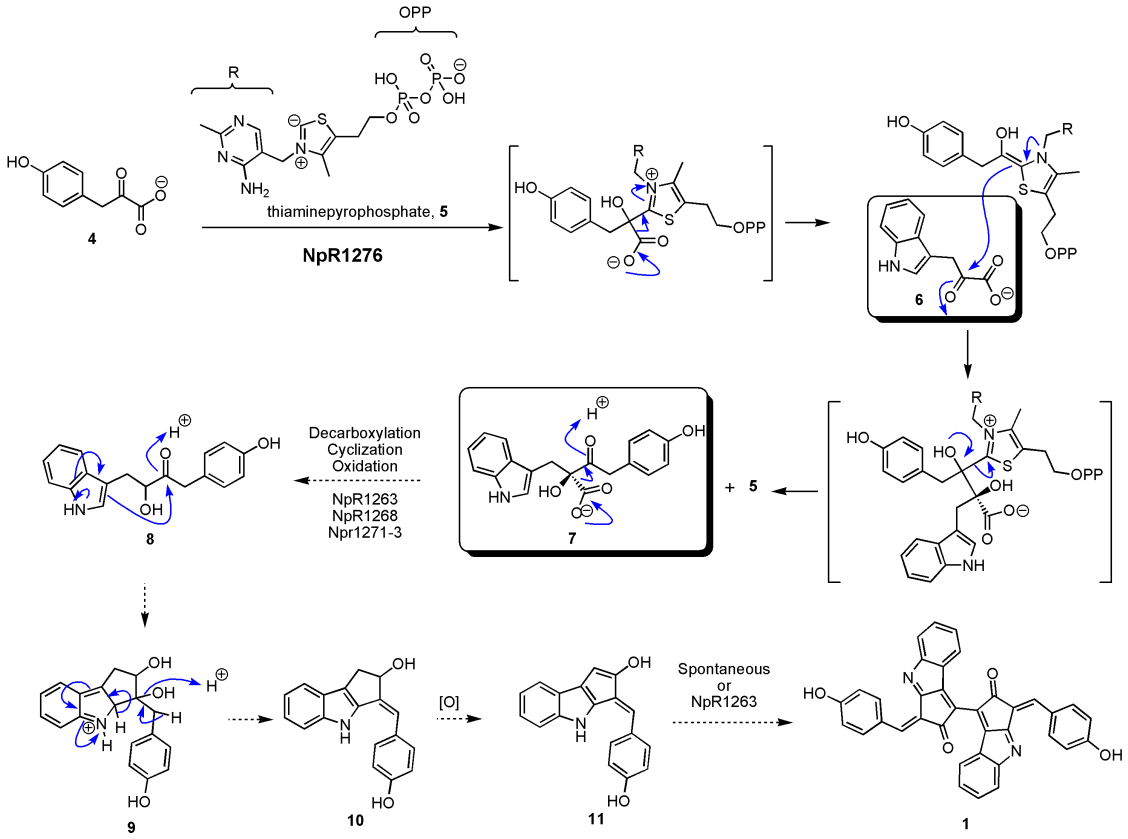

Scheme VII.3: Proposed mechanism for the biosynthesis of scytonemin (**1**) by Balsksus and Walsh[5]

Biosynthetic products that were analytically characterized (**6** and **7**) are highlighted by rectangles. Note the proposed structure of the monomer (**11**). In reality, the putative monomeric precursor is exclusively in the keto form (*vide infra*).

Garcia-Pitchel and coworkers reported the identification of the scytonemin biosynthetic gene cluster in 2007 (Scheme VII.2).[5,8] The involvement of tryptophan and chorismate in the biosynthesis were implicated by the presence of genes NpR1261-1266 and by the presence of genes NpR1260, 1267, and 1269, respectively. Subsequently, Balskus and Walsh provided biochemical evidence for the biosynthetic intermediacy of α-hydroxy ketone **7** and *p*-hydroxyphenylpyruvic acid **4**.[5] The proposed mechanism shown in

Scheme VII.3 is based on the observed activity of the ThDP (thiamine diphosphate)-dependent acetolactate synthase (NpR1276 in Scheme VII.2 and 3).

Phosphorylated thiamine is essential for the normal function of the nervous system in many species.[9] Having a ylide functionality, thiamine possesses both nucleophilicity and electrophilicity. Consequently, **5** is able to undergo nucleophilic addition to the ketone of α-ketoacid **4**, facilitate aldol condensation with another α-ketoacid **6**, and eliminate as an ylide to regenerate itself (Scheme VII.3). Decarboxylation of **7** is expected to be necessary due to the steric hindrance by the carboxylic acid in the cyclization step. Although structure **8** appears to be suitable for a rapid intramolecular cyclization reminiscent of the Pictet-Spengler reaction, catalysis is apparently necessary.[10]

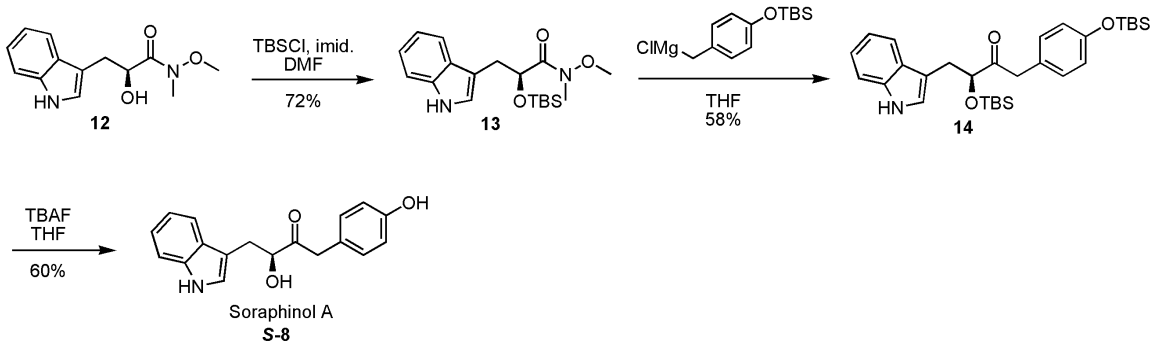

Scheme VII.4: Chemical synthesis of a putative biosynthetic precursor of scytonemin (**1**), soraphinol A (***S*-8**)

Balskus and Walsh were able to synthesize α-hydroxy ketone ***S*-8** without spontaneous cyclization through an independent route, and this material was used as a synthetic standard for comparison with the acid-catalyzed decarboxylation product of **7** (Scheme VII.4).[5]

As can be seen in Scheme VII.3, there are many steps remain to be determined in the biosynthesis of scytonemin. For example, despite genetic evidence, the intermediacy

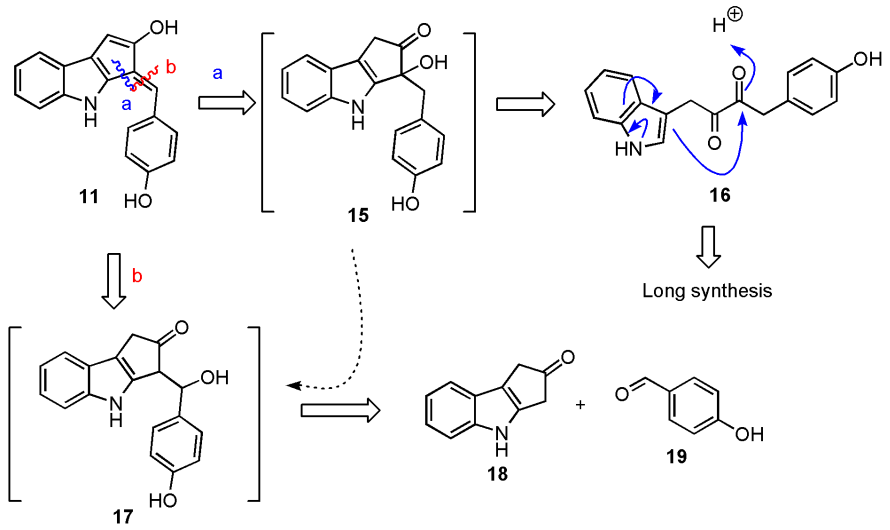

Scheme VII.5: Initially conceived synthesis of scytonemin monomer **11**

Dissection "a" represents the initially conceived approach. Dissection "b" represents the revised approach. While the biomimetic approach of "a" is attractive, the starting material **16** would require many steps to prepare.

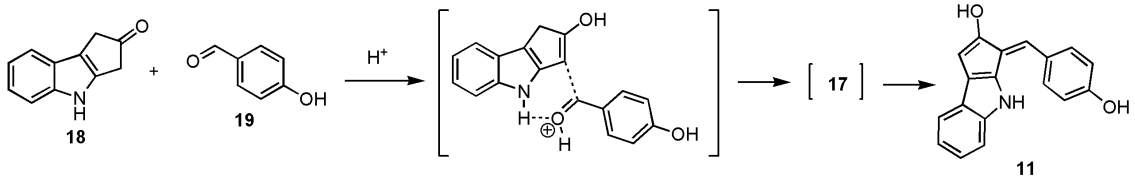

Scheme VII.6: Predicted mechanism for regioselectivity of aldol condensation between ketone **18** and aldehyde **19**

of the monomer **11** has not been established. Furthermore, it is unclear from the gene cluster analysis whether the oxidative dimerization step is enzyme-catalyzed or spontaneous under ambient conditions. The most straightforward approach to answering this question is to synthesize the putative monomer precursor. If the monomer does not dimerize spontaneously, synthetic attempts to dimerize it could provide insight into the chemistry that must occur for this important step in the biosynthesis of scytonemin (**1**).

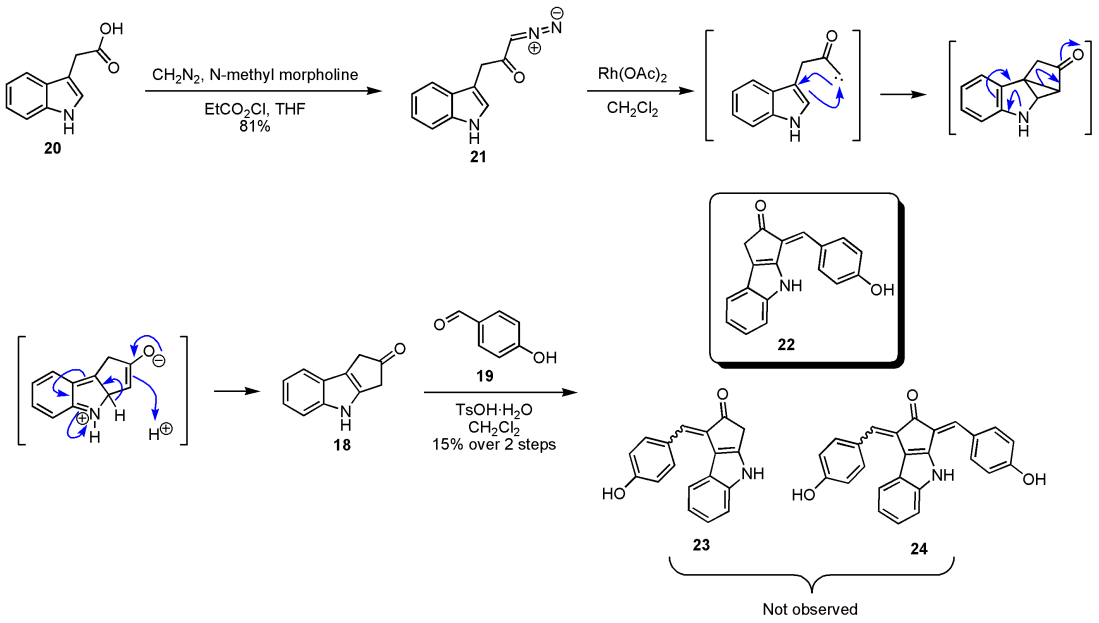

Scheme VII.7: Synthesis of scytonemin monomer

The product of the condensation of **18** and **19** was exclusively in the keto form (**22**) and not in the enol form (**11**) as predicted by others. Therefore, this product is given a new compound number (**22**).

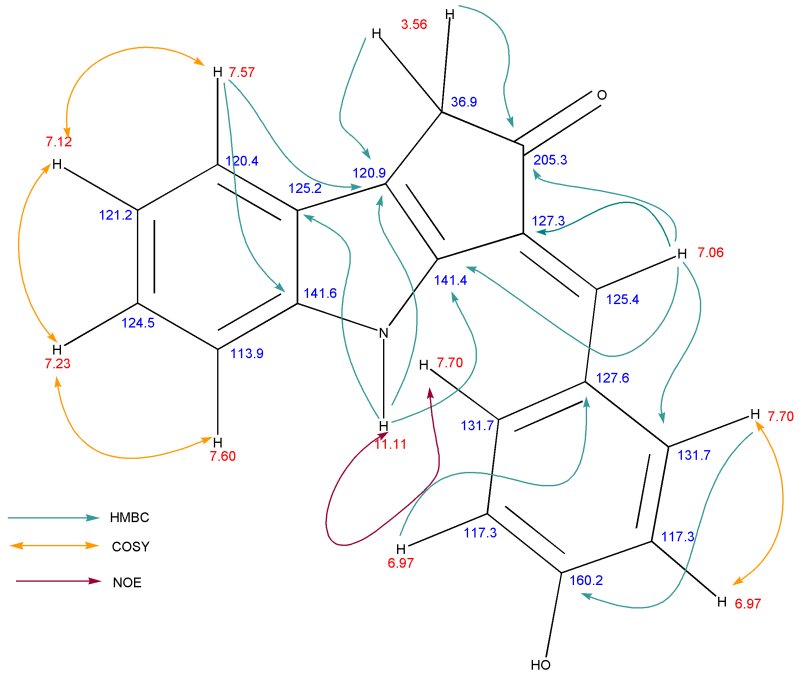

Figure VII.2: Select HMBC, COSY, and ROESY correlations of scytonemin monomer (**22**) in DMF-d_7

^{1}H NMR shifts are shown in red and ^{13}C NMR shifts are shown in blue.

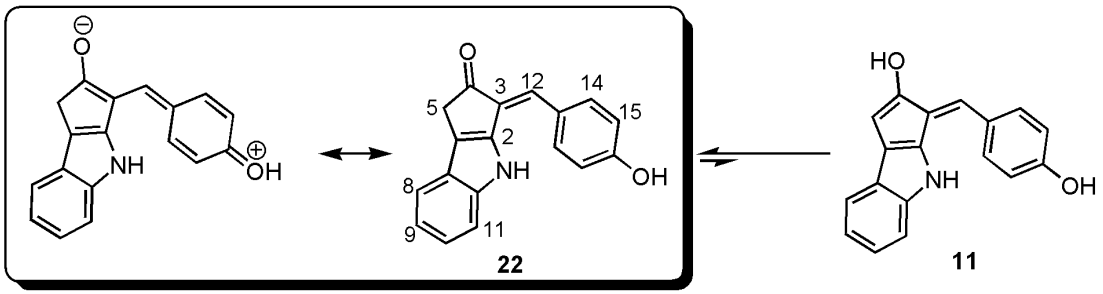

Scheme VII.8: Absence of tautomerization and resonance characteristics of scytonemin monomer (**22**)

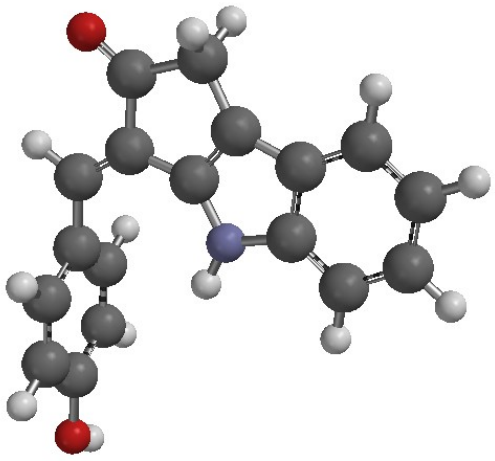

Figure VII.3: Scytonemin monomer (**22**): geometry optimized computer model

A dihedral angle constraint was placed around the single bond between the phenyl ring and the exocyclic double bond so as to keep the phenyl ring perpendicular to the tricyclic system (according to the NMR data). *Ab initio* (Hartree-Fock 3-21G*) geometry optimization was performed using Spartan®. A conformer distribution calculation at a molecular mechanics level also yielded the depicted geometry as one of the best conformers.

It has been reported that **1** possesses anti-proliferative and anti-inflammatory activities.[11] However, due to its strong metal-binding properties (especially for zinc), a pure sample of **1** could not be obtained for further biological assays. Therefore, a metal-free synthetic sample of **1** would be valuable for pharmaceutical investigation.

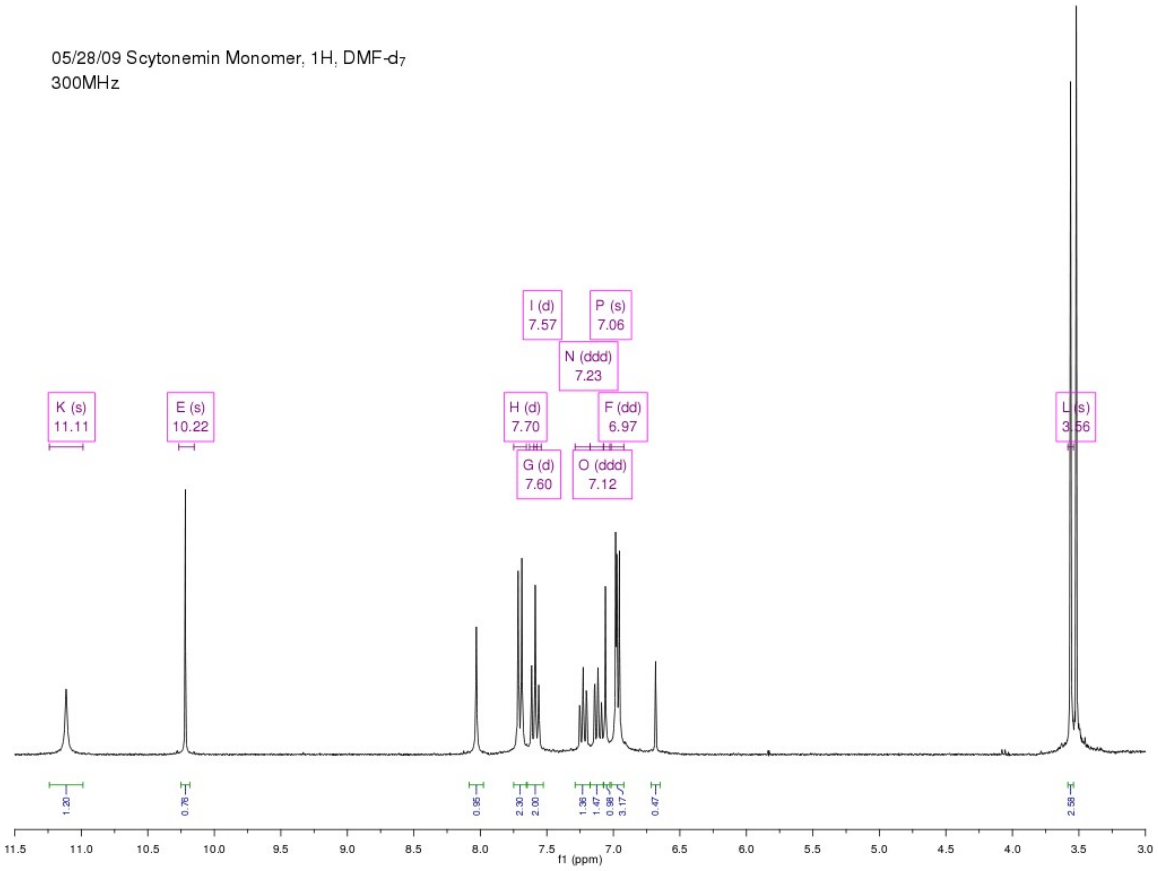

Figure VII.4: ^{1}H NMR spectrum of **22** in DMF-d_7

VII.2 Synthesis of scytonemin monomer

At the outset, a synthetic route that involves a putative biosynthetic precursor was considered for the synthesis of monomer **11** (Scheme VII.5), where diketone **16** is predicted to undergo a cyclization reaction similar to the cyclization of **8** in Scheme VII.3. However, due to the fairly large number of steps **16** would require to synthesize, another approach was conceived through the use of an alternative intermediate **17** instead of **16** (Scheme VII.5). In this strategy (dissection b), aldol condensation of ketone **18** with aldehyde **19** was envisioned. The required regioselectivity was expected based on the

predicted transition state involving a six-membered ring chelation between **18** and **19** (Scheme VII.6).

Fortunately, ketone **18** is a known compound that has been synthesized in the course of investigating rhodium-catalyzed decomposition of a diazo group.[12] Thus, the synthesis of scytonemin monomer began with indole-2-acetic acid (**20**), which was activated for acylation by ethylchloroformate and *N*-methylmorpholine to yield diazo ketone **21**. After the solvent was changed from diethyl ether (literature[12]) to THF, the yield increased to 81% from 50~60%, presumably due to the improved solubility of the starting material. The rhodium-catalyzed decomposition of the diazo group was sluggish despite the literature precedence,[12] and the product (**18**) was somewhat unstable during purification. This material (**18**) slowly converts to a pink-purple compound that further converts to an insoluble blue material upon standing in solution. The identity of these colored compounds could not be determined due to their lack of solubility.

The aldol condensation of **18** and **19** was performed by refluxing in a Soxhlet extractor equipped with a plug of glass wool and 3 Å molecular sieves for removal of water.[13] Catalysis by toluenesulfonic acid appeared to have proceeded as predicted (Scheme VII.6) and the other possible regioisomer (**22**) and over-condensed product (**23**) could not be found in the reaction mixture. The major product's color was bright yellow in a dilute solution and bright orange when dried. This solid had good solubility in DMF and DMSO, moderate solubility in pyridine and MeOH, and somewhat poor solubility in CH_2Cl_2 and EtOAc, and was insoluble in diethyl ether, hexane, and water. This material's structure was fully elucidated by NMR and HR-MS analyses (Figure VII.2). It should be noted that it was difficult to remove all of the unreacted 4-hydroxybenzaldehyde (**19**),

and complete purification was only possible by RP-HPLC or by another round of flash column chromatography.

The regiochemistry of the site of aldol condensation was determined based on HMBC and ROESY correlations. The ROESY correlation between the indole NH proton and meta-proton on the phenol indicated that the geometry of the exocyclic double bond is *E* (Figure VII.2). The ^{1}H NMR spectra in both MeOH-d_4 and DMF-d_7 revealed that the ketone was exclusively in the keto form (**22**) and not at all in the enol form (**11**), as has been suggested by others.[5] This finding is supported by the calculated energy difference between the keto and enol forms (24 kcal/mol).[14] This is possibly due to both the anti-aromaticity of the cyclopentadiene in the enol form (**11**) and the electron-donating ability of the phenol and electron-withdrawing ability of the ketone (Scheme VII.8). Due to the NMR equivalence of the two pairs of protons on the phenol moiety (H-14, H-14' and H-15, H-15'; see Scheme VII.9 for numbering), the phenyl ring is expected to be perpendicular to the tricyclic system, and not in direct conjugation with the rest of the molecule (Figure VII.3). Finally, the color of a solution of **22** could be changed to bright red when treated with a base (Figure VII.4). Upon neutralization, the color of the solution changed back to bright yellow and a TLC analysis showed that **22** was intact.

VII.3 Oxidative dimerization of scytonemin monomer

Now with the monomer **22** available, oxidative dimerization was all that was necessary for the total synthesis of scytonemin (**1**). Once the methylene carbon in **22** becomes oxidized to a methine (**25**), tautomerization should be able to render that carbon

both electrophilic and nucleophilic (Scheme VII.9). This dual property of **25** may promote spontaneous dimerization.

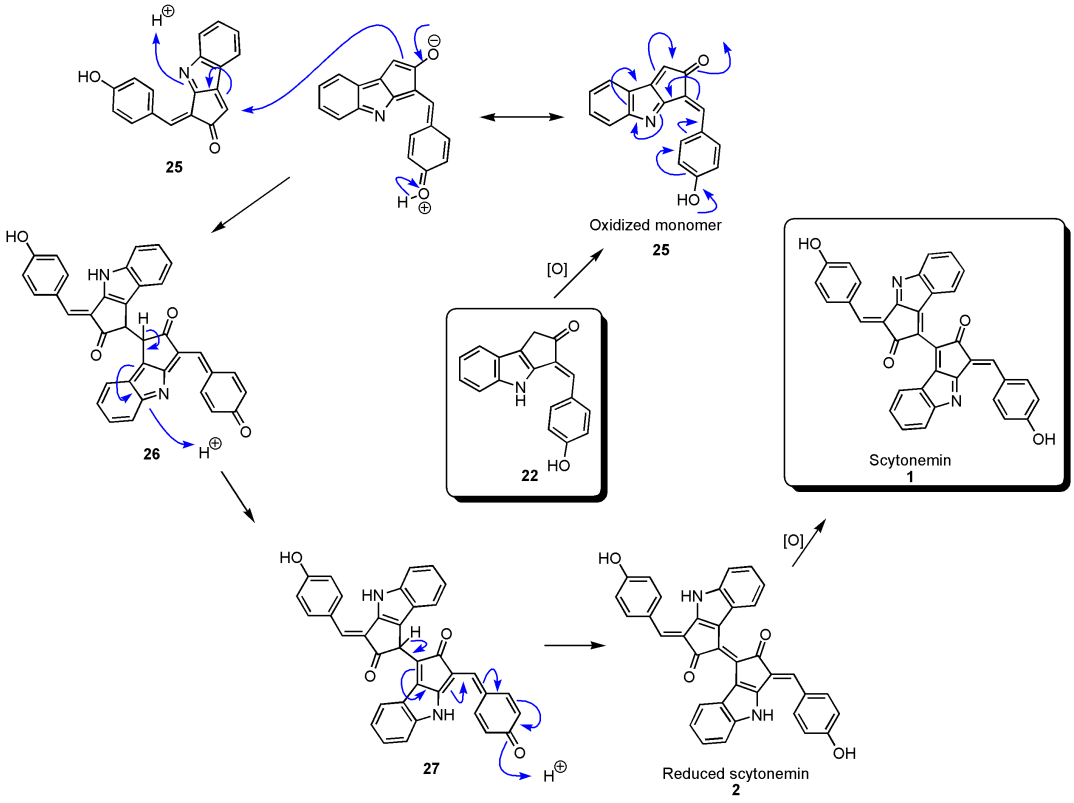

Scheme VII.9: Proposed mcehanism for dimerization of oxidized monomer **25** to reduced scytonemin **2**

Note that the conversion of **2** to **1** is known to occur spontaneously under ambient conditions.[2]

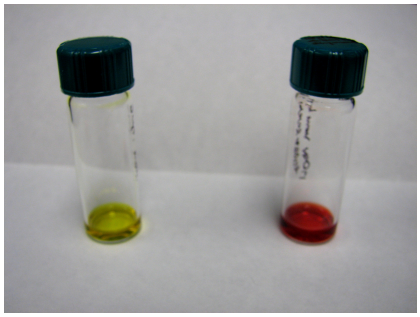

Figure VII.5: pH-dependent color change of monomer **22**

Left: a solution of **22** in MeOH. Right: a solution of **22** in MeOH that was treated with NaOH.

Inspired by the above hypothesis, **22** was initially subjected to naturally-occurring oxidative conditions, such as O_2, UV light, and the combination thereof to oxidize the methylene carbon selectively. However, even after prolonged exposure to aerial O_2 and UV light (1 week), the monomer **22** remained intact (entry 1 in Table VII.1). Therefore, it was concluded that either this oxidative dimerization step is a non-spontaneous enzymatic reaction or the oxidation of the methylene carbon occurs earlier in the biosynthesis of **1**.

In order to evaluate the two possible hypotheses, an isotope-labeled monomer (**22**) could be synthesized and fed into scytonemin-producing organisms, such as *Nostoc punctiforme*, to look for incorporation of the labeled monomer. The synthesis of **22** was repeated with [1-^{13}C] 4-hydroxybenzaldehyde[15] for the feeding study (see Scheme VII.7).[16] If incorporation occurs, it could be concluded that **22** is a true biosynthetic intermediate and that oxidation of the methylene carbon does not happen earlier in the biosynthesis. If incorporation does not occur, nothing can be firmly concluded due to the possibility that **22** cannot cross the cell membrane of the cyanobacterium.

Table VII.1: Oxidative dimerization conditions

Entry	Reagents	Result
1	UV light, air, MeOH	No Rxn
2	O_2, MeOH	No Rxn
3	Fe(III) citrate, pyridine, H_2O_2	No Rxn
4	MeOH, NaOCl	Decomp.
5	*m*-CPBA, MeOH	No Rxn
6	$Ce(SO_4)_2$, H_2SO_4	No Rxn
7	NCS, MeOH	No Rxn
8	Phosphomolybdic acid, MeOH	Green soln, but no desired products (**1** or **2**) by LCMS
9	CrO_3, AcOH, THF, H_2O	Decomp.
10	Base, $Cu(RCO_2)_2$, THF[17]	Green products, but no desired products (**1** or **2**) by LCMS
11	NaOH, DMSO, $AgNO_3$	Same mass as nostodione (**3**), but ^{1}H NMR did not match
12	DDQ, THF	Trace amount of **2** by LCMS
13	$Pd(OAc)_2$, O_2, DMSO	Mostly decomposition, but a trace of **1** was observed by LCMS
14	$Pd(OAc)_2$, O_2, pyridine	Most of **22** remained intact, the remainder decomposed
15	Fremy's salt	Decomp.
16	1. formylation 2. diazonization 3. $Rh_2(OAc)_4$	Unknown products
17	SeO_2, DMSO	Decomp.
18	$(PhCO)_2Se$, DMSO	Decomp.
19	ZrO_2, air, MeOH/DMF	
20	Rose bengal, UV, air, DMF	

Given the knowledge that the monomer **22** does not spontaneously oxidize under ambient conditions, various oxidizing reagents were tested for selective oxidation of **22** as shown in Table VII.1. These reaction conditions included two-electron oxidants, such as hypochlorite, *N*-chlorosuccinimide, *m*-chloroperbenzoic acid and one-electron oxidants, such as iron (III) and dichloro-dicyanobenzoquinone. However, none of these conditions yielded scytonemin (**1**) or its reduced form (**2**) in amounts detectable by LCMS or ^{1}H NMR except for entry 13, but because the detected amount was so little, the presence of **1** in the reaction mixture could not be unequivocally established. Moreover, even after most of **22** decomposed in this $Pd(OAc)_2$ catalyzed reaction, a significant amount of **22** was still intact, which presumably meant that oxidative decomposition of **1** (if it was formed at all) was much faster than oxidative dimerization of **22**.

In light of these failed reactions, it was hypothesized that at least some of the failed oxidation reactions were due to chemoselective oxidation of the phenol and not the cyclopentenone of **22**. This hypothesis seemed reasonable due to the electron-rich nature of the phenolic ring upon deprotonation. To overcome this potential problem, a methylated version of **22** was synthesized according to Scheme VII.10. However, even

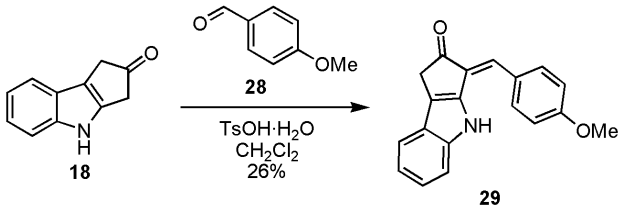

Scheme VII.10: Synthesis of methylated monomer **29**

Note that the yield could be increased to ~70% if a significant excess of **28** was used. However, the chromatographic purification became increasingly difficult due to the unreacted **28**, which almost completely coeluted with **29**.

this methylated monomer **28** could not be oxidatively dimerized under various conditions. A significantly different synthetic approach was clearly necessary.

In the gene cluster for the biosynthesis of **1** (Scheme VII.2), there are a few genes whose roles are not clearly understood in light of the proposed biosynthesis (Scheme VII.3). For example, NpR1270 (a putative glycosyltransferase) may or may not be involved in the dimerization step. One hypothesis has been brought forth in P. Proteau's thesis as follows. The enzyme from NpR1270 is hypothesized to glycosylate the ketone oxygen, converting the keto form to the enol form, and the glycosylated enol is transported across the cell membrane to be transported into the extracellular sheaths,

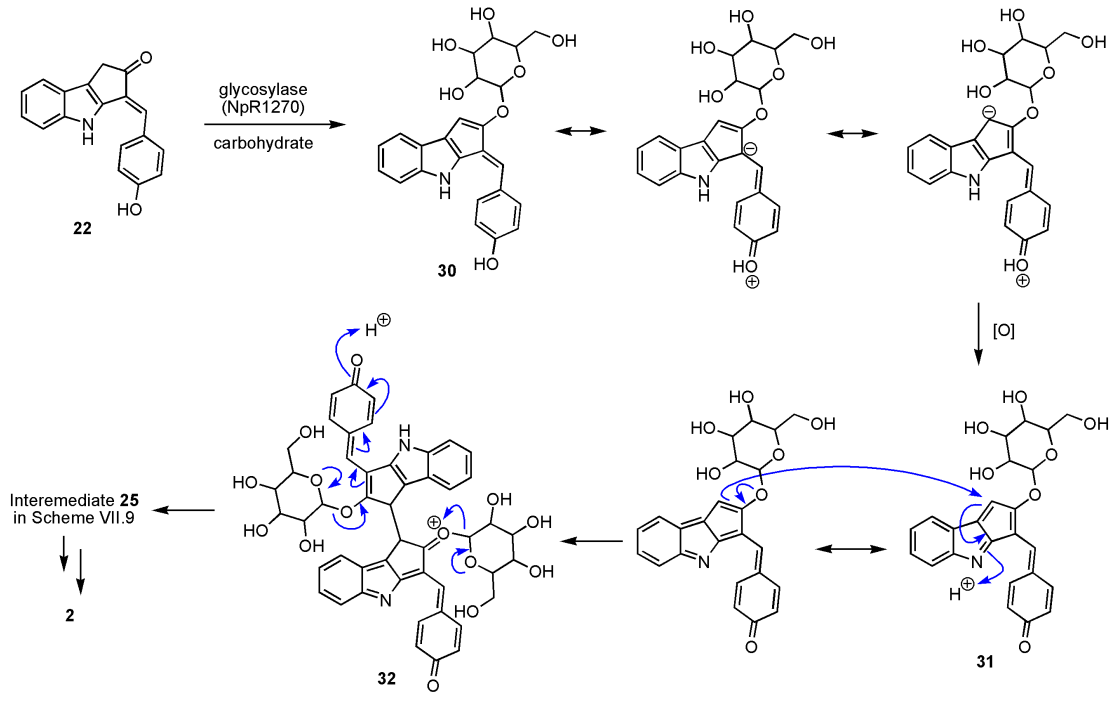

Scheme VII.11: Possible role of glycosylation in the biosynthesis of scytonemin

In **30**, resonance forms with a negative charge on the cyclopentadiene are preferred due to creation of aromaticity, which renders the ring susceptible to oxidation due to its rich electron density. Once oxidized to **31**, dimerization could occur in the same manner as in Scheme VII.9.

where the electron-rich enol α-carbon is oxidized and coupled to another monomer molecule (Scheme VII.11).[18]

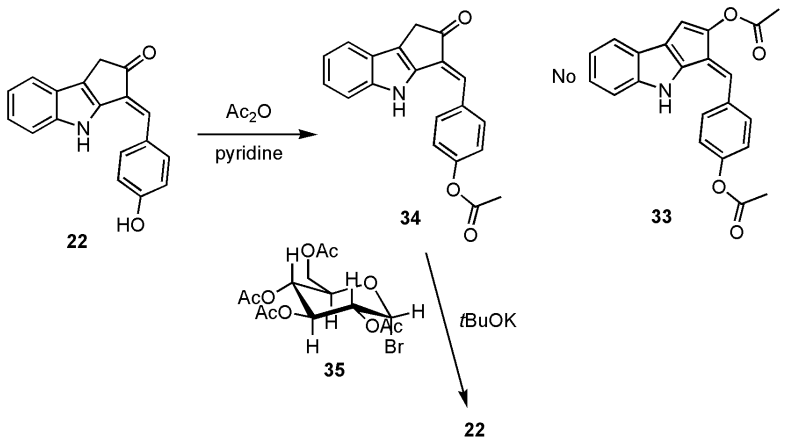

Scheme VII.12: Attempts to synthesize **30** and/or a mimic thereof (e.g. **33**)

In order to construct a mimic of the glycosylated monomer **30**, per-acetylation was attempted to form **33** (Scheme VII.12). However, the only product isolated from the reaction was a mono-acetylated monomer **34**. By taking advantage of the protection of the reactive phenolic hydroxy group in **34**, glycosylation of the corresponding enolate was attempted. It is noteworthy that there have not been rigorous synthetic studies on the glycosylation of enolate-systems even though this process appears to be widely utilized in nature.[19] Treatment of **34** with per-acetylated glucose derivative **35** and potassium *tert*-butoxide resulted in the loss of the acetyl group and reversion to monomer **22**.

Similarly, double silylation of **22** to form **36** was attempted, but it only resulted in either decomposition or mono-silylation to produce **37** (Scheme VII.14). In order to form a silyl enol ether of the ketone in **36**, it was treated with LiHMDS and TBDMSOTf. A new product was formed in this reaction, but due to its unstable nature, it could not be

isolated for full characterization. Therefore, this crude material was treated with *m*-CPBA to oxidize the α carbon. However, the resulting product showed intact methylene protons in its ^{1}H NMR spectrum.

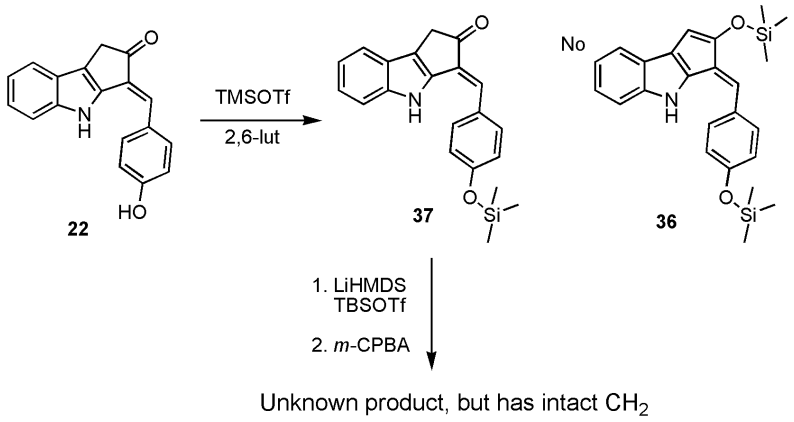

Scheme VII.13: Attempts to perform Rubottom oxidation via doubly silylation of **22**

VII.4 Chemical insights on the biosynthesis of scytonemin

After repeated failure to dimerize **22**, the legitimacy of the structure of scytonemin **1** was questioned. While the HMBC correlations noted by Gerwick et al. are fairly conclusive, they leave some room for three additional possibilities (Figure VII.6).[20] Particularly, the structure **38** is interesting because reduction and ozonolysis of **38** in the same manner as the conversion of **1** to **2** would also result in the formation of nostodione (**3**). However, there is no other way to evaluate these structures unless they are actually synthesized and their spectral data are compared with the authentic compound, which was not feasible due to time constraints.

Subsequently, the intermediacy of **22** was also questioned. Given that **22** cannot assume the enol form to enrich the electron density on C-5, presumably due to the consequential anti-aromaticity (Scheme VII.8), selective oxidation of C-5 is not readily realizable. To eliminate the anti-aromaticity problem and to be able to convert C-5 to sp^2 hybridization, a carbon other than C-5 in the cyclopentenone ring could be converted to an sp^3 carbon, thereby breaking the conjugation of the system. For example, the reason for the ketone **18** being able to undergo an aldol condensation via acid-catalyzed enolilzation is likely owing to the non-conjugated nature of the enol form of the cyclopentenone ring. The most feasible site of oxidation level change is the carbonyl carbon in the cyclopentenone ring. Thus, the synthesis of **22** was modified for the preparation of cyclopentene-ol **43** (Scheme VII.14). The execution of this synthesis is ongoing at the time of this writing.

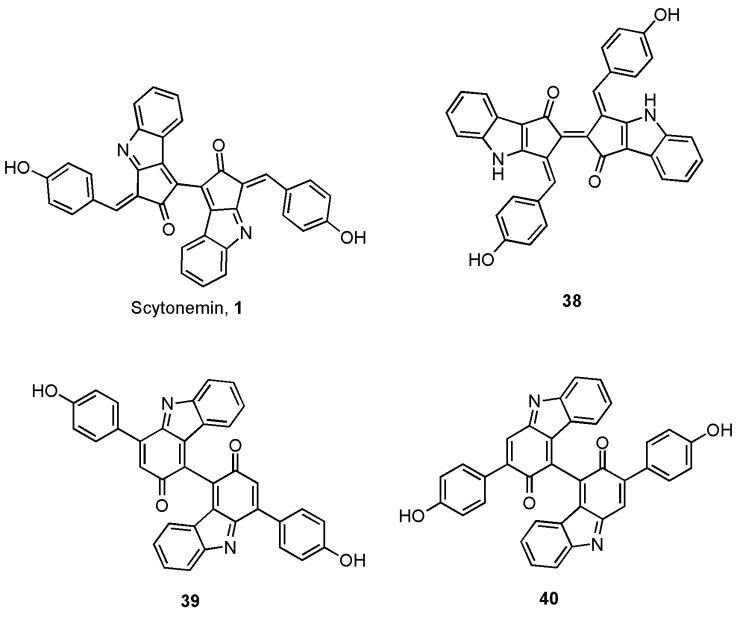

Figure VII.6: Alternative structures for scytonemin

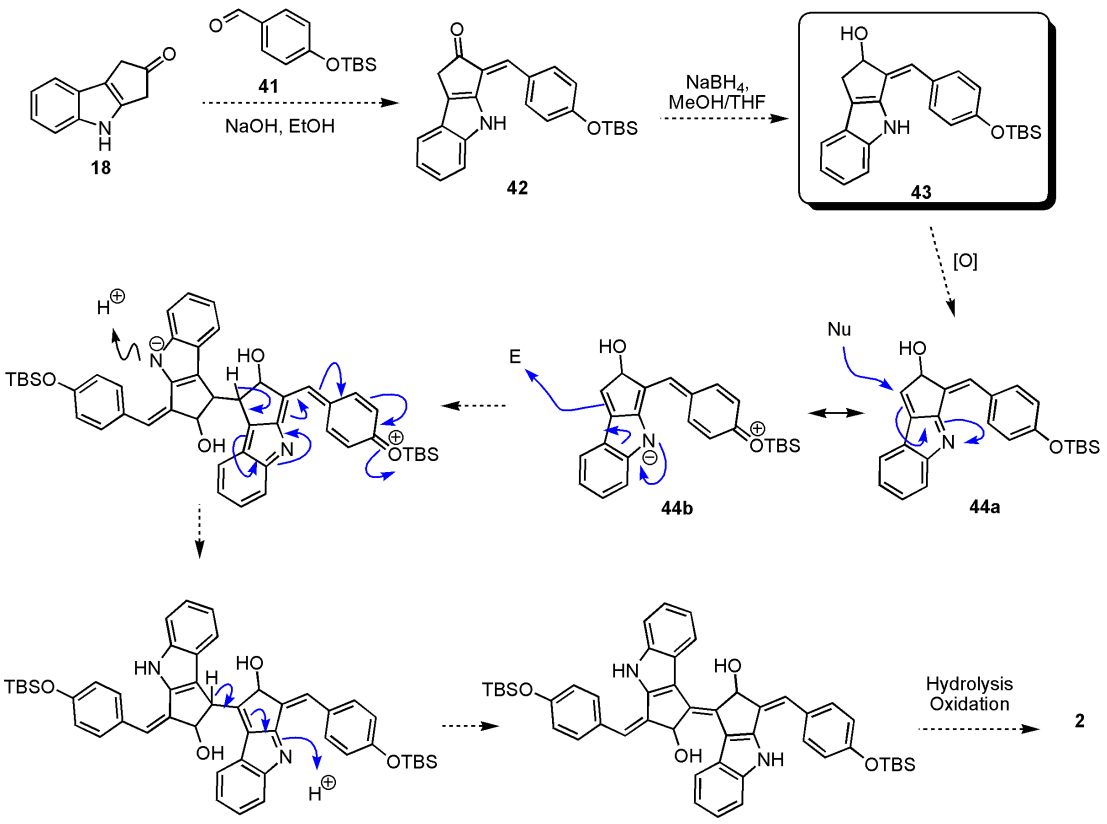

Scheme VII.14: Newly proposed route for the synthesis of **2**

Neither **44a** or **44b** suffers from anti-aromaticity. However, an important resonance form of **25** suffers from anti-aromaticity (Scheme VII.9), and it may not be possible to synthesize **25** at all. If this route is successful, credence to the intermediacy of desilylated version of **44** will be provided.

Incidentally, the desylilated version of **43** is identical to a biosynthetic intermediate (**10**) proposed by Balskus and Walsh (Scheme VII.4).[5] It is perfectly reasonable to propose that **10** is the true monomeric precursor, and not **22**, provided that C-5 of **10** is readily oxidizable (Scheme VII.14). Therefore, chemical investigations of **43** and/or **10** are expected to provide evidence for or against the alternative intermediacy of **10**. Moreover, while enolate-glycosylation of **34** was not possible, the same transformation may be possible for **42**, which would allow access to glycosylated

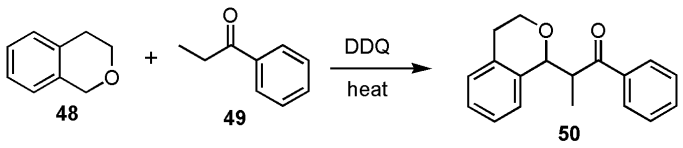

Scheme VII.15: Chemo-selective oxidation of benzylic ether by DDQ in a neat mixture

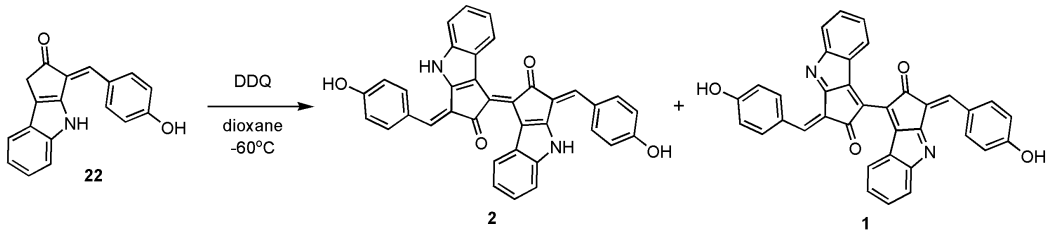

Scheme VII.16: Completion of total synthesis of scytonemin albeit very low yield

monomer **30**. Testing for incorporation of ^{13}C-labeled **30** as well as the desilylated version of **43** would be of interest with regard to the evaluation of the putative glycosylase (NpR1270) in the biosynthesis of scytonemin.

VII.4 Completion of the total synthesis of scytonemin

As seen in entry 12 of Table VII.1, treatment of **22** with DDQ produced trace amounts of **1** and **2**. The presence of these two compounds was detected by RP-HPLC coupled with ESI-MS, in which the retention time and mass spectra of **1** and **2** were matched with the crude reaction products. However, the integration of the peaks corresponding to **1** and **2** were too small to be certain that they were not due to some background noise. DDQ oxidation of a methylene carbon attached to C-3 of indole is

well known in the literature (Scheme VII.15).[21] Therefore, this reaction was revisited to improve the yield so as to determine the identity of the reaction product.

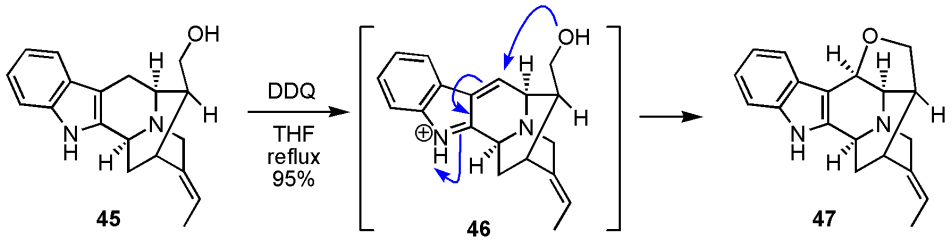

Scheme VII.17: Highly chemo-selective DDQ oxidation of (*E*)-16-epinormacusine B (**45**)

As mentioned earlier, complete purification of **22** was difficult due to **19** eluting in close proximity to **22** during flash chromatography. Therefore, many of the batches of **22** used for the oxidative dimerization studies were contaminated with significant amounts of **19**. In order to avoid any possible side reactions involving **19**, such as reduction of the oxidant by **19**, fine-tuned flash column chromatography conditions (1:19 to 1:4 THF / hexanes) were developed to completely purify **22**. Moreover, being inspired by Li and coworkers' work on so-called dehydrogenative coupling involving DDQ (Scheme VII.16),[22] a concentrated solution (0.44 M) of very pure **22** in 1,4-dioxane was used in this DDQ oxidation (Scheme VII.17). In this attempt, distinct chromatographic peaks corresponding to **1** and **2** were observed after flash column purification. Semi-prep HPLC purification of the reaction products is under way at the time of this writing. Due to the low yield, however, it is still thought that the alternative intermediacy of **43** is possible. It is possible that an unnatural reaction pathway with a high activation energy is operating in the DDQ reaction with the compound **22**.

VII.5 Conclusions

A cyanobacterial alkaloid scytonemin possesses a unique dimeric structure that raises many interesting biosynthetic questions. Through chemical synthetic investigations of this alkaloid, a few important insights into its biosynthesis were obtained. The biosynthetic precursor proposed by Walsh (**11**) was found to be a structure that does not exist because the equilibrium between **11** (enol form) and **22** (keto form) lies exclusively towards **22**. Through various failed attempts to oxidatively dimerize **22** (although a trace amount of **1** and **2** appeared to have been produced under certain conditions), this newly proposed monomeric precursor was found to have physico-chemical properties that appear to be incompatible with the oxidation required for conversion to the natural product **1**. Therefore, if **22** is a biosynthetic precursor, its dimerization must be catalyzed by an enzyme with unusual chemical properties. An alternative conclusion from this work is that a compound other than **22** is the biosynthetic precursor. In order to further evaluate the intermediacy of **22**, a stable isotope-labeled version of it is being prepared for a feeding study. The intermediacy of an alternative precursor, such as **44**, was proposed and it is being evaluated through chemical synthesis. Finally a small yield of **1** and **2** were obtained after revisiting the DDQ oxidation of **22**. Further studies are required to improve the yield of this reaction to a meaningful level.

VII.6 Experimental Section

General

Unless noted otherwise, all materials were purchased from commercial sources and were used without further purification. Anhydrous benzene, 1,4-dioxane, and 1,2-dichloroethane were purchased from EMD. Anhydrous *N*,*N*-dimethylformamide was purchased from Acros. Tetrahydrofuran (THF) was distilled from sodium / benzophenone. Pyridine, Et_3N, and CH_2Cl_2 were distilled from CaH. Ac_2O was distilled from quinone. $CHCl_3$ was passed through a column of basic alumina activity I. All reactions were carried out under dry argon atmosphere unless otherwise noted. Reaction temperatures herein recorded are external temperatures unless otherwise noted. Flash chromatorgraphy was performed using EMD silica gel (230-400 mesh) in all cases.[23] Thin layer chromatographic (TLC) analysis was performed using EM Science pre-coated silica gel plates (Merck 60 F_{254}). Melting points were determined on an Electrothermal Mel-Temp device and are uncorrected. Optical rotations were measured on a Jasco P-2000 polarimeter. IR spectra were recorded on a Nicolet Magna-IR 550. NMR spectra were recorded on a Varian Inova spectrometer (500 MHz and 125 MHz, respectively for ^1H and ^{13}C), Varian Mercury spectrometer (400 MHz and 100 MHz, respectively for ^1H and ^{13}C), Varian Mercury spectrometer (300 MHz and 75 MHz, rspectively for ^1H and ^{13}C), or Varian Inova spectrometer (300 MHz and 75 MHz, respectively for ^1H and ^{13}C). ^1H and ^{13}C spectra recorded in $CDCl_3$ were referenced to the residual solvent peaks at 7.26 ppm ($CHCl_3$) and 77.0 ppm ($CDCl_3$), respectively. ^1H and ^{13}C spectra recorded in DMF-d_7 were referenced to the residual solvent peaks at 8.03 ppm ($C\underline{H}NO(CH_3)_2$) and 163.15 ppm ($CDCl_3$), respectively. High resolution mass spectra were recorded on a ThermoFinnigan MAT900XL spectrometer.

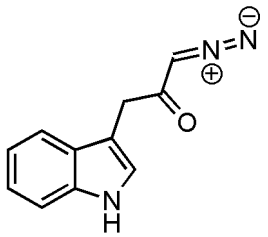

1-diazo-3-(1H-indol-3-yl)propan-2-one (21). This synthesis was done mostly according to the literature procedure[12] with minor modifications, such as the solvent and concentration. A CH_2N_2 solution in Et_2O was prepared according to a literature procedure.[24] The concentration of CH_2N_2 was determined to be 0.24 M by treatment with an excess amount of benzoic acid and back titration with NaOH in the presence of phenol red. To a solution of indole-3-acetic acid (2.500 g, 14.27 mmol) in THF (100 mL) at 0ºC were added ethyl chloroformate (1.42 mL, 14.9 mmol) and N-methyl morpholine (1.64 mL, 14.9 mmol) successively under stirring. After 15 min of stirring at 0ºC, the solution of CH2N2 was added in one portion (225 mL, 54.0 mmol). This solution was allowed to gradually warm to rt over night. A pale brown-orange solution with black tar-like residues resulted. Most of the volatiles were evaporated under a stream of N_2. The residues that dissolved in EtOAc were subjected to flash column chromatography using deactivated basic alumina (activity III) as the stationary phase (1:9 EtOAc / hexanes to 1:1) to obtain an orange oil (2.31 g, 11.6 mmol, 81% yield). TLC Rf = 0.39 (1:1 EtOAc / hexanes). 1H NMR (400 MHz, CDCl3) δ 8.64 (bs, 1H), 7.57 (d, J = 7.8 Hz, 1H), 7.36 (d, J = 8.1 Hz, 1H), 7.28 – 7.19 (m, 1H), 7.19 – 7.12 (m, 1H), 7.04 (d, J = 2.4 Hz, 1H), 5.19 (s, 1H), 3.77 (s, 2H). 13C NMR (101 MHz, CDCl3) δ 194.5, 136.2, 126.9, 123.6, 122.2, 119.7, 118.5, 111.4, 54.3, 37.9.

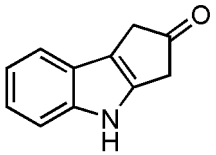

3,4-dihydrocyclopenta[b]indol-2(1H)-one (18). This synthesis was done exactly according to according to the literature procedure.[12] However, the yield was consistently lower than reported (20~40%). TLC Rf = 0.37 (3:7 THF / hexanes). ^{1}H NMR (300 MHz, $CDCl_3$) δ 8.16 (s, 1H), 7.50 (d, *J* = 7.6 Hz, 1H), 7.39 (dd, *J* = 4.7, 3.4 Hz, 1H), 7.25 – 7.12 (m, 2H), 3.54 (s, 2H), 3.53 (d, *J* = 1.0 Hz, 2H).

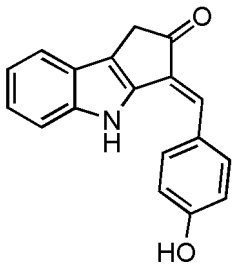

(*E*)-3-(4-hydroxybenzylidene)-3,4-dihydrocyclopenta[b]indol-2(1H)-one (22). The best overall yield was obtained when a crude mixture or **18** was used in this reaction. To a solution of the diazoketone **21** (277 mg, 1.39 mmol) in CH_2Cl_2 at rt was added $Rh_2(OAc)_4$ (6 mg, 0.014 mmol). Vigorous evolution of gas was observed. After 2 hrs, no starting material was detected by TLC analysis. A reddish orange solution resulted. The reaction mixture was filtered through a plug of silica gel, which was rinsed with 1:1 EtOAc/hexanes (100 mL). Upon removal of the solvents *in vacuo*, 155 mg of crude material was obtained (a mixture of white and orange solids). To a solution of this

material in 4:1 CH_2Cl_2/1,2-dichloroethane (10 mL) were added 4-hydroxybenzaldehyde 19 (144 mg, 1.18 mmol), toluenesulfonic acid monohydrate (16 mg, 0.080 mmol), and molecular sieves 3 Å (155 mg) at rt. This mixture was brought to reflux in a flask equipped with a condenser. After 14 hrs of refluxing, additional amounts of **19** (27 mg, 0.22 mmol) and molecular sieves 3 Å (60 mg) were added. After 4 hrs, the reaction mixture was filtered through a plug of silica gel, which was rinsed with EtOAc (200 mL). Upon concentration under vacuum, this solution was subjected to flash column chromatography (1:19 THF/hexanes to 1:4) to obtain a bright orange solid (58 mg, 0.211 mmol, 15% yield from **21** over 2 steps). Mp >210ºC. IR (film, KBr) ν_{max} 3375(br), 2963, 2921, 1712, 1599, 1483, 1441, 1274, 1231, 1165, 1123, 745 cm^{-1}. ^1H NMR (300 MHz, DMF-d_7) δ 11.11 (s, 1H), 10.22 (s, 1H), 7.70 (d, *J* = 8.5 Hz, 2H), 7.60 (d, *J* = 8.1 Hz, 1H), 7.57 (d, *J* = 8.0 Hz, 1H), 7.23 (ddd, *J* = 8.2, 7.2, 1.3 Hz, 1H), 7.12 (ddd, *J* = 7.9, 4.5, 0.6 Hz, 1H), 7.06 (s, 1H), 6.97 (dd, *J* = 6.1, 2.4 Hz, 2H), 3.56 (s, 2H). ^{13}C NMR (75 MHz, DMF-d_7) δ 205.3, 160.2, 141.6, 141.4, 131.7, 127.6, 127.3, 125.4, 125.2, 124.5, 121.2, 120.9, 120.4, 117.3, 113.9, 36.9. HRMS (EI): calcd for $C_{18}H_{13}NO_2[M^+]$: 275.0941, found 275.0945 (Δ 1.6 ppm).

(*E*)-3-(4-methoxybenzylidene)-3,4-dihydrocyclopenta[b]indol-2(1H)-one (29). This compound was synthesized in the same manner as **22**. Yellow-green solid. ^1H NMR (300 MHz, $CDCl_3$) δ 8.21 (s, 1H), 7.60 (d, *J* = 8.8 Hz, 2H), 7.55 (d, *J* = 8.0 Hz, 1H), 7.35 (d, *J* = 8.1 Hz, 1H), 7.25 (t, *J* = 7.2 Hz, 1H), 7.17 (s, 1H), 7.16 (dd, *J* = 7.4 Hz, 1H), 7.04 (d, *J* = 8.7 Hz, 2H), 3.90 (s, 3H), 3.55 (s, 2H). ^{13}C NMR (75 MHz, $CDCl_3$) δ 204.6, 160.3, 140.2, 138.8, 129.6, 128.7, 127.8, 124.3, 124.3, 120.9, 120.3, 119.8, 114.8, 111.8, 55.5,

36.5. HRMS (EI): calcd for $C_{19}H_{15}NO_2Na$ [M+Na]: 312.0995, found 312.0998 (Δ 1.0 ppm).

(*E*)-4-((2-oxo-1,2-dihydrocyclopenta[b]indol-3(4H)-ylidene)methyl)phenyl acetate (34). To a solution of **22** (21 mg, 0.076 mmol) in pyridine (200 μL) was added Ac_2O (200 μL) at rt. This solution was left at rt over night. Most of the volatiles were removed *in vacuo*, and the residues (dark orange oil) was subjected to flash column chromatography (hexanes to 1:9 acetone/hexanes) to obtain 16 mg of an yellow solid (0.050 mmol, 66% yield). TLC Rf = 0.64 (1:2 acetone/hexanes). ^{1}H NMR (400 MHz, $CDCl_3$) δ 8.29 (s, 1H), 7.64 (d, *J* = 8.7 Hz, 2H), 7.55 (d, *J* = 7.9 Hz, 1H), 7.36 (d, *J* = 8.2 Hz, 1H), 7.27 (m, 1H), 7.23 (d, *J* = 8.6 Hz, 2H), 7.16 (m, 1H), 7.14 (s, 1H), 3.56 (s, 2H), 2.36 (s, 3H). ^{13}C NMR (101 MHz, $CDCl_3$) δ 204.3, 169.5, 150.8, 139.6, 139.1, 134.0, 131.9, 129.1, 124.7, 124.0, 122.9, 122.5, 121.5, 121.0, 119.9, 112.0, 36.4, 21.2. LRMS (ESI, negative): 316 [M-H].

(*E*)-3-(4-(trimethylsilyloxy)benzylidene)-3,4-dihydrocyclopenta[b]indol-2(1H)-one (37). To a solution of 22 (40 mg, 0.145 mmol) in THF (1.1 mL) at -78ºC were added 2,6-lutidine (42 μL, 0.426 mmol) and TMSOTf (52 μL, 0.29 mmol) dropwise under stirring. After stirring for 5 min at -78ºC, the solution (orange-yellow color) was warmed immediately to rt. After stirring at rt for 3 hrs, saturated $NaHCO_3$ solution (10 mL) was added to quench, which was extracted with EtOAc (20 mL x 3). The combined organic layer was washed with H_2O (15 mL) and brine (25 mL) successively, and was dried over Na_2SO_4. This product readily decomposed to **22** on a silica gel TLC plate. Upon removal of the solvents under vacuum, 34 mg of amorphous yellow-orange solid was obtained

(0.098 mmol, 67% yield). ^{1}H NMR (300 MHz, $CDCl_3$) δ 8.26 (s, 1H), 7.55 (d, *J* = 8.3 Hz, 2H), 7.35 (d, *J* = 8.0 Hz, 1H), 7.26 (t, *J* = 7.2 Hz, 1H), 7.17 (t, *J* = 7.2 Hz, 1H), 7.16 (s, 1H), 6.99 (d, *J* = 8.6 Hz, 2H), 3.53 (s, 2H), 0.36 (s, 9H). ^{13}C NMR (75 MHz, $CDCl_3$) δ 204.6, 156.2, 140.1, 138.9, 129.6, 127.9, 125.5, 124.4, 124.3, 124.3, 120.9, 120.8, 119.8, 116.3, 111.8, 36.5, 30.3, 0.32.

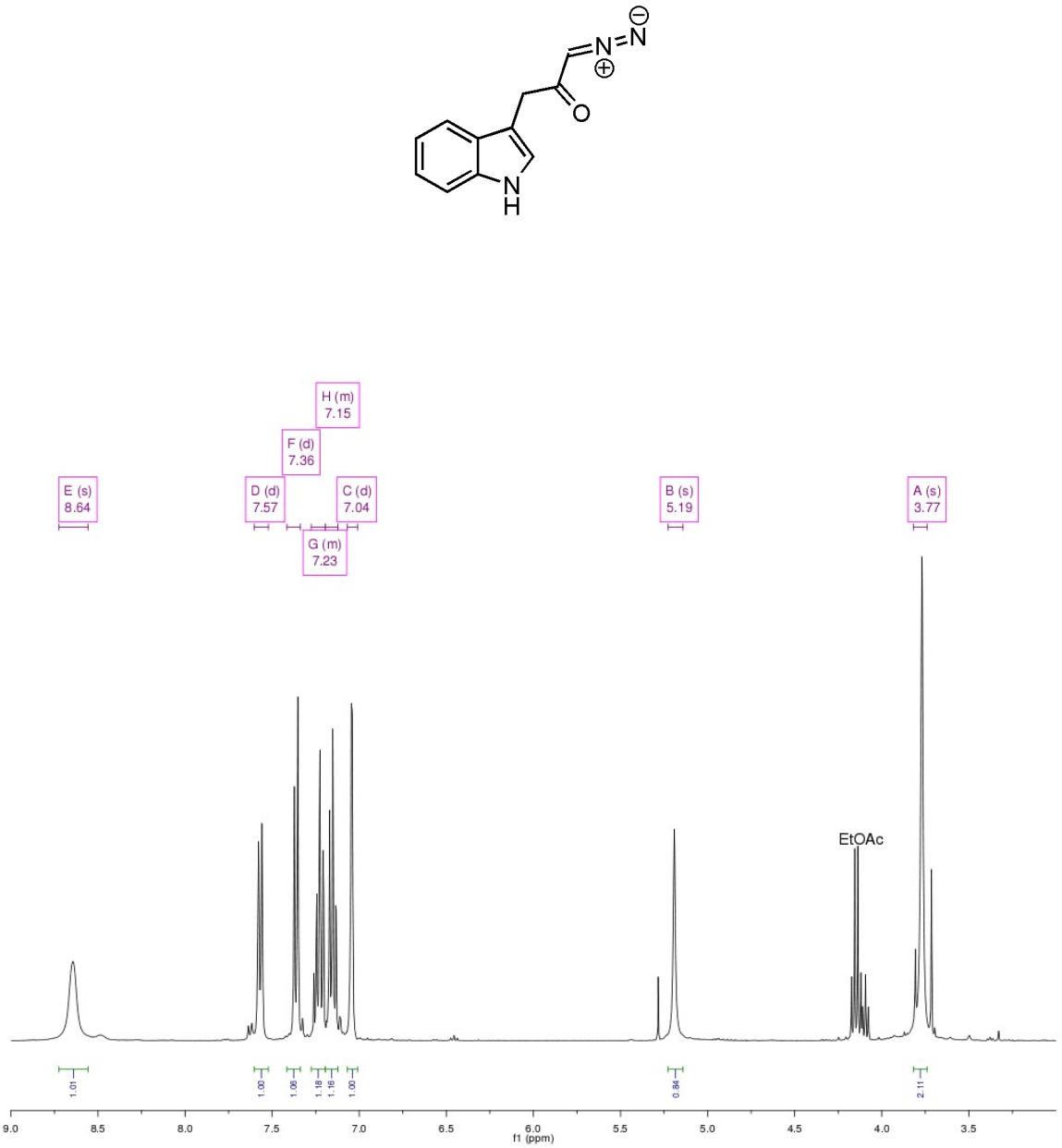

Figure VII.7: ^{1}H NMR spectrum of **21** in $CDCl_3$

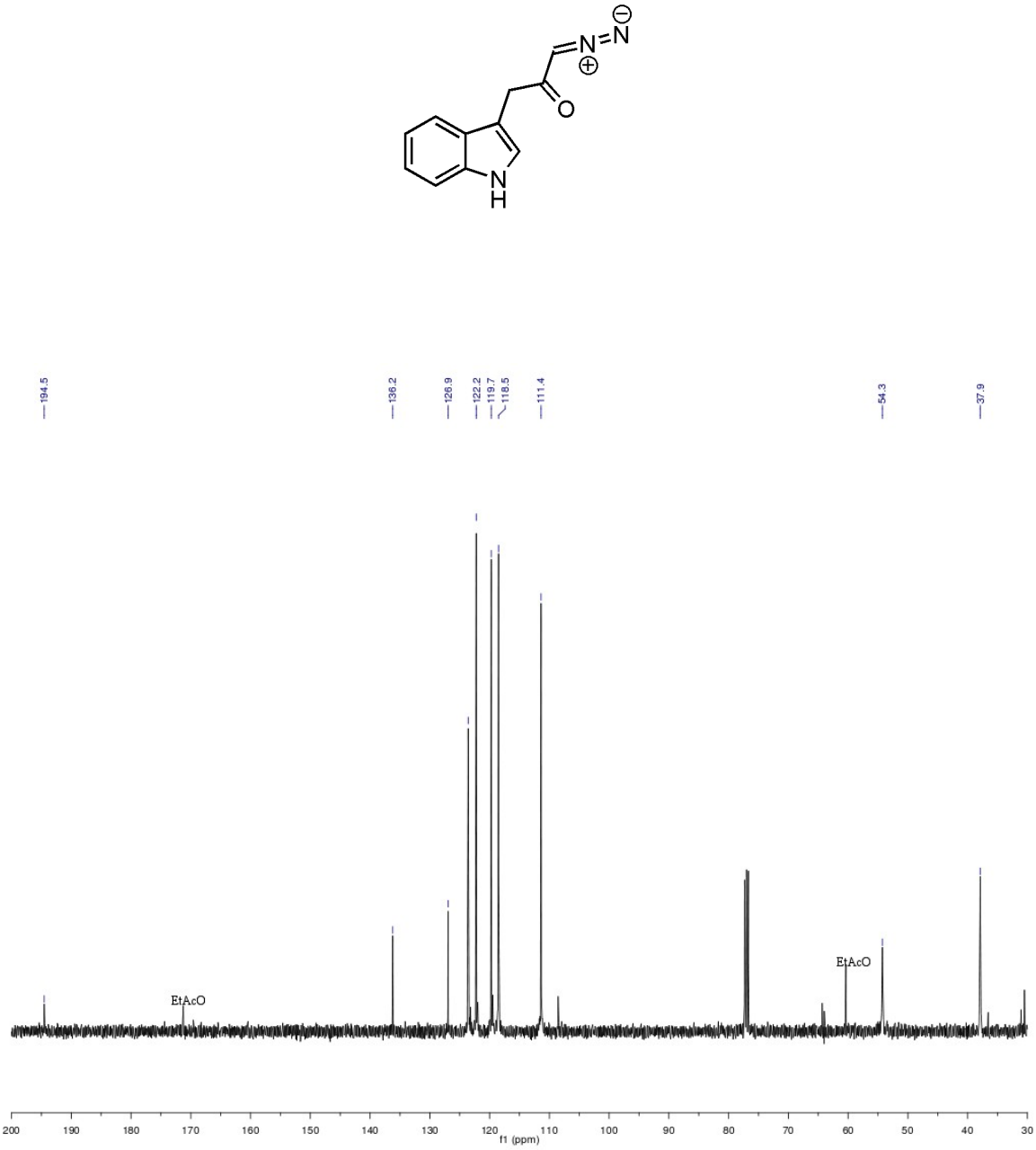

Figure VII.8: ^{13}C NMR spectrum of **21** in $CDCl_3$

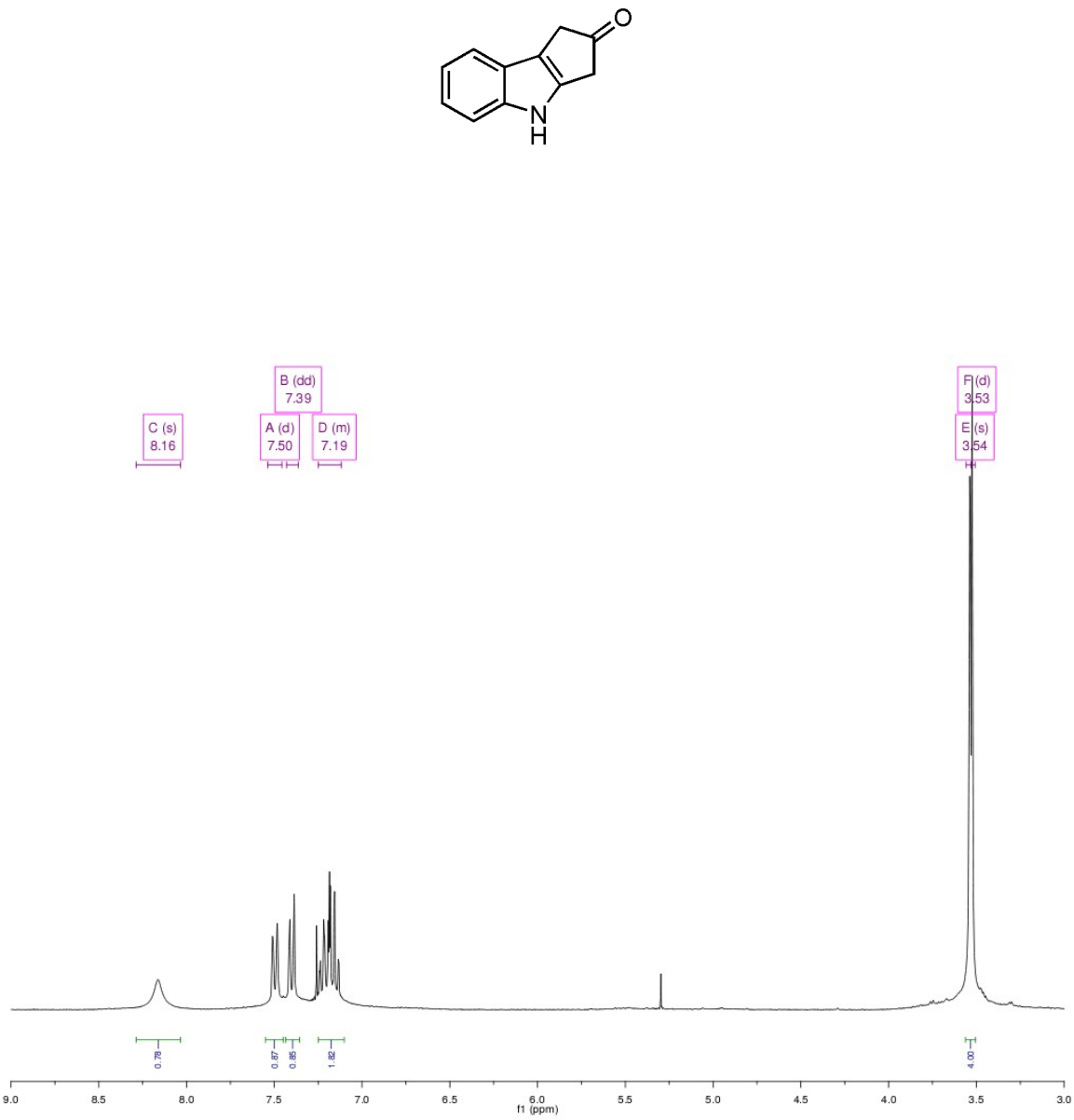

Figure VII.9: ^{1}H NMR spectrum of **18** in $CDCl_3$

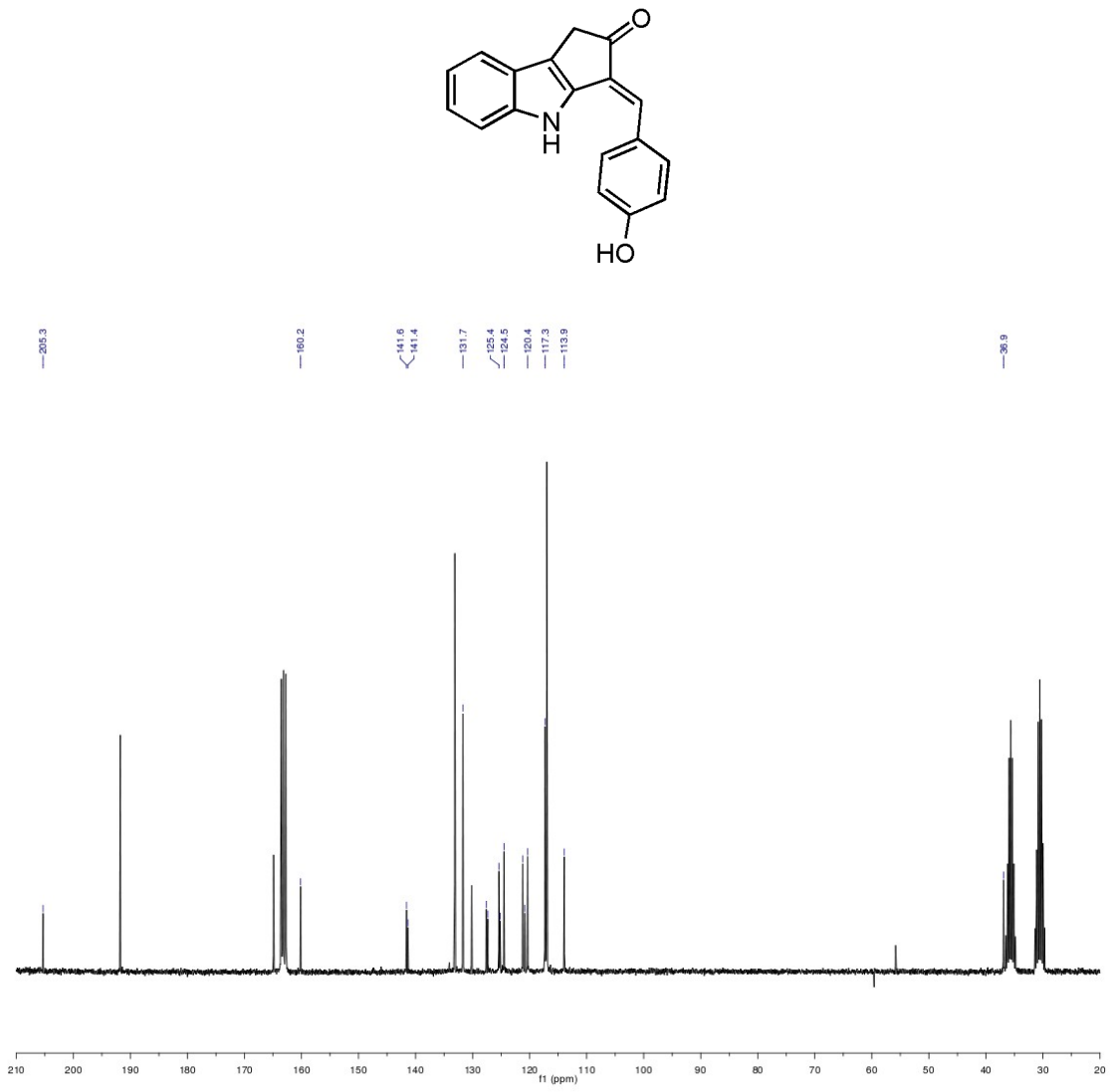

Figure VII.10: ^{13}C NMR spectrum of **22** in DMF-d_7

Note that this sample contains a significant amount of 4-hydroxybenzaldehyde (**19**), and its ^{13}C shifts include 191.8, 164.9, 133.1, 130.2, 117.0, as were established by HMBC.

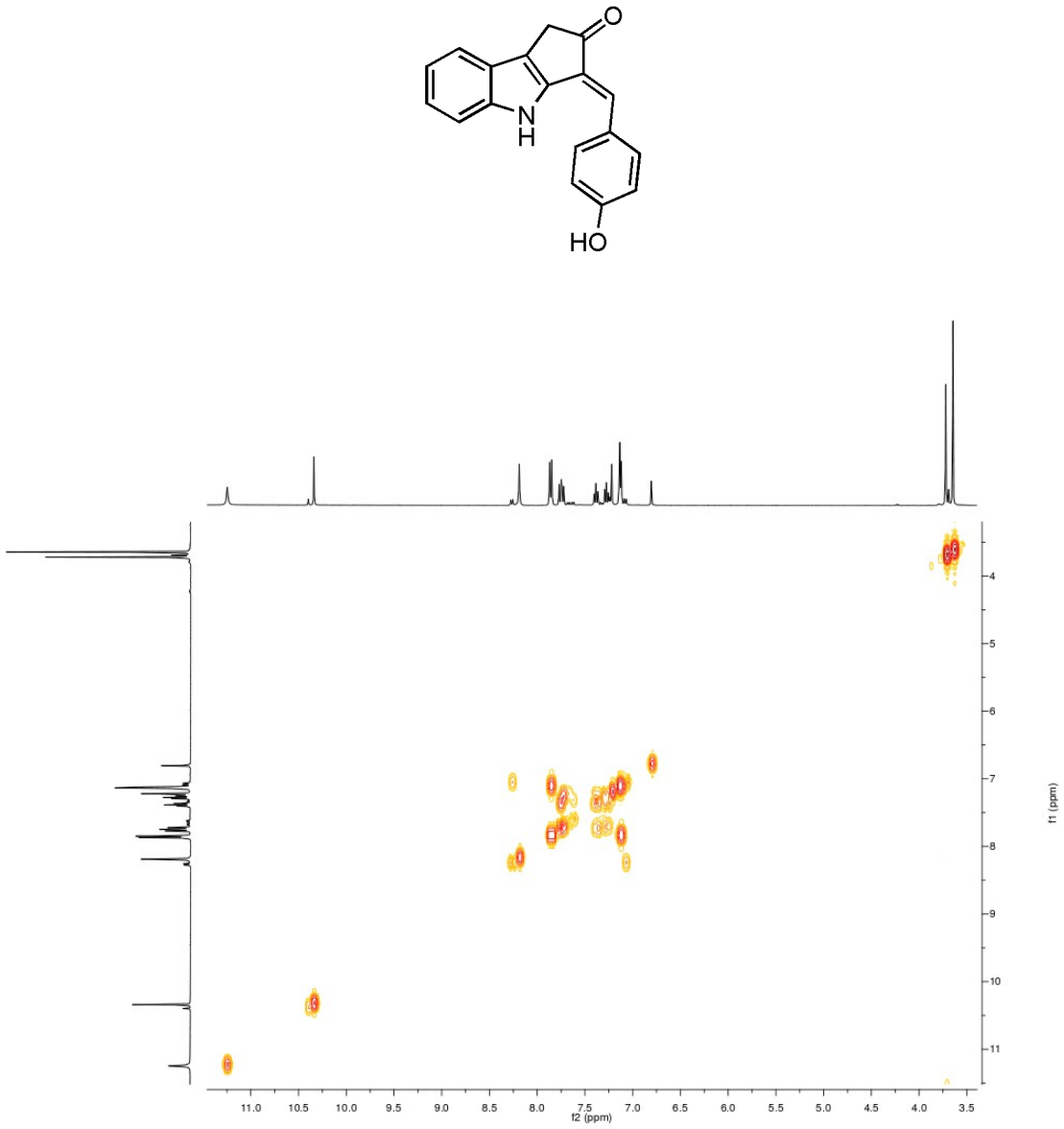

Figure VII.11: COSY NMR spectrum of **22** in DMF-d_7

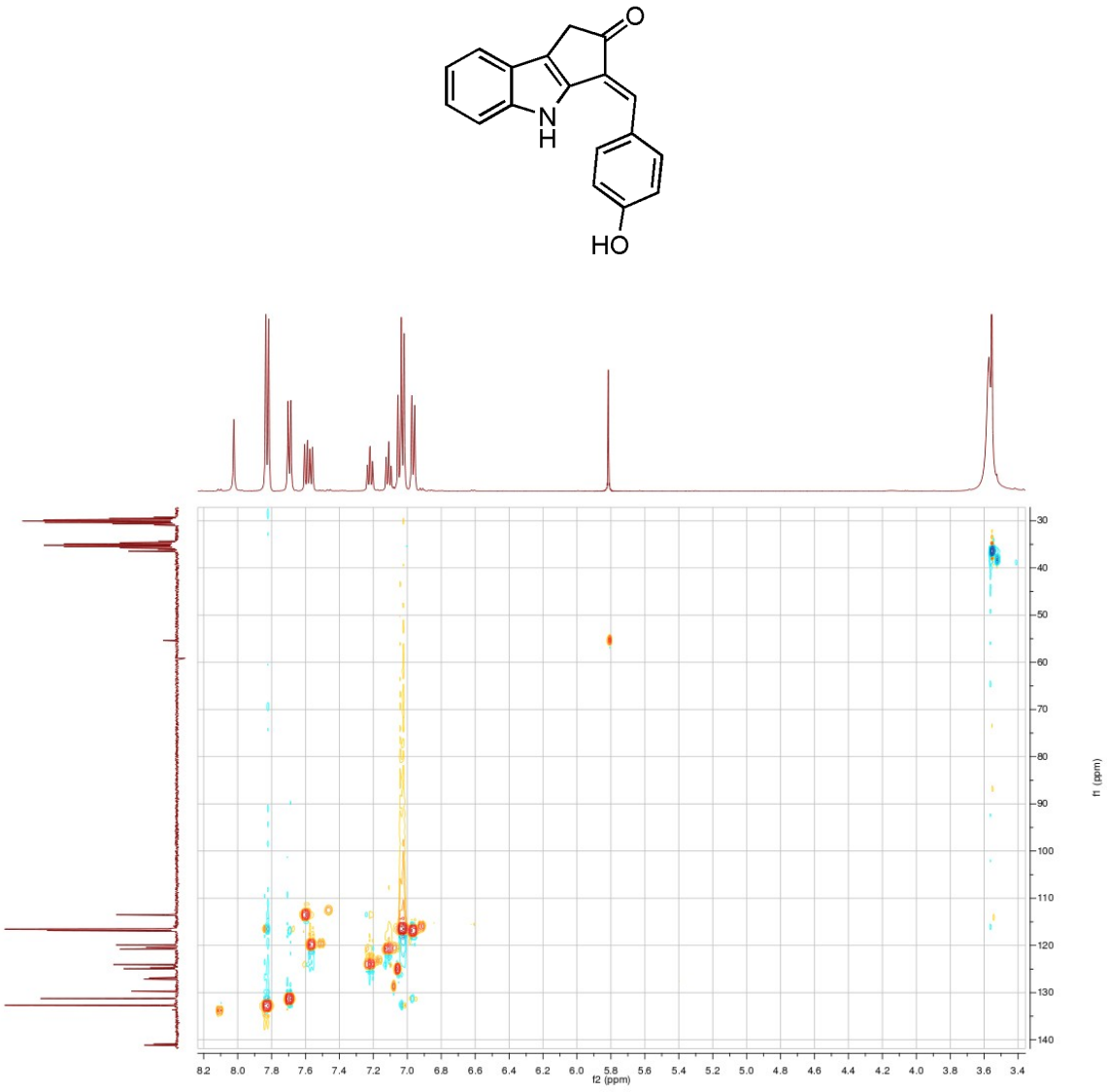

Figure VII.12: HSQC NMR spectrum of **22** in DMF-d_7

Note that this sample contains a significant amount of 4-hydroxybenzaldehyde (**19**), and its ^{13}C shifts include 191.8, 164.9, 133.1, 130.2, 117.0 ppm, as were established by HMBC. ^{1}H shifts of **19** include 9.88, 7.83, 7.04 ppm.

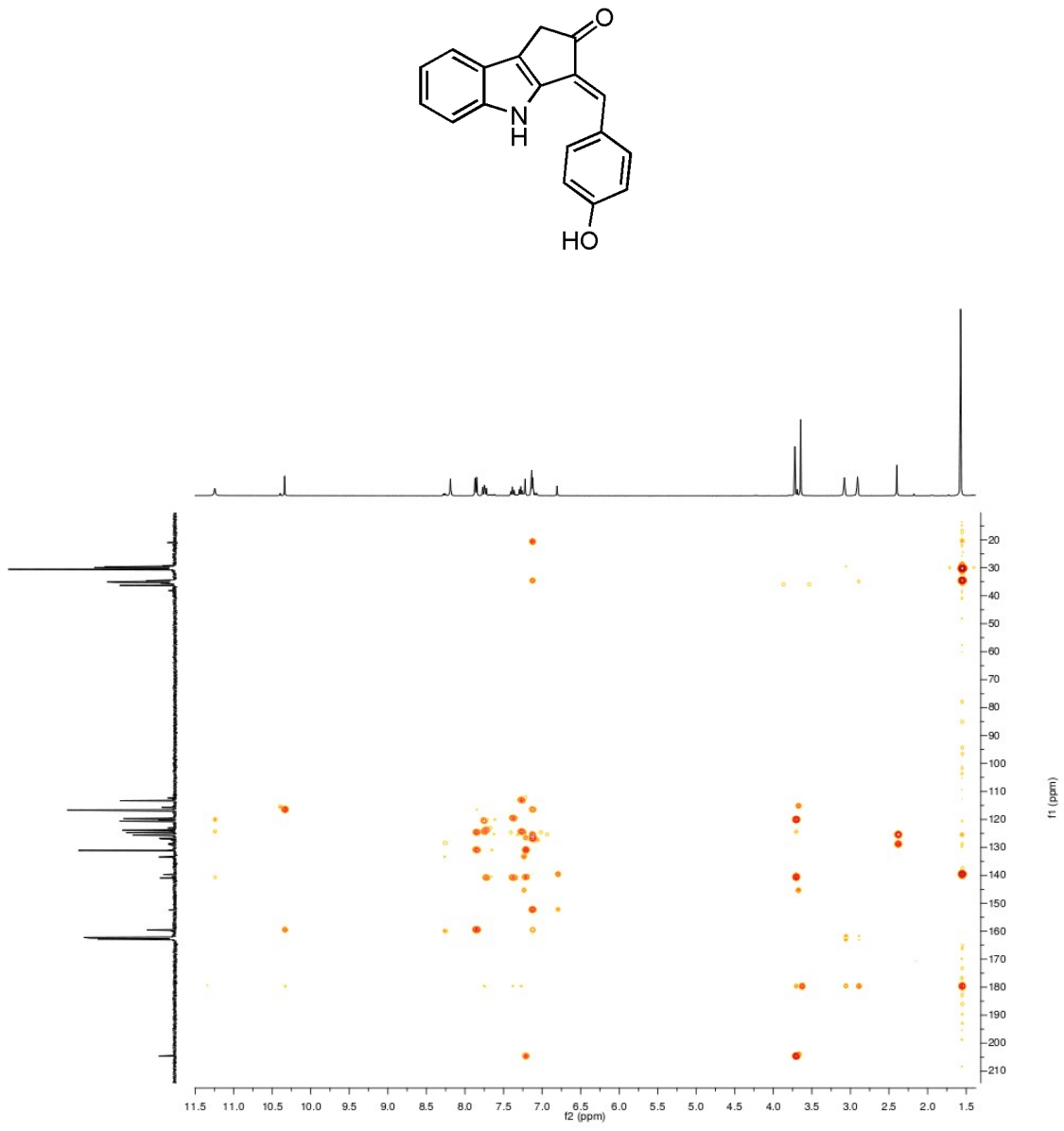

Figure VII.13: HMBC NMR spectrum of **22** in DMF-d_7

There are some impurity peaks such as the one at 1.5 ppm (^{1}H).

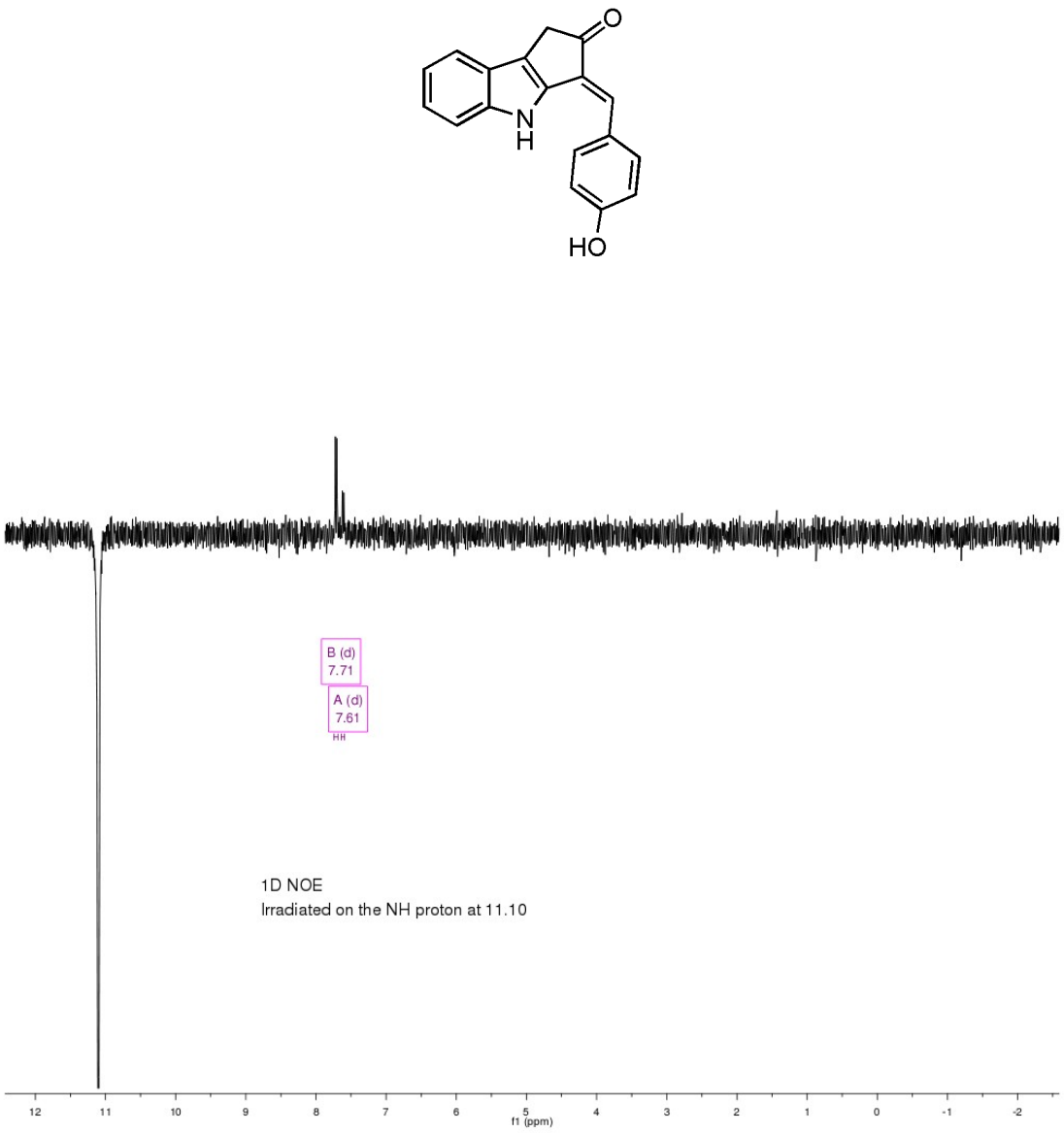

Figure VII.14: 1D NOESY NMR spectrum of **22** in DMF-d_7

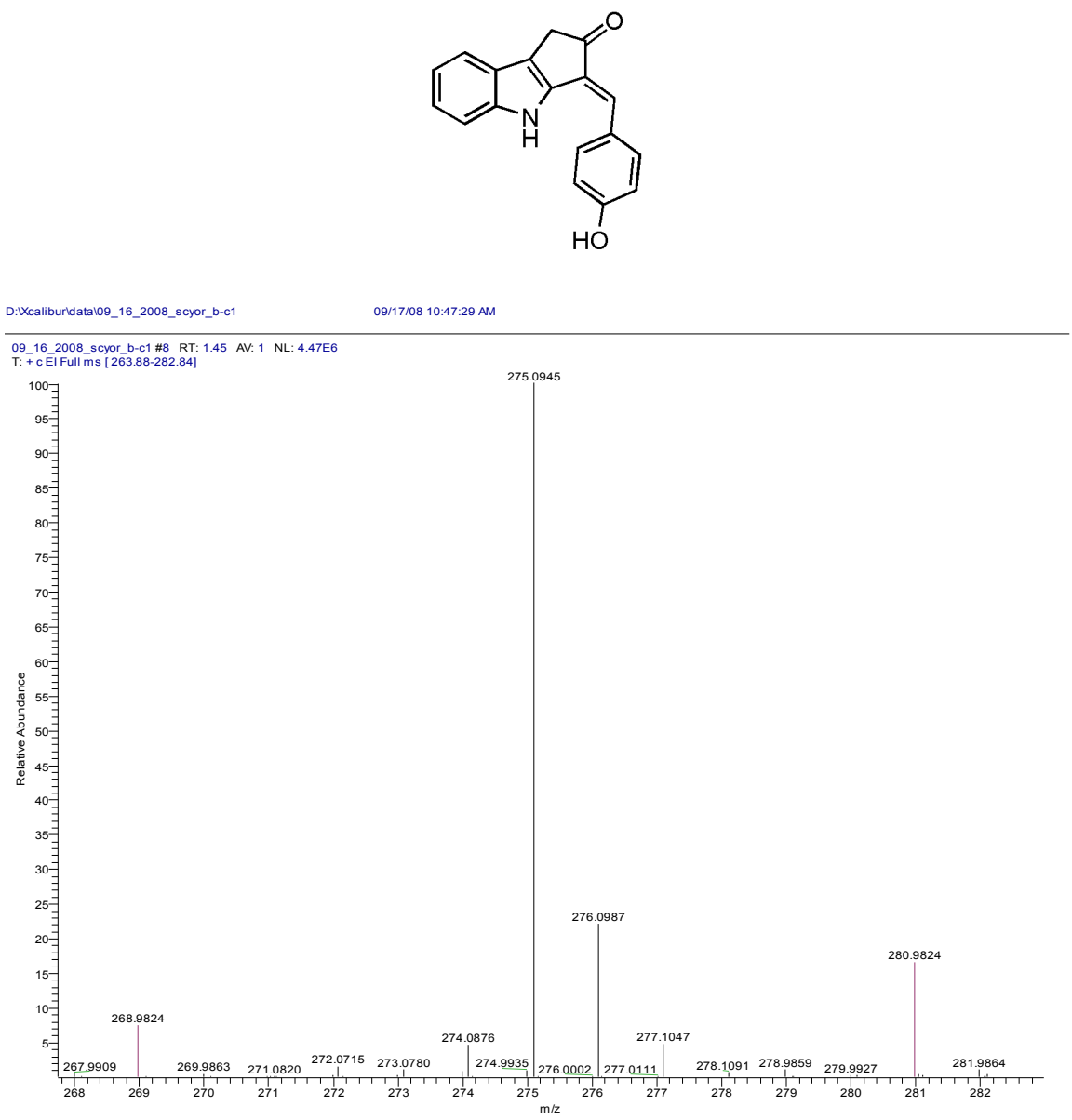

Figure VII.15: HRMS (EI) spectrum of **22**

Reference: Perfluorokerosene. Two pink lines are reference peaks.

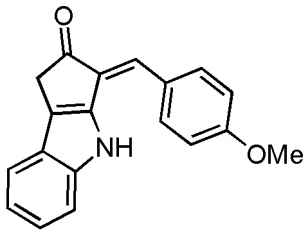

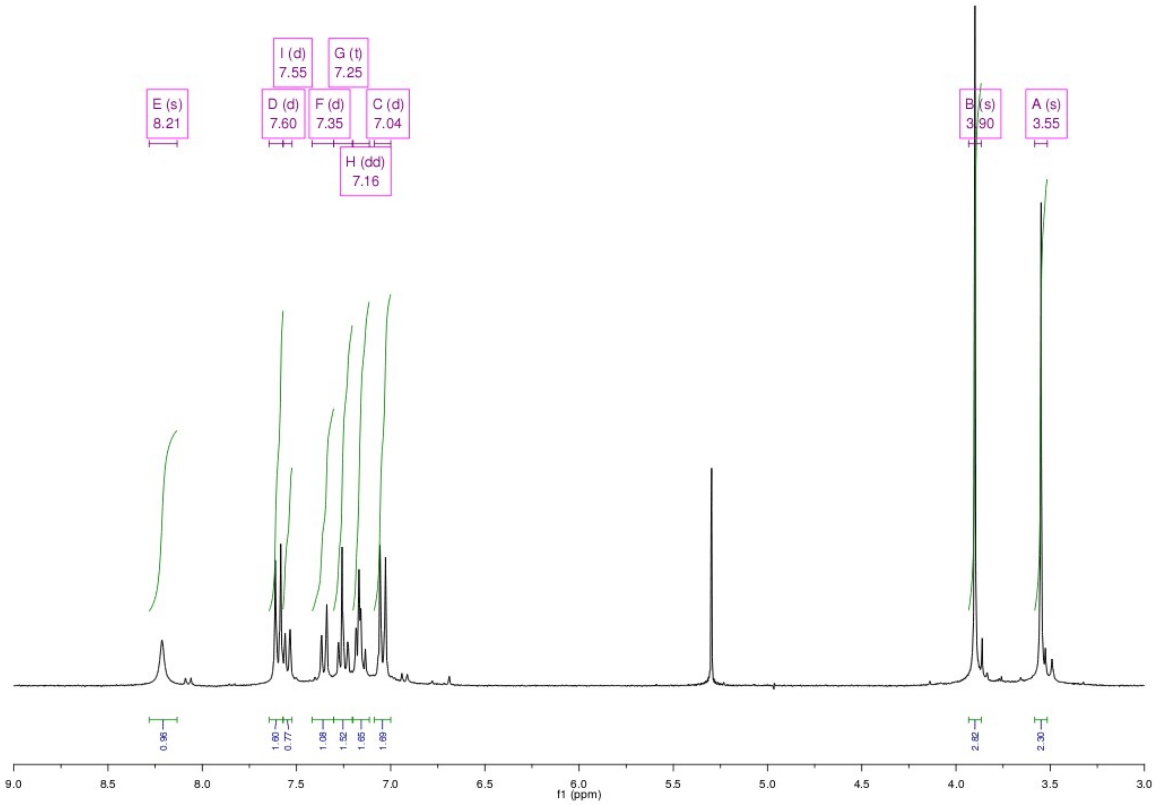

Figure VII.16: ^{1}H NMR spectrum of **29** in $CDCl_3$

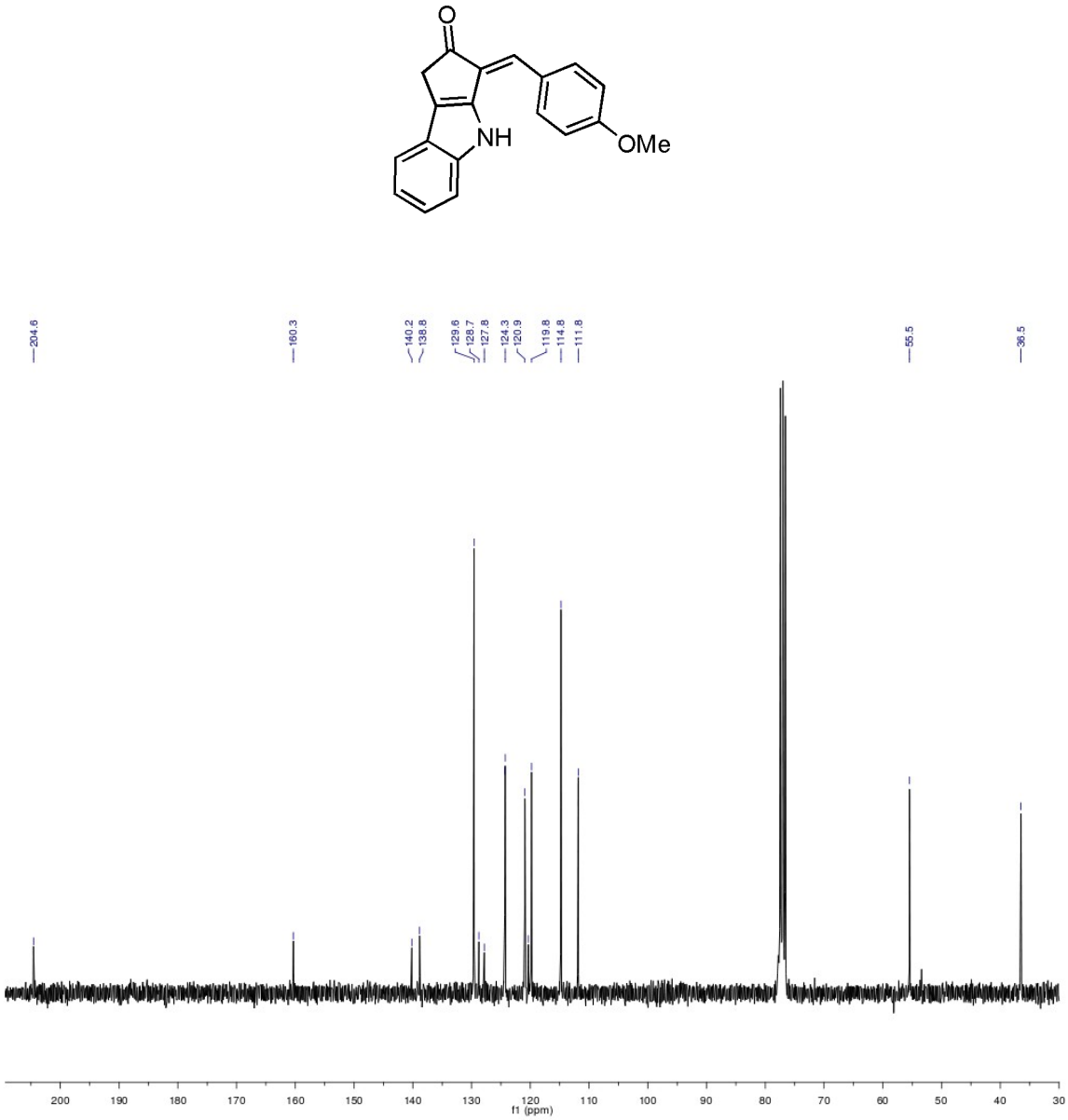

Figure VII.17: ^{13}C NMR spectrum of **29** in $CDCl_3$

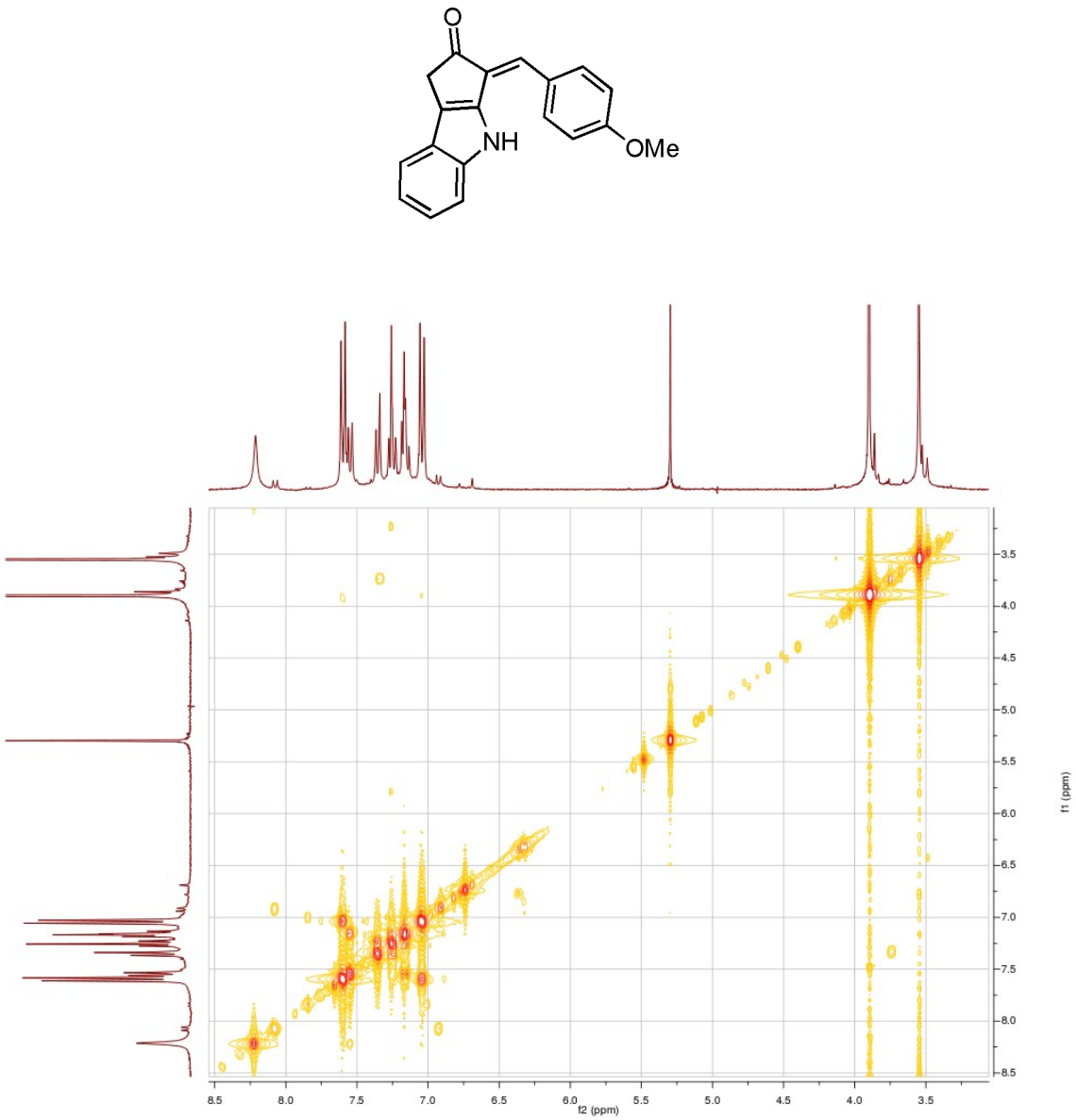

Figure VII.18: COSY spectrum of **29** in $CDCl_3$

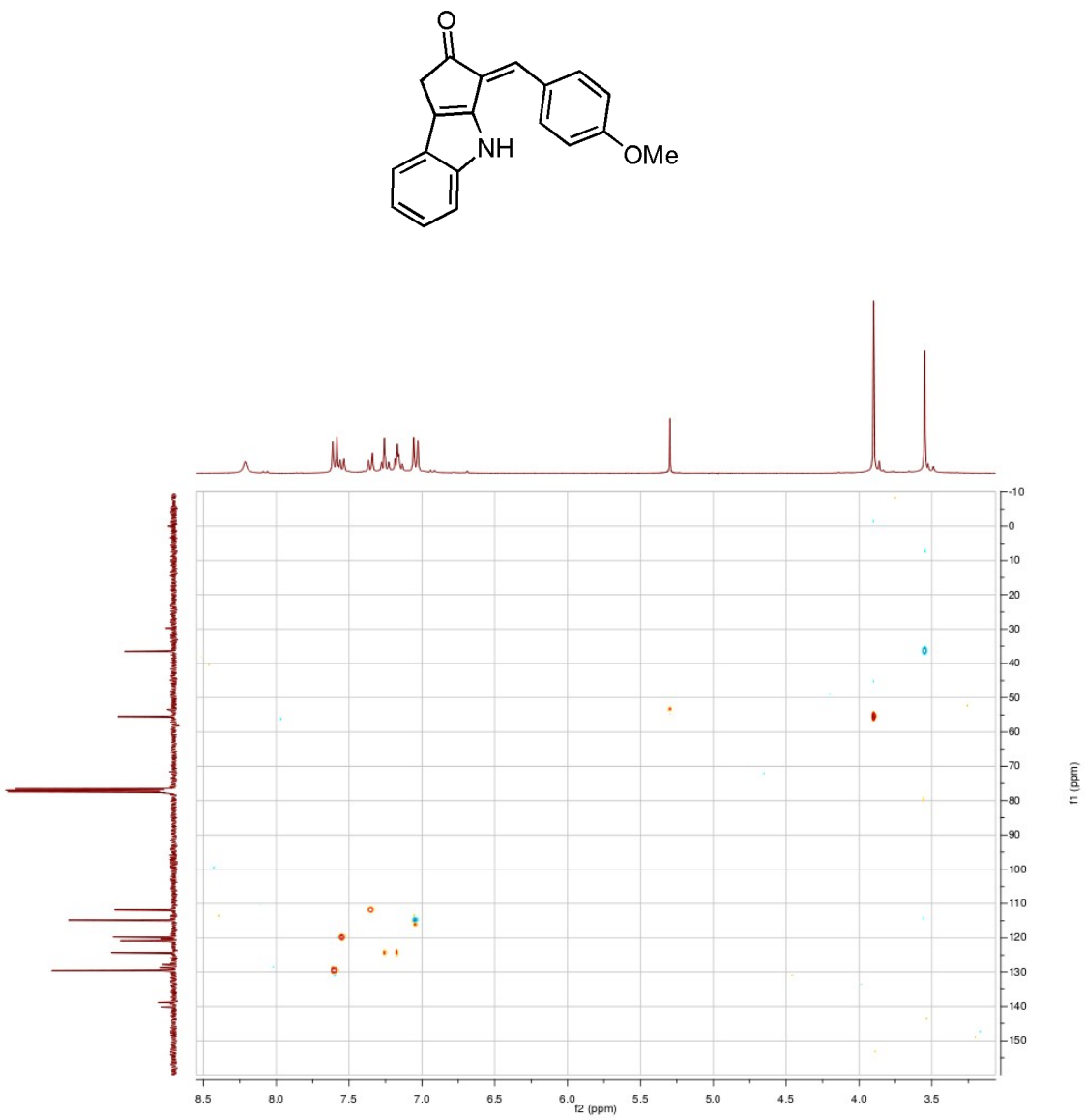

Figure VII.19: HSQC spectrum of **29** in $CDCl_3$

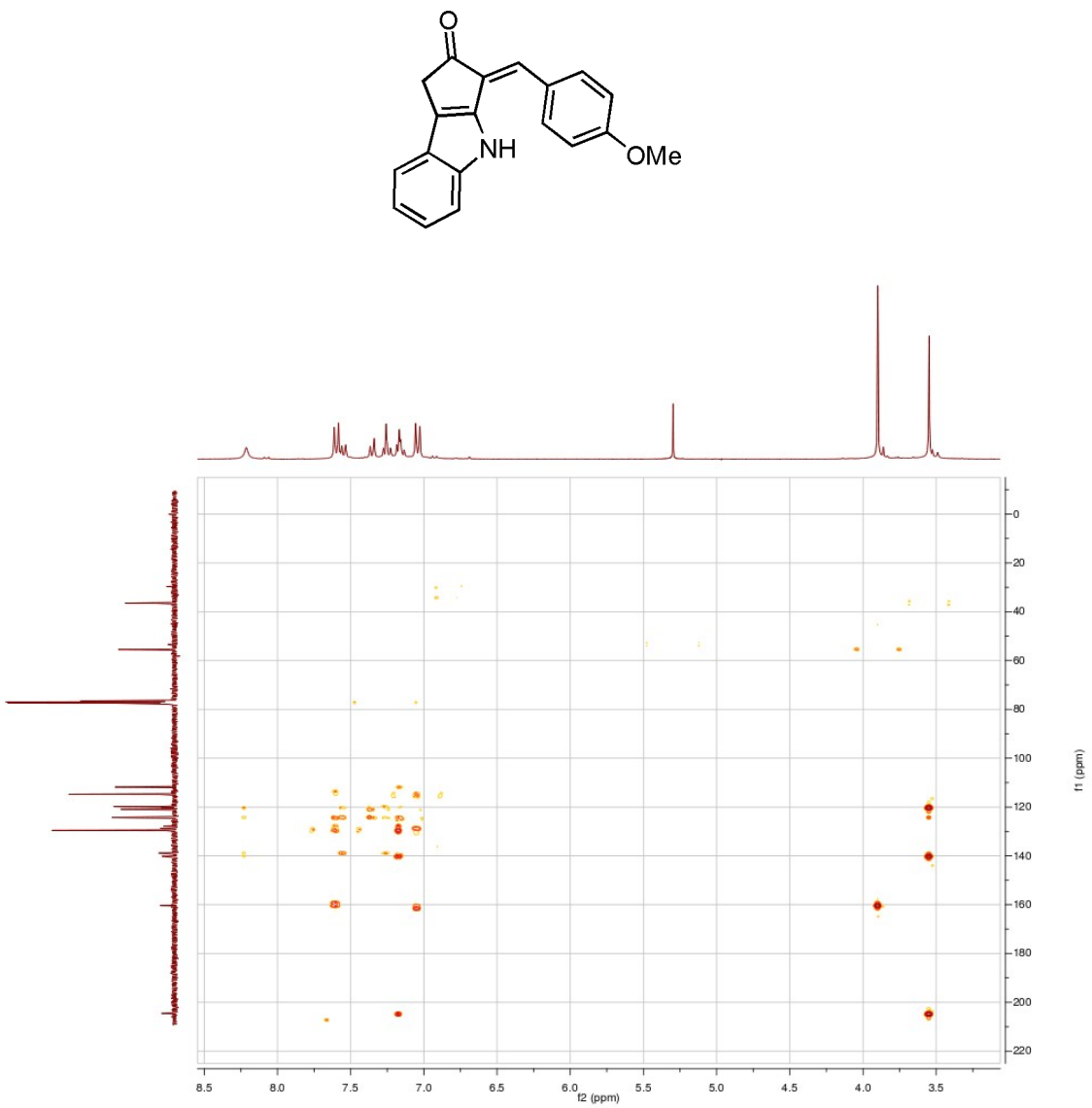

Figure VII.20: HMBC spectrum of **29** in $CDCl_3$

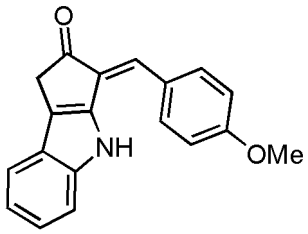

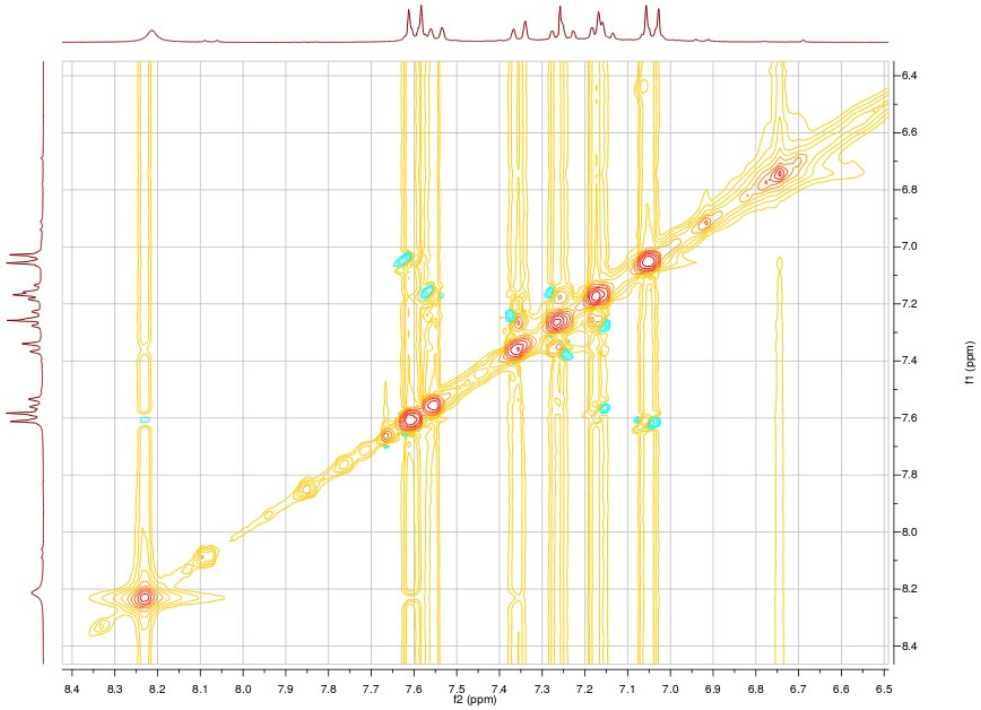

Figure VII.21: ROESY spectrum of **29** in $CDCl_3$

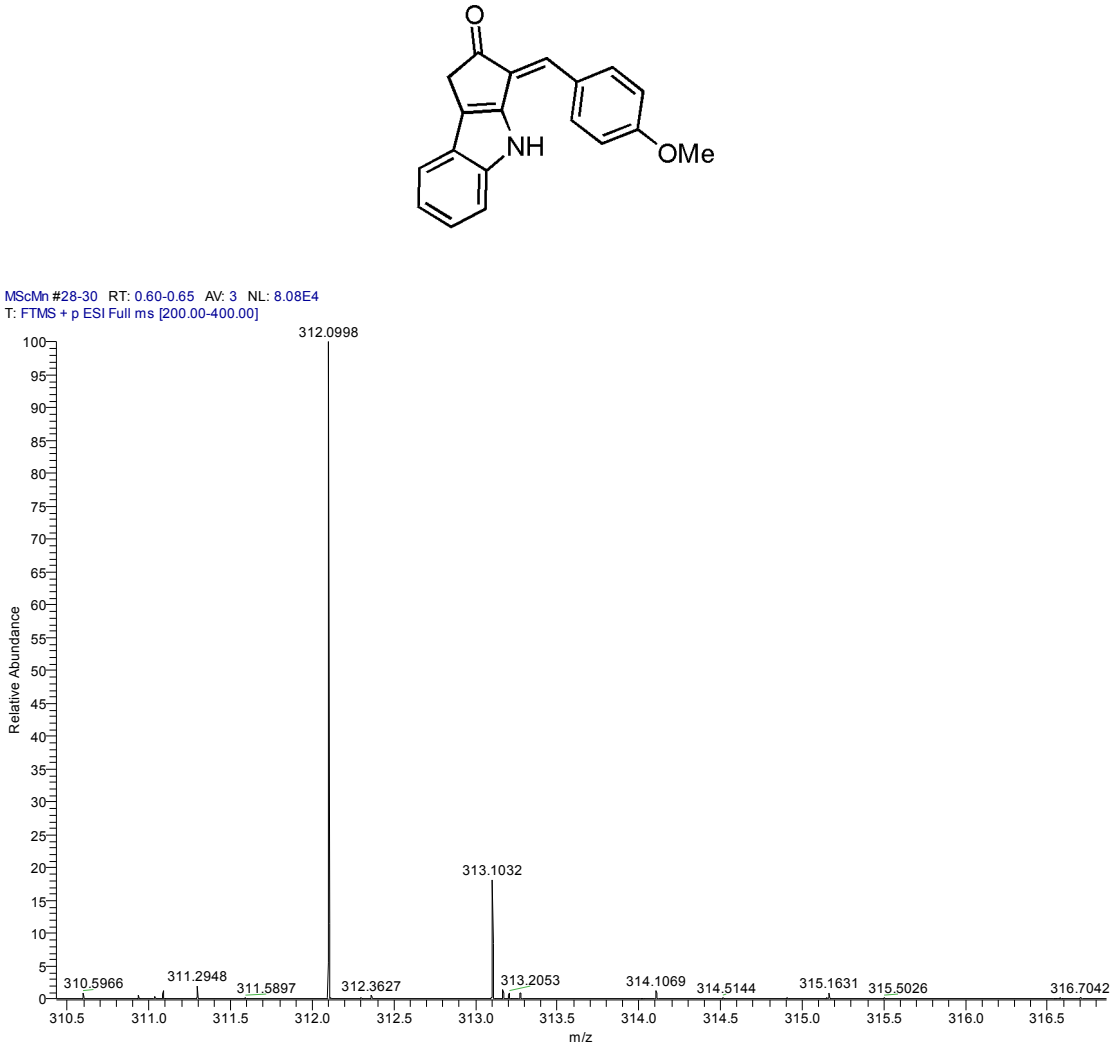

Figure VII.22: HRMS (ESI-FT) spectrum of **29** (showing [M+Na])

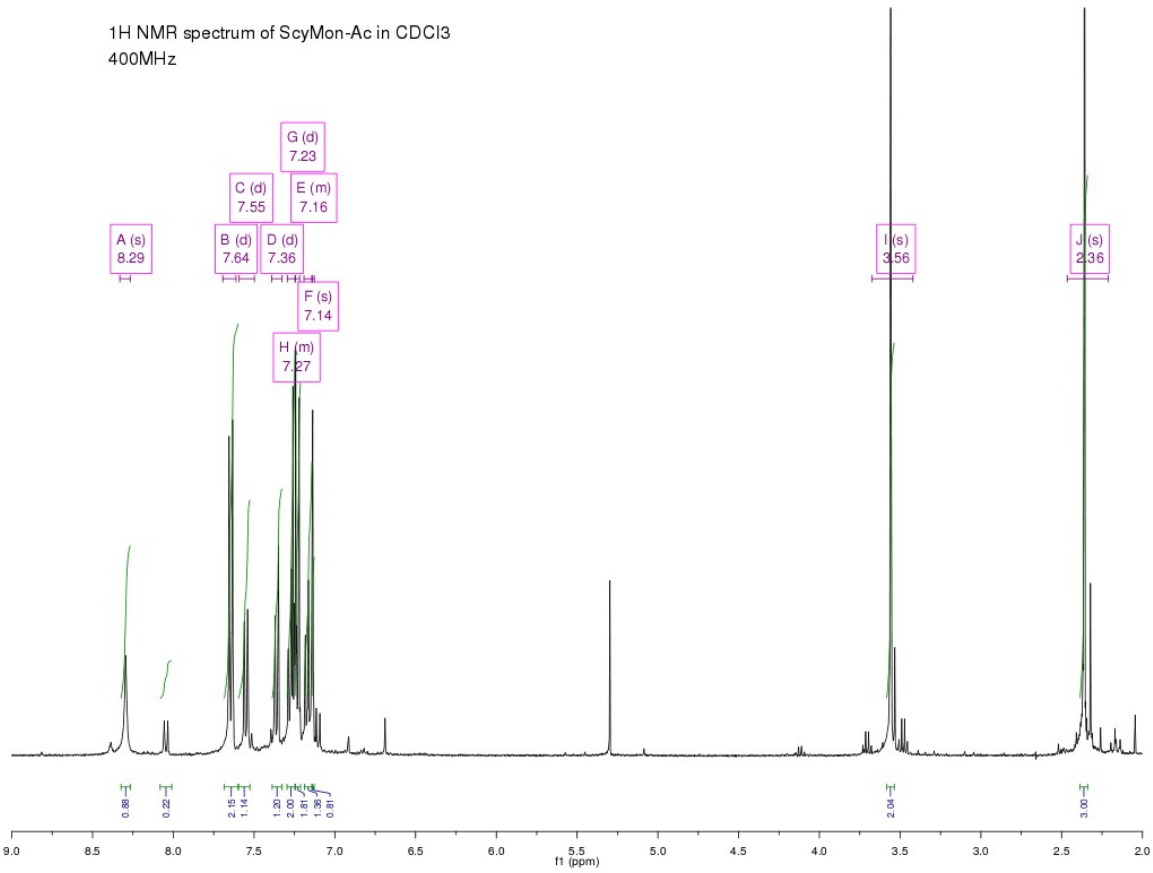

Figure VII.23: ^{1}H NMR spectrum of **34** in $CDCl_3$

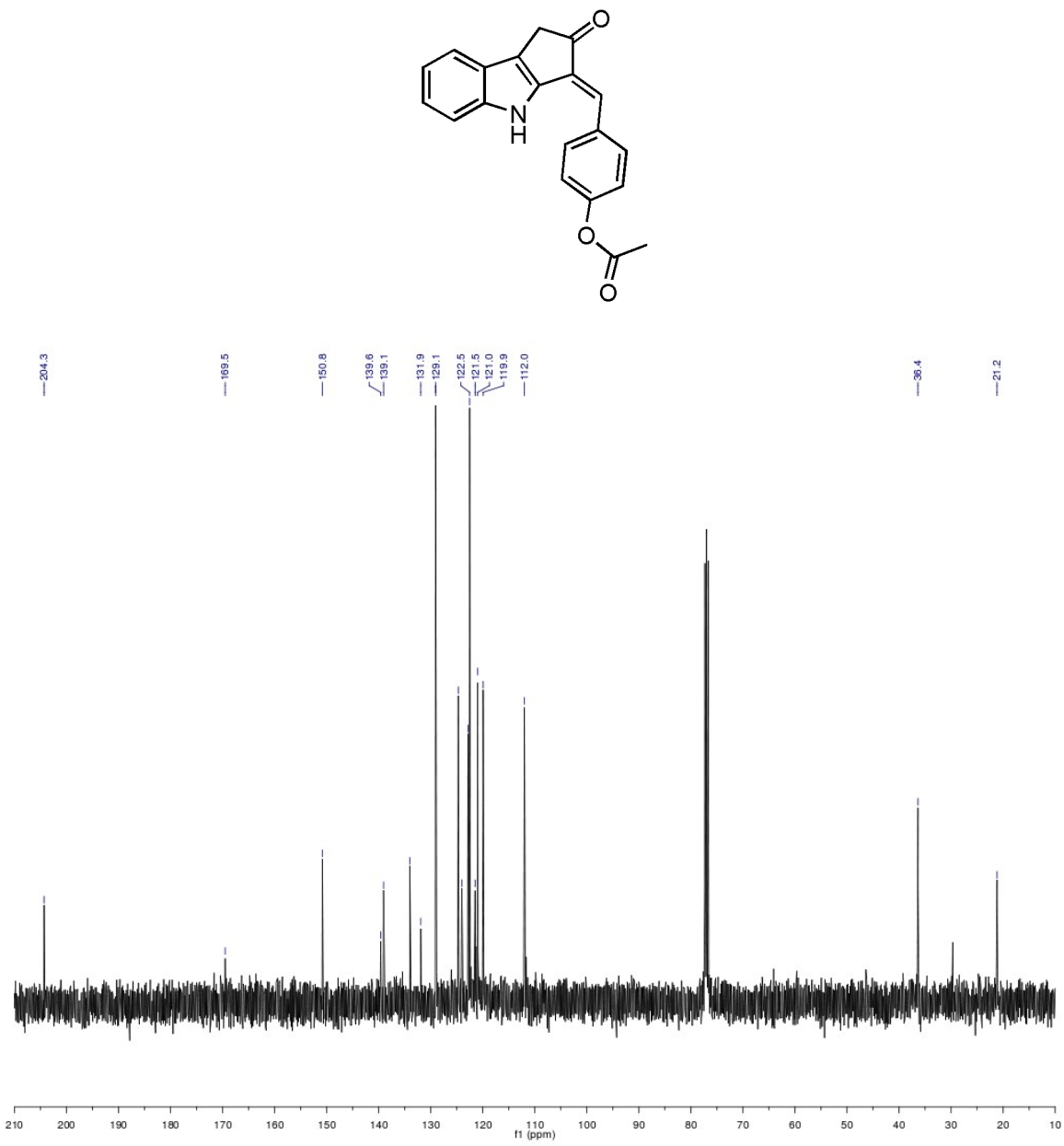

Figure VII.24: ^{13}C NMR spectrum of **34** in $CDCl_3$

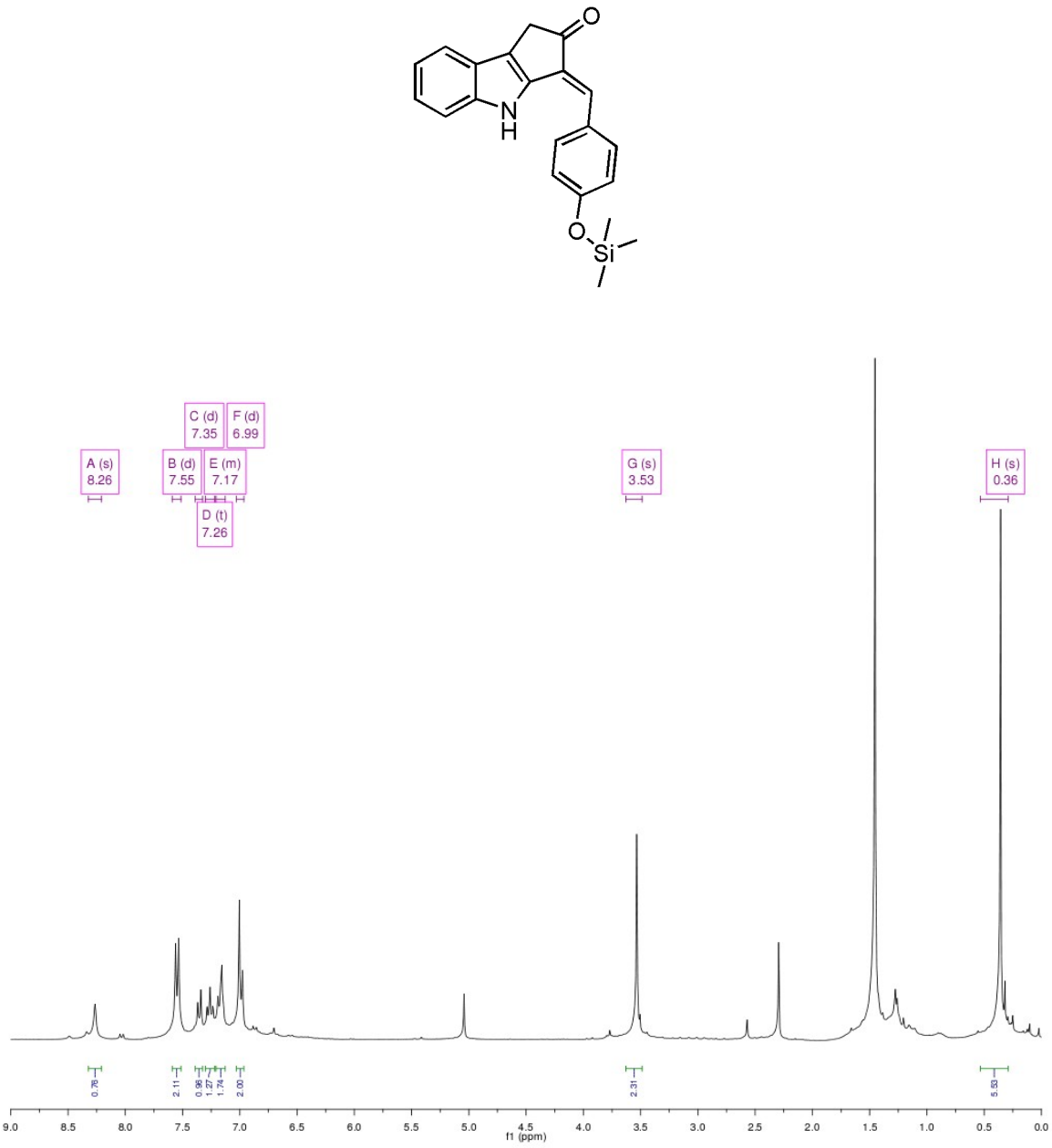

Figure VII.25: ^{1}H NMR spectrum of **37** in $CDCl_3$

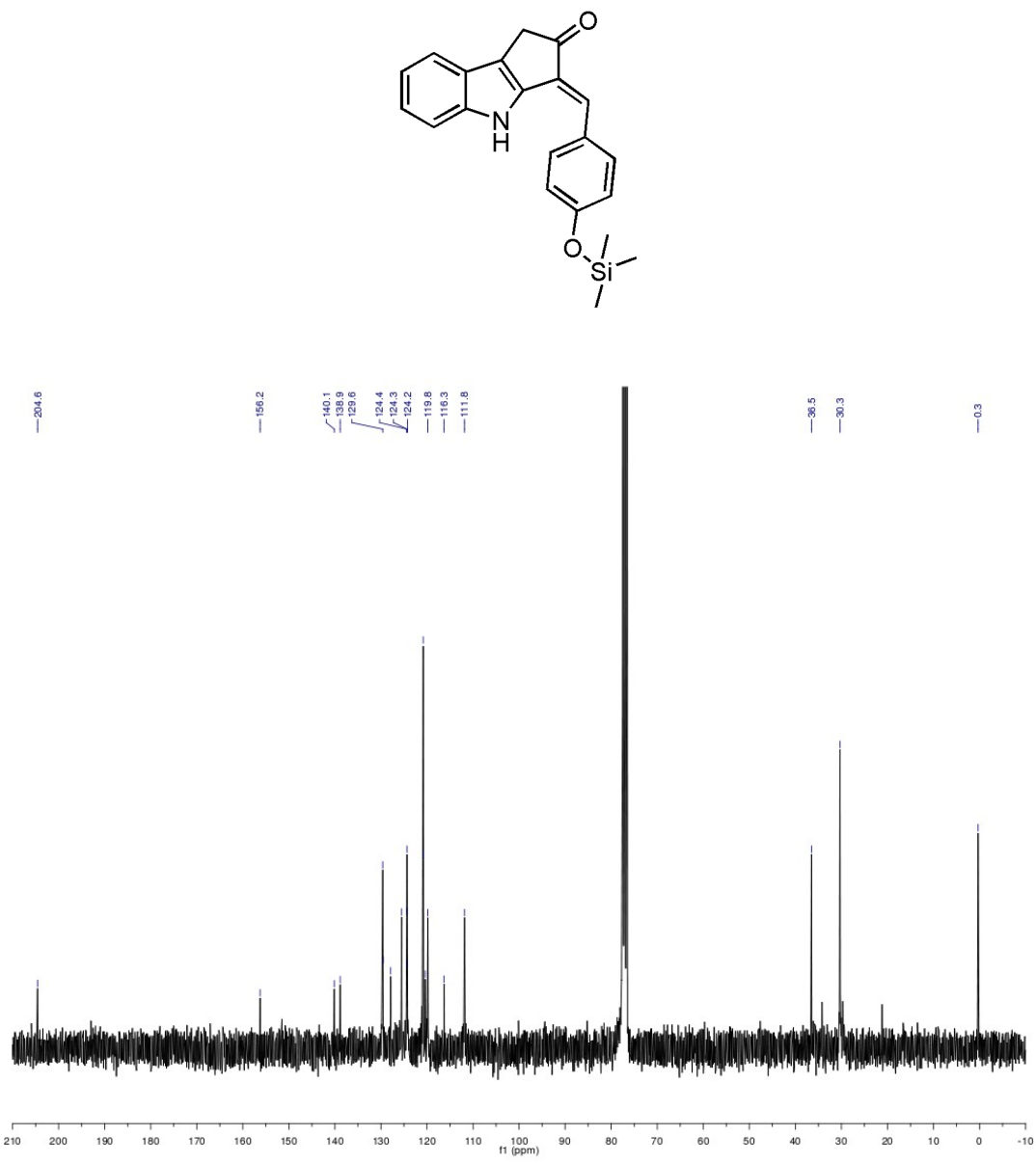

Figure VII.26: ^{13}C NMR spectrum of **37** in $CDCl_3$

References and Footnotes

1 Garcia-Pitchel, F.; Sherry, N. D.; Castenholz, R. W. Evidence for an ultraviolet sunscreen role of the extracellular pigment scytonemin in the terrestrial cyanobacterium *Chlorogloeopsis* sp. *Photochem. Photobiol.* **1992**, *56*, 17-23.

2 Proteau, P. J.; Gerwick, W. H.; Garcia-Pitchel, F.; Castenholz, R. The structure of scytonemin, an ultraviolet sunscreen pigment from the sheaths of cyanobacteria. *Experientia* **1993**, *49*, 825-829.

3 Dillon, J. G.; Castenholz, R. W. Scytonemin, a cyanobacterial sheath pigment, protects against UVC radiation: implications for early photosynthetic life. *J. Phycol.* **1999**, *35*, 673-681.

4 Sinha, R. P.; Häder, D. UV-protectants in cyanobacteria. *Plant Sci.* **2008**, *174*, 278-289.

5 Balskus, E. P.; Walsh, C. T. Investigating the initial steps in the biosynthesis of cyanobacterial sunscreen scytonemin. *J. Am. Chem. Soc.* **2008**, *130*, 15260-15261.

6 Nägeli, C. Gattungen einzelliger Algen, physiologisch und systematisch bearbeitet. *Neue Denkschrift Allg. Schweiz. Natur Ges.* **1849**, *10*, 1-138.

7 Kobayashi, A.; Kajiyama, S.; Inawaka, K.; Kanzaki, H.; Kawazu, K. Nostodione A, a novel mitotic spindle poison from a blue-green alga Nostoc commune. *Z. Naturforsch*. **1994**, *49c*, 464–470.

8 Tanya Soule, V. Stout, W. D. Swingley, J. C. Meeks, and F. Garcia-Pichel, Molecular Genetics and Genomic Analysis of Scytonemin Biosynthesis in Nostoc punctiforme ATCC 29133 . *J. Bacteriol.* **2007**, *189*, 4465-4472.

9 Matthews, C. K.; van Holde, K. E.; Ahern, K. G. *Biochemistry*, 3rd Ed. **2000**, Addison Wesley Longman, Inc.

10 Normally cyclization of indole at C-2 to form a five-membered ring is a rapid process.

11 (a) Stevenson, C. S.; Capper, E. A.; Roshak, A. K.; Marquez, B.; Grace, K.; Gerwick, W. H.; Marshall, L. A. Inflamm. Res. 2002, 51, 112–114. (b) Stevenson, C. S.; Capper, E. A.; Roshak, A. K.; Marquez, B.; Eichman, C.; Jackson, J. R.; Mattern, M.; Gerwick, W. H.; Jacobs, R. S.; Marshall, L. A. J. Pharmacol. Exp. Ther. 2002, 303, 858–866.

12 (a) Erick Cuevas-Yanez,a,* Joseph M. Muchowskib and Raymundo Cruz-Almanza , Rhodium(II) catalyzed intramolecular insertion of carbenoids derived from 2-pyrrolyl and 3-indolyl α-diazo-β-ketoesters and α-diazoketones. Tetrahedron 60 (2004) 1505–1511. (b) Mohamed Salim and Alfredo Capretta, Intramolecular Carbenoid Insertions: the Reactions of α-Diazoketones Derived from Pyrrolyl and Indolyl Carboxylic Acids with Rhodium(II) Acetate . Tetrahedron 56 (2000) 8063–8069.

13 This system worked well in the synthesis of somocystinamide A (see Chapter VI).

14 HF 3-21G* single point energy calc of dihedral angle constraint.

15 Such is available from Aldrich.

16 The feeding study is not completed at the time of writing.

17 DeMartino, M. P.; Chen, K.; Baran, P. S. Intermolecular Enolate Heterocoupling: Scope, Mechanism, and Application . *J. Am. Chem. Soc.* **2008**, *130*, 11546-11560.

18 Proteau, P. J. Oxylipins from temperate marine algae and a photoprotective sheath pigment from blue-green algae. **1993,** M.S. Thesis.

19 Sugimoto, T.; Ueda, M. Biomimetic synthesis of a leaf-opening factor, potassium isolespedezate, by direct formation of enol-glycoside. *Chem. Lett.* **2004**, *33*, 976-977.

20 All of these structures (**38-40**) require at least one four-bond HMBC correlation, which is not unheard of in a polycyclic aromatic system like scytonemin.

21 Yu, J.; Wang, T.; Wearing, X. Z.; Ma, J.; Cook, J. M. Enantiospecific Total Synthesis of (-)-(E)16-Epiaffinisine, (+)-(E)16-Epinormacusine B, and (+)-Dehydro-16-epiaffinisine as well as the Stereocontrolled Total Synthesis of Alkaloid G . *J. Org. Chem.* **2003**, *68*, 5852-5859.

22 Li, C. Cross-Dehydrogenative Coupling (CDC): Exploring C-C Bond Formations beyond Functional Group Transformations . *Accounts Chem. Res.* **2009**, *42*, 335-344.

23 Still, W. C.; Khan, M.; Mitra, A. Rapid chromatographic technique for preparative separations with moderate resolution. *J. Org. Chem.* **1978**, *43*, 2923-2925.

24 Leonard, J.; Lygo, B.; Procter, G. *Advanced Practical Organic Chemistry*, 2nd Ed. **1998**, Stanley Thomas Ltd.

Chapter VIII

Conclusions

Abstract

Conclusions drawn from the research activities described in Chapters I through VII are discussed herein.

VIII.1 Thesis

Natural products chemistry has benefited from organic synthesis in the areas of structure elucidation and confirmation, pharmaceutical application, and biosynthetic study of natural products. Simultaneously, natural products have been a major driving force for the advancement of organic synthesis. Given this rich history, direct application of organic synthesis to issues and opportunities surrounding natural products should improve productivity in all three areas mentioned above. As a significant added benefit, new chemical transformations and synthetic strategies may be discovered in the process.

VIII.2 Natural products isolated through the dissertation research

In order to evaluate the thesis that contributions from organic synthesis enhance the productivity of natural products chemistry, various studies were conducted, which included applying the techniques learned through the mastery of organic synthesis to natural product isolation and structure elucidation. The structures of the natural products that were isolated in this endeavor are summarized below in Figure VIII.1. A chemist well-trained in synthetic organic chemistry usually has mastered the art of chromatographic purification of unstable compounds. This skill most certainly increases the chance of isolating natural products of interest with a good yield and purity. Moreover, a synthetic chemist has seen a large number of NMR spectra of many different classes of compounds, which is an experience that can aid in the structure elucidation process.

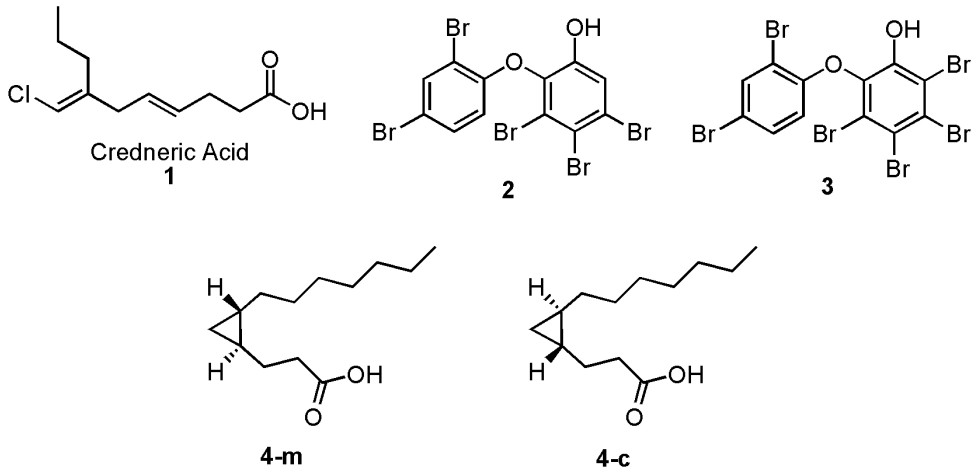

Figure VIII.1: Natural products isolated during the dissertation research

Cyclopropyl fatty acid **4-m** was isolated from a Madagascar collection of *Lyngbya majuscula*. Likewise, **4-c** was isolated from a Curaçao collection of the same organism. The stereochemistry of these two natural products are updated as per Chapter IV.

Water-soluble organic compounds are difficult to purify and to handle. Therefore, many natural products remain undiscovered due to their polarity and solubility in water. Skills nurtured through organic synthesis were utilized to isolate credneric acid (**1**), a metabolite found in the aqueous extract of a *Lyngbya* sp. from Papua New Guinea. In the pursuit to identify neurologically important marine natural products, two polybrominated diphenyl ethers (**2** and **3**) were obtained through a bioassay-guided isolation approach. The literature ^{13}C NMR values for **2** contradicted our findings, and this discrepancy was unequivocally resolved through synthesizing alternative structures to evaluate the contradicting ^{13}C NMR data.

Although unresolved, a novel concept (synthetic introduction of a stereochemical reference, SISTER method) was developed to elucidate the absolute stereochemistry of natural products that do not have a functional group appropriate for traditional derivatizations, such as synthesis of a Mosher's ester. In the course of this investigation,

an interesting concept regarding the 'phylogenetic nature' of absolute stereochemical assignments was noted.

VIII.3 Synthetic investigations of biologically important natural products

Through the total synthesis of both enantiomers of epiquinamide (**5**), a contribution was made to resolve the confusion about the identity of the potent nicotinic receptor agonist found in the skin of a rainforest frog, *Epipedobates tricolor*. Unfortunately, **5** was found to be inactive in many bioassays tested thus far. However, through the concept of using a biomimetic starting material (an ornithine derivative), a very expedient and practical synthetic route to **5** was developed. Had **5** been a bioactive molecule, this synthesis should have been able to provide sufficient quantities of the natural product for pharmaceutical investigations.

A total synthesis of a marine cyanobacterial metabolite, somocystinamide A (**7**), an exceptionally potent inhibitor of endothelial cell proliferation and angiogenesis, was also accomplished. The challenges presented by the enamide functionality were overcome after rigorous investigations. Surprisingly, the disulfide group, historically known to be a difficult functional group to synthesize, was relatively easily introduced after resorting to a somewhat biomimetic condition (molecular oxygen atmosphere in the presence of an aqueous base). Finally, a revision of the synthesis was successfully made to improve the scalability of the first synthesis, thereby providing a sufficient quantity of **7** for in vivo studies. This latter synthesis should enable future investigations of somocystinamide A analogs for development in the treatment of cancer.

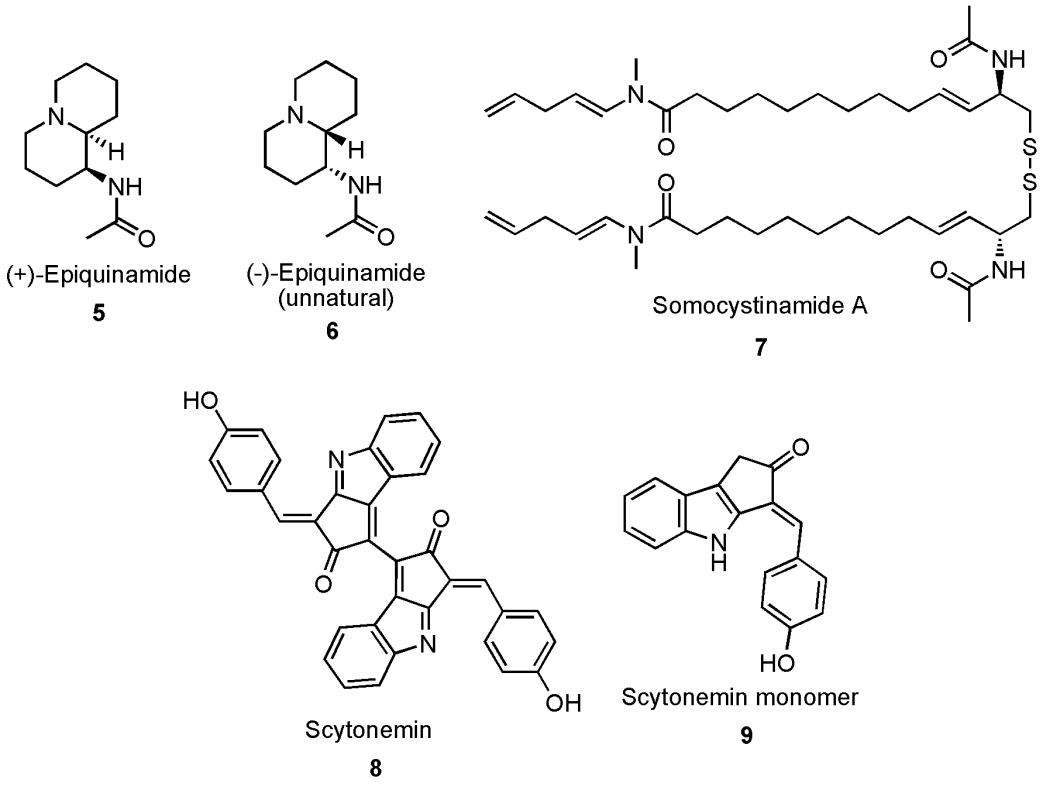

Figure VIII.2: Natural products that were synthetically investigated during the disseration research

Synthetic studies were conducted on a structurally unique alkaloid, scytonemin (**8**), a UV-blocking metabolite produced by cyanobacteria. The first synthesis of the putative monomeric precursor (**9**) of this natural product was accomplished in one step from a known indole derivative. Access to the monomer **9** allowed experiments to show that dimerization of **9** cannot occur spontaneously under ambient conditions and that such a reaction is probably enzymatically catalyzed (if it occurs at all). Moreover, many chemical and biosynthetic insights were gained through attempts to dimerize **9**, which was successful at a small yield albeit a very low yield. The synthesis of **9** and its derivatives contributed to a concurrent biosynthetic investigation of scytonemin as well.

Interestingly, pure **9** was tested in a mechanism-based anti-cancer assay and found to have unique and potentially valuable properties.

VIII.4 Final conclusions.

Through the chemical investigations of natural products mentioned above, the benefits of applying organic synthesis to natural products chemistry were clearly demonstrated. The approaches taken in this dissertation should continue to be productive in the foreseeable future.

Appendix

UV spectrum for scytonemin monomer

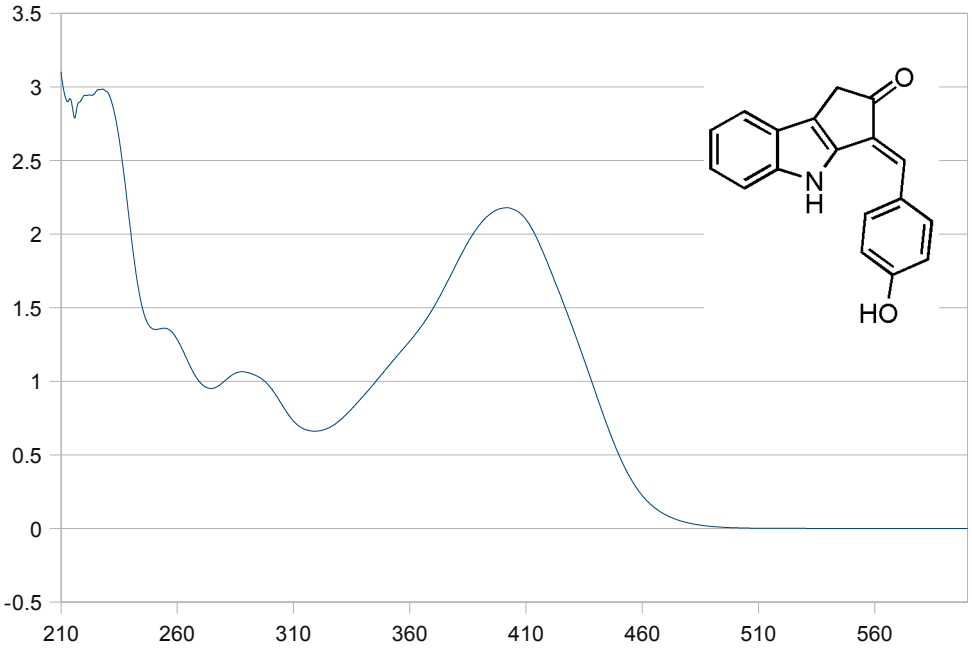

λ_{max} : 255 nm (ε = 3.8 m^2/mol); 289 nm (ε = 2.9 m^2/mol); 401 nm (ε = 6.1 m^2/mol)
Taken in 99:1 MeCN/THF (0.1 mg/ mL)

Feeding study with ^{13}C-labeled scytonemin monomer

The experimental results for the feeding study are summarized in Scheme 1. Labeled scytonemin's identity was confirmed through its retention time, which coincided with that of an authentic sample of scytonemin.

It is apparent that monomer **22** can be converted to **1** by a scytonemin-producing cyanobacterium. Moreover, two different hypotheses can be postulated based on the absence of singly labeled scytonemin (Figure 1). It is possible that presence of **22** suppressed any production of scytonemin as well as its monomer in the organism through a feedback mechanism. In this hypothesis, the observation of the unlabeled scytonemin is explained by small basal production of **1** prior to the UV radiation treatment and the

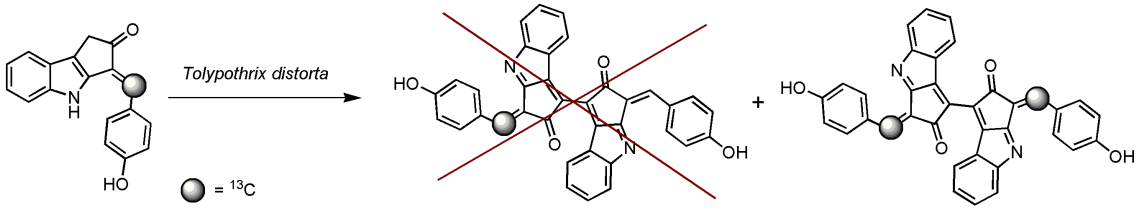

Scheme .1: *Incorporation of ^{13}C-labeled monomer **22***

Surprisingly, singly labeled scytonemin was not observed at all. However, almost equal amounts of unlabeled and doubly labeled scytonemin were observed. Tolypothrix distorta is a cyanobacterum that is known to be able to sustain moderate UV radiation through producing scytonemin.

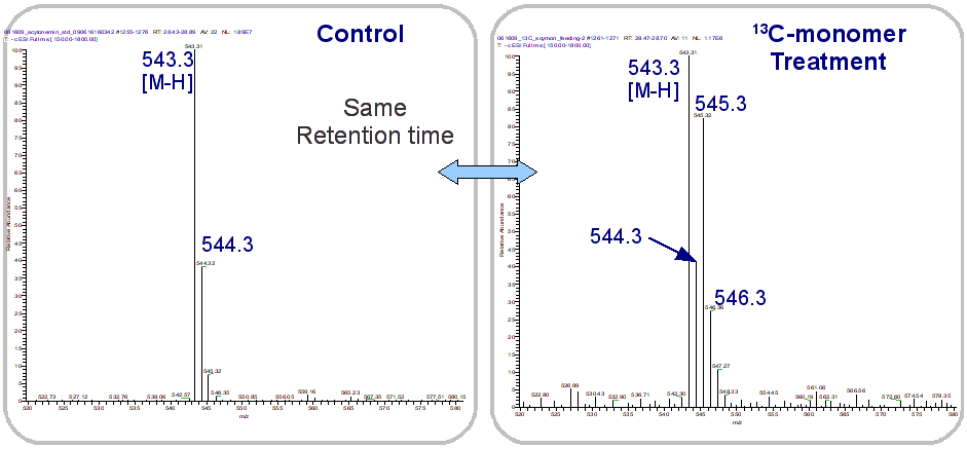

Figure 1: *ESI mass spectra of control and ^{13}C-labeled monomer treatment scytonemin*

The peak 543.3 corresponds to scytonemin ([M-H]) while the 545.3 peak corresponds to doubly labeled scytonemin ([M-H]).

introduction of **22**. Alternatively, it is possible that **22** blocked the UV radiation, which could result in suppression of the production of scytonemin in the cell. Given that most scytonemin molecules are found in the sheath and not in the cyanobacterial cell, it is

possible that the dimerization process only occurs in the sheath. If so, the labeled monomer that penetrated into the sheath would be converted only to doubly labeled scytonemin due to the suppressed production of scytonemin monomer in the cell.

Progress Report on N2024

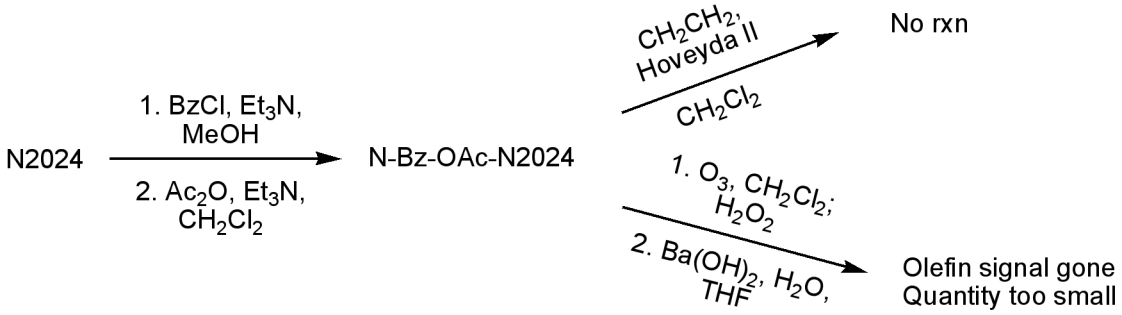

The above scheme summarizes the experiments done on N2024 so far. The ^{13}C and ^{1}H NMR spectra of N-Bz-O-Ac-N2024 were consistent with the expected structure. The decision was made to protect the free amines as amides because of the expected side reaction of the amine nitrogens attacking the ester(s) in the hydrolysis step (thereby forming lactams).

The attempt to perform ethenolysis by olefin metathesis was not successful even after prolonged reaction time. The ^{1}H NMR spectrum of the resulting material revealed olefin peaks, indicating that there was no reaction. However, oxidative ozonolysis seemed to have proceeded well based on the crude ^{1}H NMR taken on the product, in which the olefin peaks had disappeared. Subsequently, barium hydroxide mediated hydrolysis was carried out. After work-up, there were a few different compounds in the mixture and upon HPLC purification, only one of them was isolated in sufficient quantity for NMR analysis. Despite the 1.7 mm probe, it was not possible to obtain ^{1}H NMR spectrum of good quality for this material. This disappointing result may be due to two factors; 1) insufficient starting material, 2) the final product's poor solubility. The latter issue may have been worsened by the presence of an additional carboxylic acid moiety created by the oxidative ozonolysis step. For the next time, doubly reductive ozonolysis may be for performed, where the resulting ketone and aldehyde are reduced to alcohol. One complication would be the introduction of a new stereo center, the secondary alcohol.

Another approach that could be taken either independently from the above chemistry or in conjunction is to utilize the newly installed carbon-sensitive probe for ^{13}C NMR experiments. With this probe, experiments like INADEQUATE and ^{13}C-^{13}C COSY can be performed without the need for ^{13}C enrichment, thereby clarifying ^{13}C peaks through decoupling.

Experimental Details for Determination of Racemerization Rate of (*S*)-2-methylbutanal

Pier Lucio Anelli, Fernando Montanari, and Silvio Quici *Organic Syntheses*, **1993**, *8*, 367-372.

(*S*)-2-methylbutanal was synthesized according to the published procedure (above). The optical rotation was measured on a JASCO P-2000 polarimeter in the time-course measurement mode. Measurements were taken at 589 nm and at 22 ºC.

For the DMF/water run, 20.2 mg of (*S*)-2-methylbutanal was dissolved in 300 µL of DMF. Then immediately after the addition of 1.2 mL H2O, the mixture was swirled and its optical rotation was measured at 30 minute intervals.

For the MeOH run, 46.4 mg of (*S*)-2-methylbutanal was dissolved in 1.5 mL of MeOH. Immediately the mixture's optical rotation was measured at 1 minute intervals.

Below is a typical experimental result in which racemerization of (*S*)-2-methylbutanal is clearly seen through gradual decrease in the optical rotation value.